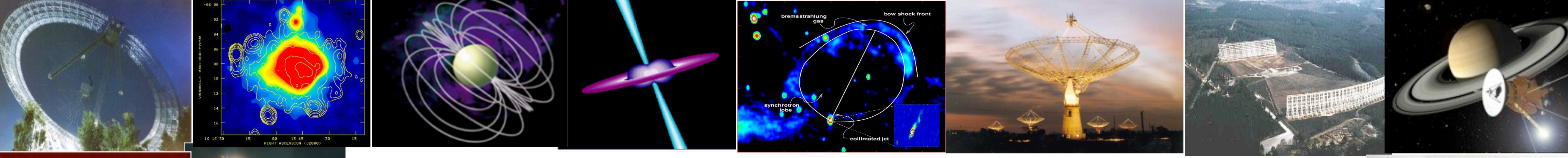

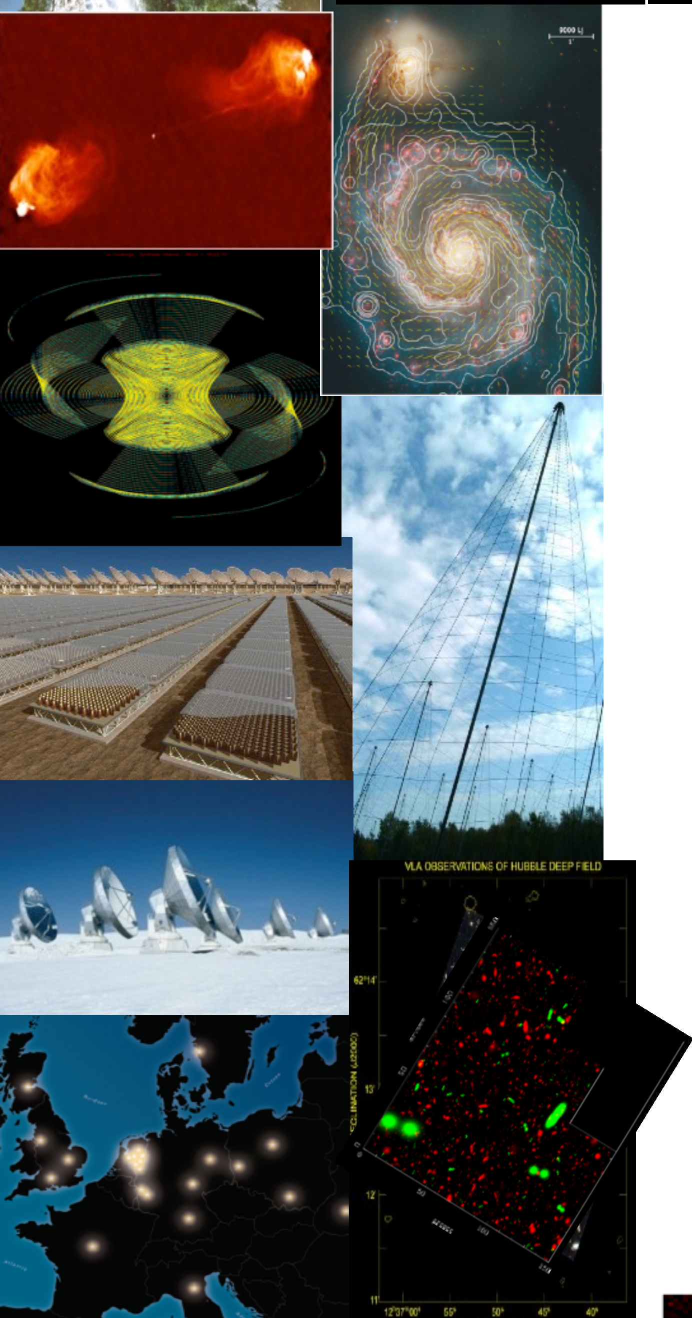

Introduction to Radioastronomy

Philippe ZARKA

<u>Outline</u> :

- Introduction (history, interest, specific features)
- Waves & Polarisation
- Plasmas & Propagation (cutoff, dispersion, Faraday effect, scintillations)
- Coherent Signal Detection (measurement theory, antenna temperature, calibration, noise)
- Receivers (heterodyne, system temperature, filtering, gain, RFI mitigation)
- Basics of Radio Astronomy Antennas: Single antennas
- Basics of Interferometry and Aperture Synthesis (phased arrays, electronic pointing, imaging, correlation, coherence, VLBI)
- Observation methods
- Large present & future ground-based radio arrays
- Basics of Space radio astronomy

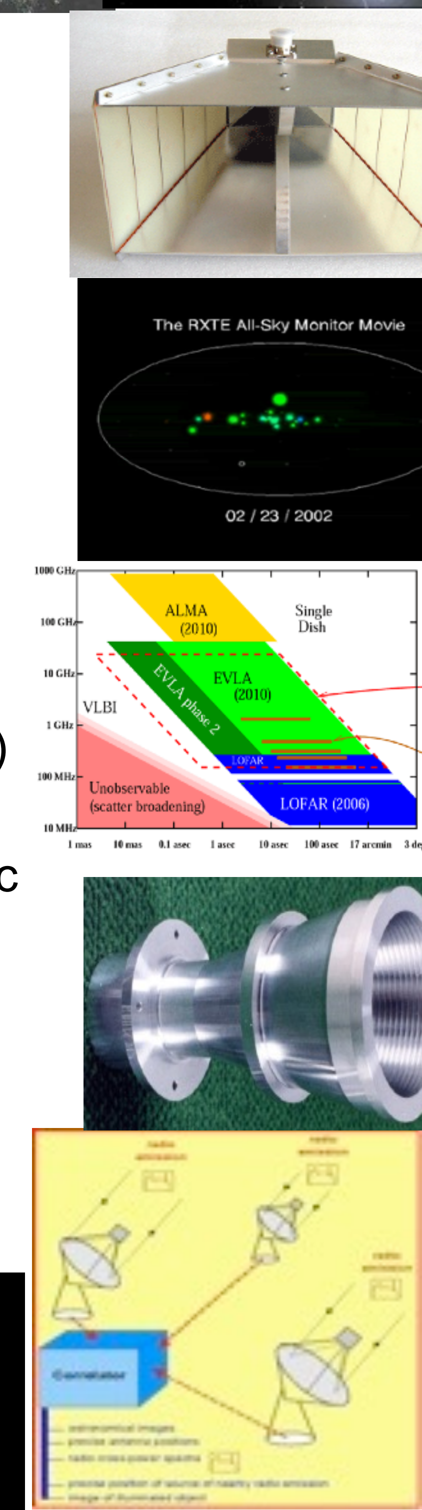

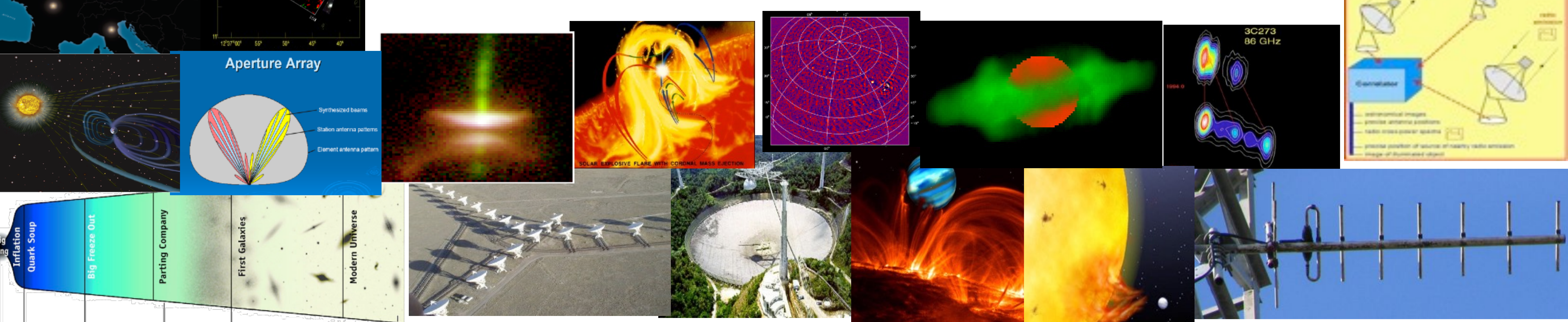

A few references

- J. D. Kraus, *Radio Astronomy*, Mac Graw-Hill, 2nd Ed., 1986.
- K. Rohlfs & T. L. Wilson, *Tools of Radio Astronomy*, Astronomy&Astrophysics Library, Springer, 2nd Ed., 1996.
- B. Burke & F. Graham-Smith, *An Introduction to Radio Astronomy*, Cambridge University Press, 1997.
- N. E. Kassim, M. R. Perez, W. Junor, P. A. Henning *(Editors)*, *From Clark Lake to the Long Wavelength Array*, ASP Conference series Vol. 345, 2005.
- R. G. Stone, K. W. Weiler, M. L. Goldstein & J.-L. Bougeret *(Editors)*, *Radio Astronomy at Long Wavelengths*, Geophysical Monograph 119, American Geophysical Union, Washington, USA, 2000.
- N. E. Kassim & K. W. Weiler *(Editors)*, *Low Frequency Astrophysics From Space*, Lecture Notes In Physics, Springer-Verlag, 1991.
- C.R. XXXth Goutelas school CNRS/INSU/SF2A, *«Radioastronomie Basses Frequences : Instrumentation, Thematiques scientifiques, Projets»*, 2007. http://www.lesia.obspm.fr/plasma/Goutelas2007/Goutelas-2007-Final.pdf
- J. P. Hamaker, J. D. Bregman, & R. J. Sault (& permutations), *Understanding Radio Polarimetry I / II / III,* Astron. Astrophys. Suppl. Series, pp. 137-165, 1996.
- O. Smirnov, *Revisiting the radio interferometer measurement equation I / II / III / IV,* Astron. Astrophys., 527(A106-A108)+531(A159), 2011.
- G. Heald, J. McKean, R. Pizo (*Editors*), *Low Frequency Radio Astronomy and the LOFAR Observatory*, ASS Library 426, 2018. https://www.astron.nl/radio-observatory/news/lofar-book/lofar-book

Internet sites:

https://www.obs-nancay.fr/	(Nançay Observatory)
https://www.obs-nancay.fr/-LOFAR-.html	(LOFAR @ Nançay)
https://nenufar.obs-nancay.fr/	(NenuFAR)
http://www.lofar.org/	(LOFAR)
http://www.astron.nl/radio-observatory/astronomers/lofar-astronomers	(LOFAR astronomers)
http://www.phys.unm.edu/~lwa/index.html	(LWA)
http://www.ece.vt.edu/swe/lwa/	(LWA memos)
https://www.mwatelescope.org/	(MWA)
https://www.skatelescope.org	(SKA)
http://www.iram-institute.org/	(IRAM)
http://www.iram-institute.org/EN/content-page-109-7-67-109-0-0.html	(IRAM millimeter interferometry summer schools)
https://www.almaobservatory.org/	(ALMA)
https://science.nrao.edu/facilities/alma/aboutALMA/Technology/ALMA_Memo_Series	(ALMA memos)
https://www.sarao.ac.za/gallery/meerkat/	(MeerKAT)
https://ngvla.nrao.edu/	(ngVLA)
https://salfconference.org	(Science at Low Frequencies conferences)
https://launchpad.net/apsynsim	(Aperture Synthesis Simulator)

- Introduction (history, interest, specific features)
- Waves & Polarisation
- Plasmas & Propagation (cutoff, dispersion, Faraday effect, scintillations)
- Coherent Signal Detection (measurement theory, antenna temperature, calibration, noise)
- Receivers (heterodyne, system temperature, filtering, gain, RFI mitigation)
- Basics of Radio Astronomy Antennas: Single antennas
- Basics of Interferometry and Aperture Synthesis (phased arrays, electronic pointing, imaging, correlation, coherence, VLBI)
- Observation methods
- Large present & future ground-based radio arrays
- Basics of Space radio astronomy

Introduction

- e.m. waves = main information vector in astronomy
  (+ cosmic rays, dust, neutrinos, gravitational waves...)

- Observation = Energy collection (of photons) + Measurement

- Atmospheric transparency : Radio window = 2nd transparent window of the atmosphere

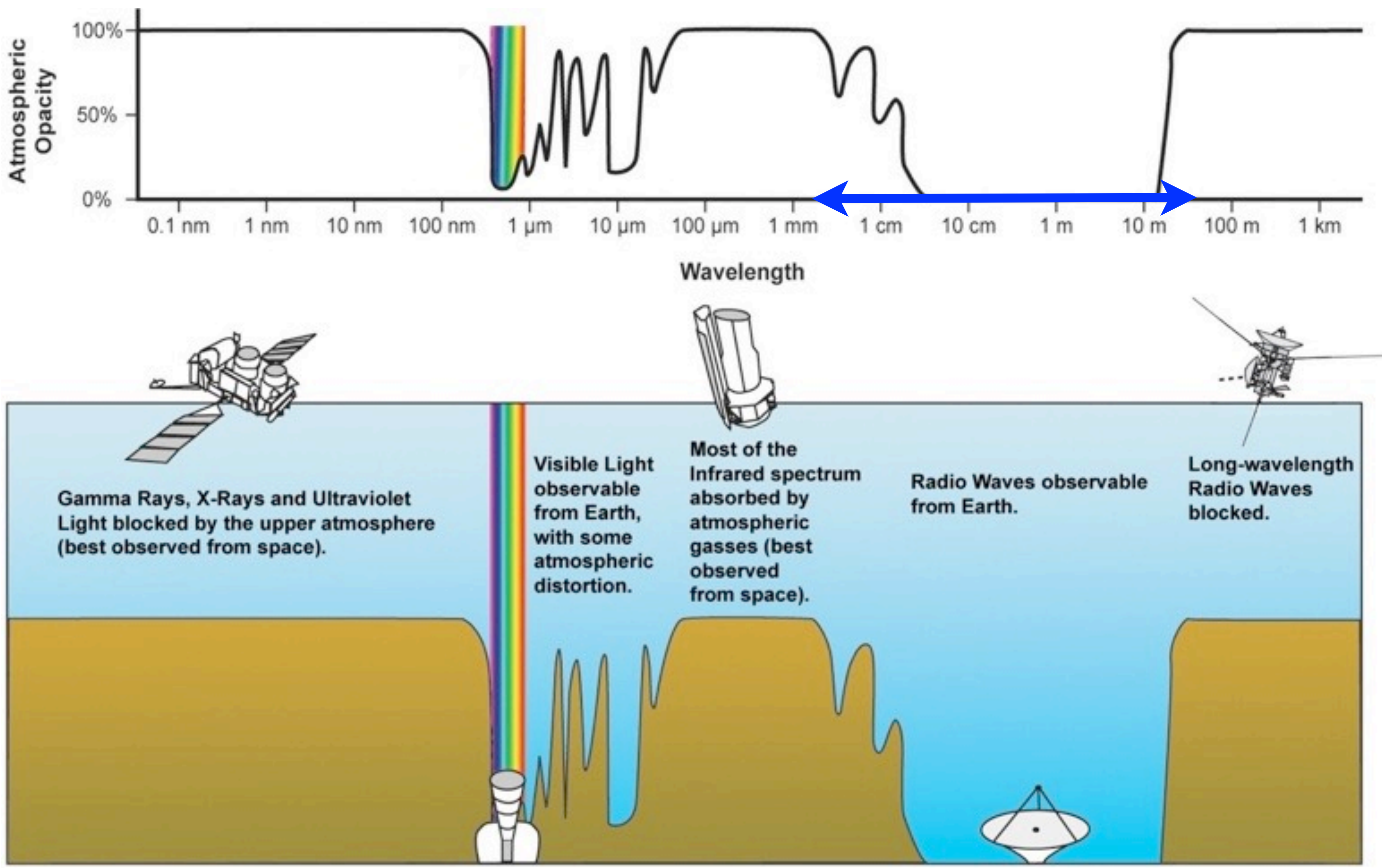

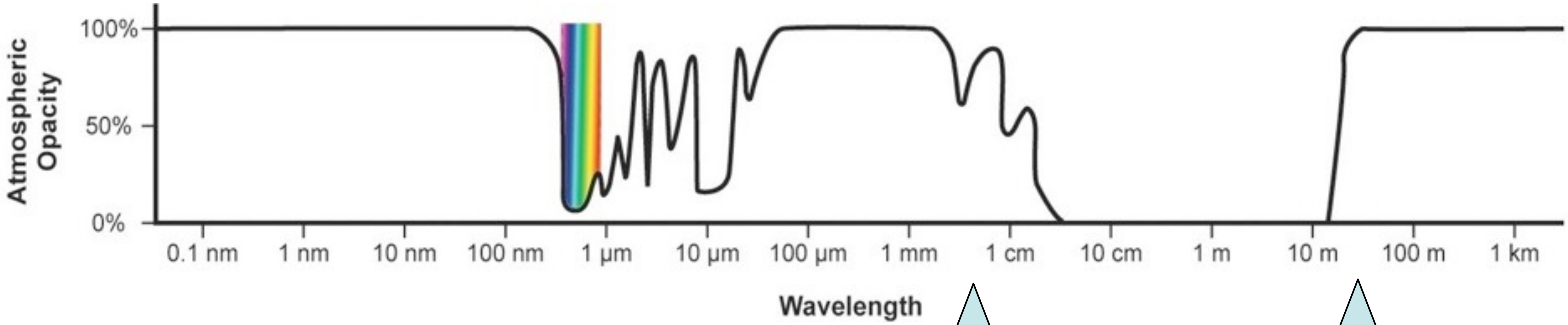

$\lambda = 0.1 - 1$ cm $\longleftrightarrow$ ~30 m

$\Downarrow$ numerous atmospheric lines $\Rightarrow$ quasi-complete extinction

$\Downarrow$ partial absorption by atmospheric O_2, H_2O …

$\Downarrow$ reflection by ionosphere ($z \approx 80\text{-}10^3$ km)

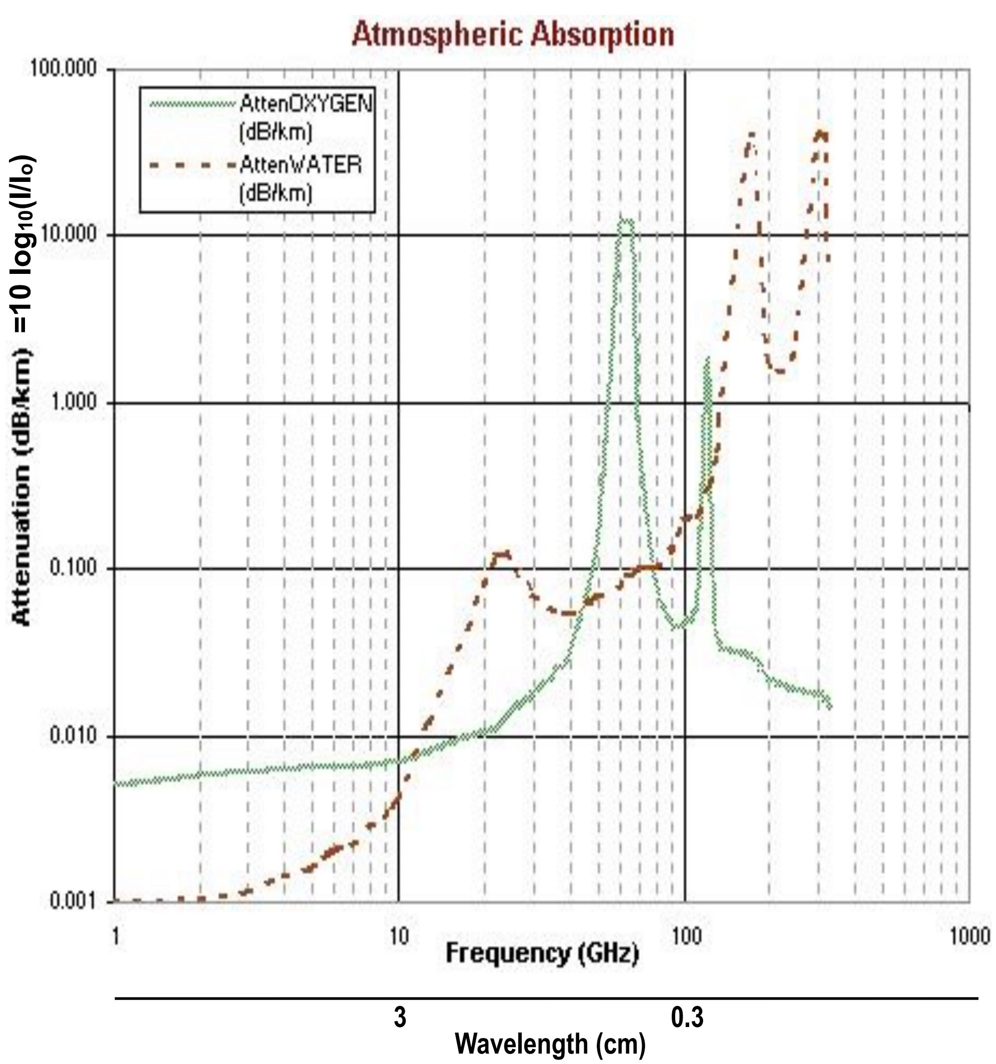

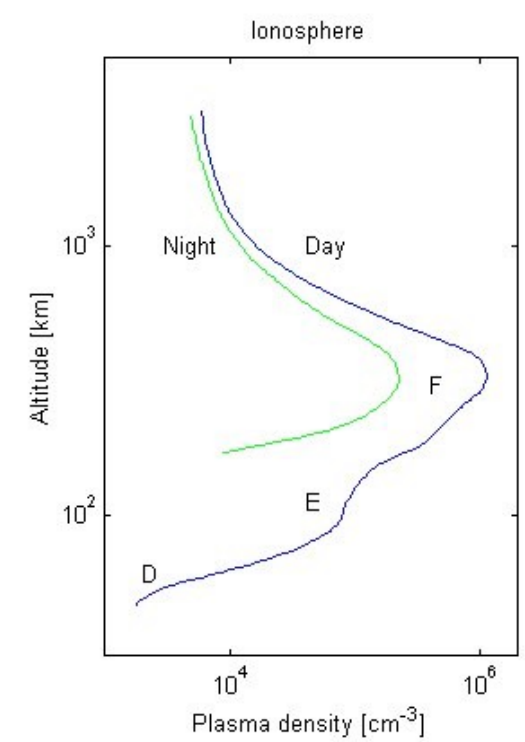

- Access to : $\lambda \leq 0.1$ cm & $\lambda \geq 30$ m $\Rightarrow$ Space

- Some definitions & reminders: Fourier transform ......

Signal (electric field) : $E(t)$

Spectrum : $\bar{E}(\nu) = \int_{\infty} E(t)\, exp(-i2\pi\nu t)\, dt = TF[E(t)]$

thus inversely : $E(t) = \int_{\infty} \bar{E}(\nu)\, exp(+i2\pi\nu t)\, d\nu = TF^{-1}[\bar{E}(\nu)]\ )$

Spectral component : $\bar{E}(\nu_o) = \int_{\infty} E(t)\, exp(-i2\pi\nu_o t)\, dt$

$\Rightarrow$ *practical calculation :* $\bar{E}(\nu_o) = (1/\Delta T) \int_{\Delta T} E(t)\, exp(-i2\pi\nu_o t)\, dt \qquad (\Delta T >> 1/2\pi\nu_o)$

$$\bar{E}(\nu_o) = |\bar{E}(\nu_o)|\, exp(i\varphi) = |\bar{E}(\nu_o)|\, (cos\varphi + i\, sin\varphi)$$

Signal at frequency ν_o *:* $E(t)|_{\nu o} = \int_{\infty} \bar{E}(\nu)\, exp(+i2\pi\nu t)\, \delta(\nu-\nu_o)\, d\nu$

$$= \bar{E}(\nu_o)\, exp(+i2\pi\nu_o t)$$

$$= |\bar{E}(\nu_o)|\, exp[+i(2\pi\nu_o t + \varphi)] \qquad (\text{but } E(t)|_{\nu o} \text{ real})$$

$$\Rightarrow \quad E(t)|_{\nu o} = |\bar{E}(\nu_o)|\, cos(2\pi\nu_o t + \varphi)$$

Spectral power : $P(\nu) = |\bar{E}(\nu)|^2$ *(often mistakenly referred to as the « spectrum »)*

$\Rightarrow$ $\bar{E}(\nu)$ *hereafter noted* $E(\nu)$

t & ν = conjugate variables

$E(t)$ & $E(\nu)$ = Fourier pairs

- Some definitions & reminders: Fourier transform ......

$E(t)$ real $\Rightarrow$ $E(-\nu) = E(\nu)^*$

Convolution product : $h(x) = \int_\infty f(y).g(x-y)\, dy = f \otimes g$

$\Rightarrow TF(h) = TF(f \otimes g) = TF(f) \times TF(g)$

Auto-correlation function : $C(\tau) = \int_\infty E(t).E(t+\tau)\, dt$

$\Rightarrow TF[C(\tau)] = C(\nu) = E(\nu) \times E(-\nu) = E(\nu) \times E(\nu)^* = |E(\nu)|^2 = P(\nu)$

= Wiener-Khintchine Theorem

The Fourier Transform conserves energy : $\int_\infty |E(t)|^2\, dt = \int_\infty |E(\nu)|^2\, d\nu$

Translation and Modulation : $E(t) \times \cos(2\pi\nu_o t) = E(t) \times \frac{1}{2}(\exp(i2\pi\nu_o t) + \exp(-i2\pi\nu_o t)) = E'(t)$

$\Rightarrow TF[\, E(t) \times \cos(2\pi\nu_o t)\,] = E'(\nu) = \frac{1}{2}\, [\, E(\nu-\nu_o) + E(\nu+\nu_o)\,]$

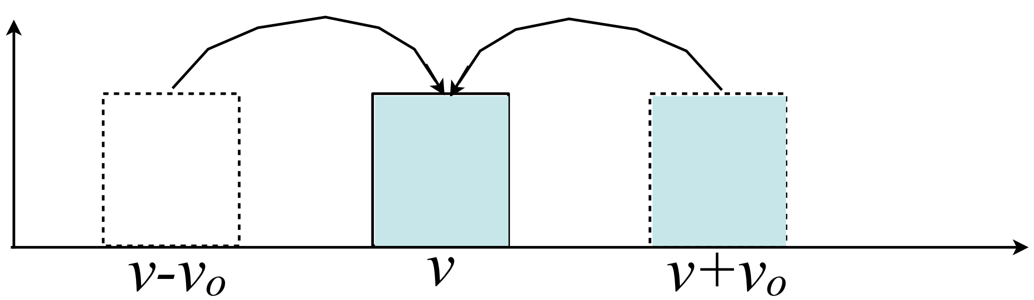

$E(t)$	1	$\cos(2\pi\nu_o t)$	$\sin(2\pi\nu_o t)$	$\Pi(t)$ $=1$ if $\lvert t\rvert \leq \frac{1}{2}$, $=0$ else	$\exp(-\pi^2 t^2)$	Random Gaussian / Uniform
$E(\nu)$	δ	$\frac{1}{2}[\delta(\nu_o)+\delta(-\nu_o)]$	$\frac{1}{2i}[\delta(\nu_o)-\delta(-\nu_o)]$	$\mathrm{sinc}(\nu)$ $=\sin(\pi\nu)/\pi\nu$	$\exp(-\nu^2)$	~Flat Random Gaussian / $+\delta$

- Coherent detection = "Radio" domain

Incoherent detection	Coherent detection
Measurement of $<E(t)^2>$ or $<E(t)\|_\nu{}^2>$ $\Rightarrow$ total flux only $\Rightarrow$ HF ($\nu \geq \nu_{IR}$) $\Rightarrow$ bolometers (1 pixel-imagery), micro-bolometer arrays, CCD, micro-channels…	Direct mesurement of $E(t)$ or $E(t)\|_\nu$ $\Rightarrow$ $\|E\|$ & ϕ $\Rightarrow$ $\nu \leq \nu_{sub\text{-}mm}$ $\Rightarrow$ Radio receivers - in baseband: ADC for $\nu \leq$ ~1 GHz - heterodyne: $E(t) \rightarrow E'(t) = E(t)\times\cos(2\pi\nu_{OL}t)$ $\Rightarrow$ translation in frequency of the spectrum, requires phase-preserving oscillators and mixers

- Techniques adapted from radar and telecommunications
- Boundary between incoherent / coherent detection = technological limit

"Visible", IR ... / Radio

rises in frequency with time (e.g. Lasers as O.L. ...)

$\rightarrow$ Current limit $\approx$ some THz = ($\lambda \leq 0.1$ mm)

Historical milestones

1800	Existence of invisible light	William Herschel
1889	Radio wave = e.m. wave = light wave : propagation in straight line at c in a vacuum, 1st emission/reception ∃? cosmic radio waves ? (but no radio technology available)	Heinrich Hertz Henri Deslandres
1900-5	1st attempts to detect the Sun (175m wire antenna + galvanometer) → failed (sensitivity, solar minimum…)	Oliver Lodge Charles Nordmann
1930-33	**Birth of Radioastronomy : ν = 20.55 MHz (λ=14.6 m)** → lightning storms + emission from galactic center (fixed sidereal time)	**Karl Jansky**

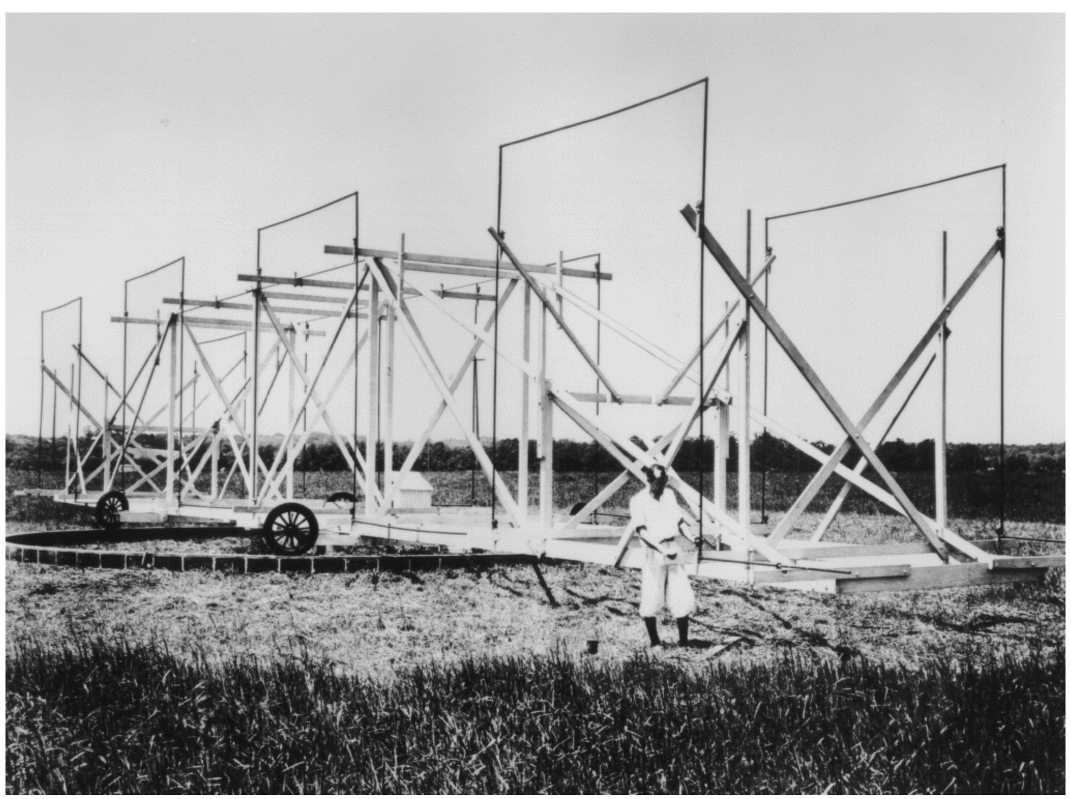

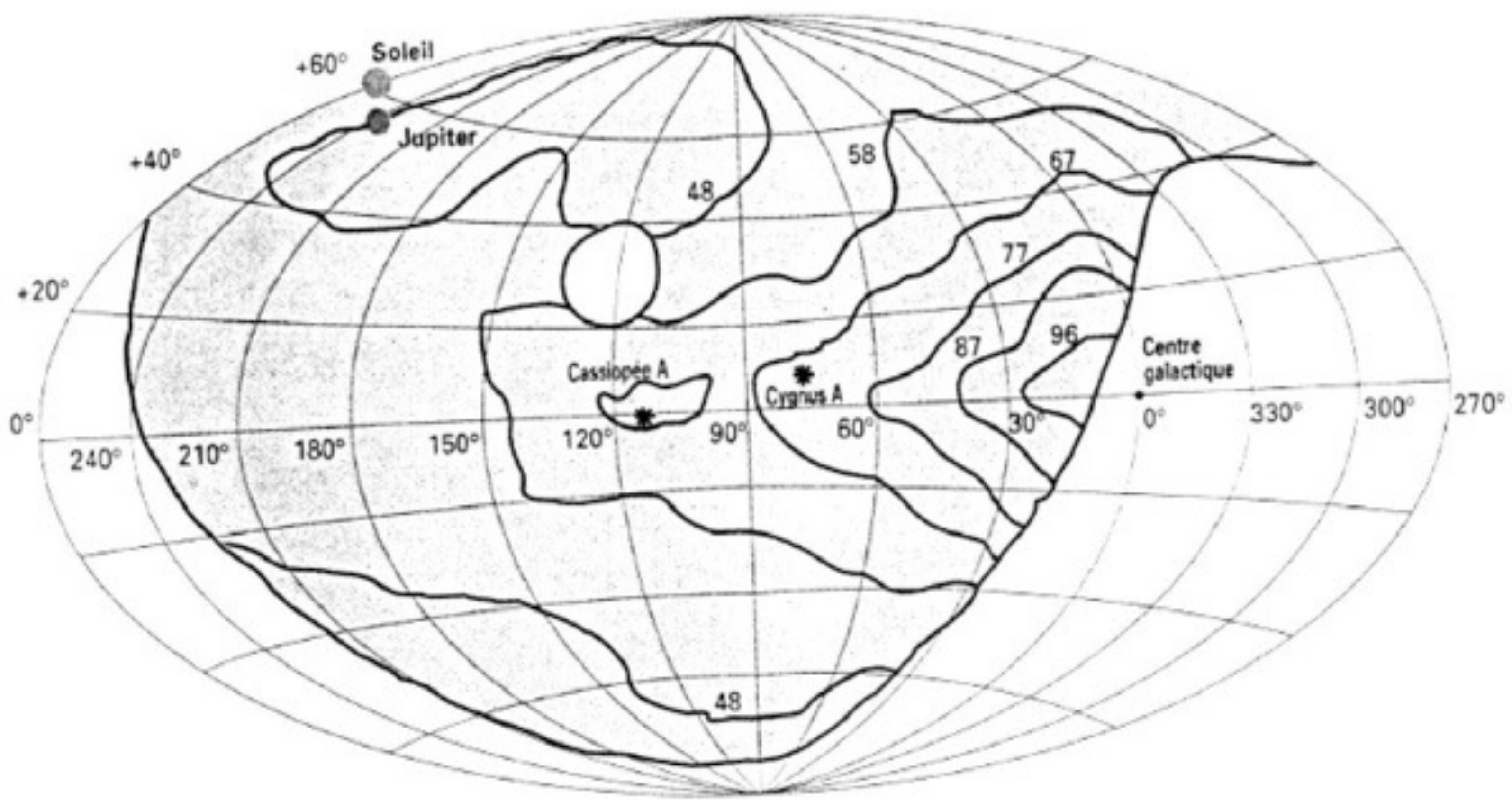

1936	Sky map at ν =160 MHz (λ=1.87 m) with a parabola $\varnothing$=10m Solar waximum $\rightarrow$ radio noise … unidentified !	Grote Reber

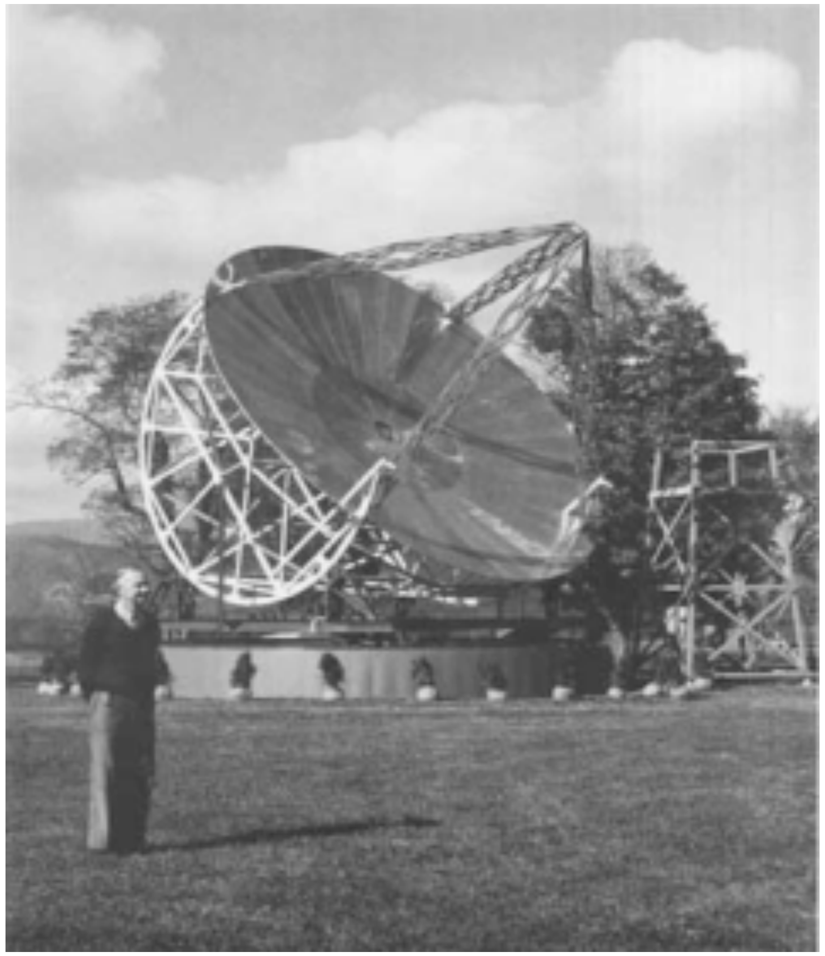

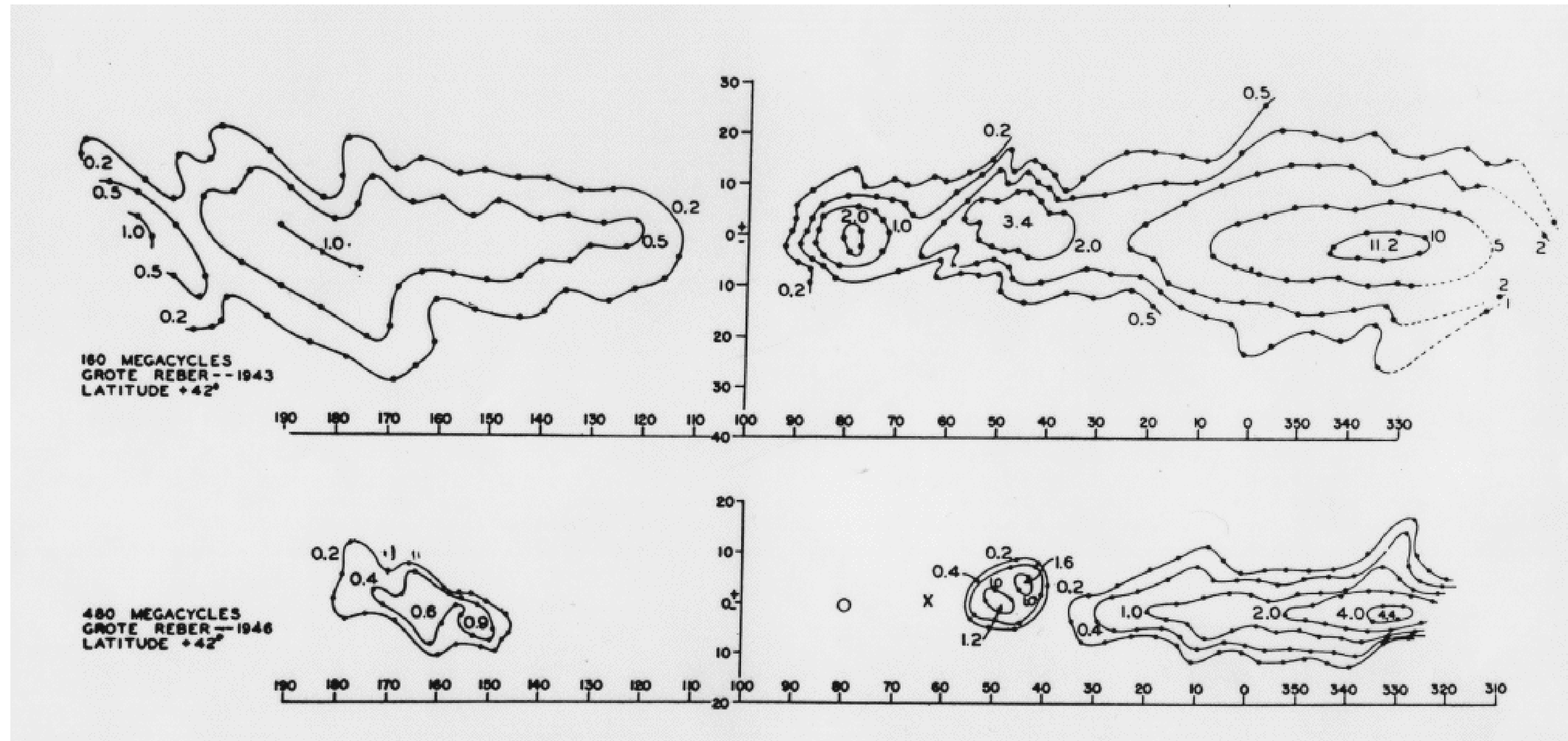

FIG. 7—Contours of constant intensity at 160 MHz and 480 MHz, taken at Wheaton, Illinois.

1940-45	Development of antenna and receiver technology for Radar	
1942-45	Detection of the Sun at ν =150 MHz (λ=2 m – Radar jamming $\rightarrow$ published in 1945 !) and at 3 & 10 GHz (λ=3 & 10 cm)	James Hey
1946	Thermal radio emission from the Moon	*US, Australia*
1946	*Start of radio astronomy in France*	*Yves Rocard*

1947	RADAR-astronomy (meteorites …)	J. Hey & G. S. Stewart
1949-60	Radiogalaxies	James Hey
1951-63	H_I line at $\lambda \sim 21$ cm (ν =1420 MHz) → ubiquitous → development of Radioastronomy → spiral structure of our Galaxy	(Hendrik van de Hulst) Harold Ewen & Edward Purcell Jan Oort

Radio Image of Cygnus-A (FR-II)

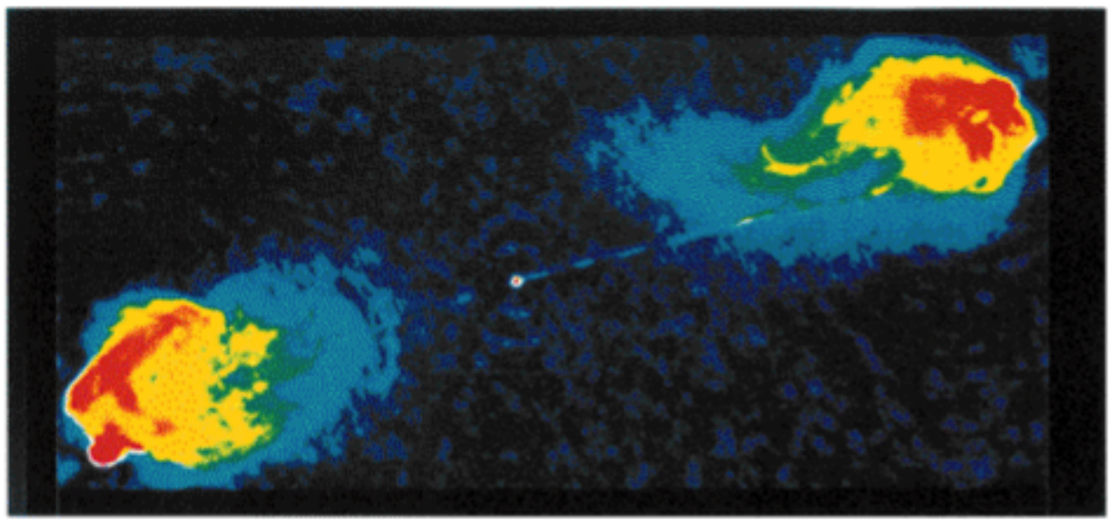

z=0.056 (d≈300 Mpc)

5 GHz image ; ∅ 200 kpc

Radio Image of 3C219 (FR-II)

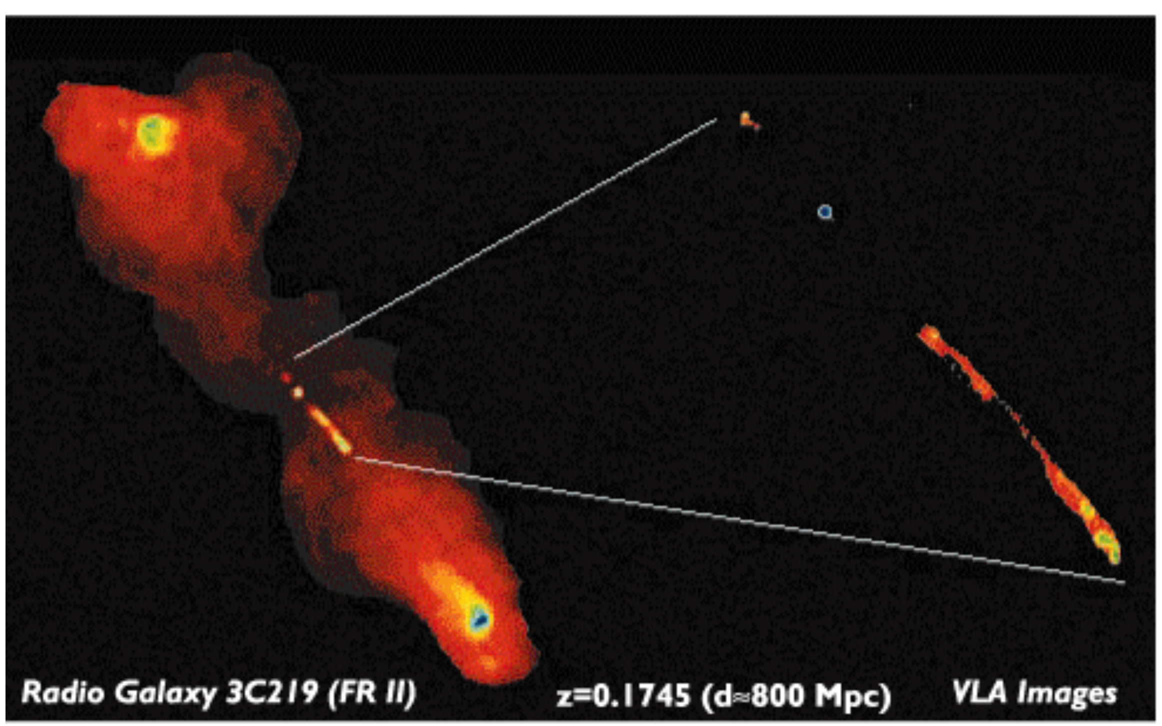

1.4+1.6 GHz combined image at 1.4 arcsec resolution

8 GHz image of jets at 0.1 arcsec resolution

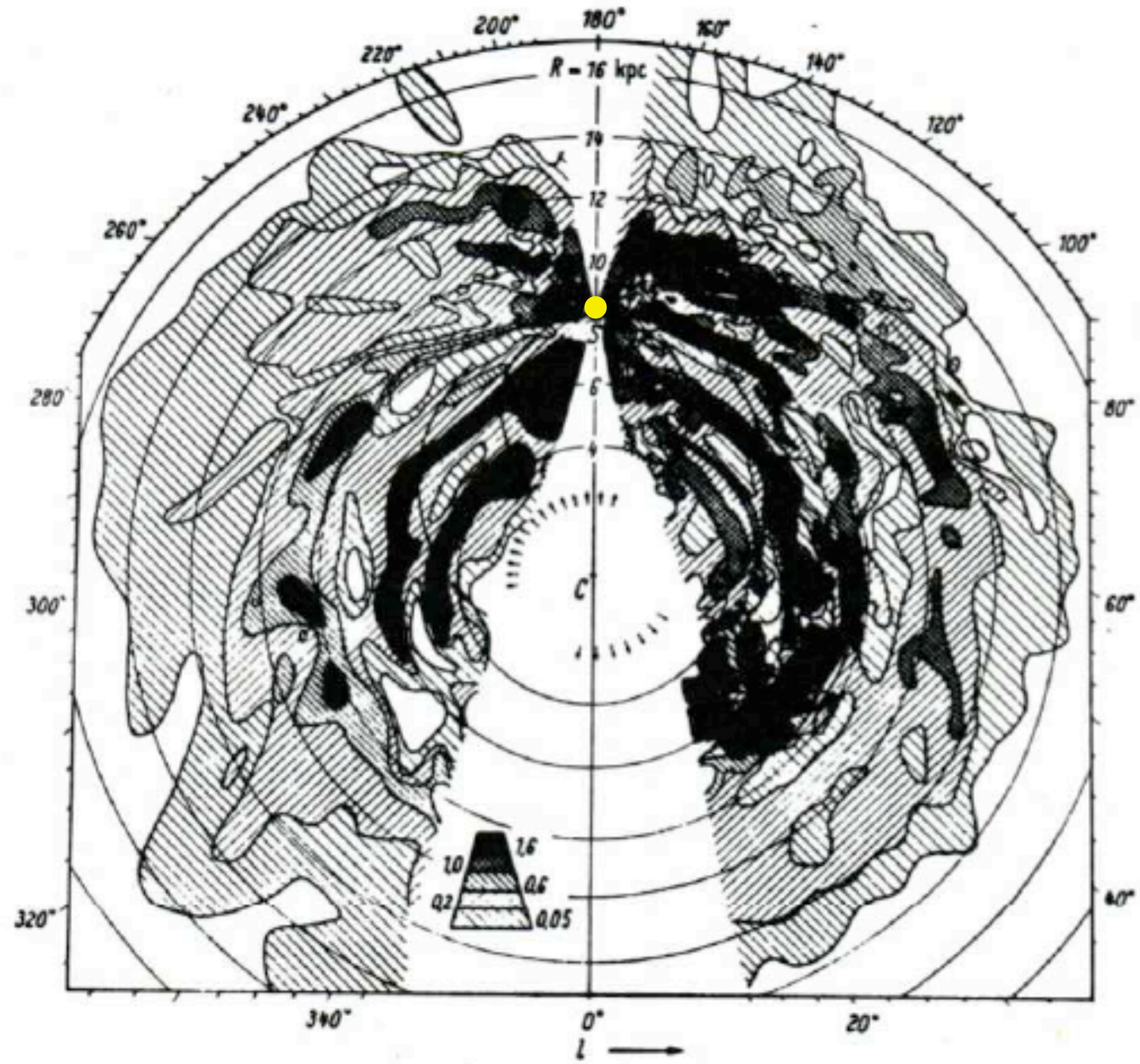

Leiden survey of HI (Oort 1958)

1950's	Radio observatories : Cambridge, Jodrell Bank, Westerbork, Parkes, Greenbank, Arecibo ...	
1953	*Foundation of the Nançay Radio Observatory*	Jean-Louis Steinberg, Jean-François Denisse
1955	First solar radiotelescopes in Nançay	Emile-Jacques Blum, André Boischot ...

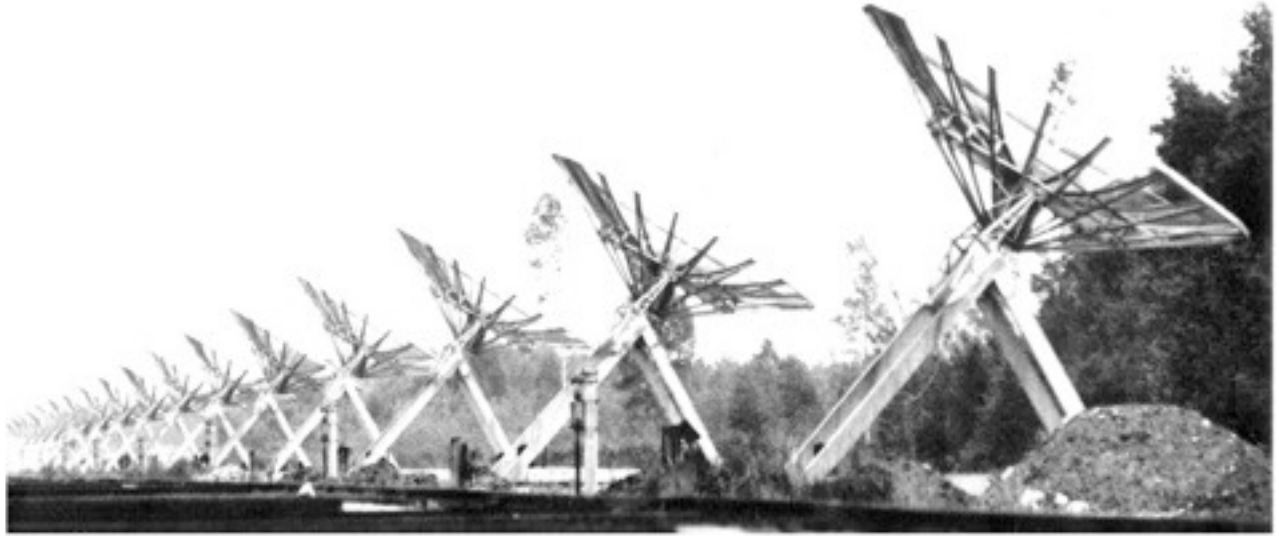

1955	Jupiter's decametric radiation (ν =22 MHz, λ=13.6 m) $\Rightarrow$ Existence and amplitude of Jovian $\lvert B \rvert$	Bernard Burke & Kenneth Franklin
1958	Jupiter's decimetric radiation (ν =3 GHz, λ=10 cm) $\Rightarrow$ Proof of existence of B Jupiter, angle (Ω,B) ~10°	Russell Sloanaker

VARIABLE RADIO SOURCE ASSOCIATED WITH JUPITER 215

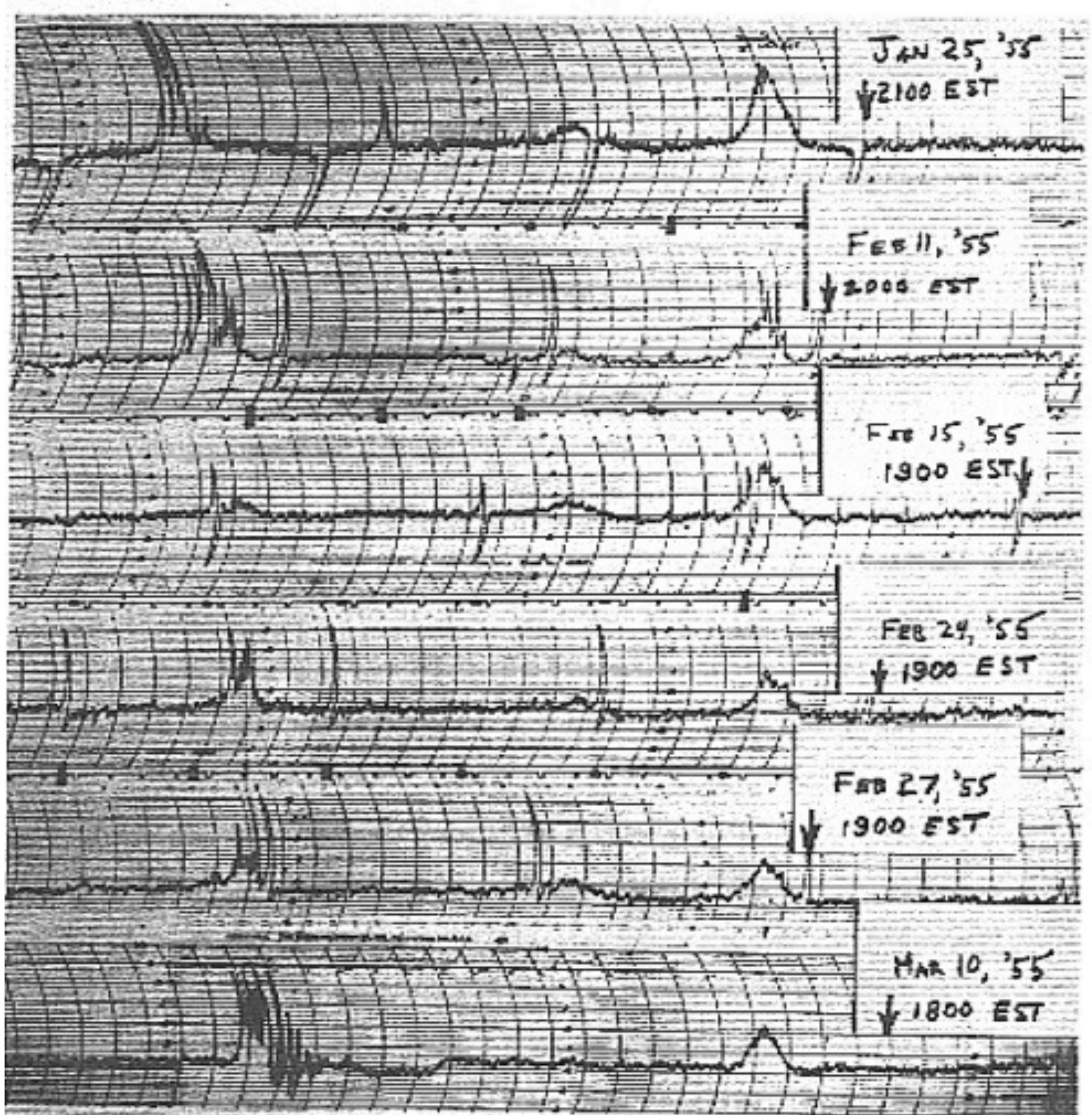

FIG. 2—Phase-switching records showing the appearance of the variable source

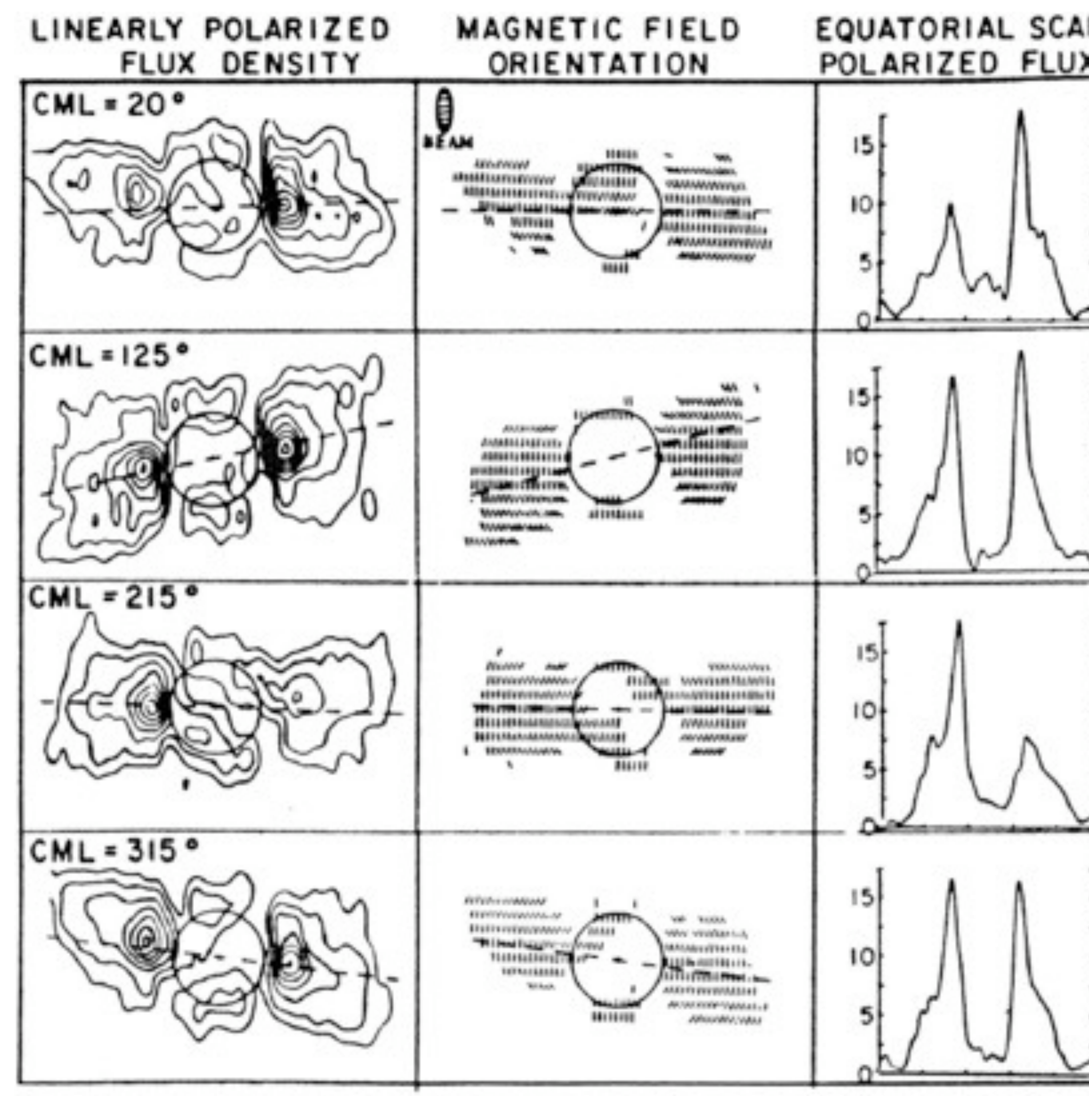

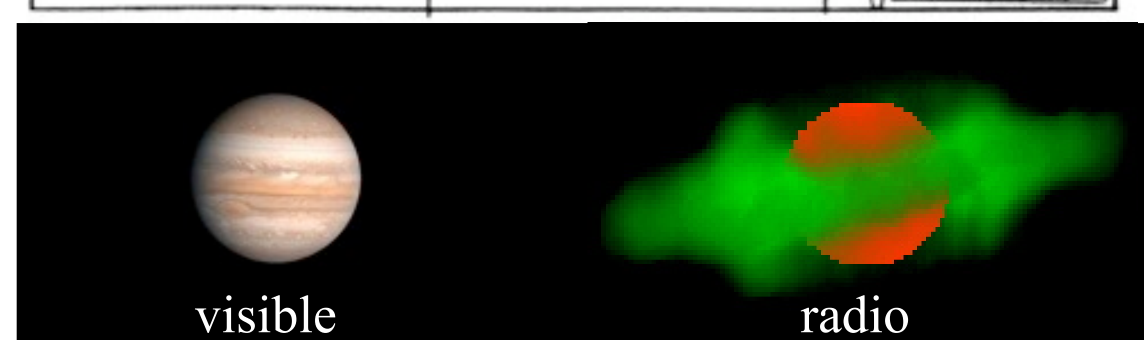

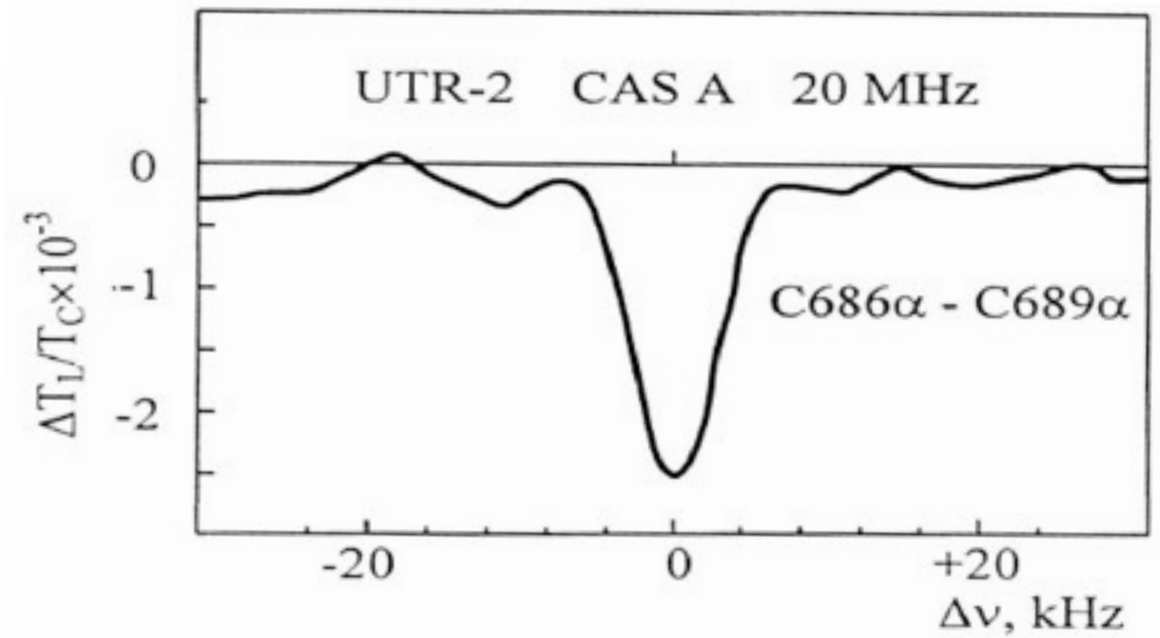

Figure 6. Carbon recombination spectral lines with most high principal quantum numbers detected on UTR-2.

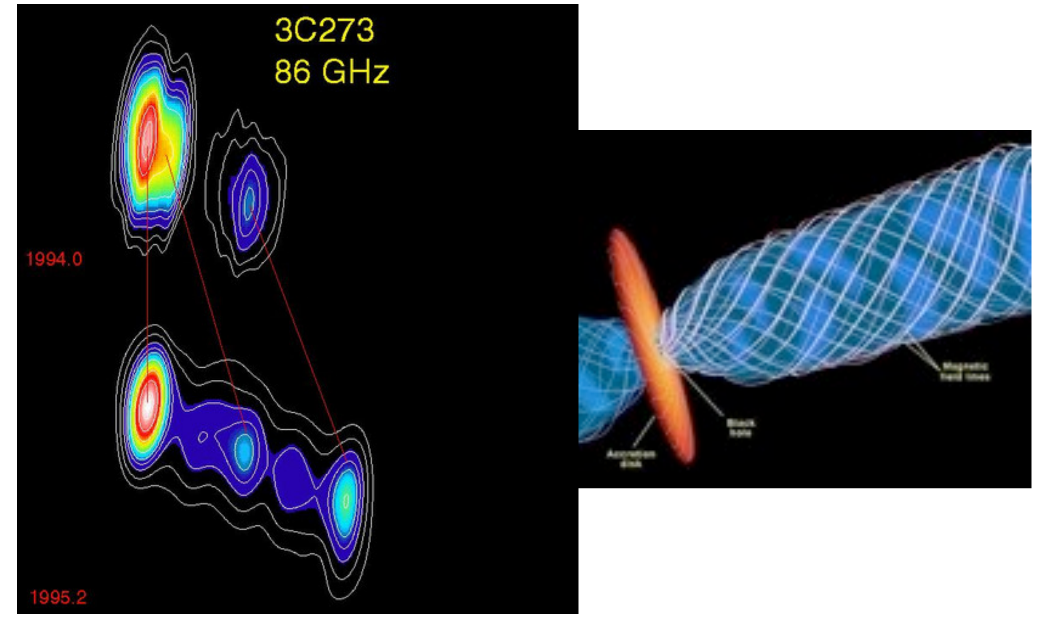

1960	Rydberg atoms : $\Delta E=(1/n_a^2 - 1/n_b^2)\times E_i$	Nikolaï Kardashev
1963	Quasars (3C273)	
1963-68	OH & complex molecules	
1964	TKR (Terrestrial Kilometric Radiation) at ν=300 kHz (λ=1 km) → Space Radioastronomy (Elektron satellite)	E. A. Benediktov
1965	Rotation of Mercury by RADAR from Arecibo (~~88~~ 59 days)	Gordon Pettengill & Rolf Dyce
1965	Cosmological background at 3 °K (λ≈mm)	Arno Penzias & Robert Wilson

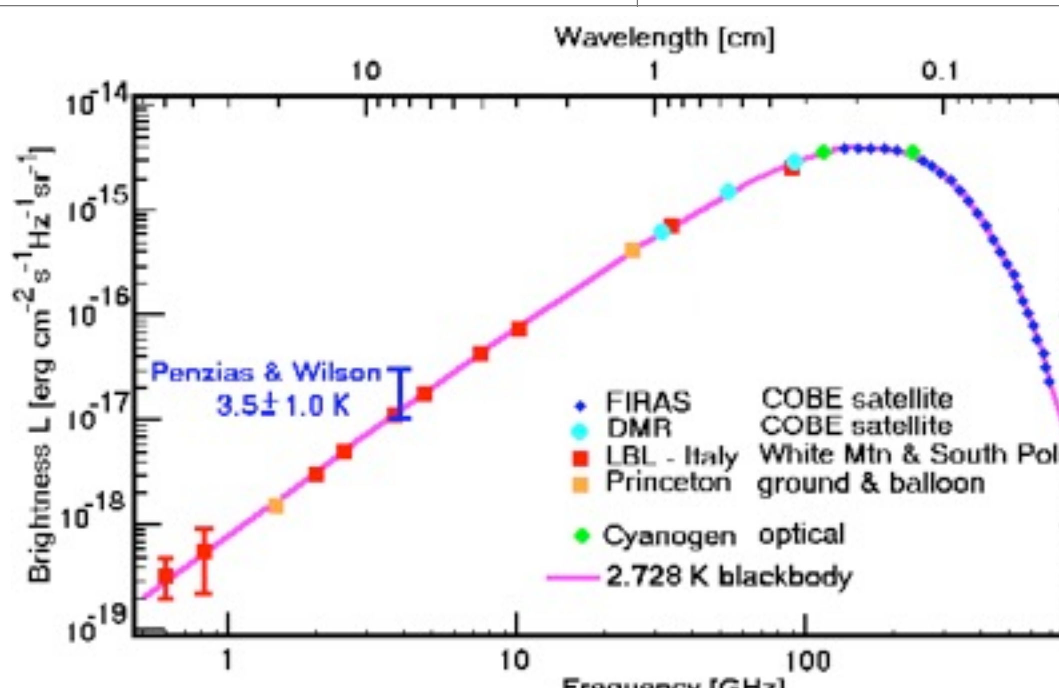

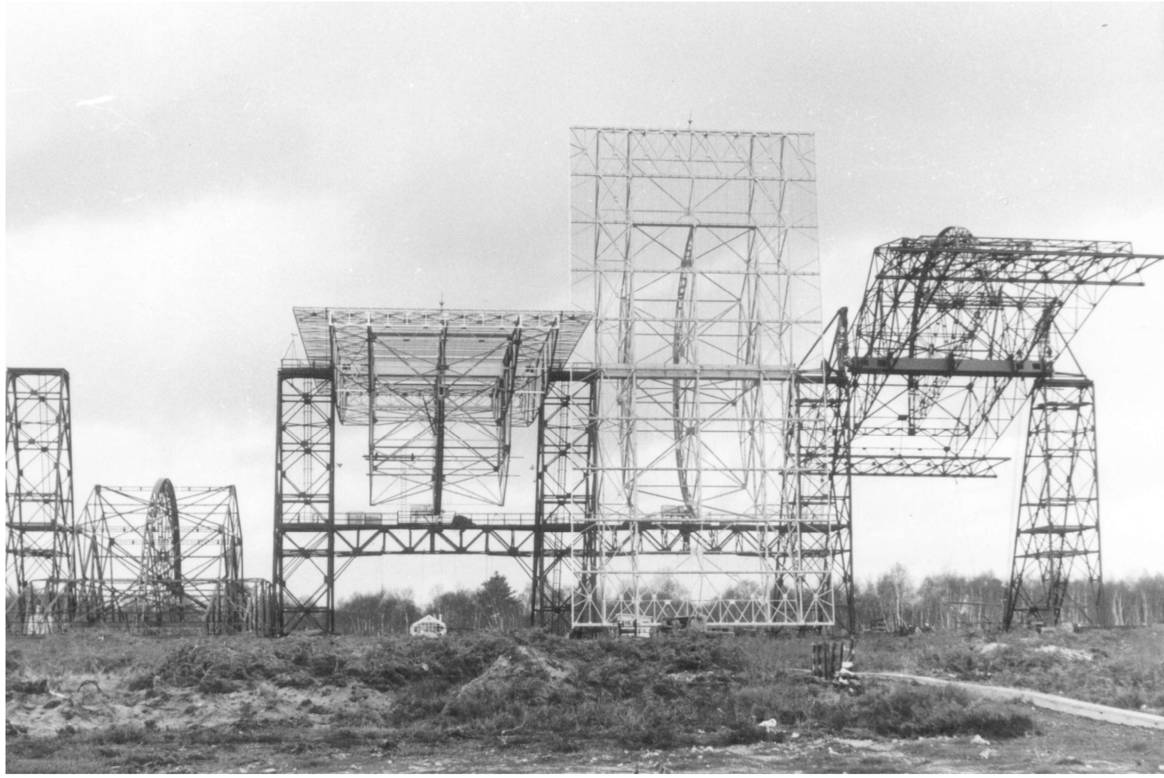

1965	*Inauguration of Nançay decimeter Radio Telescope*	
1960's	Aperture synthesis	Martin Ryle
1967-68	Pulsars	Antony Hewish & Jocelyn Bell

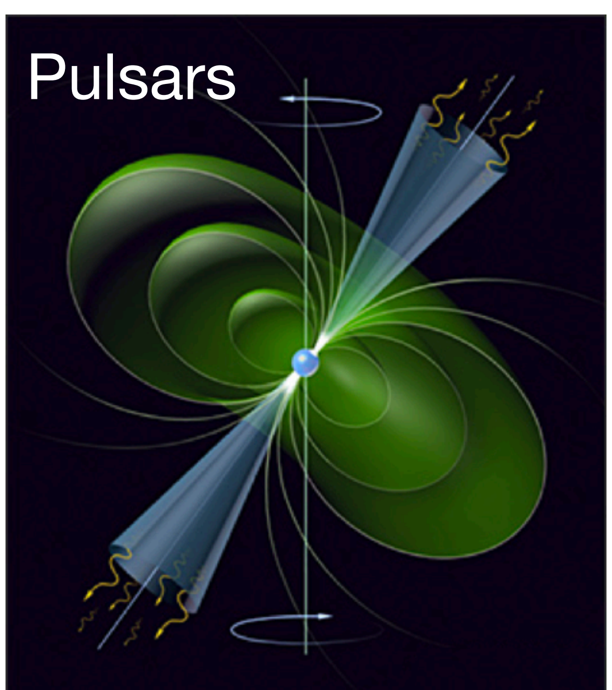

Fig. 1.1. Discovery observations of the first pulsar. (*a*) The first recording of PSR 1919+21; the signal resembled the radio interference also seen on this chart: (*b*) Fast chart recording showing individual pulses as downward deflections of the trace.

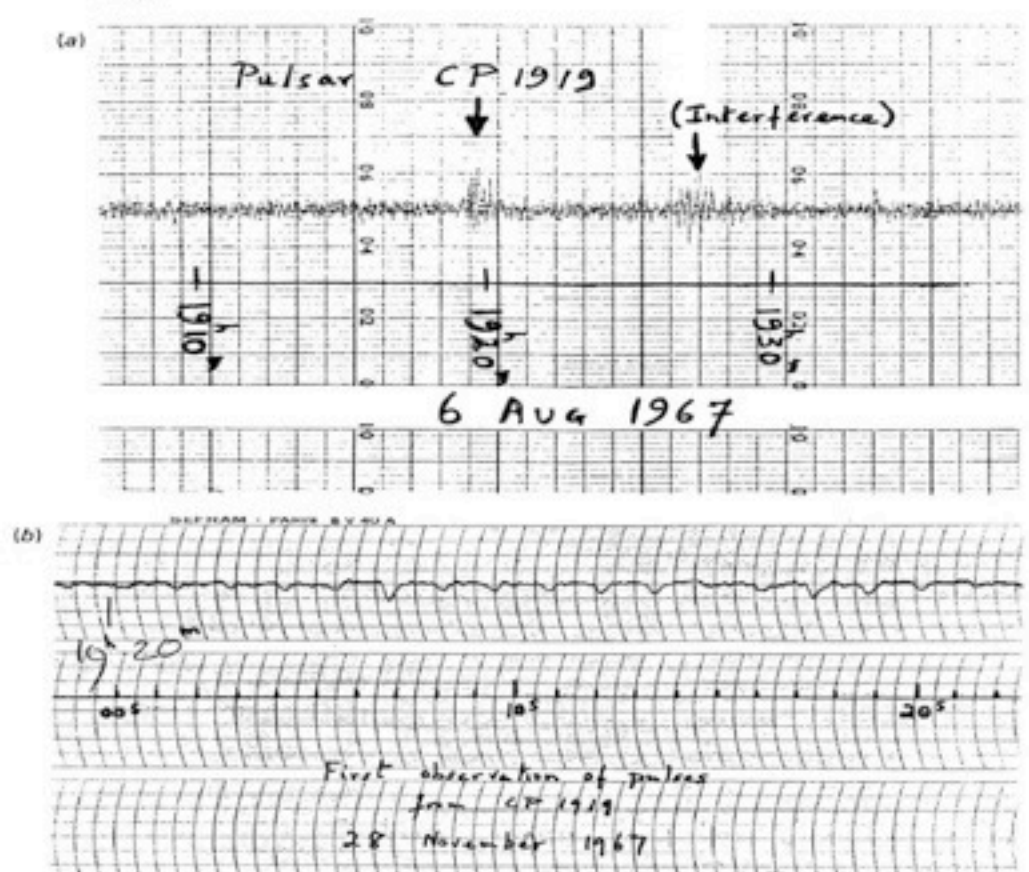

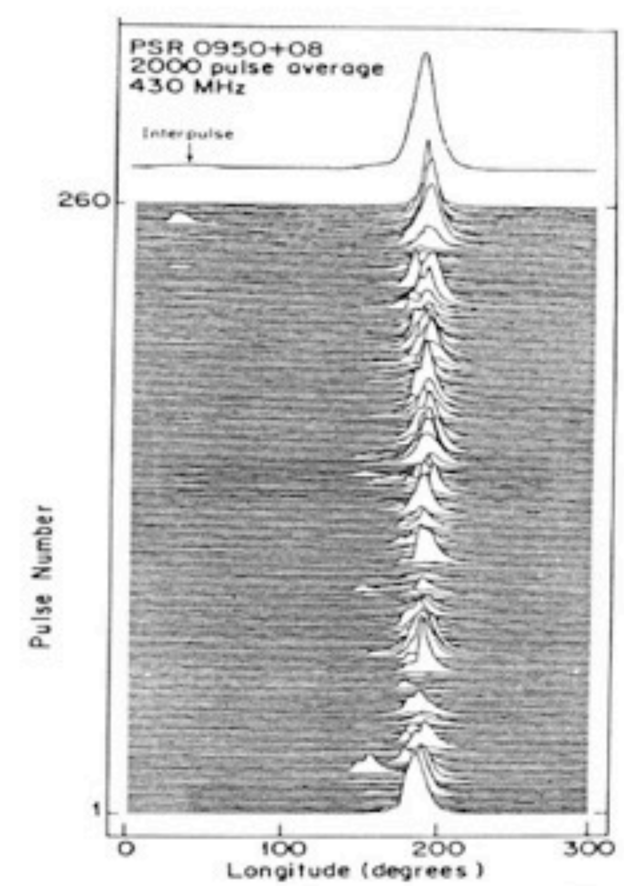

1970	LF VLBI on Jupiter : Instantaneous decameter source ≤400 km	George Dulk
1970's	LF antenna arrays (Nançay, Kharkov, Boulder, Floride) … VLBI	
1980's	Voyager (LF space planetary radioastronomy) IRAM	
1974-93	Milliseconde pulsar & gravitational waves	Russell Hulse & Joseph Taylor
1990's	Ulysses, Galileo, Cassini VLA, GMRT	

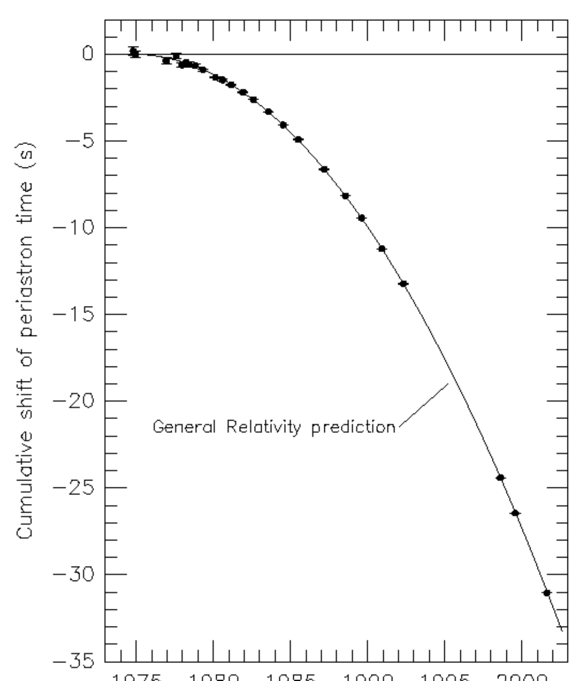

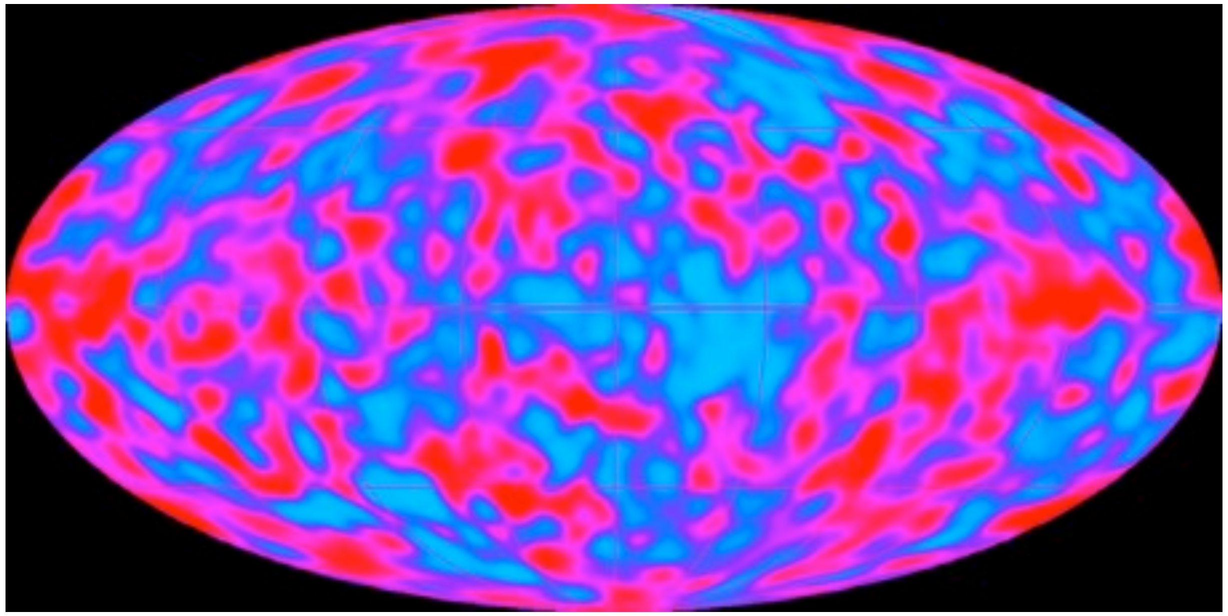

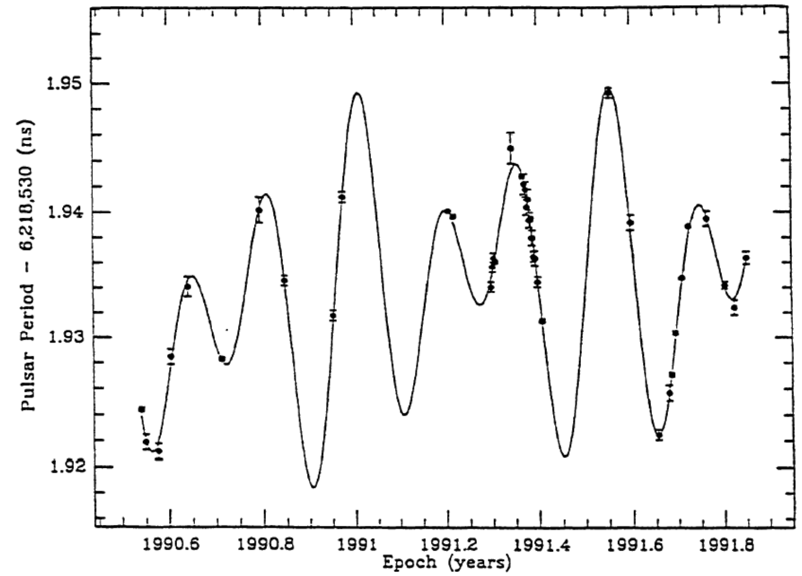

Figure 2. A comparison of period variations of PSR1257+12 (*filled circles*) with a two-planet model prediction (*solid line*).

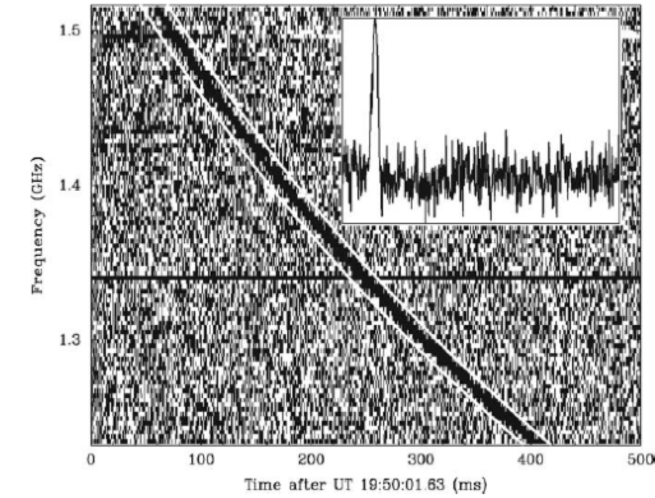

1990's	COBE: fluctuations of the cosmological background	George Smoot & John Mather
1992	1st exoplanet around a pulsar	Alexander Wolszczan
2000's	Space radio astronomy : Cassini, Stereo …	
2006-7	RRATs, FRBs	Moira McLaughlin, Duncan Lorimer
2010's	ALMA, LOFAR, Planck	

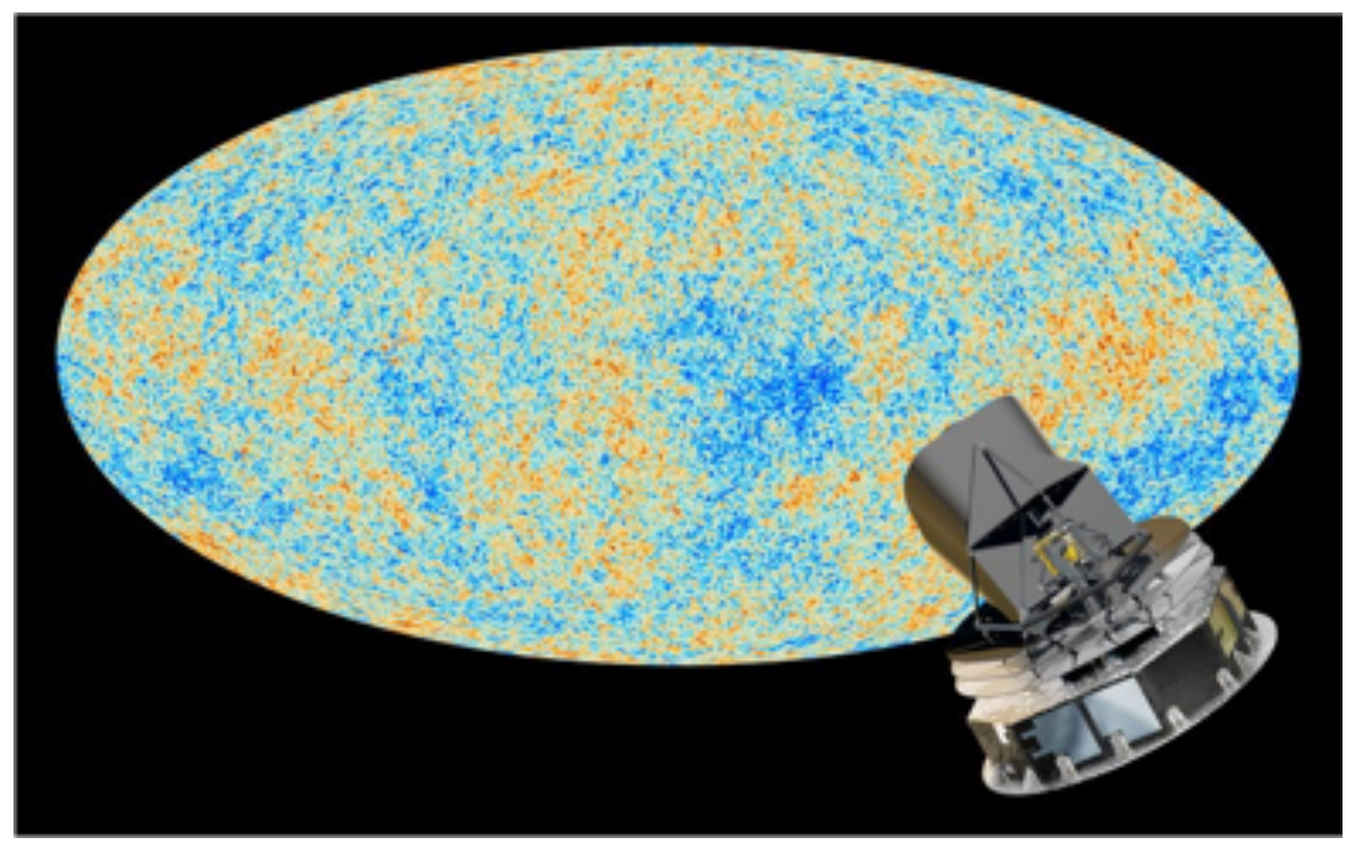

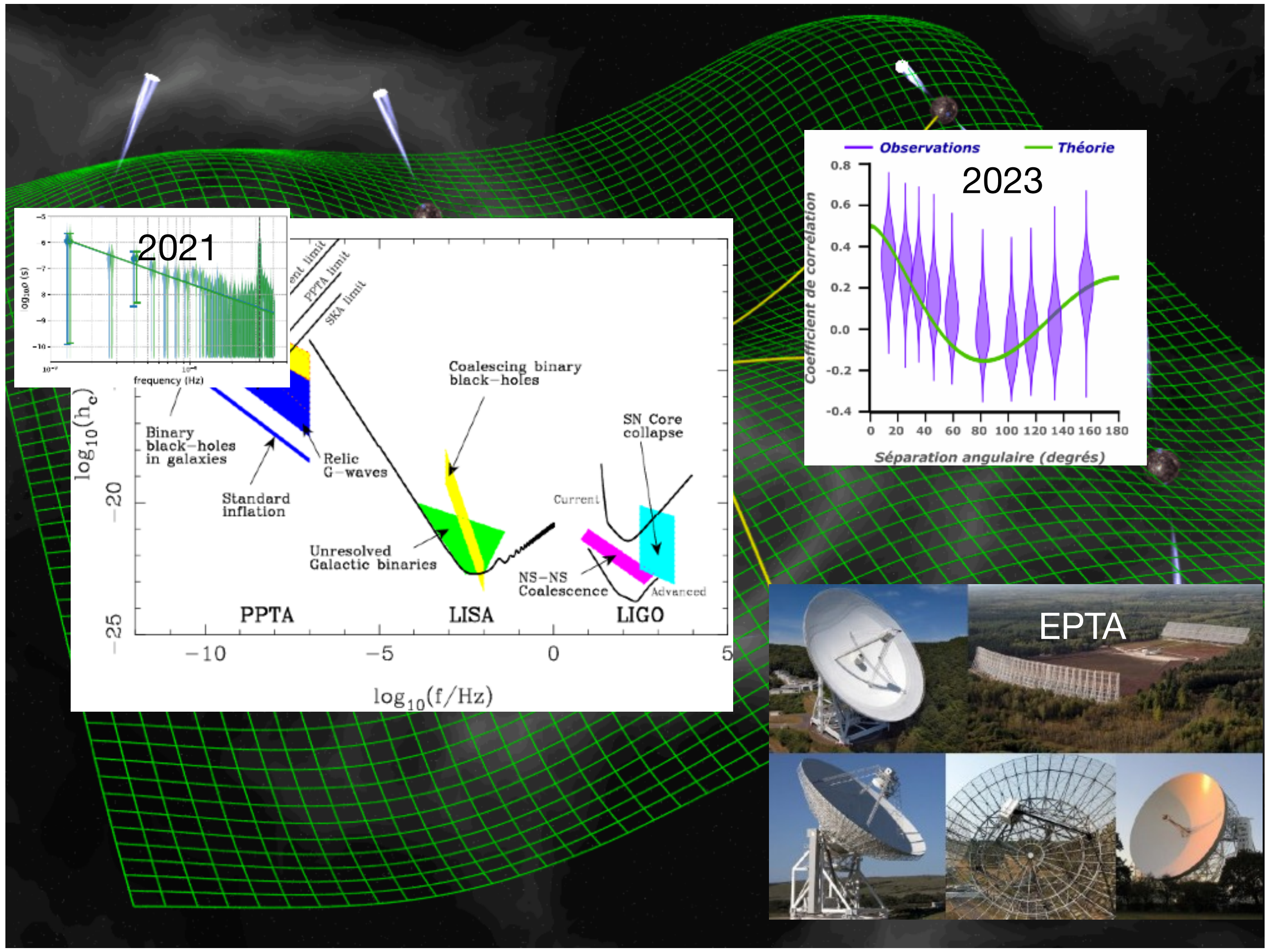

2023	Gravitational waves from galactic giant black holes	EPTA, IPTA
2020’s	SKA, Microsatellite constellations ?	
2030’s	Radioastronomy on the Moon ? …	

Specific features of Radioastronomy

- « Physical"

→ Aspect of sources ≠ from "visible" (Jupiter decimeter emission, RadioGalaxies...)

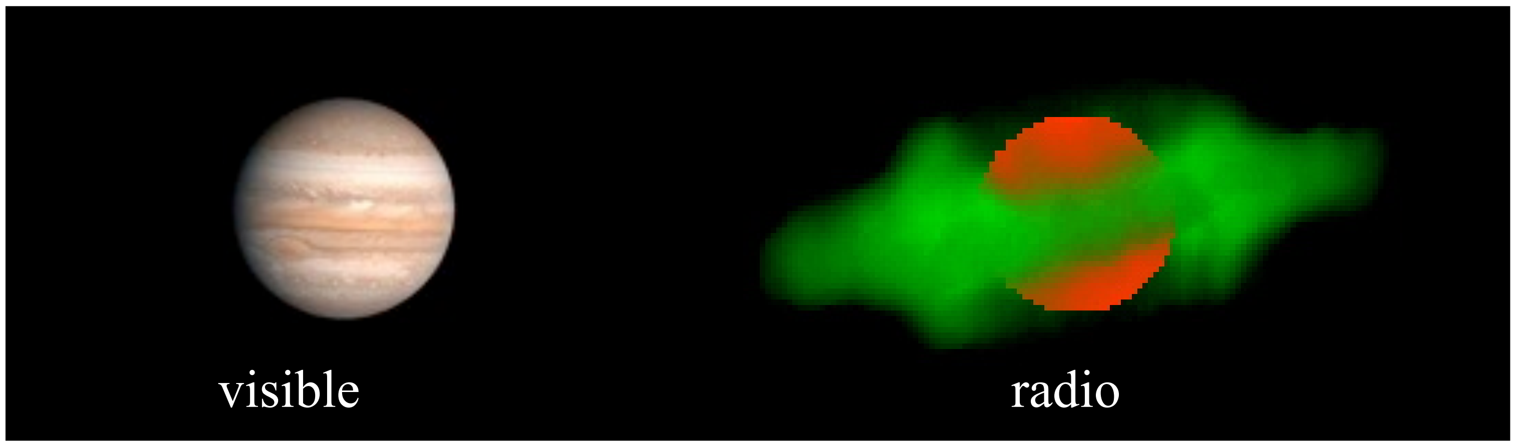

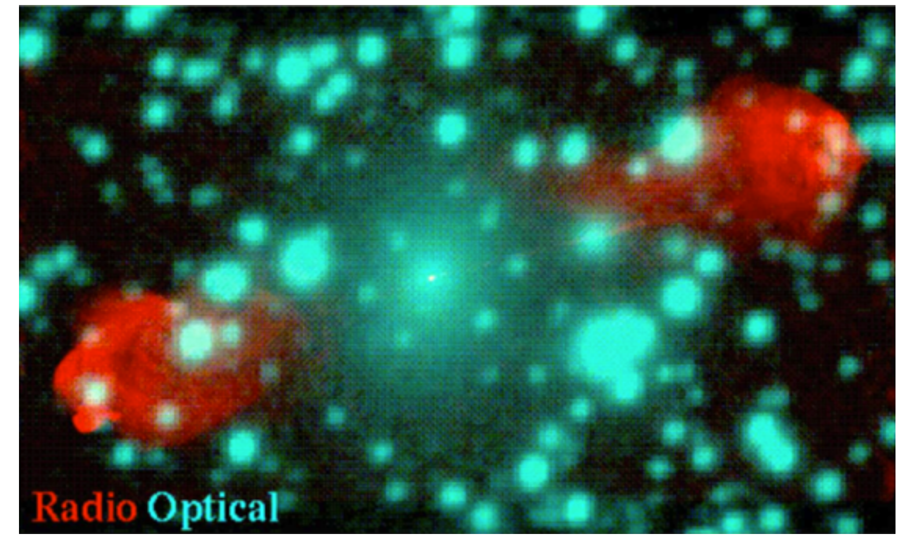

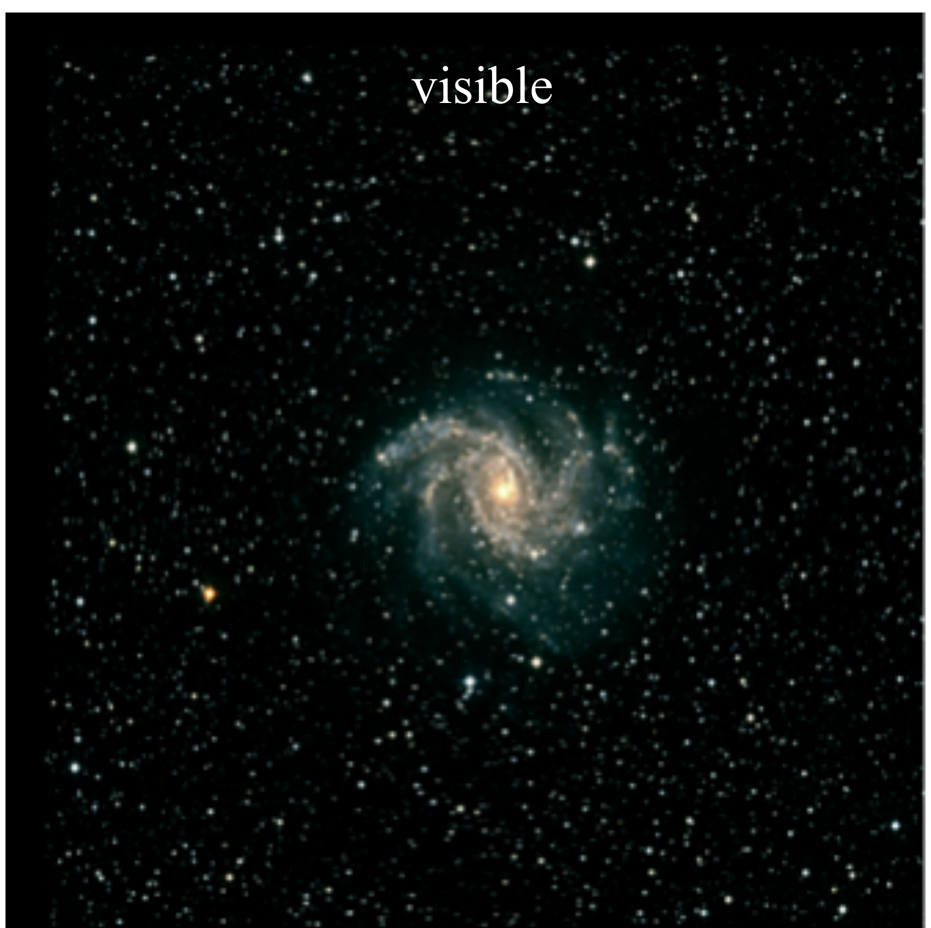

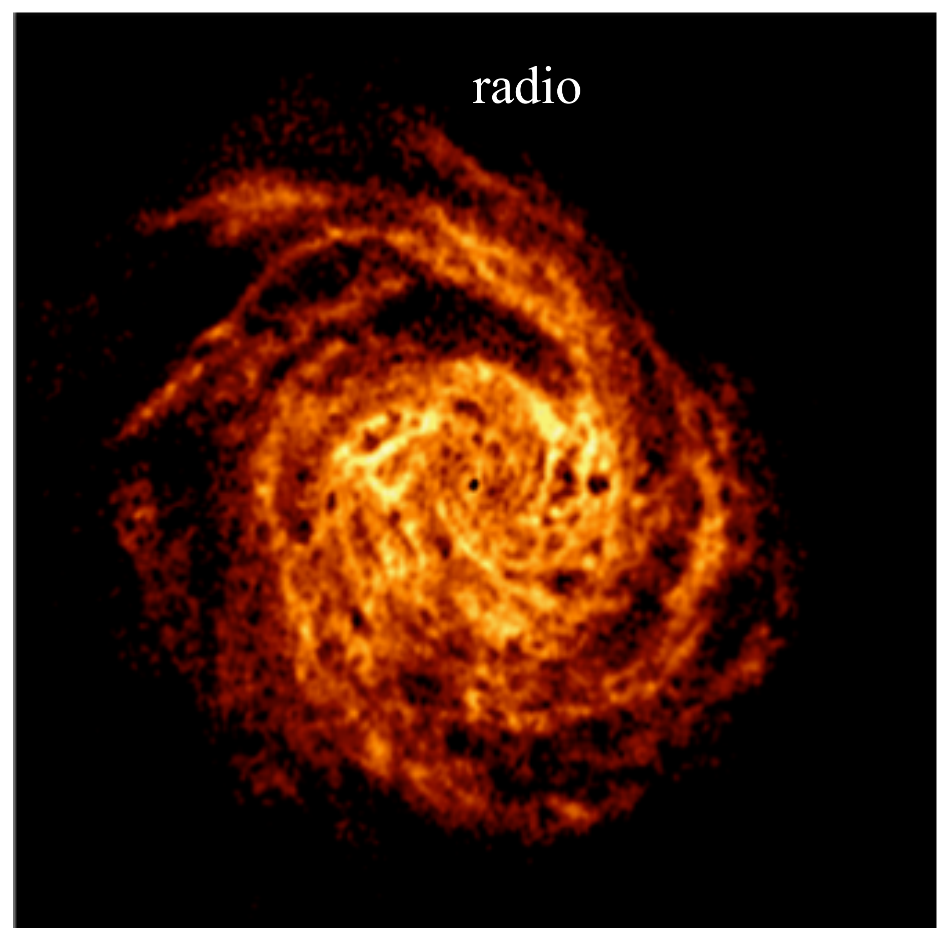

→ New sources :

- Pulsars (3473 as of today : http://www.atnf.csiro.au/research/pulsar/psrcat/)
- Radio-galaxies
- Quasars …

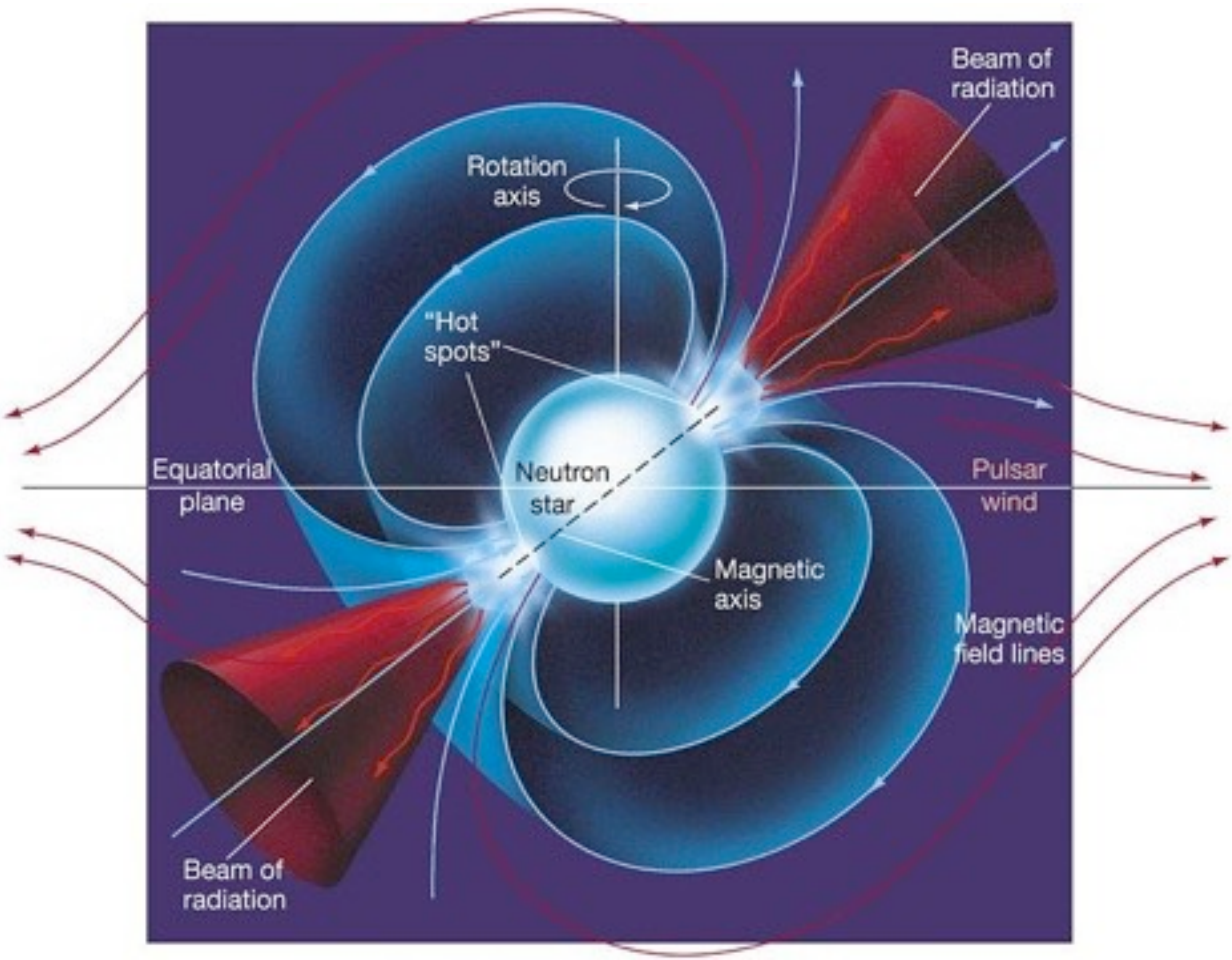

→ Thermal emission from cold objects

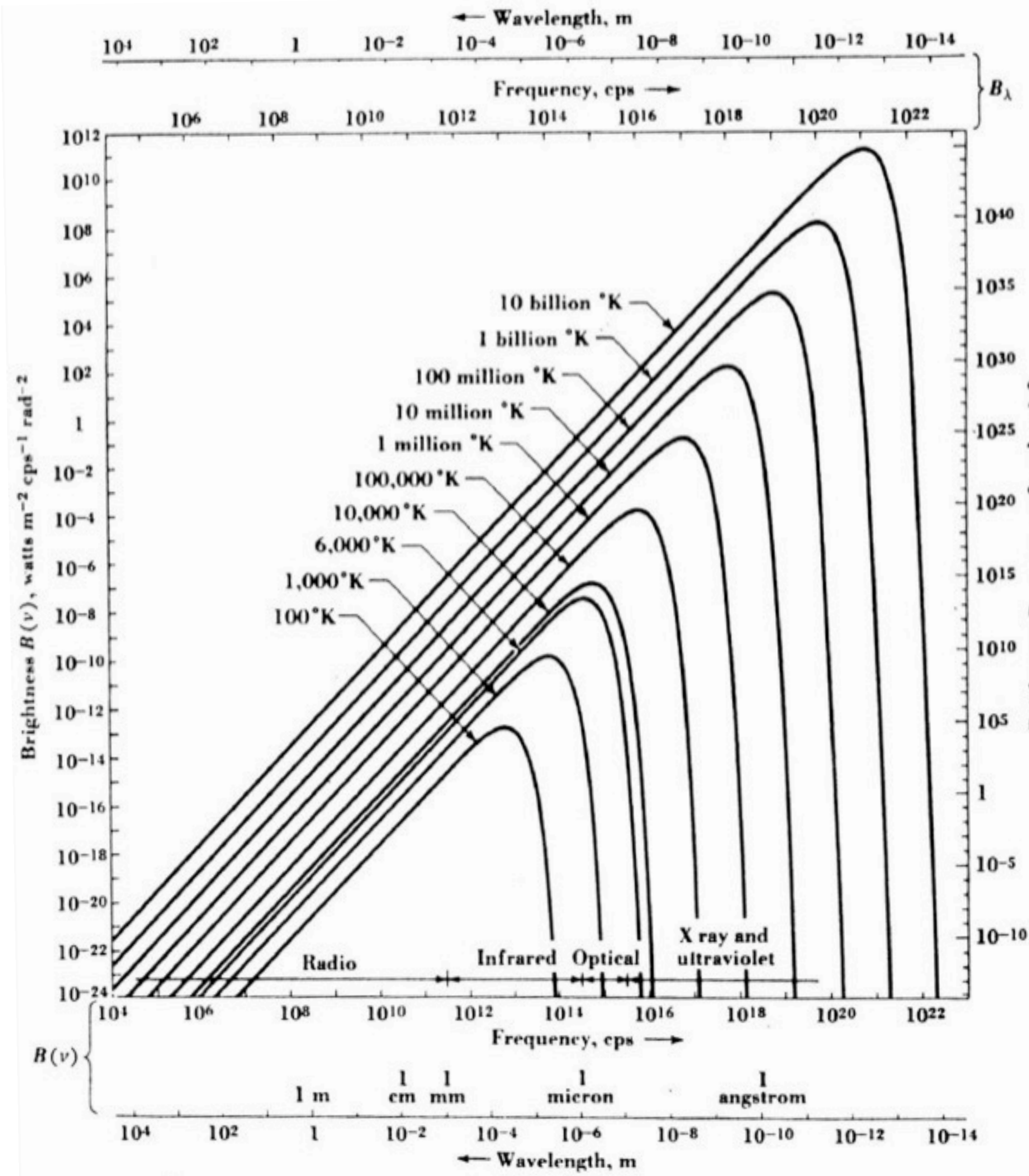

Planck-law radiation curves. $B(\nu)\,d(\nu) = B(\lambda)\,d(\lambda)$. Brightness as a function of wavelength or frequency.

Planck law (black body) :

$B(\nu) = (2h\nu^3/c^2)/(\exp(h\nu/kT)-1)$ $[W\ m^{-2}\ Hz^{-1}\ sr^{-1}]$

⇓ of source ⇓ from the source

B(ν) = Brightness (Luminance in optical photometry)

T = T_B = Brightness temperature

At low frequencies : $h\nu \ll kT$

$(h\nu/kT = 4.7\times10^{-11}\ \nu/T \Rightarrow\ \nu \ll 2\times10^{10}\ T)$

$\Rightarrow B(\nu) = 2\,k\,T_B\,\nu^2/c^2 = 2\,k\,T_B/\lambda^2$ (Rayleigh-Jeans)

$\lambda(B_{max}) = 3\times10^{-3}/T$ $[m]$ (Wien)

For $T \leq 100$ K (ISM), ~ no thermal emission for $\nu \geq 10^{14}$ Hz

⇒ invisible in optical range, but bright in IR & Radio

NB : *Flux Unit = Jansky (Jy) = f.u. =* $10^{-26}\ Wm^{-2}Hz^{-1}$

In Solar radioastronomy, one uses : Solar Flux Unit = s.f.u. = $10^{-22}\ Wm^{-2}Hz^{-1}$

→ Emission processes different from optics

- Continuum not only thermal : ∃ numerous non-thermal emission processes
  ⇒ spectrum $\neq \nu^2$ ($\nu^{-\alpha}$ notably)

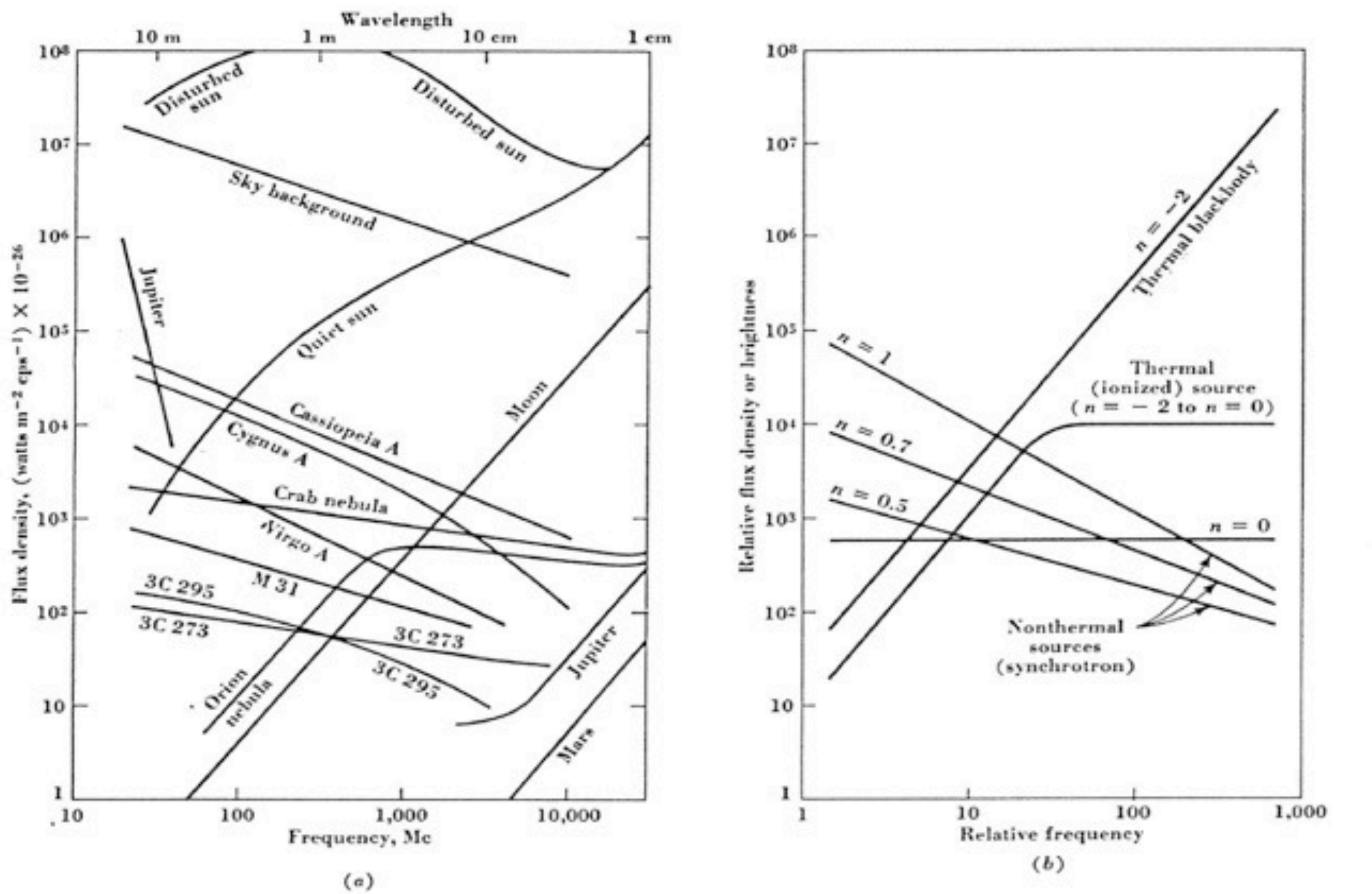

Fig. 8-6. (*a*) Spectra of typical radio sources; (*b*) calculated spectra for various values of spectral index *n*.

$T_B = B(\nu)\, \lambda^2 / 2k$ always usable in a restricted $\Delta\nu$ spectral band

= temperature of the blackbody emitting the same brightness $B(\nu)$ at this frequency

≠ physical temperature of the source if not a blackbody

Ex: $T_B \geq 10^{12}$ K for Solar radio emissions, $T_B \geq 10^{18}$ K (Jupiter), $T_B \geq 10^{22}$ K (Pulsars)

- H_I line at 21.2 cm (1420 MHz - 5×10^{-6} eV)
  = "hyperfine" structure of Hydrogen atom (preponderant in the Universe)
  "forbidden" transition ($P \sim 3\times10^{-15}$ s^{-1}, lifetime $\tau \sim 1/P$)
  $\Rightarrow$ very narrow line (natural width $\Delta\omega = 2\pi\Delta\nu \sim P$)
  $\Rightarrow$ tracer of the physical conditions in the source

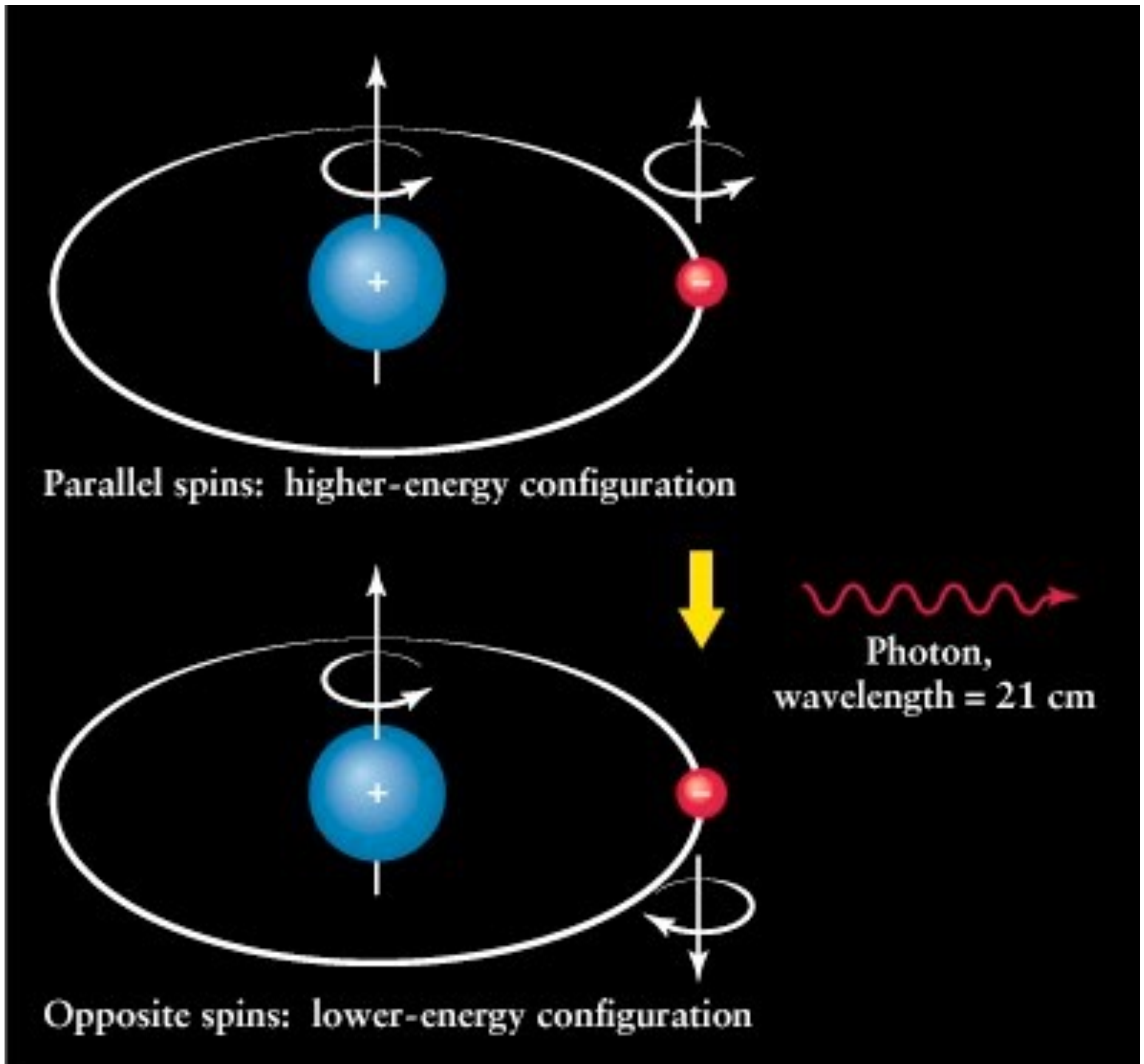

b

- Numerous molecular lines in radio
  (calculated / measured in the laboratory / observed in space from ≥1965-70)

Energy levels	Spectral domain of transitions
Electronic orbits Atomic vibrations Molecular rotations Hyperfine structure	Visible, UV IR Radio (mm → Radio → dm)

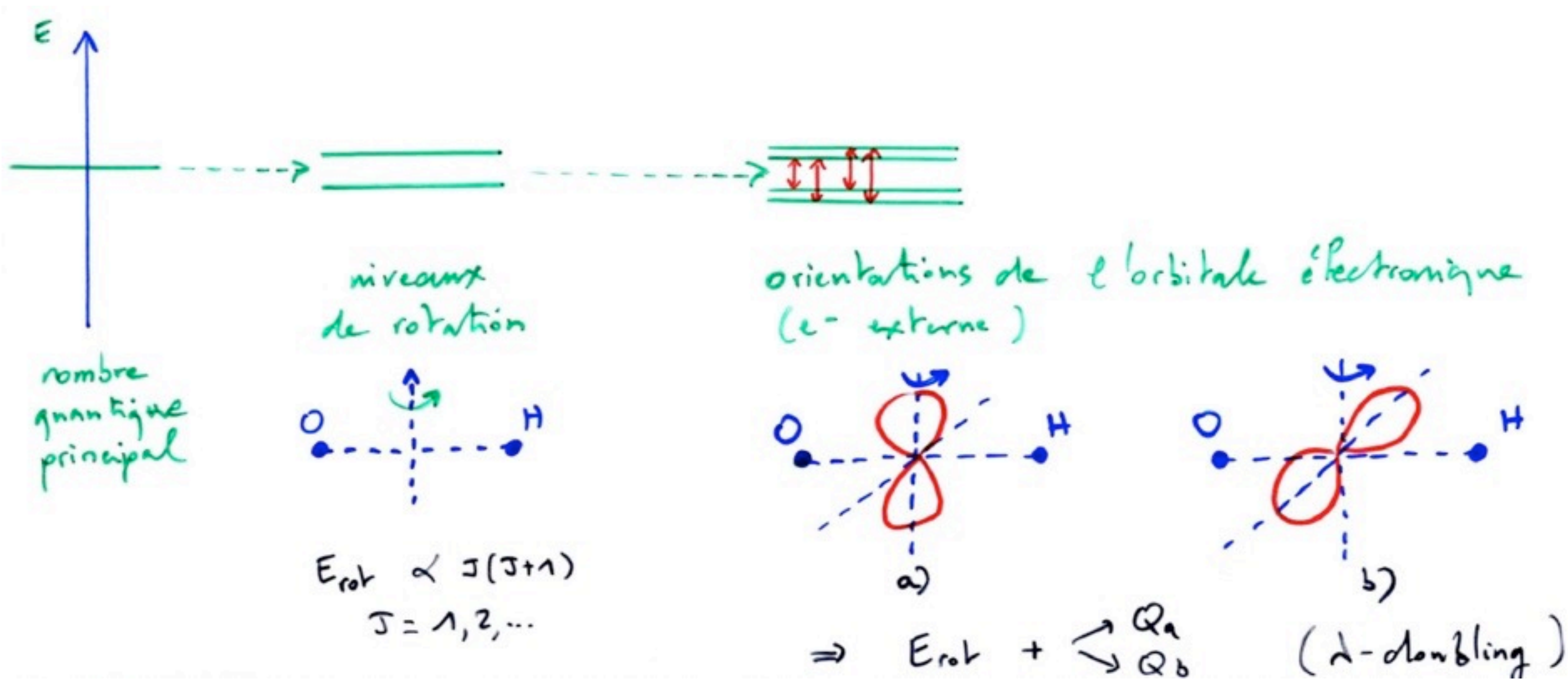

Ex: OH radical (comets, stellar envelopes, etc.)

→ ∃ 4 possible transitions between 1600 and 1670 MHz (λ~18 cm),

= "forbidden" lines with intensity ratios 1-5-9-1

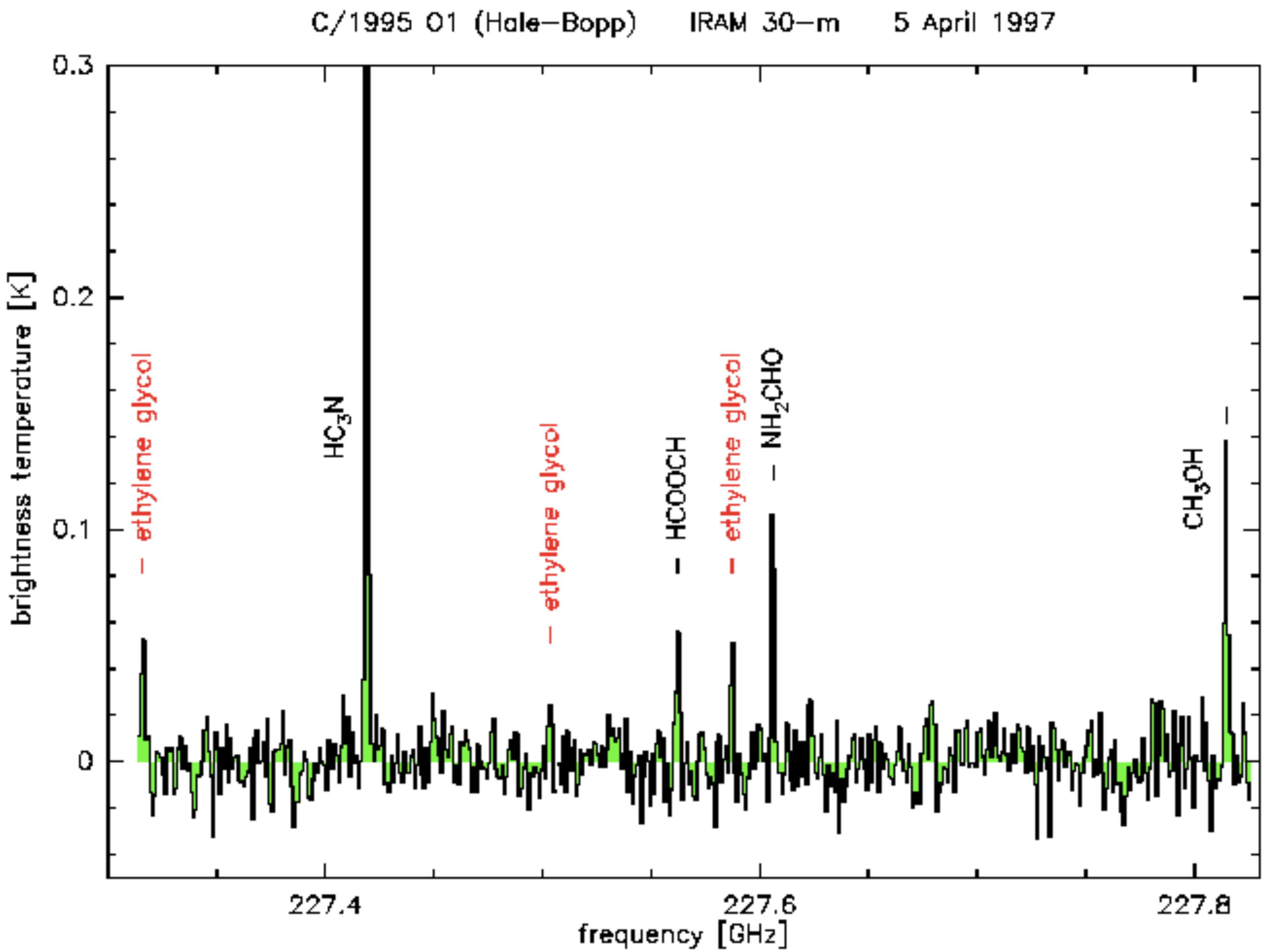

Comet Hale-Bopp observed by IRAM 30m antenna in Spain

>200 organic molecules detected to date (CO, CN, H_2CO, alcools, acids…) ⇒ astrochemistry

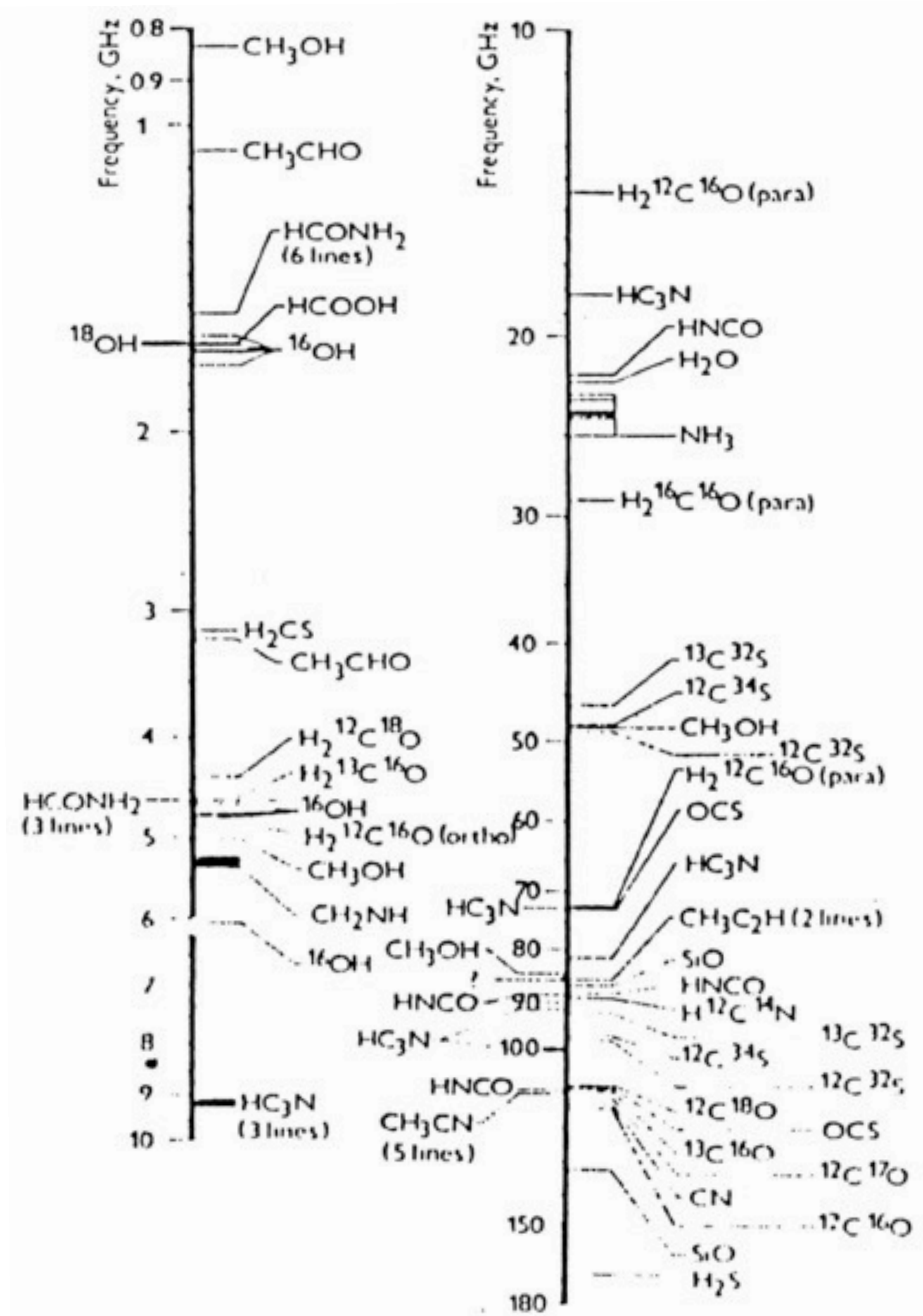

Interstellar molecules and their radio lines

Number of Atoms										
2	3	4	5	6	7	8	9	10	11	12+
H_2	C_3	c-C_3H	C_5	C_5H	C_6H	CH_3C_3N	CH_3C_4H	CH_3C_5N?	HC_9N	C_6H_6
AlF	C_2H	l-C_3H	C_4H	l-H_2C_4	CH_2CHCN	$HCOOCH_3$	CH_3CH_2CN	$(CH_3)_2CO$		$HC_{11}N$
AlCl	C_2O	C_3N	C_4Si	C_2H_4	CH_3C_2H	CH_3COOH?	$(CH_3)_2O$	NH_2CH_2COOH?		PAHs
C_2	C_2S	C_3O	l-C_3H_2	CH_3CN	HC_5N	C_7H	CH_3CH_2OH			C_{60}^+?
CH	CH_2	C_3S	c-C_3H_2	CH_3NC	$HCOCH_3$	H_2C_6	HC_7N			
CH^+	HCN	C_2H_2	CH_2CN	CH_3OH	NH_2CH_3	$HOCH_2CHO$	C_8H			
CN	HCO	CH_2D^+?	CH_4	CH_3SH	c-C_2H_4O					
CO	HCO^+	HCCN	HC_3N	HC_3NH^+						
CO^+	HCS^+	$HCNH^+$	HC_2NC	HC_2CHO						
CP	HOC^+	HNCO	HCOOH	NH_2CHO						
CSi	H_2O	HNCS	H_2CHN	C_5N						
HCl	H_2S	$HOCO^+$	H_2C_2O							
KCl	HNC	H_2CO	H_2NCN							
NH	HNO	H_2CN	HNC_3							
NO	MgCN	H_2CS	SiH_4							
NS	MgNC	H_3O^+	H_2COH^+							
NaCl	N_2H^+	NH_3								
OH	N_2O	SiC_3								
PN	NaCN	CH_3								
SO	OCS									
SO^+	SO_2									
SiN	c-SiC_2									
SiO	CO_2									
SiS	NH_2									
CS	H_3^+									
HF	H_2D^+									

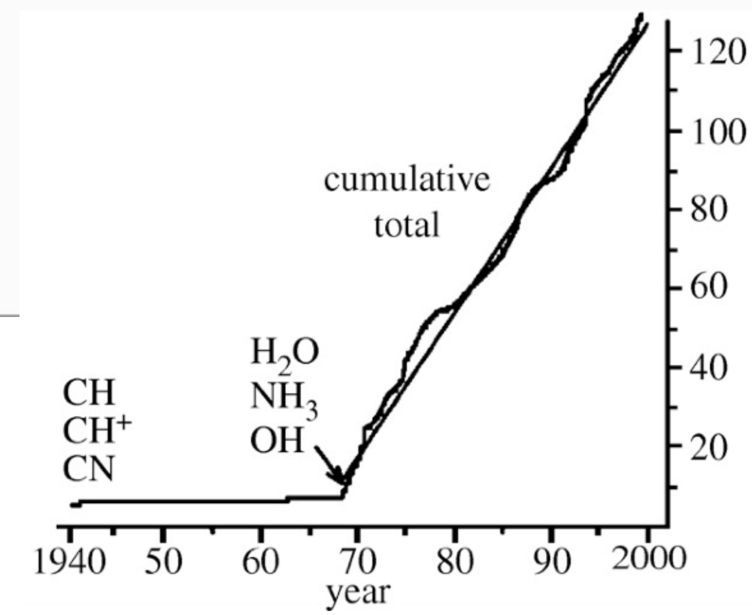

- Masers (OH, NH_3, H_2O) :

1 very intense line, revaling the existence of a "pumping" process (IR radiation from nearby stars, etc.) + induced de-excitation

→ Scattering & Opacity : the ISM contains dust grains (r ~ qq 0.1 μm) + H_I

Probability of scattering a photon λ (& fraction of incident light deflected)

$P(\lambda) \propto 1/\lambda^4$ $(r << \lambda)$ ~isotropic (Rayleigh scattering)

$P(\lambda) \propto 1/\lambda^2$ $(r \sim \lambda)$ mostly forward (Mie scattering)

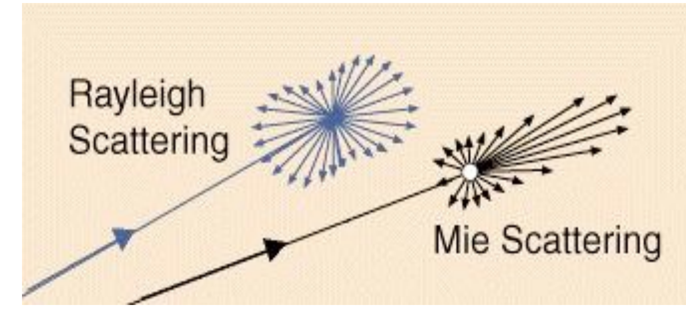

Scattering ≠ Absorption, but lengthening of photon path increases the probability of being absorbed by other processes

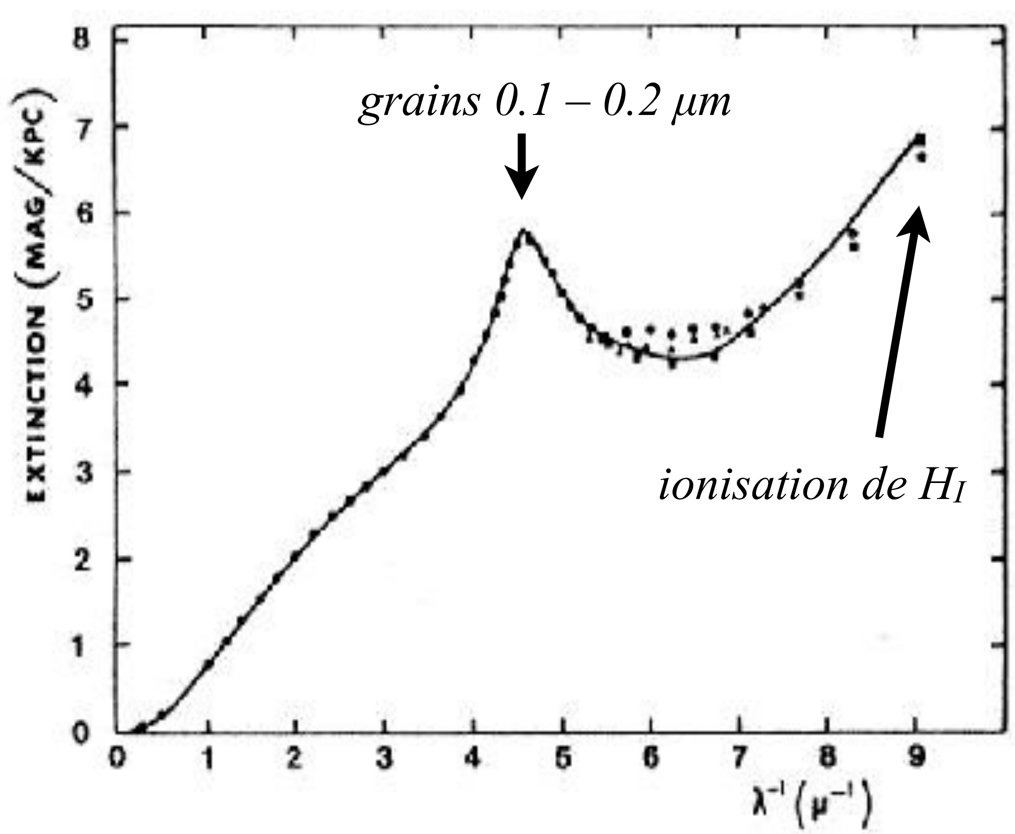

Fig. 1. Wavelength dependence of interstellar extinction normalised to 1.8 mag/kpc at λ^{-1} = 1.8 μm^{-1}. Points are astronomical observations; solid curve is for the grain model proposed here. (● average extinction data compiled from many sources by Sapar and Kuusik (1979). ▲ ESA data from Jamar *et al.* (1976). ■ OAO II data from Bless and Savage (1972).

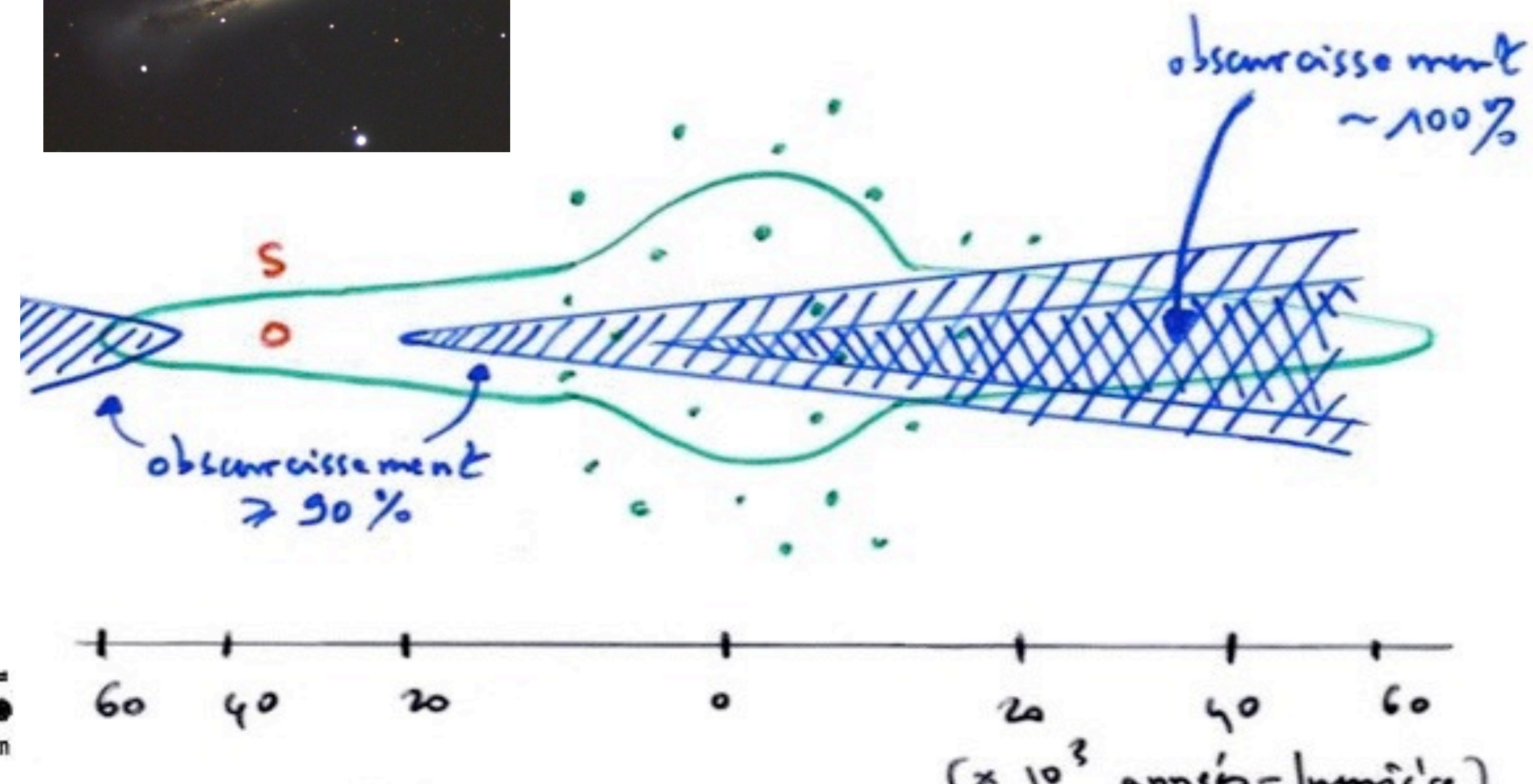

⇒ Opacity of ISM in visible light beyond ~3 kpc (<< ∅ galactic disk)

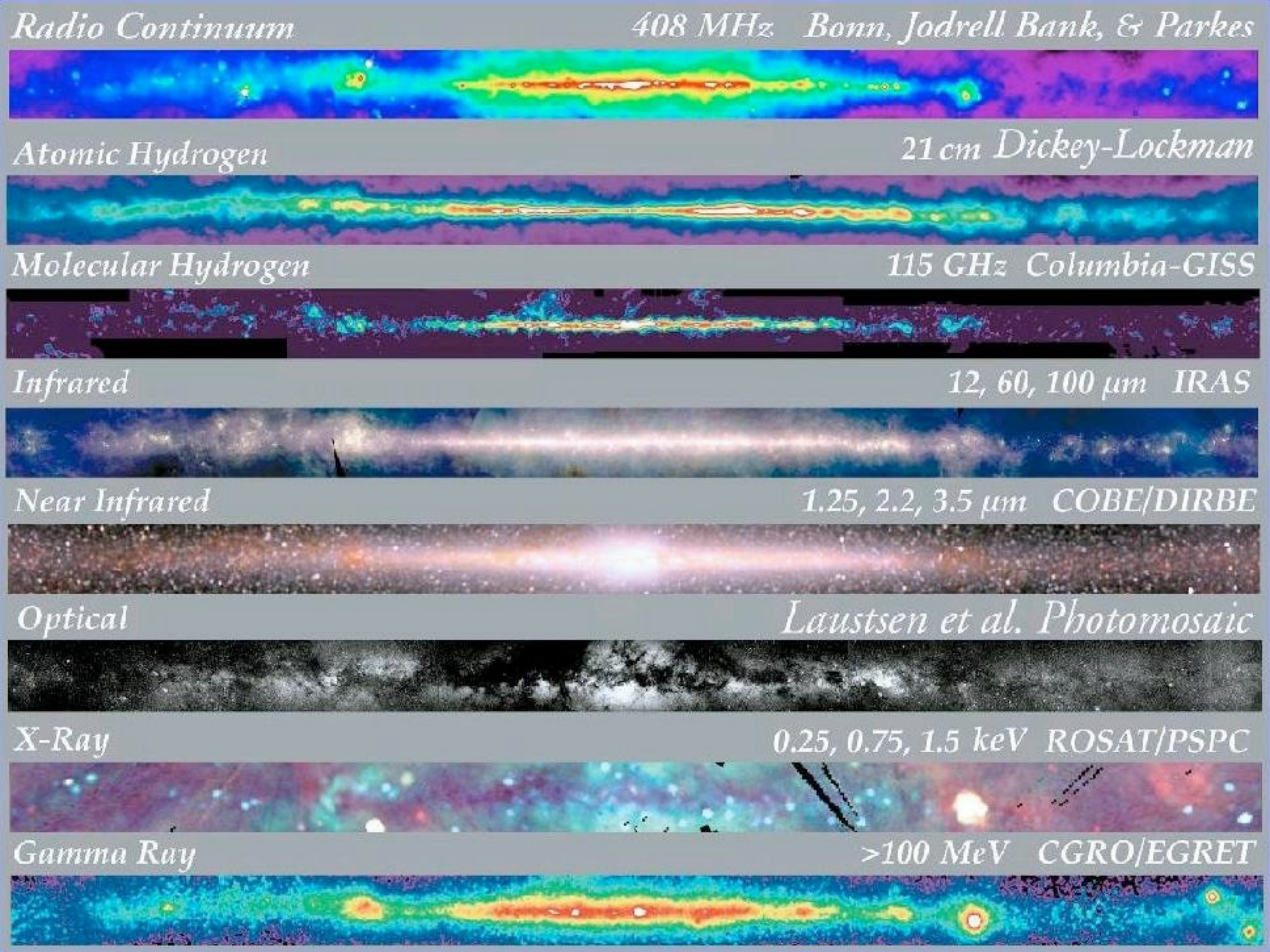
Radio Continuum
408 MHz Bonn, Jodrell Bank, & Parkes
Atomic Hydrogen
21 cm Dickey-Lockman
Molecular Hydrogen
115 GHz Columbia-GISS
Infrared
12, 60, 100 μm IRAS
Near Infrared
1.25, 2.2, 3.5 μm COBE/DIRBE
Optical
Laustsen et al. Photomosaic
X-Ray
0.25, 0.75, 1.5 keV ROSAT/PSPC
Gamma Ray
>100 MeV CGRO/EGRET

⇒ Reddening of the spectrum of distant objects → modifies the evaluation of T(source)

In Radio, $\lambda >> \Rightarrow P(\lambda) << \Rightarrow$ the Galactic disk is ~transparent
→ galactic structure
→ radio study of dark nebulae (dust)

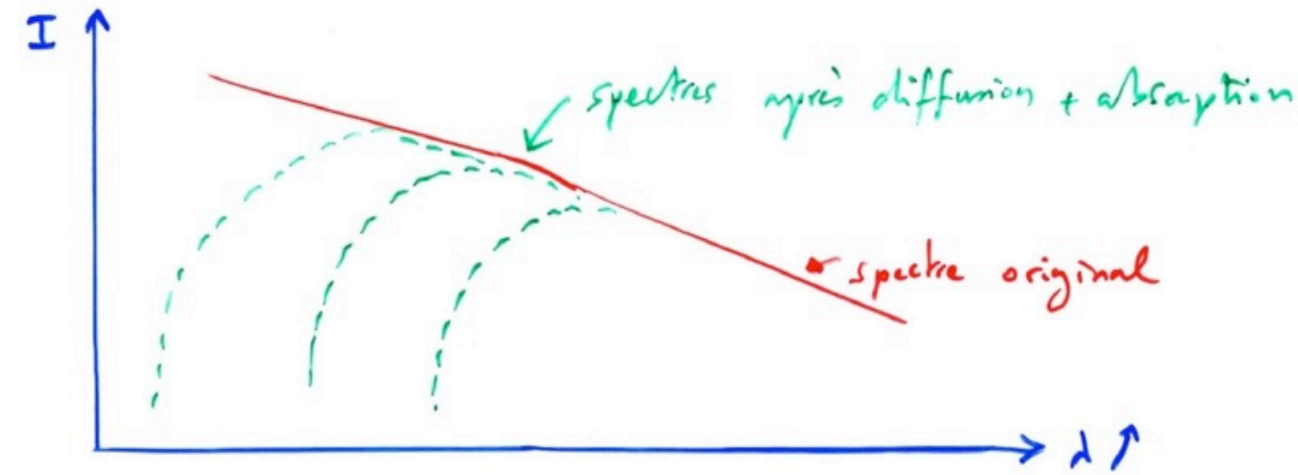

→ Propagation of a radio wave depends on the electron density N_e
(and the magnetic field **B**) of the propagation medium

⇒ probing of cosmic plasmas (Solar corona, ISM…) inaccessible in optical & IR

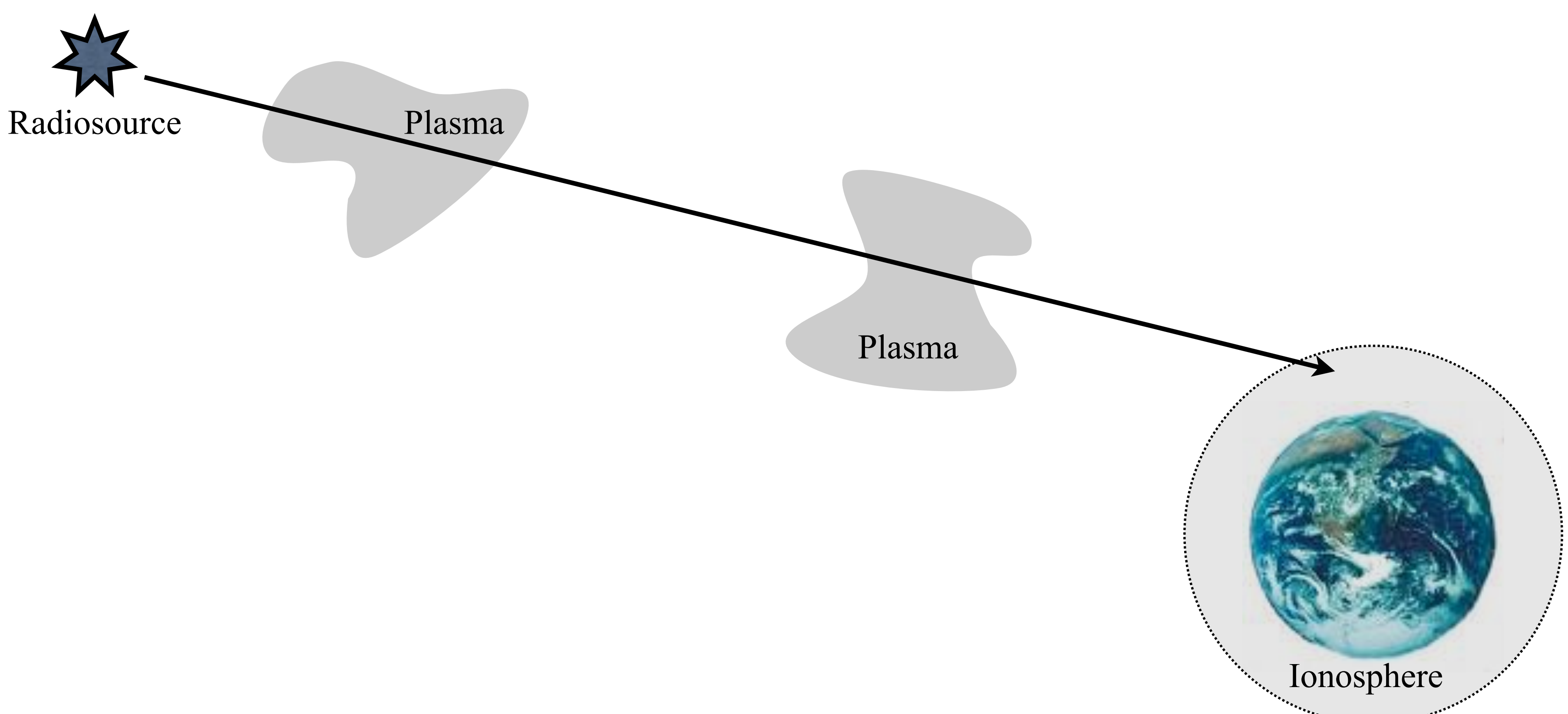

Specific features of Radioastronomy

- « Technical »

☺ Coherent detection : direct measurement of amplitude E, $|E|$ or $|E^2|$, and phase ϕ (fast electronics)

☺ Low photon noise

$n_{photons} = E / h\nu$

$\Rightarrow$ the statistical noise of photon counting (to which any flux measurement ultimately reduces) is $\propto \sqrt{n}/n \propto 1/\sqrt{n}$

Comparison Radio / Visible (at equivalent flux) :

$1/\sqrt{n_{visible}} / 1/\sqrt{n_{radio}} = (\lambda_{radio}/\lambda_{visible})^{1/2} \geq (1\ \text{mm} / 0.5\ \mu\text{m})^{1/2} \approx 45$

Example 1 : For a very weak radiosource :

$S = 10^{-30}\ Wm^{-2}Hz^{-1}$ a 100 MHz $\Rightarrow$ $S / h\nu = 1.5\times10^{-5}$ photons/m^2.s.Hz

With $b = 10$ kHz & $A_{eff} = 1000\ m^2$ $\Rightarrow$ $n = 150$ photons/s

$\Rightarrow$ statistics at ~8% accuracy in 1 second (acceptable even with $\tau < 1$ s)

Example 2 : For a very weak optical source :

$m_v = 21$ (limit magnitude for a telescope of $\varnothing$ = 4-5 m), $\lambda = 0.55\ \mu m$ (yellow),

& filter $\Delta\lambda = 0.1\ \mu m$ $\Rightarrow$ $\int_{filter} S.d\lambda = 10^{-21}\ W/m^2 = 3\times10^{-3}$ photons/m^2.s

With $A_{eff} \leq 100\ m^2$ $\Rightarrow$ $n \leq 0.3$ photons/s (+ atm. losses & in the receiver)

$\Rightarrow$ $\tau > 500$ s needed for a statistics at ~8% accuracy ($1/\sqrt{n\tau} \leq 8\%$)

$\Rightarrow$ optical measurements less sensitive to fast flux variations

☺ RADAR astronomy = Active Radioastronomy (teledetection)
Echo / t $\Rightarrow$ Relief mapping
Echo / ν $\Rightarrow$ Surface (texture)

Example: Magellan/Venus, Saturne rings, Solar corona ...

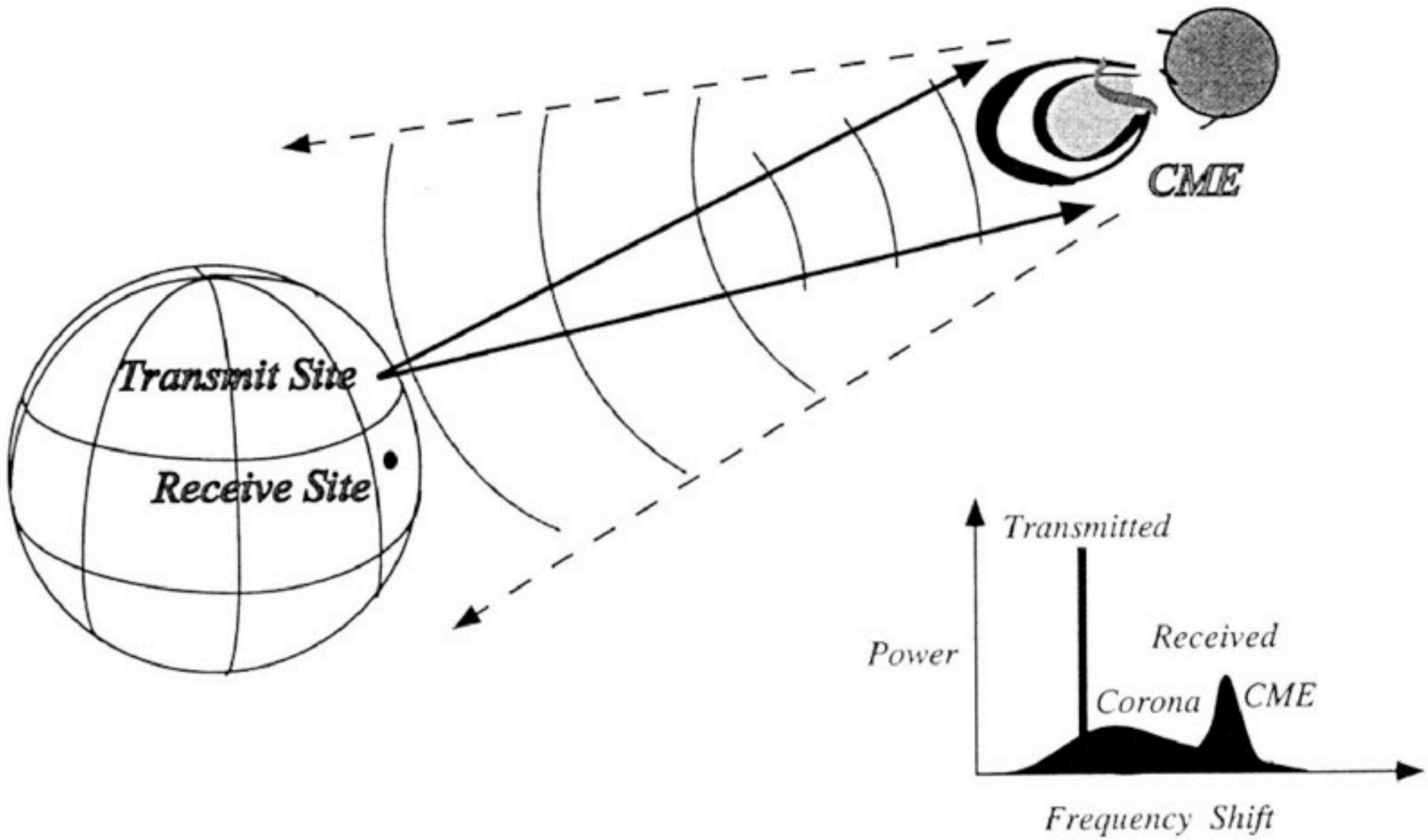

[only comparison in visible = Laser Lunar ranging]

☹ Angular resolution

• <u>Reminder</u>: diffraction at ∞ through a rectangular aperture (1D)

The phase shift of a ray passing through the aperture at distance x from O, in direction θ, is :

$\varphi = \mathbf{k.x} = k\,\Delta s = 2\pi\, x \sin\theta / \lambda \quad (\approx 2\pi\, x\, \theta / \lambda$ for small θ)

Corresponding wave (passing through M) writes : $E = E_o \exp[i(\omega t - \varphi)] = E_o \exp(i2\pi\nu t) \exp(-i2\pi\, x\, \theta / \lambda)$

The amplitude received in the θ direction (in P) is :

$\bar{E}(\theta) = \int_{-D/2}^{+D/2} E_o \exp(i2\pi\nu t) \exp(-i2\pi\, x\, \theta / \lambda)\, dx$

$= E_o \exp(i2\pi\nu t) \int_{-\infty}^{+\infty} f(x) \exp(-i2\pi\, x\, \theta / \lambda)\, dx$

with $f(x) = 1$ for $x \in [-D/2, +D/2]$, $f(x) = 0$ elsewhere

$\bar{E}(\theta) = E_o \exp(i2\pi\nu t)\ [\exp(-i2\pi\, x\, \theta / \lambda) / (-i2\pi\, \theta / \lambda)]_{-D/2}^{D/2}$

$\bar{E}(\theta) = D\, E_o \exp(i2\pi\nu t)\ \mathrm{sinc}(\pi D\, \theta / \lambda)$

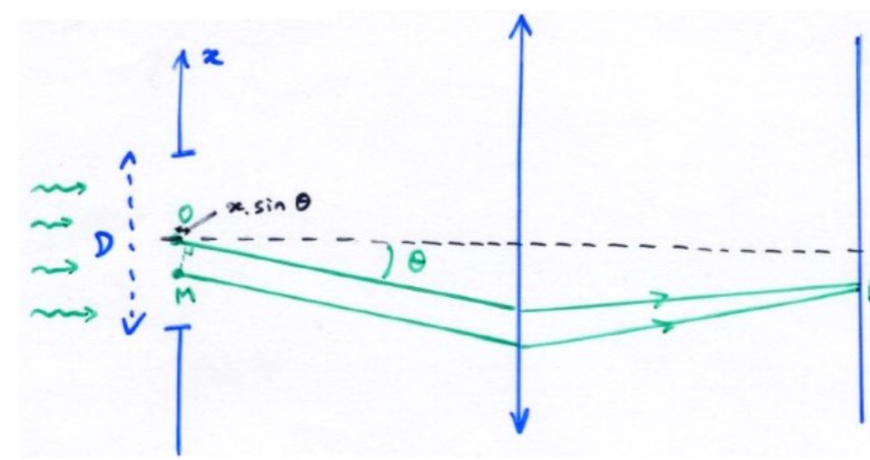

<u>*NB*</u> : $\bar{E}(\theta)$ = *TF(E(x)) where E(x) is the amplitude distribution on the aperture*

(= constant for a plane wave from ∞ near the axis)

θ and x/λ are conjugate variables

sinc(x) = sinx/x (or its normalised form: sinc(x) = sin(πx)/πx = « 1D Airy function »)

$I(\theta) \propto \bar{E}^2(\theta) \propto \mathrm{sinc}^2(\pi D\, \theta / \lambda)$ [$4J_1^2(\pi D\theta/\lambda)/(\pi D\theta/\lambda)^2$ for a 2D circular aperture]

→ Criterion for separating 2 point sources: $\theta \geq K\, \lambda / D$ [K = 1.22 for an Airy function]

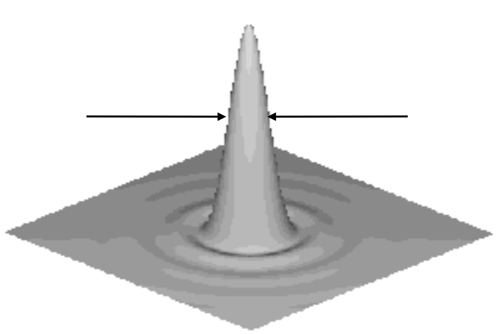

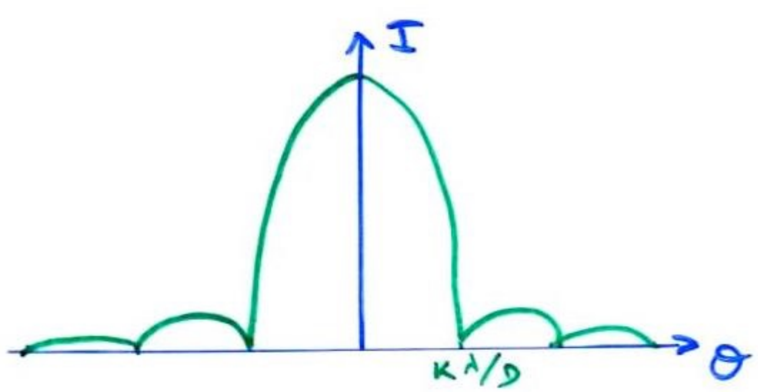

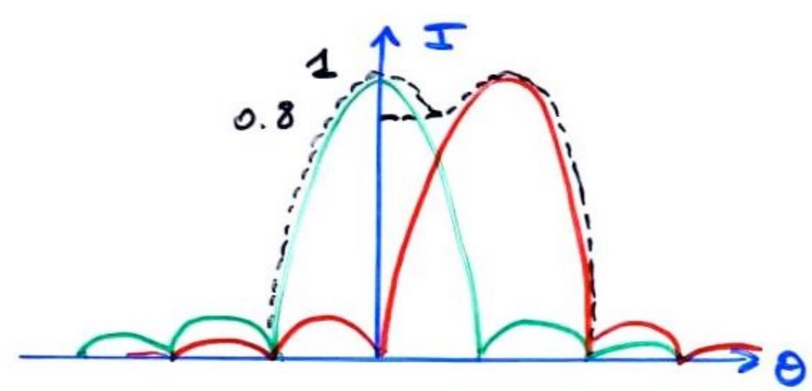

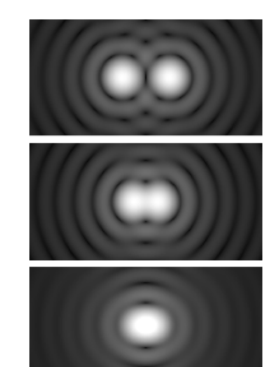

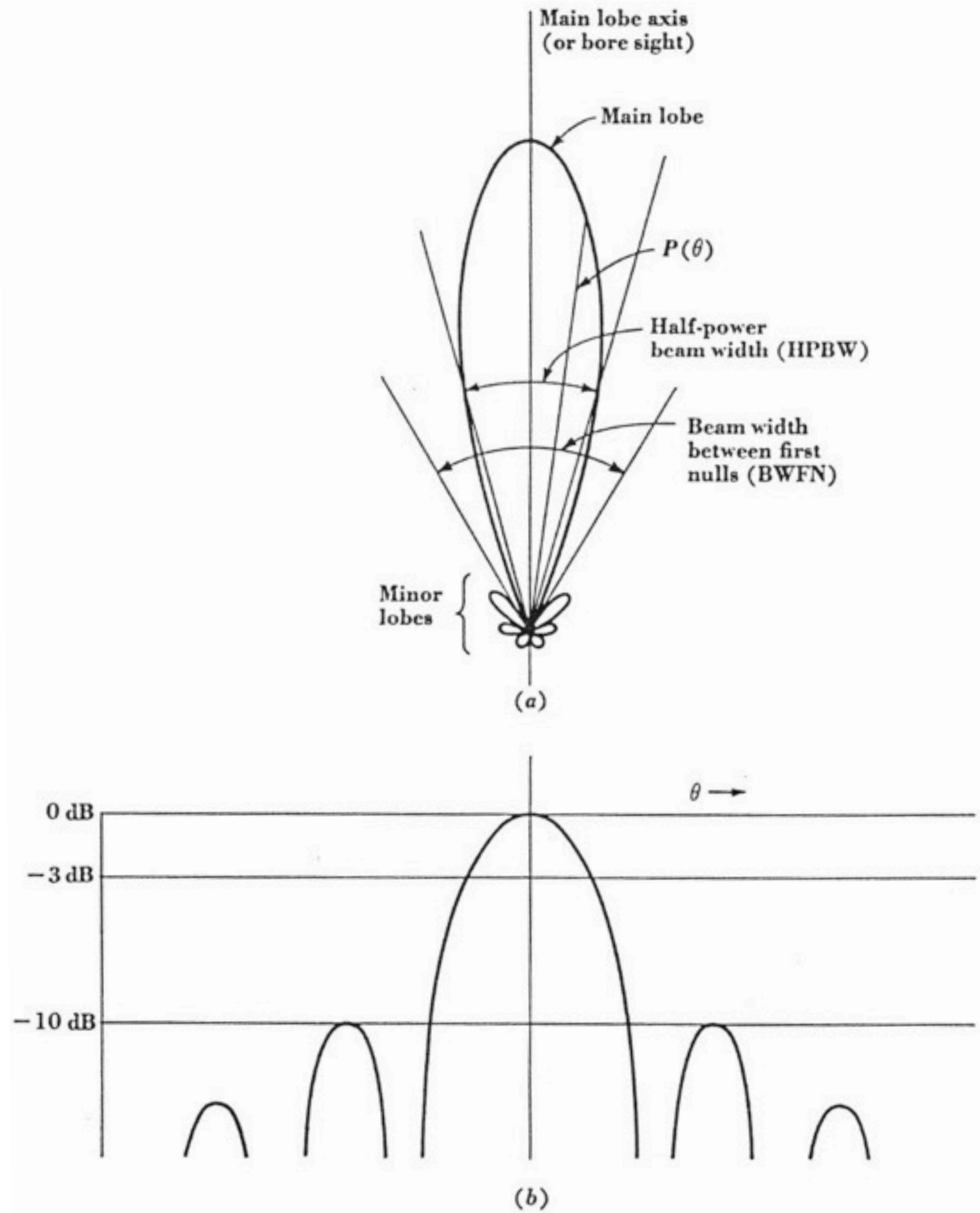

Fig. 6-1. (a) Antenna pattern in polar coordinates and linear power scale; (b) antenna pattern in rectangular coordinates and decibel power scale.

Angular resolution of an instrument of $\varnothing$ D $\sim \lambda/D \Rightarrow 10^7 \times<$ a 10m / 1 µm

$\Rightarrow$ radio instruments need to be large,

$\Rightarrow$ signal must be transporter over long distances

Ex: *Human eye :* $\varnothing(pupil) = 2\text{-}8\ mm\ (day/night) \Rightarrow \lambda/D = 0.25' - 1'$ *at* $\lambda = 0.5\ \mu m$

Same resolution at $\lambda = 1\ cm \Rightarrow D = 40 - 160\ m$

With $D = 100\ m$ *at* $\lambda = 21\ cm \Rightarrow \lambda/D = 7'$

at $\lambda = 10\ m \Rightarrow \lambda/D = 6°$ $(\varnothing Sun = 30',\ \varnothing Jupiter = 40'')$

$\Rightarrow$ very large collecting areas / very extensive instruments required,
but with modest surface precision ☺
(Rayleigh criterion $\sim\lambda/10 \rightarrow$ 1 cm wire mesh Ok at $\lambda = 21$ cm)

$\Rightarrow$ Interferometry is necessary (and "easy" : coherent detection + many baselines generally available) for reaching a correct angular resolution
($\sim\lambda/d$, with d the distance between the antennas)

$\Rightarrow$ in VLBI, one reaches $\lambda/d \sim 10^{-3}''$ (10^4 km at $\lambda = 21$ cm)

Ionosphere disturbances (same problem as ~atmosphere in optics - see below)

No radio lens (mirrors only)

No sensitive surface: focal antenna = horn or dipole

⇒ Few focal pixels (image plane) : generally only 1

(recent arrays of horns or dipoles = Focal Plane Arrays)

⇒ instantaneous imaging difficult (impossible with a single antenna)

⇒ phased array or interferometer → image synthesis

High "sky" temperature at low frequencies :

$T(K) \sim 1.15\times10^{8}/f^{\,2.5} \sim 60\,\lambda^{2.55}$ ($f \sim 3$ - 300 MHz)

f (MHz)	λ (m)	T (K)
1	300	$>10^{7}$
10	30	$\sim3\times10^{5}$
100	3	$\sim10^{3}$
1000	0.3	~5

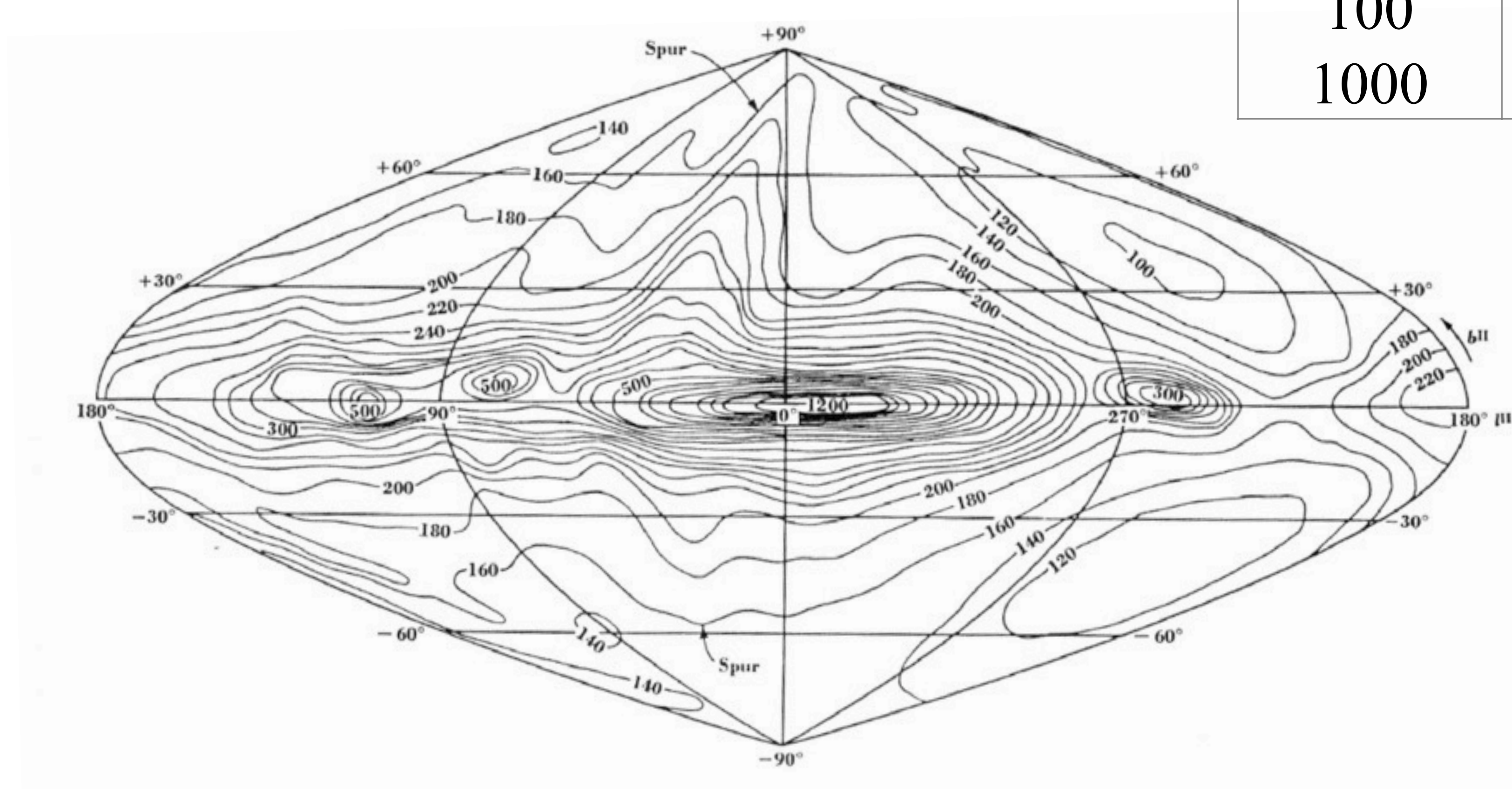

Fig. 8-51. Radio emission from the sky at 200 Mc in new galactic coordinates. Temperatures are indicated in degrees Kelvin. (*After Dröge and Priester*, 1956.)

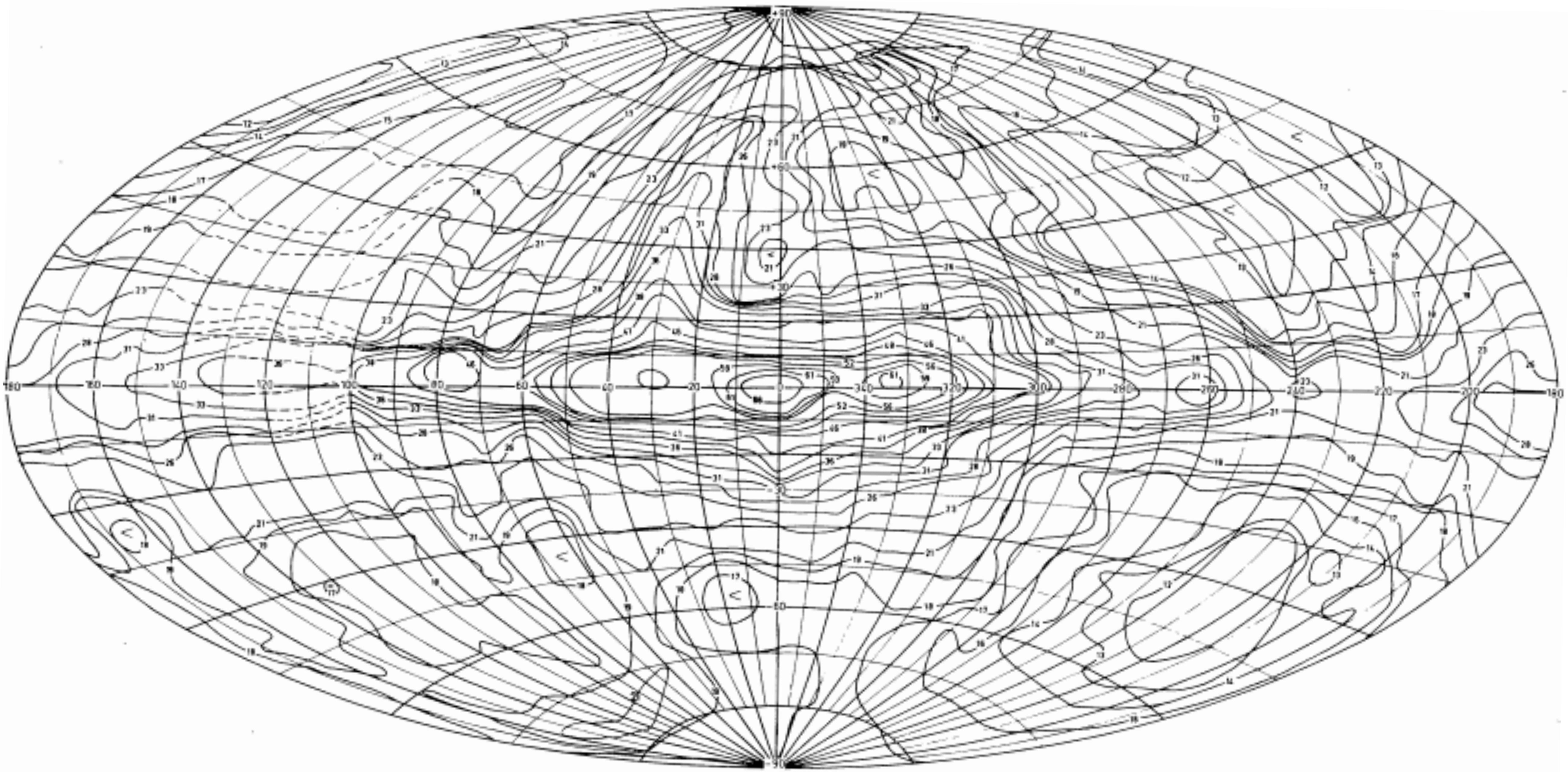

Fig. 1. Contour map of 30 MHz brightness temperatures plotted on a Hammer equal-area projection in galactic coordinates. The contour unit is 1000 K.

$T_{B,min} \sim 10^4$ K, $T_{B,max} \sim 6.6 \times 10^4$ K

$\Rightarrow$ the LF radio sky, even at night, is brighter than daytime optical sky

Radio Frequency Interference (RFI)

- Natural = lightning (broadband: <10 kHz → >10 MHz, summer, low latitudes)
- Man-made = industrial, military, telecommunications activities [4G!] (predominant)

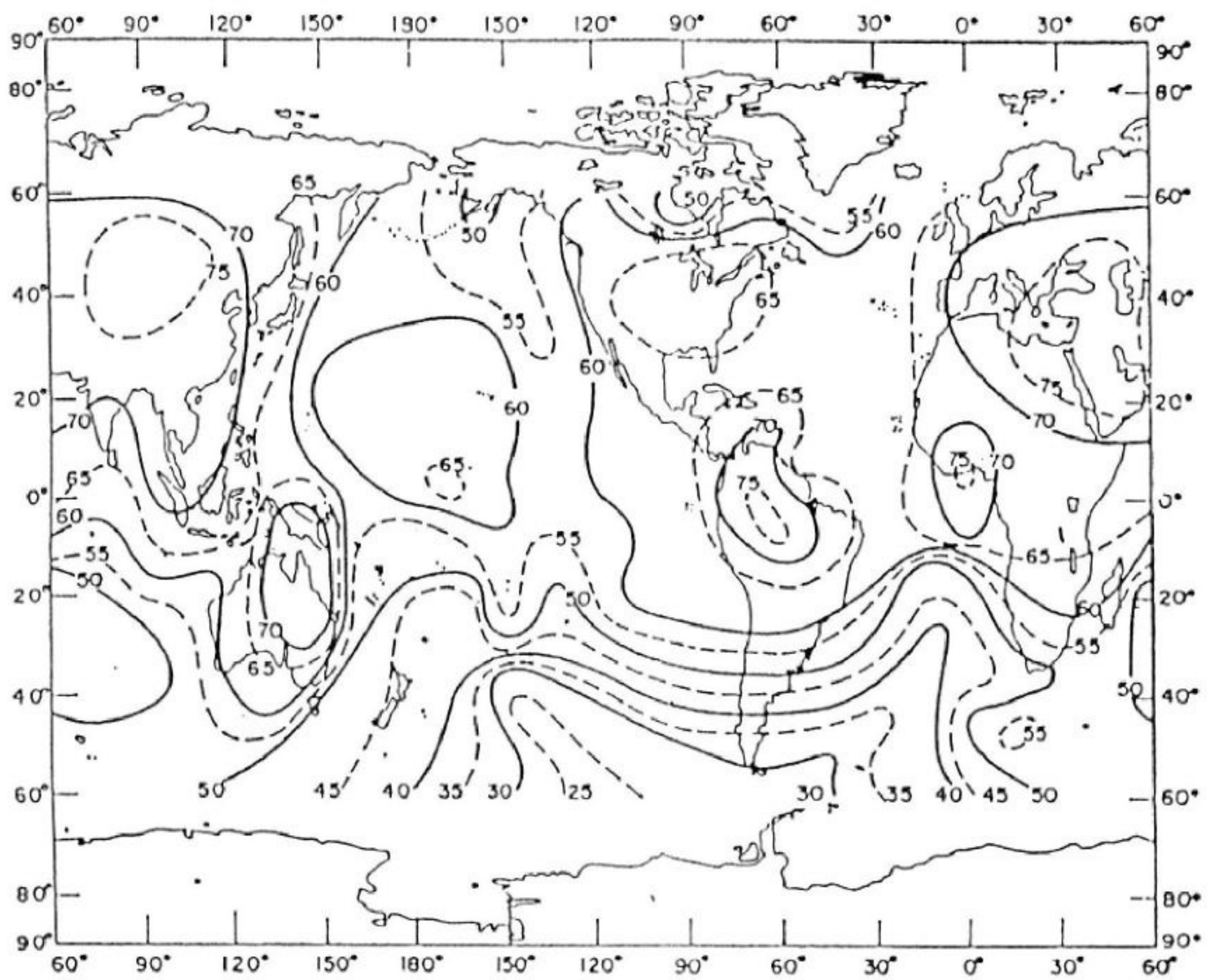

Figure 2. The terrestrial radio noise distribution derived from the RAE-1 (height 6000 km) lower "V" data at 9.18 MHz for December 2-6, 1968. The secondary peaks in activity over the mid-Pacific and northern Australia are believed to be correlated with local thunderstorm activity. Contour levels are db above 288 K. The Galactic background on this scale would be about 31 db and the receiver saturated at 75 db. (from Herman et al, 1973)

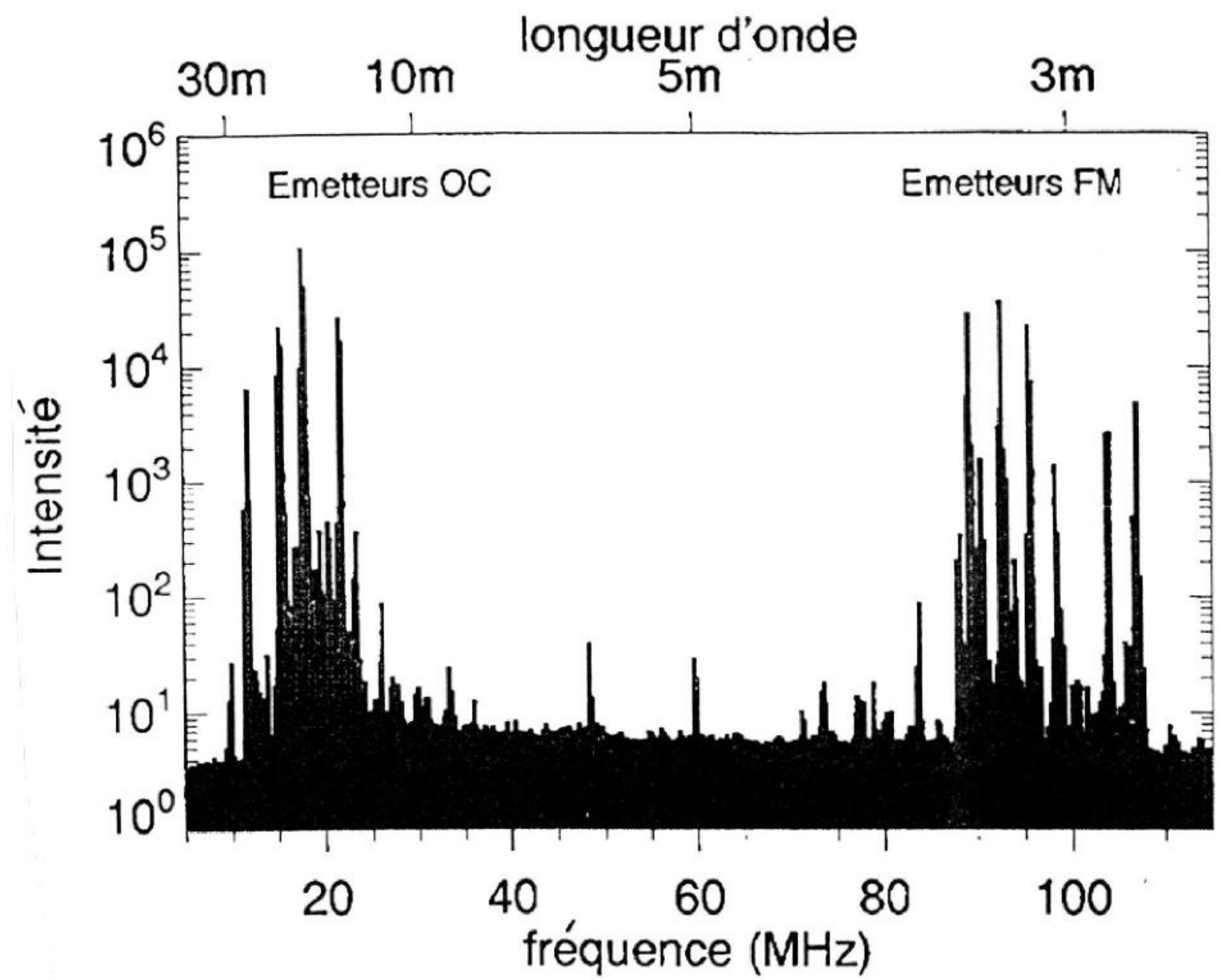

⇒ Isolated, locally protected sites (forest)

⇒ Protected frequency bands (H_I, OH ...) where all emissions are prohibited
["passive primary" WRC-ITU = World Radiocomm. Conferences of Int'l Telecomm. Union]
= growing problem due to the increasing sensitivity of observations,
and economic pressures (TV, telephone, broadcasting, radiocommunications...)

I) - Bandes de fréquence allouées au service de radioastronomie (allocations CAMR 1979) entre 10 MHz et 25 GHz.

N°	Allocation	Statut
1	13.36 - 13.41 MHz	primaire/actif
2	25.55 - 25.67 MHz	primaire exclusif
3	37.50 - 38.25 MHZ	secondaire
4	73.00 - 74.60 MHz	primaire en région 2
5	79.25 - 80.25 MHz	primaire/actif
6	150.50 - 153.00 MHz	primaire/actif
7	322.00 - 328.60 MHz	primaire/actif
8	406.10 - 410.00 MHz	primaire/actif
9	608.60 - 614.00 MHz	prim. en R2, sec. en R1/ R3
10	1330.00 - 1400.00 MHz	note d'utilisation
11	1400.00 - 1427.00 MHz	primaire passif
12	1610.60 - 1613.80 MHz	secondaire
13	1660.00 - 1660.50 MHz	primaire/actif
	1660.50 - 1668.40 MHz	primaire/actif
	1668.40 - 1670.00 MHz	primaire/actif
14	1718.80 - 1722.20 MHz	secondaire
15	2655.00 - 2690.00 MHz	secondaire
	2690.00 - 2700.00 MHz	primaire/passif
16	3260.00 - 3267.00 MHz	note d'utilisation
17	3332.00 - 3339.00 MHz	note d'utilisation
18	3345.80 - 3352.50 MHz	note d'utilisation
19	4800.00 - 4990.00 MHz	secondaire
	4990.00 - 5000.00 MHz	primaire/actif
20	10.60 - 10.68 GHz	primaire/actif
21	10.68 - 10.70 GHz	primaire/actif
22	14.47 - 14.50 GHz	secondaire
	15.35 - 15.40 GHz	primaire passif
23	22.01 - 22.21 GHz	note d'utilisation
	22.21 - 22.50 GHz	primaire/actif
24	22.81 - 22.86 GHz	note d'utilisation
25	23.07 - 23.12 GHz	note d'utilisation
26	23.60 - 24.00 GHZ	primaire passif

II) - Bandes de fréquence réellement utilisées par les radioastronomes français (F) et européens (E) depuis 1979, entre 10 MHz et 22.5 GHz.

N°	Fréquences		Intérêt astrophysique	Raie ou Continuum
1	20 - 70 MHz	(F)	Soleil et planètes (Jupiter)	C
2	150 - 450 MHz	(F,E)	Soleil	C
3	242 - 246 MHz	(E)	Pulsars	C
4	322 - 328 MHz	(E)	Interférométrie	C
5	406 - 410 MHz	(E)	Pulsars, VLBI	C
6	608 - 614 MHz	(E)	VLBI	C
7	926 - 940 MHz	(E)	Pulsars	C
8	1330 - 1400 MHz	(F,E)	Hydrogène	R
9	1400 - 1427 MHz	(F,E)	Hydrogène	R
10	1550 - 1667 MHz	(F,E)	Hydroxyle	R
11	1610 - 1722 MHz	(F,E)	Hydroxyle	R
12	2290 - 2300 MHz	(E)	VLBI	C
13	2655 - 2700 MHz	(E)	Galactique et extra-gal.	C
14	3200 - 3450 MHz	(F,E)	CH	R
15	4800 - 4990 MHz	(E)	VLBI	R,C
16	4990 - 5000 MHz	(E)	Galactique et extra-gal.	C
17	8387 - 8843 MHz	(E)	VLBI	C
18	9600 - 9620 MHz	(F)	Soleil	C
19	9.7 - 10.7 GHz	(E)	Fonds cosmique	C
20	14.5 - 15.5 GHz	(E)	Fonds cosmique	C
21	22.2 - 22.5 GHz	(E)	VLBI	C

Il faut ajouter à cette liste de nombreuses observations de raies de recombinaison sur des fréquences comprises notamment entre 1425 et 1550 MHz.

- Space observations protected by the earth's ionosphere for $\nu \leq 5$ MHz

- Moon = radio shield

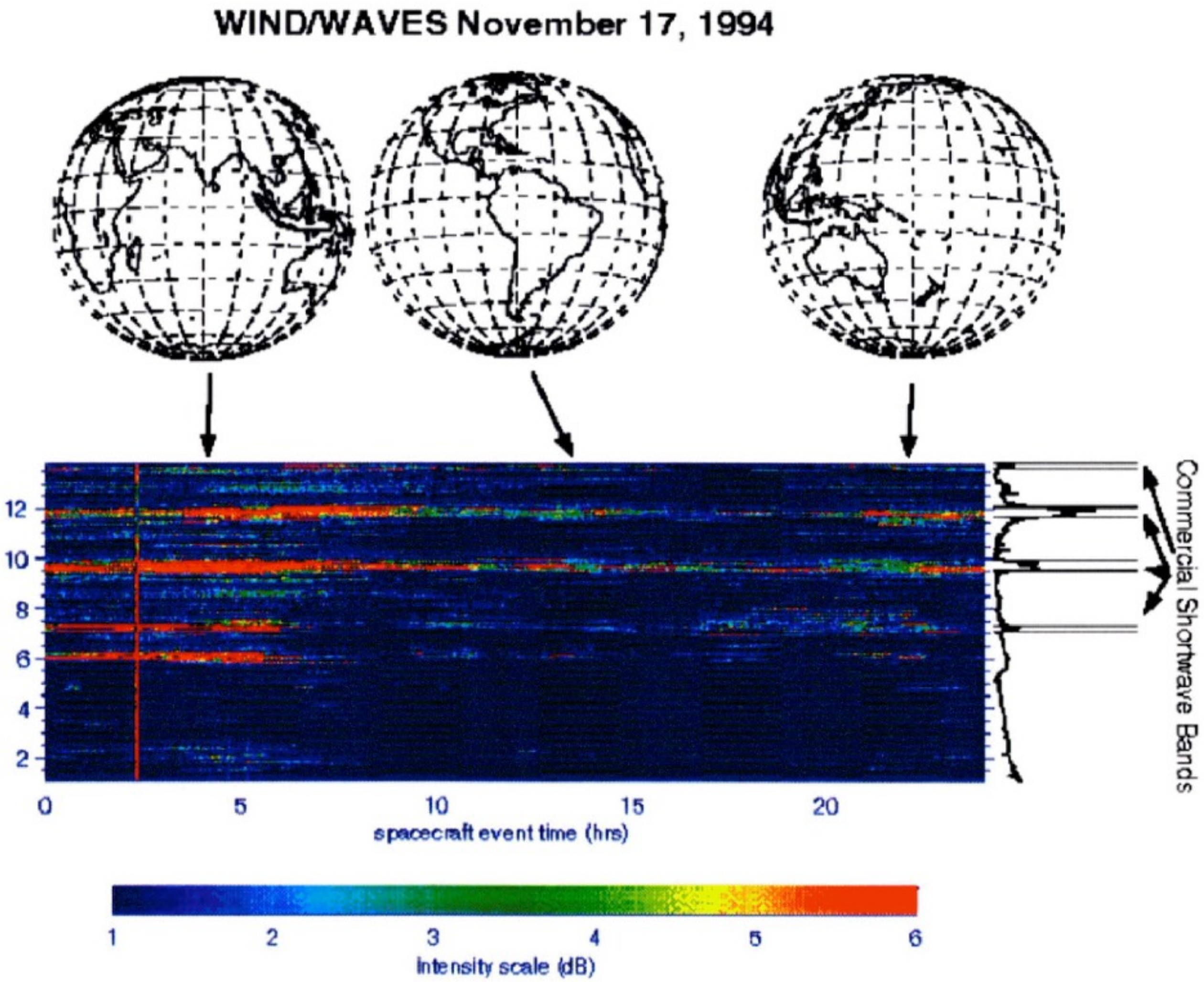

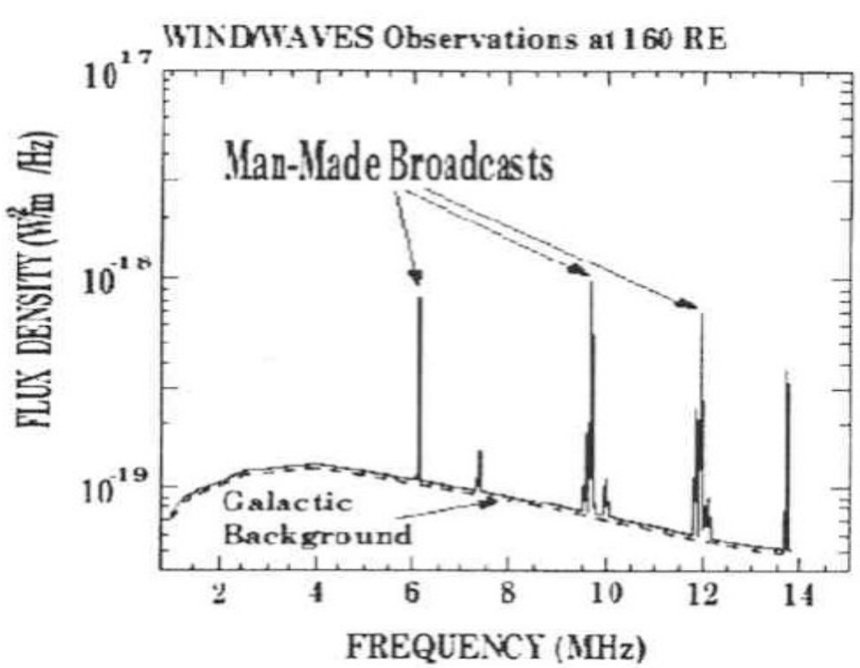

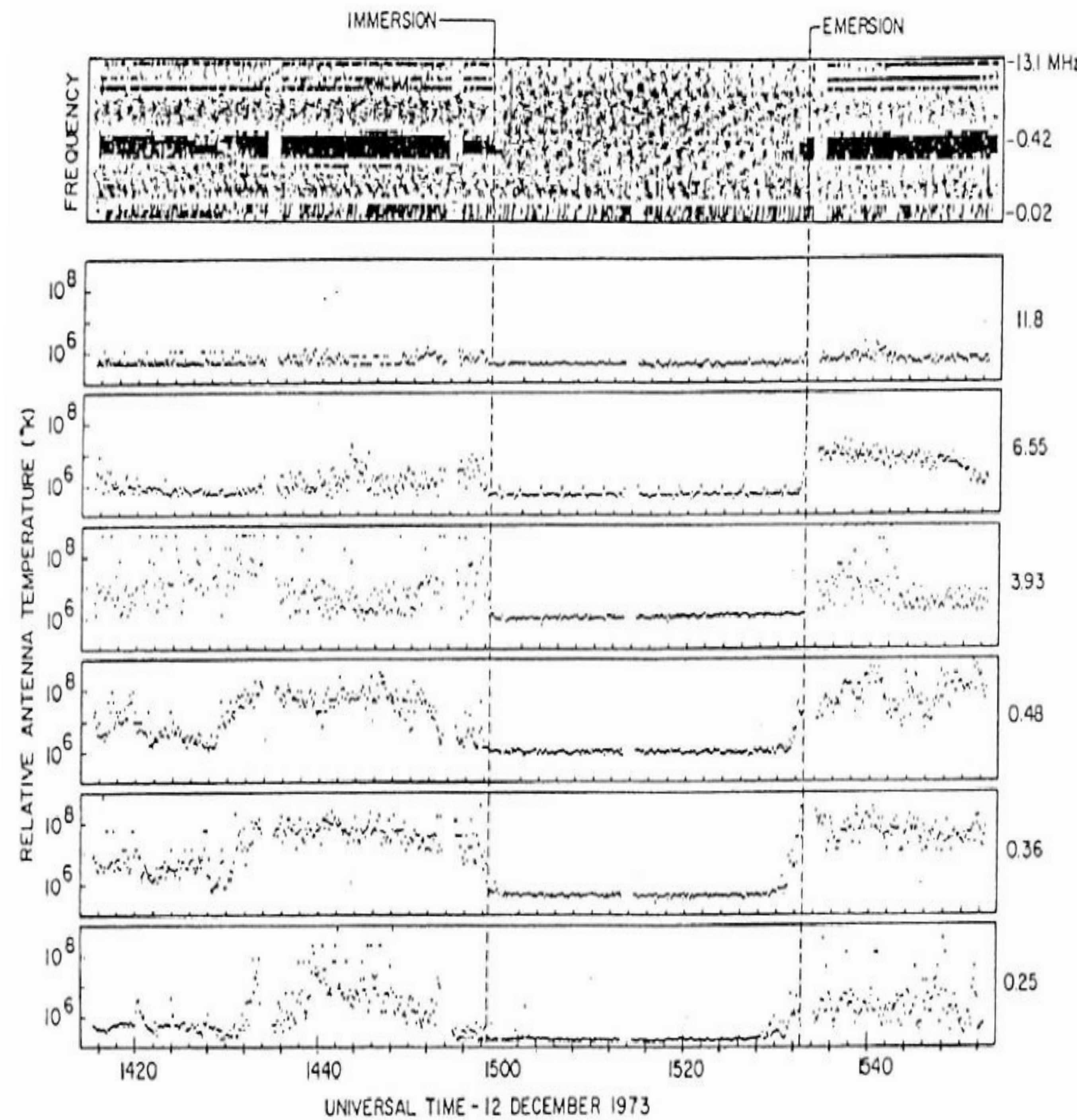

Figure 8. Data from RAE-2 in lunar orbit showing the dramatic disappearance and reappearance of interference from the Earth [*Alexander, et al.*, 1975].

- Introduction (history, interest, specific features)
- Waves & Polarisation
- Plasmas & Propagation (cutoff, dispersion, Faraday effect, scintillations)
- Coherent Signal Detection (measurement theory, antenna temperature, calibration, noise)
- Receivers (heterodyne, system temperature, filtering, gain, RFI mitigation)
- Basics of Radio Astronomy Antennas: Single antennas
- Basics of Interferometry and Aperture Synthesis (phased arrays, electronic pointing, imaging, correlation, coherence, VLBI)
- Observation methods
- Large present & future ground-based radio arrays
- Basics of Space radio astronomy

Wave

- Radio wave = transverse e.m. wave (**E**, **B** $\perp$ **k**) → propagation in straight line at c in vacuum

Pulsation : $\omega = 2\pi f$
Wave vector : $k = 2\pi/\lambda$

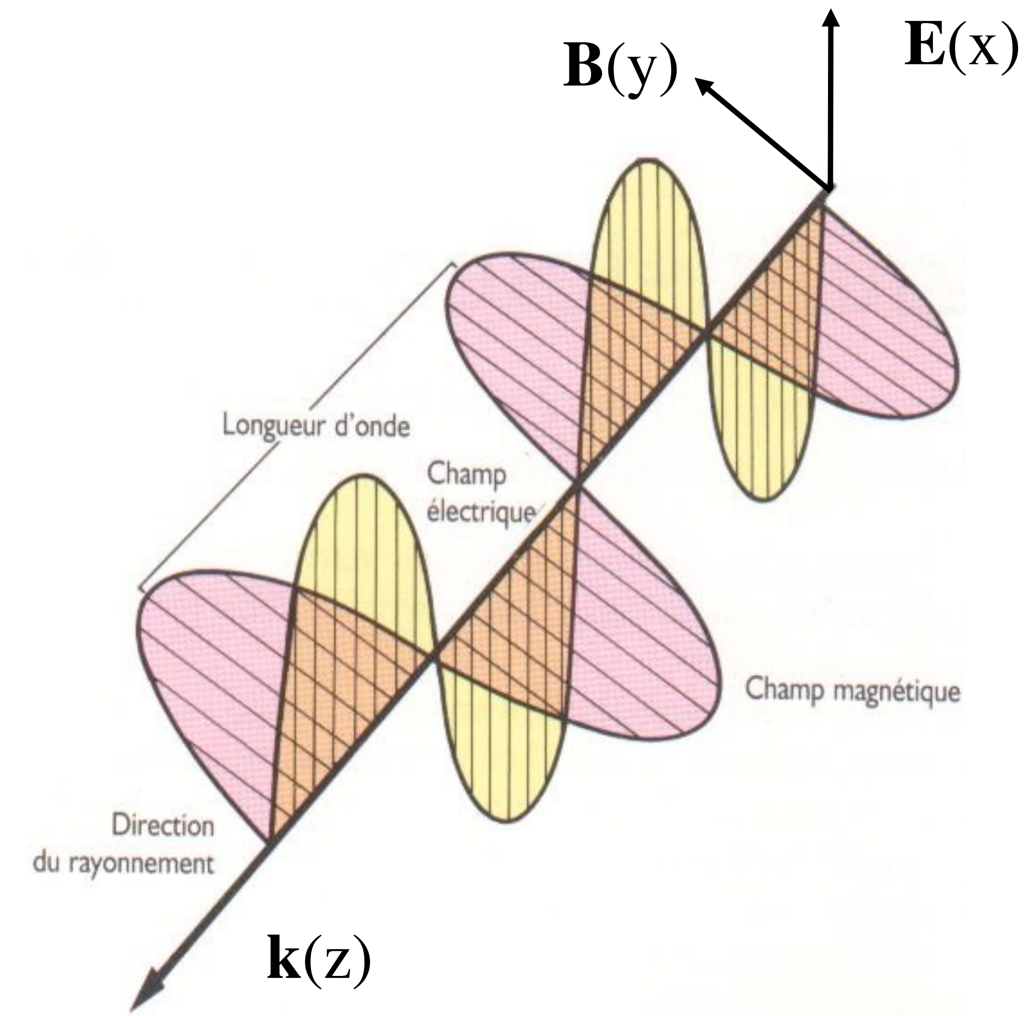

NB: ∃ *"plasma" waves, e.s., longitudinal: $B = 0$, $E \,//\, k$*
→ *excited near the resonance frequencies of the medium*
~ f_{pe}, f_{ce} (generally VLF / radio frequencies)
→ *no propagation outside their medium of origin*
→ *e.m. / e.s. distinction e.g. via magnetic antennas*

• Electric field $\rightarrow \mathbf{E} = E_o \, \mathbf{x} \cos(kz - \omega t)$ $\quad T = 2\pi/\omega \quad f = \omega/2\pi$

$k = 2\pi/\lambda \quad \lambda f = c$ (in vacuum)

$\mathbf{E}$ unchanged for $(kz - \omega t) = C^t \Rightarrow k\,dz - \omega\,dt = 0 \Rightarrow v_\phi = dz/dt = \omega / k$

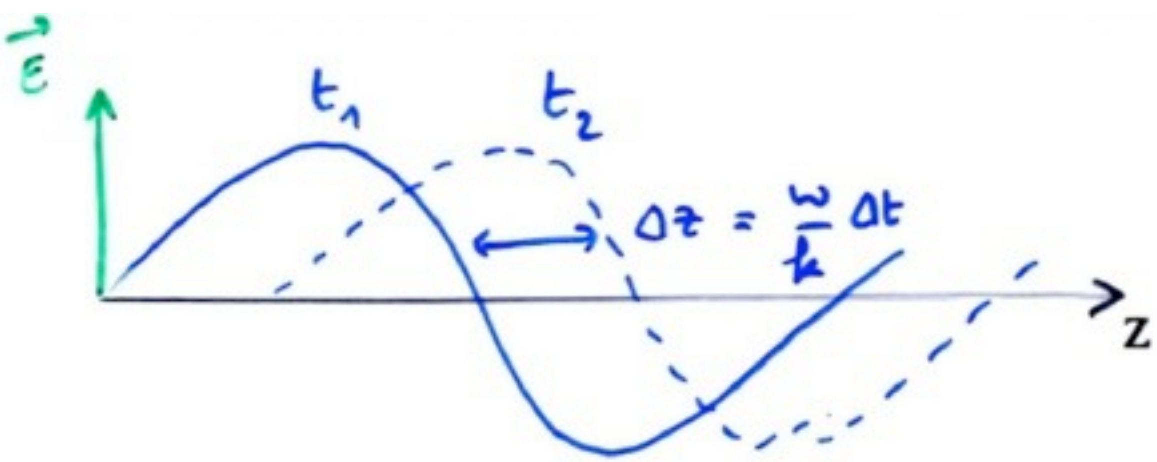

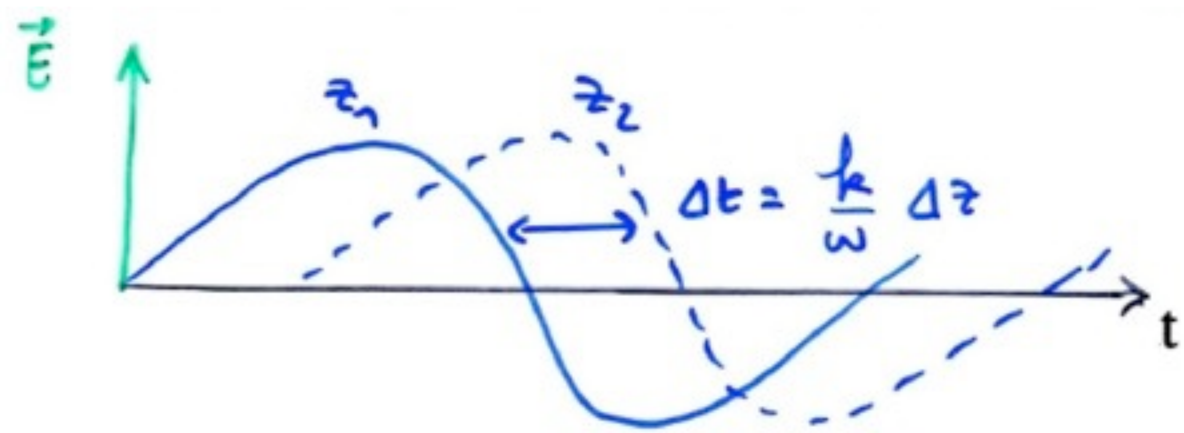

$\Rightarrow E_o \, \mathbf{x} \cos(kz - \omega t)$ represent a monochromatic harmonic wave propagating without deformation at speed $v_\phi = \omega / k$

[v_ϕ is determined by the physical characteristics of the propagation medium (= c = C^t in a vacuum)]

→ In a medium ≠ vacuum, ω is generally a function of $\mathbf{k}$

→ energy carried by a wave (= intensity = modulus of the Poynting vector)

- instantaneous : $|\mathbf{P}| = |\mathbf{E} \wedge \mathbf{B}| / \mu_o = |E(t,z)|^2 / Z$ $\quad [\, B = E / c = E / \sqrt{(\varepsilon_o \mu_o)} \,]$
- average : $<|\mathbf{P}|> = E_o^2 / 2Z$

in a vacuum, $Z = Z_o = \sqrt{(\mu_o/\varepsilon_o)} = 120\,\pi = 377\ \Omega$ (impedance of free space)

- <u>complex wave equation</u>

$$U = E_o \exp[i(kz - \omega t)] = E_o [\cos(kz - \omega t) + i \sin(kz - \omega t)]$$

$\rightarrow$ Re(U) only represents the wave amplitude

$\rightarrow$ the energy transported is then $\langle |\mathbf{P}| \rangle = U.U^* / 2Z$

Energy is transported at group velocity $v_g = \partial\omega / \partial k$

$v_g \neq v_\phi$ (velocity of individual monochromatic components)

$\rightarrow$ a detector responds to wave energy

The medium is non-dispersive if $v_g = C^t \Rightarrow \partial^2\omega/\partial k^2 = 0$ (ex: $\omega/k = C^{te} = v_\phi = c$ in vacuum)

or $\Delta k = 0$ (monochromatic wave $\Rightarrow v_g = \partial\omega / \partial k \,|_{k=ko}$)

If $v_g(k) \neq C^t \Rightarrow$ dispersion of a narrow pulse during propagation

(conversely, signal spread allows us to trace the dispersion characteristics of the medium)

Polarisation

→ Linear Polarisation : **E** maintains a constant orientation (e.g. // O**x**)

Polarisation plane = trace of **E** in **x**O**y** plane

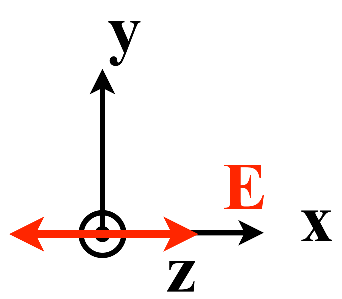

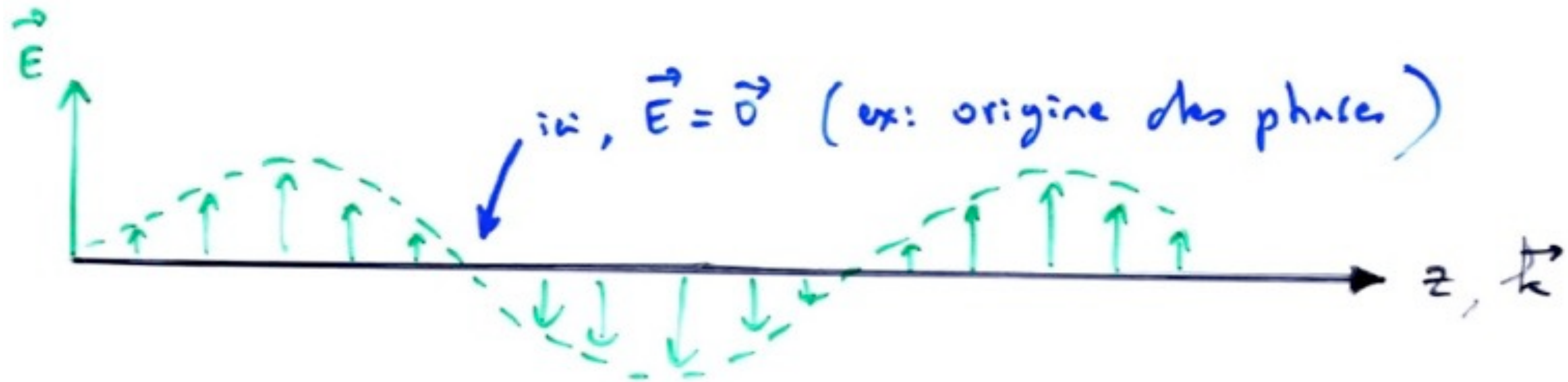

Ex: Pulsars, Jupiter's decimeter emission (synchrotron) …

Σ 2 linear polarisations in phase = linear polarisation

$U_1 + U_2 = \mathbf{E_1} \exp[i(kz\text{-}\omega t)] + \mathbf{E_2} \exp[i(kz\text{-}\omega t)] = (\mathbf{E_1} + \mathbf{E_2}) \exp[i(kz\text{-}\omega t)]$

Σ 2 linear polarisations with a pjhase shift of ±π/2 :

$U_1 + U_2 = \mathbf{E_1} \exp[i(kz\text{-}\omega t)] + \mathbf{E_2} \exp[i(kz\text{-}\omega t \pm \pi/2)]$

Si $|\mathbf{E_1}| = |\mathbf{E_2}| = E_o$ ($\mathbf{E_1} = E_o\,\mathbf{x}$; $\mathbf{E_2} = E_o\,\mathbf{y}$)

$U_1 + U_2 = E_o \exp[i(kz\text{-}\omega t)]\ (\mathbf{x} \pm i\mathbf{y})$

$\Rightarrow \mathrm{Re}(U_1 + U_2) = E_o\,(\mathbf{x} \cos(kz\text{-}\omega t) \mp \mathbf{y} \sin(kz\text{-}\omega t)) = E_o\,(\mathbf{x} \cos\phi \mp \mathbf{y} \sin\phi)$

$\Rightarrow U_1 + U_2$ is a circularly polarised wave

(constant amplitude & direction rotates with t or z)

→ Circular Polarisation : **E** rotates / **k** during propagation, by one turn per period or wavelength.

Origin of phases = direction of **E** in **xOy** plane at fixed z

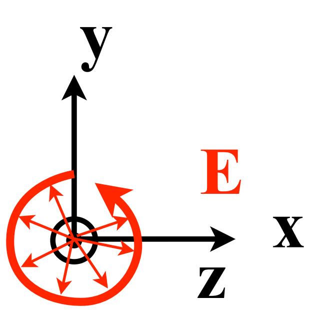

Ex: auroral radio emissions from planets …

Direction of rotation : IRE convention (international radio-electricity) [1942]

(L)eft (LHC) → rotation of **E** in the direct sense when looking along **k** (⊗)

(R)ight (RHC) → inverse sens (= sense of gyration of electrons around **B** // **k**)

<u>NB</u>: opposite rule in optics.

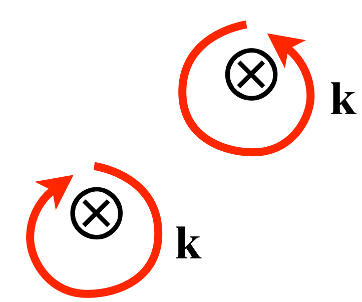

Any circular wave can be decomposed into Σ of 2 linear ones (above)
or conversely, any linear wave in 2 opposite circular waves (L + R) of equal amplitude

If their phase shift is $\Phi = 0 \Rightarrow$ trivial :

$U_R = U_+ = E_o\,(\mathbf{x} + i\mathbf{y}) \exp[i(kz-\omega t)]$

$U_L = U_- = E_o\,(\mathbf{x} - i\mathbf{y}) \exp[i(kz-\omega t)]$

$\Rightarrow U_R + U_L = 2E_o\,\mathbf{x} \exp[i(kz-\omega t)]$ linear !

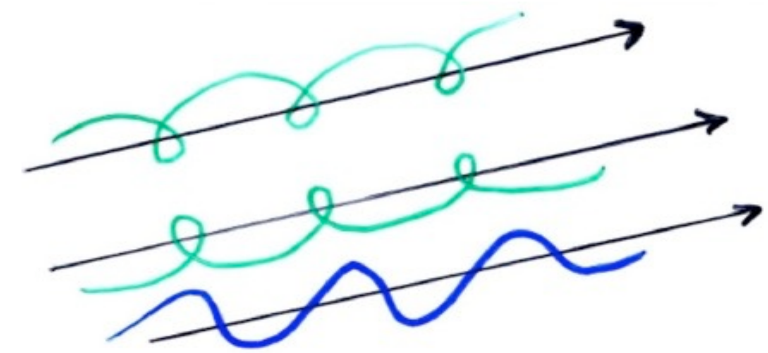

If $\Phi \neq 0$:

$U_R = U_+ = E_o\,(\mathbf{x} + i\mathbf{y}) \exp[i(kz-\omega t)]$

$U_L = U_- = E_o\,(\mathbf{x} - i\mathbf{y}) \exp[i(kz-\omega t+\Phi)]$

$\quad = E_o\,(\mathbf{x}\cos\Phi + \mathbf{y}\sin\Phi + i(\mathbf{y}\cos\Phi - \mathbf{x}\sin\Phi)) \exp[i(kz-\omega t)]$

$\Rightarrow U_R + U_L = E_o\,[\mathbf{x}(1+\cos\Phi) + \mathbf{y}\sin\Phi + i(\mathbf{y}(1+\cos\Phi) - \mathbf{x}\sin\Phi)] \exp[i(kz-\omega t)]$

Wave amplitude

$\mathrm{Re}(U_R + U_L) = E_o\,\mathbf{x}\,[(1+\cos\Phi)\cos\phi + \sin\Phi\sin\phi] + E_o\,\mathbf{y}\,[\sin\Phi\cos\phi - (1+\cos\Phi)\sin\phi]$

with $\phi = kz - \omega t$

$\mathrm{Re}(U_R + U_L) = E_o\,[\,\mathbf{x}\,(\cos\phi + \cos(\phi-\Phi)) + \mathbf{y}\,(\sin(\phi-\Phi) - \sin\phi)\,]$

$\quad = 2E_o\,[\,\mathbf{x}\cos\Phi/2\,\cos(\phi-\Phi/2)) + \mathbf{y}\sin\Phi/2\,\cos(\phi-\Phi/2)\,]$

$\Downarrow \qquad \Downarrow$

the 2 components are in phase

$\Rightarrow (U_R + U_L)$ is linearly polarised

Amplitudes are different on $\mathbf{x}$ & $\mathbf{y}$

$\rightarrow$ the linear polarisation plane makes an angle $\Phi/2$ with O$\mathbf{x}$

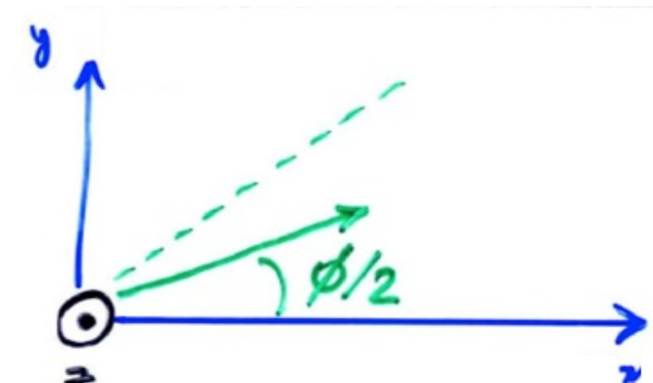

The sum of 2 circular waves of equal amplitude and opposite direction, dephased by Φ, is a linearly polarised wave whose plane of polarisation is at $\Phi/2$ from the phase origin.

<u>NB</u>: 2 opposite circular waves, or 2 $\perp$ linear waves = orthogonal bases on which the decomposition of any polarised (elliptical) wave is unique

→ <u>Elliptical Polarisation</u> = Σ 2 circular waves L & R with $\neq$ amplitudes
= Σ 2 linear waves phase shifed by $\varphi \neq 0, \pm\pi/2$, or non $\perp$
= Σ 1 linear wave & 1 circular wave

Characterised by : direction (L or R)
ellipticity (circular/linear)
orientation of major axis of ellipse

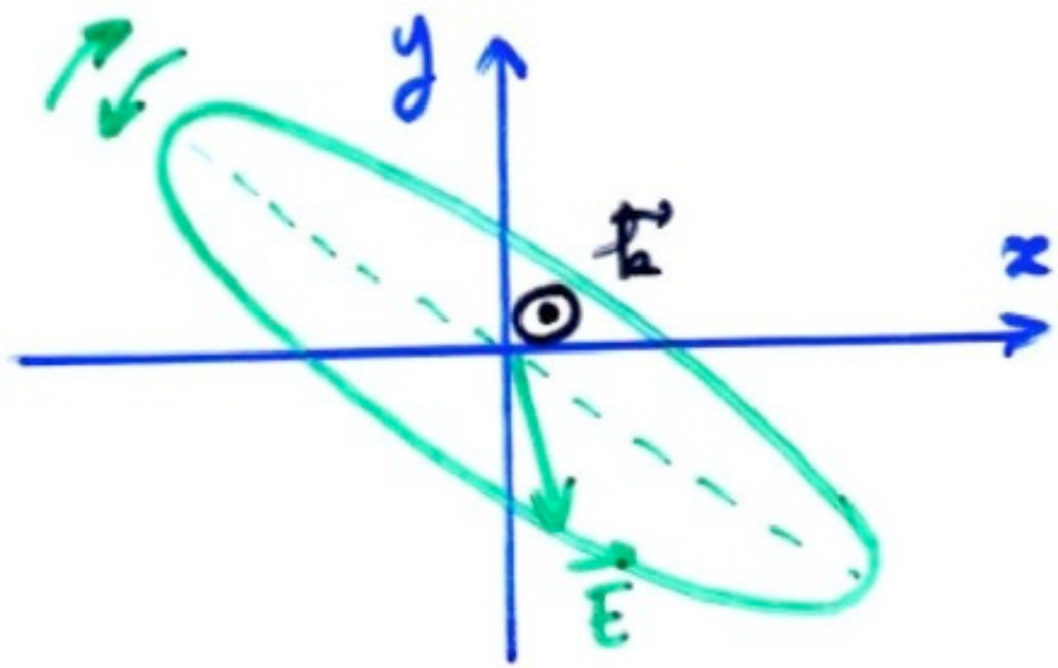

Ex: decameter radio emission from Jupiter ...

→ <u>Stokes Parameters</u> : S, Q, U, V

complete wave polarisation	$U_x = E_1 \exp[i(kz-\omega t)]$ $U_y = E_2 \exp[i(kz-\omega t+\phi)]$
S = total intensity (flux) Q, U : linear polarisation V = circular polarisation (G→V>0 ; D→V<0)	$S = < E_1^2 + E_2^2 >/2Z_o$ $Q = < E_1^2 - E_2^2 >/2Z_o$ $U = < E_1E_2\cos\phi >/Z_o$ $V = < E_1E_2\sin\phi >/Z_o$

For a fully polarised monochromatic wave : $(Q^2+U^2+V^2)^{1/2} = S$

If partially polarised : $(Q^2+U^2+V^2)^{1/2} < S$

$(Q^2 + U^2 + V^2)^{1/2}$ = polarisation fraction of the wave

$S - (Q^2+U^2+V^2)^{1/2}$ = unpolarised fraction of the wave (or randomly polarised)

Polarisation of radiation from an electron in a circular orbit

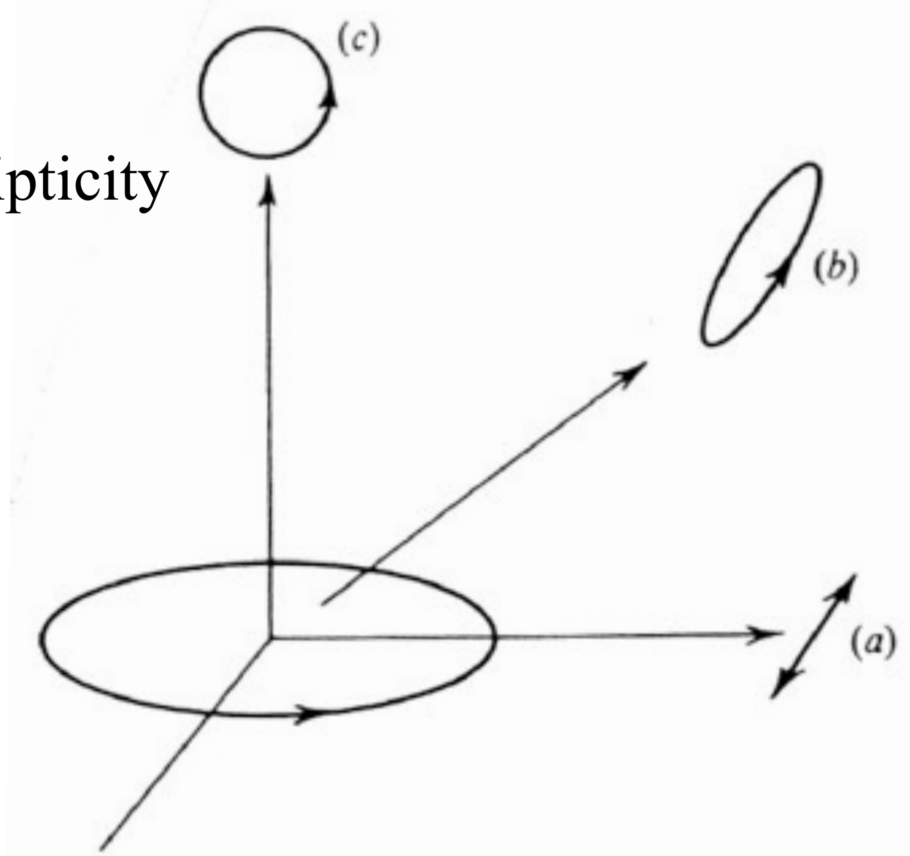

T defined by $V = 2T/(1+T^2)$ characterises ellipticity

$T = \cos\theta \quad = (1 - (1-V^2)^{1/2})/V$

We also use normalised quantities : $q = Q/S$, $u = U/S$, $v = V/S$

$\Rightarrow$ graphic representation on the "Poincare sphere"

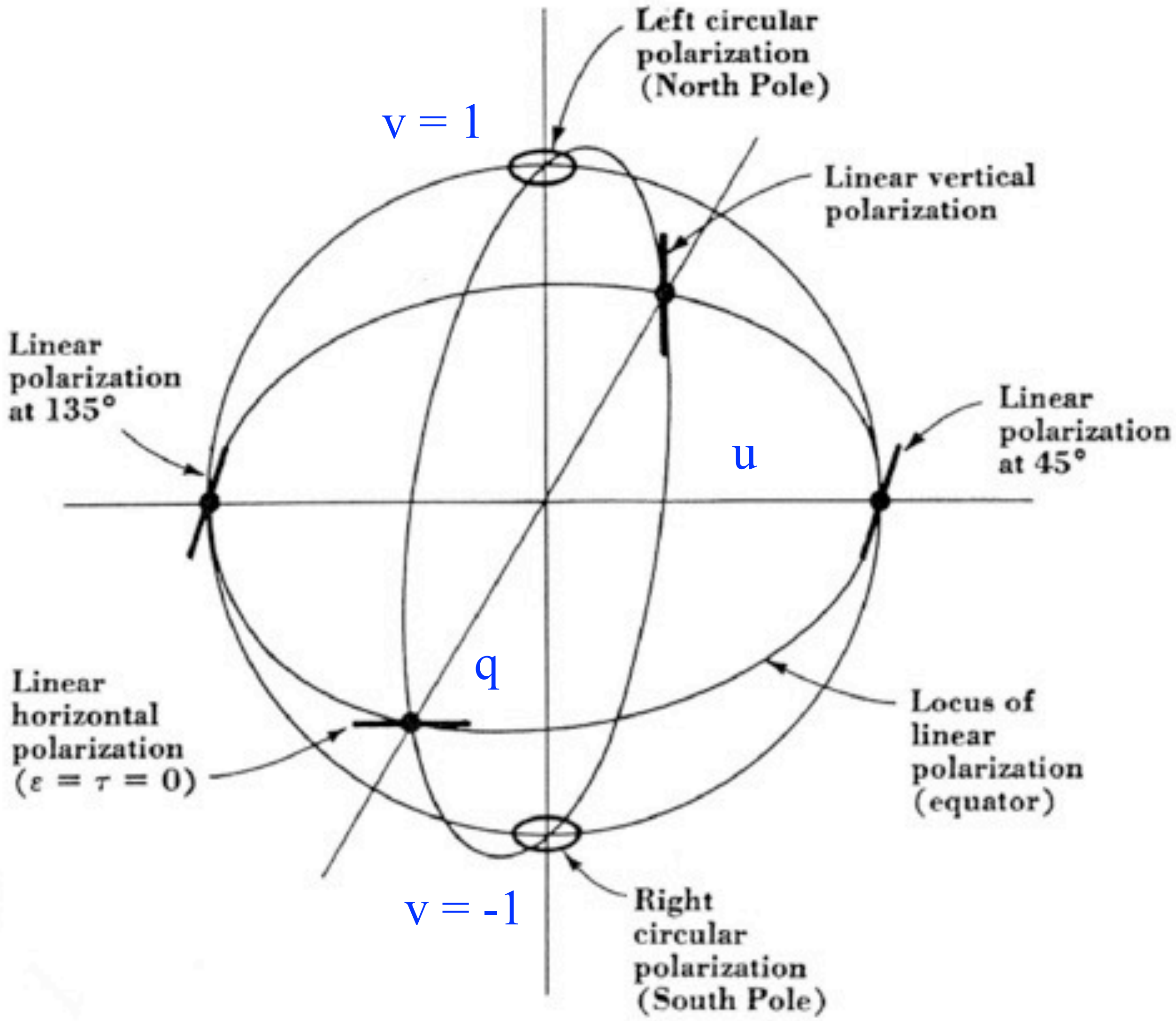

Polarization at cardinal points of Poincaré sphere.

Non-polarised radiation (cosmic thermal radiation, galactic background, etc.)

$\Rightarrow$ the orientation of **E** in the plane $\perp$ **k** varies randomly (as does $|\mathbf{E}|$ or $|\mathbf{E}|^2$)

= succession of wave packets of any and variable amplitude and polarisation

(e.g. elliptical polarisation rapidly fluctuating in direction, ellipticity and orientation)

$\Rightarrow$ Q, U, V = 0 (on average)

- Introduction (history, interest, specific features)
- Waves & Polarisation
- Plasmas & Propagation (cutoff, dispersion, Faraday effect, scintillations)
- Coherent Signal Detection (measurement theory, antenna temperature, calibration, noise)
- Receivers (heterodyne, system temperature, filtering, gain, RFI mitigation)
- Basics of Radio Astronomy Antennas: Single antennas
- Basics of Interferometry and Aperture Synthesis (phased arrays, electronic pointing, imaging, correlation, coherence, VLBI)
- Observation methods
- Large present & future ground-based radio arrays
- Basics of Space radio astronomy

Plasmas

Basic notions :

→ medium containing free charges (e^-, p^+, ions)

→ large-scale global electrical neutrality

→ partial or total ionisation

- radiative $h\nu \geq E_{ionisation}$
- collisional $kT \geq E_{ionisation}$ ($\sim e^2/8\pi\varepsilon_o r_{Bohr} \sim 13.6$ eV for the most external e^-)
- via energetic particle bombardment

→ conductor-like behavior for e.m. waves

→ collective effects = ∃ natural frequencies of the plasma

Plasma frequency (oscillation e^- / ions)	Cyclotron frequency (gyration e^- / **B**)
ω_{pe} (Hz) $= (N_e e^2/\varepsilon_o m_e)^{1/2}$ f_{pe} (Hz) $= (1/2\pi)\,(N_e e^2/\varepsilon_o m_e)^{1/2}$ $= 9\ N_e^{1/2}$ with N_e in m^{-3}	ω_{ce} (Hz) $= (eB/m_e)$ f_{ce} (Hz) $= (1/2\pi)\,(eB/m_e)$ $= 2.8\times10^6$ B with B in Gauss (10^{-4} T)

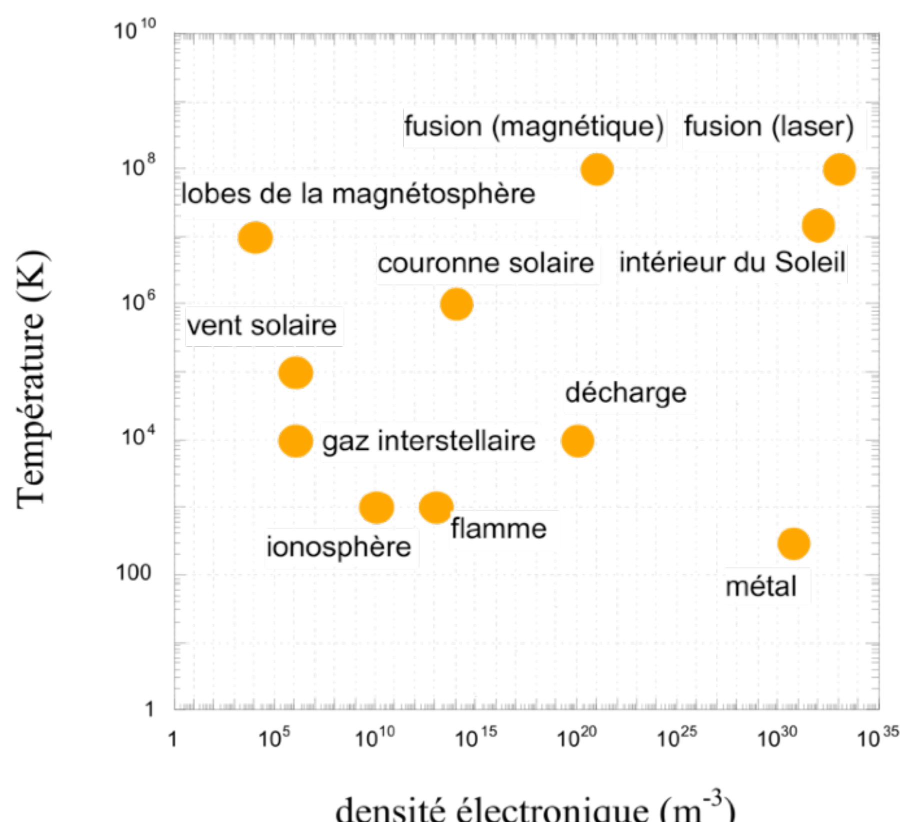

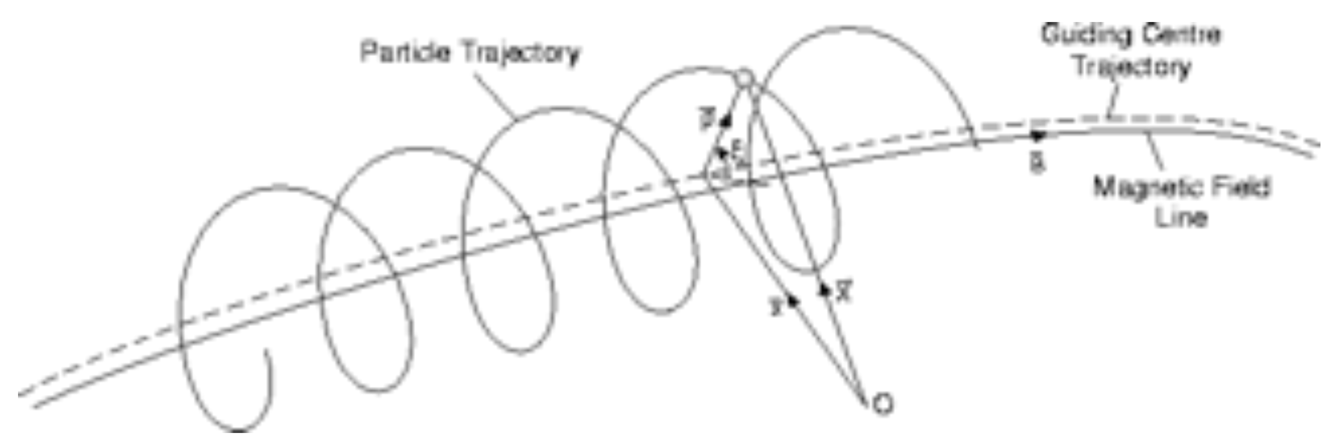

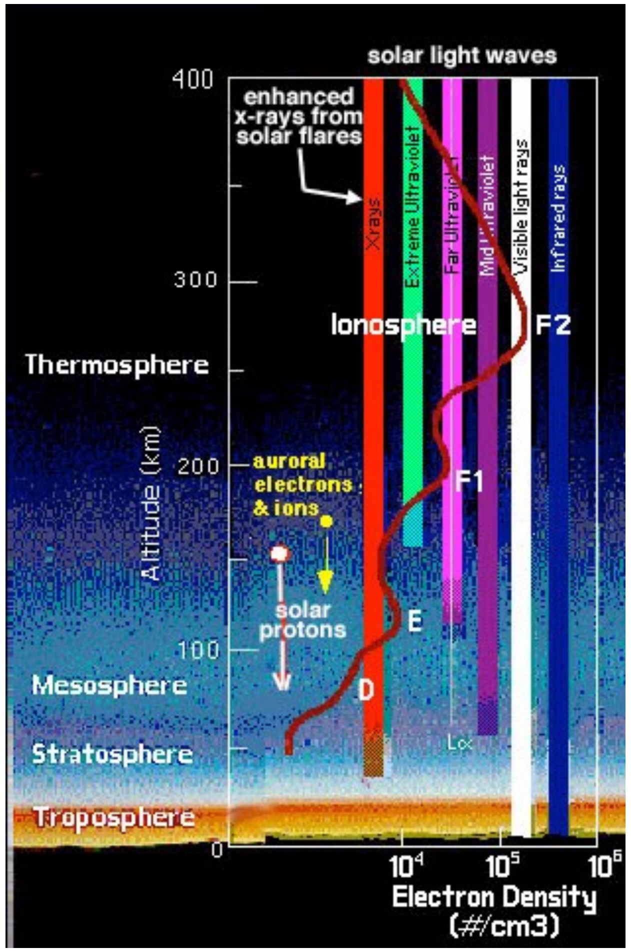

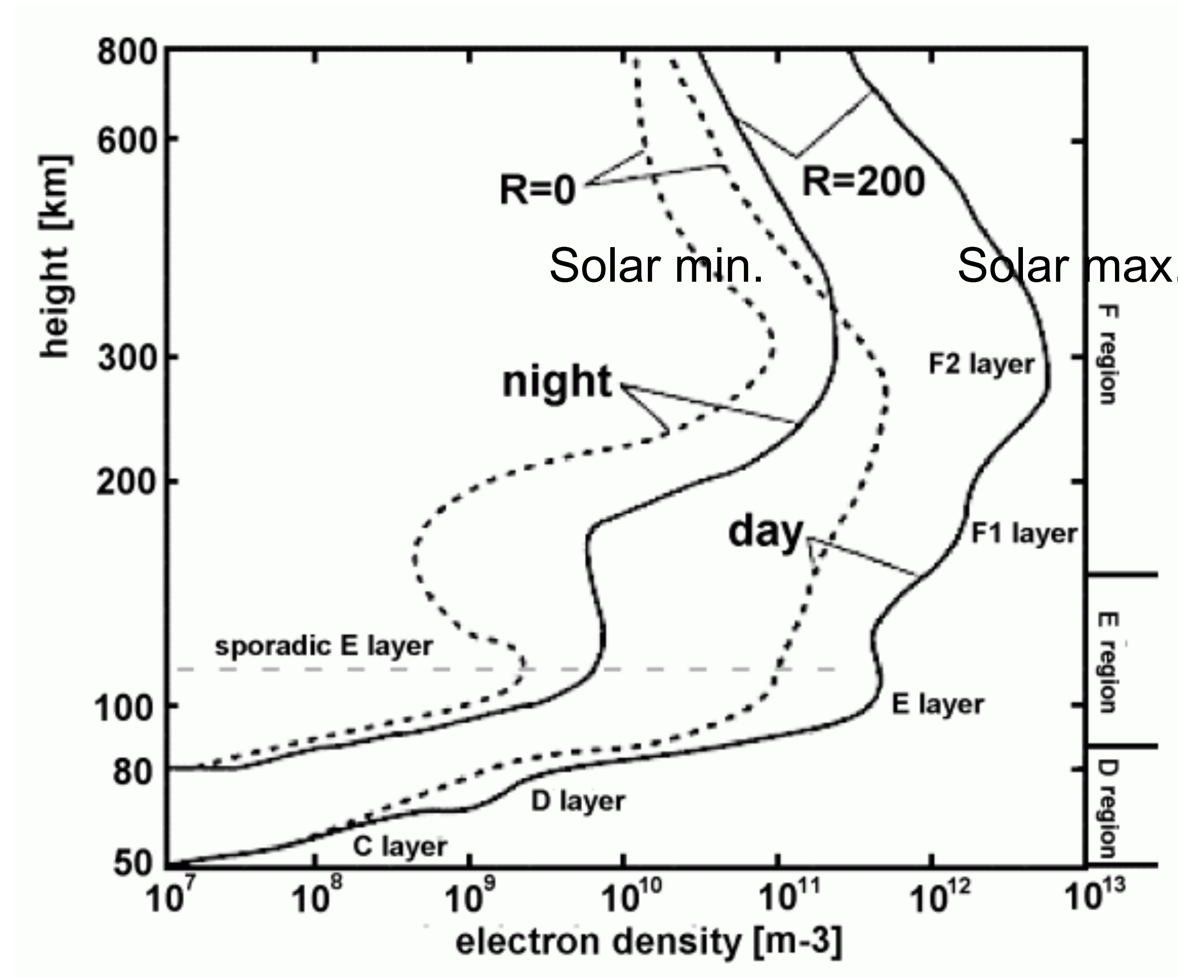

<u>Examples</u>:

- *Earth's ionosphere : $N_o=10^{14}$ cm^{-3}, $N_e/N_o \sim 10^{-9}$ (ionisation via Solar X & UV), $T \sim 900$ K*

  $N_e \approx 10^{5\text{-}6}$ cm^{-3} (day) $\Rightarrow f_{pe} \approx$ 3-10 MHz

  $N_e \approx 5\times10^{4\text{-}5}$ cm^{-3} (night) $\Rightarrow f_{pe} \approx$ 2-6 MHz

  (function of season, latitude, solar activity ...)

- *Solar corona : $N_o \sim N_e \approx 10^{8\text{-}9}$ cm^{-3} (complete ionisation)*

  $\Rightarrow$ $f_{pe} \approx$ 100-300 MHz, $T \sim 10^6$ K

- *Inter Planetary Medium (solar wind at Earth orbit) : $N_o \sim N_e \approx$ 5-10 cm^{-3} (variable)*

  $\Rightarrow$ $f_{pe} \approx$ 20-30 kHz, $T \sim 4\times10^5$ K

- *Inter Stellar Medium : $N_o=1$ cm^{-3}, $N_e \approx 0.03$ cm^{-3}, $N_e/N_o \sim 3\%$ $\Rightarrow$ $f_{pe} \approx 1.5$ kHz*

  (except H_{II} regions near hot stars)

Propagation

Plasma = dispersive medium
Wave/Plasma interactions along wave propagation:

- ➡ Cutoff at f_{pe}
- ➡ Dispersion
- ➡ Faraday Effect
- ➡ Scintillations

Non-magnetised plasma (**B**=**0**)

E.m. wave (**E**, **B**) induces electron motion in the plasma : $\mathbf{F} = -e\,(\mathbf{E} + \mathbf{v} \times \mathbf{B})$

w define the electric displacement : $\mathbf{D} = \varepsilon\,\mathbf{E} = \varepsilon_r\,\varepsilon_o\,\mathbf{E} = \varepsilon_o\,\mathbf{E} + \mathbf{P}$
with ε, ε_r, ε_o = electrical permittivites (total, of matter, of vacuum)
and **P** the polarisation vector (of the medium) hence : $\varepsilon_r = 1 + |\mathbf{P}|/|\varepsilon_o\,\mathbf{E}| = 1 + \chi_e$

similarly : $\mathbf{B} = \mu_r\,\mu_o\,\mathbf{H} = \mu_o\,\mathbf{H} + \mathbf{M}$ (**B** & **H** = magnetic induction & field)
with μ = magnetic permeability and **M** the magnetisation vector

$\Rightarrow$ Maxwell equations for harmonic perturbations **E** & **B** :

rot $\mathbf{H} = \mathbf{j} + \partial\mathbf{D}/\partial t$ $\Rightarrow i\,k\,B / \mu_r\,\mu_o = j + i\,\omega\,\varepsilon_r\,\varepsilon_o\,E$ $\Rightarrow E / B = k / \omega\,\mu_r\,\mu_o\,\varepsilon_r\,\varepsilon_o$

rot $\mathbf{E} = -\partial\mathbf{B}/\partial t$ $\Rightarrow i\,k\,E = i\,\omega\,B$ $\Rightarrow E / B = \omega / k$

d'où $\omega / k = (\varepsilon_o\,\mu_o\,\varepsilon_r\,\mu_r)^{-1/2} = c / (\varepsilon_r\,\mu_r)^{1/2} = c / n = v_\phi$

(v_ϕ = propagation velocity of an e.m. field disturbance of frequency $\omega/2\pi$ and wave vector **k**)

and $n = (\varepsilon_r\,\mu_r)^{1/2}$ refraction index ($\mu_r^{1/2} = 1$ for a non-magnetised medium)

Calculation of **P** :

→ oscillatory motion of plasma electrons (ions assumed to be immobile, $|\mathbf{B}| \sim |\mathbf{E}/c| << |\mathbf{E}|$)

$$m_e\, d^2z/dt^2 = -e\, E = -e\, E_o \cos \omega t = -\, m_e\, \omega^2\, z \quad \Rightarrow \quad z = e\, E / m_e\, \omega^2$$

→ the dipole moment of an (e^- - ion) pair separated by **z** is $(-e.\mathbf{z})$ thus

$$\mathbf{P} = -N_e\, e\, \mathbf{z} = -\,(N_e\, e^2 / m_e\, \omega^2)\, \mathbf{E} \quad \Rightarrow \varepsilon_r = 1 + |\mathbf{P}|/|\varepsilon_o\, \mathbf{E}| = 1 - N_e\, e^2 / \varepsilon_o\, m_e\, \omega^2 = 1 - \omega_{pe}^2/\omega^2$$

hence
$$\boxed{\begin{array}{l} n = (1 - \omega_{pe}^2/\omega^2)^{1/2} = (1 - f_{pe}^2/f^2)^{1/2} < 1 \\ v_\phi = \omega / k = c / n \quad > c \end{array}}$$

(but "non-physical" speed, since a monochromatic wave of constant amplitude carries no information)

the transport speed of energy/information is $v_g = d\omega/dk$

we have : $c^2\, k^2 = \omega^2\, n^2 = \omega^2 - \omega_{pe}^2 \Rightarrow 2\, c^2\, k\, dk/d\omega = 2\omega$

$$\Rightarrow \quad \boxed{v_g = d\omega/dk = c^2\, k / \omega = c\, n < c}$$

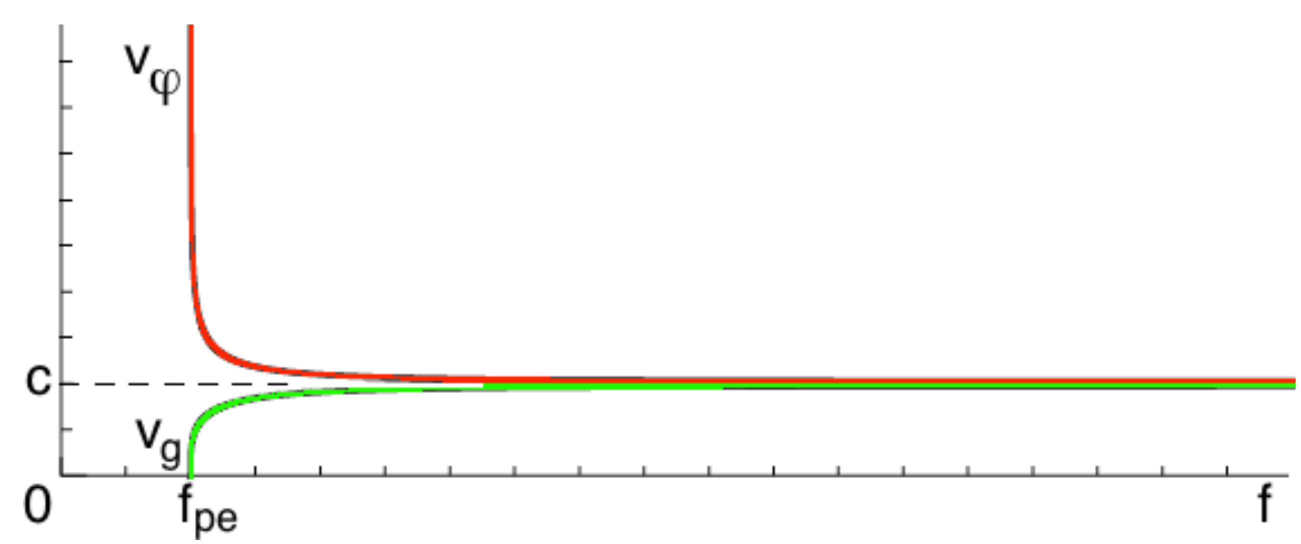

NB: $v_g\, v_\phi = c^2$

• Wave propagation in non-magnetised plasma : LF cutoff at f_{pe}

plasma restoring force   *wave excitation*

$$\frac{d^2z}{dt} + \omega_{pe}^2 z = \frac{-eE_0}{m_e}\cos\omega t$$

$$z(t) = \frac{eE_0}{m_e(\omega^2 - \omega_{pe}^2)}\cos\omega t$$

Incident wave ⇒ setting e^- in motion :

→ 3 propagation regimes :

(1) $f >> f_{pe}$

⇒ the e.m. wave induces forced oscillations at f of the plasma e^- (HF therefore low amplitude)

$n \approx 1$ ⇒ free propagation at $v_g = c\, n \approx c$ ⇒ the medium is ~transparent

(2) $f \approx f_{pe}$

⇒ e.m. wave induces resonant oscillations at f_{pe} (large amplitude) + energy dissipation through collisions

$n=0$ ⇒ absorbing medium *[a fraction of the energy is re emitted at ~f_{pe} as e.s. waves in the plasma]*

(3) $f \lesssim f_{pe}$

⇒ the e.m. wave induces non-resonant LF oscillations, but with amplitude > case (1)

n imaginary ⇒ $|E| \propto \exp[i(kz - \omega t)] \propto \exp[ik(z - ct/n)] \propto \exp(-\alpha)$ with α real

⇒ damped wave beyond a surface layer (skin depth) + re-emission at f by the e^- having not sustained any collision

⇒ reflecting medium (+ absorbing)

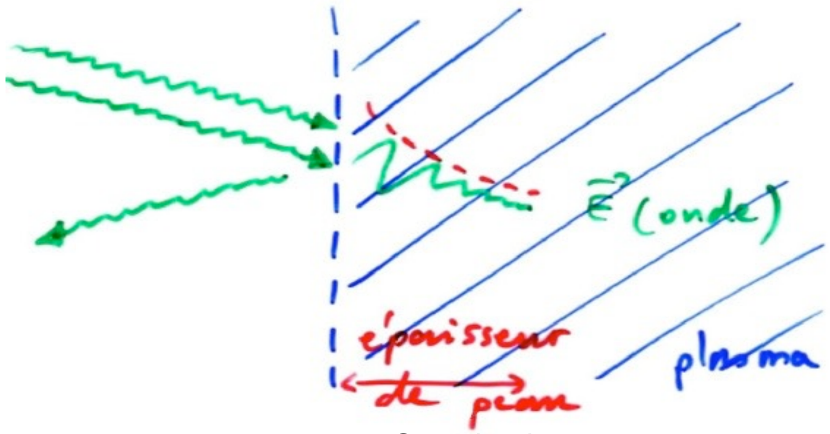

Skin depth

Example: Earth ionosphere = high-pass filter *sky ←→ ground*

Ionospheric sounding: exploiting the cut-off frequency $f_c = f_{pe}$ at ~normal incidence

→ sending variable-frequency radio radiation to the zenith,
and measuring the delay between transmission and reception $\Delta t = t_R - t_E$

As f ↑, the radiation penetrates higher and Δt ↑
⇒ we deduce $N_e(z) = f_{pe}^2/81 = f^2/81$ *with* $z = c\,\Delta t / 2$

The latest reflected frequency gives $N_{e\text{-}max}(z_{max})$

For the profile at $z>z_{max}$ *the same procedure is followed from an orbiting satellite*

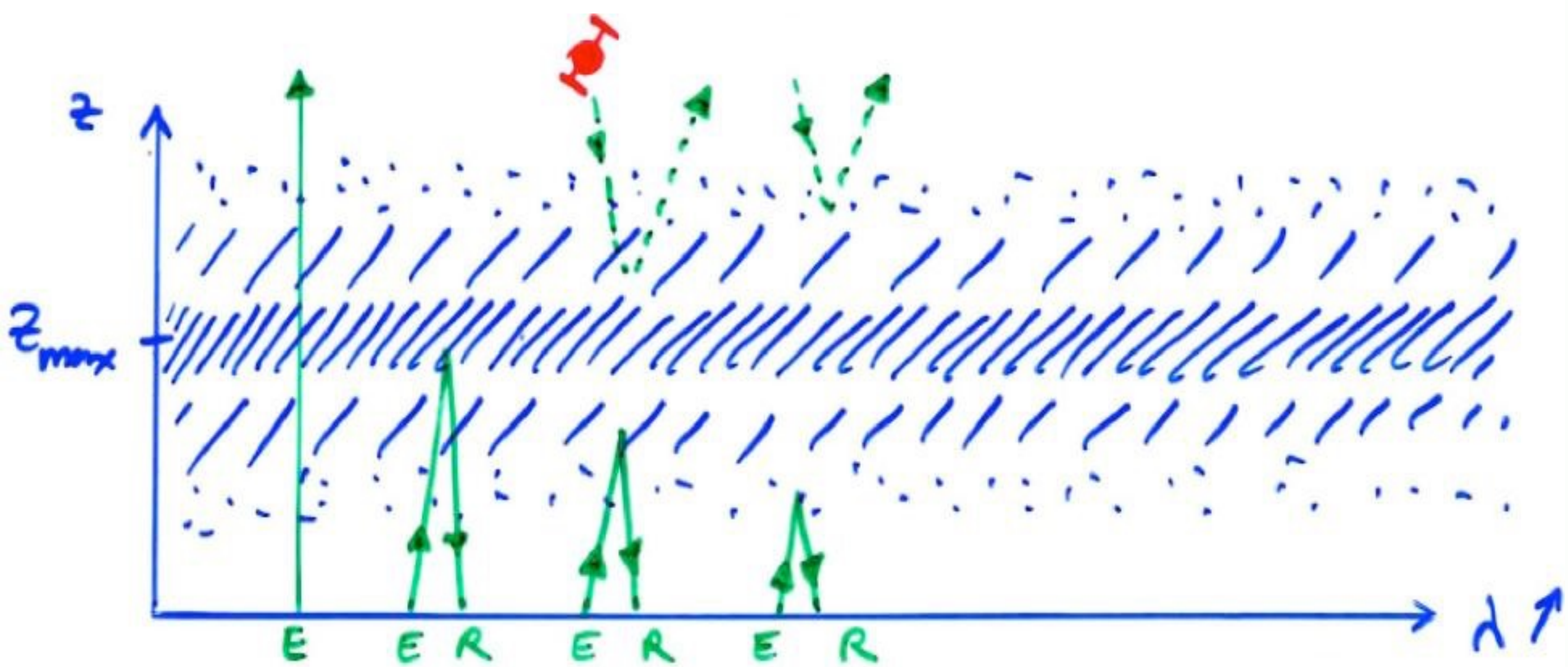

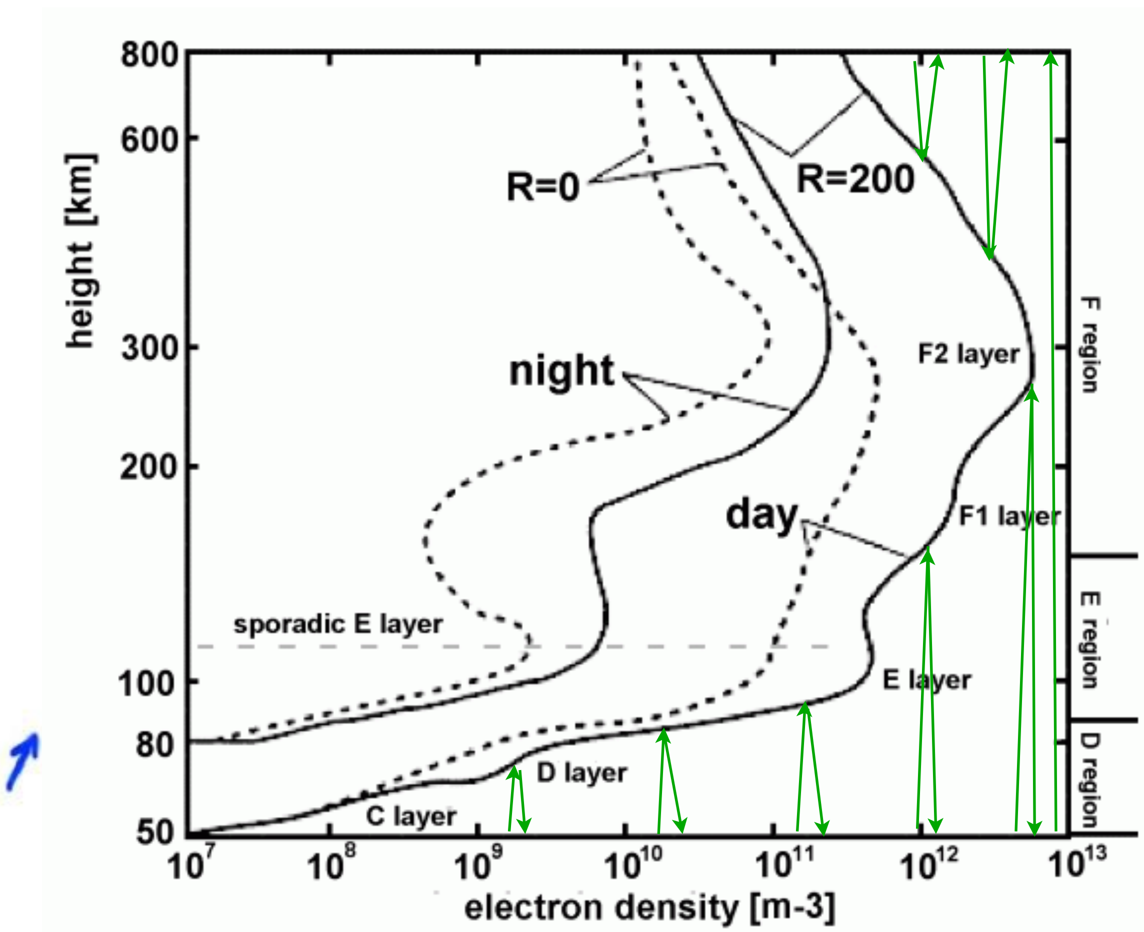

Example: *Solar wind* : N_e = 5-10 cm^{-3} / L^2
(with L in UA) → f_{pe} = 20-30 kHz / L

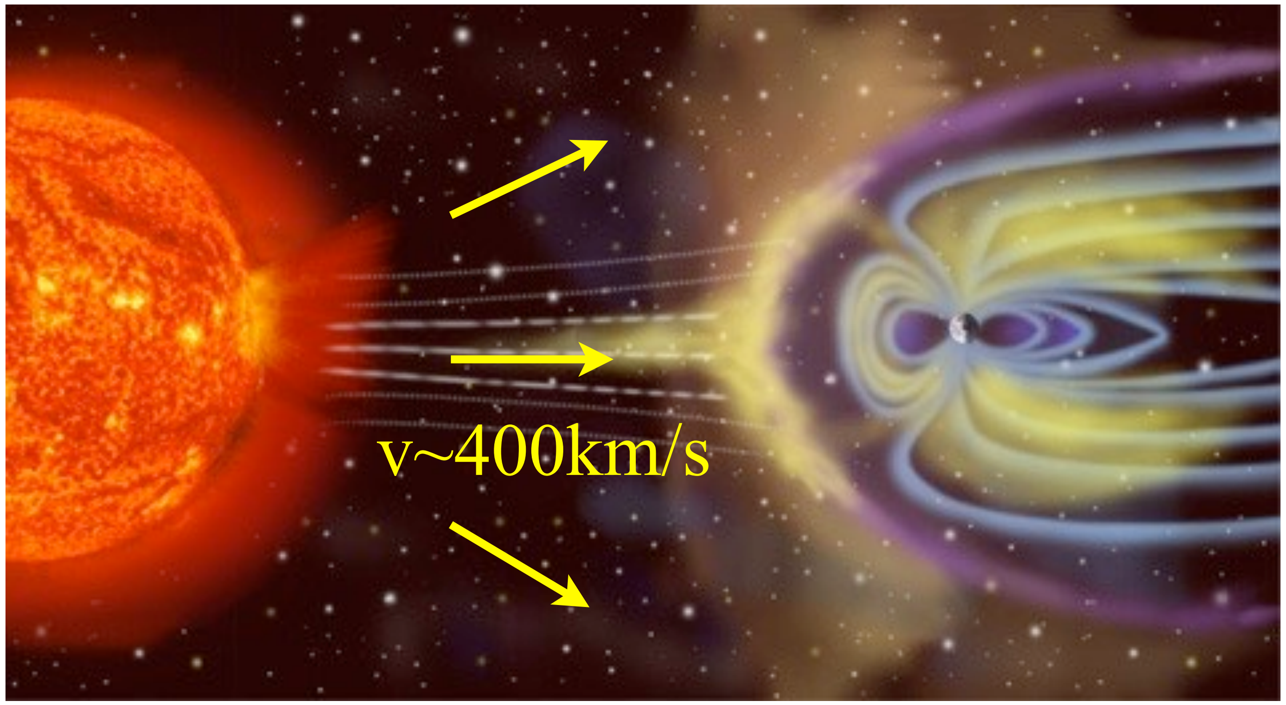

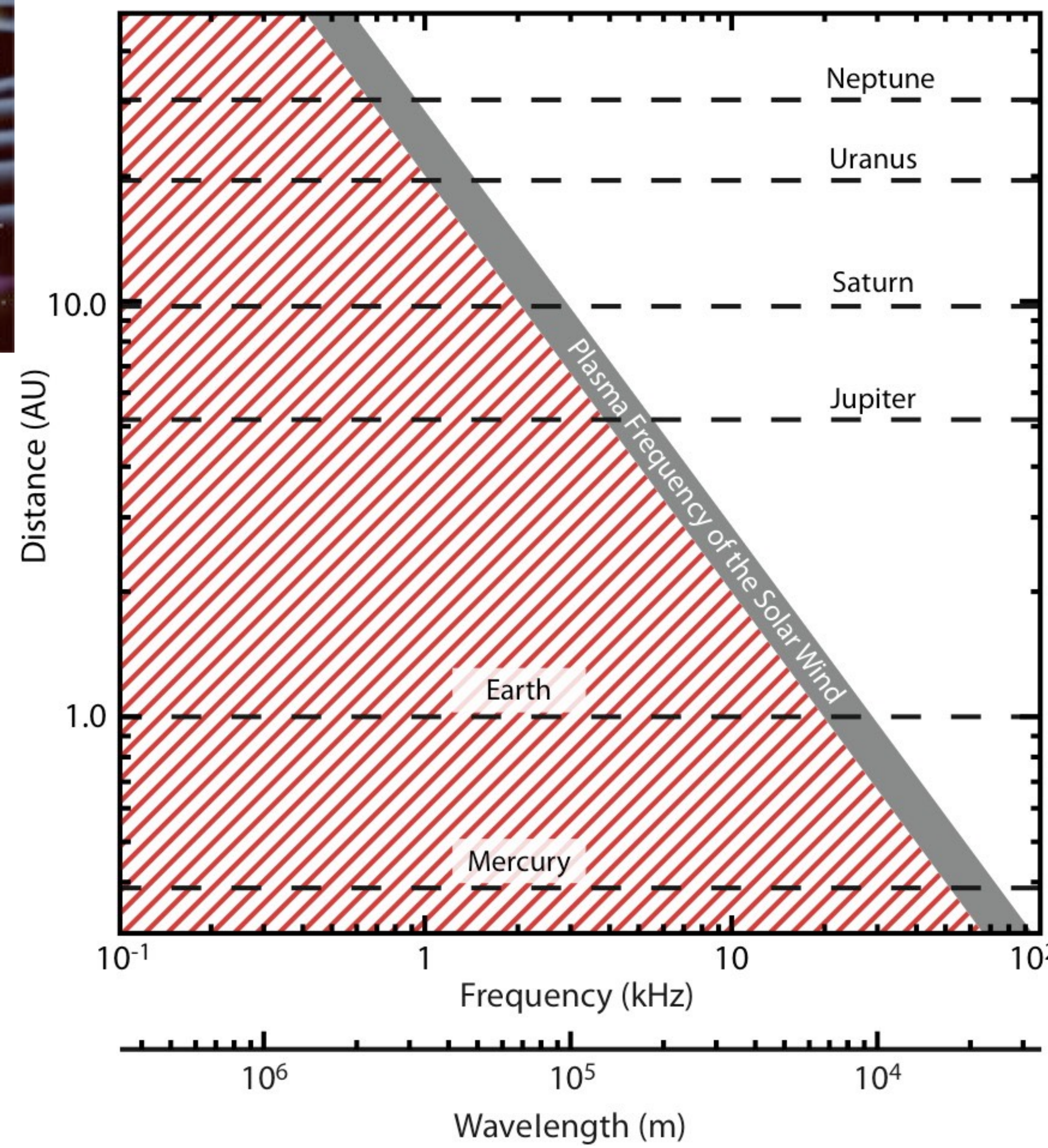

→ Cutoff frequency f_c for an angle of incidence θ / normal to the plasma layer :

Total reflection for $1.\sin\theta = n.\sin(\pi/2)$

⇒ $n^2 = 1 - f_{pe}^2/f_c^2 = \sin^2\theta$

⇒ $f_c = f_{pe} / \cos\theta$

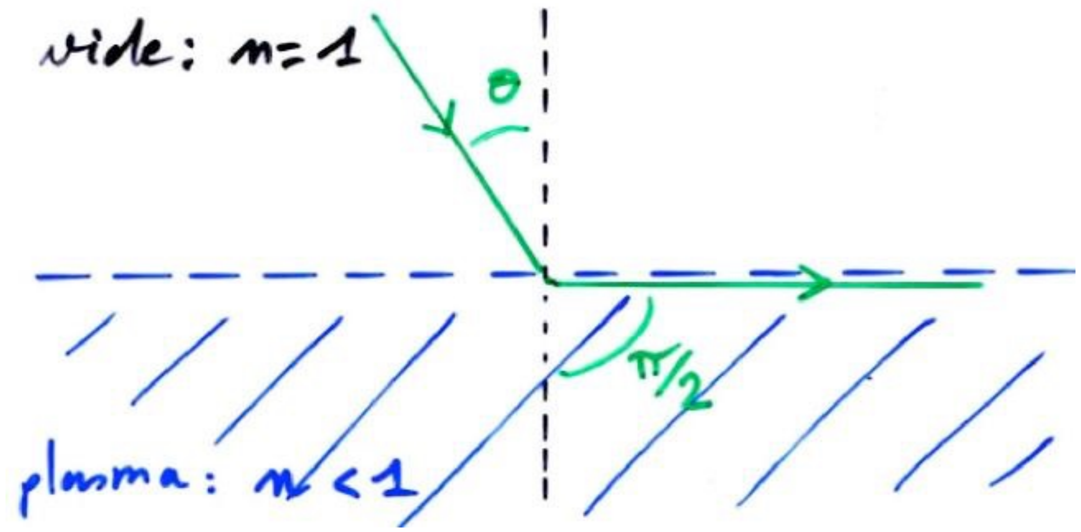

⇒ possibility of terrestrial radio-communications on "short waves" ($f \leq 30$ MHz) : propagation beyond the horizon by reflection under the ionosphere for $f < f_{pe}/\cos\theta$

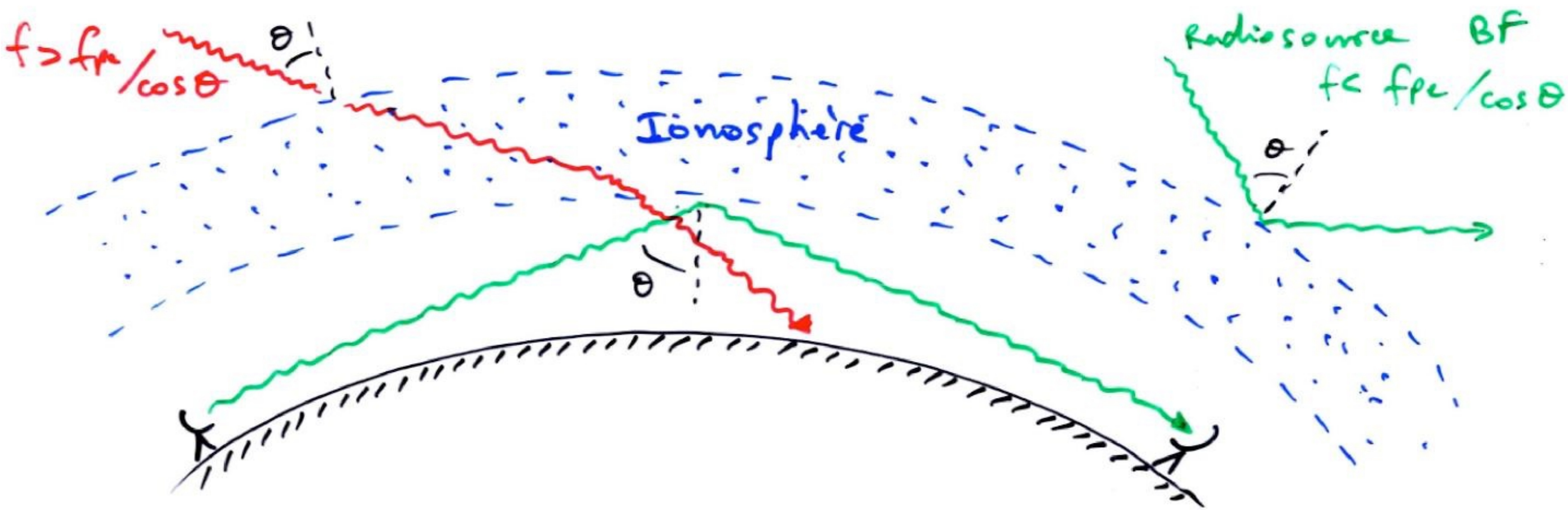

Example: *Mirror → metal's free e^- reflects incident e.m. waves.*

$r_{atom} \approx 1$ Å & 1 free e^- libre pooled per atom

$\Rightarrow N_e \approx 1/(2\text{ Å})^3 \approx 10^{29}\ m^{-3}$

$\Rightarrow f_{pe} \approx 3\times10^{15}$ Hz $\lambda \approx 100$ nm (UV)

→ a metallic mirror reflects visible light but not X-rays

(except for specular reflection, $\theta \approx 90° \Rightarrow f_c = f_{pe} / \cos\theta \uparrow\uparrow$)

- Wave propagation in a non-magnetised plasma : Dispersion

→ $v_g = d\omega/dk = c^2 k / \omega = c\, n \approx c\,(1 - \omega_{pe}^2/ 2\omega^2)$ for $\omega_{pe}^2 << \omega^2$
(typically $f \geq 100$ kHz in natural plasmas)

$v_g = v_g(\omega) \Rightarrow$ plasma is a dispersive medium for radio waves

→ For a broad-spectrum radiosource at distance L from the observer :
$t(\omega) = L / v_g(\omega) \approx (1 + \omega_{pe}^2/ 2\omega^2)\, L / c$ assuming that $\omega_{pe} = C^t$ along the path L
$\Rightarrow \quad \Delta t(\omega) = t(\omega) - t(\omega\rightarrow\infty) \approx \omega_{pe}^2\, L / 2\omega^2 c = N_e\, L\, e^2 / 2\varepsilon_o m_e \omega^2 c$

or more strictly, if $N_e \neq C^{te}$ along the path L
$\Delta t(\omega) \approx \left(\int_L N_e dL\right) e^2 / 2\varepsilon_o m_e \omega^2 c = \langle N_e L \rangle\, e^2 / 2\varepsilon_o m_e \omega^2 c$

We call « Dispersion Measure" [DM] the quantity $\int_L N_e dL$ integrated along the wave path

Hence : $\boxed{\begin{array}{ccc} \Delta t(f) \approx & 4.15\times10^3 \; [DM] & f^{-2} \\ \Downarrow & \Downarrow & \Downarrow \\ [\text{sec}] & [\text{pc.cm}^{-3}] & [\text{MHz}] \end{array}}$

$\Delta t(f_1) - \Delta t(f_2) \approx 4.15\times10^3\; [DM]\; (f_1^{-2} - f_2^{-2})$

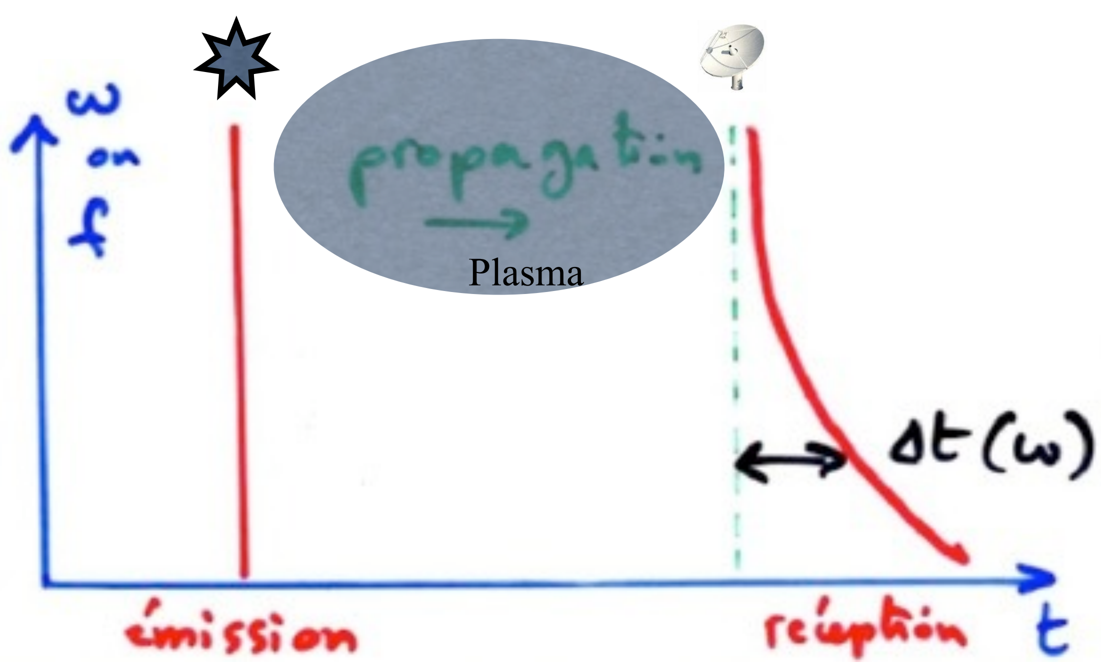

Fig. 3.1. Frequency dispersion in pulse arrival time for PSR 1641−45, recorded in 64 adjacent frequency channels, each 5 MHz wide, centred on 1540 MHz.

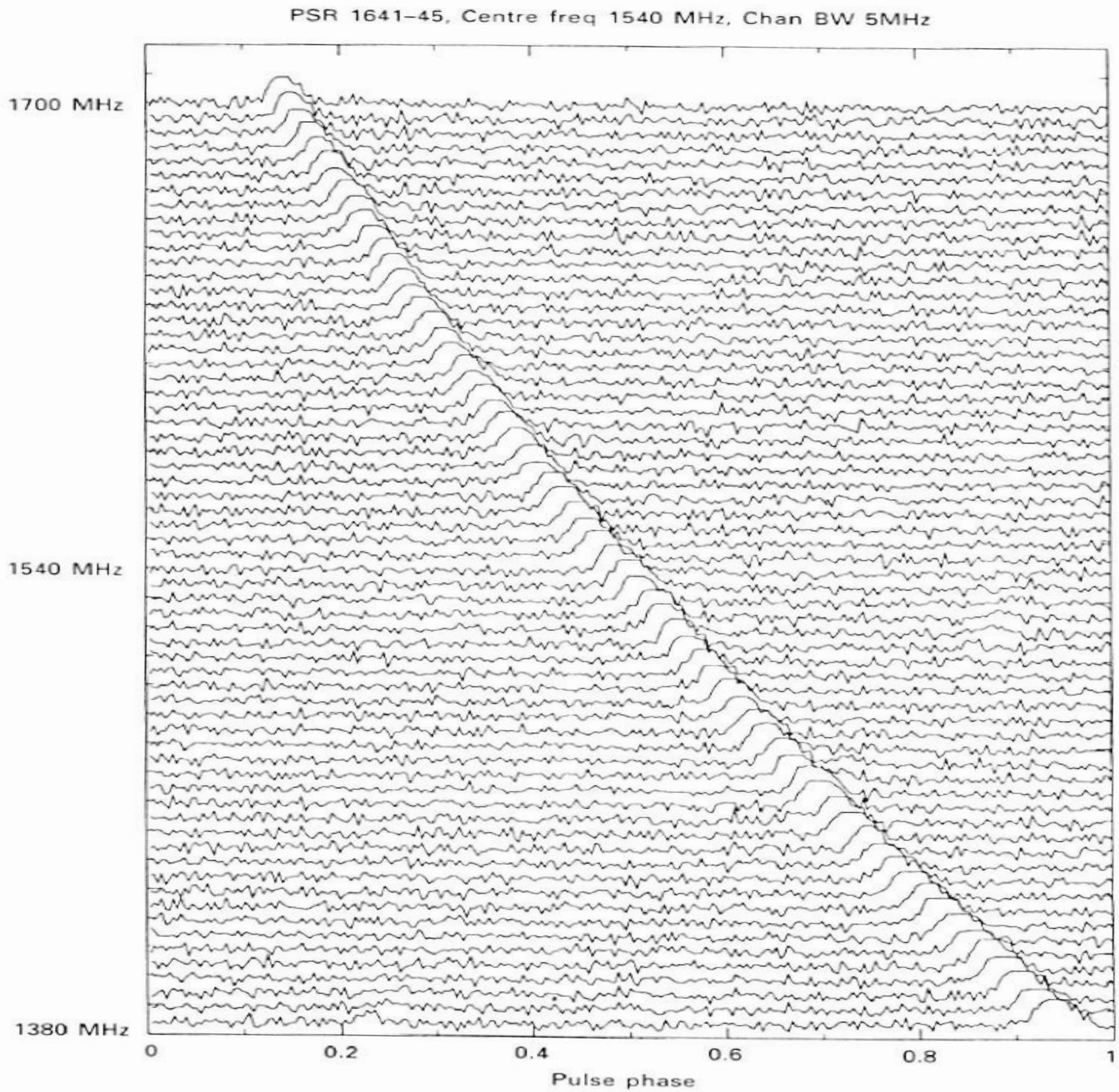

→ Measuring $\Delta t(f)$ gives information on N_e and L of the traversed plasma.

• Wave propagation in a magnetised plasma : Faraday effect

→ we show for a magnetised plasma (with collisions = general case) that the refraction index writes (Appleton-Hartree equation) :

$$n^2 = 1 - X / \{1 - iZ - \tfrac{1}{2}Y_T/(1-X-iZ) \pm [\tfrac{1}{4}Y_T^4/(1-X-iZ) + Y_L^2]^{1/2} \}$$

with $X = f_{pe}^2/f^2$

$Y_T = (f_{ce}/f)\sin\theta$ & $Y_L = (f_{ce}/f)\cos\theta$ où $\theta = (\mathbf{k},\mathbf{B})$

$Z = f_{coll}/2\pi f$ where $f_{coll} \propto N_e T^{-3/2}$ for collisions e^--ions

$\Rightarrow n = \mu - i\,\chi$ où $\mu = \mathrm{Re}(n)$ characterises refraction

and $\chi = \mathrm{Im}(n)$ characterises damping/amplification

If we neglect collisions, i.e. $f_{coll} << f_{pe}, f_{ce}, f \Rightarrow Z \approx 0$ and consider propagation quasi-// **B** (actually not strictly ⊥ **B**) $\Rightarrow Y_T^2/2 << Y_L$

$$n^2 = 1 - X / (1 - \tfrac{1}{2}Y_T \pm Y_L) = 1 - \omega_{pe}^2 / (\omega(\omega - \tfrac{1}{2}\omega_{ce}\sin\theta \pm \omega_{ce}\cos\theta))$$

$$\Rightarrow n_\pm = [1 - \omega_{pe}^2 / (\omega(\omega - \tfrac{1}{2}\omega_{ce}\sin\theta \pm \omega_{ce}\cos\theta))]^{1/2}$$

$n_+ \rightarrow$ LHC wave propagation, $n_- \rightarrow$ RHC wave propagation

(demonstration by considering ***E*** *rotating, L or R, and recalculating* ***P****,* ε_r*,* $n_\pm$*)*

*NB: **B** introduces anisotropy that makes the plasma birefringent*

(≡ crystal where the anisotropy comes from the crystalline structure)

$\rightarrow v_{\phi\pm} = c / n_\pm$

$\Rightarrow \Delta v_\phi = |v_{\phi+} - v_{\phi-}| = c\ |1/n_+ - 1/n_-|$

$\approx c\ \omega_{pe}^2 / 2\omega\ |1/(\omega - \frac{1}{2}\omega_{ce}\sin\theta + \omega_{ce}\cos\theta) - 1/(\omega - \frac{1}{2}\omega_{ce}\sin\theta - \omega_{ce}\cos\theta)|$

$= c\ \omega_{pe}^2 \omega_{ce}\cos\theta / \omega[(\omega - \frac{1}{2}\omega_{ce}\sin\theta)^2 - (\omega_{ce}\cos\theta)^2]$

thus for $\omega >> \omega_{pe}, \omega_{ce}$ $\quad \Delta v_\phi \approx c\ \omega_{pe}^2 \omega_{ce}\cos\theta / \omega^3 = c\ \omega_{pe}^2 \omega_{ce//} / \omega^3$

For 2 circular waves (L & R), initially in phase ($\propto \exp[i(kz-\omega t)] \propto \exp[ik(z-v_\phi t)]$)

$\Rightarrow \Delta\phi(t) = k\ \Delta v_\phi\ t = 2\pi/\lambda\ \ c\omega_{pe}^2\omega_{ce}/\omega^3\ \ t = e^3\ \lambda^2\ B_{//}\ N_e\ t / (4\pi^2 c^2\ m_e^2\ \varepsilon_o)$

with $t \approx L/c$ for a source at distance L

$\rightarrow$ the Faraday Effect is the rotation of the linear polarisation plane of a wave propagating parallel to **B** in a magnetised plasma. The polarisation plane rotates from :

$\theta\ (\mathrm{rad}) = \Delta\phi/2 = e^3\ \lambda^2 < N_e\ L\ B_{//} > / (8\pi^2 c^3\ m_e^2\ \varepsilon_o) = e^3\ \lambda^2 < [\mathrm{DM}]\ B_{//} > / (8\pi^2 c^3\ m_e^2\ \varepsilon_o)$

$\theta\ (\mathrm{rad}) = \mathrm{RM}\ \lambda^2$ with λ in m and RM = Rotation Measure = $0.8 \int_L \underbrace{N_e}_{\mathrm{cm}^{-3}}\ \underbrace{B_{//}}_{\mu\mathrm{G}}\ \underbrace{dL}_{\mathrm{pc}}$

or $\boxed{\underbrace{\theta}_{[°]} = 4\times10^{12} < \underbrace{[\mathrm{DM}]}_{[\mathrm{pc.cm}^{-3}]}\ \underbrace{B_{//}}_{[\mathrm{G}]} > \underbrace{f^{-2}}_{[\mathrm{MHz}]}}$

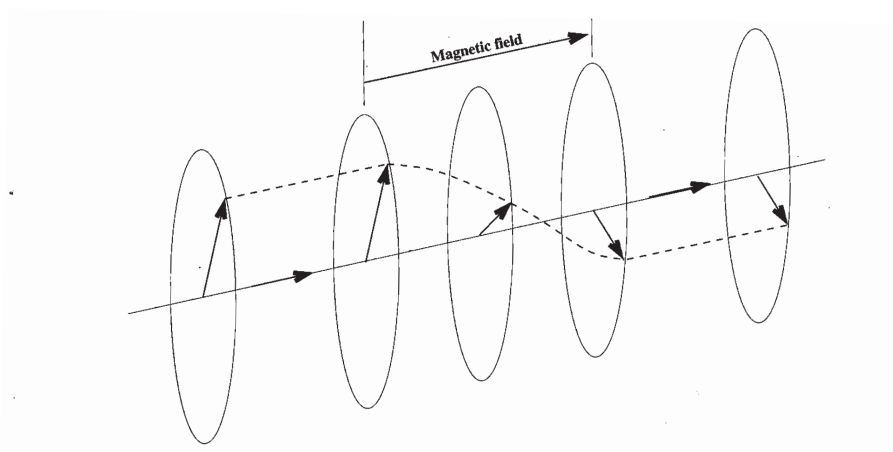

$\Delta\theta = \theta(f_1) - \theta(f_2) \approx 4\times10^{12}\ [\mathrm{DM}]\ B_{//}\ (f_1^{-2} - f_2^{-2})$

Example : *Faraday fringes are observed in the dynamic spectrum of Jupiter's decametric emission (observed with a linear antenna).*
Fringe separation at 27 MHz is ~0.15 MHz → origin ?

$$\Delta\theta\ (°) = d\theta/df.\Delta f = 4\times10^{12}\ [DM]\ B_{//}\ 2\ f^{-3}\ \Delta f \quad \Rightarrow \quad \Delta f = \Delta\theta\ f^{3} / (8\times10^{12}\ N_e\ L\ B_{//})$$

$\Delta\theta$ between 2 consecutive fringes (bright or dark) = 180°

- *Io's plasma torus : N_e~1000 cm^{-3}, L~2$R_{Jupiter}$ (1R_J =7×10^4 km), $B_{//}$ ~ 0.003 G*
  $\Rightarrow \Delta f \approx 31$ MHz
- *IPM : N_e~5 cm^{-3}, L~5 UA (1 UA =1.5×10^8 km), $B_{//}$ ~ 3 nT*
  $\Rightarrow \Delta f \approx 118$ MHz
- *Earth's ionosphere : N_e~5×10^5 cm^{-3}, L~500 km, $B_{//}$ ~ 0.3 G*
  $\Rightarrow \Delta f \approx 0.18$ MHz

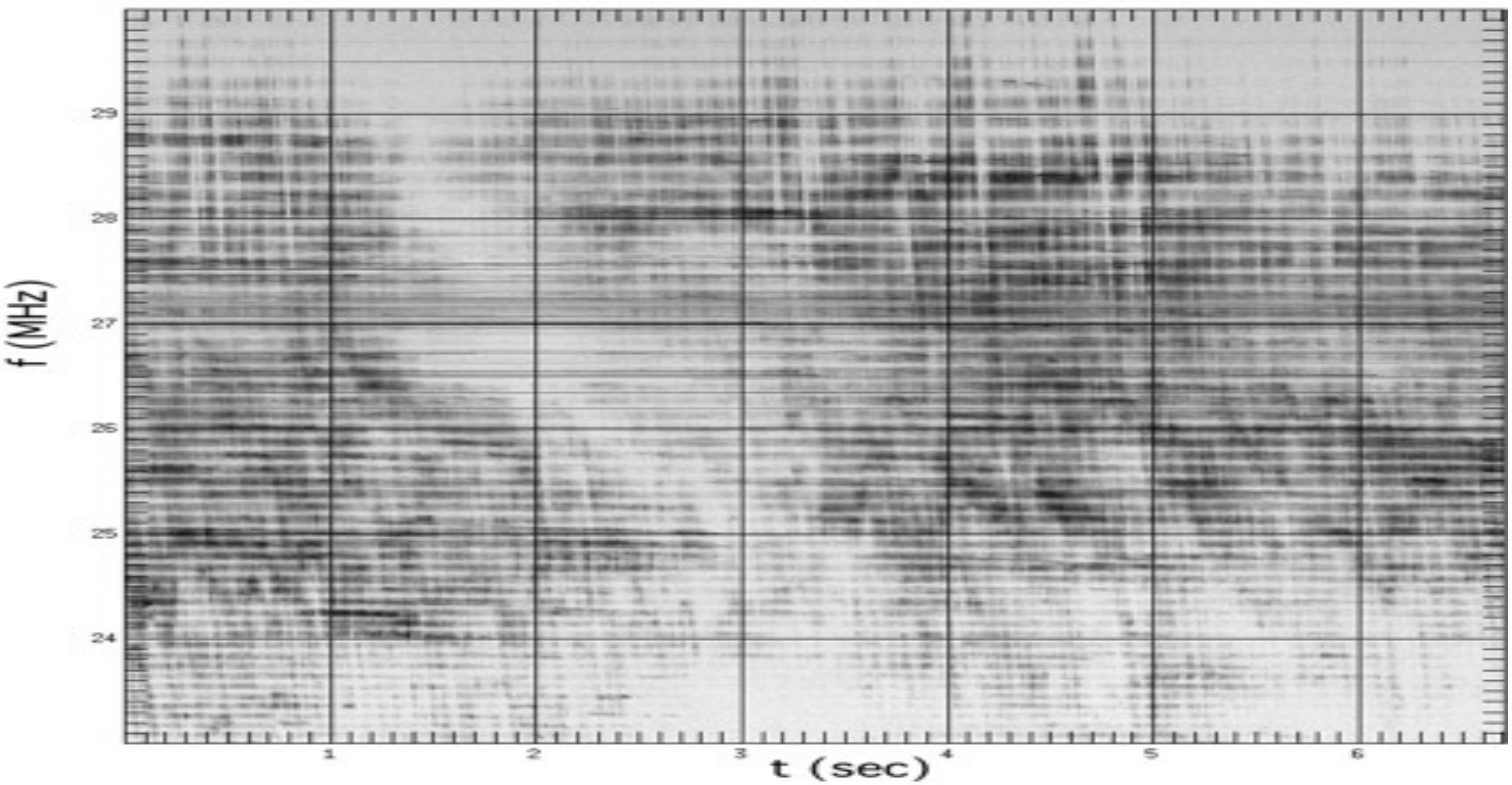

Fig. 8.2. The positions of the 316 pulsars in the uniform sample, projected onto the plane of the Galaxy. The galactic centre is at the centre of the diagram. The pulsars are clustered round the Sun, at a distance of about 8 kpc from the centre.

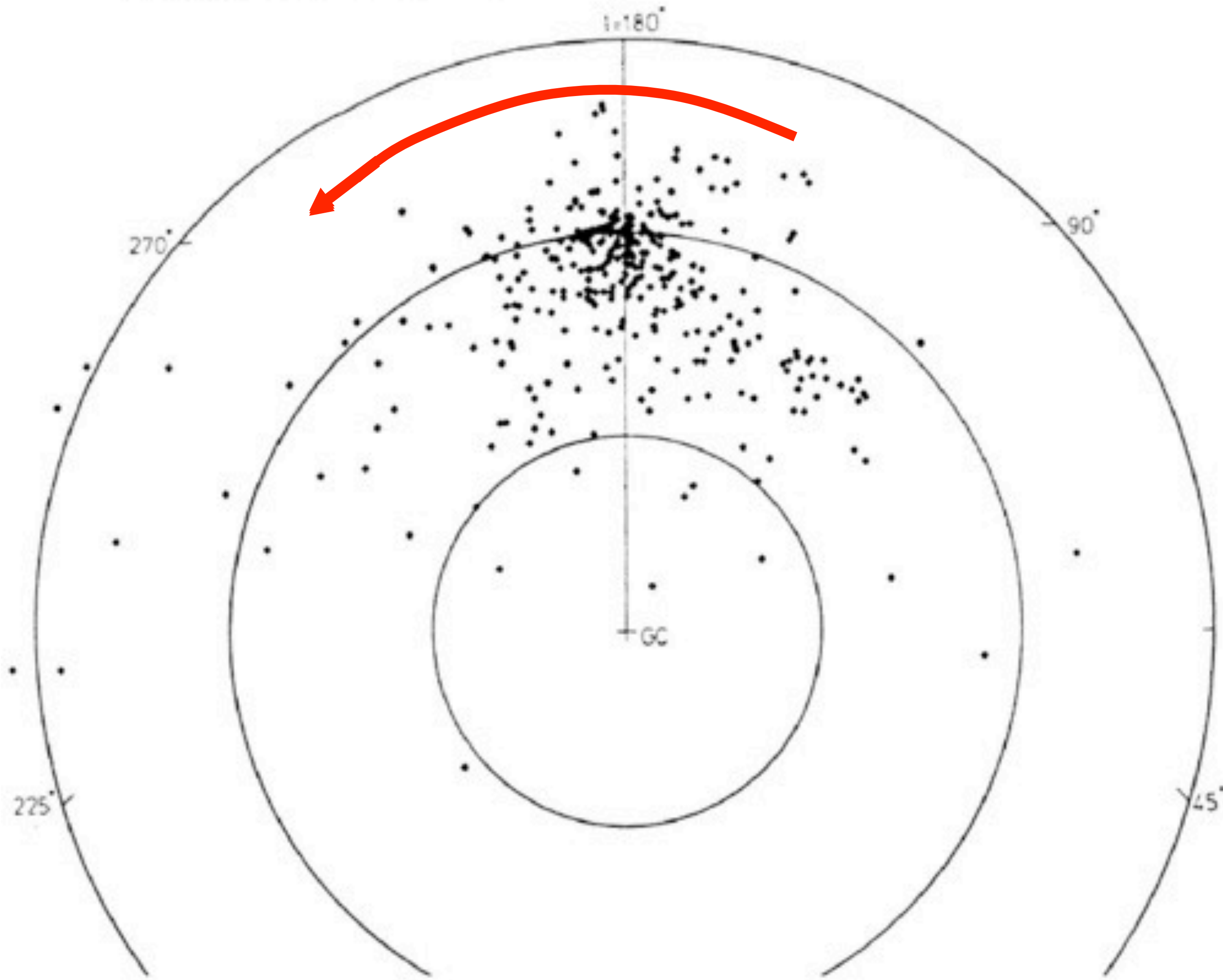

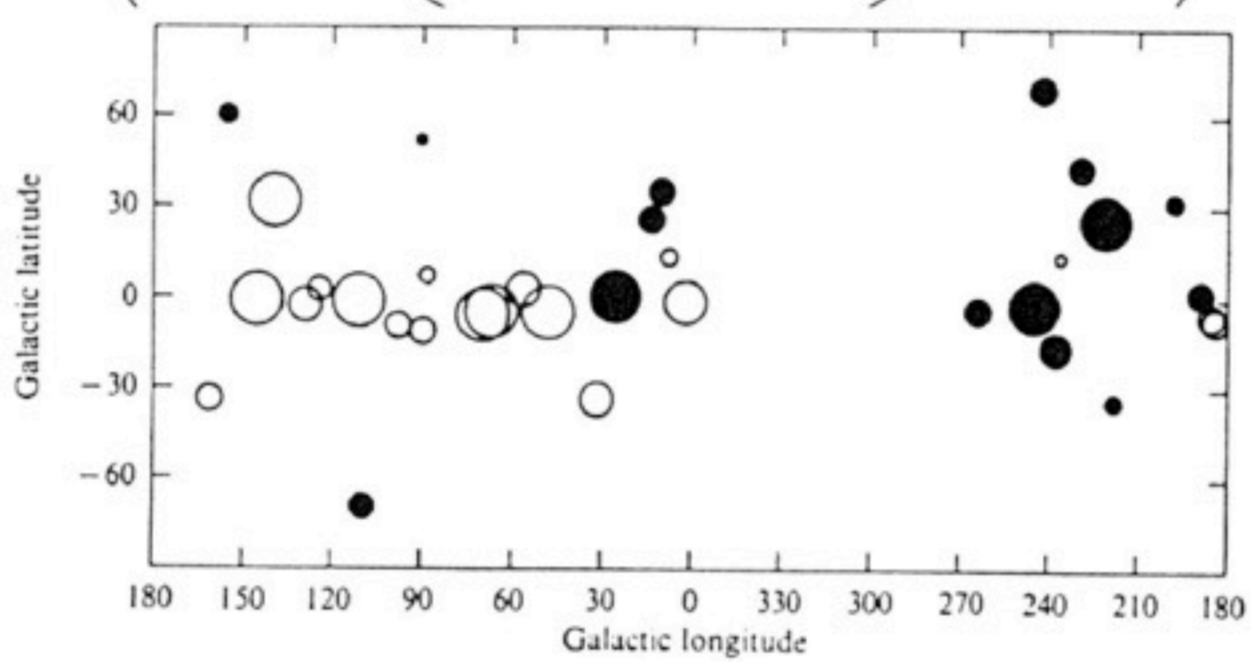

Direction (& amplitude) of B_z in the galactic plane

• Wave propagation in an inhomogeneous plasma : IP & IS scintillations

$n^2 = 1 - f_{pe}^2/f^2 = 1 - N_e e^2/4\pi^2\varepsilon_o m_e f^2$

but the IPM and ISM are in fact inhomogeneous : $N_e = \langle N_e \rangle + \delta N_e$

$\Rightarrow 2n\, \delta n = (-e^2/4\pi^2\varepsilon_o m_e f^2)\, \delta N_e$

$\Rightarrow$ index variations $\delta n \approx (1/2n)\,(e^2/4\pi^2\varepsilon_o m_e f^2)\, \delta N_e$

$\Rightarrow$ phase variation introduced by an inhomogeneity δn of size L :

$\delta\varphi \approx \omega\, \delta t = \omega\, \delta(L/v_\phi) = 2\pi f\, (L/c)\, \delta n = (e^2/4\pi c \varepsilon_o m_e)\, L\, \delta N_e / (f\, n)$

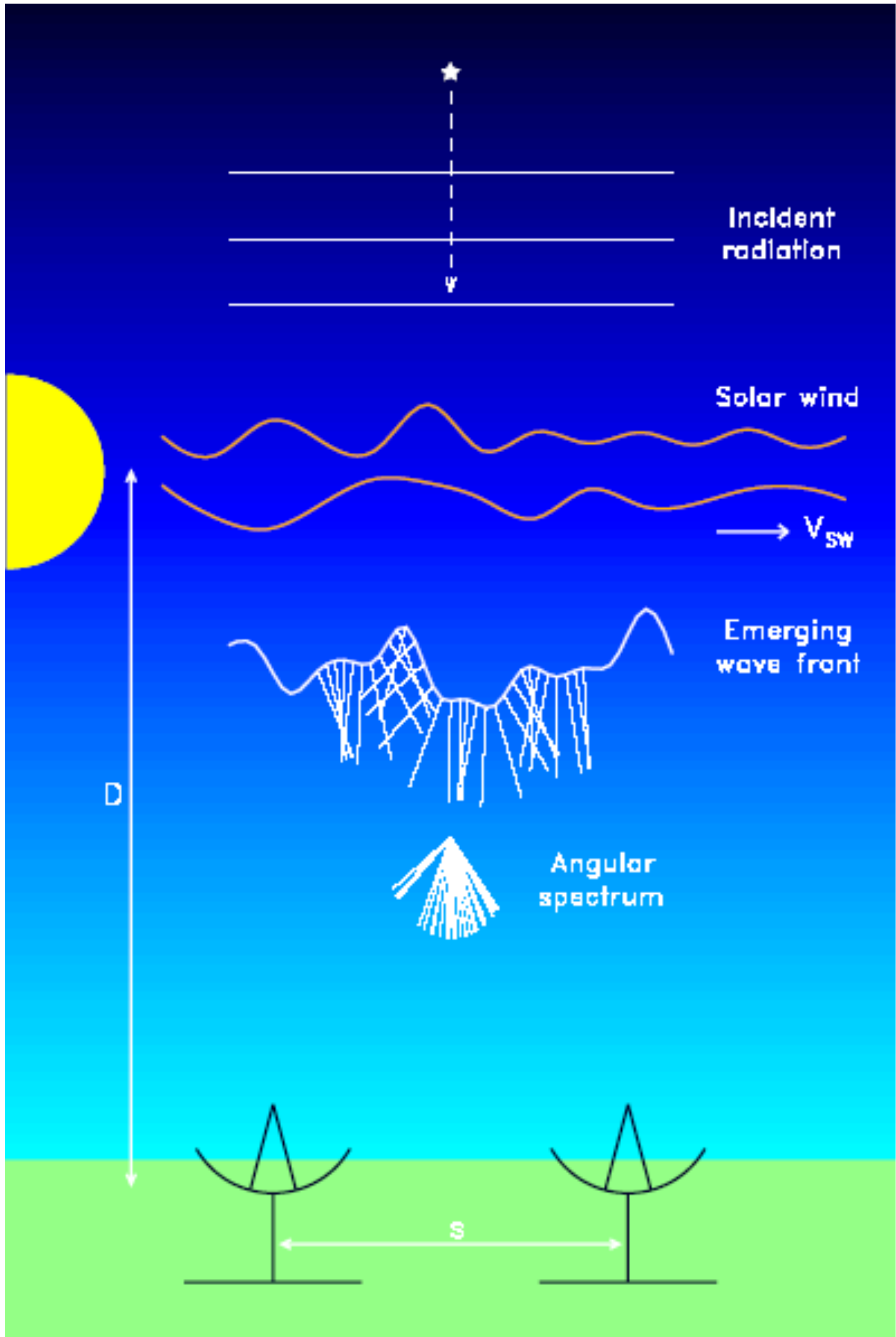

- $\delta N_e \ll N_e$, large spatial scales (N_e gradients), high frequencies $\Rightarrow$ weak scintillations $\Rightarrow$ refractive effects (fluctuations in intensity, position, temporal dispersion)

- $\delta N_e \sim N_e$, small spatial scales (turbulence) $\Rightarrow$ diffractive effects (intensity fluctuations, angular, temporal, spectral spreading)

REFRACTION PHENOMENA

Phenomenon	Quantity	Typical Values (DM~100) 400 MHz	30 MHz	10 MHz	
Slow scintillations	$\sigma_I/I \propto \lambda^{-1.1}$	20%	1	0.3	
	$\Delta t_r \propto \lambda^{2.2}$	1 yr	300	3000	$\Delta t_r(\sigma_I/I)$
Time-of-arrival variations	$\Delta t_{DM} \propto \lambda^2$	10μs	2 ms	16 ms	Dispersion
$\Delta t_{1D}(\Delta\theta_r)$	$\Delta t_\theta \propto \lambda^{1.6}$	1μs	60	400	time scale of erratic displacement
$\Delta t_{2D}(\Delta\theta_r)$	$\Delta t_{\theta^2} \propto \lambda^{3.3}$	1μs	5 ms	200 ms	
Angular wandering	$\Delta\theta_r \propto \lambda^{1.6}$	1 $m.a.s.$	60	400	

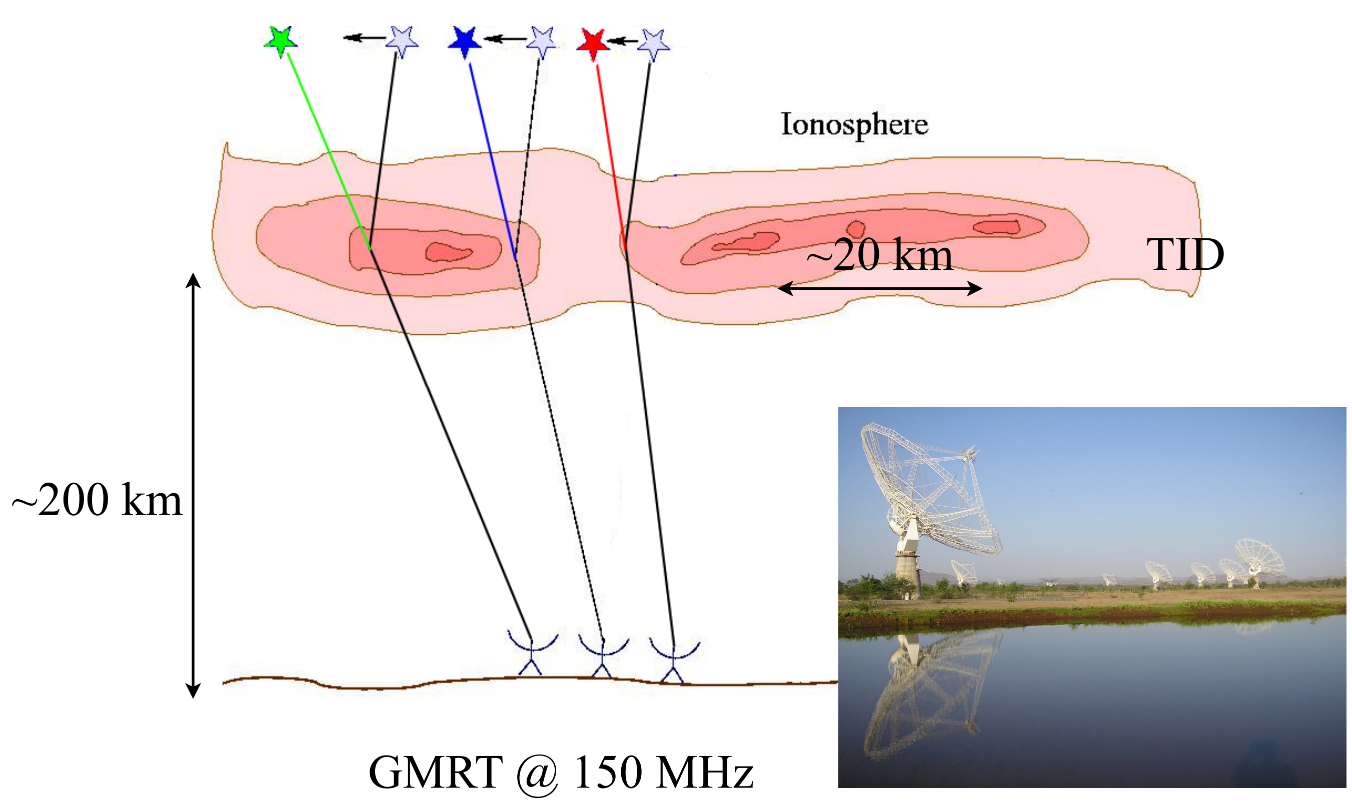

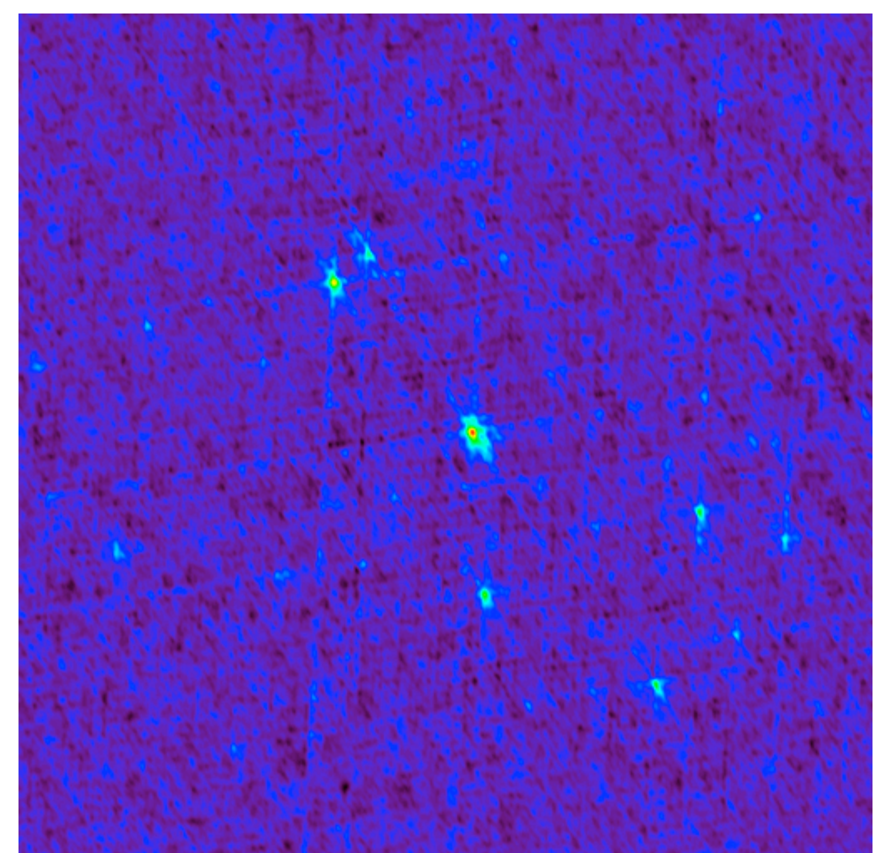

DIFFRACTION PHENOMENA

Phenomenon	Quantity	Typical Values (DM~100) 400 MHz	30 MHz	10 MHz	
Intensity Scintillations $\sigma_I \sim I$	$\Delta\nu \propto \lambda^{-4.4}$	10 kHz	10^{-2}	10^{-7}	spectral and temporal scales of fluctuations $\sigma_I \sim I$
	$\Delta t_d \propto \lambda^{-1.2}$	60 sec	3	0.7	
Temporal broadening	$\tau_d \propto \lambda^{4.4}$	1 ms	1 min	3 hr	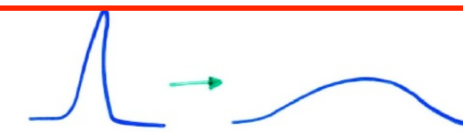
Angular broadening	$\theta_d \propto \lambda^{2.2}$	10 $m.a.s.$	$3''$	$33''$	$\bullet \rightarrow$ O
Spectral broadening	$\Delta\nu_s \propto \lambda^{1.2}$	1 Hz	22	83	Doppler on scattering inhomogeneities

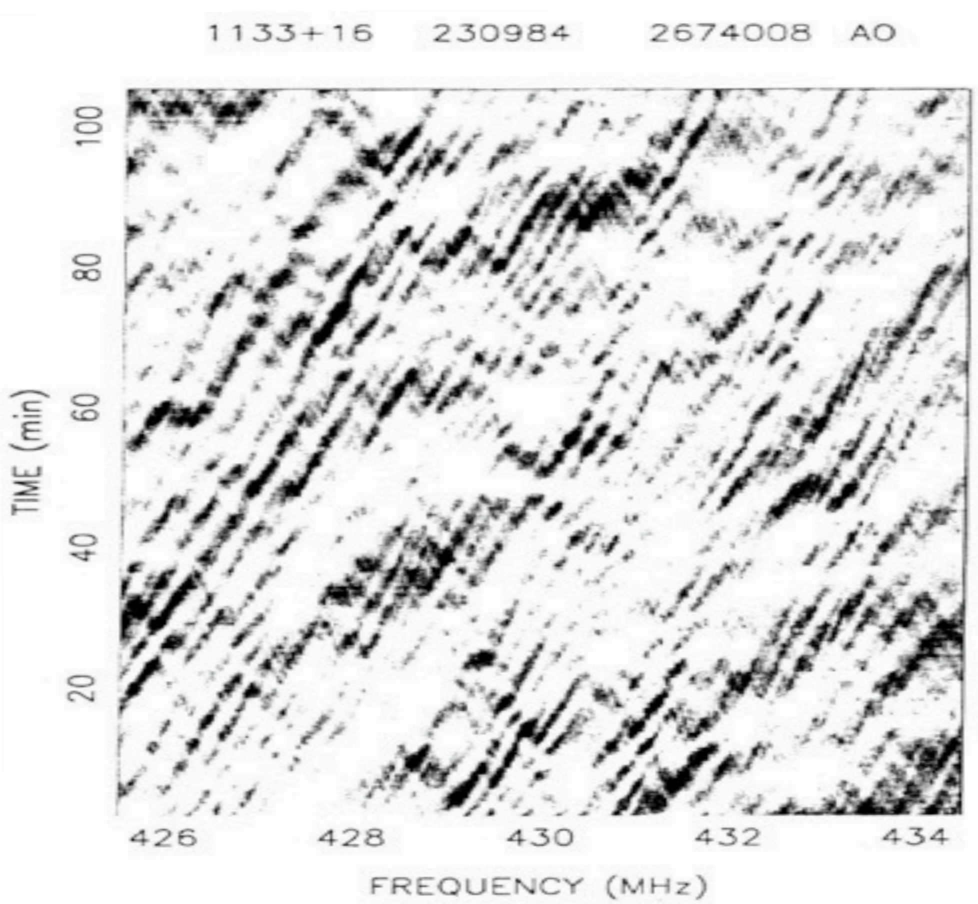

Figure 3. Dynamic spectrum $I(\nu, t)$ for PSR B1133+16 that shows constructive and destructive interference from multipath propagation. (DM ~ 5)

Maximum DM for time resolution δt: $\delta t \leq \tau_d$

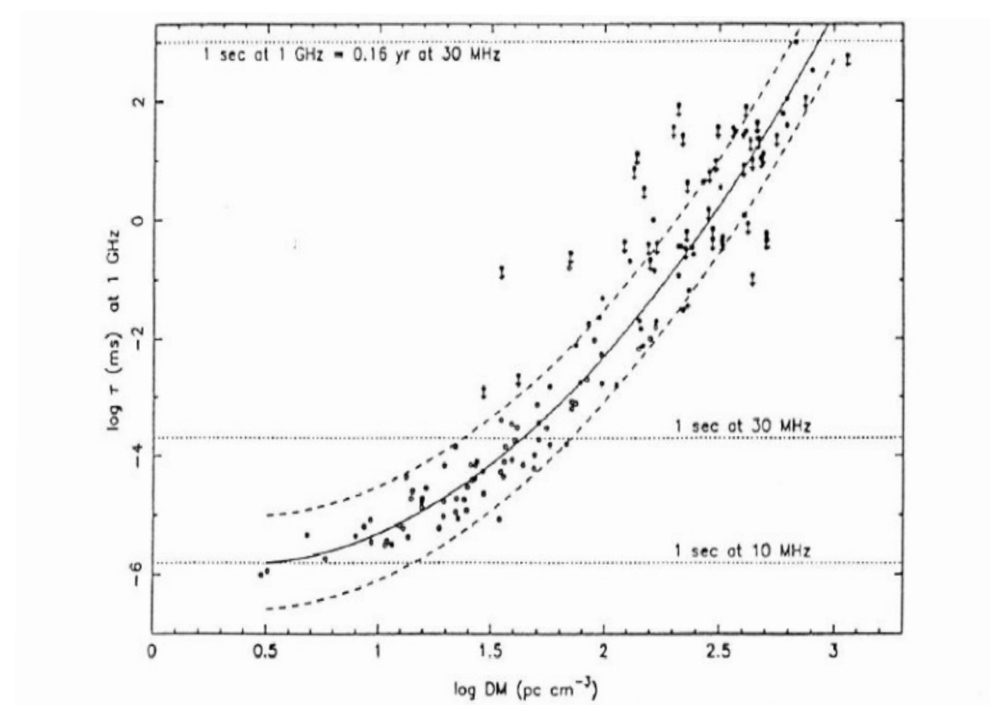

Figure 4. Pulsar temporal broadening times plotted against dispersion measure, DM. The solid line is a least squares fit to the data; the dashed lines are $\pm 1\sigma$ deviations from the fit. Downward arrows denote upper limits, which were excluded from the fit.

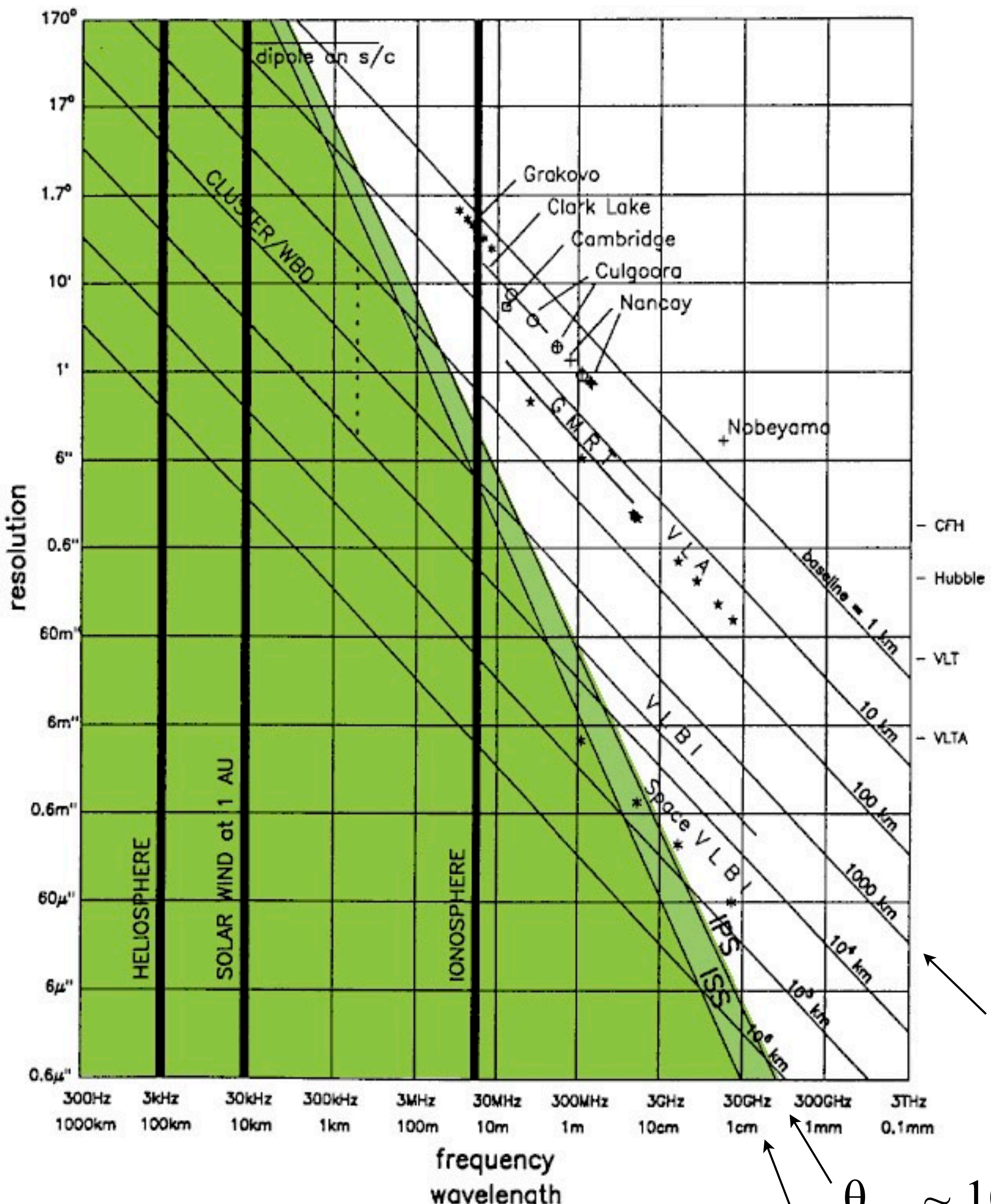

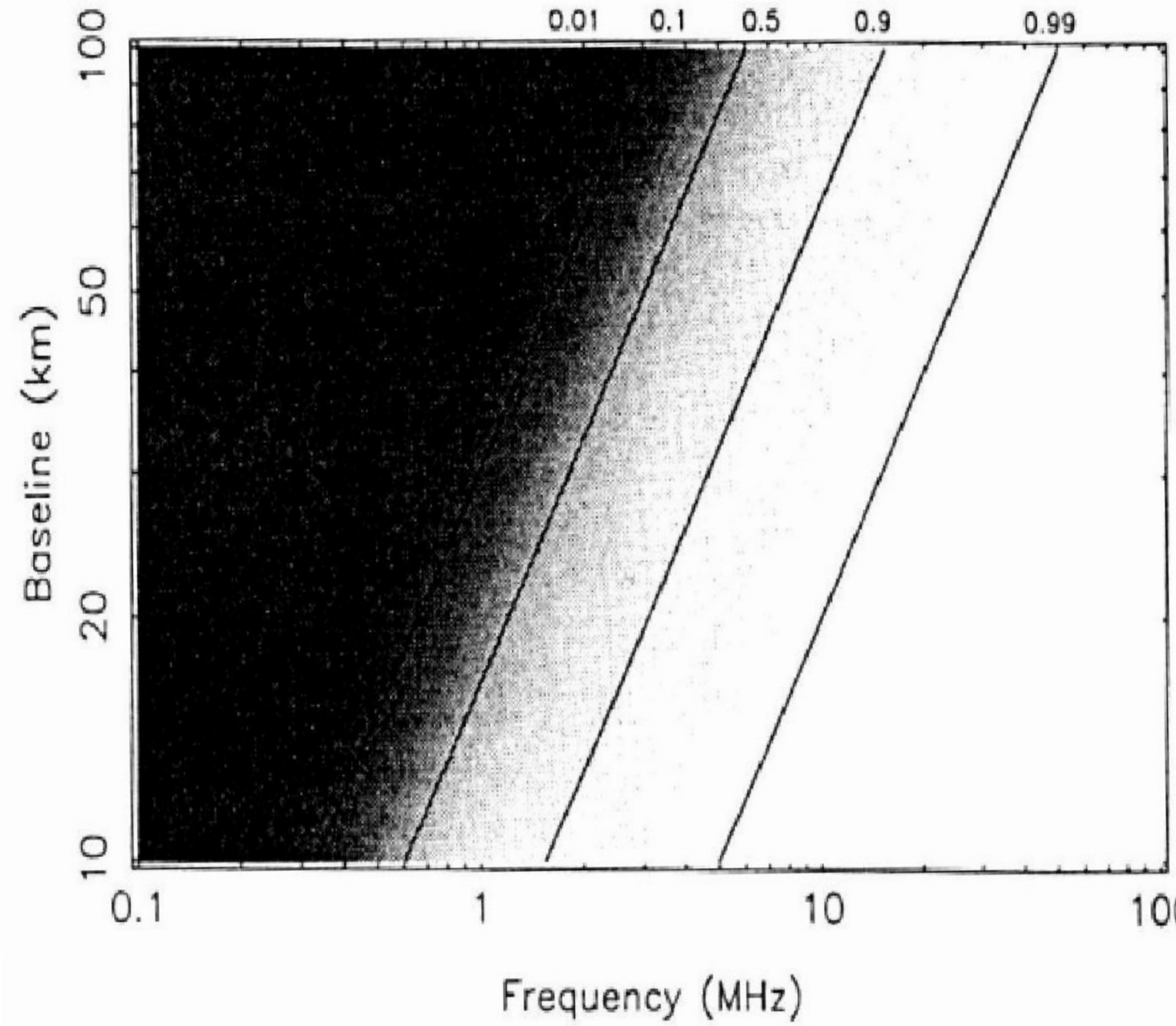

Figure 2. A graphical representation of the loss of visibility due to scattering in the IPM for observations at about 90° from the Sun. Contours of visibility amplitude are shown at 0.99, 0.9, 0.5, 0.1 and 0.01

$\theta_{min} \sim \lambda/d \sim c/fd$

$\theta_{IPS} \sim 100'/(Pf)^2$ (MHz)

P = minimun distance to Sun (UA)

$\theta_{ISS} \sim 22'/f^2$ (MHz)

$d_{max}(km) \simeq c/f\,\theta_{min} \sim c/f\,\theta_{IPS}$

$\simeq 10\,P^2 \times f$ (MHz)

$\sim 10 \times f$ (MHz)

- Introduction (history, interest, specific features)
- Waves & Polarisation
- Plasmas & Propagation (cutoff, dispersion, Faraday effect, scintillations)
- Coherent Signal Detection (measurement theory, antenna temperature, calibration, noise)
- Receivers (heterodyne, system temperature, filtering, gain, RFI mitigation)
- Basics of Radio Astronomy Antennas: Single antennas
- Basics of Interferometry and Aperture Synthesis (phased arrays, electronic pointing, imaging, correlation, coherence, VLBI)
- Observation methods
- Large present & future ground-based radio arrays
- Basics of Space radio astronomy

- Problems posed by radioastronomy observation

  - weak signal (~$10^{-4} \rightarrow 1$ Jy), "HF" ($\rightarrow$ GHz, THz …), with zero mean ($\langle V \rangle$)
    - $\Rightarrow$ amplification
    - $\Rightarrow$ frequency change ($\rightarrow$ LF)
    - $\Rightarrow$ positive values / detection

  - intense noise sources :
    - $\rightarrow$ sky background (Galaxy)
    - $\rightarrow$ nearby transmitters (thunderstorm lightning, artificial transmitters)
    - $\rightarrow$ noise from receiver system electronics

  - calibration of received intensity in physical units $\rightarrow$ reference radio source ?

- Schematic diagram of a radiotelescope

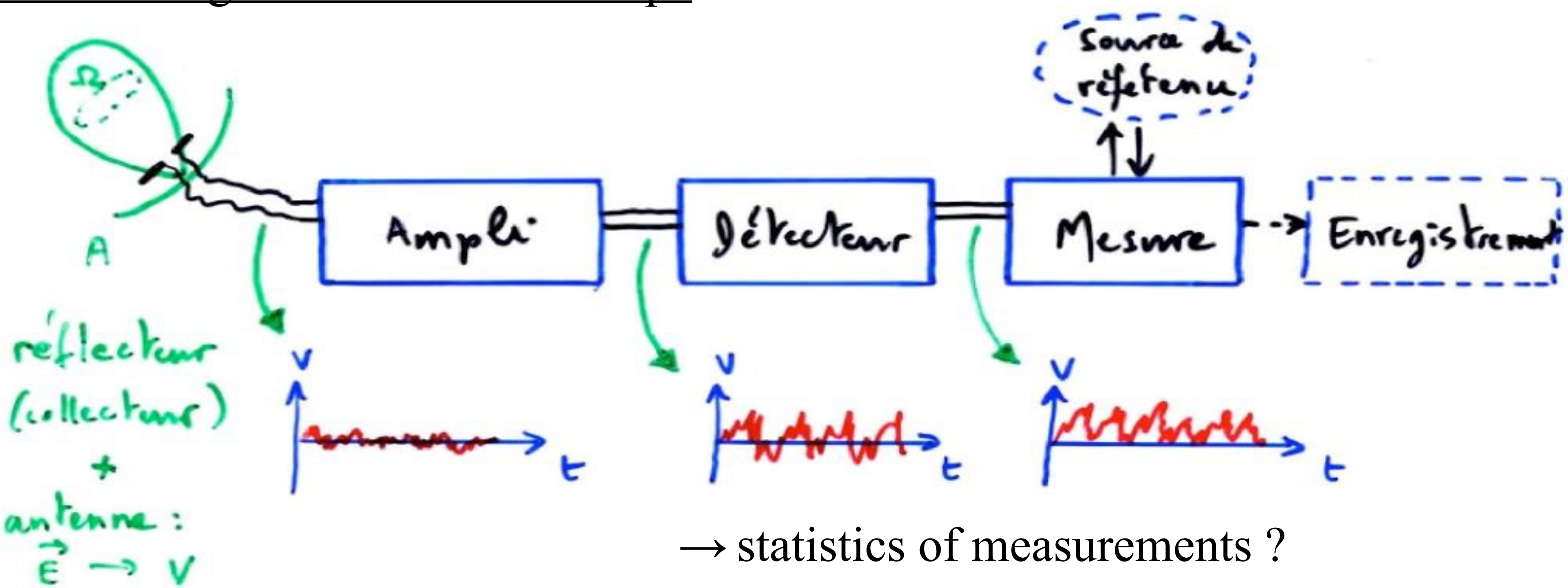

$\rightarrow$ statistics of measurements ?
$\rightarrow$ effect of filtering (band selection)
$\rightarrow$ how to separate RFI from the emission of interest ?

- <u>Nature of the signal received</u>

- artificial signal → narrow band, sustained/coherent emission, modulated (AM, FM...)

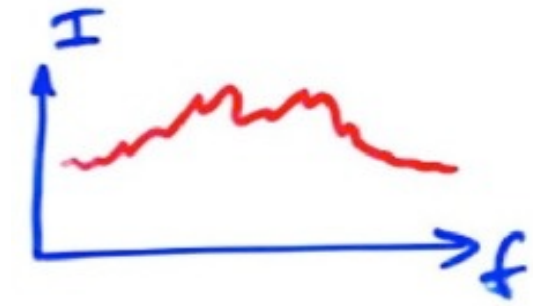

- natural signal = "noise", <u>generally</u> broadband, stationary, with gaussian statistics (incoherent source with $\varnothing >> \lambda$)
$P(x) = 1/(\sigma \sqrt{2\pi}) \exp[-(x-x_o)^2/2\sigma^2]$ $\quad (x = E, \ |E|, I \ ...)$

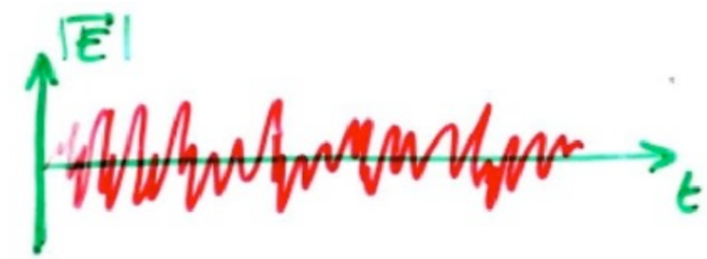

⇒ amplitude & phase of **E** (broadband) vary randomly vs. t, z
$|\mathbf{E}(z)|_{to}$ and $|\mathbf{E}(t)|_{zo}$ are random functions, $\langle E\rangle=0$, $\langle E^2\rangle\neq 0$

The spectral (Fourier) decomposition of E provides E(f) components with any relative phase
⇒ energies carried in disjoint frequency bands add up.

⇒ <u>Working hypothesis</u> : the received signal ris a white noise ($I(f) \propto |E(f)|^2 = C^t$)
We can always return to this case by studying the spectrum of the signal in narrow bands where the noise is - to 1st approximation - white

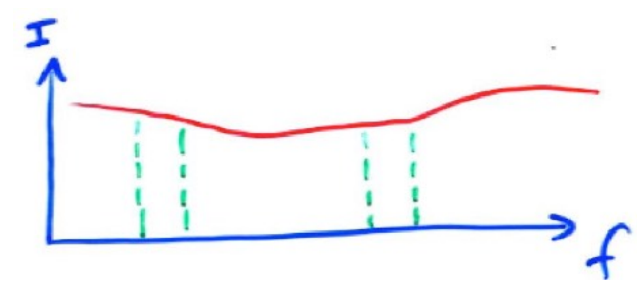

⇒ <u>Thermodynamical formulation</u> employed in Radioastronomy measurement theory

• <u>Basic Notions on Radio Astronomical Antennas</u>

<u>Relation A ⟵⟶ Ω (preliminary derivation)</u>

For any single dish (≠interferometer) of size (∅) D,
we have : $\theta_{min} \sim \lambda/D \Rightarrow \theta_{min}^2 \sim \Omega \sim \lambda^2/D^2 \sim \lambda^2/A$

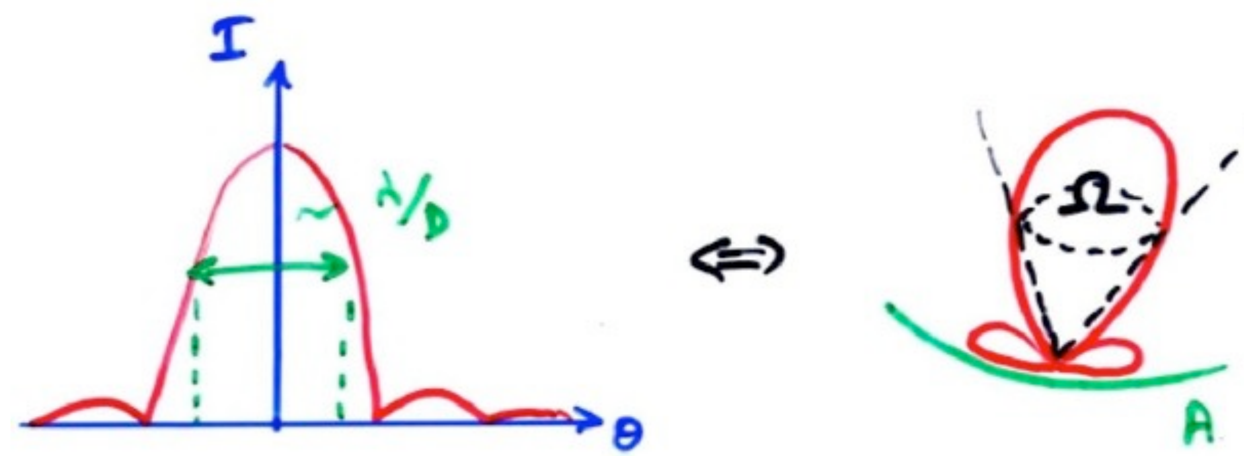

More generally, for any antenna of effective area A_{eff} and main lobe Ω, we show that :

$$\boxed{A_{eff}\,\Omega = \lambda^2 \quad \Rightarrow G = 4\pi / \Omega = 4\pi A_{eff} / \lambda^2}$$

<u>NB</u> : A is not necessarily the geometrical area of the collector, but its "effective" area = "effective cross-section" of the radiotelescope / incident radio radiation (taking losses into account ...) in the direction of the main lobe.

<u>Example</u> : Lossless dipolar antenna : $A_{eff} = 3\lambda^2 / 8\pi$
→ unrelated to its geometric surface

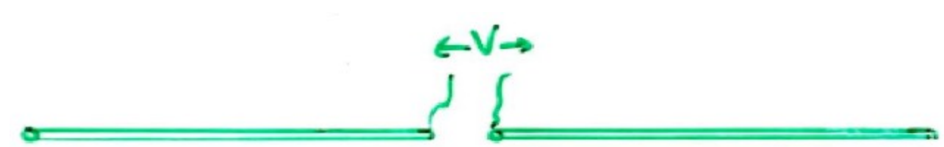

Antenna temperature

→ Observation of an extended black body ($/\Omega$), of brightness $B = 2kT_B/\lambda^2$ [$W\ m^{-2}\ Hz^{-1}\ sr^{-1}$]

$\Downarrow$ of source $\quad \Downarrow$ from the source

Source "seen" by the radiotelescope (Ω) : $A_s = \Omega d^2$

Solid angle subtended by the RT as seen from the source : $\Omega_A = A_{antenna}/d^2 = A/d^2$

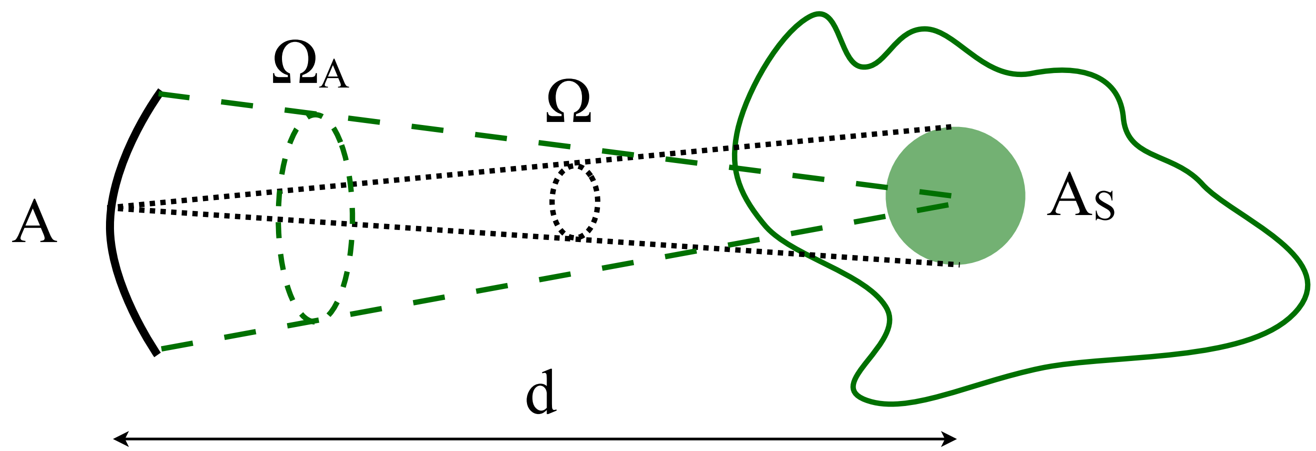

⇒ Spectral power received by the radiotelescope from an extended black body :

$P(\nu)\, d\nu = B(\nu)\, A_S\, \Omega_A\, d\nu = (2kT_B/\lambda^2)\,(\Omega d^2)\,(A/d^2)\, d\nu \quad = 2\, k\, T_B\, d\nu$

⇒ $\boxed{P(\nu) = (2)\, k\, T_B \quad [W\ Hz^{-1}]}$

$\Downarrow$

relative polarisation antenna / wave

$\forall$ A, d, λ... : $A \uparrow \Rightarrow \Omega \downarrow$

$d \uparrow \Rightarrow \Omega d^2 \uparrow$

$\lambda \uparrow \Rightarrow \Omega = \lambda^2/A \uparrow$ but $B \propto 1/\lambda^2 \downarrow$

⇒ Flux density received from an extended black body :

$S(\nu) = P(\nu) / A_{eff} = (2)\, k\, T_B / A_{eff} \quad [W\ m^{-2}\ Hz^{-1}]$

$\Downarrow$

of antenna

$\rightarrow$ If $\omega_{source} < \Omega_{antenna}$ (with $\omega_{source} = A_{source}/d^2$)

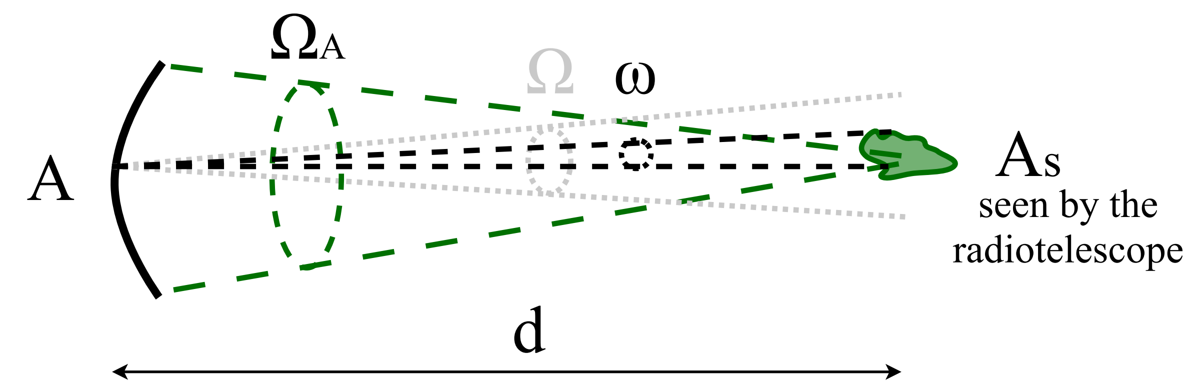

$\Rightarrow$ $P(\nu) = (2)\,k\,T_B\,(\omega_{source}\,/\,\Omega) = (2)\,k\,T_A$
and $S(\nu) = (2)\,k\,T_B\,\omega_{source}\,/\,A_{eff}\,\Omega = (2)\,k\,T_A\,/\,A_{eff}$

$\Rightarrow$ definition of "Antenna temperature" : $T_A = S(\nu)A_{eff}\,/\,(2)\,k = P(\nu)/\,(2)\,k$

T_A is a measure of the received power (or flux density)
[for a source polarised ≡ antenna $\Rightarrow T_A \times 2$*]*

In the case of an extended black body, we have : $T_A = T_B = T_{physical}$
In the case of a non-extended source : $T_A = T_B\,\omega_{source}/\Omega \ll T_B$

For a point source, we can measure S and T_A but not T_B, for which we can only obtain a lower/upper limit if there is an upper/lower limit on ω_{source}

<u>Example</u> : Jupiter observed with the Nançay Decameter Array $(A \approx 3000\ m^2)$
$S \approx 10^{-19}\ W\,m^{-2}\,Hz^{-1}$ *at 10 MHz* $\Rightarrow$ $T_A = A\,S\,/\,2\,k \approx 10^7\ K$
In addition, VLBI measurements show that $\varnothing$*(source at 10 MHz)* ≤ 400 *km*
thus $\omega_{source} < \pi\varnothing^2/4d^2$ $(d \sim 4.2\ UA)$
$\Rightarrow T_B > T_A\,\Omega/\omega_{source} = (AS\,/\,2k)\,(\lambda^2/A)\,(4d^2/\pi\varnothing^2) = 10^{19}\ K \Rightarrow$ *coherent emission !*

- <u>Measuring the received signal</u>

Source is never isolated

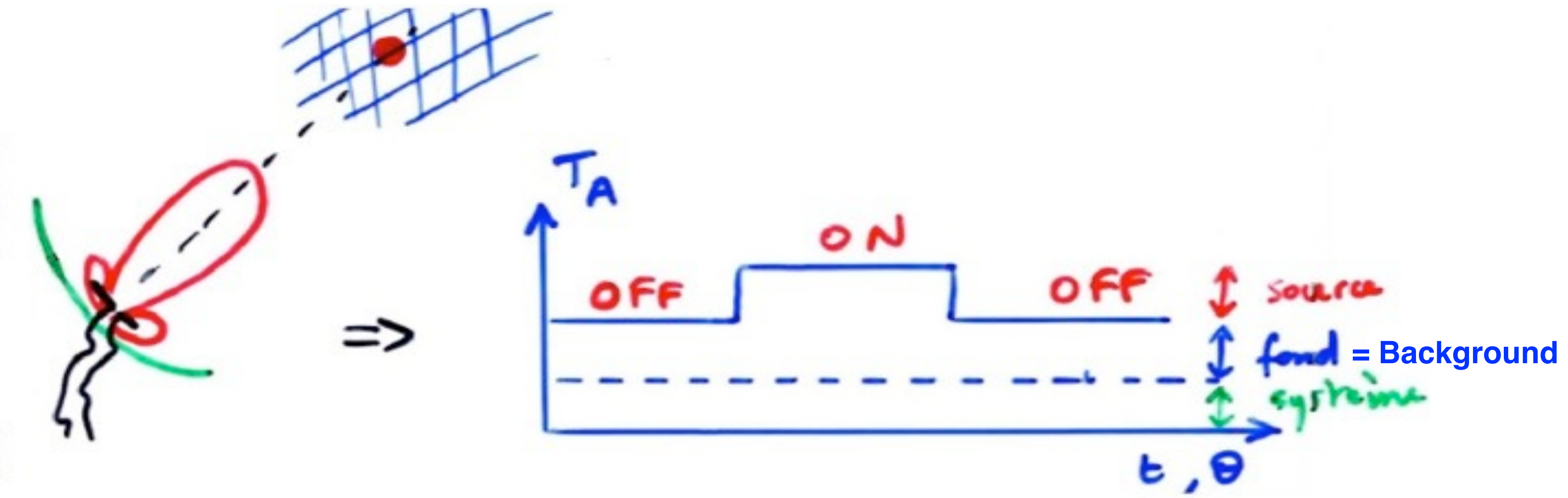

⇒ received signal = signal of interest (source)
+ "background"
+ RFI (from main or side lobes)
+ Nyquist/Johnson noise (due to antenna and receiver's resistive elements)
+ …

Eliminating the "background" : observations "ON" – "OFF"
T_A (RFI + Nyquist + …) = T_{system}
depending in particular on the physical temperature of the receiving system

If $\omega_{source} << \Omega$ $\quad$ $T_{A(signal)} = T_B\ \omega_{source}/\Omega$ $\quad$ may be $\quad$ $<< T_{system}$, $T_{backgound}$

⇒ difficulty = measuring weak signals superimposed on stronger signals
limits = instrument accuracy, and above all <u>random fluctuations in received signals (= noise)</u>

Examples: • *Radio emission from a Jupiter-like exoplanet ?*
$T_A = T_{A(Jupiter)} \times (d_{Jupiter}/d_{exoplanet})^2 \approx 10^7 \times (5\ UA\ /\ 5\ pc)^2 \approx 4{\times}10^{-3}\ K$
with $T_{sky\ background} \geq 10^5\ K$ *at 10 MHz* *(+ RFI…)*
• *Cosmological background at 2.7 K, whereas* $T_{system} \approx 10 - 100\ K$
at $\lambda \in$ *[cm, dm] and impossible to point « OFF-source" !*

• <u>The case of noise</u>

All signals follow random fluctuations
(quantisation of e.m. energy → photons ⇒ statistical fluctuations of $n_{photons}$ received)

Main sources of noise :

- Photon noise (= S / hν) → ~ negligible in radio
- Noise in 1/f (S(ν) ∝ 1/ν) universal, affects ~ all physical phenomena
- Shot noise (hν ⇒ V ⇒ e^- in detector with an energy distribution + potential barrier (e.g. transistor) ⇒ random fluctuations in output current = e- flow)
- External interference (RFI)
- Nyquist/Johnson noise
  = fluctuating power delivered by any resistive circuit, even in the absence of a signal

Nyquist noise

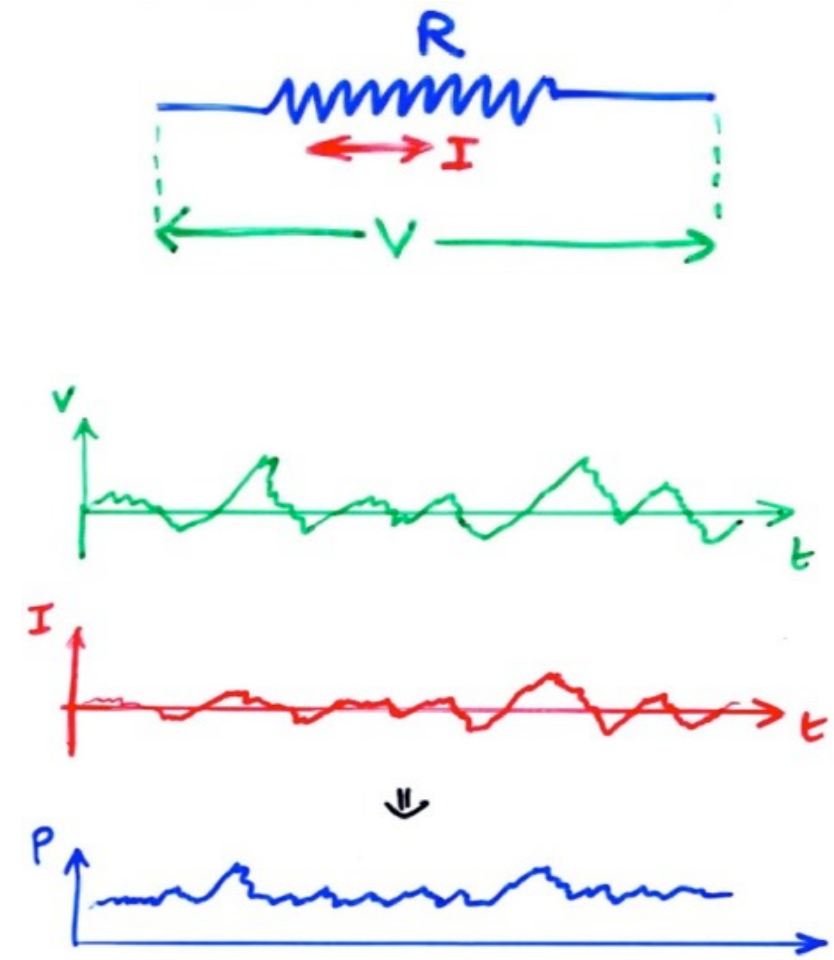

Passive circuit passif (no generator) at $T \neq 0$

$\Rightarrow$ thermal agitation of e^- (Brownian motion)

$\Rightarrow$ non-uniform distribution of free e^- in the conductor

$\Rightarrow$ a random voltage drop (V) appears at conductor terminals

an a random current (I, correlated with V) in the conductor,

$\langle V \rangle = 0$ and $\langle I \rangle = 0$ but $\langle P \rangle = \langle V \times I \rangle \neq 0$

$\Rightarrow$ Power P dissipated in resistor R: source = thermal agitation of e^-

$\Rightarrow$ T(R) $\downarrow$ unless resistance absorbs energy from its environment

The thermal motion of e^- generates white noise, which is independent of ν

$\rightarrow$ on what depends power P supplied "spontaneously" by R ?

Experience 1 : thermostated cavity at T

∃ spontaneous power exchanges between R_1 and R_2
but $T(R_1)=T(R_2)$
$\Rightarrow P(R_1 \rightarrow R_2) = P(R_2 \rightarrow R_1)$
[1st principle of Thermodynamics]

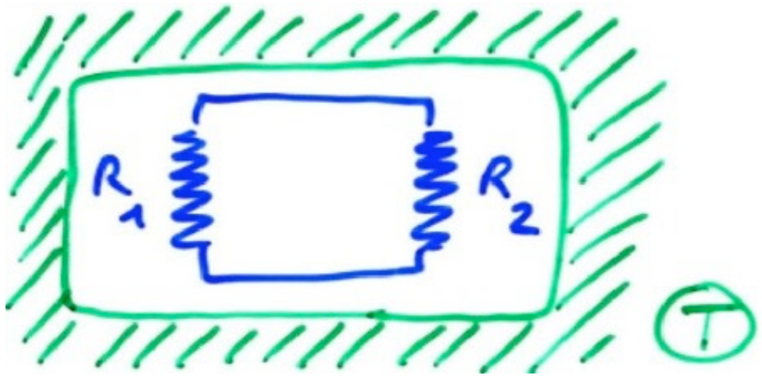

Experience 2 : thermostated cavities at T_1 and T_2

$\Delta P = P(R_1 \rightarrow R_2) - P(R_2 \rightarrow R_1) \propto (T_1 - T_2)$ only
$\Rightarrow$ P supplied by R
$\rightarrow$ independent of R value (∀ resistive system)
$\rightarrow \propto$ T only

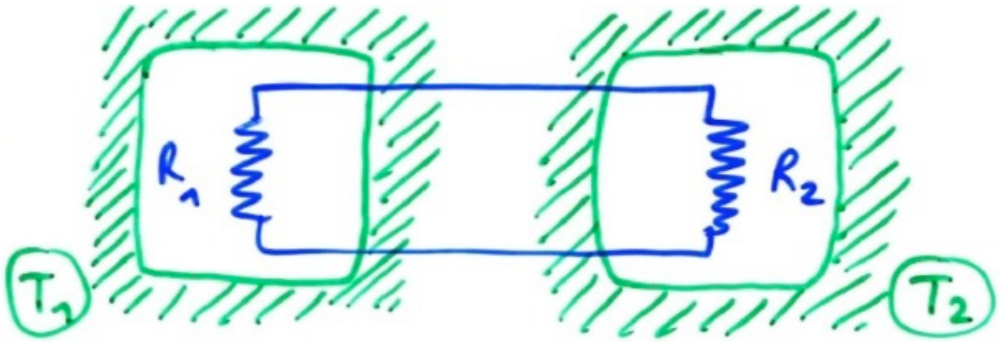

Nyquist Theorem : $P(\nu) = k\,T$ is the average power at the terminals of a resistive circuit at temperature T $\Rightarrow$ *"System Temperature"* T_S

[Johnson, Phys. Rev. 1928 ; Nyquist, Phys. Rev. 1928]

White noise $\Rightarrow$ fluctuations at 2 ≠ frequencies ν are uncorrelated

$\Rightarrow$ spectral powers add up : $P(\nu)\,\Delta\nu = k\,T\,\Delta\nu$

Notes: all passive resistive system (the elements of the measurement system - antennas, receivers, etc.) contribute to its resistive noise ≈ noise generators

T_{system} of a system is $\leq T_{physical}$ (∃ radiative dissipation…)

T_{system} typically ~150 K for an uncooled antenna+receiver system

$T_{OFF} = T_{system} + T_{background} = T_S + T_F$

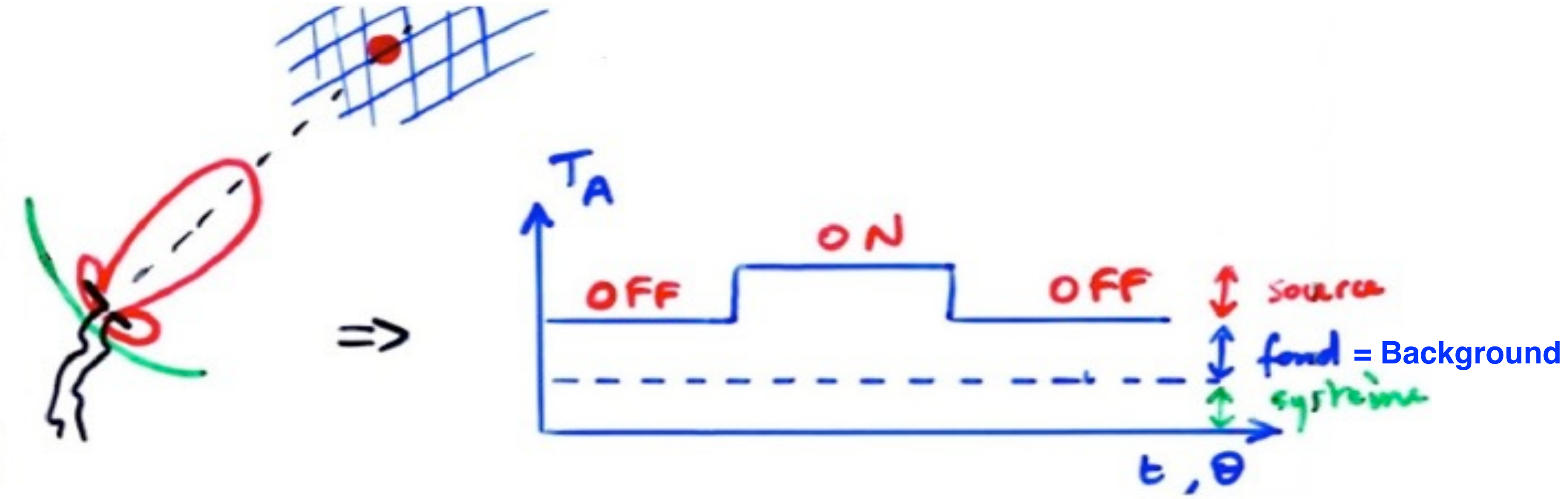

T_{OFF} sometimes improperly noted T_S
dominated by $T_{background}$ at LF (≤0.5 - 1 GHz), by T_{system} at HF (≥0.5 - 1 GHz)

→ Various contributions to T_F

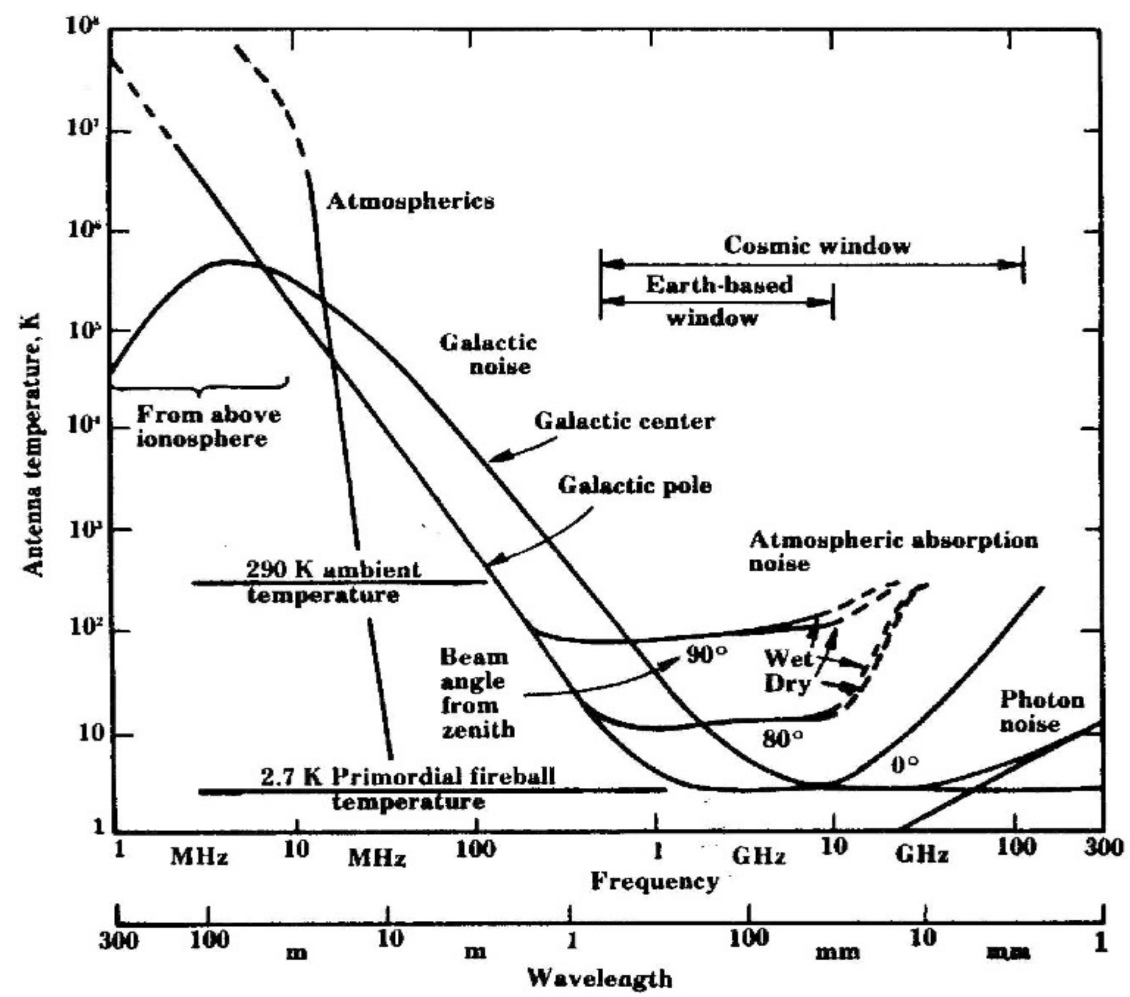

The "quality factor" or "sensitivity" of a system is defined by : $F = A_e / T_S$

Ex: For the Nançay radiotelescope : $A_e / T_S \sim 5000 / 25 \sim 200\ m^2/K$

For SKA, we aim for : $A_e / T_S = 20\,000\ m^2/K$

→ How to reduce T_S ?

[~1 , ~100 MHz] $T_S << T_F$ → transistor amplifiers + high-dynamic electronics
(to avoid saturation in the presence of interference)

[0.1 , 1 GHz] low-noise electronics (field-effect transistors, etc.)

[1– 100 GHz] cooled electronics (FET, HEMT) with liquid N_2 (77 K) or He (4 K)
→ reduces Nyquist noise, which is very high at the input stages, up to 1st amplification
→ T_S = 20-25 K reached in Nançay (down to 10 K at e.g. Goldstone/JPL)

[≥ 100 GHz] No more direct amplification → shift to Lower Frequencies via local oscillator
+ low-noise mixer

⇒ rapid technological progress :

- specific integrated circuits at room temperature

- approaching ultimate limits 2.7 K and photon noise
($k T_S = h \nu$)

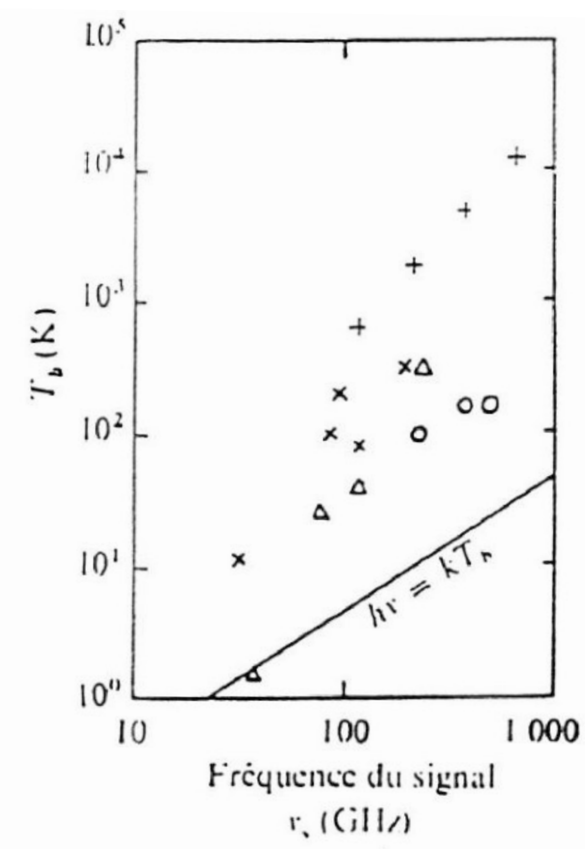

- <u>Effect of random fluctuations on measurement / How to reduce fluctuations ?</u>

More realistic situation : if T_A (source) << fluctuations of ($T_S + T_F$)
→ the signal will be undetectable (hidden in noise)

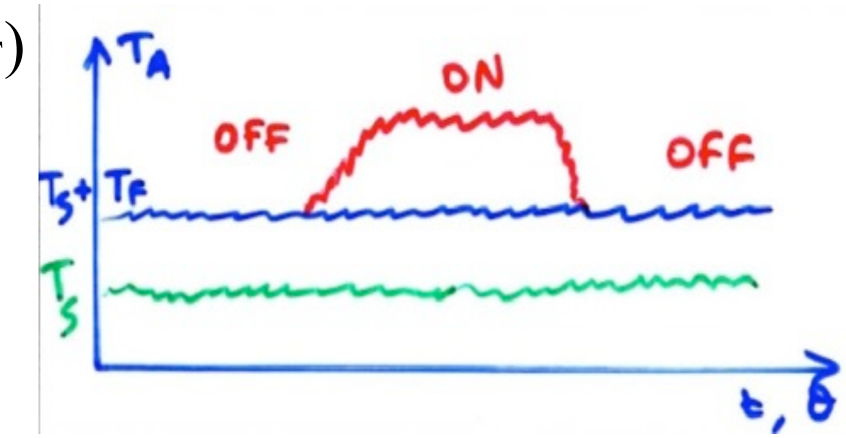

Gaussian signal E(t) : $P(E) = 1/(\sigma\sqrt{2\pi})\, exp[-(E-<E>)^2/2\sigma^2]$

with $<E> = 0$ *et* $\sigma^2 = <(E-<E>)^2> = <E^2>$

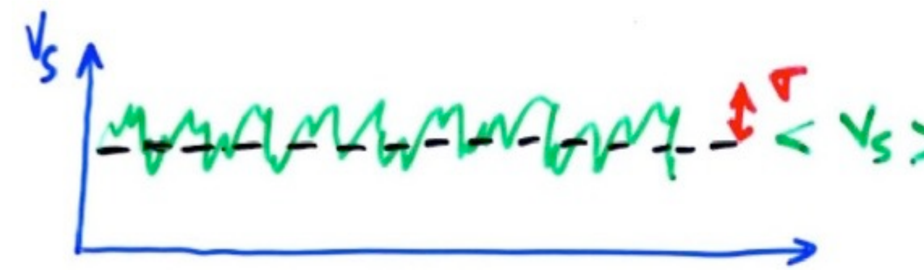

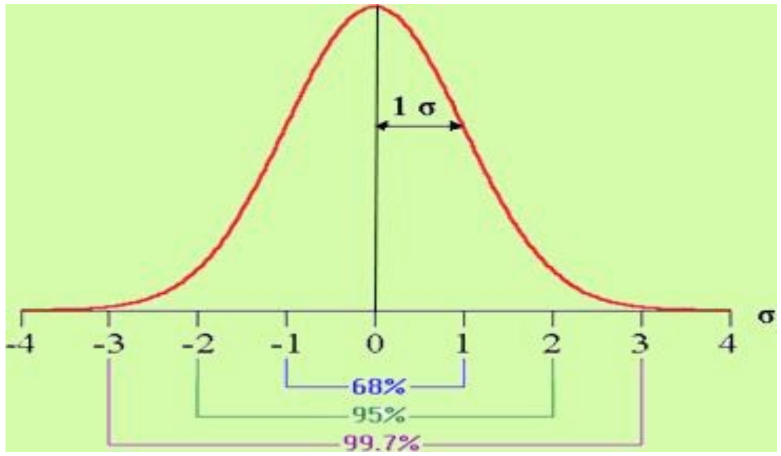

Measurement of E : E $\rightarrow V_{in}$ ($=V_e$) $\propto$ E
$\rightarrow V_{out}$ ($=V_s$) $\propto$ |E| or $|E^2|$

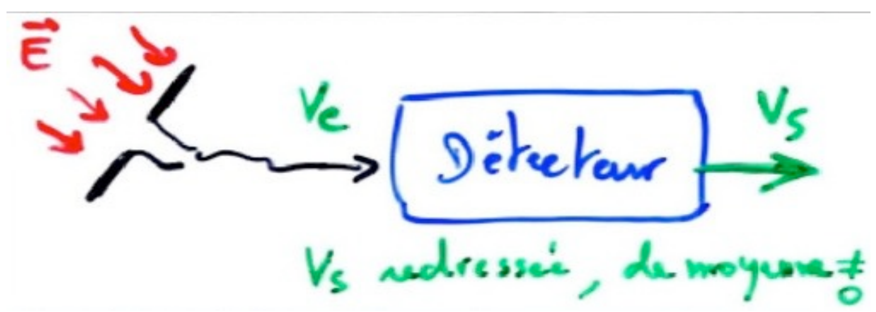

⇒ Statistics of fluctuations of V_{out} : we show that in both cases : $\sigma \propto <V_{out}>$

Linear detection : $V_{out} \propto |E|$

$P(E) \propto \exp(-E^2/2\langle E^2\rangle)$

$\Rightarrow$ *Rayleigh distribution = "rectified" Gaussian*

$P(V_{out}=V) = (2V/\langle V^2\rangle)\exp(-V^2/\langle V^2\rangle) \quad \Rightarrow \quad \int_0^\infty P(V)dV = 1$

$\Rightarrow \langle V\rangle = \int_0^\infty V\,P(V)\,dV = (\pi\langle V^2\rangle/4)^{1/2}$

$\Rightarrow \sigma = (\langle V^2\rangle - \langle V\rangle^2)^{1/2} = (\,(1-\pi/4)\langle V^2\rangle\,)^{1/2}$

$\sigma = 0.52\,\langle V\rangle$

Quadratic detection : $V_{out} \propto |E^2| \propto S$

$P(V_{out}=V) = (1/\langle V\rangle)\exp(-V/\langle V\rangle) \quad \Rightarrow \quad \int_0^\infty P(V)dV = 1$

$\Rightarrow \langle V^2\rangle = \int_0^\infty V^2\,P(V)\,dV = 2\,\langle V\rangle^2$

$\Rightarrow \sigma = [\langle V^2\rangle - \langle V\rangle^2]^{1/2} = [2\langle V\rangle^2 - \langle V\rangle^2]^{1/2}$

$\sigma = \langle V\rangle$

→ Reduction of fluctuations (thus of σ) :

Let A_i *(i=1,N) be independent random variables :* $B = (1/N)\ \Sigma_{i=1,N}\ (A_i)$

$\sigma_{Ai}^2 = \sigma_A^2 = <Ai - <Ai>>^2 \qquad \Rightarrow \sigma_B^2 = \Sigma_{i=1,N}\ \sigma_A^2 / N^2 = \sigma_A^2 / N$

$\Rightarrow \sigma_B = \sigma_A / \sqrt{N}$

Let us consider a large number of independent measurements of V_S, with mean $M = <V_S>$ and dispersion $\sigma \propto M$

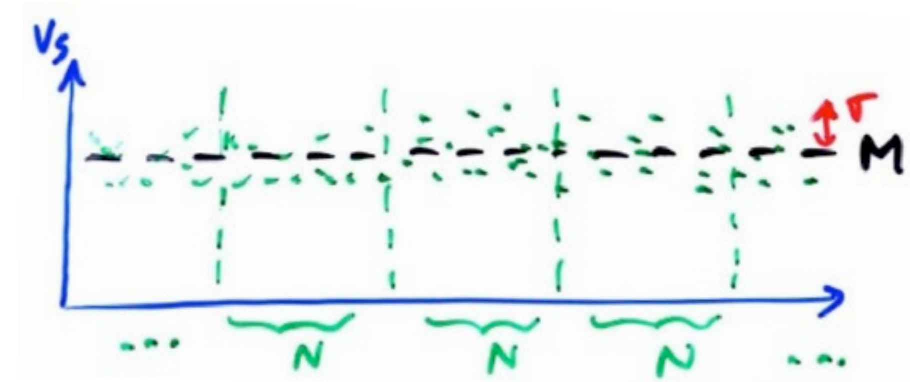

Each measurement lasts δt_o and is performed by a receiver of band $\delta\nu_o$

Average of measurements in groups of N time steps $\delta t_o \times$ P frequency bands $\delta\nu_o$:
independent random fluctuations $\Rightarrow$ new random distribution of mean M and dispersion $\sigma' = \sigma/\sqrt{NP}$

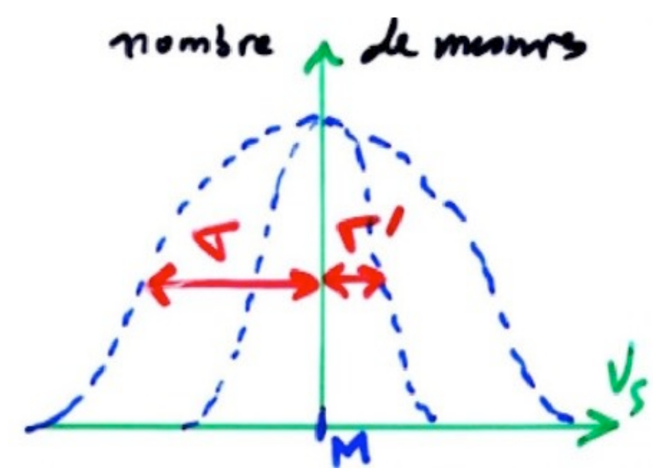

$N\times\delta t_o = \tau$ = total integration time of a measurement
$P\times\delta\nu_o = b$ = total measurement bandwidth

$\Rightarrow \sigma'(\tau,b) = \sigma(\delta t_o, \delta\nu_o)/(NP)^{1/2} = \sigma(\delta t_o, \delta\nu_o)\ (\delta t_o\times\delta\nu_o)^{1/2} / (b\times\tau)^{1/2} \approx M\ (\delta t_o\times\delta\nu_o)^{1/2} / (b\times\tau)^{1/2}$

= uncertainty in measurement of M

What are "independent measurements"?

For a fixed τ, the stochastic fluctuations of V_S are affected by fluctuations such that : $\sigma \propto \tau^{-1/2}$

If τ is such that $\sigma << M$, successive V_S measurements are "correlated" around M
(e.g. $P(V_S = <V_S> \pm 1\sigma) \sim 68\%$) $\rightarrow$ not totally independent

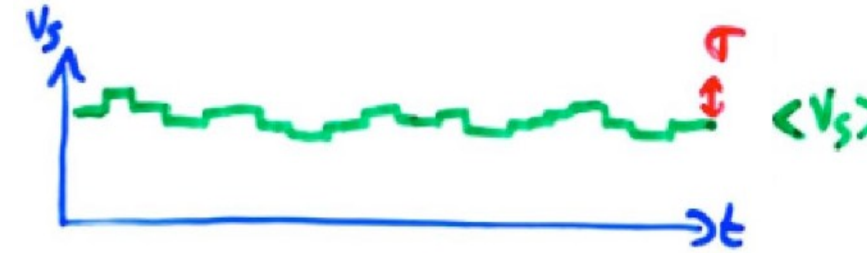

When $\tau \downarrow$, $\sigma \uparrow$ $\Rightarrow$ for τ sufficiently small, we reach : $\sigma = M$

$\Rightarrow$ measurements often reach zero, consecutive values become uncorrelated

$\Rightarrow \tau = \delta t_o$

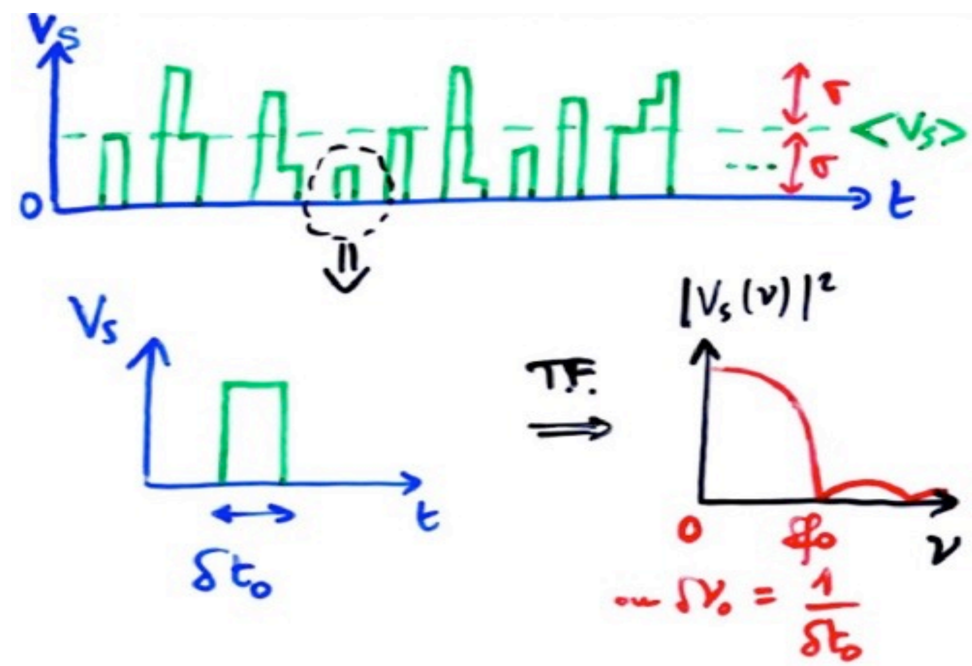

Consider a pulse of duration δt_o (interval of constant $V_S(t)$)
the spectrum of this pulse is:

$$TF(V_S(t)) = V_S(\nu) = 1/\delta t_o \int V(t) \exp(-i\omega t)\, dt \propto \mathrm{sinc}(\pi\nu\delta t_o)$$

$\rightarrow$ the useful part of the spectrum is the interval $[0, \delta\nu_o = 1/\delta t_o]$
to which the receiver must be sensitive to detect the $V_S(t)$ pulse

$\Rightarrow \delta t_o \times \delta\nu_o \approx 1$

For white noise and observation conditions such that $\delta t_o \times \delta\nu_o \approx 1$, successive measurements constitute a sequence of random, independent values of mean M and dispersion $\sigma \approx M$

hence : $\sigma(b,\tau) \approx M\, (\delta t_o \times \delta\nu_o)^{1/2} / (b \times \tau)^{1/2} \approx M \times 1 / (b \times \tau)^{1/2}$

$\Rightarrow \quad \sigma \approx M / \sqrt{(b\tau)}$

NB :

- In general, for any function, "useful" spectral width $\times$ temporal length $\approx$ 1
(ex: sin $\omega t \rightarrow$ zero spectral width and temporal length ∞)

A more detailed (complicated) analysis shows that for any detection system, we have :

$\sigma = K \times M / \sqrt{(b\tau)}$ with $1/\sqrt{2} \leq K \leq 2$

NB :

- When $\tau\uparrow$, fluctuations diminish but we lose temporal resolution, hence sensitivity to rapidly varying signals (pulsars, Jupiter bursts...)

- When $b\uparrow$, fluctuations decrease but spectral resolution is lost, which limits the analysis of narrow lines (H_I , OH...) and makes it more difficult to eliminate artificial, generally narrow-band interference

• <u>Noise temperature & minimum detectable flux</u>

→ Realistic radioastronomy measurement

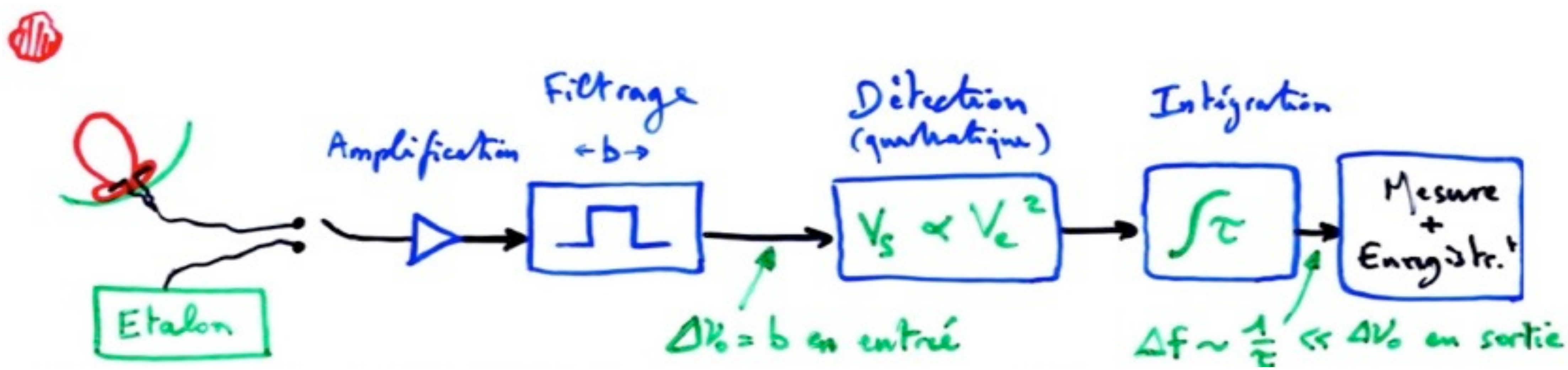

$\sigma = (T_S+T_F) / \sqrt{(b\tau)} = T_N$

= definition of "Noise temperature"

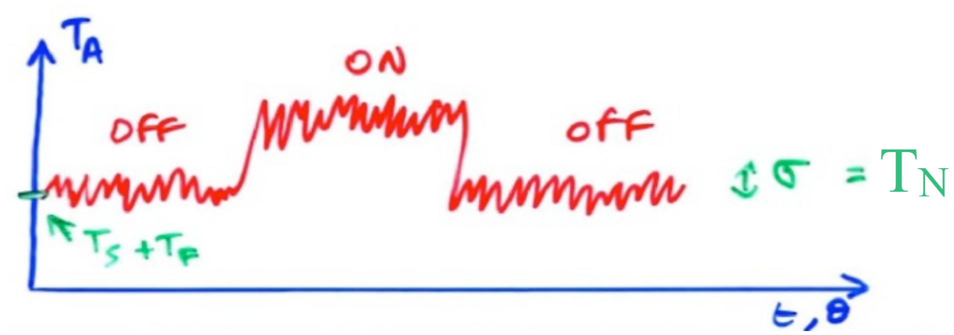

⇒ condition for detecting a radiosource in the sky background (+ system noise) :
$T_A(\text{source}) > n\times T_N$ with $n = 2$ to 5 depending on required confidence level and difficulty of the measurement

Definition of the signal-to-noise ratio : $S / N = T_{A(\text{source})} / T_N$

Similarly, we define : $P_N = k\, T_N$ = "Noise power"

and : $S_N = 2\, k\, T_N / A = 2\, k\, (T_S + T_F) / A\, (b\tau)^{1/2} = S_{min}$

minimum detectable unpolarised flux density (S/N = 1)

If the source radiation is polarised ≡ antenna : $S_{min} = S_N / 2$

Example : *Nançay decimeter radiotelescope :*

Flat reflector $A_{eff} \approx (200 \times 35\ m^2) \times 0.8 \approx 5600\ m^2$

$\Downarrow$

focal antenna efficiency (matching, losses)

Observation at 1420 MHz ($\lambda = 21.2$ *cm*) *with* $b = 5$ *MHz*, $\tau = 10$ *s*

$T_S = 25$ *K*, $T_F \sim 3$ *K*, *1 polarisation detected*

$\Rightarrow \quad T_N = T_S / \sqrt{(b\tau)} = 4$ *mK*

$S_{min} = 2\ k\ T_S / A_{eff} \sqrt{(b\tau)} = 2$ *mJy*

Example :

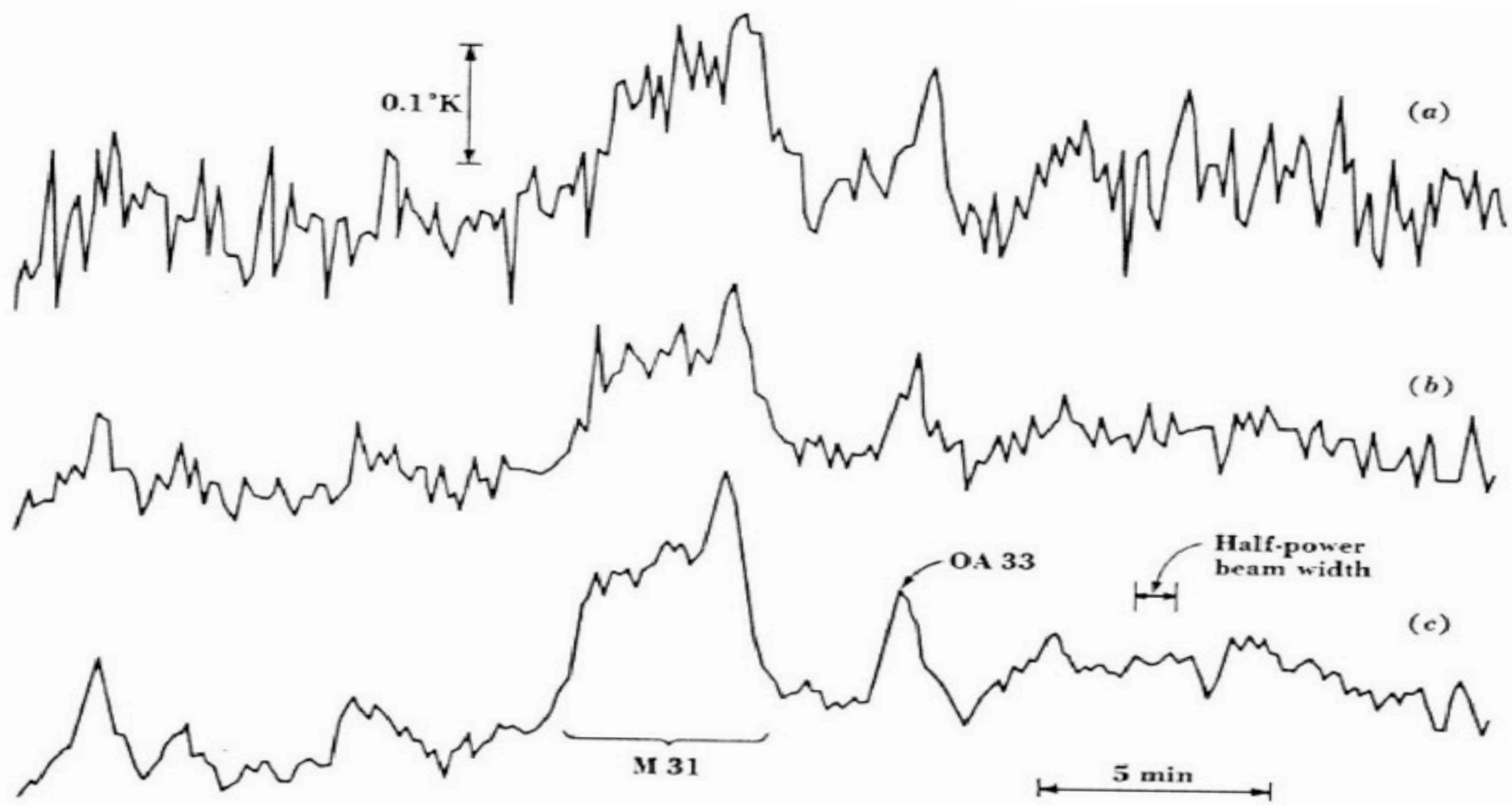

Fig. 3-26. Drift profiles through the nucleus of the Andromeda galaxy (M 31), made at 1,415 Mc with the Ohio State University 260-ft radio telescope, illustrating the reduction in noise fluctuation in going from one record (*a*) to the average of four records (*b*) and then to a threefold increase in integration time (*c*). In the bottom record M 31 stands out clearly with source OA 33 preceding it by several minutes.

• <u>Confusion</u>

Survey VLA 1.4 GHz at 5" resolution

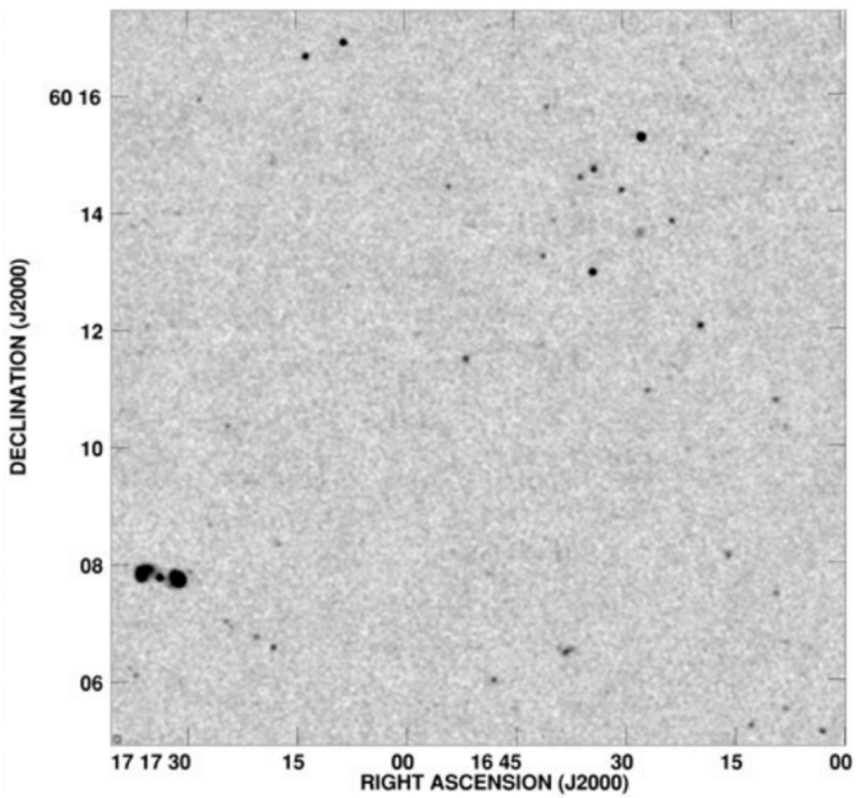

~Isotropic source distribution in
NVSS (NRAO VLA Sky Survey)
$\delta > 75°$, $S > 2.5$ mJy

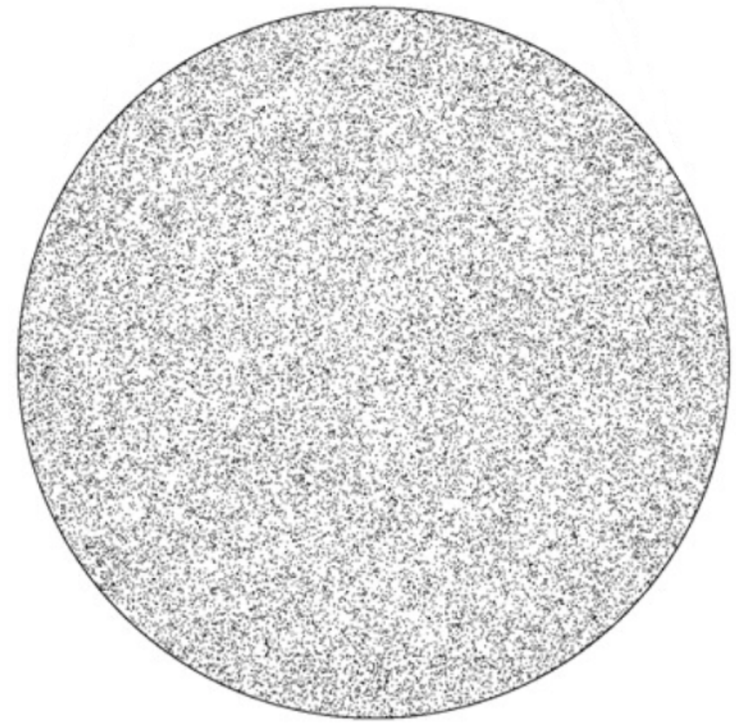

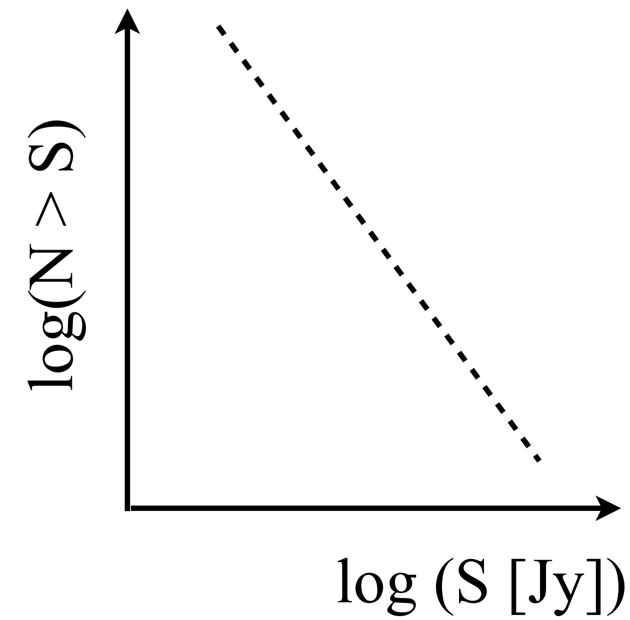

Confusion = spatial noise (imagery)
$\Longrightarrow$ empirical formulas

σ_c [mJy/beam] $\sim 0.2\ (\nu\ /\ \mathrm{GHz})^{-0.7}\ (\theta\ /\ \mathrm{arcmin})^2$
σ_c [K] $\sim 0.07\ (\nu\ /\ \mathrm{GHz})^{-2.7}$

[Condon 1974, 2002, 2005, 2012 ; Cohen, 2004]

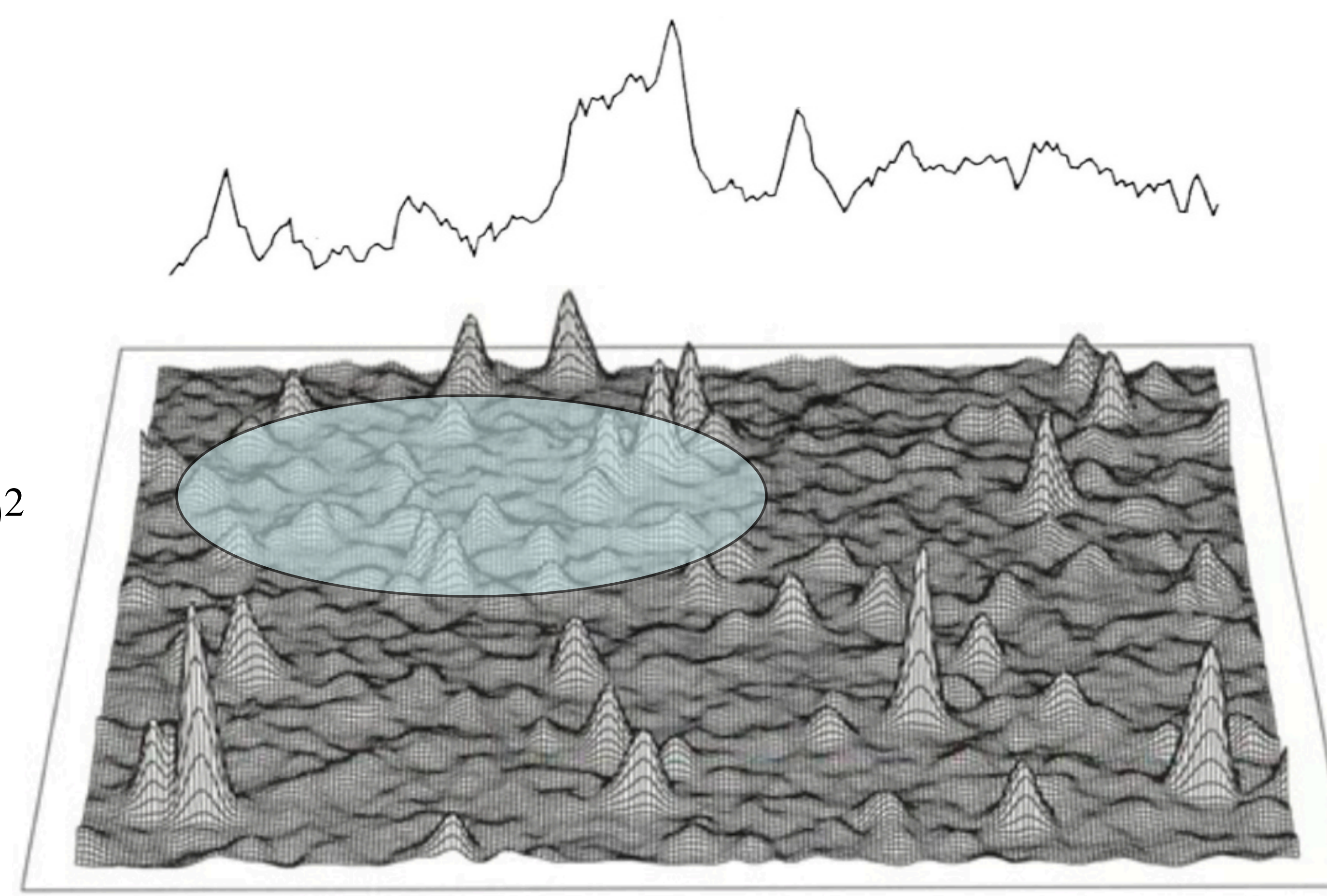

- <u>Primary calibration of radio astronomical measurements</u>

Thermostated resistor (T_R) connected to an antenna placed in an isotropic radiation field at T (black body)
$P(\nu)$ [R→antenna] = k T_R
$P(\nu)$ [transmitted by the (polarised) antenna →R] = k T

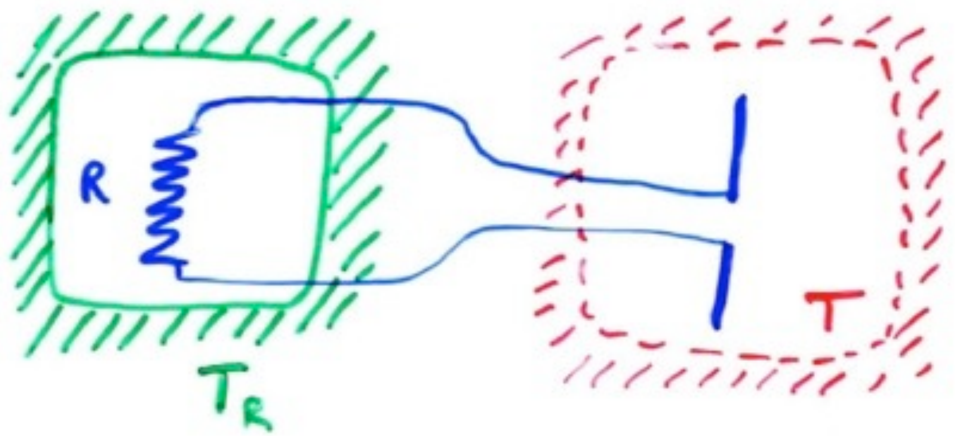

Energy exchange balance : $\Delta P = k\ |T - T_R|$
equilibrium for $T = T_R$

⇒ New definition of the antenna temperature of a radiation field : $T_A = T_R$
⇓
temperature of a resistor delivering the same spectral power as the antenna

⇒ radio astronomy measurement standard: black body and thermostated standard with known variable T (antenna or simple resistor in an enclosure at T)
→ T is adjusted to balance the signal ⇒ $T = T_A$ (source)

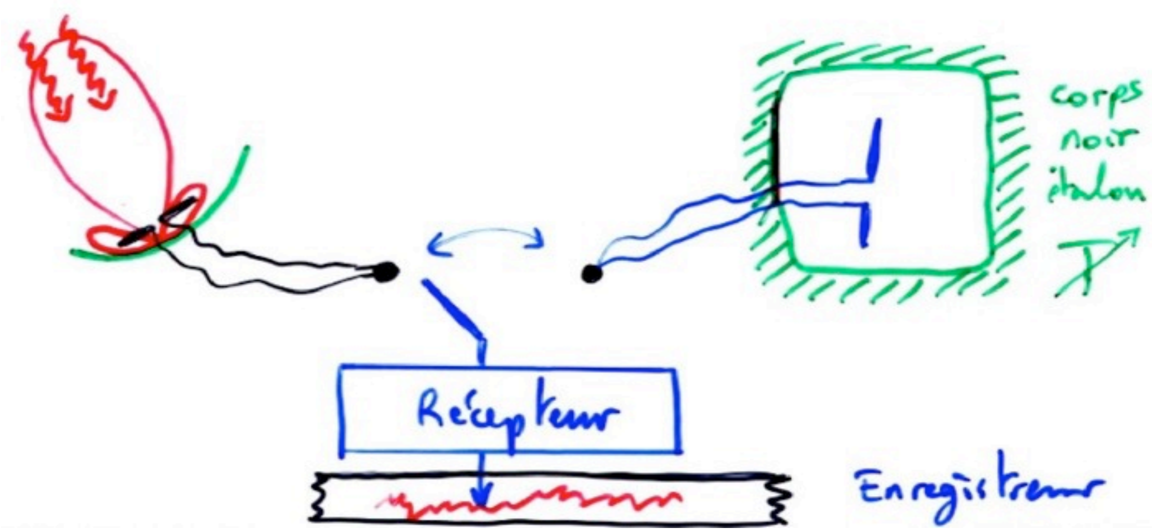

• <u>In practice, secondary standards are used:</u>

- well-calibrated radiosources (e.g. LOFAR flux calibrators)

Source	Kind	Band	RA (h m s)	DEC (° ' ")	I at 150 MHz	spectral index
3C196	Seyfert 1 Galaxy	LBA+HBA	08 13 36.07	+48 13 02.58	83.084	-0.699, -0.110
3C295	Seyfert 2 Galaxy	HBA	14 11 20.52	+52 12 09.86	97.763	-0.582,-0.298, 0.583,-0.363
3C147	Seyfert 1 Galaxy	LBA+HBA	05 42 36.26	+49 51 07.08	66.738	-0.022,-1.012,0.549
3C48	Quasar	LBA+HBA	01 37 41.30	+33 09 35.12	64.768	-0.387,-0.420,0.181
3C286	Quasar	LBA+HBA	13 31 08.3	+30 30 33	27.477	-0.158,0.032,-0.180
3C287	Quasar	LBA+HBA	13 30 37.7	+25 09 11	16.367	-0.364
3C380	Quasar	LBA+HBA	18 29 31.8	+48 44 46	77.352	-0.767

- radiosource catalogues (global sky models) :
VLSS (VLA LF -74 MHz- Source Survey)
MSSS (LOFAR's Multi-Snapshot Source Survey →
150 MHz, 60 MHz)
NED (NASA Extragalactic Database)

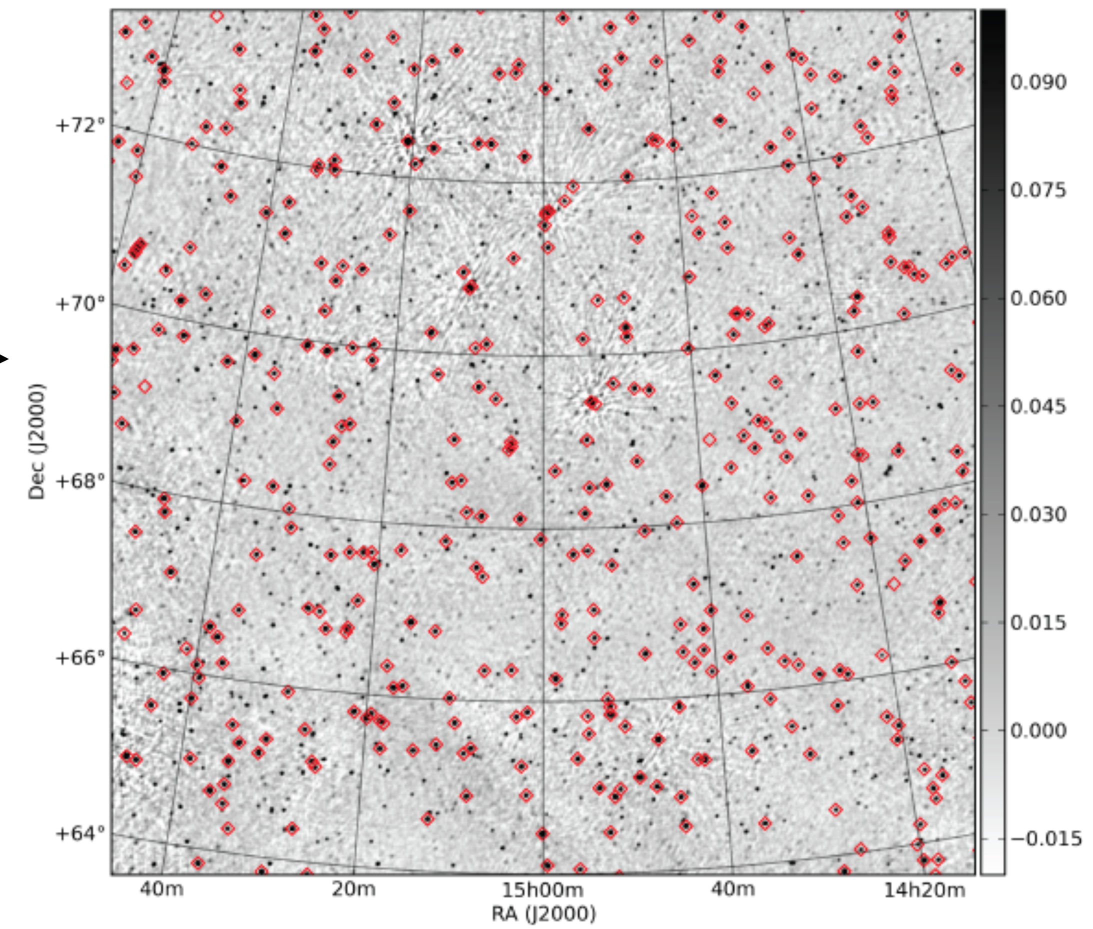

- noise sources (diodes) calibrated on reference radiosources

- Introduction (history, interest, specific features)
- Waves & Polarisation
- Plasmas & Propagation (cutoff, dispersion, Faraday effect, scintillations)
- Coherent Signal Detection (measurement theory, antenna temperature, calibration, noise)
- Receivers (heterodyne, system temperature, filtering, gain, RFI mitigation)
- Basics of Radio Astronomy Antennas: Single antennas
- Basics of Interferometry and Aperture Synthesis (phased arrays, electronic pointing, imaging, correlation, coherence, VLBI)
- Observation methods
- Large present & future ground-based radio arrays
- Basics of Space radio astronomy

• <u>Types of receivers:</u> measurement of S (or I), Q, U, V as a function of t, f, θ, φ

Spectrometry : *Spectral power density* $I\ (f,t)$

Polarimetry : *Stokes parameters* $I,Q,U,V\ (t)$

Imaging (e.g. interferometric): *Radio image* $I,Q,U,V\ (\theta, \varphi)$

Phase addition / Beamforming :

Formation of N 'independent' beams $I,Q,U,V\ (f,t)$

Waveform : *Amplitude and phase of E versus t*

Interference processing (RFI)

Dedispersion pulsars, detection of fast signals ...

} *«Intelligent» Receivers*

Combination of modes:

Ex: Multi-beam radio imager with N spectral channels

• Narrow-band spectrometry ⇒ Heterodyne receiver

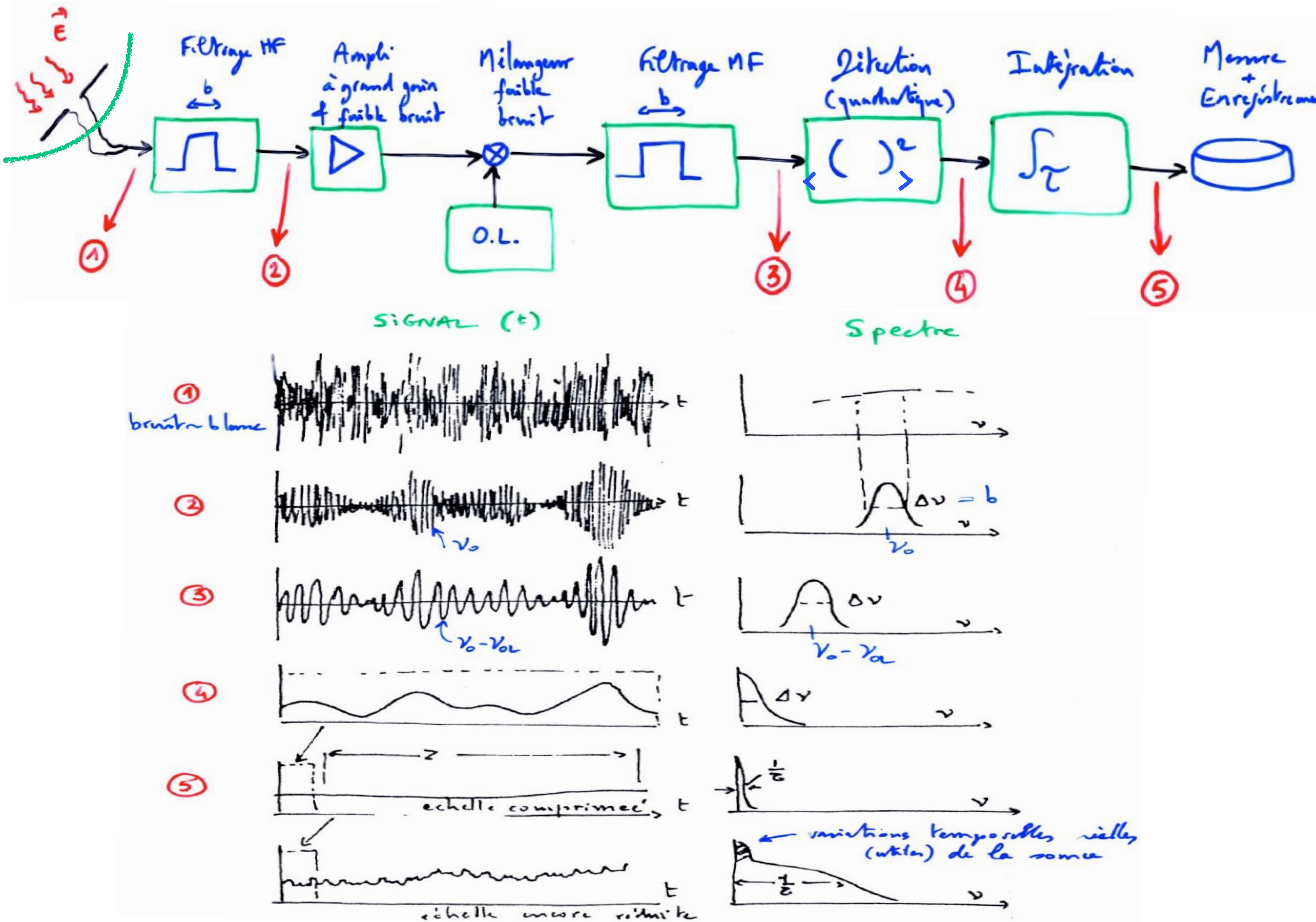

- <u>Narrow-band spectrometry ⇒ Heterodyne receiver</u>

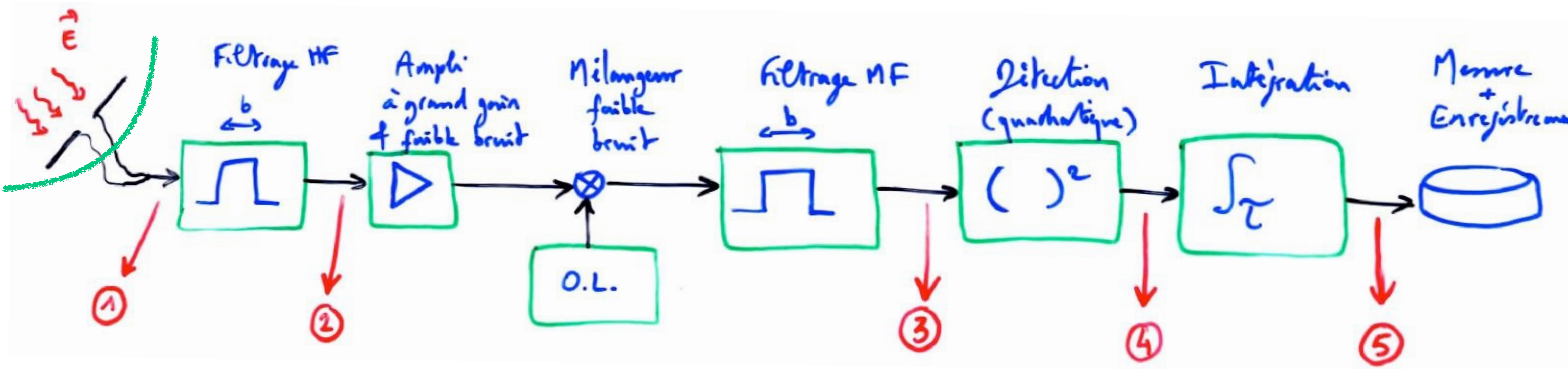

→ broadband incoming **E** ⇒ V_{in} broadband too

→ HF filtering ⇒ band selection $\nu_o \pm b/2$

→ 1st amplification (low noise)

} *Reverse order a HF*

→ × LO (local oscillator)

⇒ $\nu_o - \nu_{OL} \pm b/2 = \nu_{MF} \pm b/2$ (same fluctuations spectrum)

→ MF filtering

→ Detection, integration ...

Gain

$\rightarrow$ Input power is generally very low

Example : $T_A = 10\ K$ *in* $b = 10\ kHz \quad \Rightarrow P_e = k\, T_A\, b = 1.4\times10^{-18}\ W$

If you want to measure V ~1 mV at 50 Ω, you need an output power : $P_S = V^2 / 50 = 2\times10^{-8}$ W

$\Rightarrow$ Gain required $> \times10^{10}$ $\quad (G(dB) = 10 \log_{10}(P_S/P_e) = 100$ dB)

After detection (quadratic) and integration : $\langle V_S\rangle \propto P_S \propto G\, P_e$

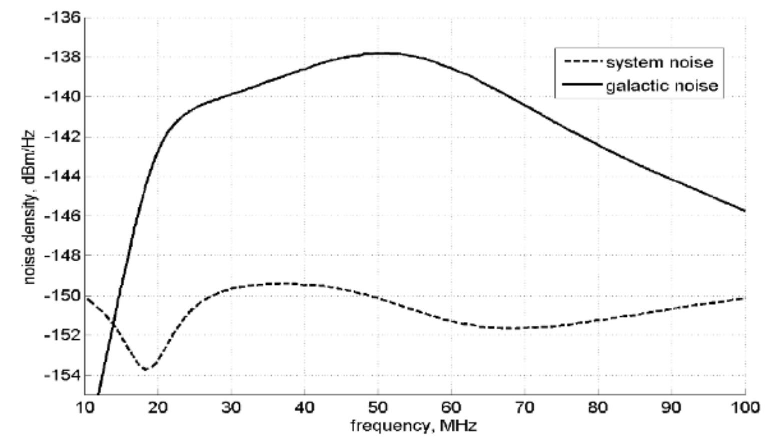

For a real receiver : $\langle V_S\rangle = \underline{\alpha\, G\, k\, b}\ (T_A + T_S)$

$\Downarrow$

can be calibrated with a reference source

Multi-stage receiver : $\langle V_S\rangle \propto G_n (\ldots G_2 (G_1 (T_A + T_1) + T_2) + \ldots + T_n) \sim \Pi G_i\, (T_A + T_S)$

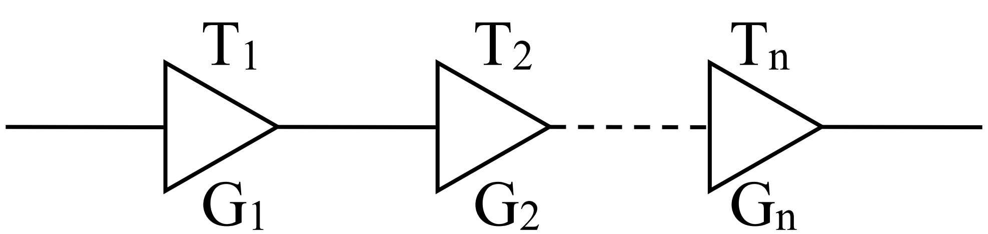

$$T_S = T1 + \frac{T2}{G1} + \frac{T3}{G1G2} + \ldots \frac{Tn}{\prod_{i=1}^{i=n-1} Gi}$$

Friis formula for n stages of gain G_i with noise temperature T_i

Only the first stage (G_1,T_1) should be ultra-low-noise

G_i must be high enough for T_i (i>1) be negligible $\Rightarrow$ in general $G_1 \geq 30$ dB is required

Notes :

- *In a receiver, gain is provided by the amplifiers; all other stages create losses.*
- *The linear operating range is the range where G does not depend on input power.*

Stability

$\Rightarrow$ Fluctuations : $\Delta \langle V_S \rangle / \langle V_S \rangle \;=\; \Delta(T_A + T_S)/\,(T_A + T_S) \;+\; \Delta G/G$

if $T_A \ll T_S$ $\qquad \approx\; \Delta T_S/T_S \;+\; \Delta G/G \;\approx\; 1/\sqrt{(b\tau)} \;+\; \Delta G/G$

Theoretical sensitivity $T_S/\sqrt{(b\tau)}$ is only achieved if the relative stability of gain / t

$\Delta G/G \ll \Delta T_S/T_S \;=\; 1/\sqrt{(b\tau)}$

If G fluctuates too much (thermal fluctuations, power supply ...), its fluctuations may mask those of T_A due to a possible source.

Example : *if* $\Delta G/G = 0.1\%$ *with* $\tau = 100$ *sec,* $b = 1$ *MHz*

$\Rightarrow \quad \Delta G/G = 10^{-3} \;\gg\; \Delta T_S/T_S \;=\; 1/\sqrt{(b\tau)} = 10^{-4}$

If $T_S = 150$ *K,* $\Delta T_G = 0.15$ *K* $\;\gg\; T_S/\sqrt{(b\tau)} = 0.015$ *K* *hence* $T_{A\text{-}min} \approx \Delta T_G$

$\rightarrow$ Solutions used :

- quality of components used

- thermal regulation & receiver power regulation

- differential ON / OFF or sky / calibrator measurements :
    rapid permutation $\gg 1/\Delta t_{Gain}$
    simultaneously in multiple beams
    or at slightly different frequencies (spectral measurements)

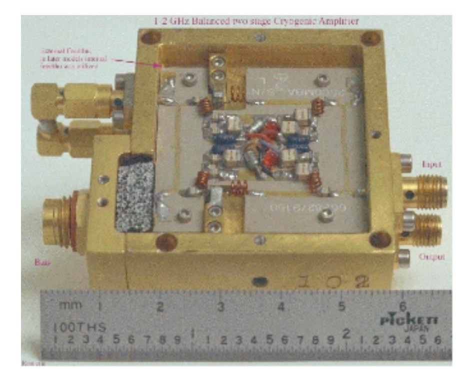

discrete components

LNA

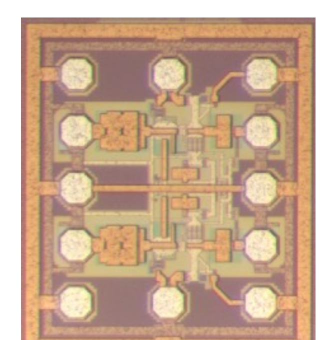

integrated circuit ($0{,}63 \times 0{,}73$ mm^2)

→ *Measuring receiver stability*

The "Allan variance" describes the competitive behaviour of statistical functions with different spectra involved in real measurements
= Variance of a series of N measurements Vi_τ of integration time τ (total duration = $N\times\tau$)
as a function of the value of τ : $\sigma^2(\tau) = (1/N)\,\Sigma\,(Vi_\tau - \langle Vi_\tau \rangle)^2$

It can be shown that if the spectrum of the measured signal is : $P(\nu) \propto \nu^\beta$ then $\sigma^2(\tau) \propto \tau^{-\beta-1}$

$\beta = 0 \;\Rightarrow\; P(\nu) = C^t$ *(white noise)* $\;\Rightarrow\; \sigma^2(\tau) = C^t/\tau$

$\beta = -1 \;\Rightarrow\; P(\nu) \propto 1/\nu$ *("1/f" noise)* $\;\Rightarrow\; \sigma^2(\tau) = C^t$

$\beta = -2 \;\Rightarrow\; P(\nu) \propto 1/\nu^2$ *(noise ↑ at LF)* $\;\Rightarrow\; \sigma^2(\tau) = C^t \times \tau \;\Rightarrow\; \uparrow$ *with* τ

(generally due to the slow drift of the system's gain)

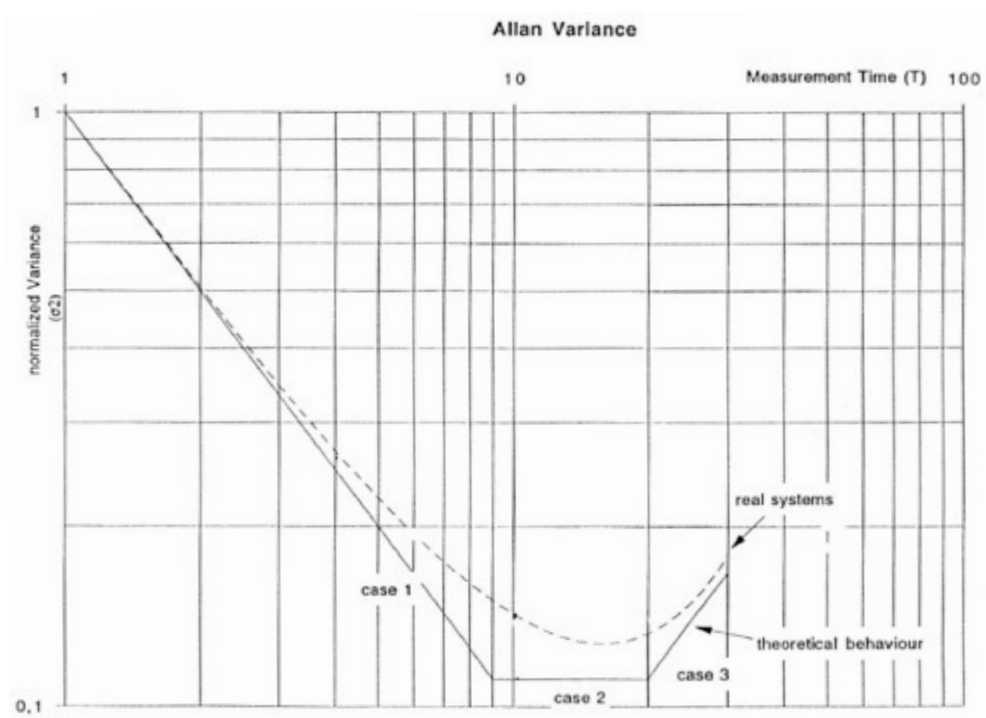

⇒ *$\sigma^2(\tau)$ characterises the receiver's stability and is used to select the optimum operating range = min($\sigma^2(\tau)$) which gives the maximum time during which the receiver can be used without recalibration*

Filtering

- Low pass (LP) : cuts $\nu > \nu_2$
- High pass HP) : cuts $\nu < \nu_1$
- Band pass (BP) : cuts $\nu < \nu_1$ and $\nu > \nu_2$
- Rejection : cuts $\nu_1 < \nu < \nu_2$

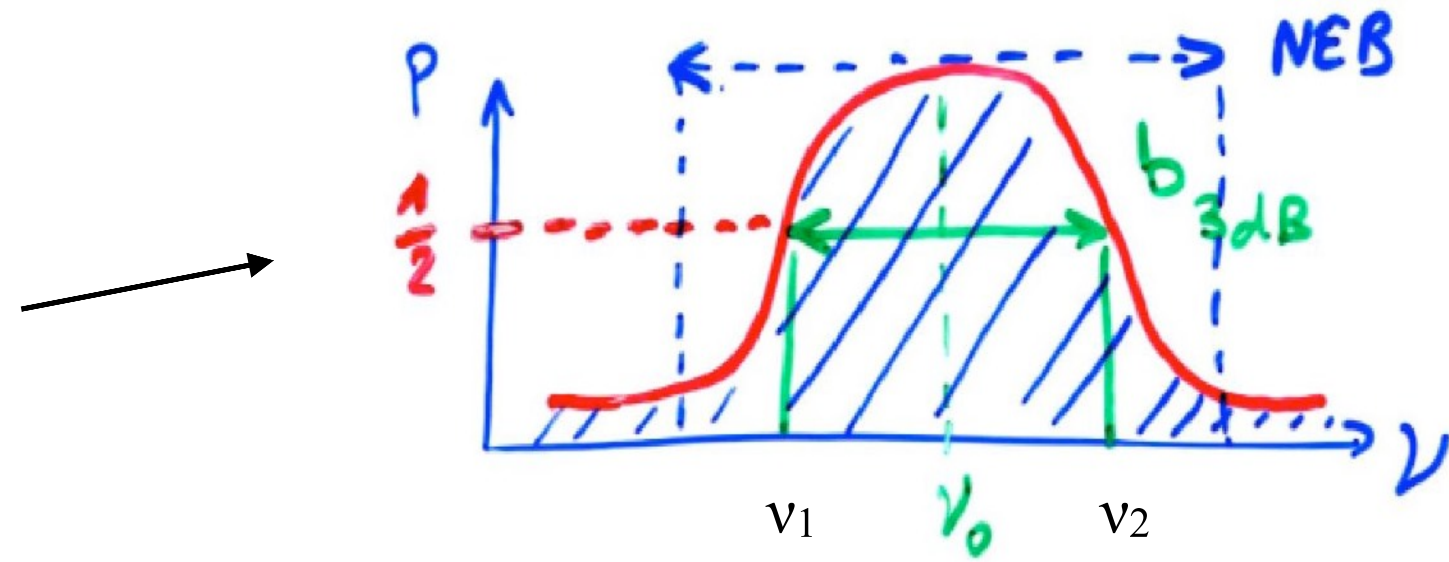

ν_1 and ν_2 define the bandwidth, generally at - 3 dB : $b_{3\ \mathrm{dB}} = \int_{P(\nu)\geq P(\nu o)/2} P(\nu)\, d\nu \,/\, P(\nu_o)$

$\forall$ filter shape, we can define an equivalent band : $b_{eq} = {}^{+\infty}\!\int_{-\infty} P(\nu)\, d\nu \,/\, P(\nu_o)$

$\rightarrow$ It can be measured via : $b_{eq} = <V_S>^2 / \sigma^2 \tau$ = NEB (Noise Equivalent Band)

($b_{3\ \mathrm{dB}} <$ NEB)

<u>Filtering</u>

Characteristics :

- ripple in the frequency band
- in-band delay or phase shift (important for interferometers and phased arrays)
- out-of-band rejection value
- selectivity = slope of transition zone between passband and rejected band
- losses

(5,2×2,3 mm²)

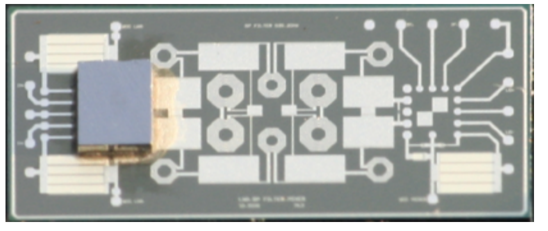

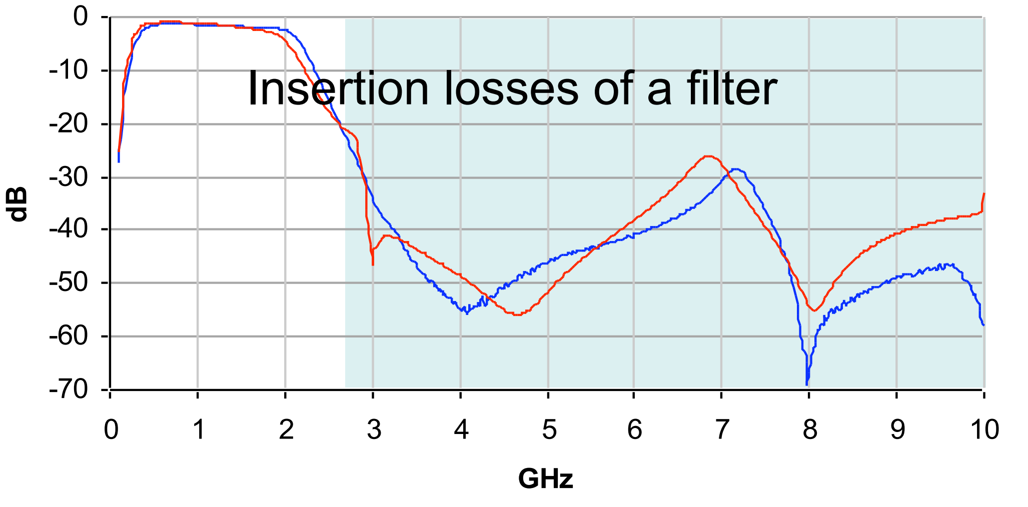

A filter is necessary :

- before a mixer: elimination of the image band
- at each stage: reduction of the band that contains noise

  ⇒ dynamic range increase + noise/RFI filtering

- before LNA in LF (elimination of noise picked up by the antenna) <u>BUT not in HF</u> because losses increase T_S (-0.5 dB ↔ T_S + 35 K !) unless superconducting filter+cryogenics are used

Frequency transposition

→ Mixer (×) and local oscillator (LO)

> Reminder : $TF[\ E(t)\ ] = E(\nu)$
>
> $TF[\ E(t).\cos(2\pi\nu_{LO}t)\ ] = ½\ [\ E(\nu\text{-}\nu_{LO}) + E(\nu+\nu_{LO})\ ]$
>
> $E(-\nu) = E(\nu)^* \quad \Rightarrow \quad P(-\nu) = P(\nu)$

Mixer = non-linear element giving an output frequency $\nu = \nu_{MF} = \pm\, m\times\nu \pm n\times\nu_{LO}$

- if we keep $\nu_{MF} = \nu + \nu_{LO}$ the receiver is called supradyne
- if we keep $\nu_{MF} = \nu - \nu_{LO}$ or $\nu_{LO} - \nu$ depending on whether $\nu > \nu_{LO}$ or $\nu < \nu_{LO}$ the receiver is called infradyne

We also have : $|\varphi_{MF}| = |\varphi_o\text{-}\varphi_{LO}|$

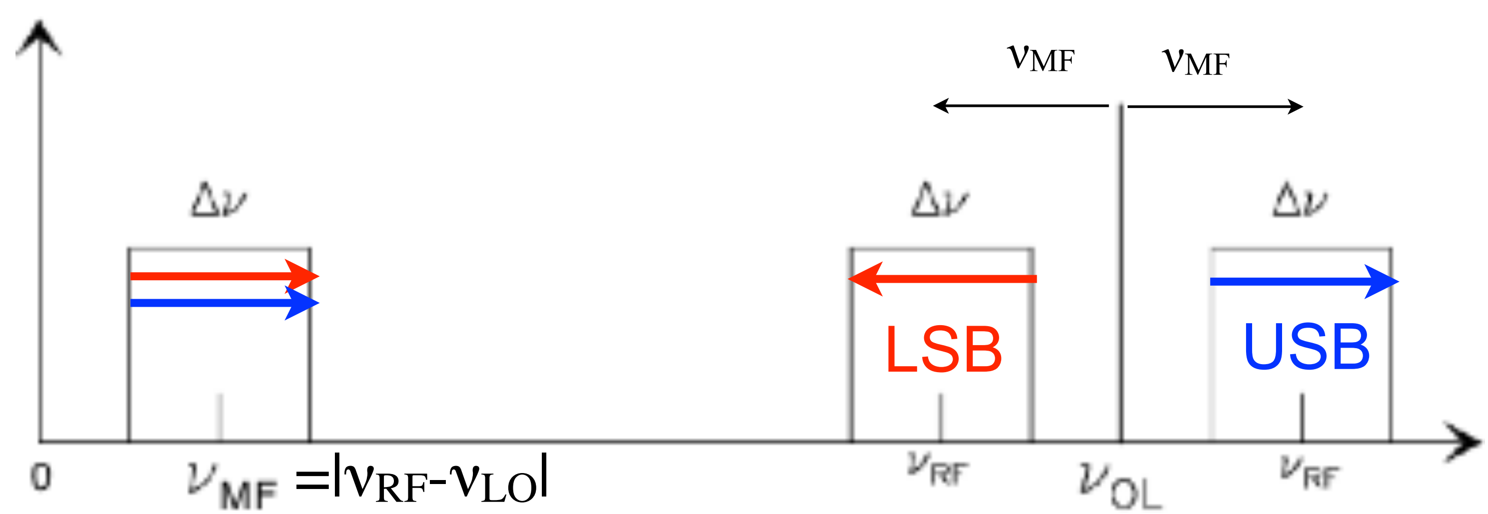

Notes :

- *the same MF frequency can be given by* $\nu_{MF} = \nu_1 - \nu_{LO} = \nu_{LO} - \nu_2$ *= folding*
- *if the 2 RF frequencies are used (which then overlap and are indistinguishable), the indistinguishable) the receiver is "double side band" (DSB).*
- *in general, only one is used (single side band = SSB) ; a distinction is made between upper side band = USB and lower side band = LSB.*

Local Oscillator (LO)

- fixed or adjustable (at least one adjustable stage s required to bring a broadband signal to a fixed ν_{MF})

Super-heterodyne receiver : 2 frequency changes (2 LO)

1) transition to HF : $\nu \rightarrow \nu_{LO1}-\nu$ (steeper anti-aliasing filtering possible), ν_{LO1} can be variable

2) transition to MF : $\rightarrow \nu_{LO2}-(\nu_{LO1}-\nu)= \nu-(\nu_{LO1}-\nu_{LO2})$,

- must be very stable :

→ in single dish : minimum spectral resolution required

(Ex: $\Delta\nu = 10$ Hz with $\nu_{LO} = 10$ GHz $\Rightarrow$ stability 10^{-9})

→ in interferometer and phased array : must preserve phase and coherence

⇒ much more severe constraints

⇒ LO time reference based on atomic clock

(Rubidium : $\approx 5\times10^{-12}$, Cesium : $\approx 10^{-12}$, Hydrogen Masers : $\approx 10^{-13/-14}$)

Detection, integration

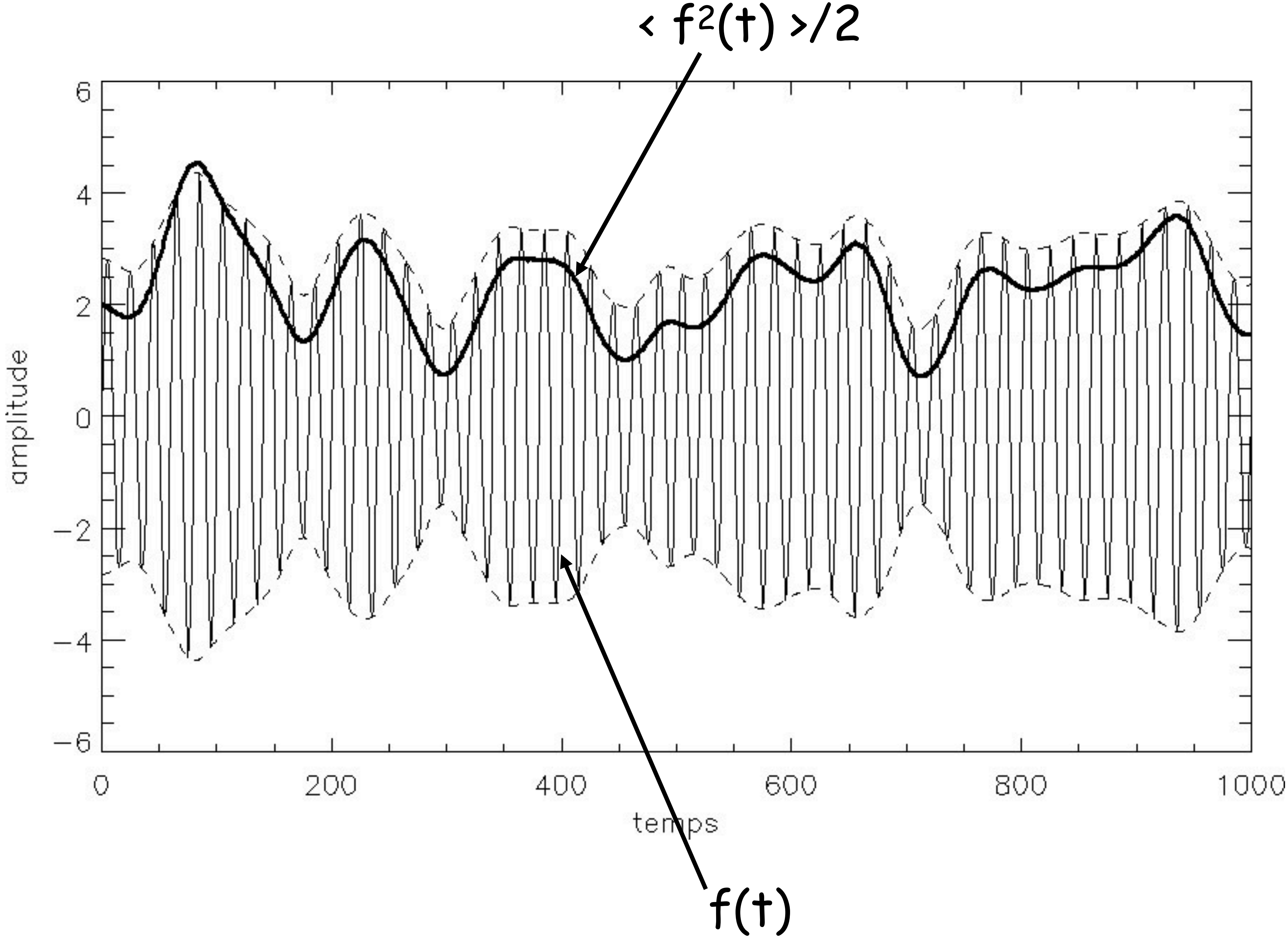

Analog $\rightarrow$ Digital conversion

Classic sampling : $\nu_{sampling} \geq 2\ \nu_{max}$ (Shannon)

What sampling actually does : $E(t) \rightarrow E(t-nt_o) = E(t) \times \delta(t-nt_o)$ $n = -\infty, +\infty$

$E(\nu) \rightarrow E(\nu) \otimes \delta(\nu-n\nu_o)$ with $\nu_o = 1/t_o$

$= E(\nu) + E(\nu - \nu_o) + E(\nu + \nu_o) + E(\nu - 2\nu_o) \ldots$

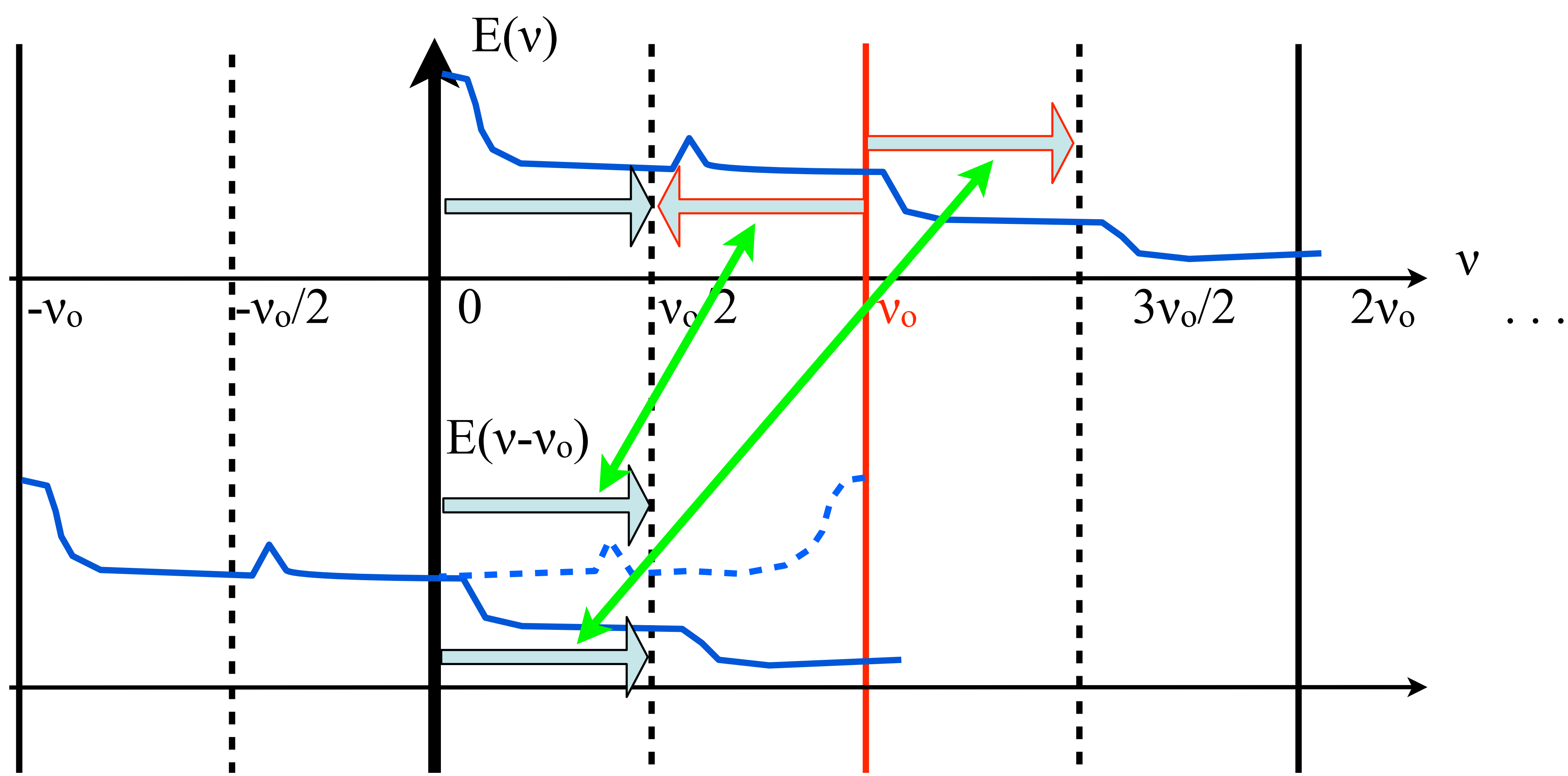

Nyquist Zones : I II III IV V . . .

Analog → Digital conversion

Classic sampling : $\nu_{sampling} \geq 2\ \nu_{max}$ (Shannon)

What sampling actually does : $E(t) \rightarrow E(t\text{-}nt_o) = E(t) \times \delta(t\text{-}nt_o)$ $n = -\infty, +\infty$

$E(\nu) \rightarrow E(\nu) \otimes \delta(\nu\text{-}n\nu_o)$ with $\nu_o = 1/t_o$

$= E(\nu) + E(\nu - \nu_o) + E(\nu + \nu_o) + E(\nu - 2\nu_o) \ldots$

⇒ Spectrum folding

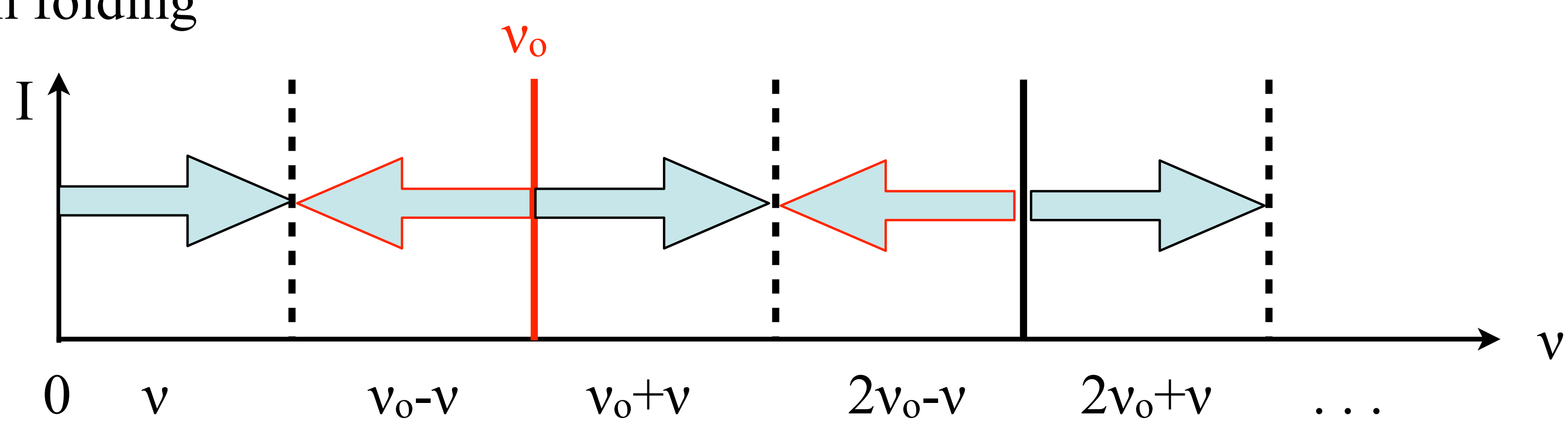

Nyquist Zones : I II III IV V . . .

⇒ Subsampling possible

⇒ Analog input filtering required to avoid aliasing

ex: LOFAR

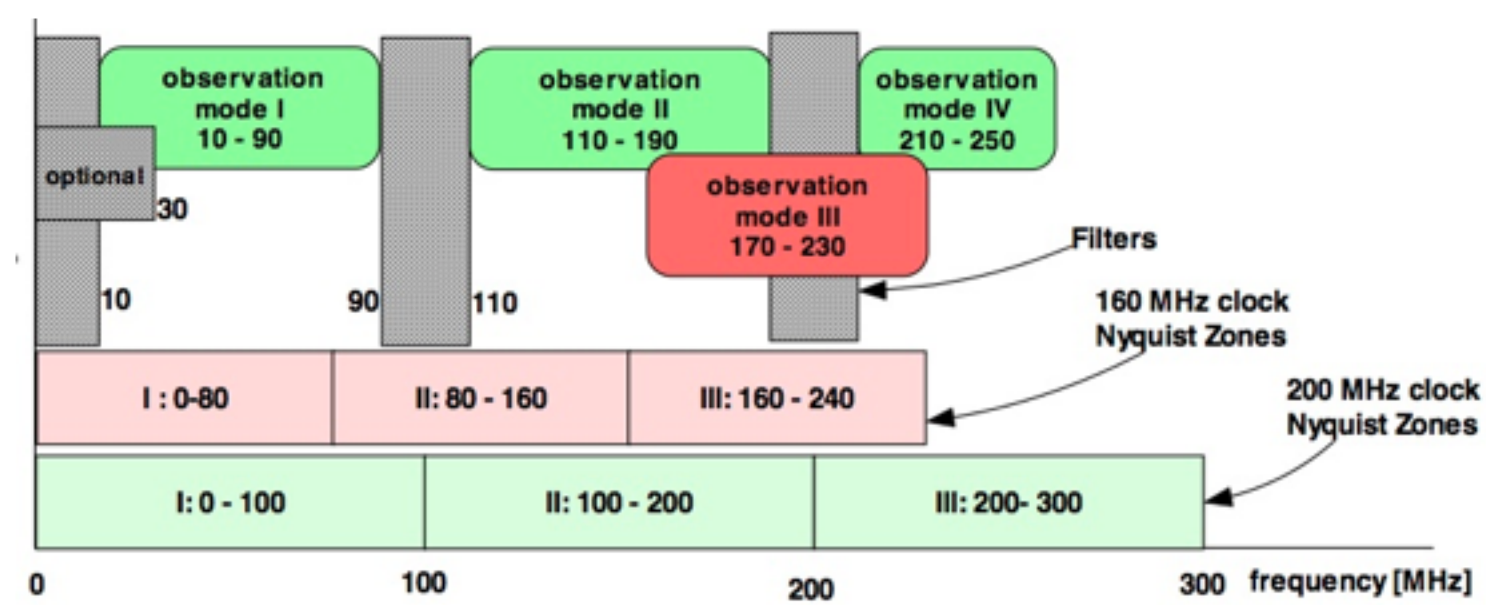

Analog → Digital conversion

Discretises an analog signal into $k = 2^N$ levels (for binary coding)

Signal → ADC → Signal + **noise** and spectrum duplications

- discretisation noise
  (S/N ≈ 3 or 6 dB × Nbits → see dynamics)
- noise due to clock jitter
- non-linearities ...

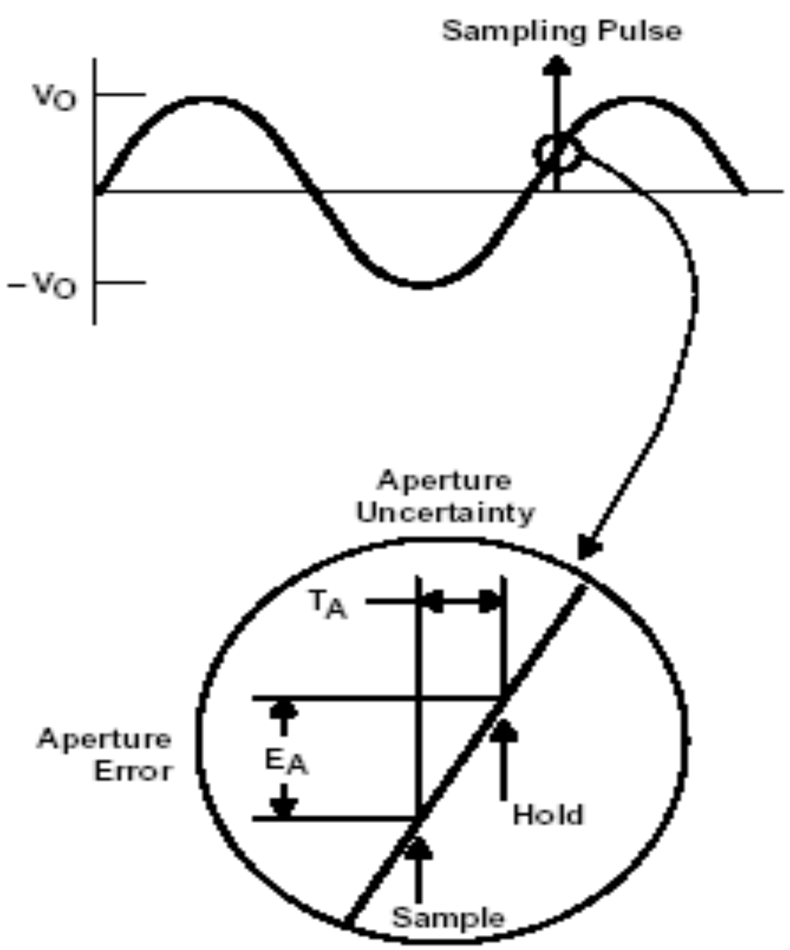

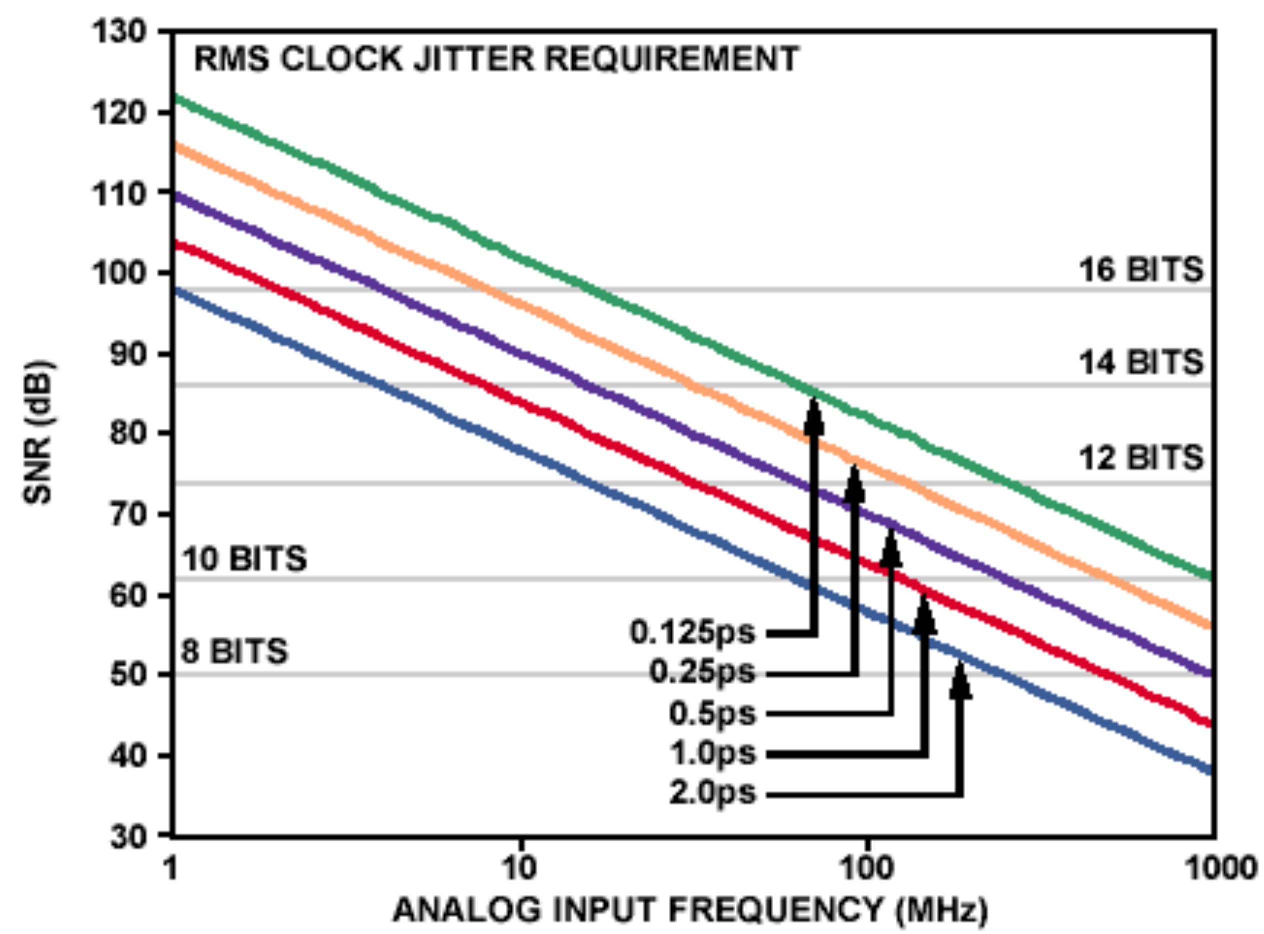

• <u>Parameters defining receiver efficiency</u>

→ Overall / instantaneous spectral band covered : Δf

Limited by the « front end »
(input electronics)
Ex: - Nançay RT : 1,06 GHz - 3,5 GHz
- LOFAR : 30 - 90 MHz et 110 - 250 MHz
- SKA-mid : ~300 MHz - 20 GHz

Fixed by MF & analysis means
Ex: - Nançay RT : 4 ×50 MHz max.
- LOFAR : 2 ×48 MHz
- SKA : 200 MHz a qq GHz

→ Spectral resolution (absolute, relative) : δf ($\approx$ or $\neq$ b), $\delta f/f$
$\Rightarrow N_{freq} = \Delta f / \delta f$ number of frequency channels (per spectrum)

→ Temporal resolution : δt between 2 successive measurements
at the same frequency (i.e. from one spectrum to the next)
$\Rightarrow$ $\delta t \approx N_{freq} \times \tau$ (swept-frequency receiver)
or $\delta t \approx \tau$ (multichannel)

$\Rightarrow$ Data rate = $N_{bit} \times N_{freq} / \delta t$ (bits/sec)

→ Maximum continuous observation time : Δt

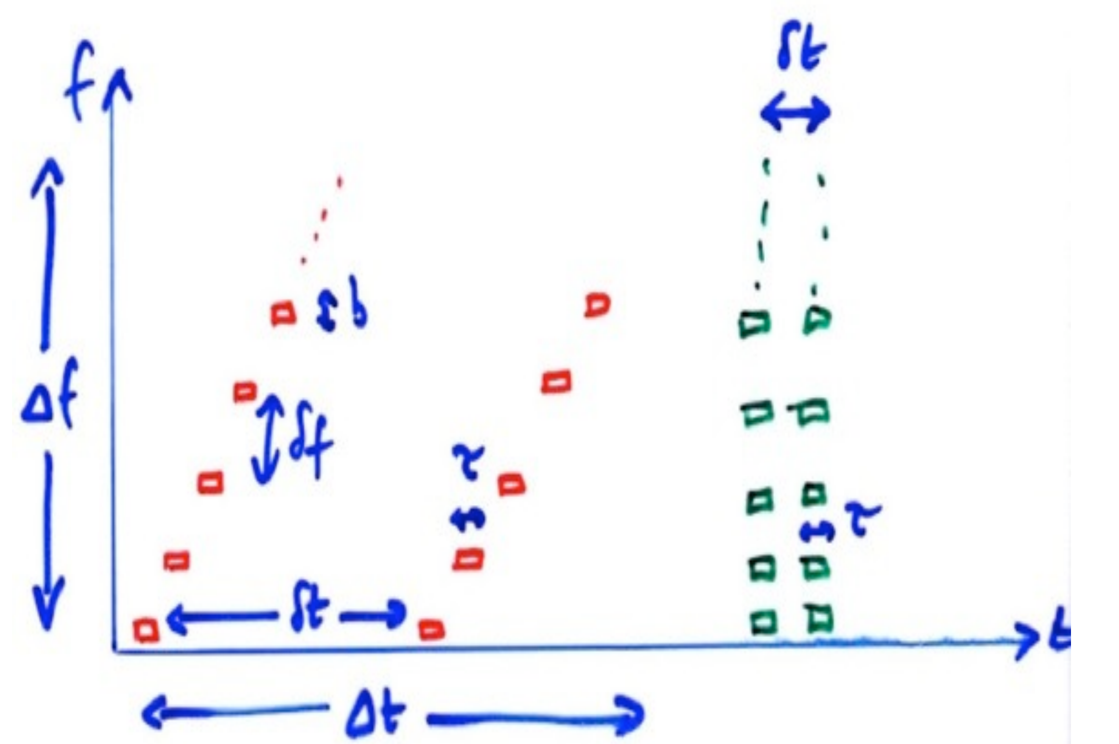

→ Noise temperature : $T_N = K\, T_S / \sqrt{(b\tau)}$ with $K \sim 1$

Noise factor (NF) = $10 \log_{10} (T_S/T_o + 1)$ (in dB)
with by definition : $T_o = 290$ K

Ex: $T_S = 290\ K \Rightarrow F = 3\ dB$
$T_S = 75\ K \Rightarrow F = 1\ dB$
$T_S = 50\ K \Rightarrow F = 0{,}7\ dB$
$T_S = 7\ K \Rightarrow F = 0{,}1\ dB$

NF of an integrated LNA for SKA

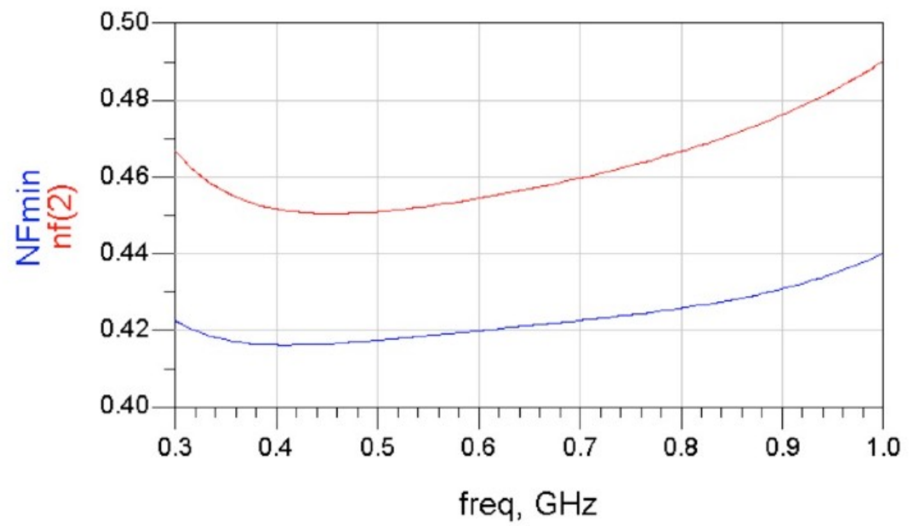

The state of the art (cryogenics) is $T_S \approx$ 1-2 K / GHz

<u>*Ex*</u> : *SKA sensitivity* = $A_e/T_S = 20\,000\ m^2/K$
Specification : $T_S = 50\ K$
If we manage to reduce T_S *to 45 K, we obtain the same sensitivity for* $A_e = 9 \times 10^5\ m^2$ *instead of* $10^6\ m^2 \Rightarrow$ *large cost saving !*

→ Dynamic range :

Analog : $D = T_{max}/T_{min}$ measurable without distortion
(limited upwards by saturation and downwards by noise)

Digital : $D = N_{bit} \times 3$ dB for a quadratic receiver
$T_{dB} = 10\times\log_{10}(T_{max}/T_{min}) = 10\times\log_{10}(V_{max}/V_{min})$

$N_{bit} \times 6$ dB for a linear receiver
$T_{dB} = 10\times\log_{10}(T_{max}/T_{min}) = 10\times\log_{10}(V^2_{max}/V^2_{min}) = 20\times\log_{10}(V_{max}/V_{min})$

If T_N is sampled on > 1 bit, better dynamic resolution at low levels, but reduced dynamic range
If T_N is sampled on << 1 bit, discretisation error and lower sensitivity at low levels.

Linearity :

- Constant gain in the linear range drops off at saturation
- Compression point at - 1dB, where gain drop = 1 dB
$\Rightarrow D = P_{-1dB} / kT_S\, b\, G$

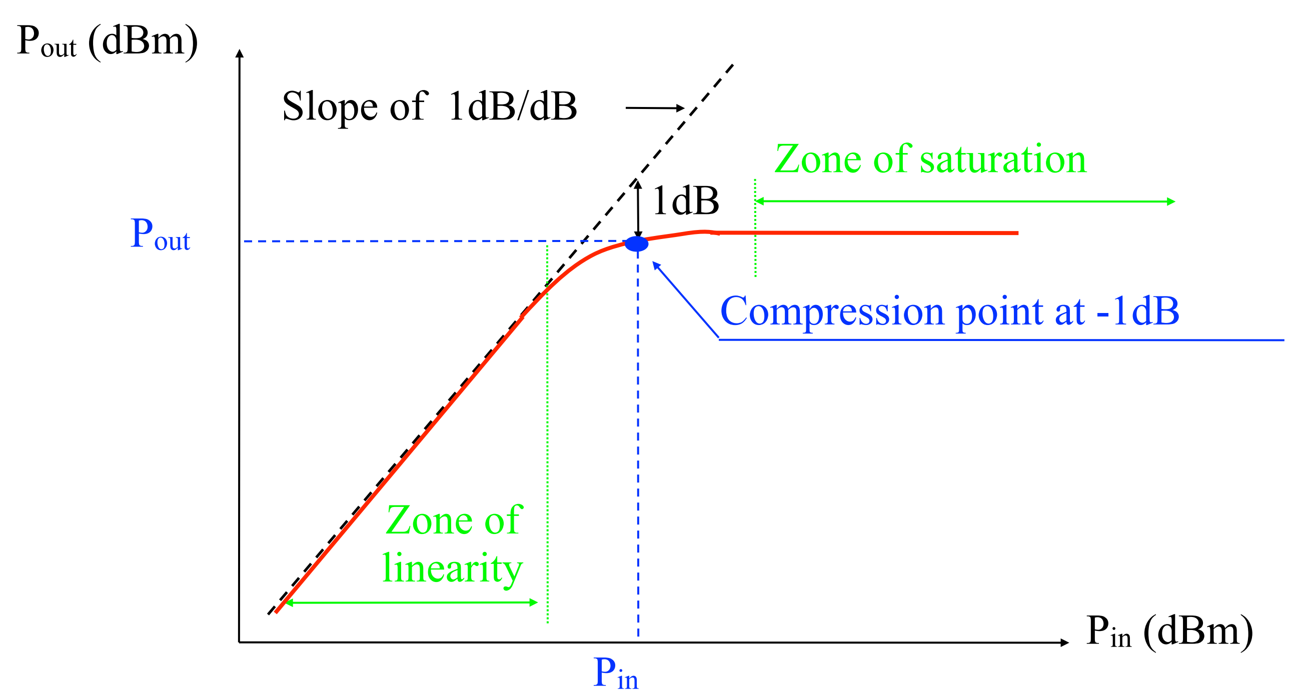

Ex : Input stage of Embrace (SKA demonstrator) :
- LNA with an equivalent noise band : NEB = 700 MHz, G = 18 dB, T_S = 50 K
P-1dB = 0 dBm = 1 mW $\Rightarrow$ *D = 75 dB*

- <u>Types of spectrometers</u>

	D	Δf	δf, $\delta f/f$	N_{freq}	δt	Δt	Rate	Remarks
Filter bank (multichannel)		–		dozens	+			heavy, cumbersome, not flexible, expensive
Frequency scanning spectrum analyser (SFA, SFR) = (Super-)heterodyne receiver with variable O.L.	+ ≥ 60 dB	+ ~f	+ ≤%	+ $\sim\Delta f/\delta f$	– $\delta f \times \tau \gg 1$ $\Rightarrow$ $\delta t \gg N/\delta f$ ~sec	+	~ ko/s	stability Ok, low t-f plane coverage, sensitivity $\propto 1/N$
Acousto-Optical Spectrograph (SAO)	– ≤ 25 dB	+ ~f, up to 1 GHz	+ ~%	+ hundreds	+ msec	–	01-1 Mo/s	low stability (~min), compact, complete coverage of t-f plane
• Correlators (digital): TF spectrum of the autocorrel function (Wiener-Khintchine) • TF receivers (digital - FFT, Welch estimator) • Polyphase filters	++ N_{bit}, ≥65 dB	+ ALMA 2 GHz, GBT 800 MHz	+ ≤%	+ thousands	+ msec	–	a few × Mo/s	flexibility in band selection and resolution, stability
Waveform sampler	N_{bit}	$\leq f_{sampling}/2$ ~100 MHz	++ only limit : $\delta f \times \delta t \gg 1$			– –	a few 100s Mo/s	snapshots

• <u>Autocorrelation spectrometers</u>

Discrete calculation of $C_{xx}(\tau) = \langle x(t).x(t-\tau)\rangle$ Δt between 2 samples

$\Rightarrow$ $C_{xx}(n\times\Delta t) = 1/(n+1) \; {}_{k=0}\Sigma^{n} \; x(k\times\Delta t).x((k-n)\times\Delta t)$

then of the spectrum $P(f)$ [WHz^{-1}] = $TF(C_{xx}(\tau))$ [Wiener-Khintchine Theorem]

$\Rightarrow$ $P(p\times df) = {}_{k=0}\Sigma^{n-1} \; C_{xx}(k.\Delta t)\times exp(-i2\pi f.k.dt)$ *with* $p = 0, 1, ..., n-1$

$f = p\times\Delta f$, $\Delta f = 1/(n\times\Delta t) = F_{sampling}/n$

Digital vs. analog correlation :

- Depends on signal discretisation at correlator input (Number of levels & $F_{sampling}$)

- 1-bit correlation (2 levels): only the sign of the signals is retained during digitisation

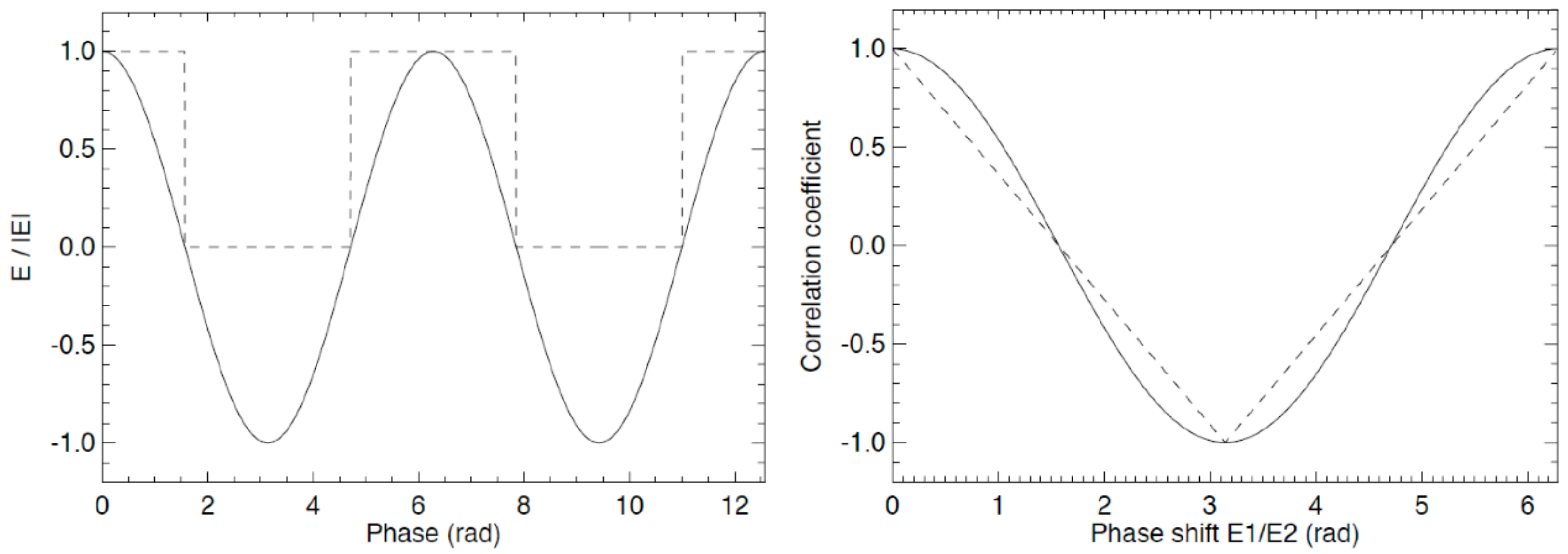

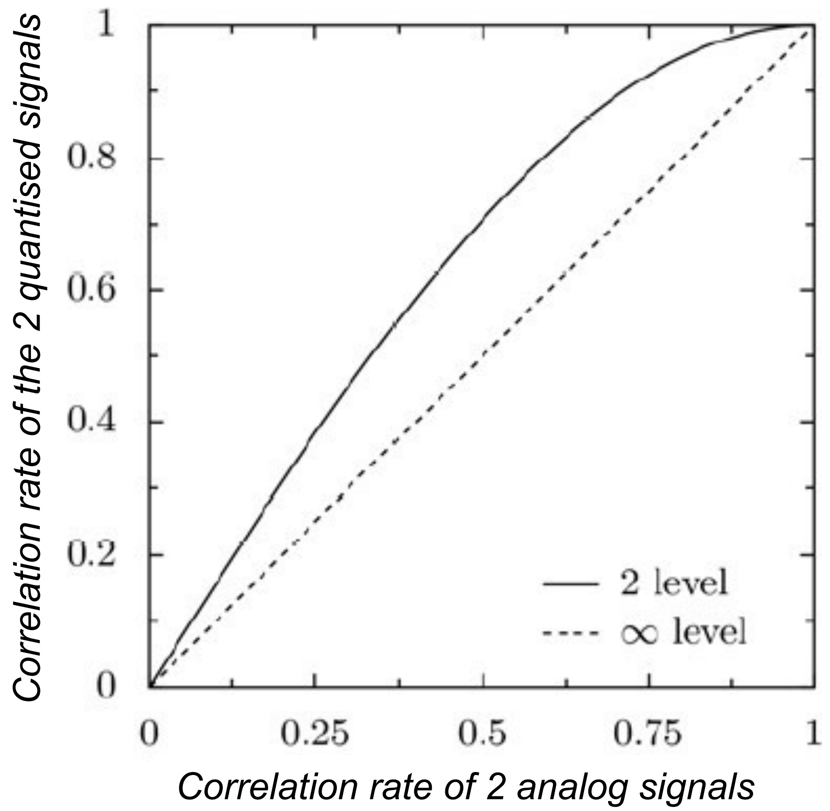

- *Van Vleck* correction to linearise autocorrelation result before FFT

- <u>Direct TF spectrometers</u>

  - Spectral response (Power Spectral Density) = $|FFT|^2$, depends on the weighting window used which modifies the width of the lobe at half power, the level of the secondary lobes and the gain.

Rectangular (porte) : $h(t)=1$ *for* $t \in [0,T]$ $\Rightarrow$ $h(f) \sim sinc(x)$ *with* $x = \pi f T$

Triangular (Bartlett): $h(t)=2t/T$ *for* $t \in [0,T/2[$ $\Rightarrow$ $h(f) \sim sinc^2(x/2)$
$h(t)=2(T-t)/T$ *for* $t \in [T/2,T]$

Hann: $h(t)=0.5-0.5\times\cos(2\pi t/T)$ *for* $t \in [0,T]$
Hamming: $h(t)=0.54-0.46\times\cos(2\pi t/T)$ *for* $t \in [0,T]$ $\Rightarrow$ *broader, no secondary lobe*

Blackman-Harris: $h(t)=0.42-0.5\times\cos(2\pi t/T)+0.08\times\cos(4\pi t/T)$ *for* $t \in [0,T]$ $\Rightarrow$ *intermediate, steeper*

Time profile of window

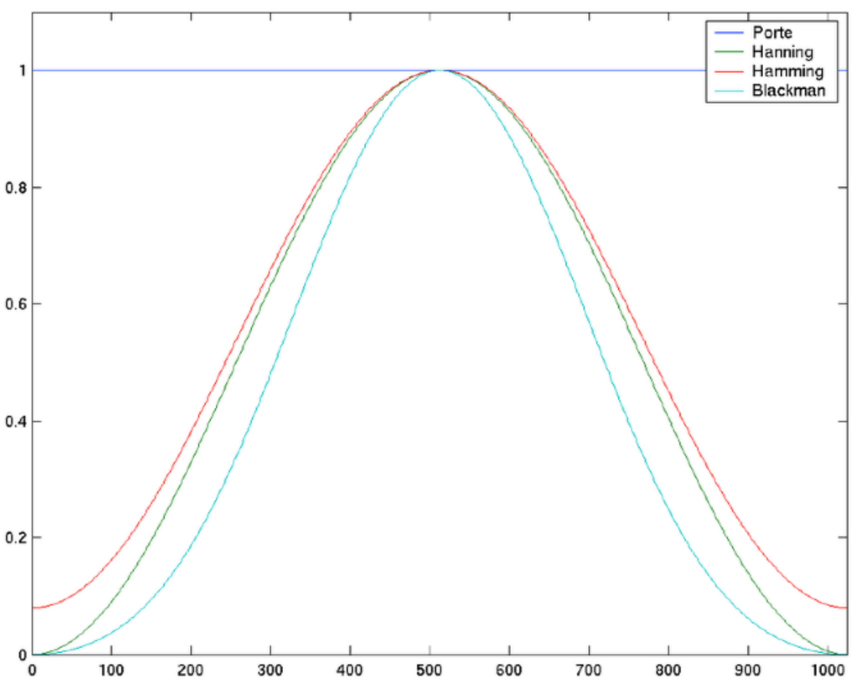

Spectral profile of window

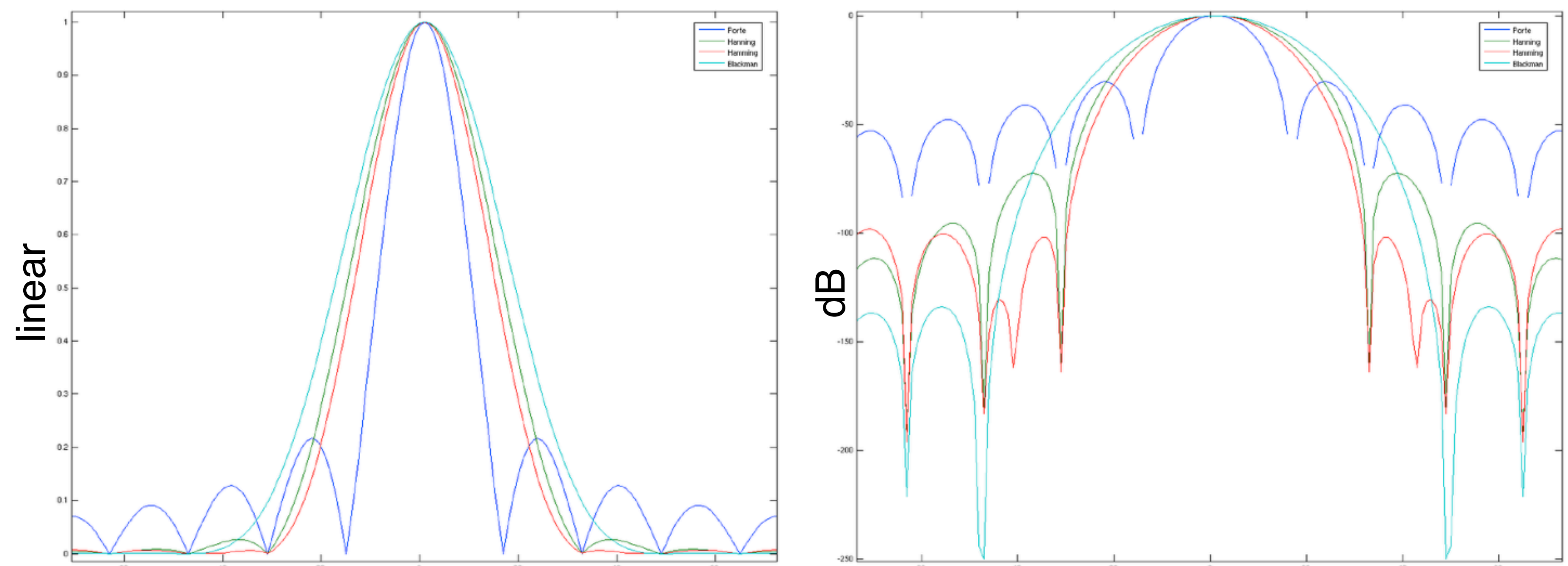

Window	Level of secondary lobe (dB)	Slope (dB/octave)	Bandpass (bins)
Rectangular	-13	-6	1.21
Triangular	-27	-12	1.78
Hann	-32	-18	2.00
Hamming	-43	-6	1.81
Blackman-Harris	-67	-6	1.81

- <u>Direct TF spectrometers</u>

For a time sequence of kN samples, the PSD on N channels is the average (weighted & normalised) of the (2k-1) FFTs generated with 50% overlap of sample intervals.

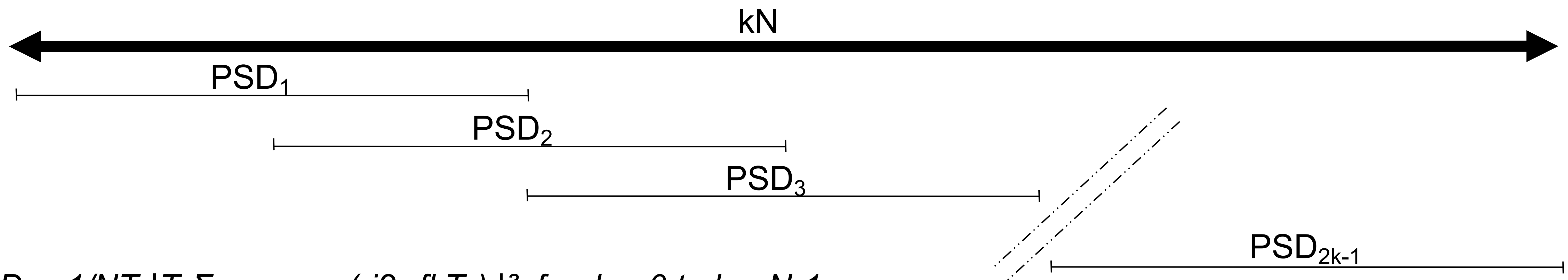

$PSD_i = 1/NT_e|T_e\Sigma w_k.x_k.exp(-j2\pi fkT_e)\,|^2$ for $k = 0$ to $k = N-1$

$PSD = 1/\,(2k-1)(Norm)\ \Sigma\ DSPi$ for $i = 0$ to $2k-1$, with $Norm = T_e/N\ \Sigma\ w_m^2$ for $m = 0$ to $N-1$

→ N channel spaced by $\Delta f = 1/2N\Delta t$

- <u>Polyphase filter spectrometers</u>

- equivalent to an M-channel FFT with an n.M-point weighting window

 & to a bank of M discrete digital filters (with optimised calculations)

n coefficients / filter ⇒ total of n.M coefficients

- Outputs $X_i(nM\Delta t)$ are the time series of samples from the M spectral channels (i=0, M-1)

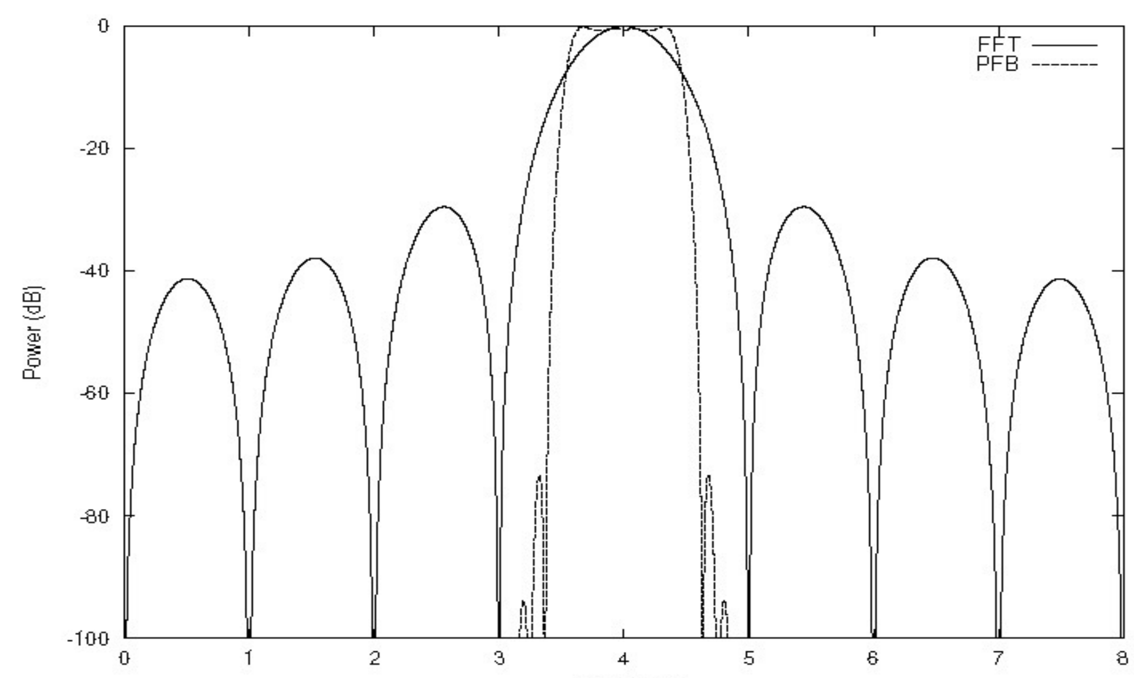

→ Independent adjustment of side lobe rejection and channel width.

• Evolution of spectroscopy of Jupiter's decametric emission over ~35 years

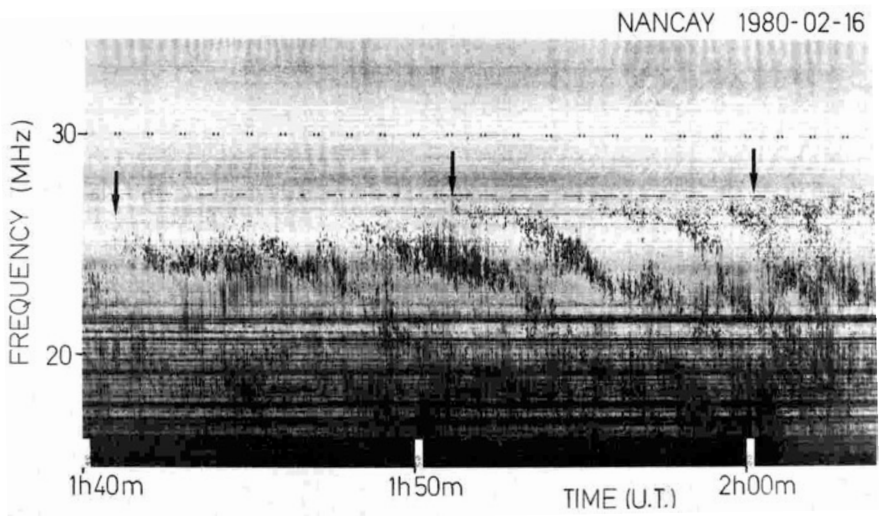

SFR (1980's)

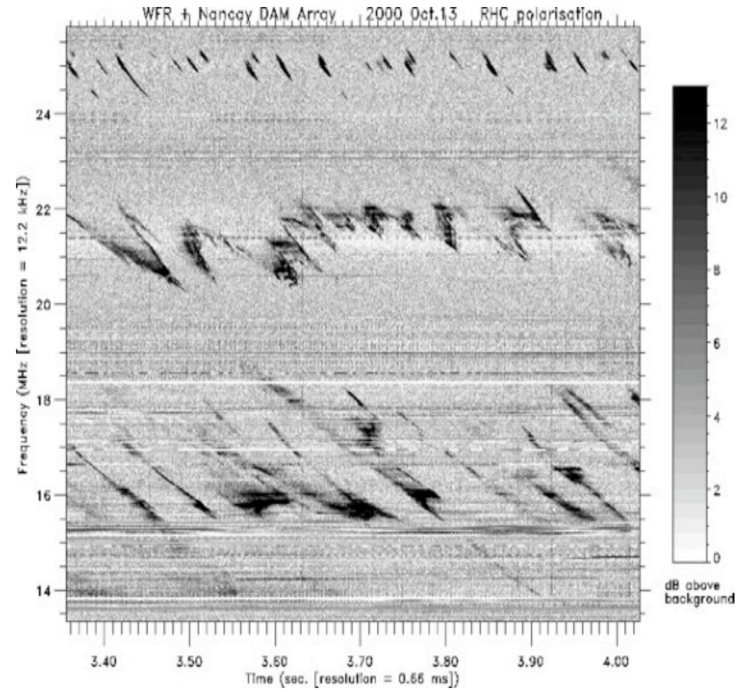

FFT (2000's)

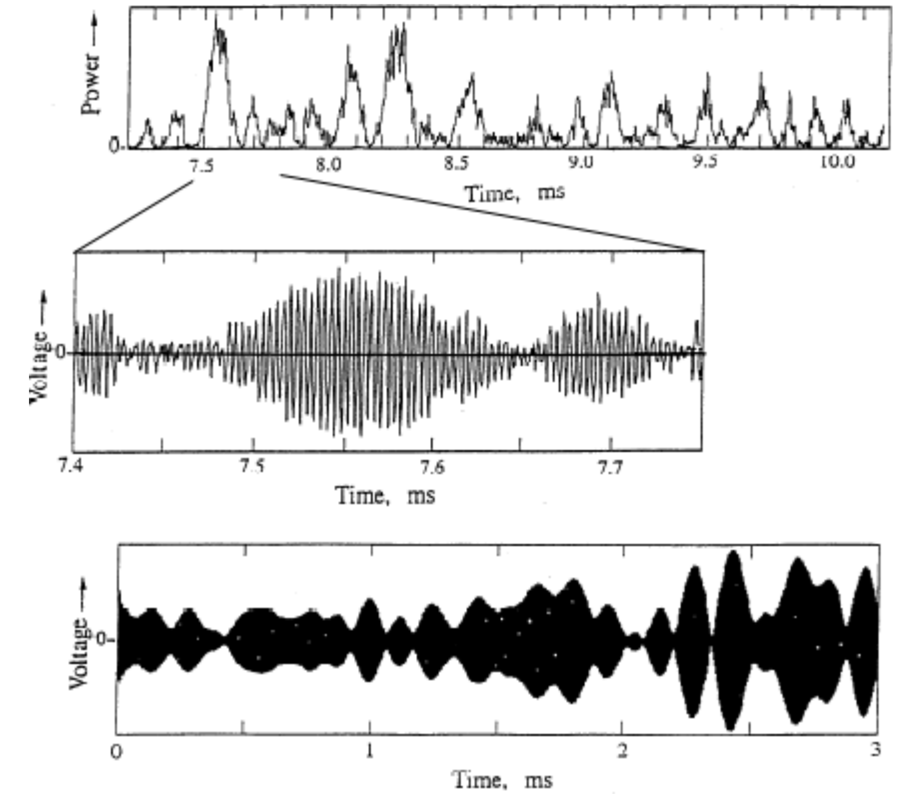

LF waveform (2000's)

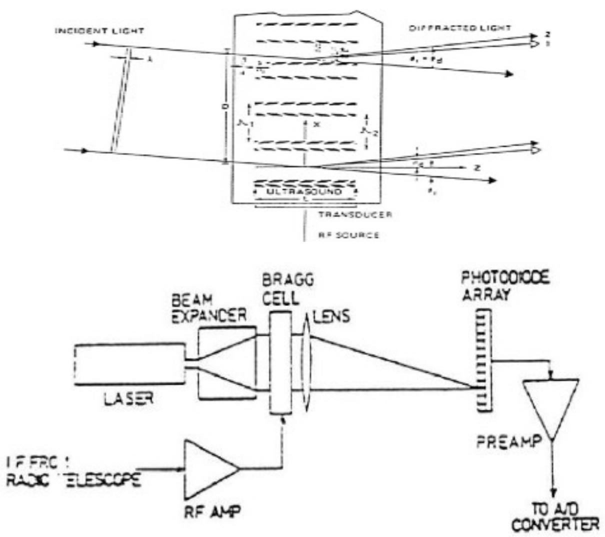

Block diagram of an acousto-optical spectrometer

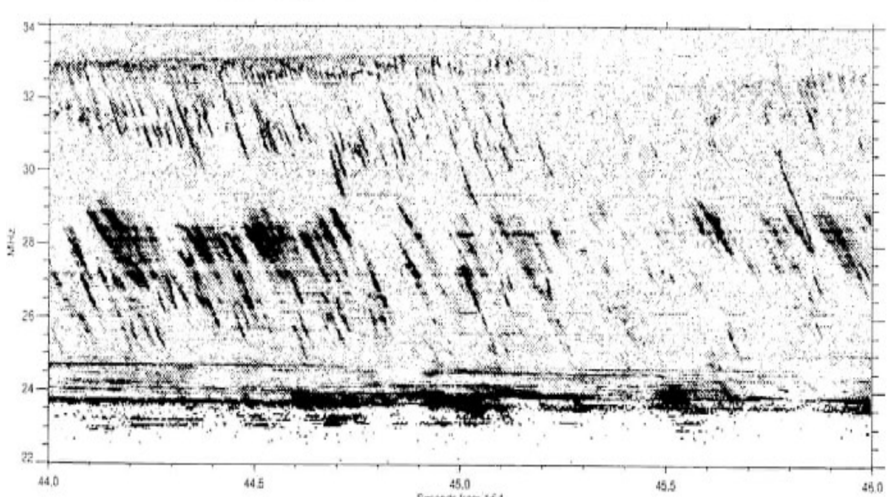

AOS (1990's)

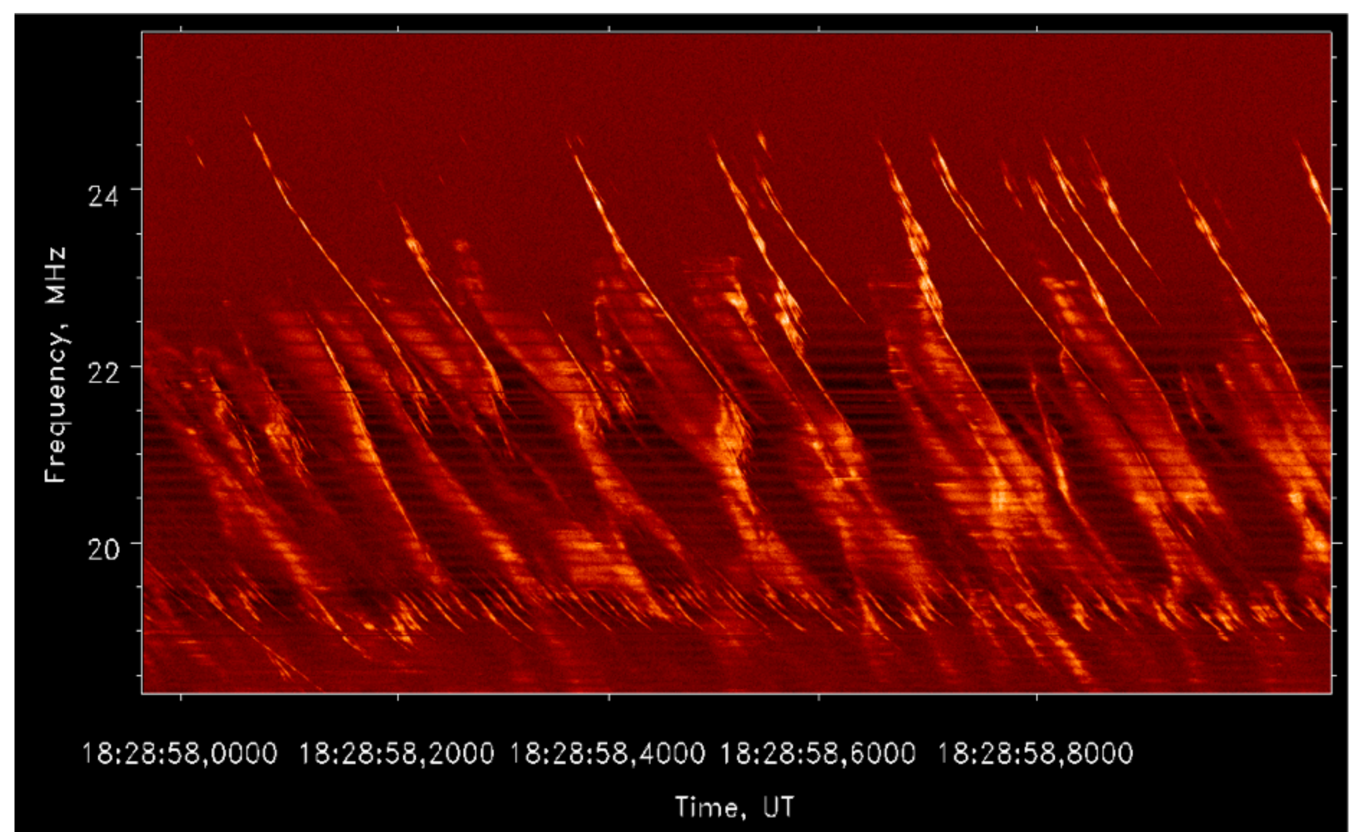

HF waveform (2010's)

• Spectroscopic measurements

(1) wide-spectrum "continuous" sources, ~constant or slowly varying (over $\Delta t >> \tau$)
⇒ measurements with large τ flux in narrow δf bands
→ swept-frequency spectrum analysers (+ filter banks)

(2) emission/absorption spectral lines
+ offset (Doppler), broadening (Doppler, collisional), splitting (Zeeman)
⇒ need for spectral resolution ($\delta f << f$) and sensitivity
→ multichannel receivers, correlators, FFT spectrographs

(3) rapidly changing spectra / t ($\delta t \leq$ or $<<$ 1 sec)
+ fine spectral structures ($\delta f << f$) on broad bands ($\Delta f \approx f$)
= "dynamic spectra" (solar & magnetospheric planetary emissions)
⇒ need for spectral resolution ($\delta f << f$) and temporal resolution ($\delta t \leq$ or $<<$ 1 sec)
→ multichannel receivers, SAO, FFT spectrometers, polyphase, waveform samplers

• Combination of techniques (DDC, Polyphase, FFT):
Ex: SETI spectrometer with 128 million channels
Analysis bandwidth: 200 MHz, frequency resolution: 2 Hz

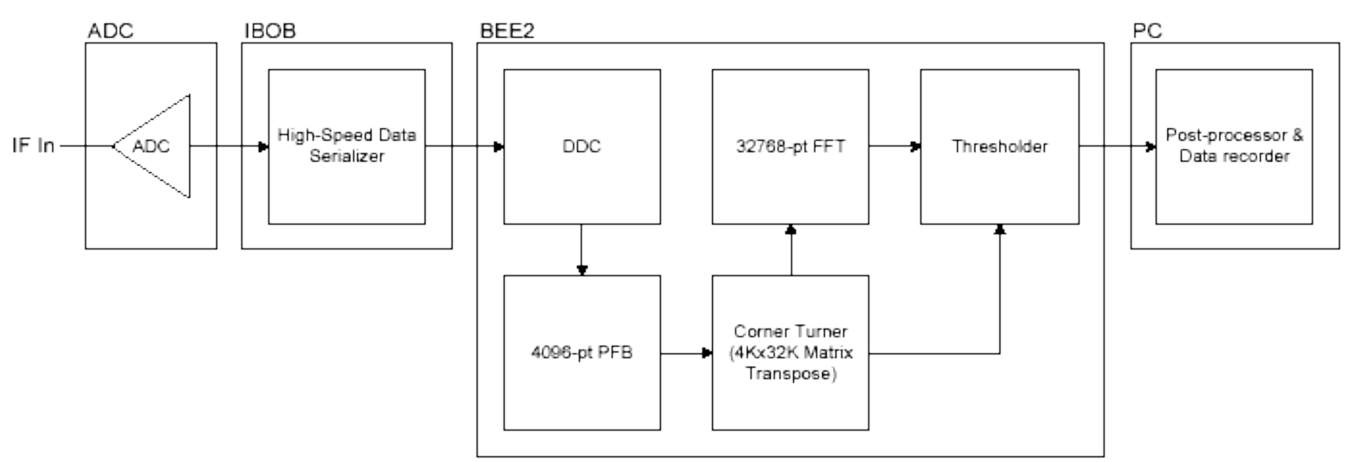

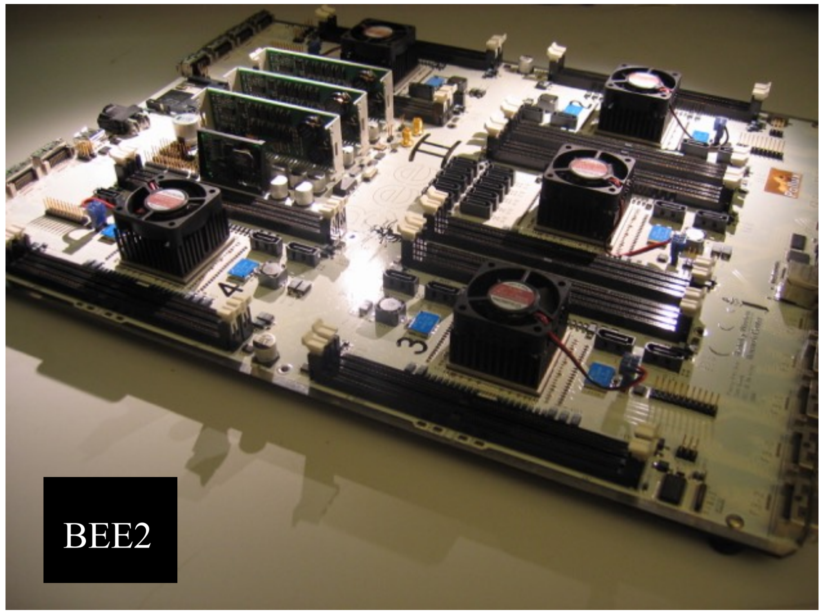

- <u>Polarimetry</u>: *determination of Stokes parametres S (or I), Q, U, V*

Measurement of the electric fields Ex and Ey in two perpendicular directions normal to the direction of propagation (antenna giving both linear polarisations): $E_x(t)$ et $E_y(t)$

$$E_x = e_x\cos(\omega t+\phi_x) \text{ et } E_y = e_y\cos(\omega t+\phi_y)$$

$S = \langle E_x^2(t)\rangle + \langle E_y^2(t)\rangle$
$Q = \langle E_x^2(t)\rangle - \langle E_y^2(t)\rangle$
$U = 2 \langle E_x(t).E_y(t).\cos(\phi_x - \phi_y)\rangle$
$V = 2 \langle E_x(t).E_y(t).\sin(\phi_x - \phi_y)\rangle$

Measurement of auto-correlations $E_x^2(t)$ and $E_y^2(t)$ allows to compute S and Q
Measurement of cross-correlations $E_x(t).E_y(t)$ and $E_x(t).E_y^*(t)$ allows to compute U and V

Linear polarisation fraction: $(Q^2 + U^2)^{1/2} / I$
Circular polarisation fraction: V / I
Total polarisation fraction: $(Q^2 + U^2 + V^2)^{1/2} / I$
Linear polarisation angle: $\frac{1}{2} \tan^{-1}(U / Q)$

• <u>Interference (RFI) mitigation</u>

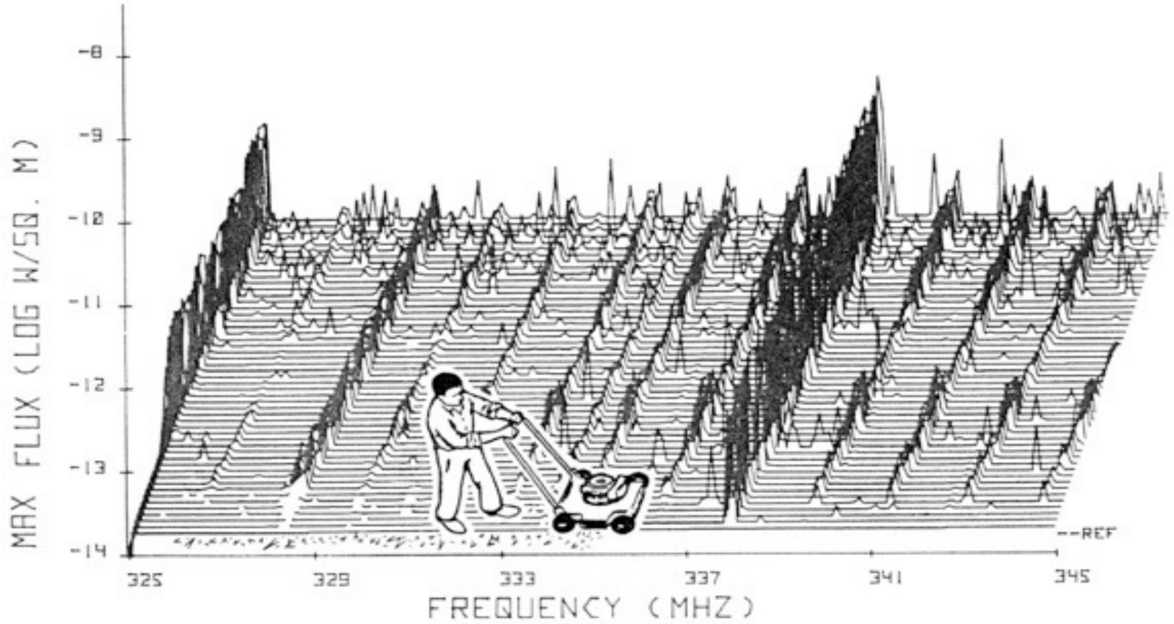

→ Intermittent RFI :

- "Waveform blanking" before detection (in real time) = interruption of waveform capture based on a pre-defined criterion (usually intensity threshold).

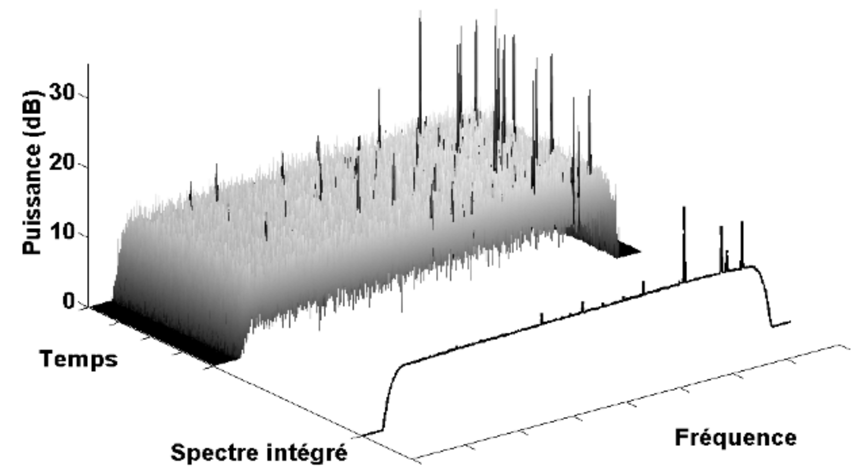

- Statistical analysis of dynamic spectrum and masking (t,f) in real-time or after detection

→ Continuous RFI : Estimation, reduction/ cancellation or nulling (imaging)

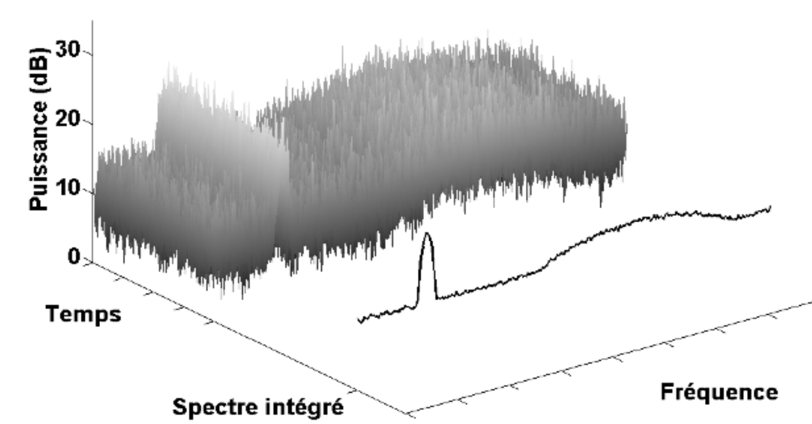

→ + legal protection

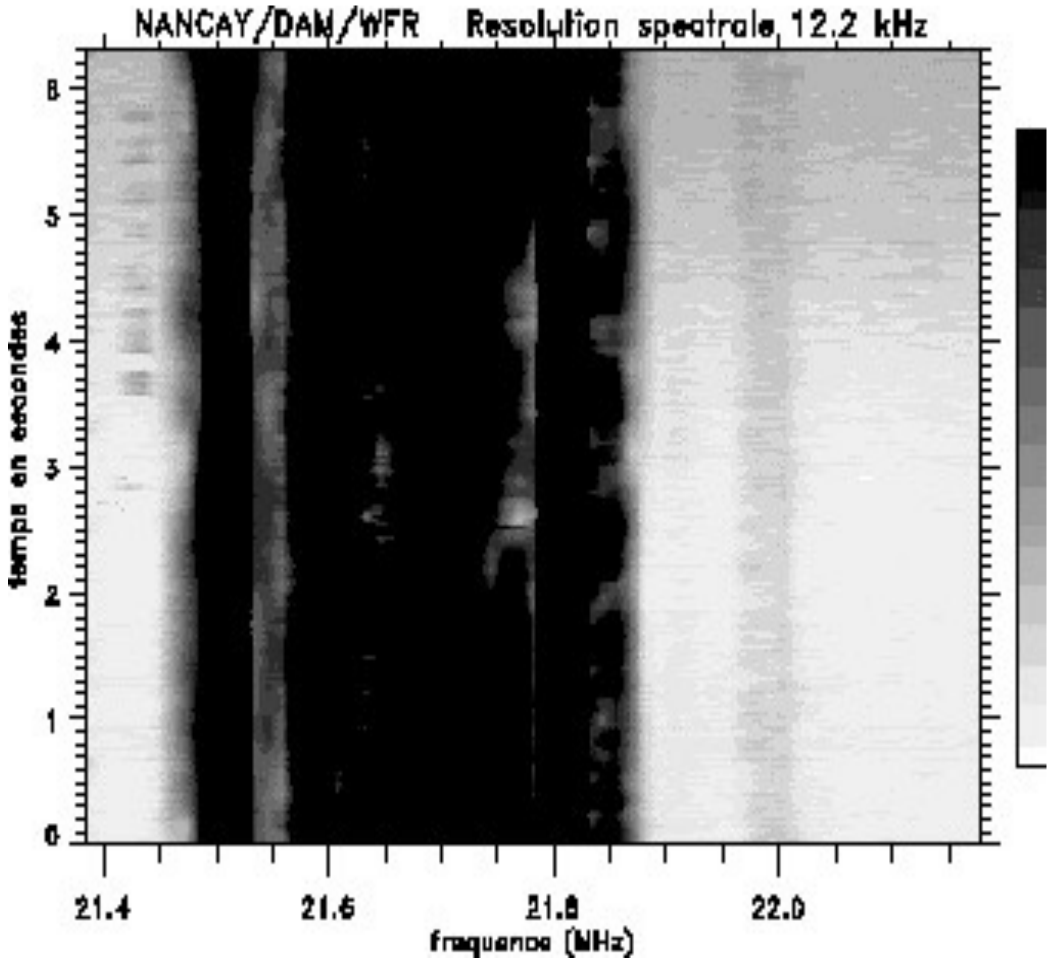

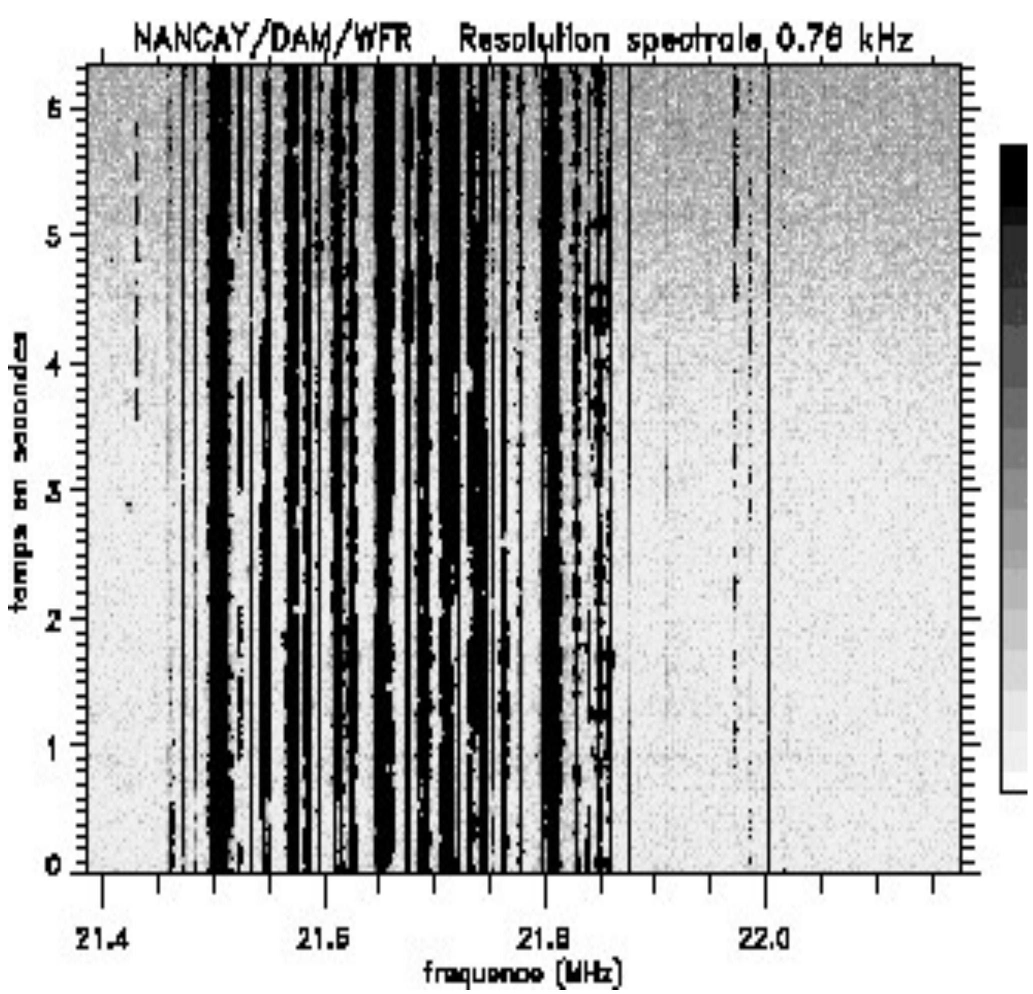

% unpolluted channels vs. spectral resolution

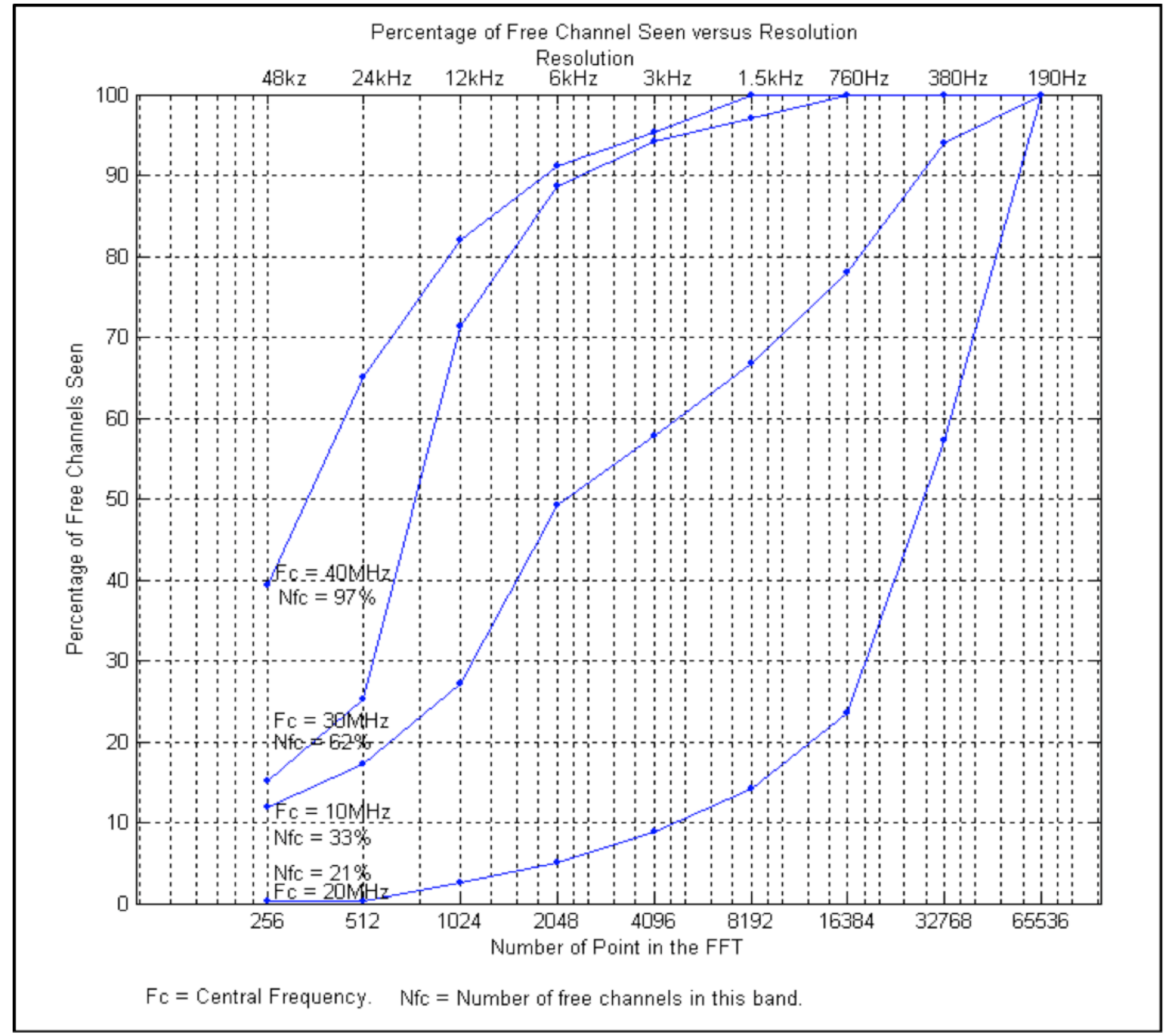

90% availability in the band :

- 35-45 MHz, requires 6.25 kHz resolution
- 25-35 MHz, requires 1.6 kHz resolution
- 15-25 MHz, requires 190 Hz resolution

Statistical analysis of dynamic spectrum and masking (t,f) in real-time or after detection, before further integration

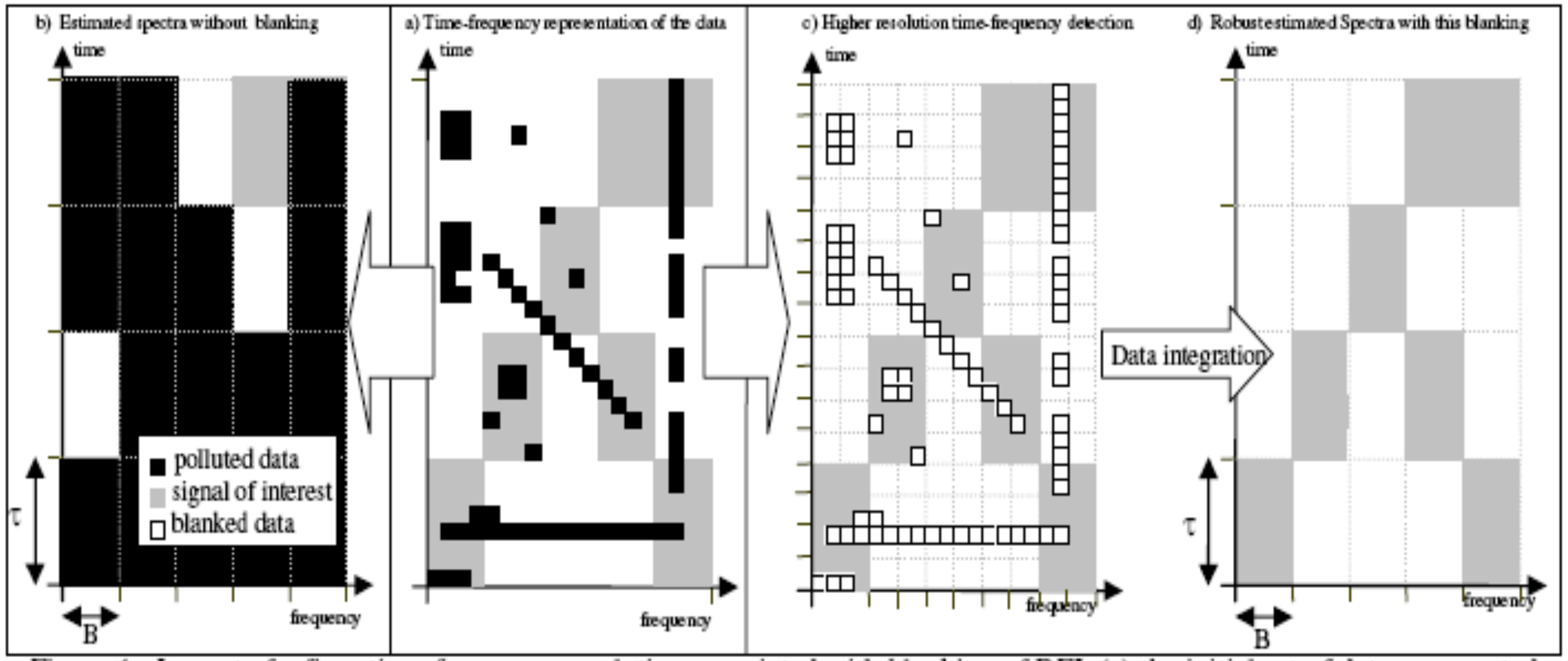

Figure 1 : Impact of a finer time-frequency resolution associated with blanking of RFI. (a) the initial set of data represented in the time-frequency plane. (b) Estimated spectra obtained with classical receiver. (c) RFI detection and blanking with finer time-frequency resolution. (d) Estimated spectra after blanking. The SOI can be recovered which was not the case in (a).

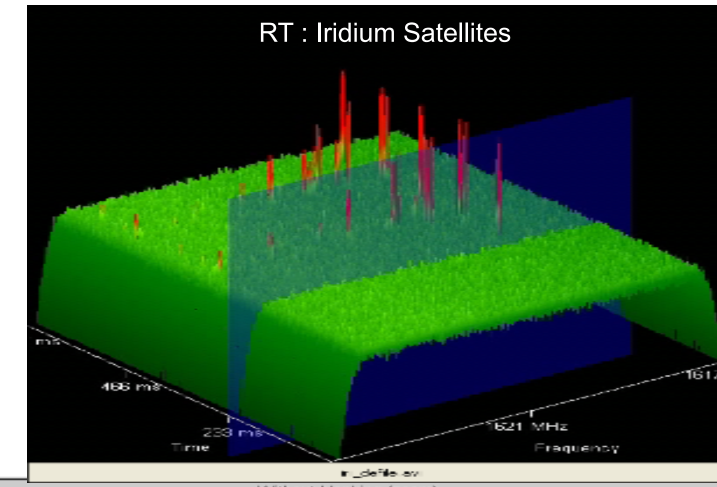

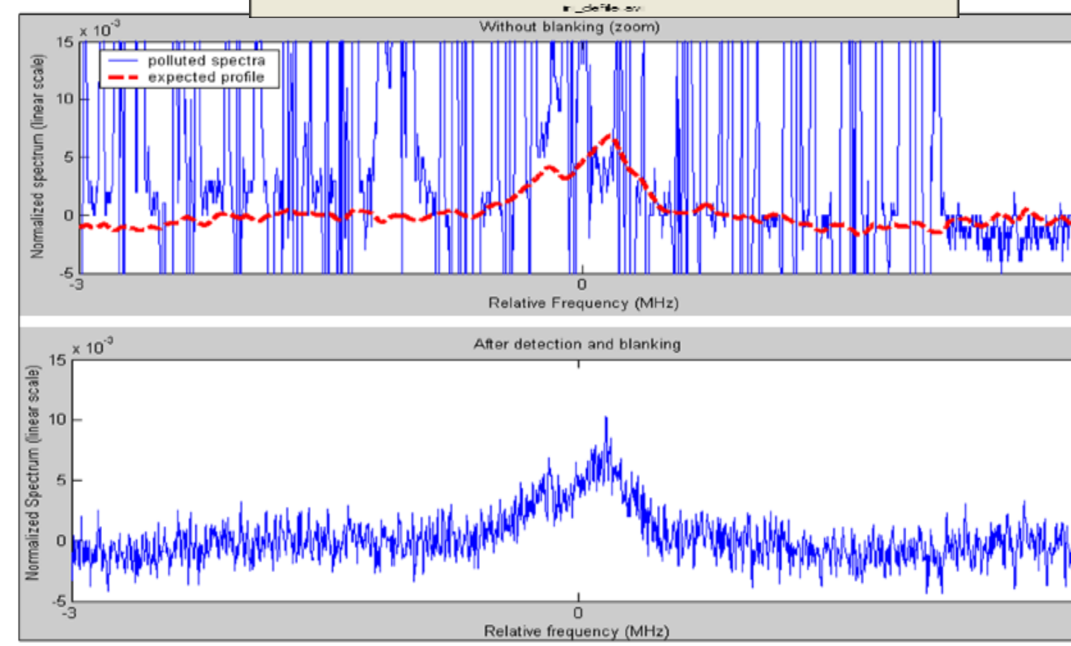

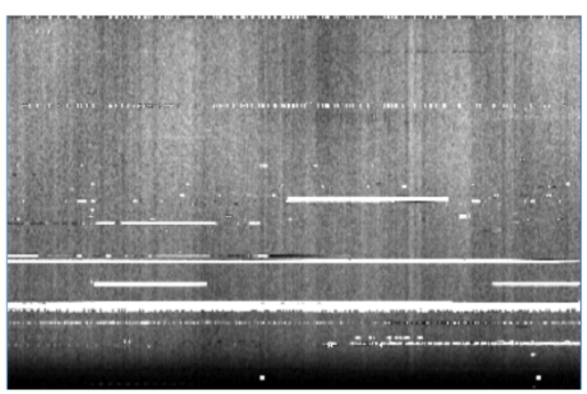

(a) Original

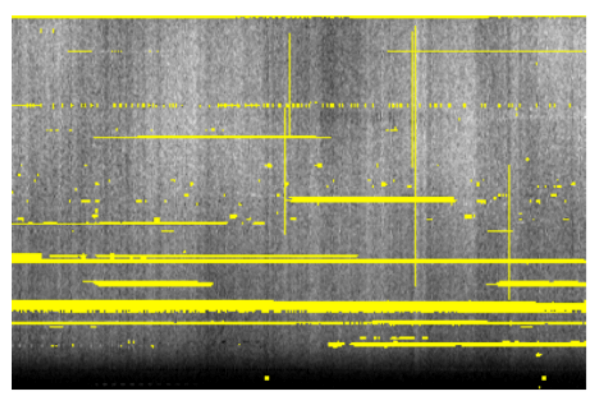

(b) Automated flagging result

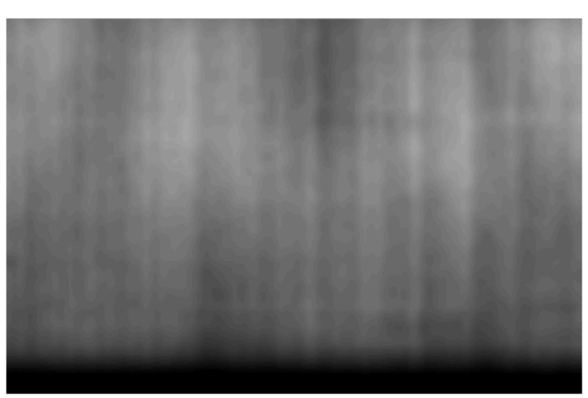

(c) Smoothed

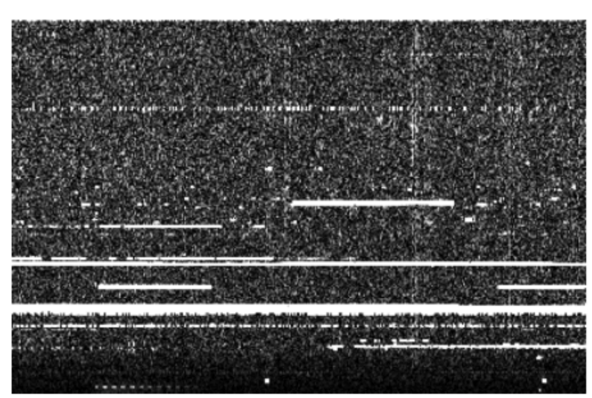

(d) Difference

[Offringa, 2012]

- <u>Pulsars dedispersion</u>

→ detection, timing

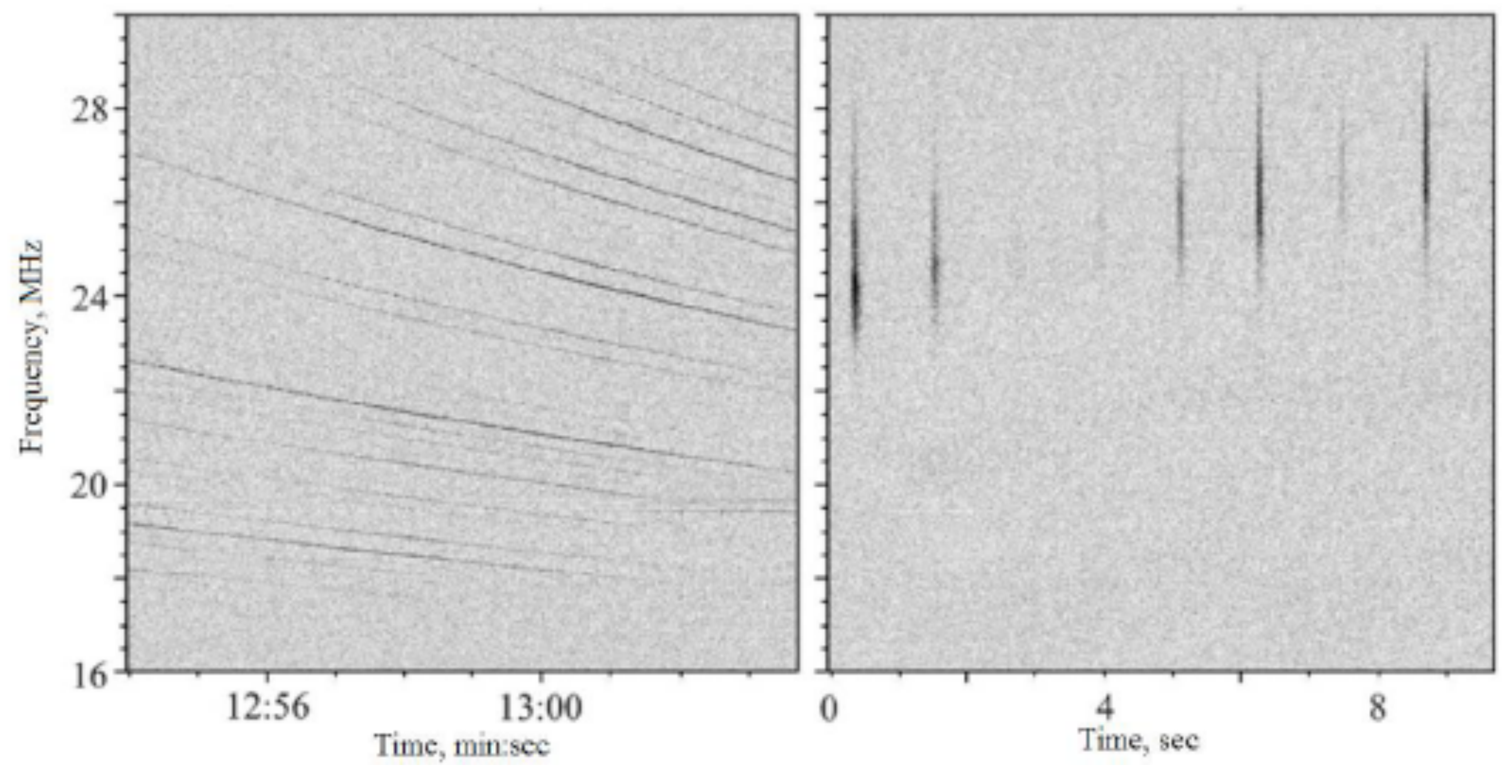

- <u>Detection of fast bursts</u>

→ high-speed recording

Example of a time-frequency topological criterion

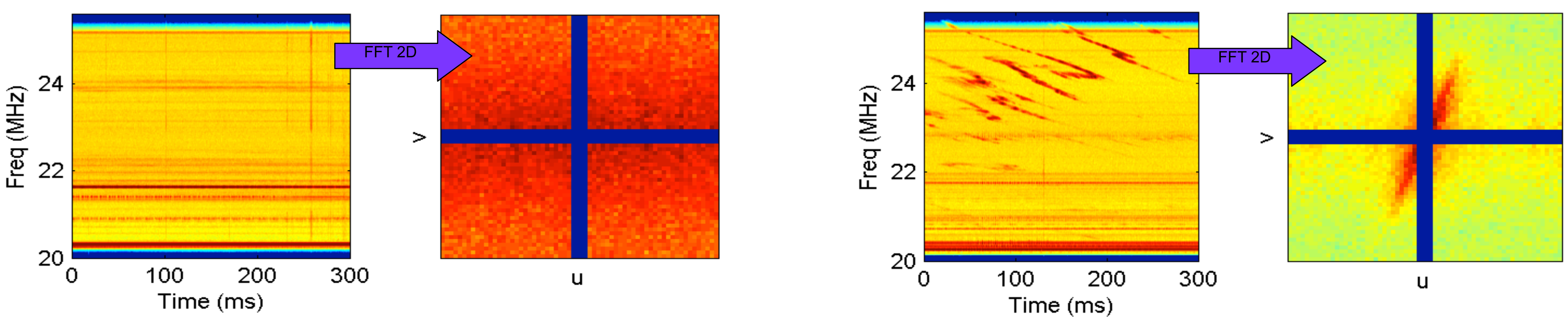

- Introduction (history, interest, specific features)
- Waves & Polarisation
- Plasmas & Propagation (cutoff, dispersion, Faraday effect, scintillations)
- Coherent Signal Detection (measurement theory, antenna temperature, calibration, noise)
- Receivers (heterodyne, system temperature, filtering, gain, RFI mitigation)
- Basics of Radio Astronomy Antennas: Single antennas
- Basics of Interferometry and Aperture Synthesis (phased arrays, electronic pointing, imaging, correlation, coherence, VLBI)
- Observation methods
- Large present & future ground-based radio arrays
- Basics of Space radio astronomy

• <u>Definitions</u> :

An antenna is a device that transmits energy between a wave propagating in free space and a power transmission line.

Reciprocity theorem applied to antennas (Carson's theorem): The properties of an antenna can be indifferently used, defined and evaluated in transmission or reception.

3 radiation zones :

- Rayleigh zone (near field)
- Fresnel zone (intermediate)
- Fraunhoffer zone (far field) : E,B in 1/r, S in $1/r^2$

$\Rightarrow r_{min} > 2D^2/\lambda$ with D the size (diameter) of the antenna

Ex: *Nançay Decimeter Radiotelescope : $D = 200$ m at $\lambda = 0{,}21$ m $\Rightarrow r_{min} = 380$ km*

Nançay Radio Heliograph : $D = 10$ m at $\lambda = 1$ m $\Rightarrow r_{min} = 200$ m

- <u>Antenna in reception</u> $\rightarrow$ <u>Effective area</u>

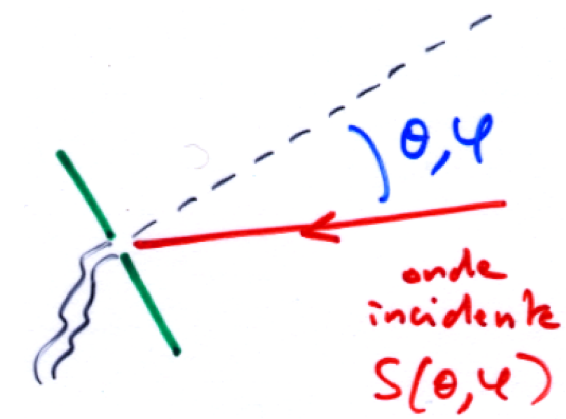

Spectral power received from (θ,ϕ) in $d\Omega$:

$dP_\nu(\theta,\phi) = P_\nu(\theta,\phi)\, d\Omega = dS_\nu(\theta,\phi).A_{eff}(\theta,\phi)$ $[W.Hz^{-1}]$

<u>NB</u> : we have seen that the spectral power received by an antenna can be written as :

$P_\nu = B_\nu\, \Omega_A\, A_{source\text{-}seen\text{-}by\text{-}antenna} = B_\nu\, A_{antenna}/d^2\, A_{source\text{-}seen\text{-}by\text{-}antenna}$

$= B_\nu\, A_{antenna}\, \omega_{source\text{-}seen\text{-}by\text{-}antenna} = S_\nu\, A_{antenna}$

hence : $S_\nu = B_\nu\, \omega_{source\text{-}seen\text{-}by\text{-}antenna} = B_\nu\, min(\omega_{source}, \Omega)$

which generalises as : $B_\nu(\theta,\phi) = dS(\theta,\phi)/d\Omega$ or $dS(\theta,\phi) = B_\nu(\theta,\phi)\, d\Omega$

hence $dP_\nu(\theta,\phi) = P_\nu(\theta,\phi)\, d\Omega = B_\nu(\theta,\phi)\, .\, A_{eff}(\theta,\phi)\, d\Omega$ $[W.Hz^{-1}]$

with $A_{eff}(\theta,\phi) = \eta\, A\, p(\theta,\phi)$

A = Physical area $\Rightarrow \eta A$ = Geometrical effective area

η = efficiency ≤ 1 (antenna illumination, energy not intercepted, surface defects, losses)

$p(\theta,\phi)$ = directional sensitivity (normalised : $p_{max} = 1$)

Ex: 2D Airy figure for a circular reflector
or $p(\theta,\phi) = 1$ for an isotropic antenna
(impossible to build in practice)

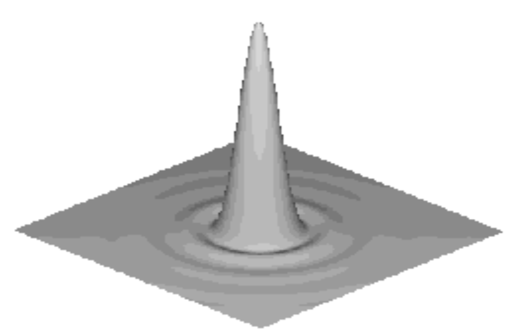

Antenna of effective area A_{eff} in equilibrium in an isotropic blackbody radiation field at temperature T :

$B_\nu(\theta,\phi) = ½ \times 2kT_B/\lambda^2$ & $P_{\nu\text{-tot}} = k\,T_B$

$\Rightarrow \quad P_\nu(\theta,\phi)\,d\Omega = B_\nu(\theta,\phi)\,.\,A_{eff}(\theta,\phi)\,d\Omega = k\,T_B/\lambda^2\,.\,A_{eff}(\theta,\phi)d\Omega$

$\int_{4\pi} P_\nu(\theta,\phi)\,d\Omega = k\,T_B/\lambda^2 \int_{4\pi} A_{eff}(\theta,\phi)d\Omega \quad = P_{\nu\text{-tot}} = k\,T_B$

hence whatever the antenna, regardless of its nature, we obtain : $\int_{4\pi} A_{eff}(\theta,\phi)\,d\Omega = \lambda^2$

<u>NB</u> : A is not necessarily the geometrical area of the collector, but its "effective" area (or collection surface) = "effective cross-section" of the radiotelescope with respect to the incident radio radiation (taking losses into account ...).

• Antenna in emission → Gain

$P_{\nu\text{-total}}$ injected at terminals $\Rightarrow dP_\nu$ = fraction emitted in $d\Omega$ in the direction (θ,ϕ)

$dP_\nu(\theta,\phi) = P_\nu(\theta,\phi)\, d\Omega = (P_{\nu\text{-total}}/4\pi) \times g(\theta,\phi)\, d\Omega$

with $g(\theta,\phi)$ = antenna radiation pattern or directional gain or directivity
(=1 for an isotropic antenna)
$\Rightarrow g(\theta,\phi) = 4\pi/P_{\nu\text{-total}} \times P_\nu(\theta,\phi)$

hence $\int_{4\pi} g(\theta,\phi)\, d\Omega = 4\pi/P_{\nu\text{-total}} \int_{4\pi} P_\nu(\theta,\phi)\, d\Omega = 4\pi/P_{\nu\text{-total}} \int_{4\pi} dP(\theta,\phi)$
$\Rightarrow \quad \int_{4\pi} g(\theta,\phi)\, d\Omega = 4\pi$ by definition of g

Reciprocity theorem : $p(\theta,\phi) = g(\theta,\phi) / g_{max} = A_{eff}(\theta,\phi) / \eta A$
$\int_{4\pi} A_{eff}(\theta,\phi)\, d\Omega = \lambda^2$ and $\int_{4\pi} g(\theta,\phi)\, d\Omega = 4\pi \quad \Rightarrow \quad g(\theta,\phi) = 4\pi A_{eff}(\theta,\phi) / \lambda^2$

→ Directional antenna : all energy is emitted in Ω (main lobe), with a ~constant gain (or $p = p_{max} = 1$) on Ω

$\int_{4\pi} p(\theta,\phi)\, d\Omega = \Omega$
$\int_{4\pi} g(\theta,\phi)\, d\Omega = 4\pi$
$\Rightarrow g_{max}(\theta_o,\phi_o) \approx g \approx C^t = 4\pi/\Omega$
$g \uparrow$ when $\Omega \downarrow$
$g = 4\pi A_{eff} / \lambda^2 \quad \Rightarrow \quad A_{eff} \,.\, \Omega = \lambda^2$
$\Downarrow$
effective area in the direction of the main lobe

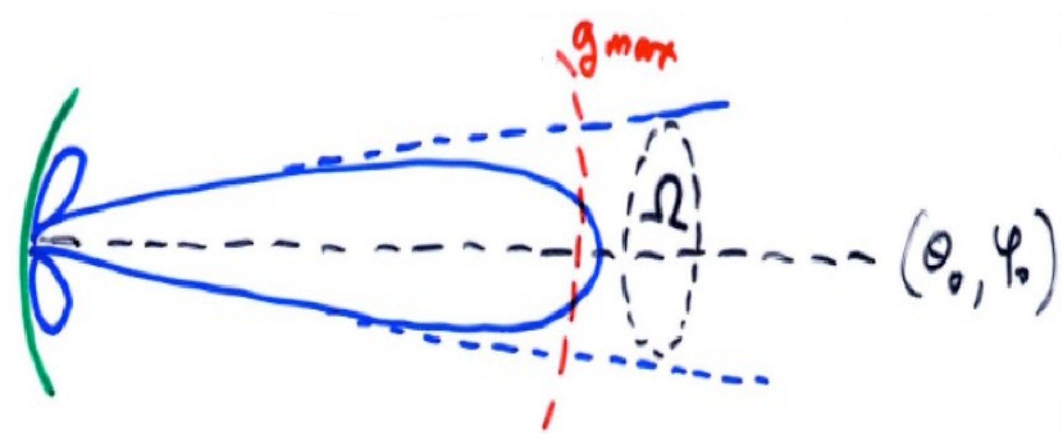

• <u>Antenna temperature</u>

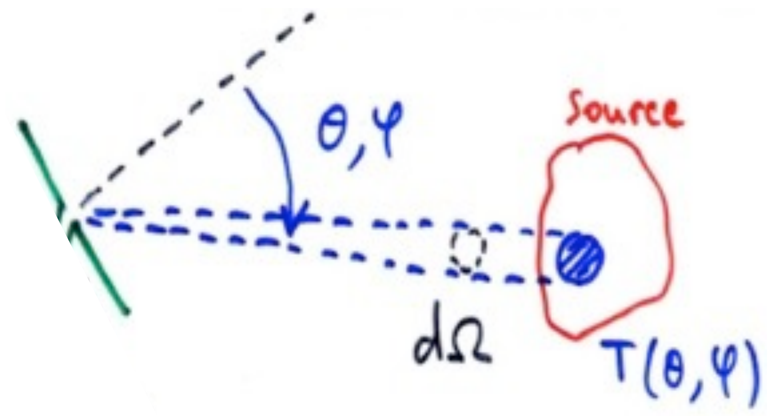

The antenna receives radiation from the source at T_B

$\Rightarrow$ in $d\Omega$ from the direction (θ,ϕ), the received power is :

$P_\nu(\theta,\phi)\, d\Omega = k\, T_B / \lambda^2 \,.\, A_{eff}(\theta,\phi)\, d\Omega = k\, T_B / 4\pi \times g(\theta,\phi)\, d\Omega$

For any T_B(source), not necessarily uniform :

$P_\nu(\theta,\phi)\, d\Omega = kT_B(\theta,\phi)/4\pi \times g(\theta,\phi)\, d\Omega$

$\Rightarrow \int_{4\pi} P_\nu(\theta,\phi)\, d\Omega = P_{tot} = k\, T_A = k/4\pi \int_{4\pi} T_B(\theta,\phi) \times g(\theta,\phi)\, d\Omega$

$\Rightarrow T_A = 1/4\pi \int_{4\pi} T_B(\theta,\phi) \times g(\theta,\phi)\, d\Omega$

For a finite-dimensional source, the antenna temperature of the source writes :

$$T_A = 1/4\pi \times \int_{source} \underbrace{T(\theta,\phi)}_{\text{characterises the source}} \times \underbrace{g(\theta,\phi)}_{\text{characterises the antenna}}\, d\Omega$$

→ Consequences :

1) $\omega_{source} > \Omega$ (antenna lobe) and $T(\theta,\phi) \approx C^t$ on Ω

if we only receive energy from the source (and not from the secondary lobes)

$\Rightarrow$ T and $g \neq 0$ only in Ω)

$\Rightarrow T_A = 1/4\pi \times \int_{source} T(\theta,\phi) \times g(\theta,\phi)\, d\Omega$

$= T(\theta,\phi)/4\pi \times \int_{lobe} g(\theta,\phi)\, d\Omega$

$= T(\theta,\phi)/4\pi \times (\int_{4\pi} g(\theta,\phi)\, d\Omega)$

$\Rightarrow T_A = T(\theta,\phi)$

2) $\omega_{source} << \Omega$ (main lobe, >> secondary lobes)

if we only receive energy from the source $\Rightarrow g(\theta,\phi) \approx C^t \approx g = 4\pi/\Omega$

$\Rightarrow T_A = g/4\pi \times \int_{source} T(\theta,\phi)\, d\Omega = \langle T\rangle_{source}\, \omega_{source} / \Omega$

- <u>Radiation diagram</u>

Representation of $g(\theta,\phi)$ or $g(\theta,\phi)/g_{max}$ as a function of θ and/or ϕ in polar or rectangular coordinates, in 2D or 3D

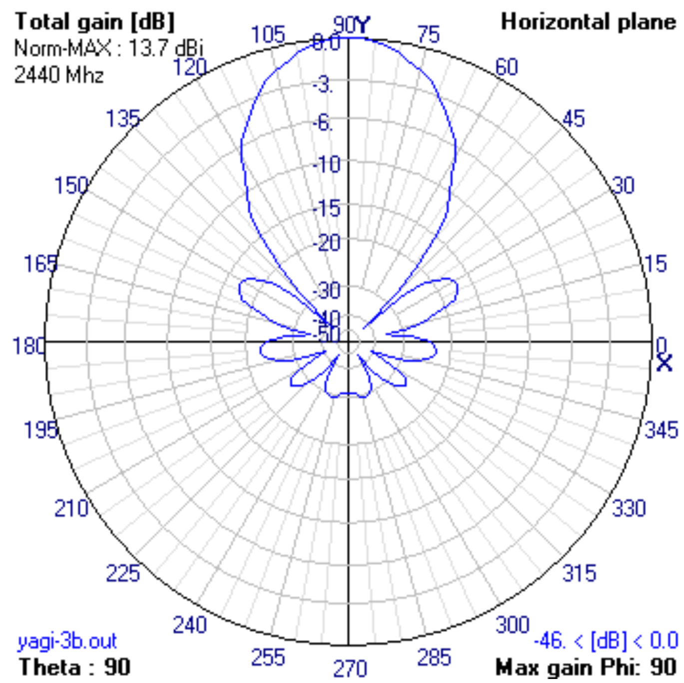

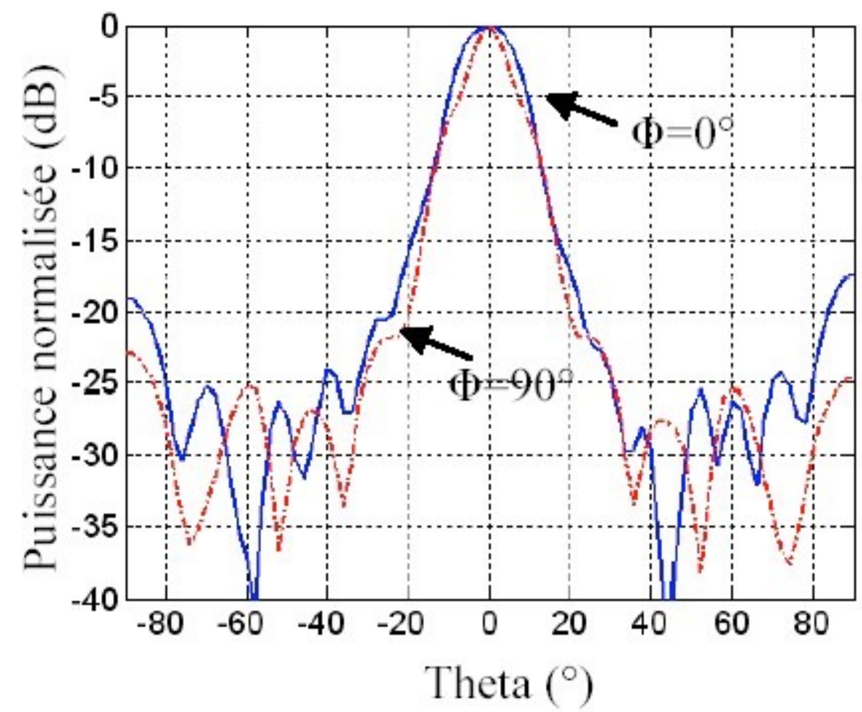

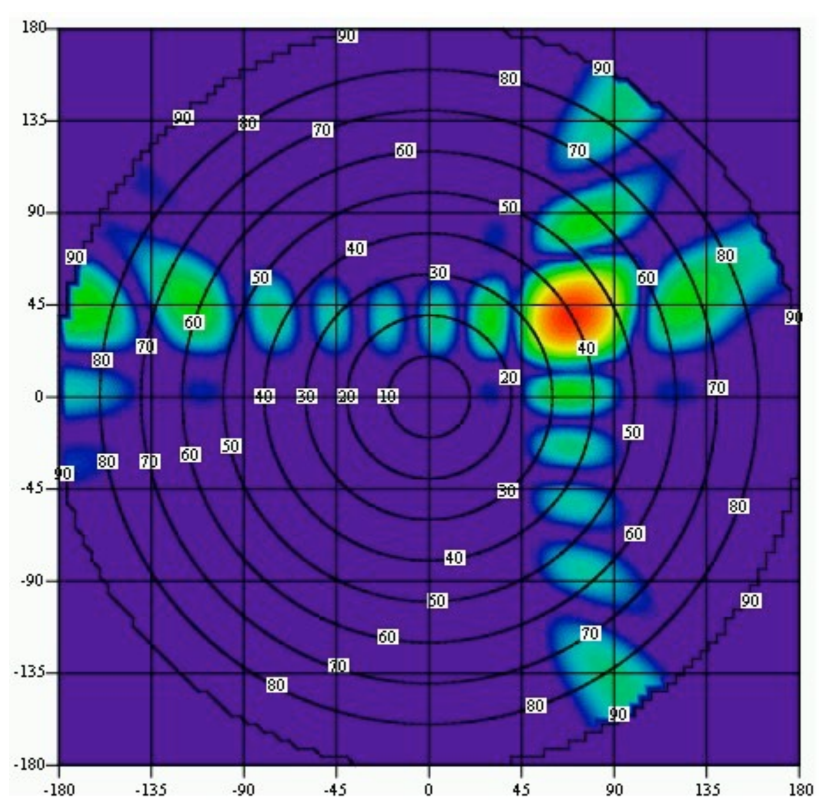

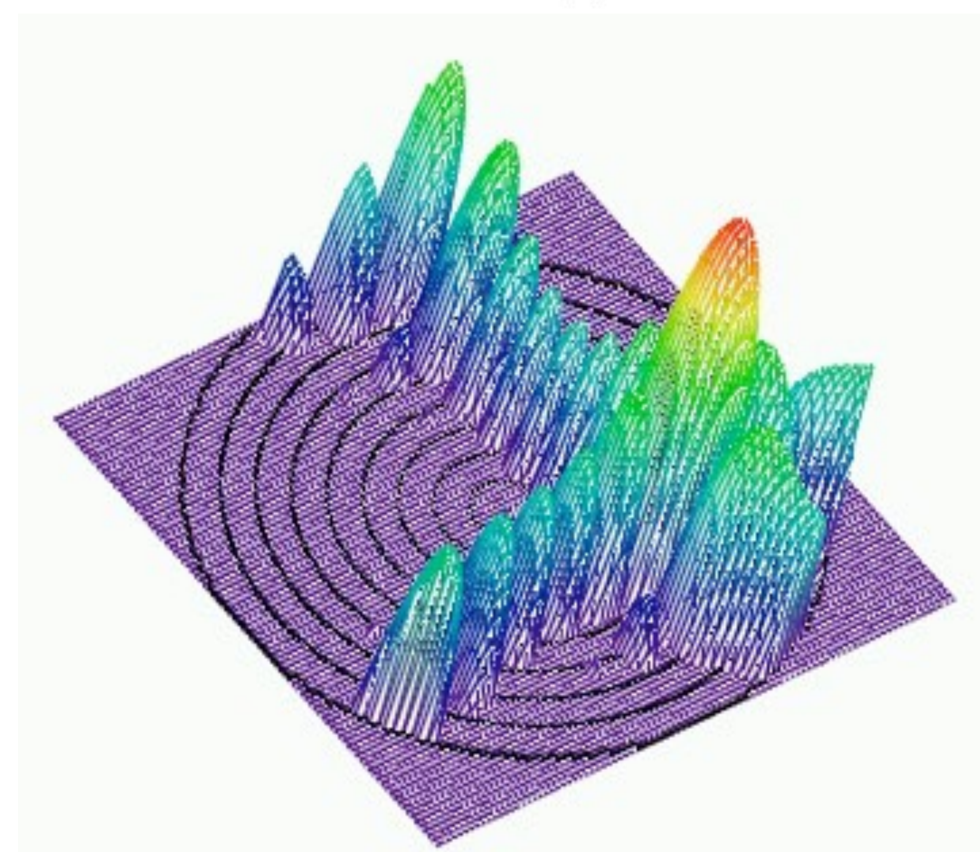

$g(\theta,\phi)$ is expressed in dBi (dB / isotropic) = $10 \log_{10}(g(\theta,\phi))$
or in dBc (dB / maximum gain) = $10 \log_{10}(g(\theta,\phi)/g_{max})$

Ex: - *for the Nançay radiotelescope, with* $A_e = 5600\ m^2$ *at 21 cm,* $g_{max} = 62$ *dBi*
- *for a uniformly illuminated rectangular aperture (* $g(\theta) \propto \mathrm{sinc}(\pi D\theta/\lambda)^2$ *), the 1st secondary lobe is at -13,26 dBc)*
- *for a uniformly illuminated circular aperture (* $g(\theta)=[2J_1(\pi D\theta/\lambda)/(\pi D\theta/\lambda)]^2$ *), the 1st secondary lobe is at -17,6 dBc*

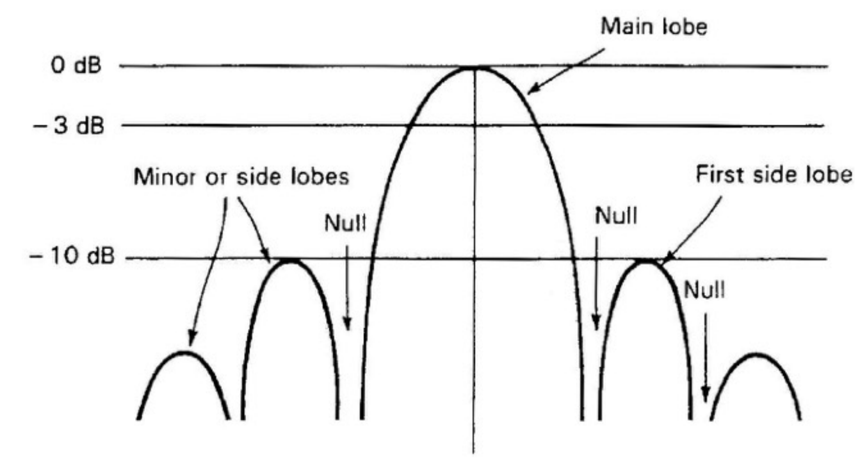

Characteristic features of the $g(\theta,\phi)$ diagram :
- main lobe
- secondary lobes
- rear lobes
- half-power width (= lobe aperture at maximum-3 dB)

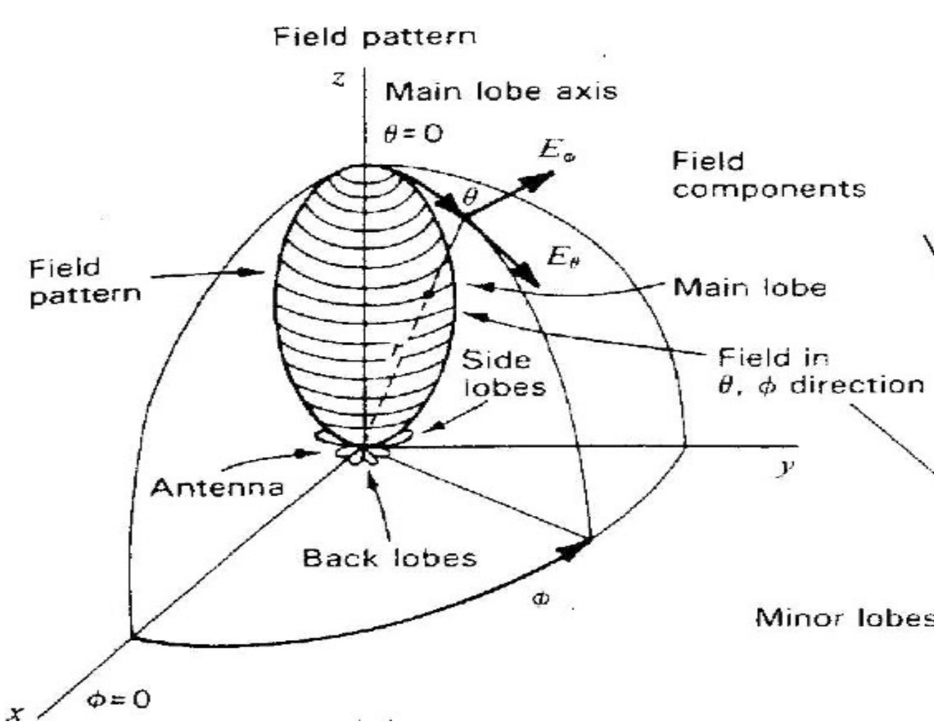

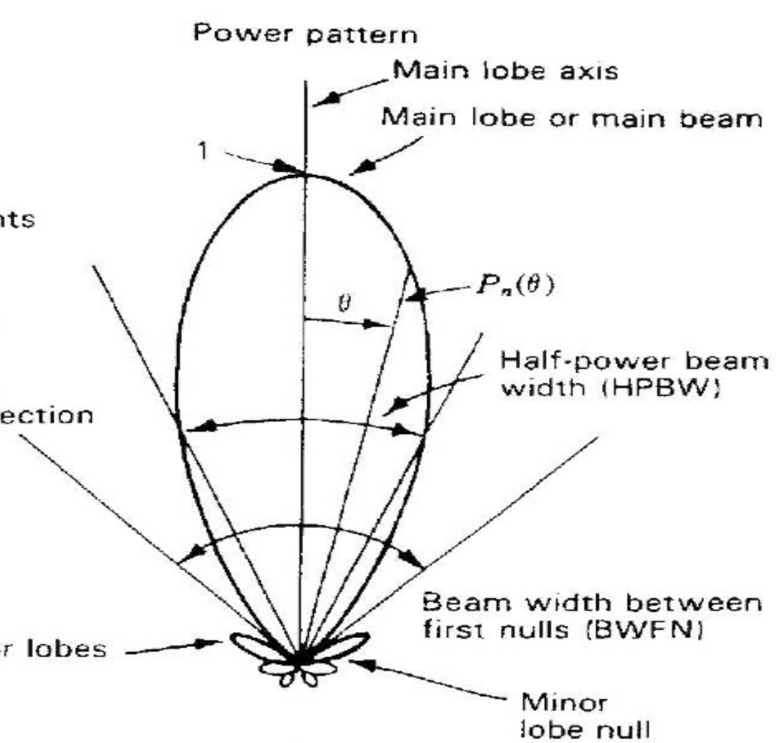

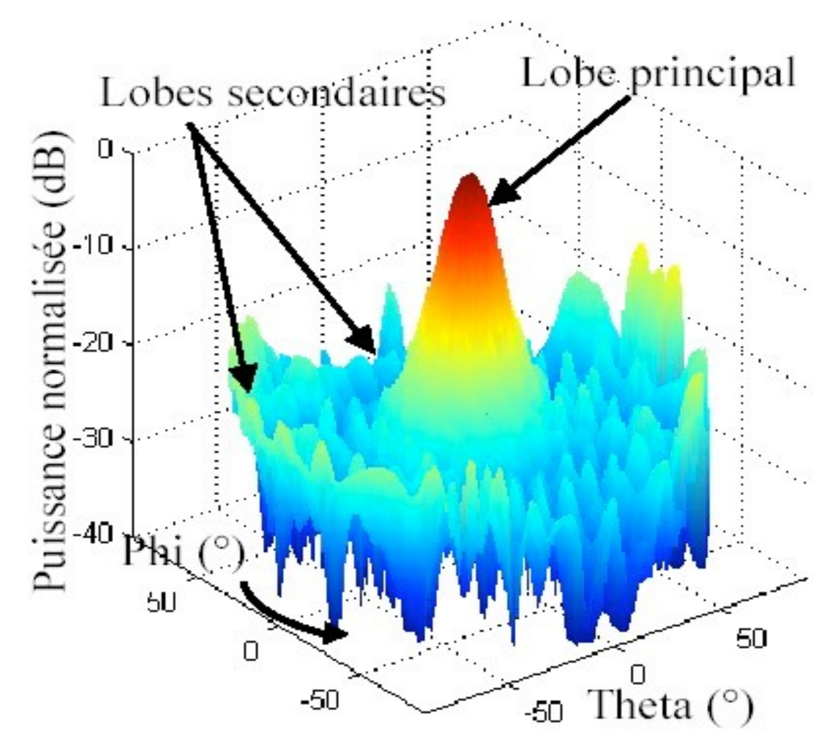

• <u>Practical design</u>

No radio lens → Reflector necessary, or directly collecting antennas
$\lambda \uparrow \Rightarrow D \uparrow$, very large collector areas required, but with limited surface precision ($\sim\lambda/10$ - $\lambda/20$)
Geometry often ≠ parabola for technical reasons (mechanical ...)

Ex : D_{max} = 100 m for the largest steerable dish (Effelsberg / Bonn)
$\Rightarrow A \approx 7850\ m^2$

Nançay dm radiotelescope = Meridian instrument : pointing in declination (δ) by a plane mirror 200×35 m² + focusing by a spherical mirror of radius R
⇒ focus on the sphere R/2
⇒ tracking via movable focal system for 1h around the meridian

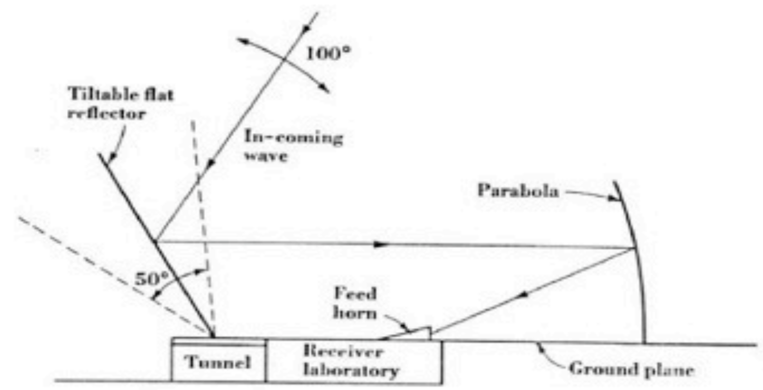

Fig. 6-43. Elevation cross section through standing-parabola tiltable-flat-reflector radio telescope of the Ohio State University.

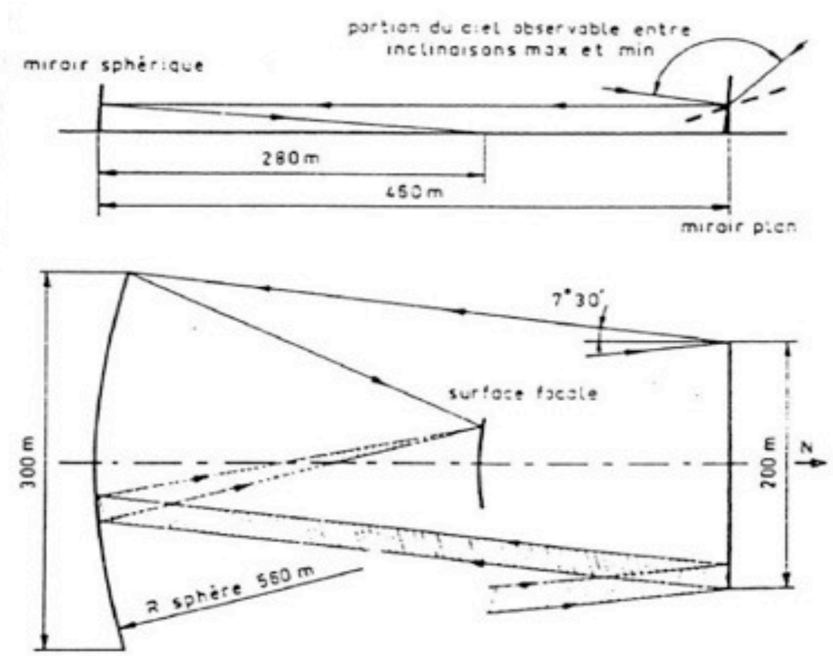

Largest instruments dm-cm = Fixed antenna :
- Arecibo : ∅ ~ 300 m (collapsed in 2020)
- FAST : ∅ ~ 500 m (300 m used instantaneously)

Reflector shaped in a natural bowl (limited motion of the focus)

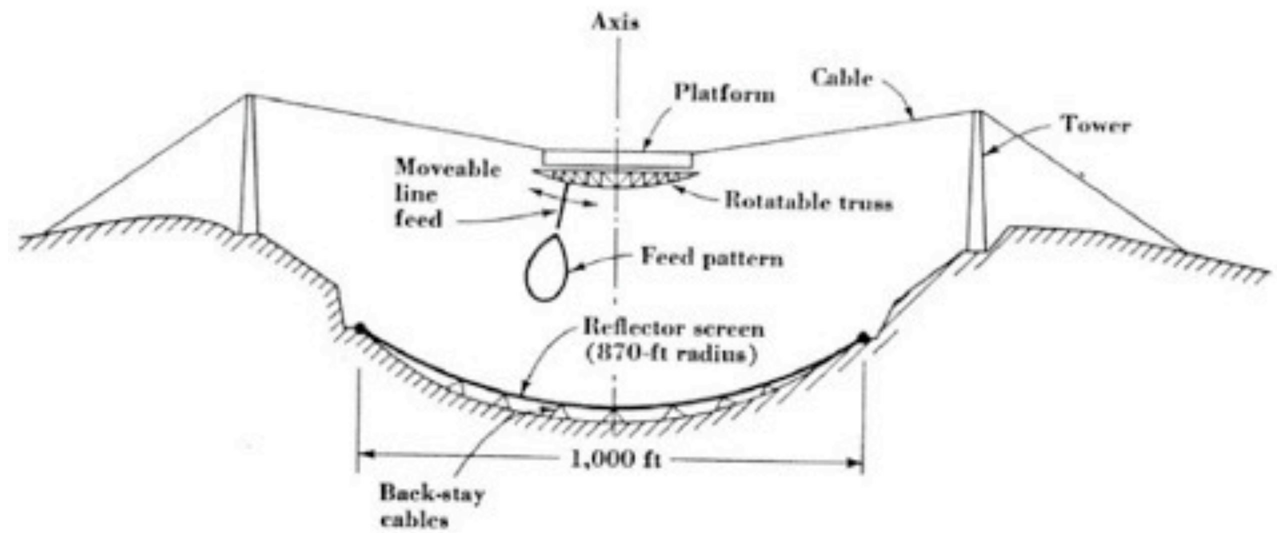

Fig. 6-54. Elevation cross section of fixed 1,000-ft-diameter spherical reflector of radio telescope at Arecibo, Puerto Rico.

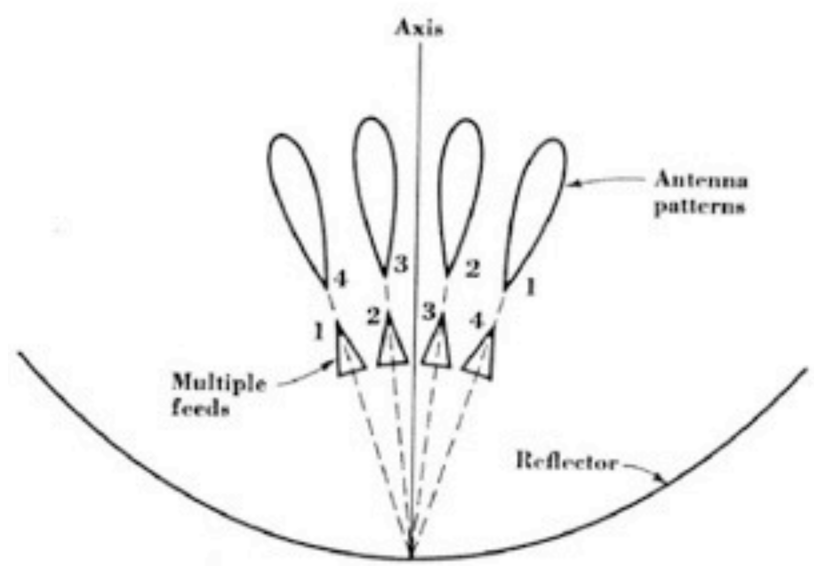

Fig. 6-55. Antenna with multiple feeds for producing multiple beams.

For a uniformly illuminated aperture in phase and amplitude: $A_e = A$ (physical area)

General case : $A_e = \eta A$ with efficiency $\eta = \eta_{\text{illumination}} \times \eta_{\text{non-intercepted energy}} \times \eta_{\text{surface irregularities}}$

« Spillover »

$\exp[-(4\pi\sigma_{RMS}/\lambda)^2]$

For a circular aperture

TYPE OF DISTRIBUTION $0 \le r \le 1$	DIRECTIVITY PATTERN E(u) $u=\pi D\theta/\lambda$	HALF POWER BEAMWIDTH IN DEGREES	ANGULAR DISTANCE TO FIRST ZERO	INTENSITY OF Ist SIDELOBE db BELOW MAX.	GAIN FACTOR
$f(r)=(1-r^2)^0=1$	$\pi a^2 \frac{J_1(u)}{u}$	$58.9\frac{\lambda}{D}$	$69.8\frac{\lambda}{D}$	17.6	1.00
$f(r)=(1-r^2)$	$2\pi a^2 \frac{J_2(u)}{u^2}$	$72.7\frac{\lambda}{D}$	$93.6\frac{\lambda}{D}$	24.6	0.75
$f(r)=(1-r^2)^2$	$8\pi a^2 \frac{J_3(u)}{u^3}$	$84.3\frac{\lambda}{D}$	$116.2\frac{\lambda}{D}$	30.6	0.56

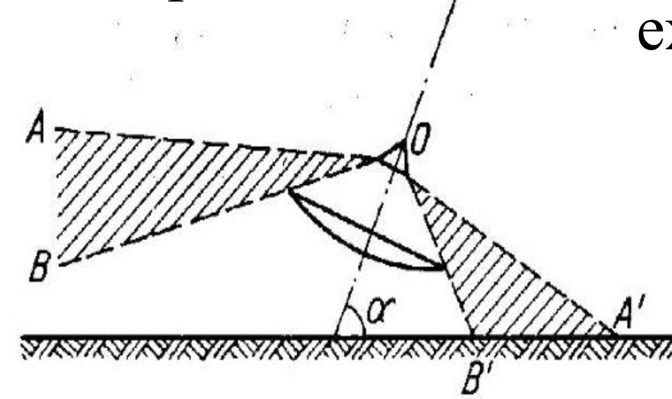

Primary focus : high $T_{A\text{-ground}}$

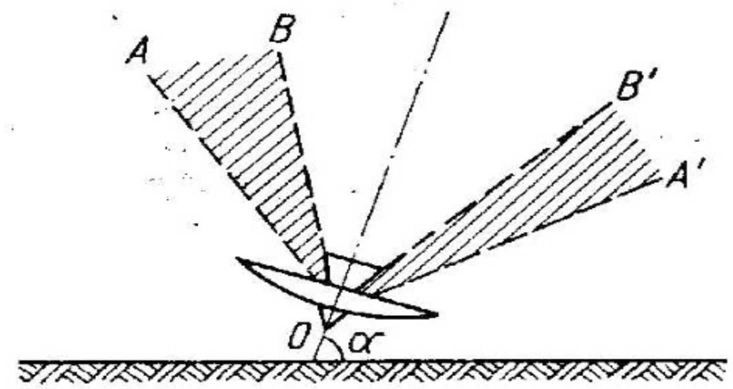

Cassegrain focus : lower $T_{A\text{-sky}}$

$\rightarrow \eta = \sim 0{,}7$ for a good parabolic antenna

• <u>Focal systems</u>

no sensitive surface (focal antenna = horn or dipole = 1 pixel)
Dipole or horn ⇒ receives energy from diffraction pattern of collector → detector
⇒ instantaneous imaging difficult with a single antenna
Since 2010's, Focal Plane Arrays = focal antenna arrays (cf. + below)

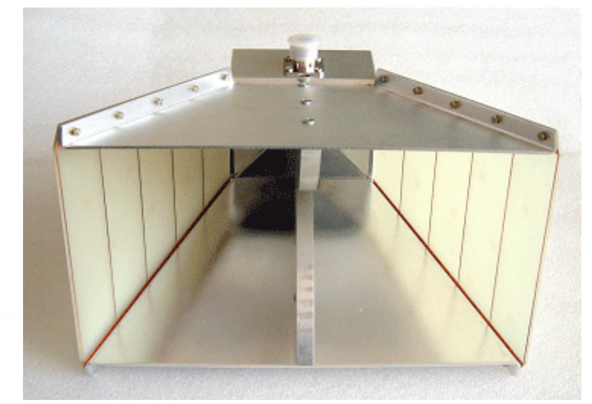

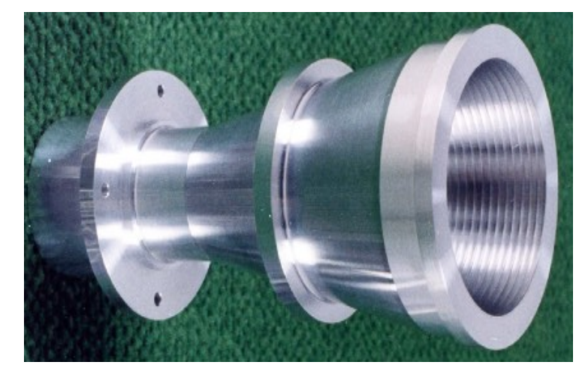

Focal antennas are generally polarised (linearly or circularly)
Linear focal antenna orientation / E ⇒ antenna polarisation
(Horizontal & Vertical polarisations are often used)

⇒ each polarisation receives/transmits S/2 for a non-polarised incident signal S

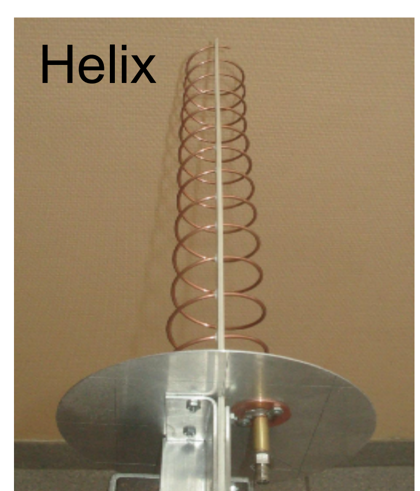

Main planes ⊥, = E and B (or H) for a linearly polarised antenna: radiation pattern generally different in these 2 planes
⇒ response generally ≠ in the 2 polarisations

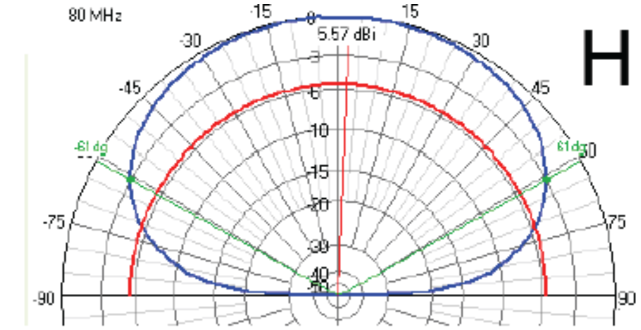

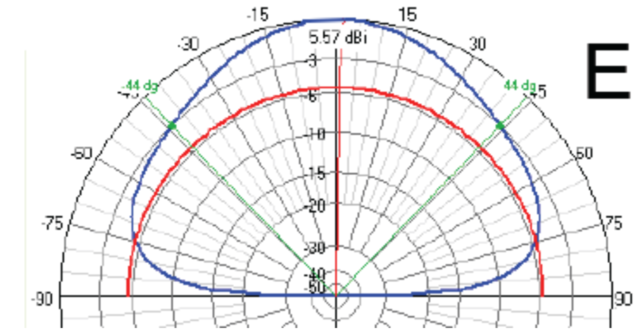

Polarisation cross-talk : response of an antenna to polarisation ⊥ to its nominal reception polar.

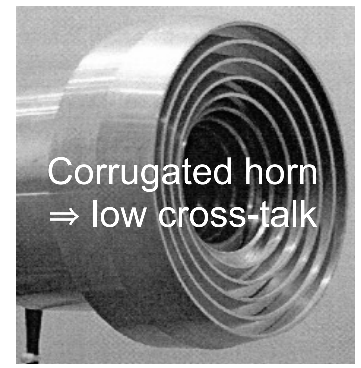

Operating band: limited by variations in $g(\theta,\phi)$ with frequency ⇒ often ≤ 1 octave

Broadband antennas :

- short dipole $L<\lambda/10$ (active if integrated preamplifier)
- « log-periodic » antennas

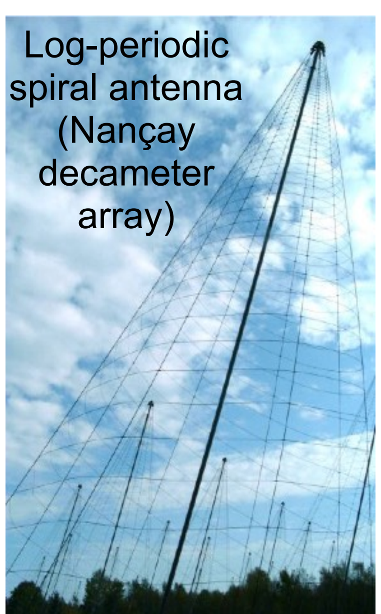

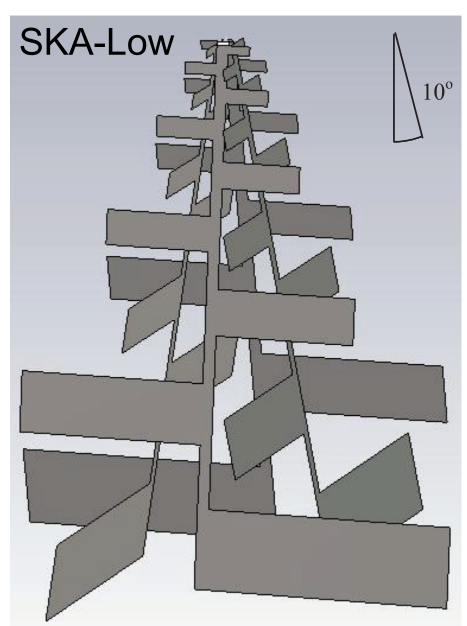

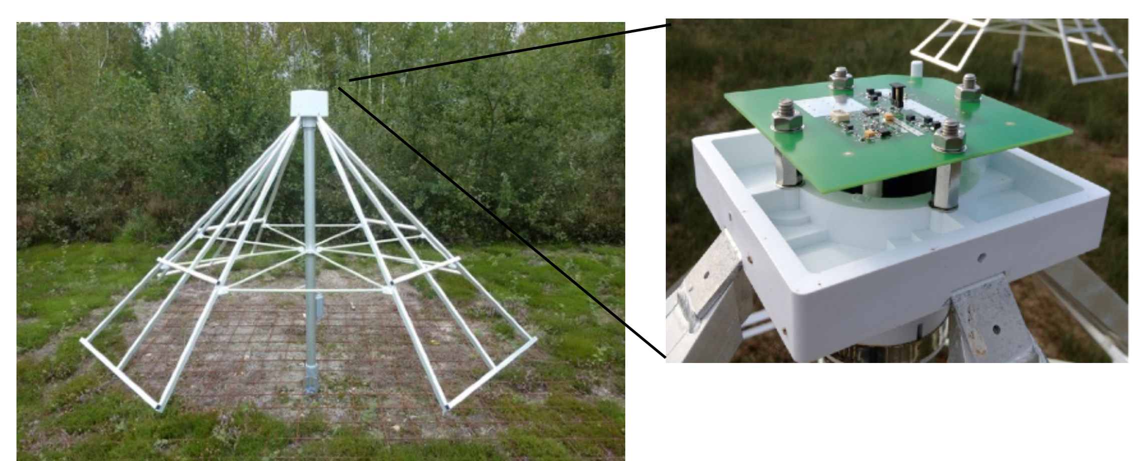

- Introduction (history, interest, specific features)
- Waves & Polarisation
- Plasmas & Propagation (cutoff, dispersion, Faraday effect, scintillations)
- Coherent Signal Detection (measurement theory, antenna temperature, calibration, noise)
- Receivers (heterodyne, system temperature, filtering, gain, RFI mitigation)
- Basics of Radio Astronomy Antennas: Single antennas
- Basics of Interferometry and Aperture Synthesis (phased arrays, electronic pointing, imaging, correlation, coherence, VLBI)
- Observation methods
- Large present & future ground-based radio arrays
- Basics of Space radio astronomy

High angular resolution required on Jupiter, Sun, RadioGalaxies, Quasars...

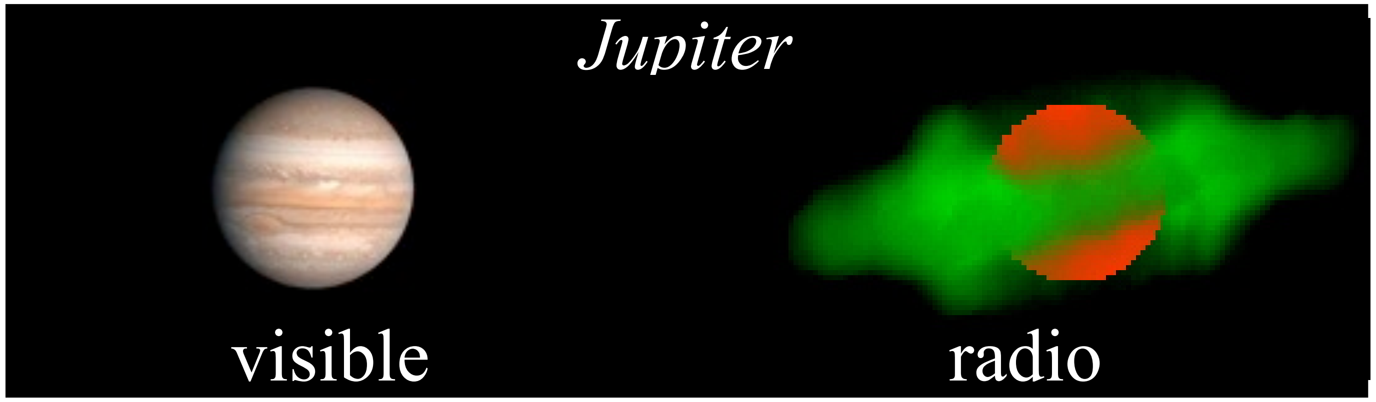

40”

Radio Image of Cygnus-A (FR-II)

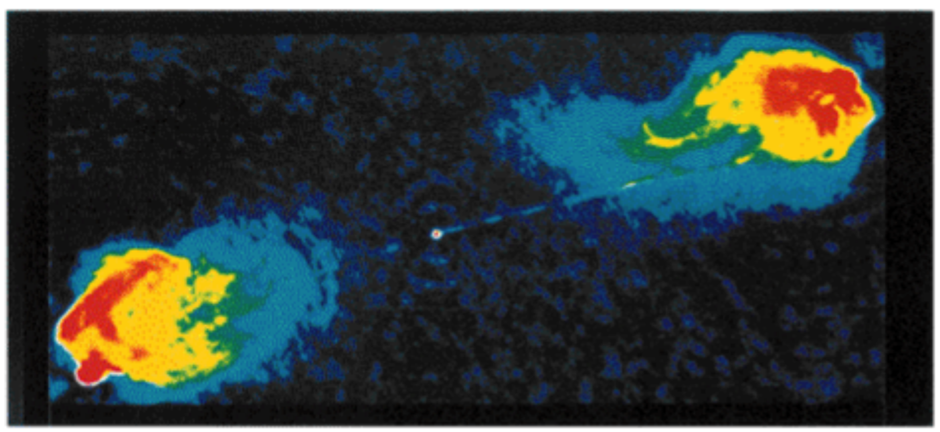

z=0.056 (d≈300 Mpc)

5 GHz image ; ∅ 200 kpc

2’

Radio Image of 3C219 (FR-II)

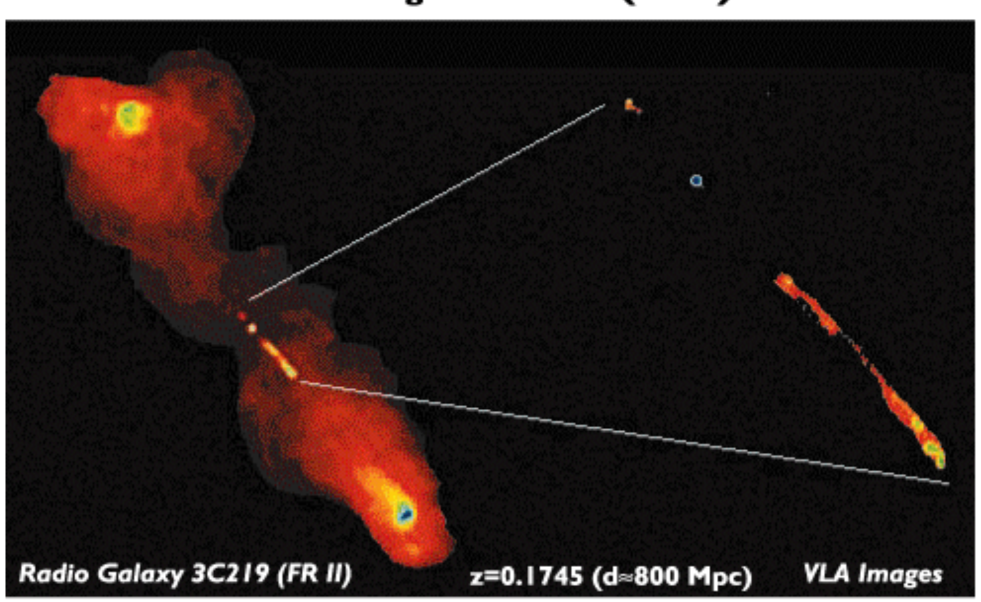

1.4+1.6 GHz combined image at 1.4 arcsec resolution

8 GHz image of jets at 0.1 arcsec resolution

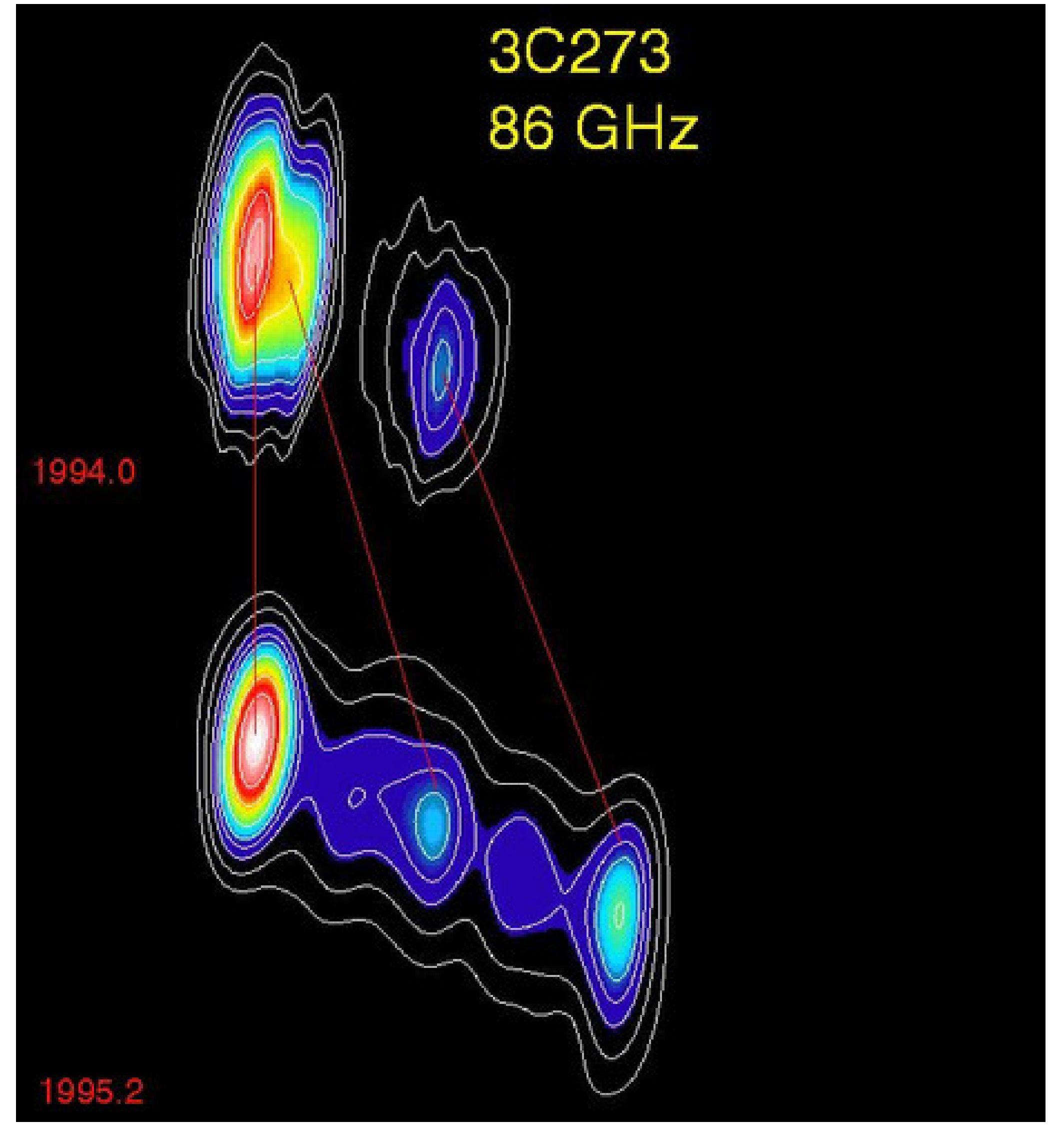

0.001”

+ Possible existence of spatially coherent sources (e.g. Jupiter, Masers...), linked to non-thermal coherent mechanisms.

• Maximum resolution of single antennas ~ λ / D_{max} ≈ 1'

• To increase angular resolution ⇒ Interferometry

• Point source (in the direction θ)

2-antenna array (or interferometer) in sum (Σ)

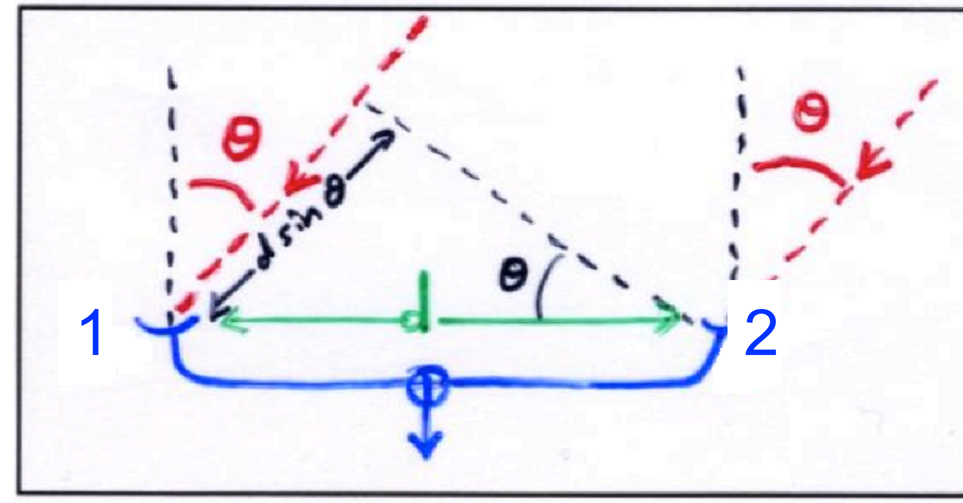

Relative phase shift :

$$\psi = \mathbf{k} \cdot \mathbf{x}$$
$$= 2\pi d \sin\theta / \lambda$$
$$\approx 2\pi d\theta/\lambda \quad \text{for } \theta \text{ small}$$

Identical & omnidirectional antennas :

$E_1 = E_o \exp(i2\pi\nu t)$ $\qquad$ $E_2 = E_o \exp[i(2\pi\nu t-\psi)]$

$$E_\oplus = E_o \exp(i2\pi\nu t)\,[1 + \exp(-i\psi)]$$
$$= E_o \exp(i2\pi\nu t-i\psi/2)\,[\exp(i\psi/2) + \exp(-i\psi/2)]$$
$$= 2E_o \exp(i2\pi\nu t-i\psi/2) \cos(\psi/2)$$
$$\Rightarrow \; P_\oplus = E_\oplus . E_\oplus^*$$
$$P_\oplus = 2\,E_o^2\,(1+\cos\psi) = 4\,E_o^2 \cos^2(\psi/2) = 4\,E_o^2 \cos^2(\pi d\theta/\lambda)$$

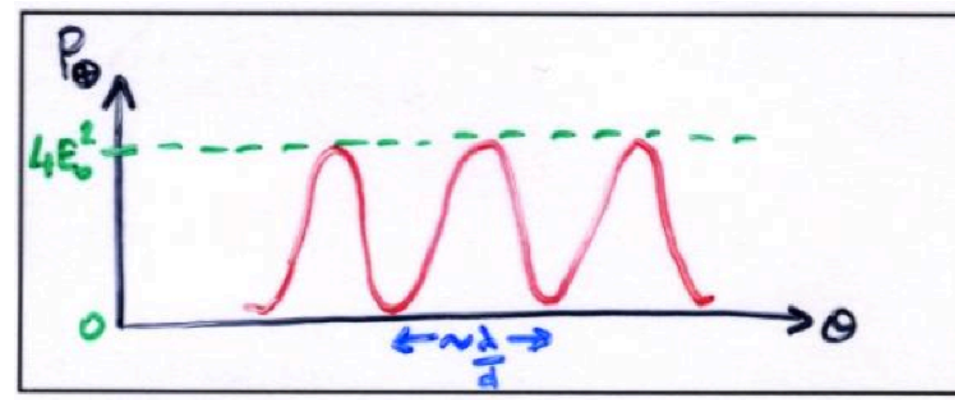

Contrast $|V(d,\theta)| = (P_{\oplus max} - P_{\oplus min}) / (P_{\oplus max} + P_{\oplus min}) = 1$

Antennas with ≠ gains : $E_1{}^2 = g_1\,E_o{}^2$ & $E_2{}^2 = g_2\,E_o{}^2$

$$\Rightarrow \; P_\oplus = E_1{}^2 + E_2{}^2 + 2E_1E_2\cos\psi$$
$$\Rightarrow \; |V| = 2(g_1g_2)^{1/2}/(g_1+g_2)$$

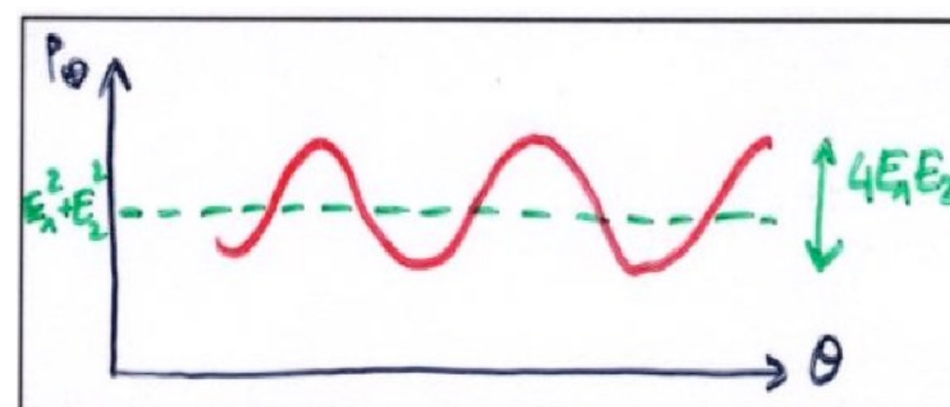

For non-omnidirectional antennas :

$\Rightarrow$ Diagram multiplication theorem :

If $g(\theta,\phi)$ represents the radiation pattern of an antenna A, and $R(\theta,\phi)$ the radiation pattern of an array R of isotropic antennas, the radiation pattern of an array R made up of these antennas A is (in the far field) : $F(\theta,\phi) = g(\theta,\phi) \times R(\theta,\phi)$

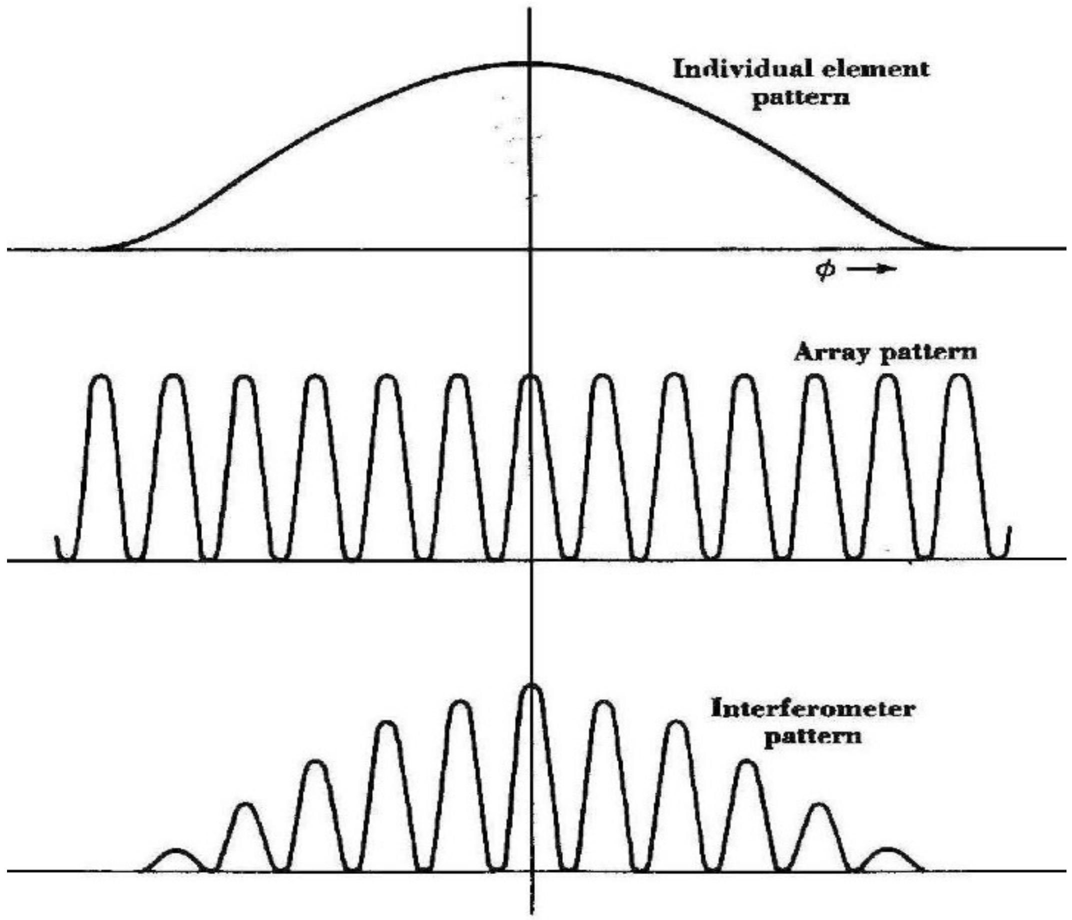

$E_o \rightarrow E_o(\theta)$ = antenna diffraction pattern = interference pattern envelope

e.g. for 2 rectangular 1D apertures :

$P_\oplus \rightarrow P_\oplus \times sinc^2(\pi D\theta/\lambda)$

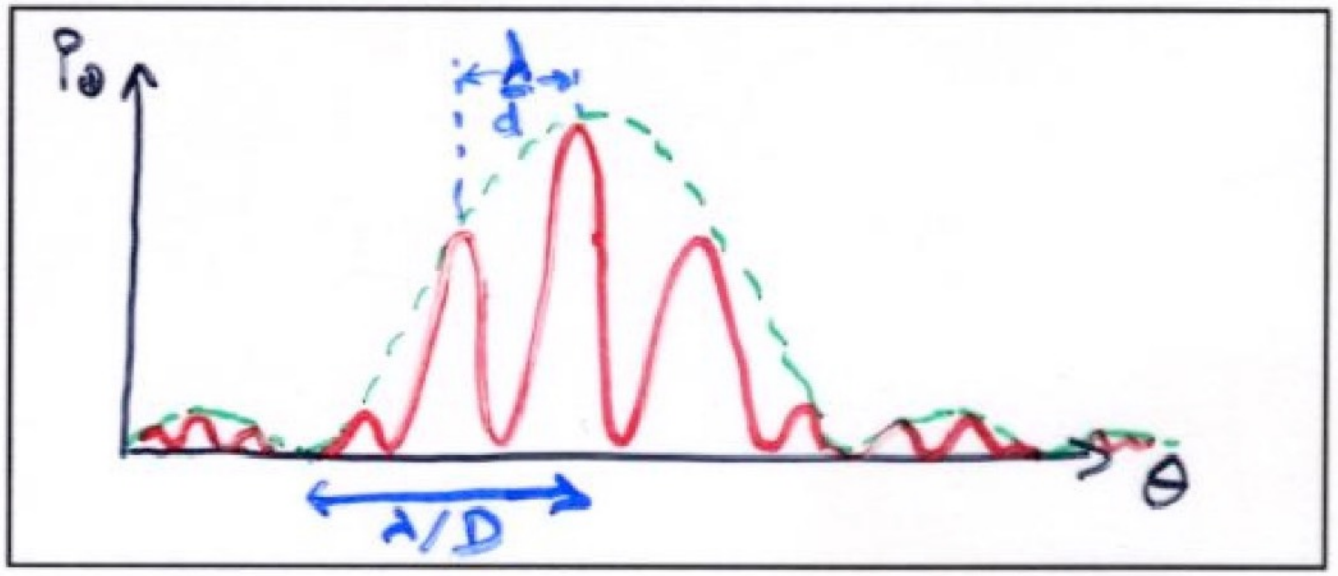

2-antenna interferometer in product (Π) or correlation

Identical antennas : $P_\otimes = E_1.E_2^* = E_o^2 \exp(i\psi)$
$\mathrm{Re}(P_\otimes) = E_o^2 \cos\psi$
Antennas with ≠ gains : $P_\otimes = E_1.E_2.\exp(i\psi)$

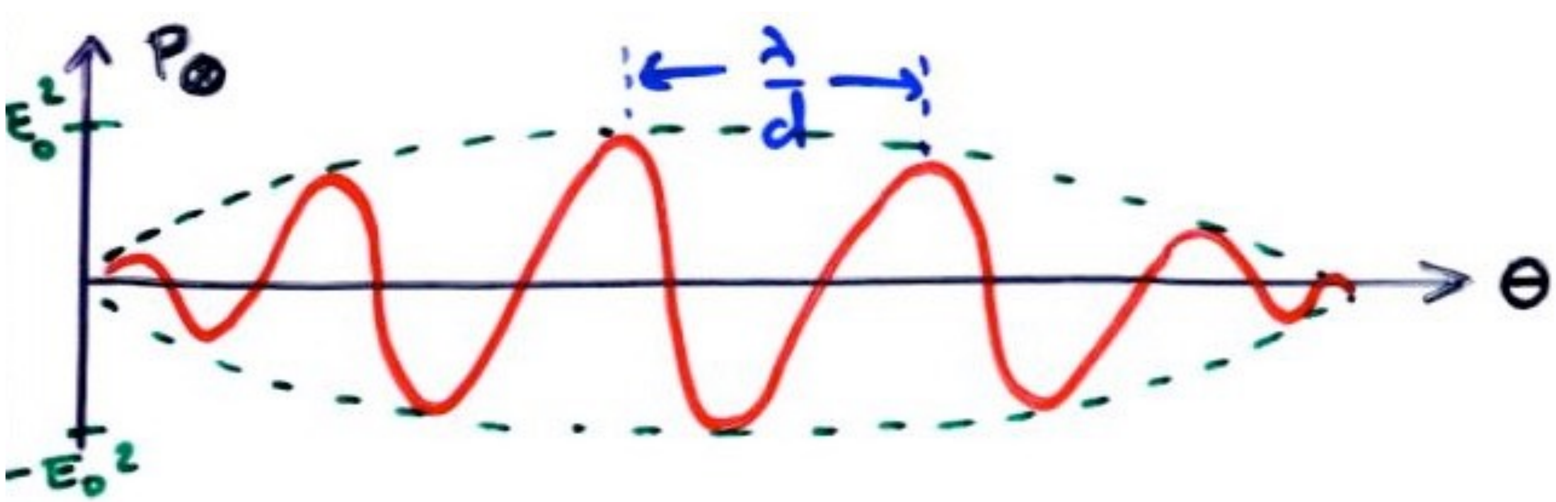

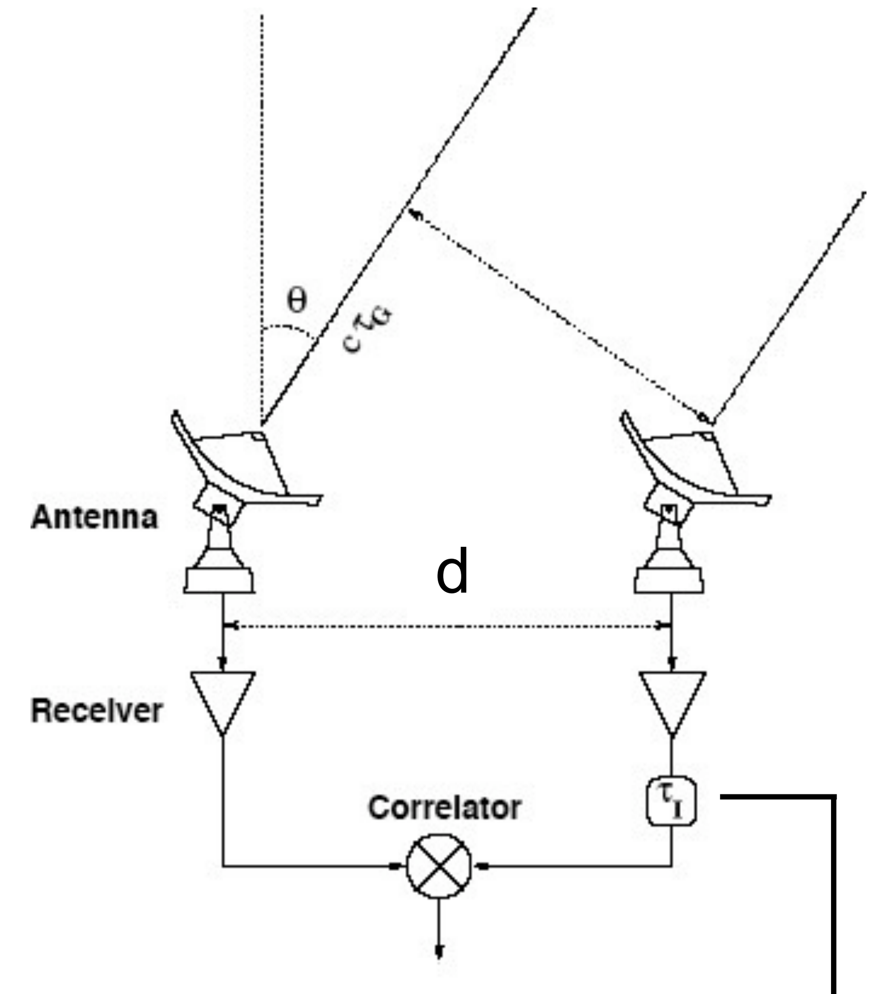

A simple, two-antenna interferometer

We define the complex visibility : $V(d) = \exp(i\psi)$
with modulus = the fringe contrast of the interference pattern (=1 for a point source),
and phase = the position of the central fringe relative to a path difference = zero

$\mathrm{Re}(P_\otimes)$ can be obtained directly in digital, or in analog by phase modulation :

$$\mathrm{Re}(P_\otimes) = 1/4\ (P_\oplus - P_\ominus) = 1/4\ [\ \underbrace{(E_1^2+E_2^2+2E_1E_2\cos\psi)}_{\text{sum in phase}} - \underbrace{(E_1^2+E_2^2+2E_1E_2\cos(\psi+\pi))}_{\text{sum in phase opposition}}\ ]$$

$$= E_1.E_2.\cos\psi$$

<u>NB</u>:

- *the response of an interferometer in product is ≠ power*
- *in all cases, we have* $|V| = 1$
- *in fact, we calculate responses (in* Σ *or* Π*) as* $< E_1(t).E_2^*(t)>|_{\Delta t >> 1/\nu}$

  or $< U_1(t).U_2^*(t)>|_{\Delta t >> 1/\nu}$

For a 2-antennas interferometer: the central fringe is ~λ/d, but the relative contribution of sidelobes ↑ when λ/d ↓ ⇒ compromise resolution/sensitivity/... ?

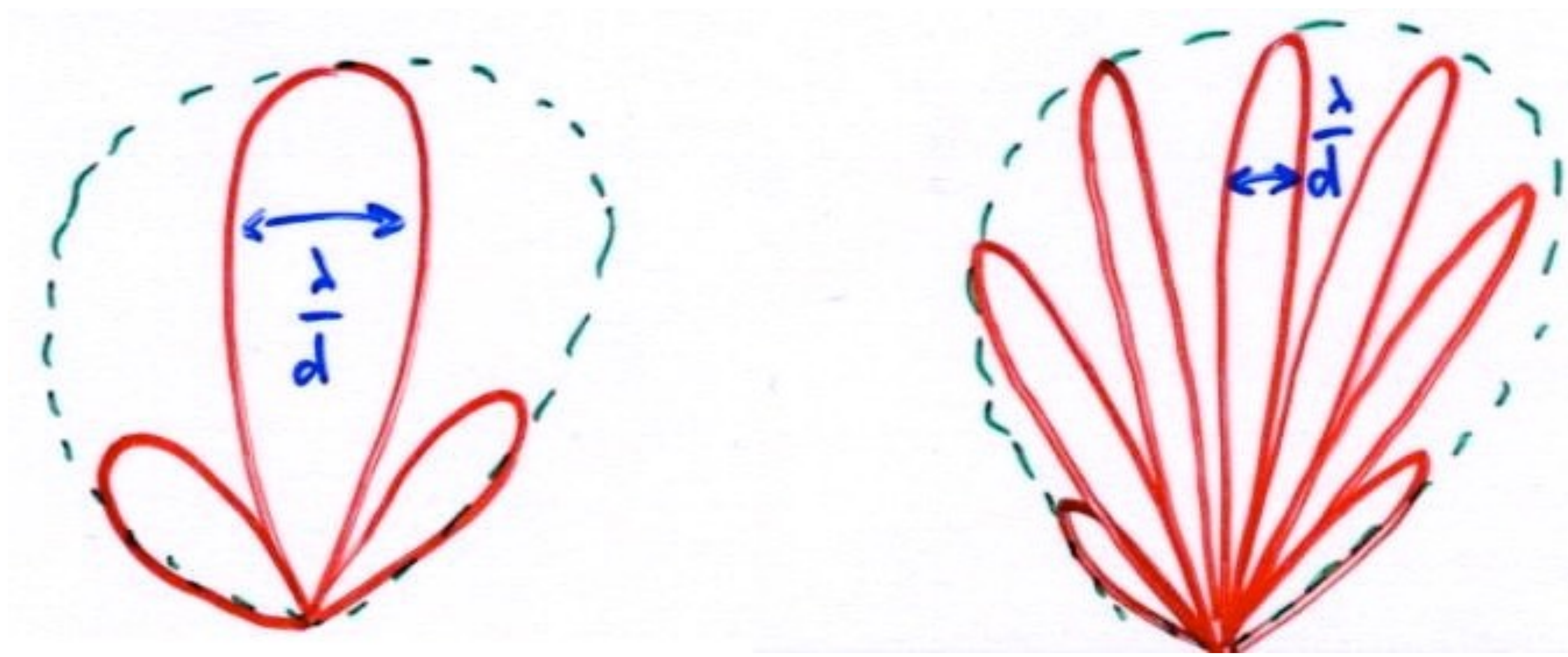

Composite interferometers (X, T …) : composed of any, non-identical antennas

If the 2 antennas are symmetrical with respect to their common phase center(X) :

$$\mathrm{Re}(P_\otimes) = E_1.E_2.\cos(\psi)$$

$$\psi = 0 \;\Rightarrow\; \mathrm{Re}(P_\otimes) = E_1.E_2 \propto \mathrm{sinc}(\pi D_1\theta/\lambda) \times \mathrm{sinc}(\pi D_2\theta/\lambda)$$

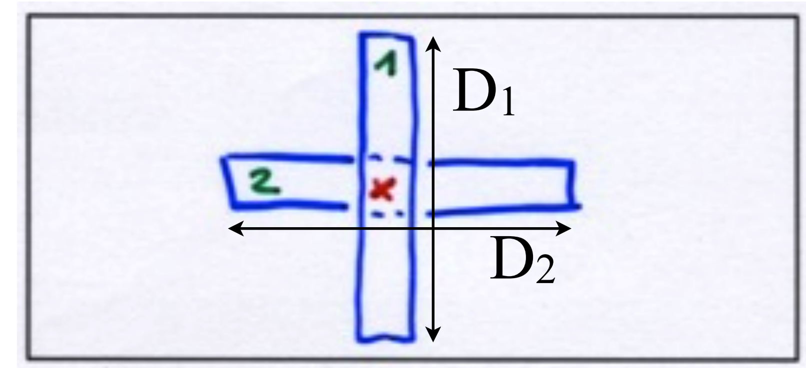

Mills cross

If the 2 antennas have distinct phase centers (here separated by $D_2/4$):

$$P_\otimes = E_1.E_2 \cdot \exp(2\pi D_2\theta/4\lambda)$$

$$\mathrm{Re}(P_\otimes) \propto \mathrm{sinc}(\pi D_1\theta/\lambda) \times \mathrm{sinc}(\pi D_2\theta/2\lambda) \times \cos(\pi D_2\theta/2\lambda)$$

$$\propto \mathrm{sinc}(\pi D_1\theta/\lambda) \times \mathrm{sinc}(\pi D_2\theta/\lambda)$$

(same lobe as symmetrical antenna D_2, but sensitivity ÷2)

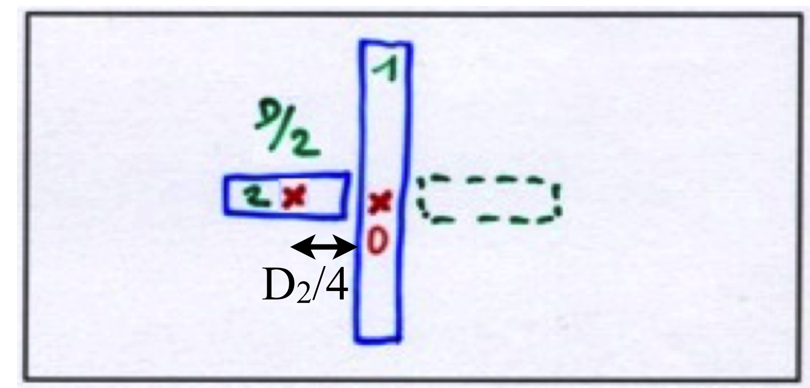

UTR-2/Kharkov array

Linear composite interferometer :

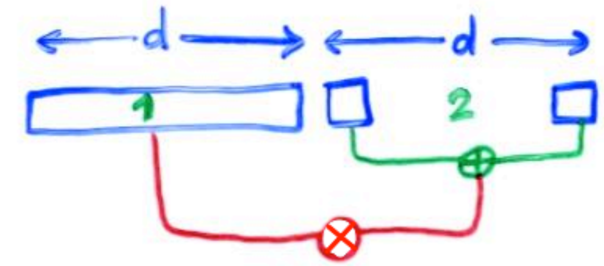

$E_1 \propto \mathrm{sinc}(\psi/2)$ $\quad$ $E_2 \propto \cos(\psi/2)$ $\quad$ with $\quad \psi = 2\pi d\theta/\lambda$

$\Rightarrow \mathrm{Re}(P_\otimes) = E_1.E_2.\cos\psi \;\propto\; \mathrm{sinc}(\psi/2)\cos(\psi/2)\cos\psi \propto \mathrm{sinc}(2\psi)$

$\Rightarrow$ same as antenna with length 2d (but lower sensitivity)

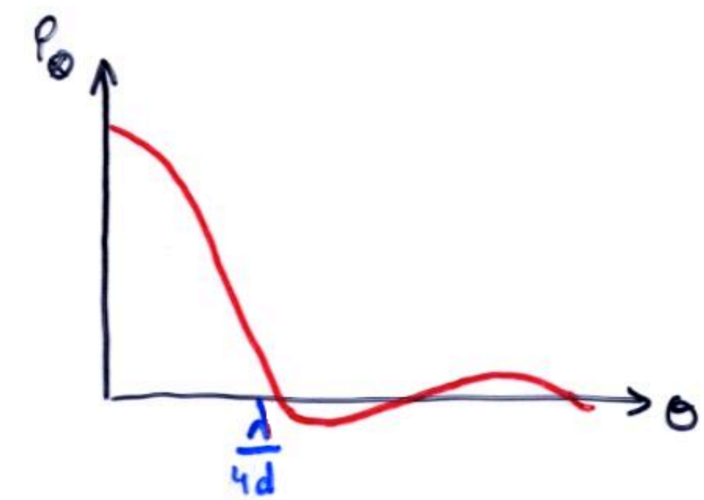

N-antenna interferometer in sum (all in phase)

Phase shift between 2 antennas : $\psi = 2\pi d\theta / \lambda$

$$E = E_o \, \Sigma_{k=0}^{N-1} \exp(ik\psi) \quad \times \, \mathrm{sinc}(\pi D\theta / \lambda) = E_o \, (1 - \exp(iN\psi)) \, / \, (1 - \exp(ik\psi)) \quad \times \, \mathrm{sinc}(\pi D\theta / \lambda)$$

$$= E_o \exp(i(N-1)\psi/2) \times [\sin(N\psi/2) \, / \, \sin(\psi/2)] \quad \times \, \mathrm{sinc}(\pi D\theta / \lambda)$$

$$\Rightarrow P_\oplus = E_o^2 \, [\sin^2(N\psi/2) \, / \, \sin^2(\psi/2)] \qquad \times \, \mathrm{sinc}^2(\pi D\theta / \lambda)$$

$\Rightarrow$ better angular resolution and reduced sidelobes $\Rightarrow$ S/N $\uparrow$

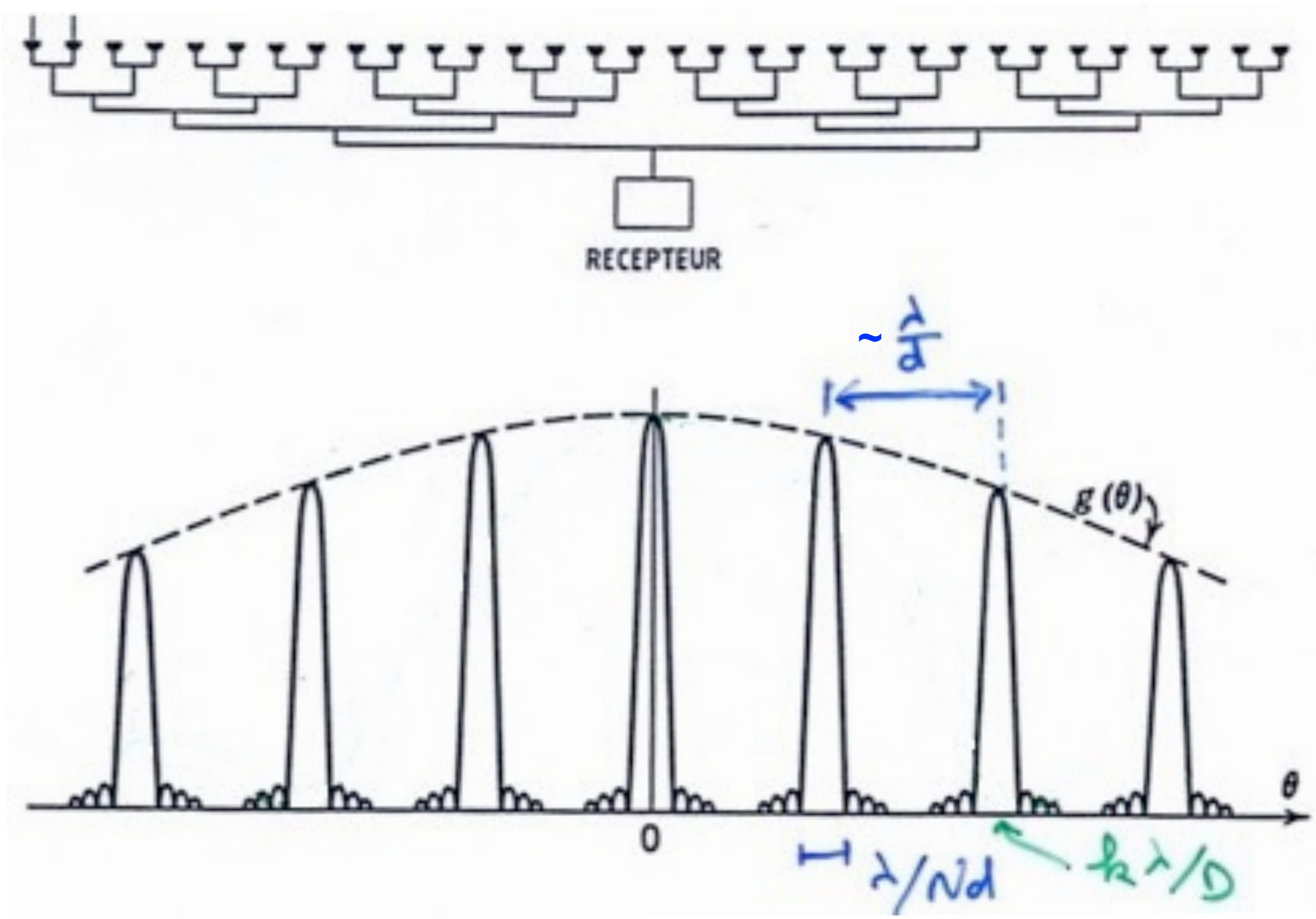

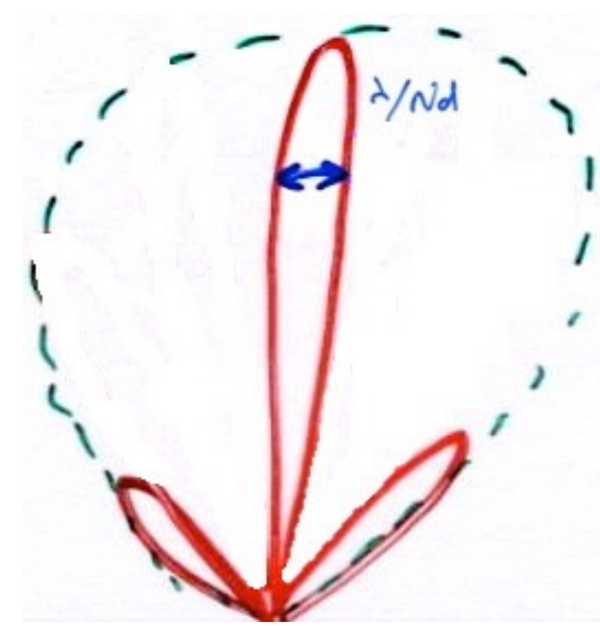

Optimising the radiation pattern:

N $\uparrow \Rightarrow \lambda/Nd \downarrow$ so resolution $\uparrow$

d $\downarrow \Rightarrow \lambda/d \uparrow$ so fewer side lobes

limit = single antenna: $N \to \infty$, $d \to 0$

• <u>Phased array</u>

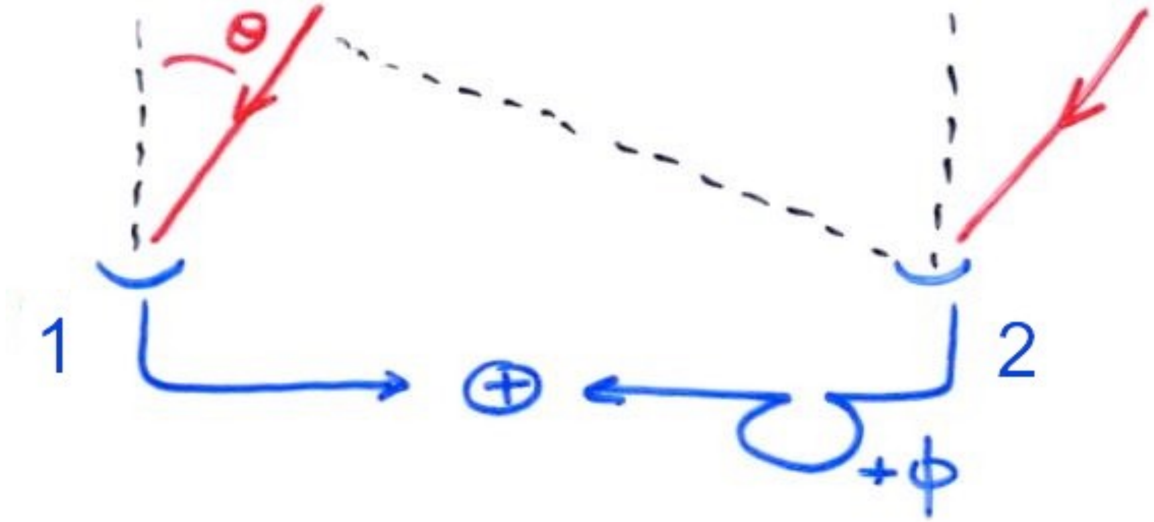

= N-antenna interferometer in sum
⇒ synthesis of a narrow beam, total flux measurement

<u>Electronic pointing of a phased array</u> :
Principle with 2 antennas ⇒ response $R \propto \cos(\psi/2)$
If the antennas are in phase ⇒ R maximum for $\theta = 0$ ⇒ central fringe in the bisector plane of the 2 antennas
If we introduce a phase shift φ of antenna 2 / antenna 1
⇒ response $R \propto \cos((\psi + \varphi)/2) = \cos((2\pi d \sin\theta / \lambda + \varphi)/2)$
maximum for $\theta_o = \arcsin(-\lambda\varphi/2\pi d) \neq 0$ ⇒ shifted central fringe

NB: for a small FoV : $R \propto \cos((2\pi d\, \theta / \lambda + \varphi)/2)$ *maximum for* $\theta_o = -\lambda\varphi/2\pi d$

⇒ same formulas apply for a N antennas array
A relative phase shift allows to point without mechanical movement

The benefits of electronic pointing :
→ rapidity (< 1 sec)
→ fiability (no moving parts)
→ flexibility (simultaneous ON/OFF, e.g. at UTR-2)

Array (linear, 1D) with N (isotropic) antennas :

$\Rightarrow$ we introduce a constant phase shift φ between 2 successive antennas to point in the direction θ_o :

$$\psi = 2\pi d \sin\theta / \lambda + \varphi = 2\pi d \sin\theta / \lambda - 2\pi d \sin\theta_o / \lambda$$

$\Rightarrow P_\oplus = E_o^2 \, [\sin^2(N\psi/2) / \sin^2(\psi/2)]$

Periodic main lobes = array lobes, for ψ multiple of 2π

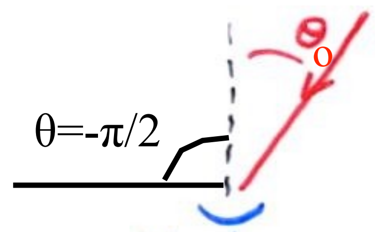

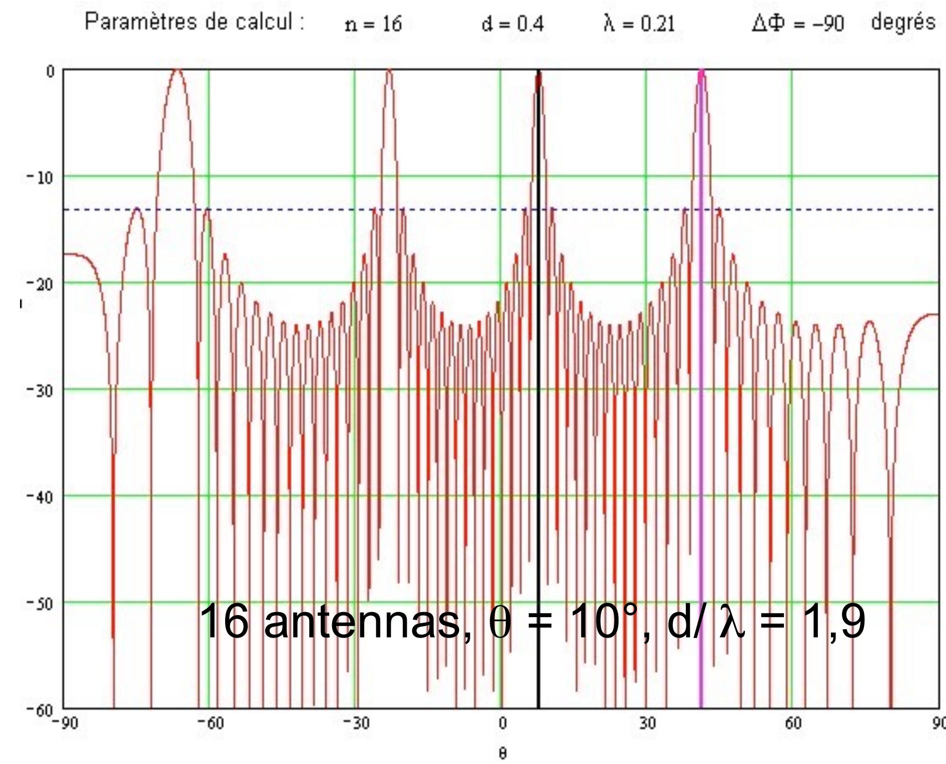

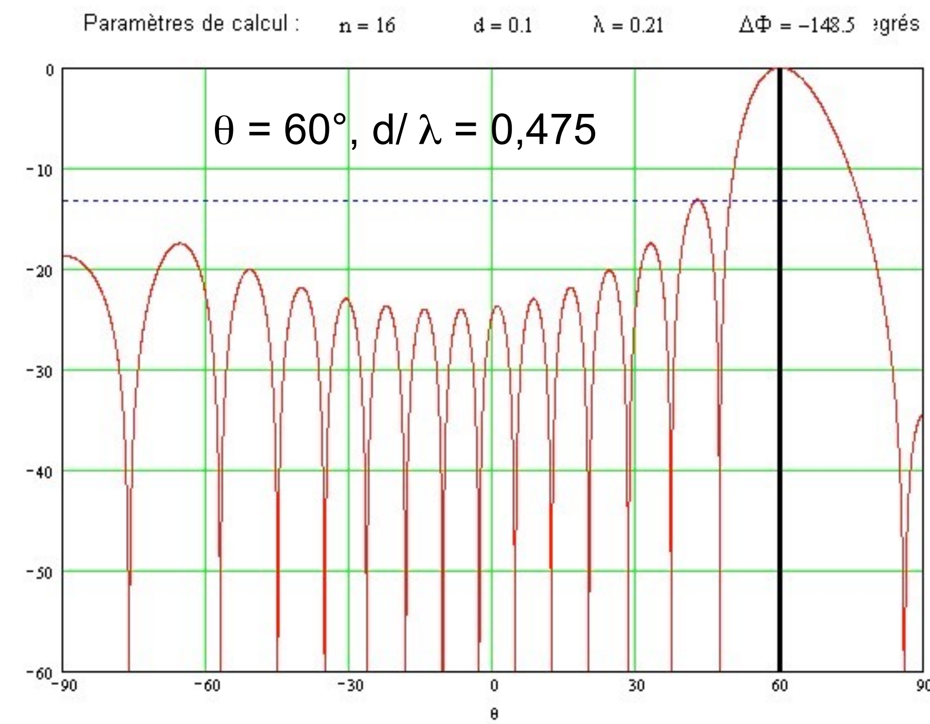

Choice of the distance between antennas such that no grating lobes appear when pointing in the θ_o direction :

$\psi > -2\pi$ pour $\theta = -\pi/2 \Rightarrow d < \lambda/(1+\sin\theta_o)$

$d < \lambda$ for a pointing to the zenith

$d < \lambda/2$ $\forall$ pointing

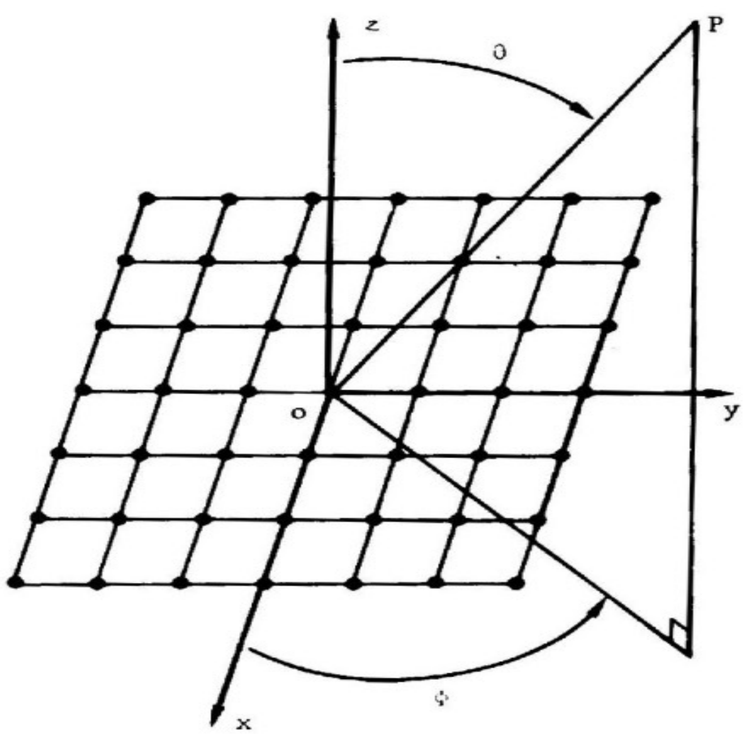

Planar array (rectangular, 2D) with $N_x \times N_y$ antennas (isotropic) :

$\Rightarrow P_\oplus = E_o^2 \, [\sin^2(N_x\psi_x/2) / \sin^2(\psi_x/2)] \times [\sin^2(N_y\psi_y/2) / \sin^2(\psi_y/2)]$

Dense array: elements very close to each other, $A_e \sim A$
Sparse array: elements widely separated, $A_e << A$
Aperiodic array : non-regular grid to suppress array lobes

Ex: Nançay Decameter Array : phased array in Σ, compact ("filled aperture", space between antennas < λ)
φ between blocks of 8 antennas (9 blocks / array / circular polarisation) introduced by "delay lines"

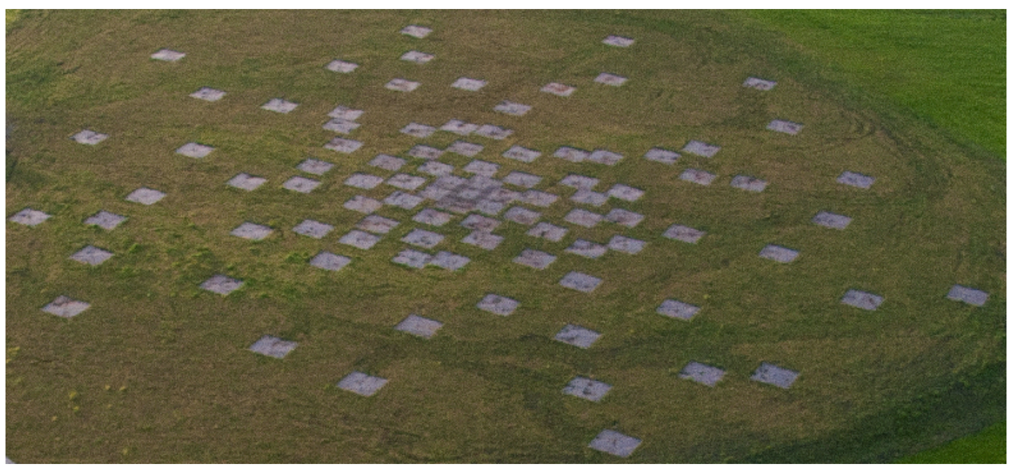

Ex: LOFAR-LBA field: phase array in Σ, random distribution ~Gaussian, overlap A_{eff}~20%
φ between antennas introduced numerically by channelisation + phase shifts

Additional degree of freedom: distribution of the gains of the N antennas for the best compromise
Ex: in-phase antennas λ/2 apart

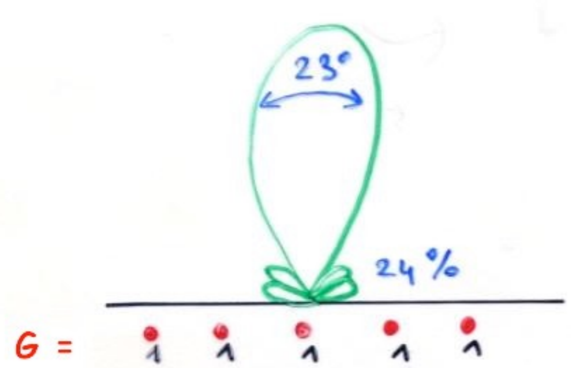

(Uniform distribution)

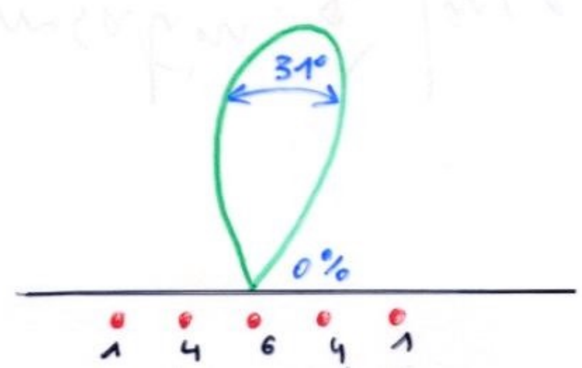

(Binomial distribution)

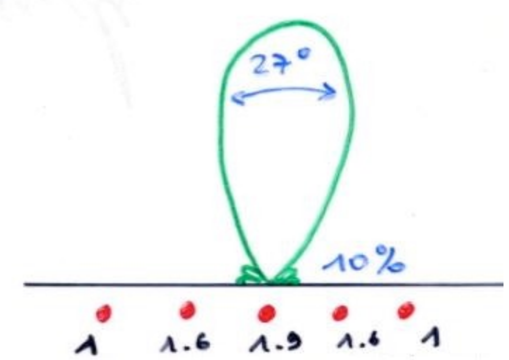

(Optimal «Dolph-Tchebychev» distribution)

Determining the gains and phase shifts to be applied to each antenna

⇒ beamforming

- main lobe width
- array lobes suppression
- position of zeros (deterministic nulling / adaptative in real-time)
- secondary lobes level

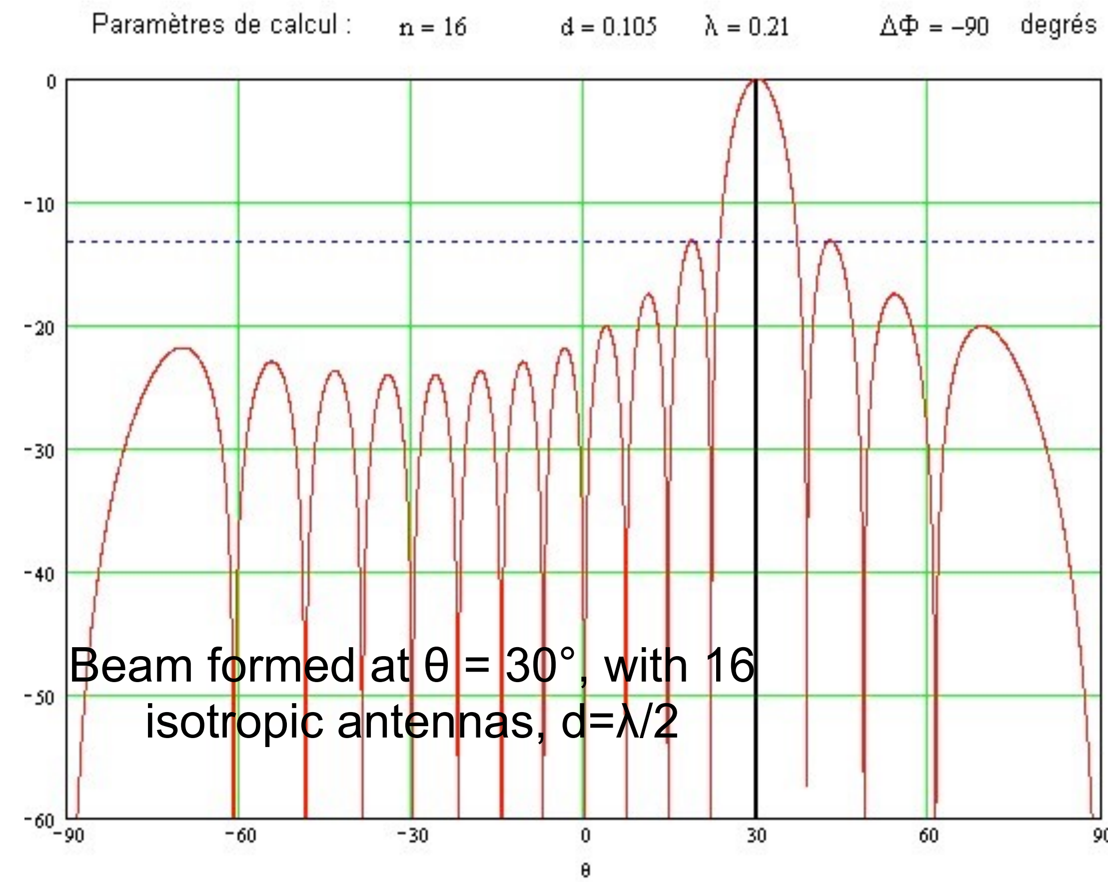

Delay lines : $\varphi = 2\pi\nu\tau \Rightarrow \psi + \varphi = 2\pi d \sin\theta/\lambda + 2\pi c\tau/\lambda = 0$

for $\theta = \arcsin(-c\tau/d)$ independent of λ

⇒ achromatic pointing

Phase-shifting circuits : $\psi + \varphi = 2\pi d \sin\theta/\lambda + \varphi = 0$

for $\theta = \arcsin(-\lambda\varphi/2\pi d)$ dependent of λ

⇒ chromatic pointing

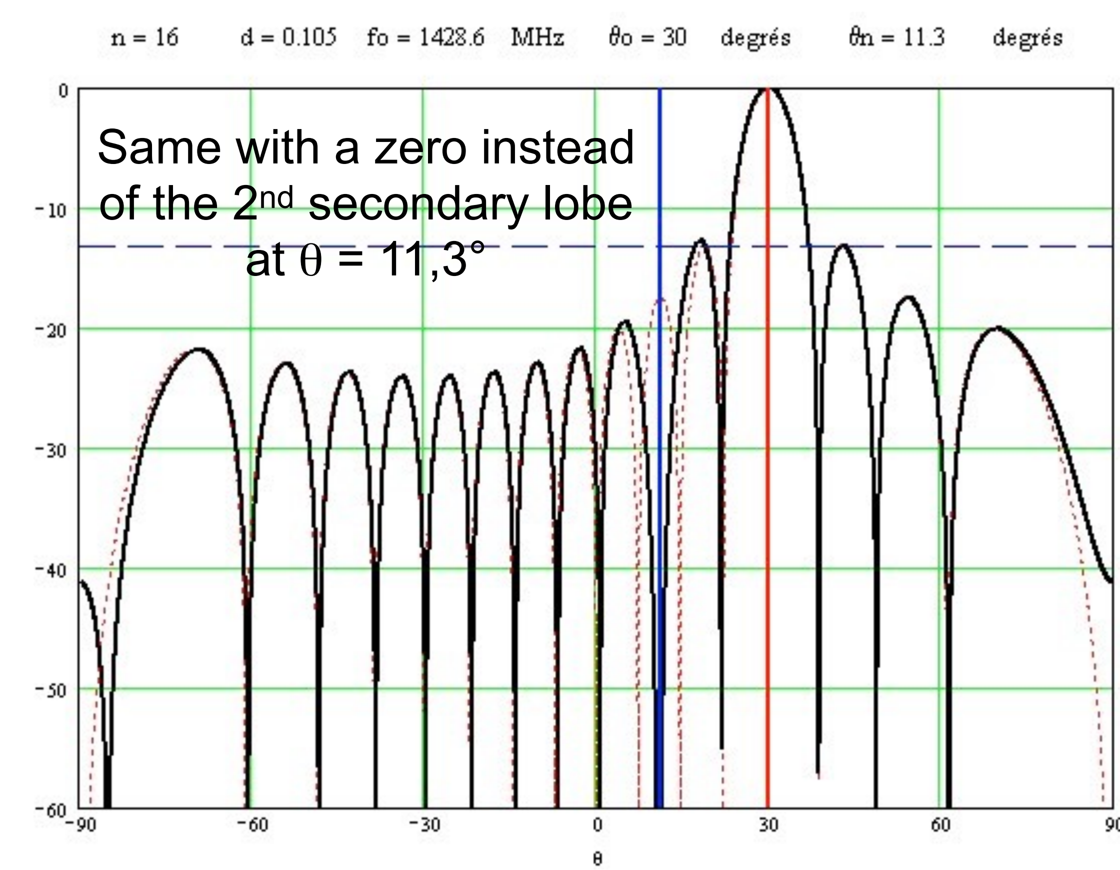

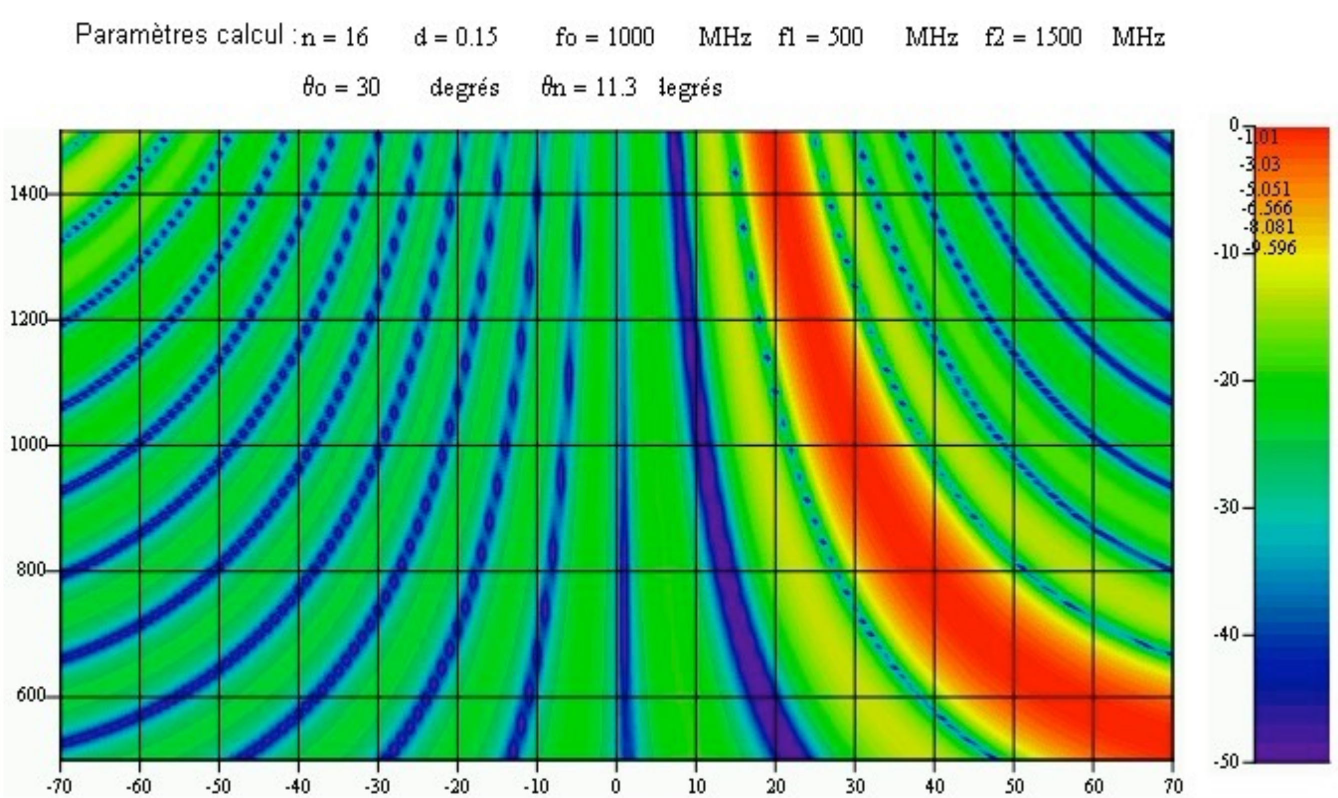

• <u>Field of view</u> (=FoV)

The narrow lobe formed by the array has as its envelope the lobe of each constituent element of the array (consequence of the diagram multiplication theorem).

→ FoV generally defined by the -3 dB lobe of an element

$$\text{FoV (sr)} = \int_0^{\theta_{3dB}/2} 2\pi \sin\theta \, d\theta = 2\pi \left(1 - \cos\left(\theta_{3dB}/2\right)\right) \approx \pi\, \theta_{3dB}^2/4$$

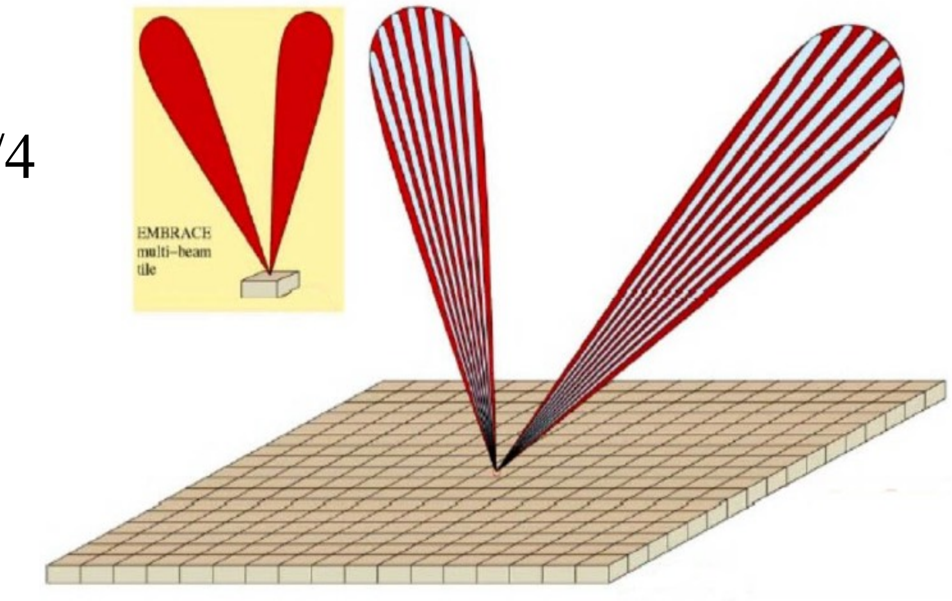

Ex : *For a 6m diameter dish at 1 GHz : FoV ≈ 9°²*

For a 1m × 1m tile at 1 GHz : FoV ≈ 350°²

• Multi-beam systems

Focal Plane Arrays - Horn arrays (1 / beam)

- Focal phased arrays

Direct sampling of the incident wavefront by a dense phase array (Aperture Array)

<u>NB</u> : with phased arrays, all elements contribute to all beams

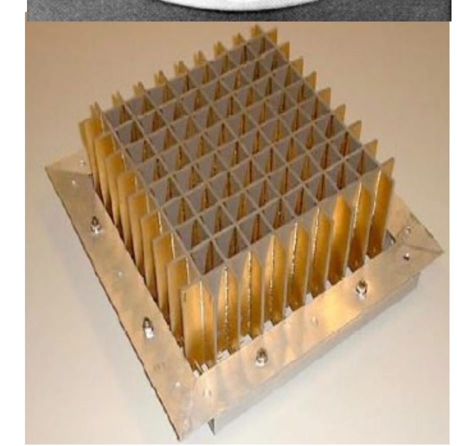

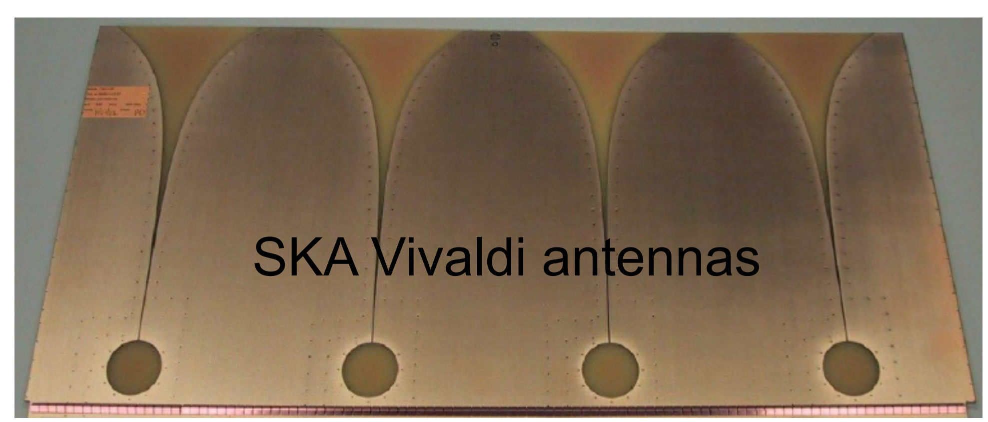

• <u>Antennas in imagery</u>

→ *Intuitive* approach to the Visibility as a function of the dimension of an extended source
An extended source drifts in front of the instrument (2-antenna interferometer) → θ(t)

- for a point source (∅ << λ/d), I(θ(t)) is simply the response of the instrument R(θ)

- for an extended source of ∅ < λ/d, the response of the interferometer never falls to 0, but there are still fluctuations in I(θ(t)) (I = convolution of R by the brightness distribution of the source)

⇒ contrast is defined as the amplitude of the modulation:

$|V(d)| = [I_{max}(\theta) - I_{min}(\theta)] / [I_{max}(\theta) + I_{min}(\theta)]$

$|V|=1$ for a point source,

↓ when the source size ↑

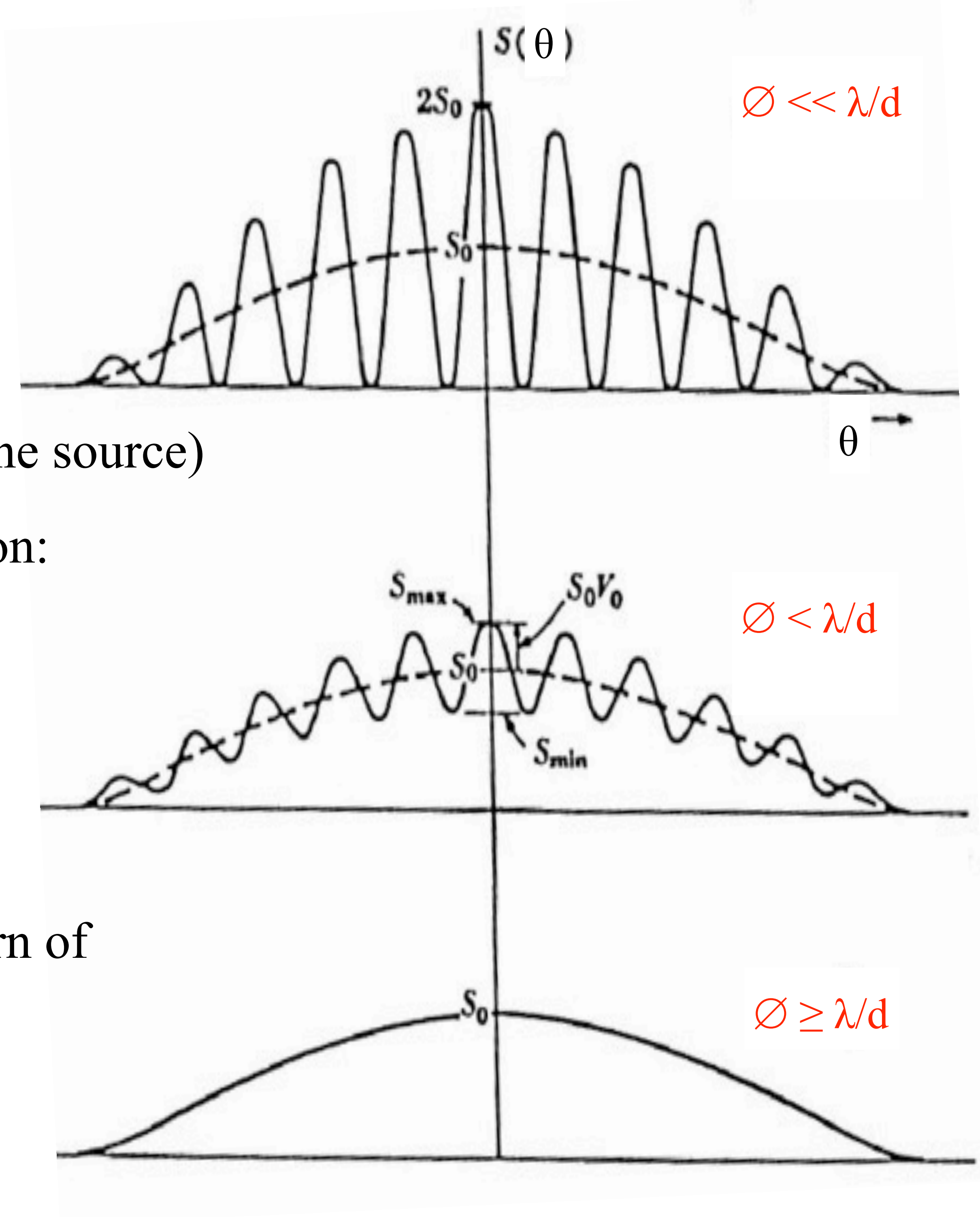

- for an extended source of ∅ ≥ λ/d, the response of the interferometer is reduced to the diffraction pattern of each telescope

⇒ no fringes are observed anymore: $|V|=0$

⇒ resolution of interferometric observations is lost

⇒ a 2-antenna interferometer is only sensitive to angular resolutions ~λ/d (the "useful" information is the measurement of the contrast V, in amplitude and phase)

• Imagery of an extended source

2-antenna interferometer in sum (Σ) [identical & omnidirectional antennas]

$E_\oplus = \exp(i2\pi\nu t) \int_{source} E(\theta) [1 + \exp(-i\psi)] \, d\theta$ *(in 2D $d\theta d\varphi$)*

$\psi = 2\pi d \sin\theta / \lambda$
$\approx 2\pi d\theta/\lambda$

$\Rightarrow P_\oplus = < E_\oplus . E_\oplus^* >|_{\Delta t >> 1/\nu}$

$= \int_{source} 2\, E(\theta)^2 [1 + \cos\psi] \, d\theta$

$= \int_{source} 2\, E(\theta)^2 \, d\theta + \int_{source} 2\, E(\theta)^2 \cos\psi \, d\theta$

$= 2 \int_{source} T_A(\theta) \, d\theta + 2 \int_{source} T_A(\theta) \cos\psi \, d\theta$

$P_\oplus = 2 <T_A>|_{source} + 2\mathrm{Re}(\int_{source} T_A(\theta) \exp(i\psi) \, d\theta)$

$T_A(\theta) \approx E(\theta).E(\theta)^*$
$\approx |E(\theta)|^2$

We define the complex visibility:

$V(d) = (\int_{source} T_A(\theta) \exp(i\psi) \, d\theta) / (\int_{source} T_A(\theta) \, d\theta)$

$V(d) = (\int_{source} T_A(\theta) \exp(i\psi) \, d\theta) / <T_A>|_{source}$

$\Rightarrow P_\oplus = 2 <T_A>|_{source} [1 + \mathrm{Re}(V(d))]$

2-antenna interferometer in product (Π) or correlation [identical & omnidirectional antennas]

$P_\otimes = < E_1.E_2^* >|_{\Delta t >> 1/\nu} = \int_{source} E(\theta)^2 \exp(i\psi) \, d\theta = (\int_{source} T_A(\theta) \exp(i\psi) \, d\theta)$

hence

$P_\otimes = V(d) <T_A>|_{source}$ or $V(d) = P_\otimes / <T_A>|_{source}$

- Notion of spatial frequency

Reminder: for a ray from a direction θ ray passing through the aperture at M a distance x from O, the phase shift is:

$$\psi = \mathbf{k.x} = 2\pi\, x \sin\theta / \lambda \approx 2\pi\, x\, \theta / \lambda$$

the corresponding wave (passing at M) writes: $E = E_o \exp[i(\omega t - \psi)] = E_o \exp(i2\pi\nu t) \exp(-i2\pi\, x\, \theta / \lambda)$

The amplitude received in the direction θ is :

$$E(\theta) = \int_{aperture} E_o \exp(i2\pi\nu t) \exp(-i2\pi\, x\, \theta / \lambda)\, dx = E_o \exp(i2\pi\nu t) \int_{-\infty}^{+\infty} f(x) \exp(-i2\pi\, x\, \theta / \lambda)\, dx$$

with $f(x) = 1$ *for* $x \in$ *aperture,* $f(x) = 0$ *elsewhere*

$E(\theta) = TF(E(x))$ where $E(x) = [\, E_o \exp(i2\pi\nu t)\,] \times f(x)$ *is the amplitude distribution over the aperture*

θ *(or sinθ)* and x/λ are conjugate variables

$u = x/\lambda$ is the spatial frequency associated with the characteristic angular scale $\theta = u^{-1}$

In two dimensions (u,v) are the spatial frequencies, defined on the pupil plane (the aperture), conjugated to the angular coordinates (θ,ϕ)

$(u = x/\lambda,\ v = y/\lambda)$ are expressed in [rad^{-1}] or [°$^{-1}$], with (x,y) = coordinates in the pupil plane

$\Rightarrow E(\theta,\phi) = F.T.\,[E(u,v)] \Leftrightarrow E(u,v) = F.T.^{-1}\,[E(\theta,\phi)]$

More generally (in 2D) complex visibility therefore writes:

$$V(u,v) = \left(\int_{source} T_A(\theta,\phi) \exp[i2\pi(u\theta+v\phi)]\, d\theta d\phi \right) / \left(\int_{source} T_A(\theta,\phi)\, d\theta d\phi \right)$$

$\Rightarrow V(u,v) = t_A(u,v) / \langle T_A \rangle|_{source}$

Zernike-Van Cittert Theorem : the complex visibility (or coherence factor) is the Fourier Transform of the source's spatial intensity distribution normalised by its mean intensity.

As: $V(u,v) = P_{\otimes} / \langle T_A \rangle|_{source} \quad \Rightarrow \quad V(u,v) = \langle E(0,0).E(u,v)^* \rangle / \langle T_A \rangle|_{source}$

the complex visibility is measured as correlations on the aperture (to a constant factor)

• <u>Imaging an extended source with any antenna (or array of antennas)</u>

An antenna $g(\theta,\phi)$ pointing in the direction (θ_o,ϕ_o) to observe a source of brightness distribution $T(\theta,\phi)$ produces an image

$$\Rightarrow T_A(\theta_o,\phi_o) = 1/4\pi \times \int_{source} T(\theta,\phi) \times g(\theta_o-\theta,\phi_o-\phi)\, d\Omega = 1/4\pi \times [\, g \otimes T \,]\, (\theta_o,\phi_o)$$

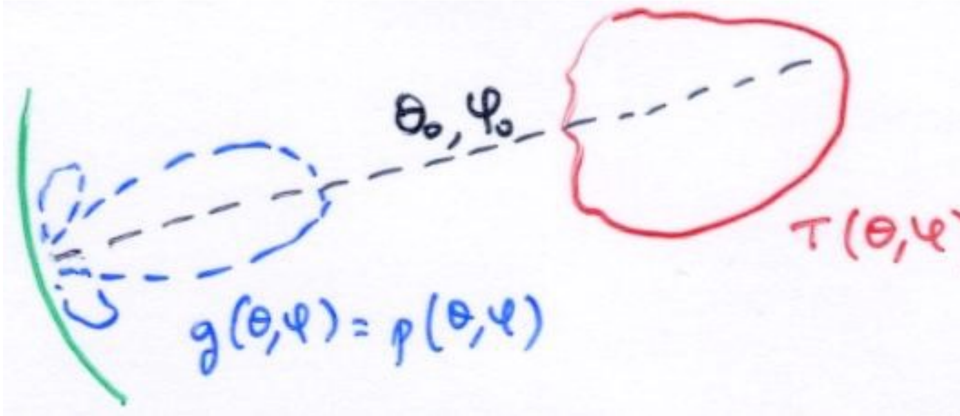

The object $T(\theta,\phi)$ can be decomposed by 2D spatial (angular) Fourier Transform

$$T(\theta,\phi) = F.T.\,[t(u,v)] \quad \Leftrightarrow \quad t(u,v) = F.T.^{-1}\,[T(\theta,\phi)]$$

$$\Rightarrow t_A(u,v) = G(u,v)\,.\,t(u,v)$$

with $T_A(\theta,\phi) = F.T.\,[t_A(u,v)] \Leftrightarrow t(u,v) = F.T.^{-1}\,[T(\theta,\phi)]$

and $G(u,v) = 1/4\pi \times TF[g(\theta,\phi)]$ = "transfer function" of the antenna

$\Downarrow$

"antenna impulse response" $[\, t(u,v)=1$ for $T(\theta,\phi)=\delta \,]$

The antenna is a complex linear filter of the source's spatial frequencies.

<u>NB</u> : $G(0,0) = 1/4\pi \times \int g(\theta,\phi)\, e^{-iu\theta}\, e^{-iv\phi}\, d\Omega = 1/4\pi \times \int g(\theta,\phi)\, d\Omega = 1$
corresponds to the fact that the antenna goes into thermodynamic equilibrium with an extended source (for $\omega_{source} > \Omega$, main lobe $\rightarrow T_A = T_{source}$)

How to calculate G(u,v) ?

For a point source : $T(\theta,\phi) = \delta(\theta_o,\phi_o) \;\Rightarrow\; T_A(\theta,\phi) = 1/4\pi \times g(\theta_o,\phi_o)$

$t(u,v) = 1 \;\Rightarrow\; t_A(u,v) = G(u,v)$

And we have seen that for a point source:

$$E(\theta,\phi) = \text{F.T. } [E(u,v)] = \text{F.T. } [\, E_o \exp(i2\pi\nu t) \,] \times f(u,v) \,]$$

$\Downarrow$ field distribution at ∞ $\qquad$ $\Downarrow$ field distribution on the antenna

$$T_A(\theta,\phi) = E(\theta,\phi).E(\theta,\phi)^* = |E(\theta,\phi)|^2 \qquad \text{(radiation diagram in power)}$$

$$\Rightarrow \; t_A(u,v) = G(u,v) = E(u,v) \otimes E^*(u,v)$$

The Fourier Transform of the image of a point source is the transfer function of the instrument = autocorrelation function of the field distribution over the aperture = autocorrelation of the pupil.

The image of a point source (the PSF) is the Fourier Transform of the pupil autocorrelation.

- Comparison of temporal and spatial domains :

Temporal (electronics, 1D)	Spatial (optics, 2D)
Temporal frequency ν	Spatial frequencies (u,v)
Low-pass filter	Single dish
Band-pass filter	2 antennas interferometer
Transfer function	Point Spread Function

Ex: Circular aperture

$E(u,v) = 1$ for $(u^2+v^2)^{1/2} \leq D/2$, $= 0$ elsewhere

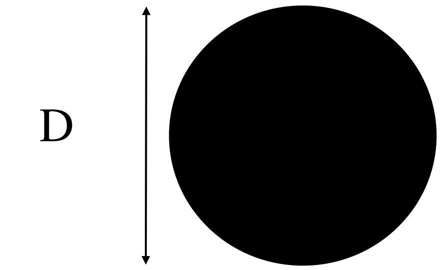

$G(u,v) = 2/\pi\ [\arccos(r) - r(1-r^2)^{1/2}]$ with $r = (\lambda/D)\ (u^2+v^2)^{1/2}$

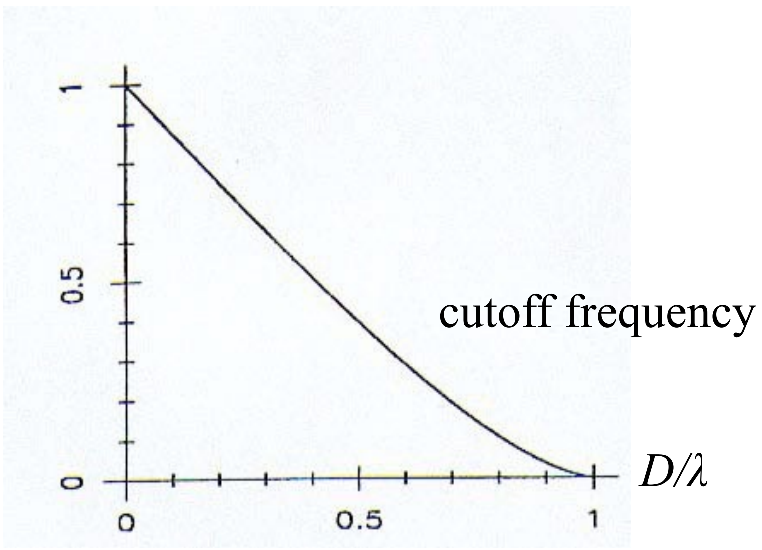

$g(\alpha) = [2J_1(\pi D\alpha/\lambda)/(\pi D\alpha/\lambda)]^2$ with $\alpha = (\theta^2+\varphi^2)^{1/2}$

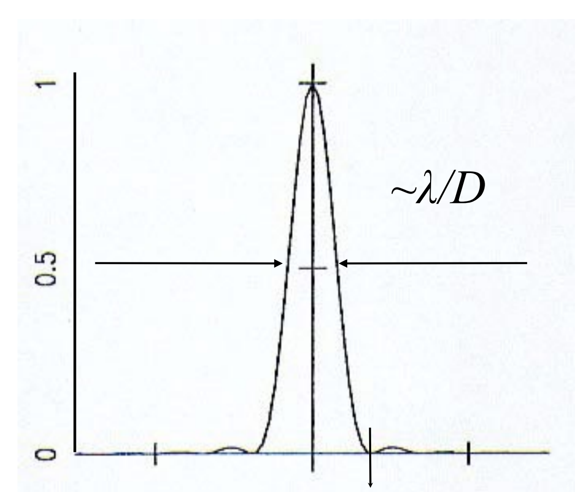

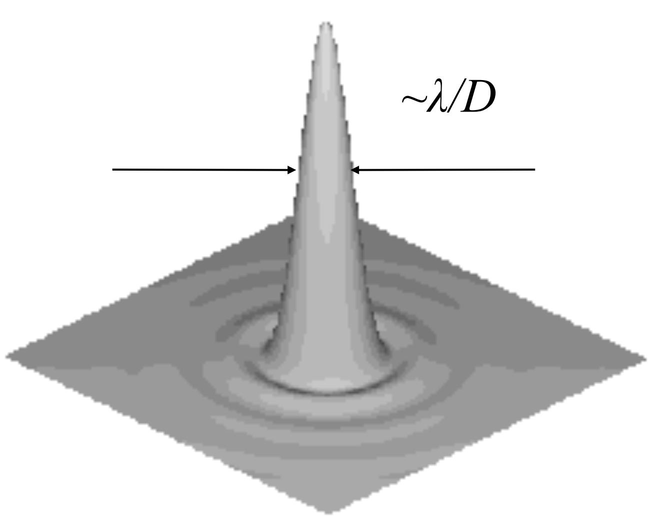

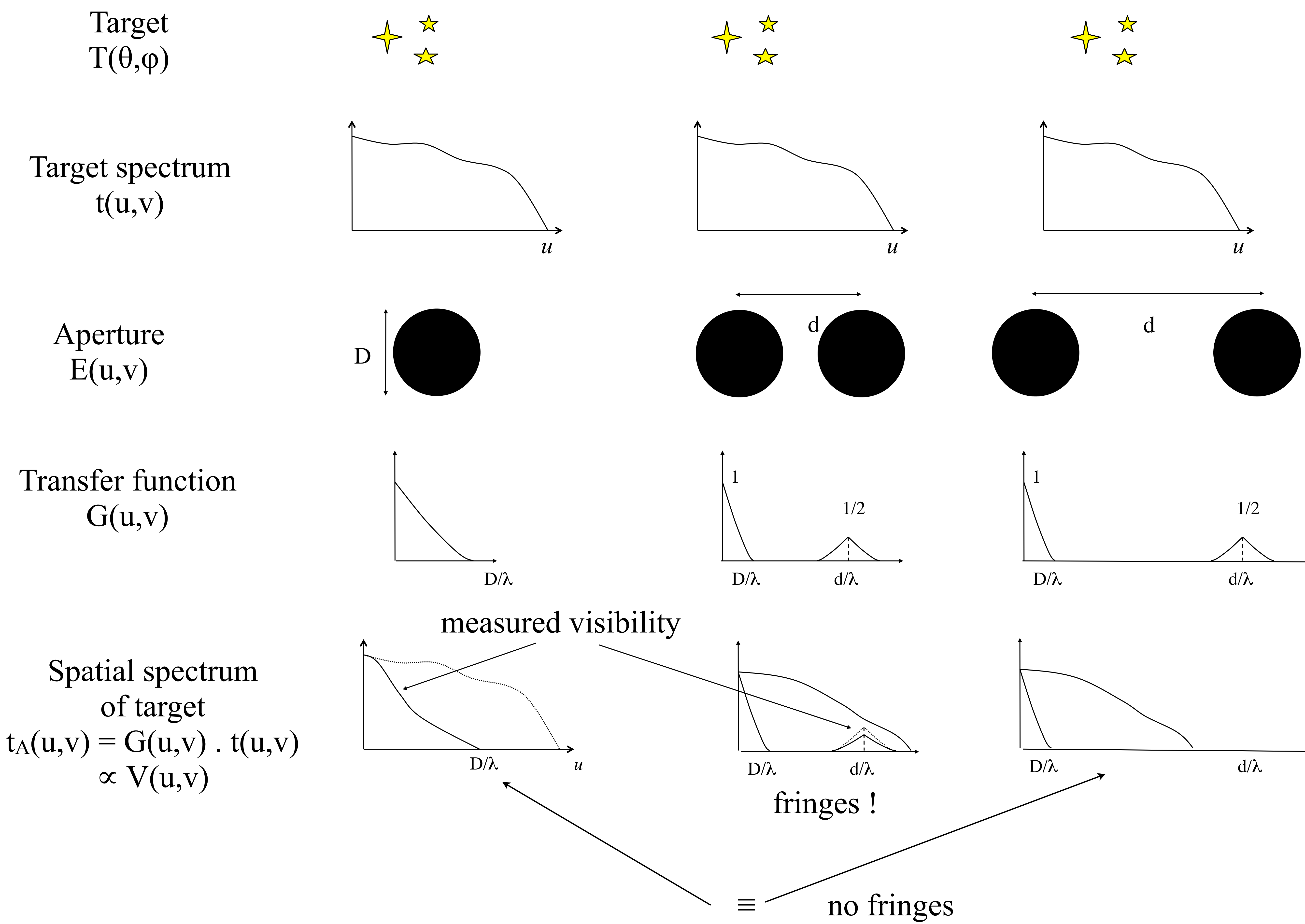
Target
T(θ,φ)
Target spectrum
t(u,v)
u
u
u
Aperture
E(u,v)
D
d
d
Transfer function
G(u,v)
D/λ
1
1/2
D/λ
d/λ
1
1/2
D/λ
d/λ
measured visibility
Spatial spectrum
of target
tA(u,v) = G(u,v) . t(u,v)
∝ V(u,v)
D/λ
u
D/λ
d/λ
fringes !
D/λ
d/λ
≡
no fringes

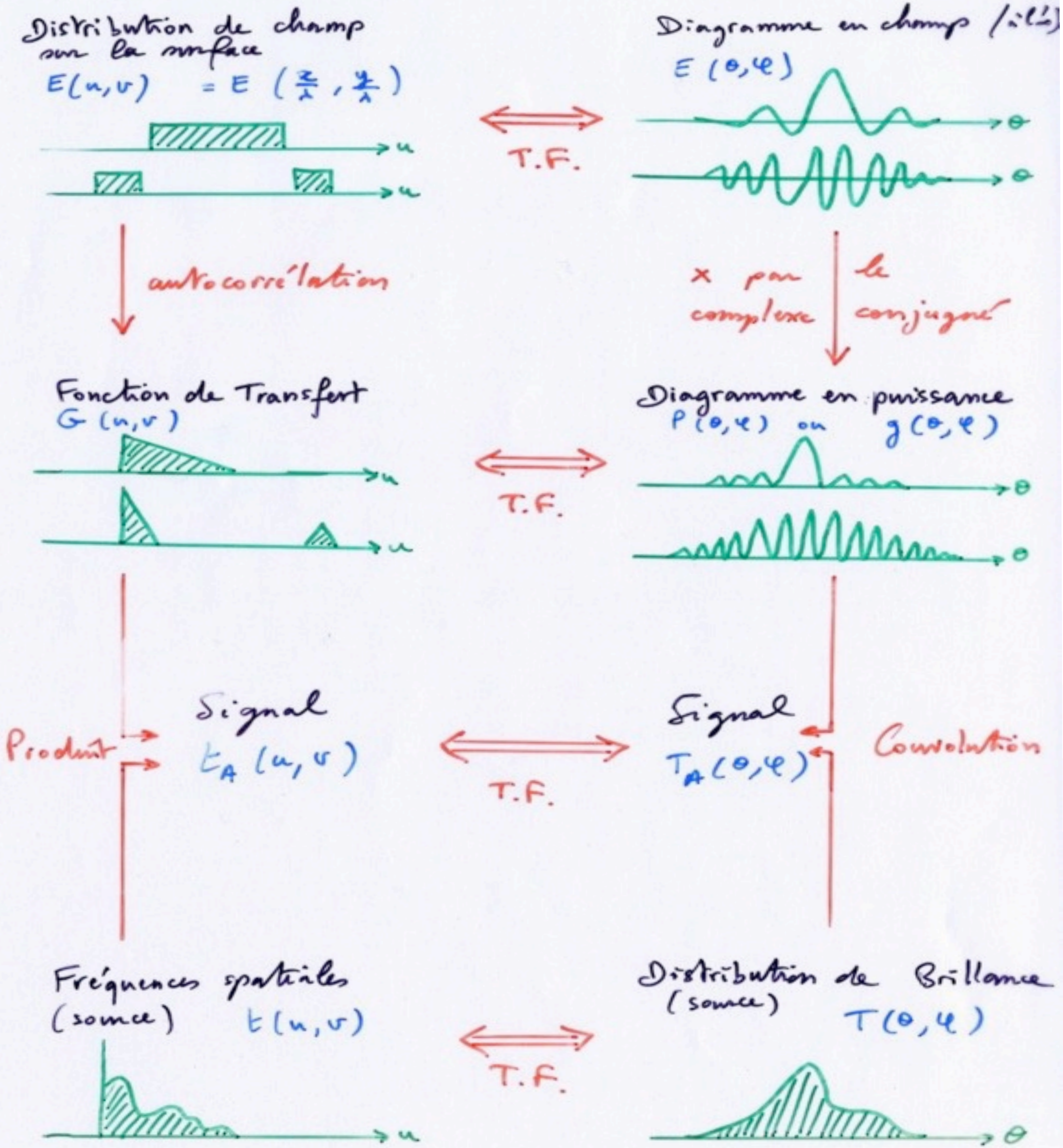

Distribution de champ sur la surface
E(u,v) = E (x/λ, y/λ)
Diagramme en champ (à l'∞)
E (θ,φ)
T.F.
autocorrélation
× par le complexe conjugué
Fonction de Transfert
G (u,v)
Diagramme en puissance
P (θ,φ) ou g (θ,φ)
T.F.
Produit
Signal
t_A (u,v)
T.F.
Signal
T_A (θ,φ)
Convolution
Fréquences spatiales (source)
t (u,v)
Distribution de Brillance (source)
T (θ,φ)
T.F.

• <u>Binary star</u> :

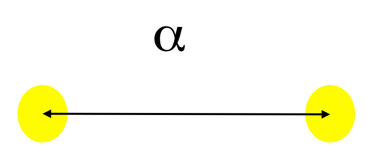

Brightness distribution : $T(\theta) \propto \delta(-\alpha/2) + \delta(\alpha/2)$

$\Rightarrow$ spectrum : $t(u) \propto \cos(\pi \alpha u)$

Visibility function of 2 antennas separated by d :

$$G(u) = \delta(u) = \delta(d/\lambda) \quad \Rightarrow \quad t_A(u) \propto V(u) = V(d/\lambda) = \cos(\pi \, \vec{\boldsymbol{\alpha}} \, . \, \vec{\mathbf{d}} \, /\lambda)$$

$|V(u)|$ for d // α :

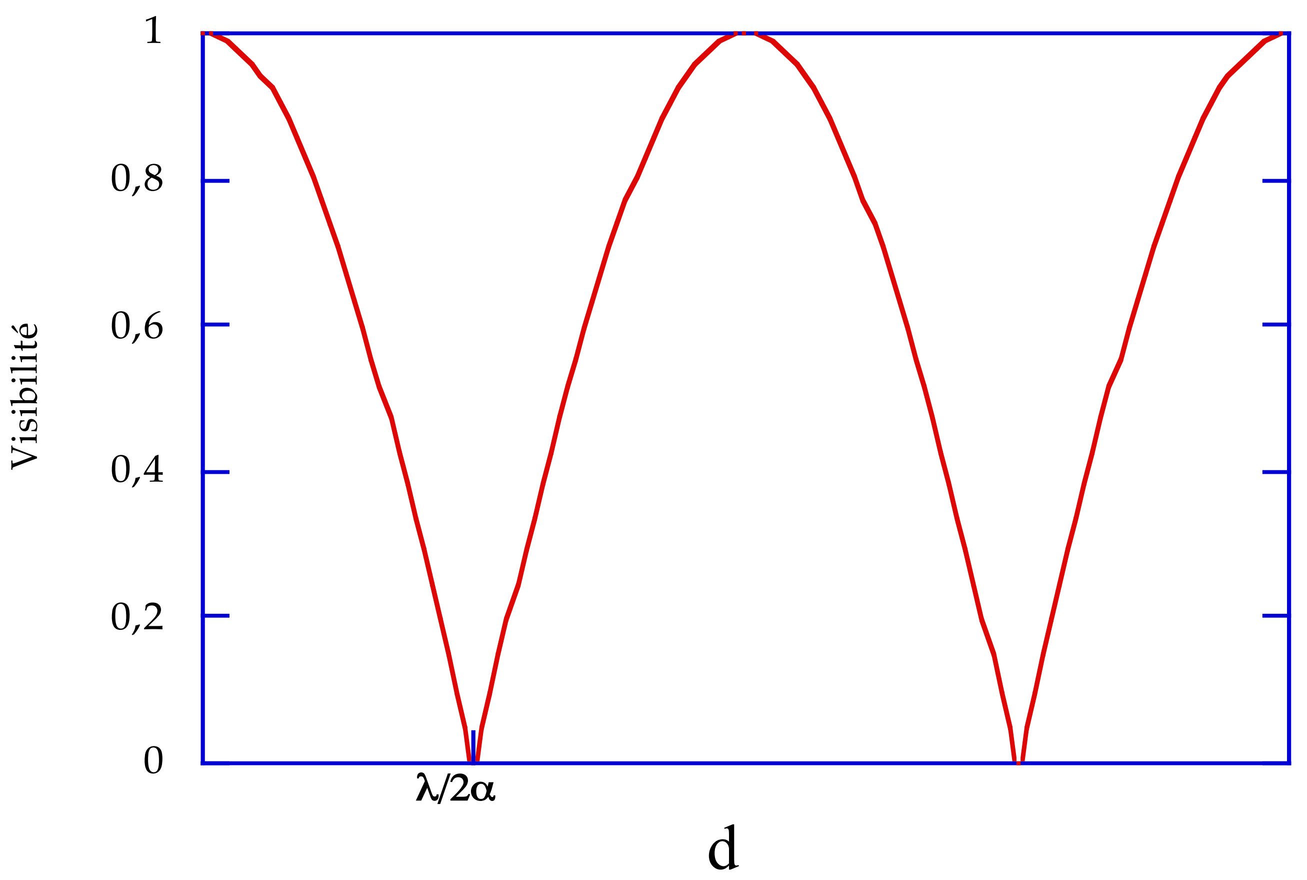

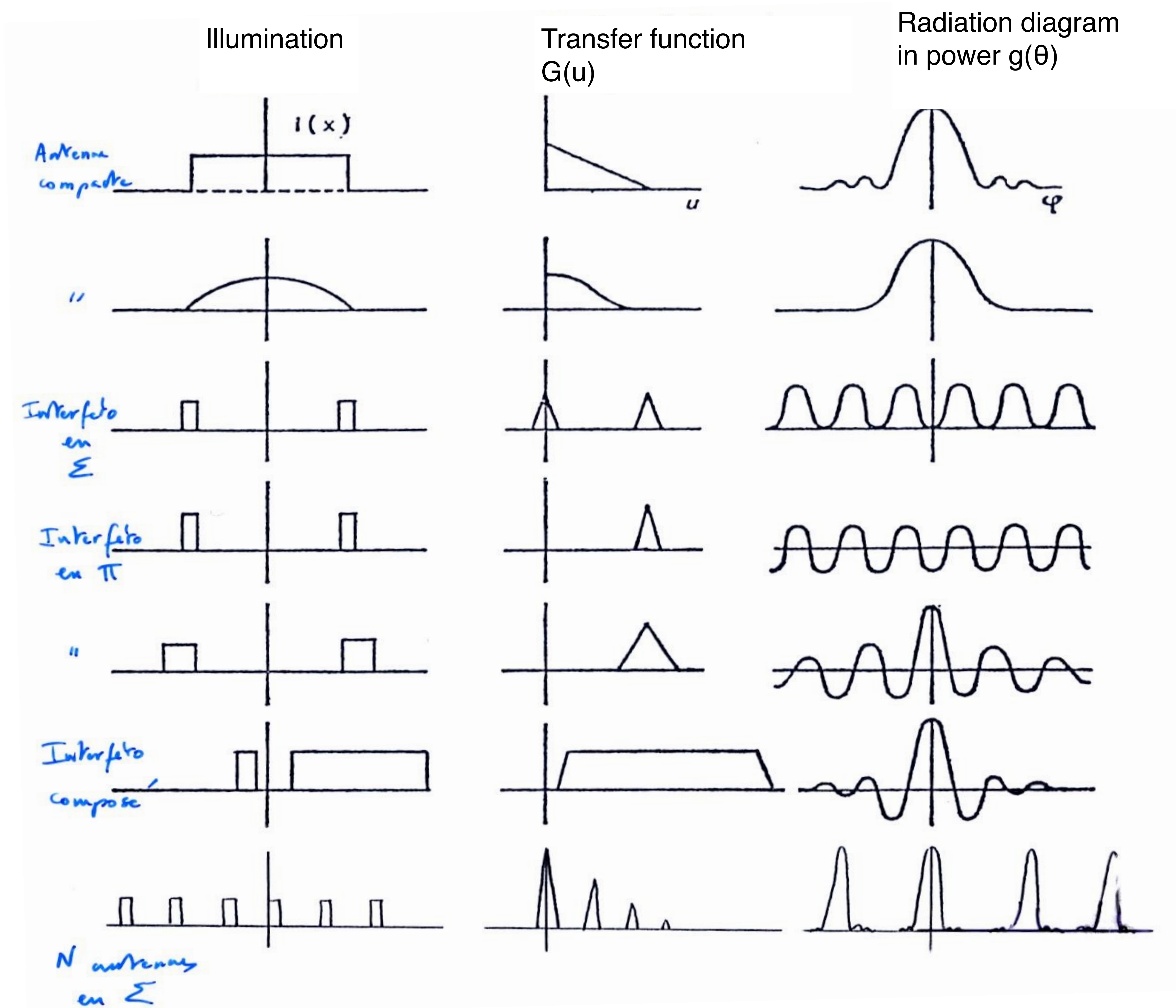

Illumination
Transfer function
G(u)
Radiation diagram
in power g(θ)
i(x)
u
φ
Antenne compacte
''
Interfero en Σ
Interfero en π
''
Interfero composé
N antennes en Σ

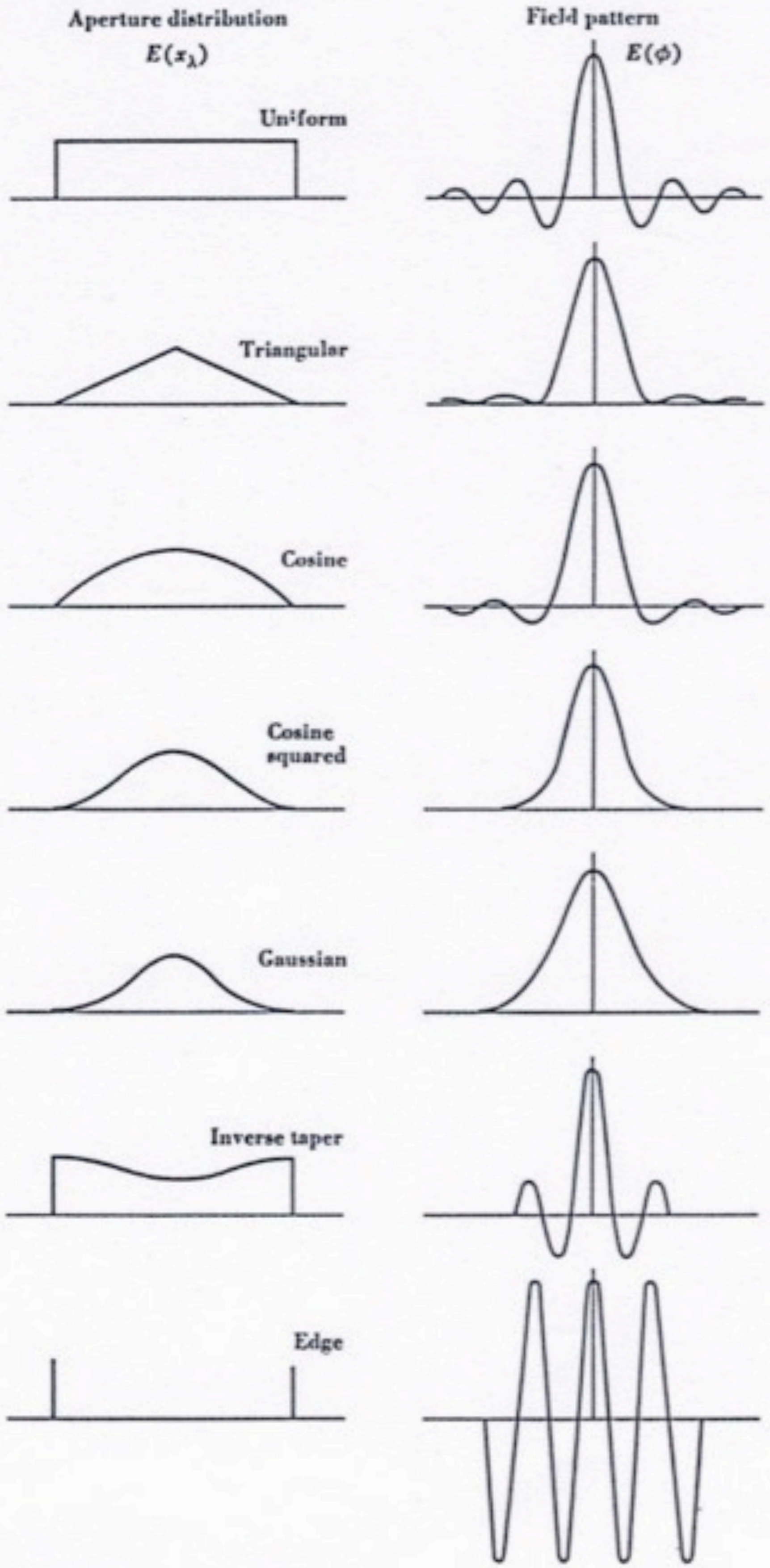

Fig. 6-9. Different aperture distributions with associated antenna patterns.

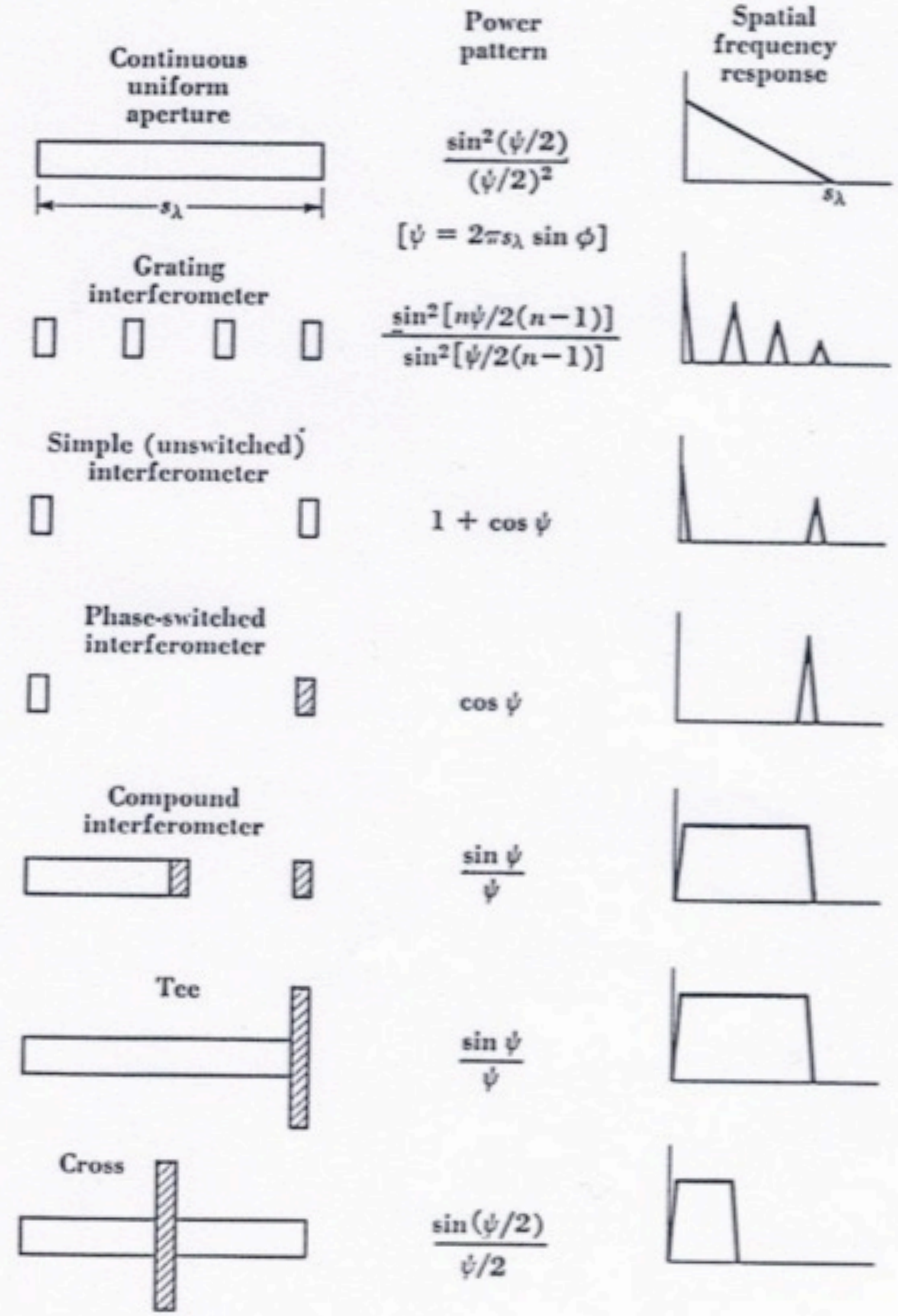

Fig. 6-31. Spatial-frequency characteristics and power-pattern expressions for a continuous uniform aperture and various interferometer arrangements. The switched portions of the interferometers are shaded. The width of the narrow interferometer elements is neglected in the pattern expressions.

- Measurement of the complex visibility $t_A(u,v) \propto V(u,v)$

Complex visibility (or spatial coherence factor) is expressed as the correlation rate between the fields at the two points (1 & 2) defining the base (u,v):

$V(u,v) = \mathrm{Corr}(E_1(t),E_2(t)) = \langle E_1(t).E_2^*(t) \rangle / (\langle |E_1(t)|^2 \rangle . \langle |E_2(t)|^2 \rangle)^{1/2}$

with $\langle \ldots \rangle = \langle \ldots \rangle|_{\Delta t \gg 1/\nu}$

$V(u,v) = P_\otimes / E_1.E_2 \approx \exp(i\psi)$ for each point of the source

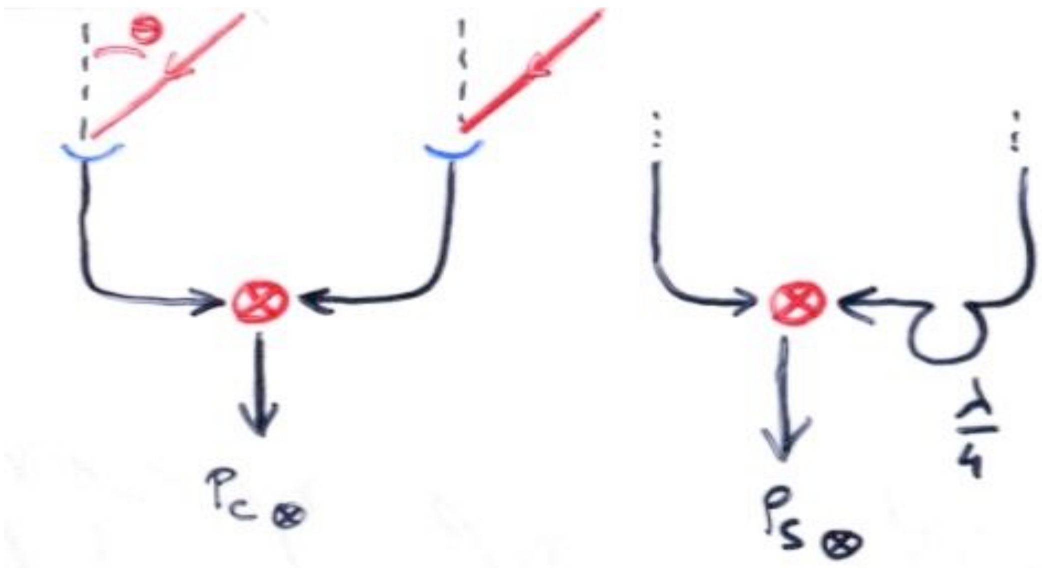

Analog measurement provides $\mathrm{Re}(P_\otimes / E_1.E_2) \approx \cos(\psi) = P_{c\otimes}$

and, after insertion of an additional phase shift (cable length) $\lambda/4$ on the path from the 2nd antenna to the correlator, we obtain (successively or simultaneously with 2 correlators)

$\mathrm{Re}(P'_\otimes / E_1.E_2) \approx \cos(\psi+\pi/2) = \sin(\psi) = P_{s\otimes}$

from which we derive : $P_\otimes = P_{c\otimes} + i\, P_{s\otimes}$

Digitally, we can directly measure P⊗ (amplitude and phase of the correlation).
We have seen that we can limit ourselves to a 1-bit correlation (sign of $E_1(t)$ and $E_2(t)$) for signals with low dynamic range.

$\Rightarrow$ $P_{c\otimes 1\text{-bit}}(t) = 1-2\psi/\pi \rightarrow$ estimator of $P_{c\otimes}(t) = \cos(\psi)$

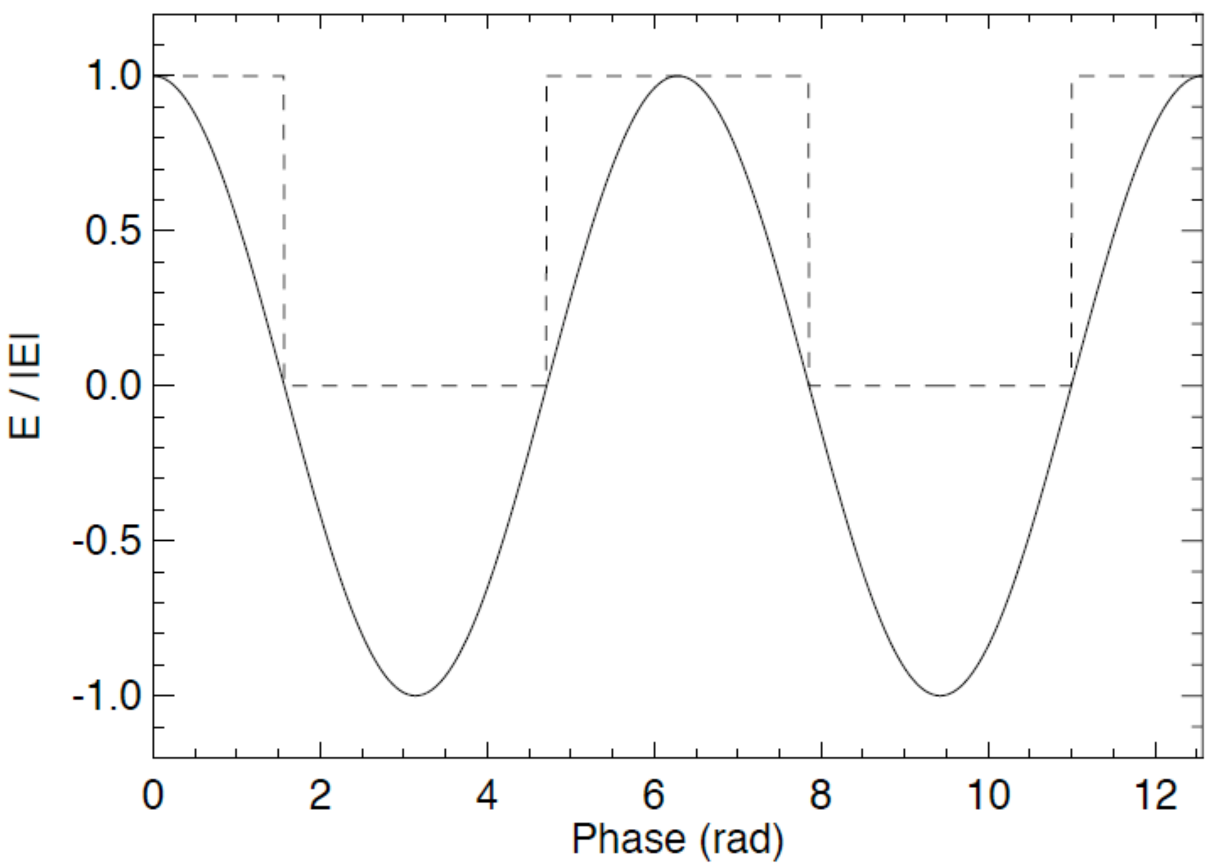

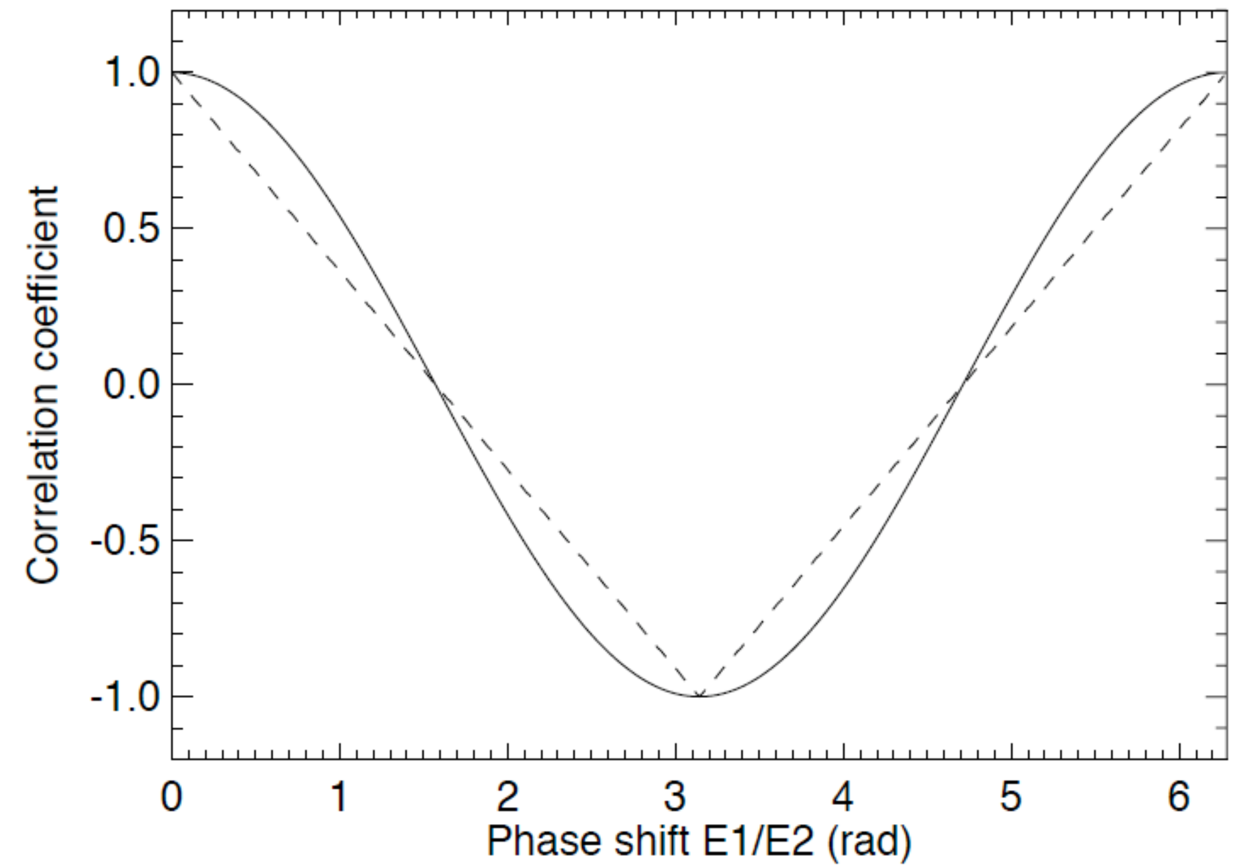

NB :

- if the gains (g_i) and phases (ϕ_i) of the interferometer antennas are not identical, we actually measure $g_1 g_2 . \exp[i(\phi_1-\phi_2)] \times t_A(u,v)$

$\Rightarrow$ *need to calibrate / t the g_i et ϕ_i by observing « reference" radiosources (intense, known - ex: Cyg A)*

- <u>Time coherency</u>

The preceding calculations assume monochromatic signals.
For a finite spectrum of width $\Delta\nu$, Eo changes into a variable amplitude :
$E_o(t) = E_o \times TF(E(\nu)) = E_o \times \mathrm{sinc}(\pi t\, \Delta\nu)$ e.g. for a rectangular spectral band
$\tau \sim 1/\Delta\nu$ = characteristic duration of a coherent wave packet

$E_1 = E_o(t) \times \exp(i2\pi\nu t)$ $E_2 = E_o(t-\tau) \times \exp[i(2\pi\nu(t-\tau))] = E_o(t-\tau) \times \exp[i(2\pi\nu t-\psi)]$
with $\psi = 2\pi\nu\, \tau$ and $\tau = d \sin\theta / c$
whence $P_\otimes = < E_1.E_2^* > = < E_o(t).E_o(t-\tau) > \times \exp(i\psi) = E_o^2 \exp(i\psi) \times c(\tau)$
with $c(\tau)$ the "coherence function"
Ex: $c(\tau) = (\int E^2(\nu) \exp(i2\pi\nu\tau)\, d\nu) / (\int E^2(\nu)\, d\nu) = \mathrm{sinc}^2(\pi\tau\, \Delta\nu)$ for $\Delta\nu$ rectangular

To limit the loss of coherence, and therefore the decrease in the correlation coefficient, "delay lines" (cable lengths) that are multiples of λ are inserted to approximately compensate for the difference in rate $c\tau$:
$\tau \rightarrow \tau' = \tau - nT = \tau - n\lambda/c \sim 0$
and remain in the regime where $c(\tau') \approx 1$

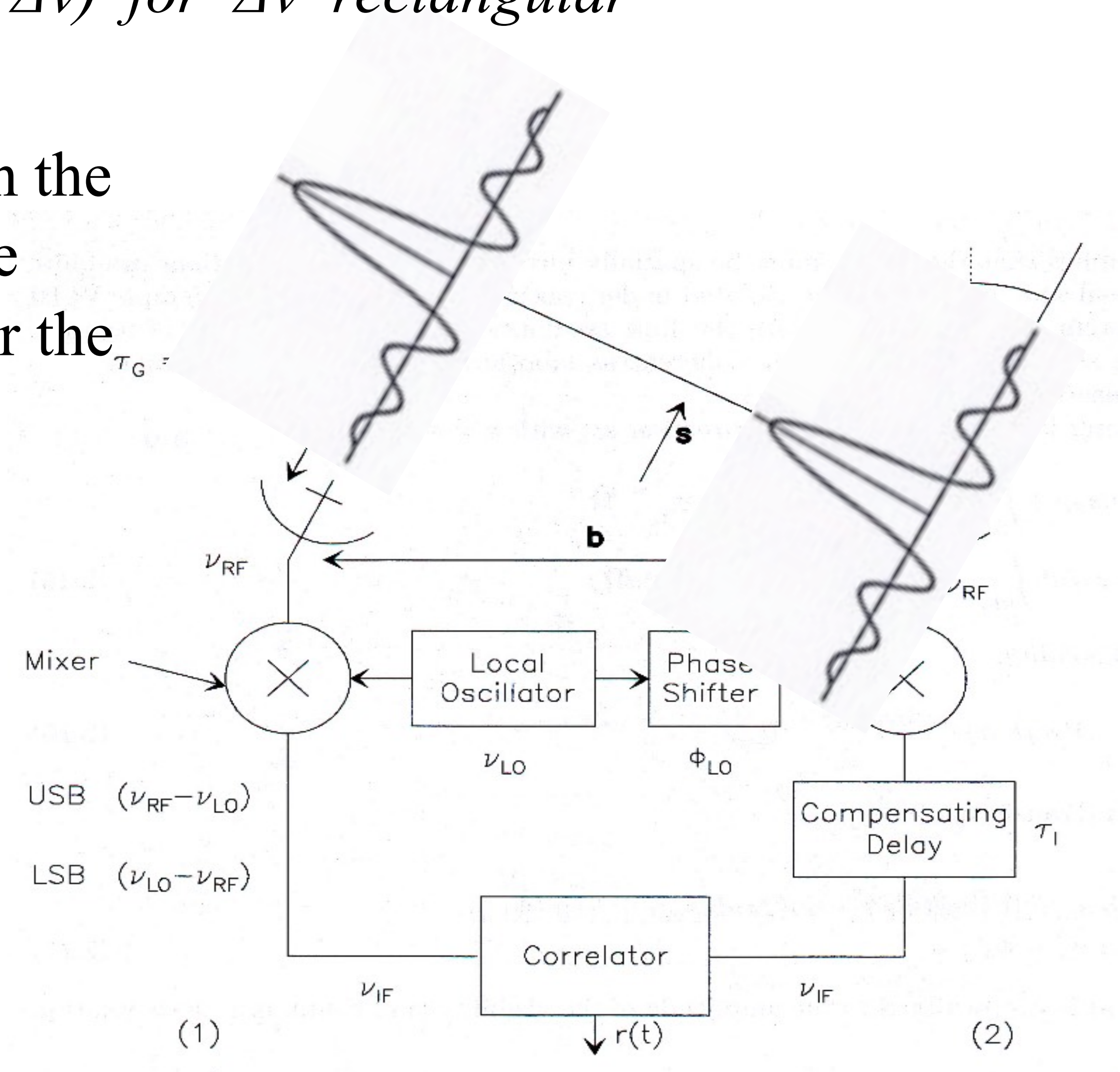

→ equivalent to the electronic pointing of the central fringe of the interferometer ~ in the direction of the source = "fringe stopping" during source tracking.

- Aperture synthesis

A linear interferometer (1D) provides a cross-section through the (u,v) plane of the source's spatial frequencies, parallel to the direction of its projected base on the sky

Multiple 2D bases are thus required to image a two-dimensional source
→ good sampling of complex visibility measurements $t_A(u,v)$
⇒ reconstruction of an "image" $T(\theta,\phi)$ by TF

The information on the source structure is contained in each non-zero component of $t_A(u,v)$
⇒ the important thing is the coverage of the (u,v) plane, redundancies are useless (except for SNR).

With a filled aperture, low frequencies are favoured over high frequencies (images with greater contrast at low frequencies than at high spatial frequencies).

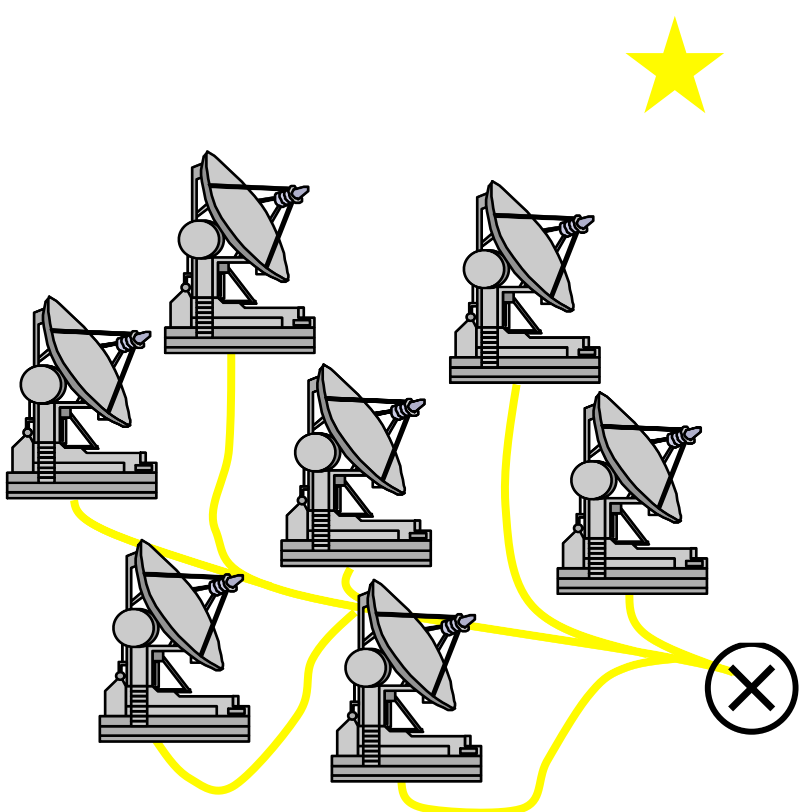

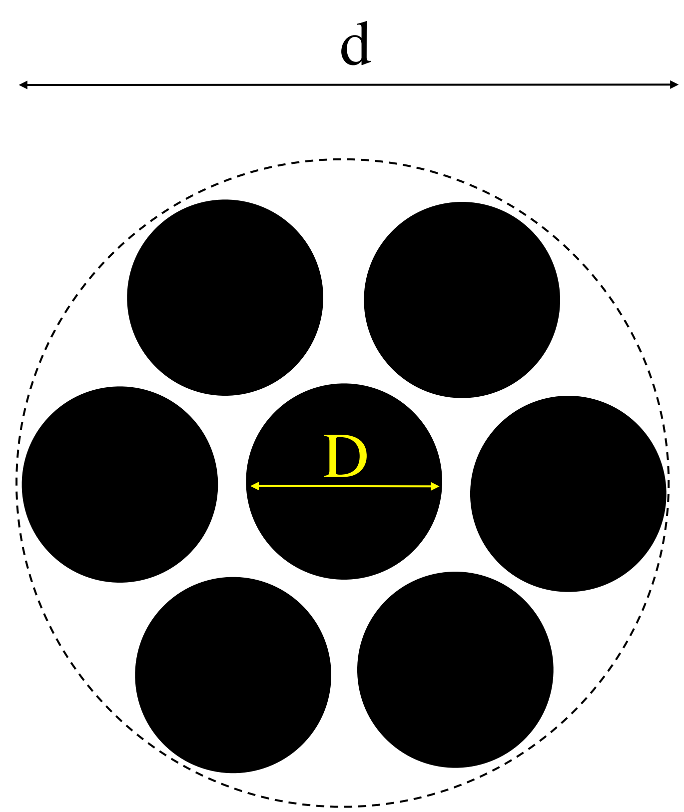

Synthesised aperture

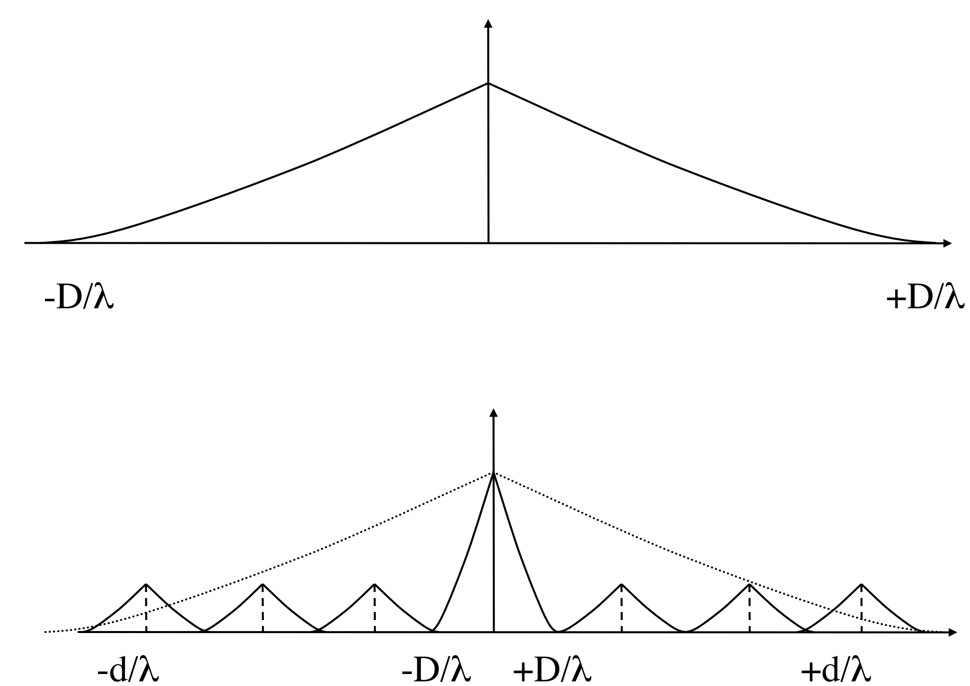

Non redundancy

Aperture

Transfer function

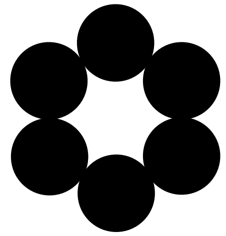

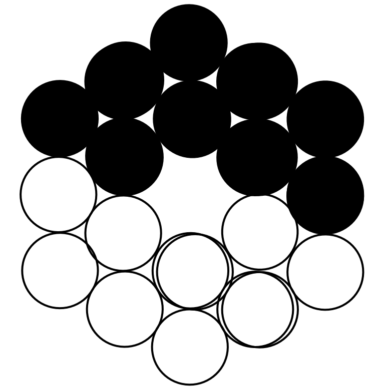

9 spatial frequencies measured

N(N-1)/2 independent baselines

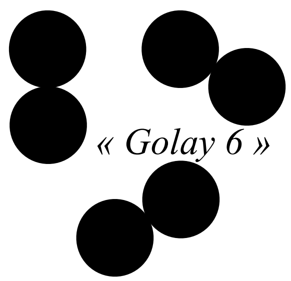

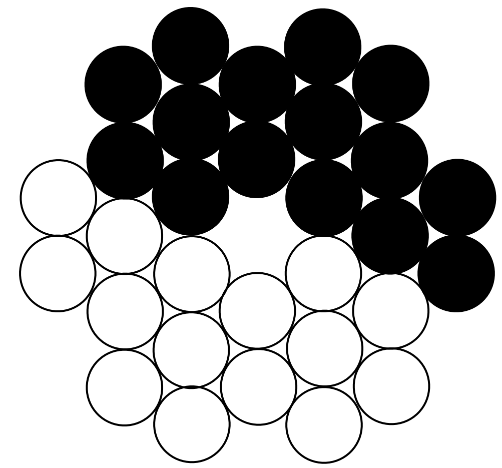

15 spatial frequencies measured

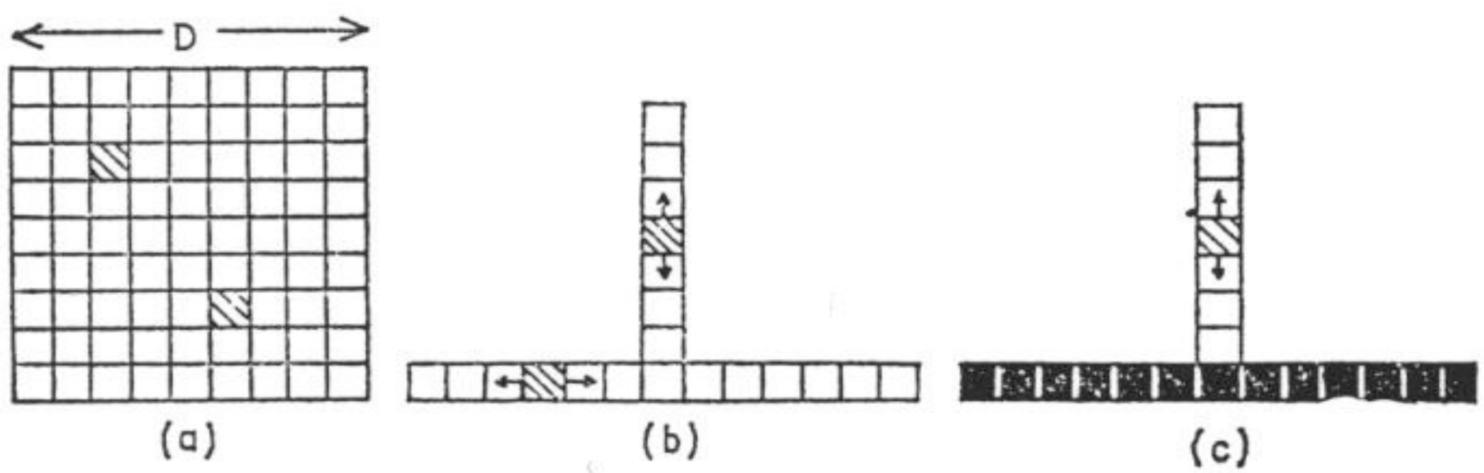

Fig. 9. — Principe des antennes synthétiques de Ryle

a) On obtient l'équivalent d'une antenne de dimensions D en utilisant deux petites antennes (carrés hachurés) et en leur donnant toutes les positions possibles ;
b) Le même résultat peut être obtenu en déplaçant seulement les antennes sur deux branches formant un T ;
c) Pour diminuer le temps d'observation nécessaire dans le cas *b)*, Ryle utilise une ligne continue d'antennes orientées est-ouest, et déplace une petite antenne sur une ligne nord-sud.

→ Real 2D configurations : « Y » (ex: VLA, 27 antennas × 25 m ∅, d_{max} ~ 25 km)
« O »
« T » (ex : Nançay RadioHeliograph)

A 2D interferometer has only a limited number of baselines (e.g. ~350 for the VLA).
+ incomplete knowledge of complex visibilities
+ measured visibilities affected by instrument & propagation effects (g_i, ϕ_i)
+ problem of short bases, necessarily > ∅
+ problem of secondary lobes
⇒ image reconstructed by Fourier Transform has artefacts
⇒ need for a posteriori processing of the $t_A(u,v)$ map to correct these effects
(see "Observation methods" chapter).

Nançay Radioheliograph array configuration

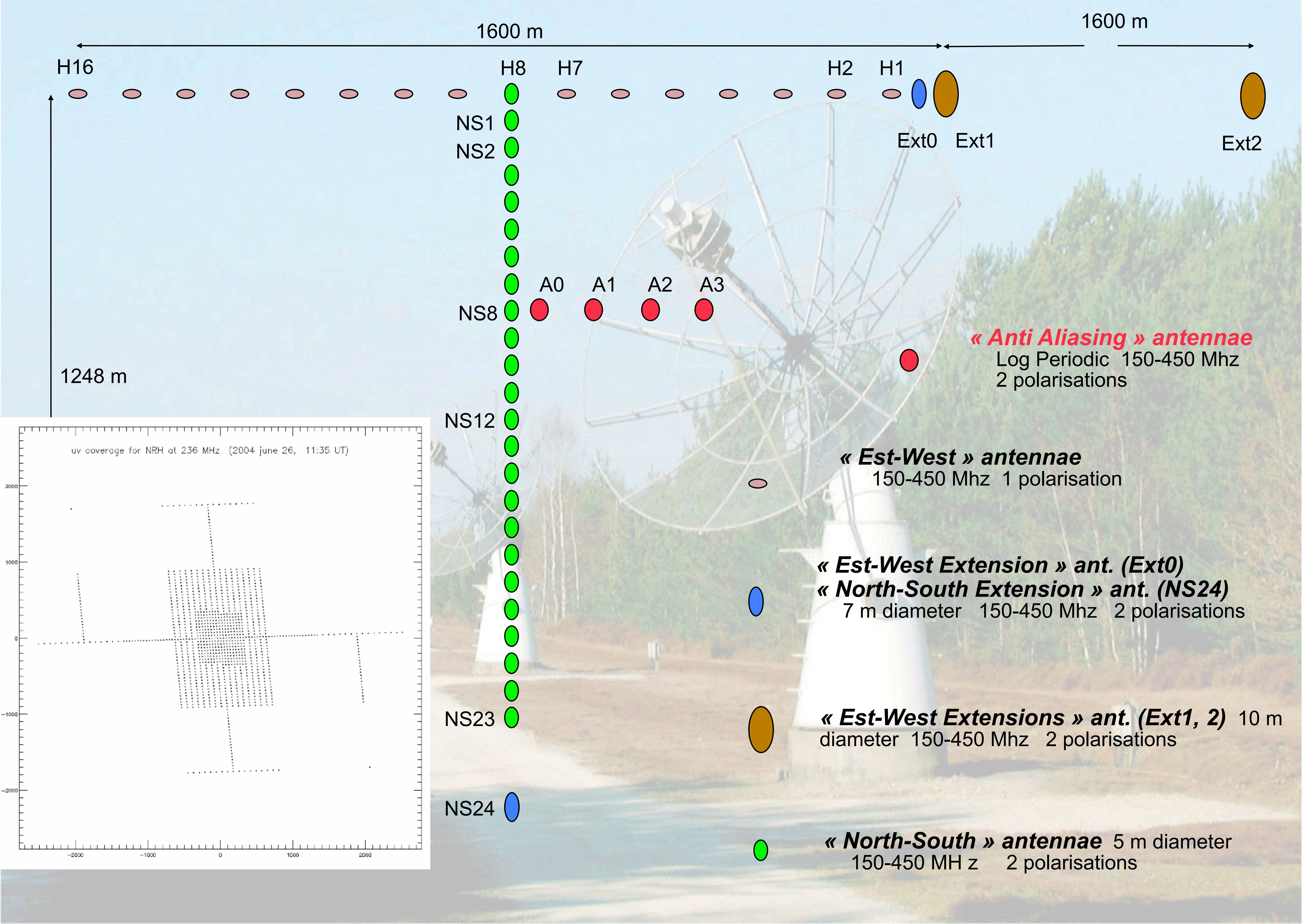

• <u>Optimisation of the configuration of an interferometer</u>

→ depends on the type of observation / desired (u,v) coverage
Direct trial-and-error approach very costly and inefficient (≠ ideal solution?)

⇒ Example of inverse approach: *Boone algorithm [A&A, 2001, 2002]*

= iterative displacement of antennas with $D_i = \gamma\, \Sigma_{i=1}^{N-1}\, M(AH,\delta,\lambda)\, P(u_i,v_i)$

γ = gain, M = matrix of passage (u,v) → ground plane (via source coordinates AH,δ and latitude λ of the array)

$P(u,v) = \nabla(G(u,v)-G_m(u,v))$ analog to a pressure force, resulting from the gradient between actual and modelled transfer function (uniform, Gaussian...)

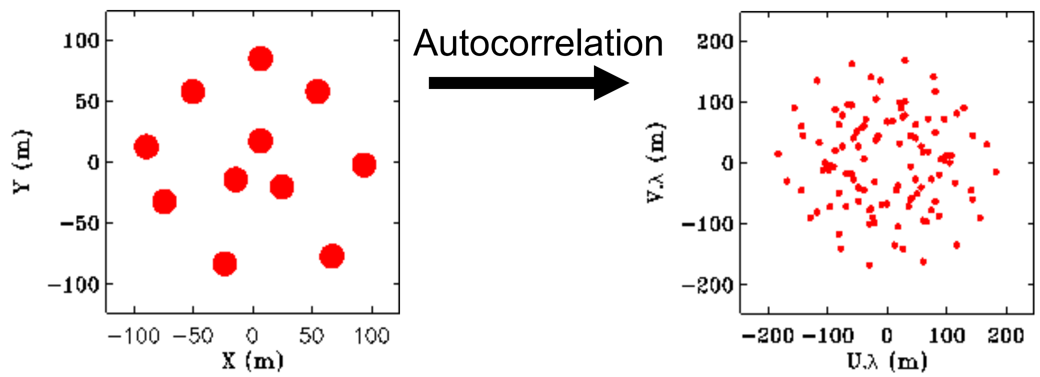

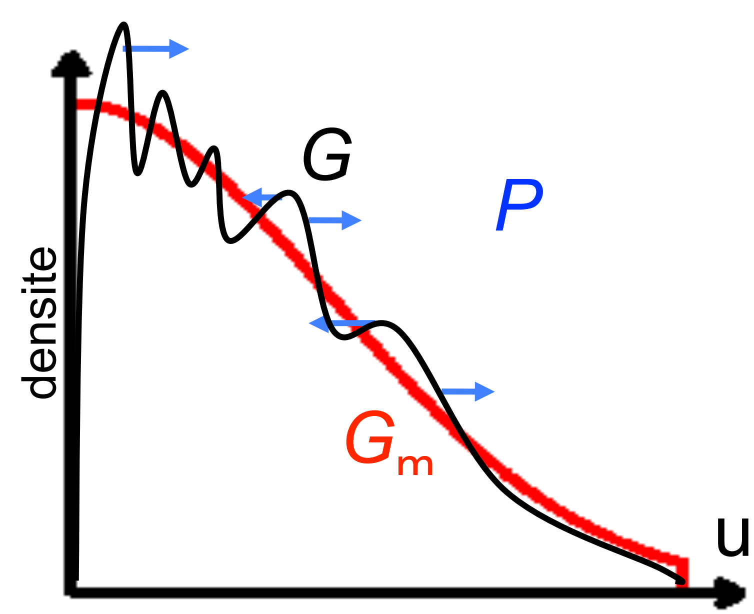

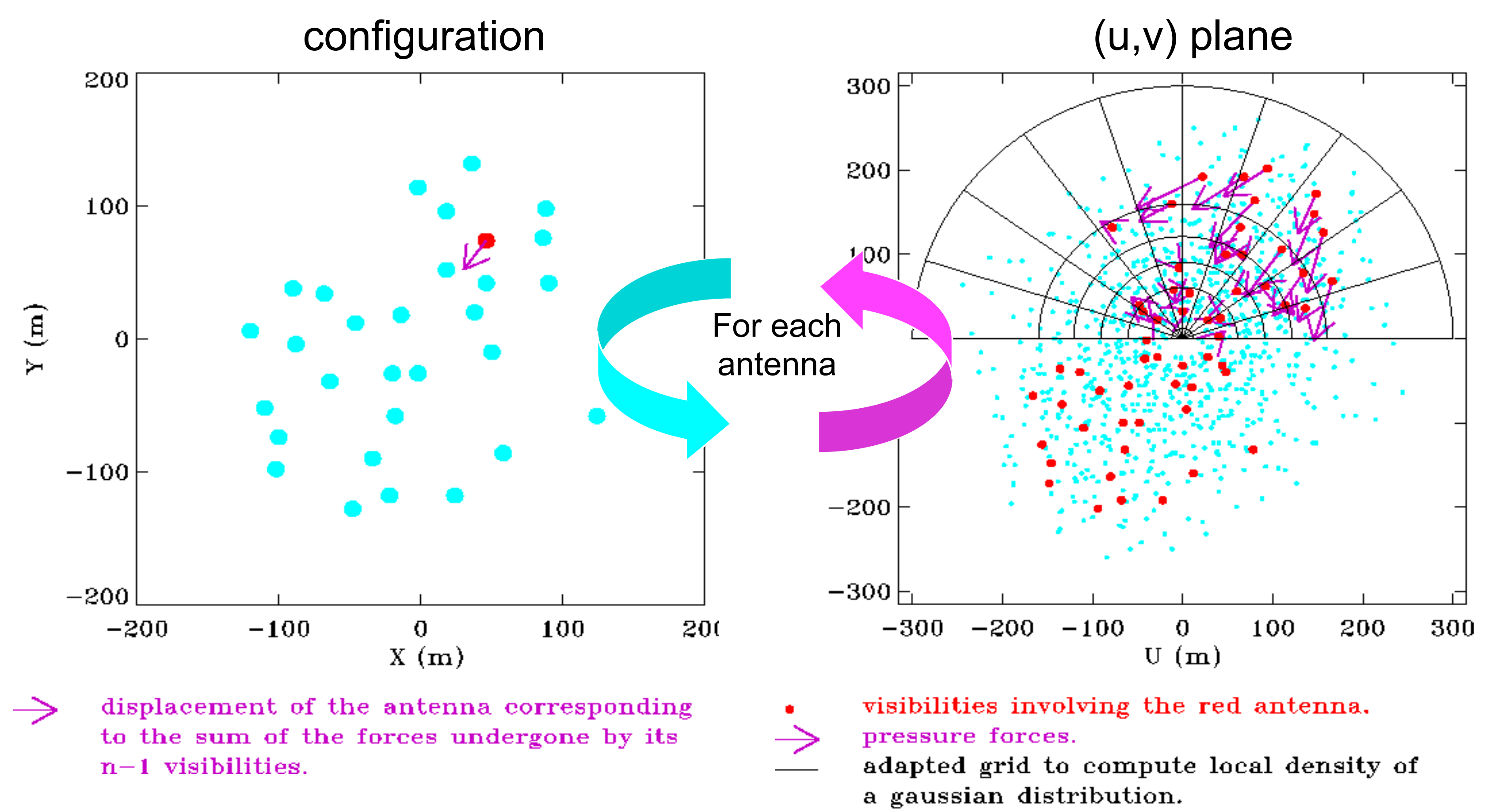

• Optimisation of the configuration of an interferometer

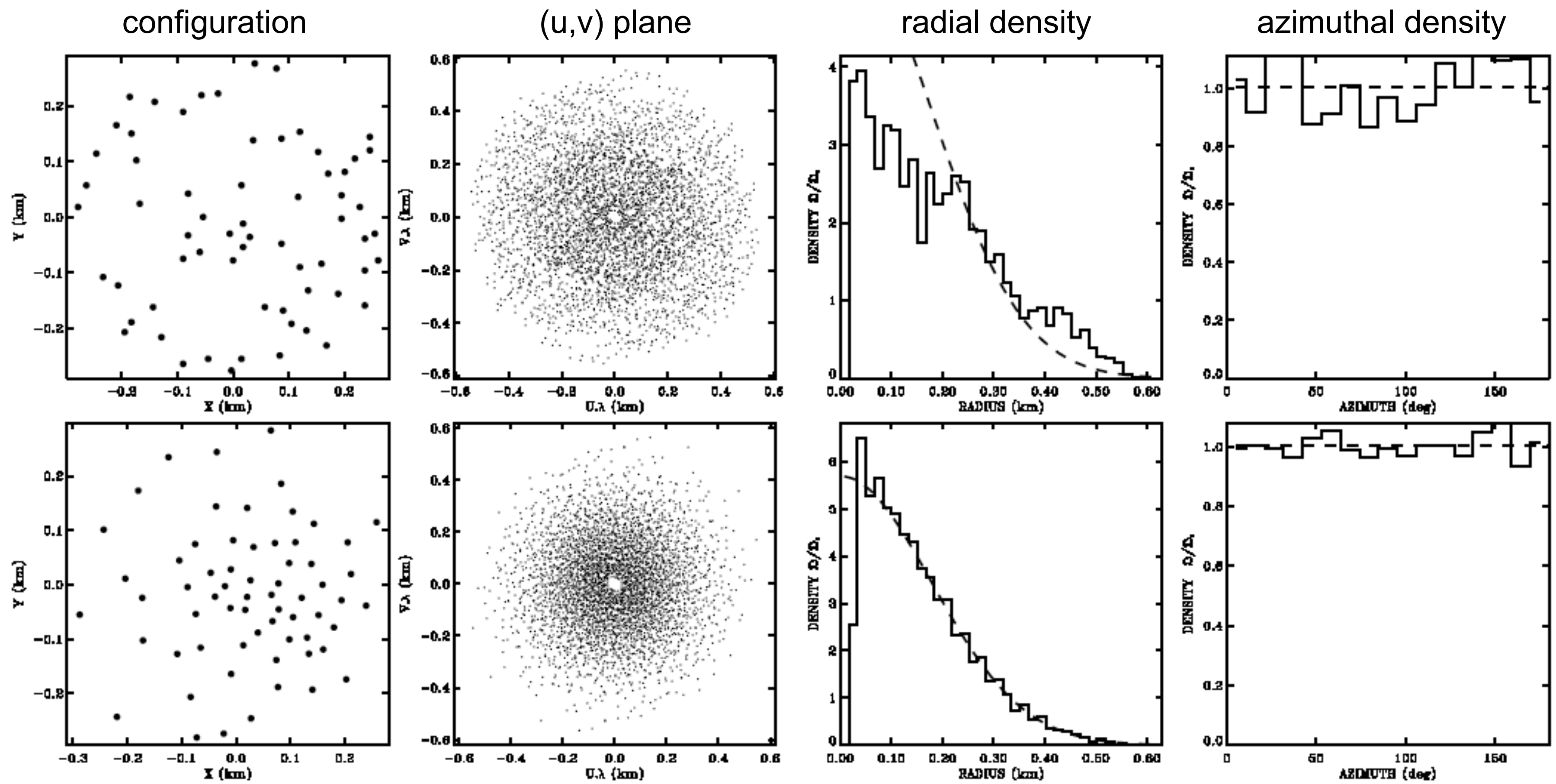

NenuFAR

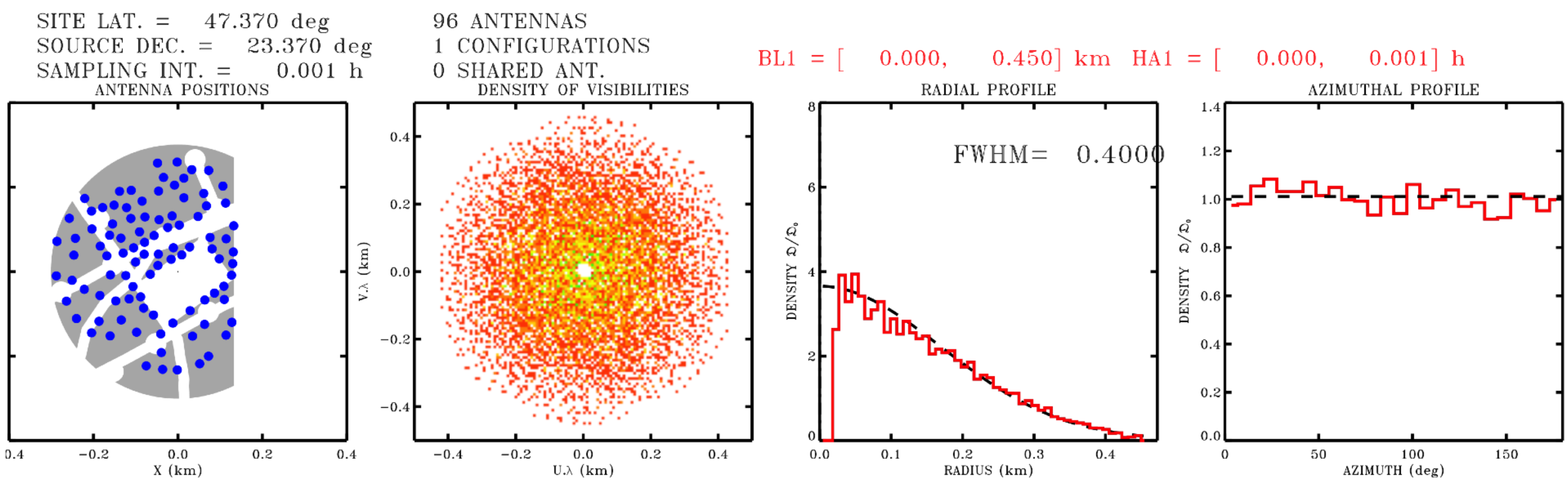

• <u>Super-synthesis</u>

If the observed source is stationary on a timescale of a few hours to 1 day (e.g. "quiet" Sun, galactic and extragalactic radio astronomy)

⇒ possible use of Earth's rotation

⇒ baselines rotation in the sky = ellipses in the (u,v) plane

⇒ image synthesis possible with a reduced number of baselines
(or increased image quality for a given number of baselines)

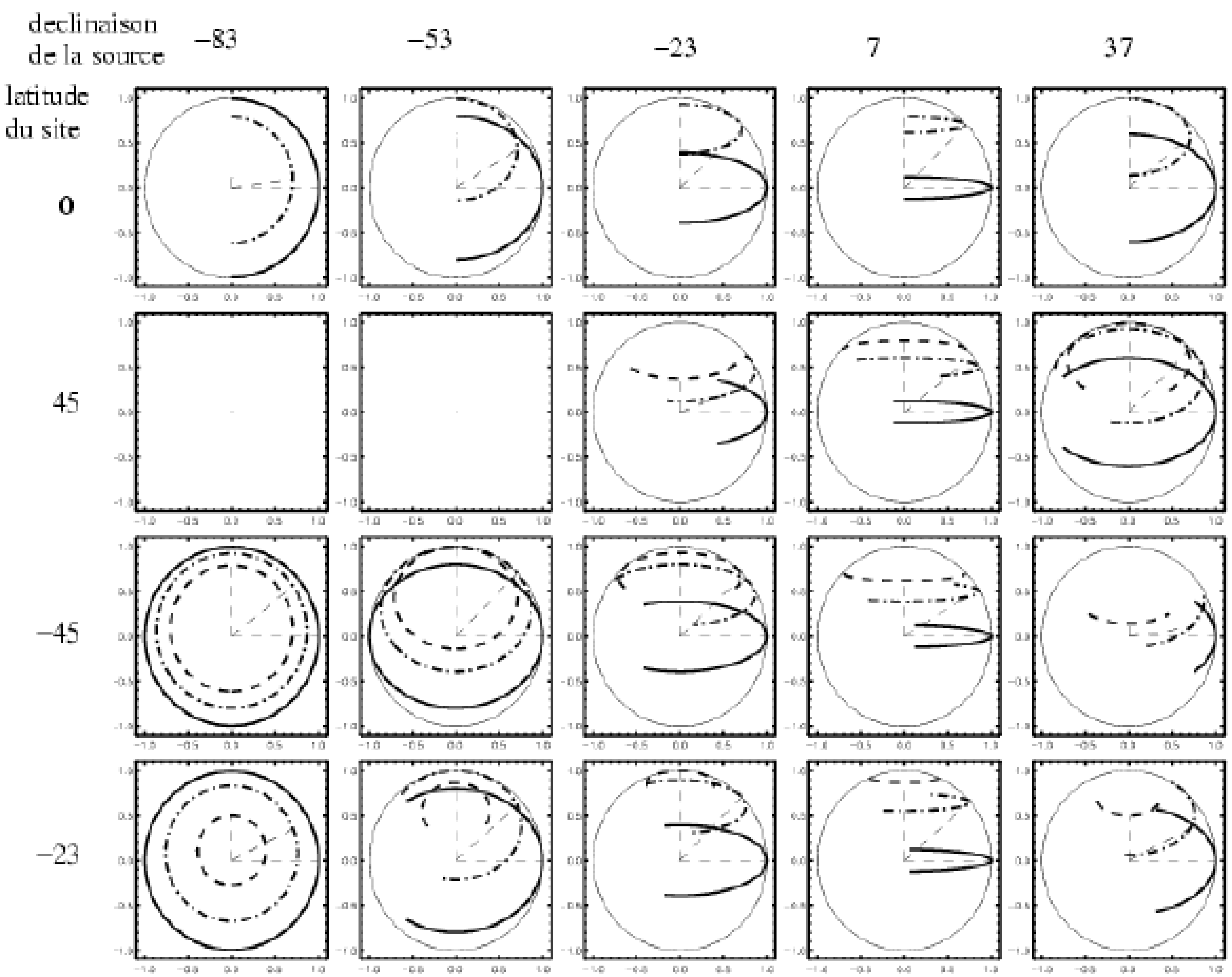

Nançay Radioheliograph

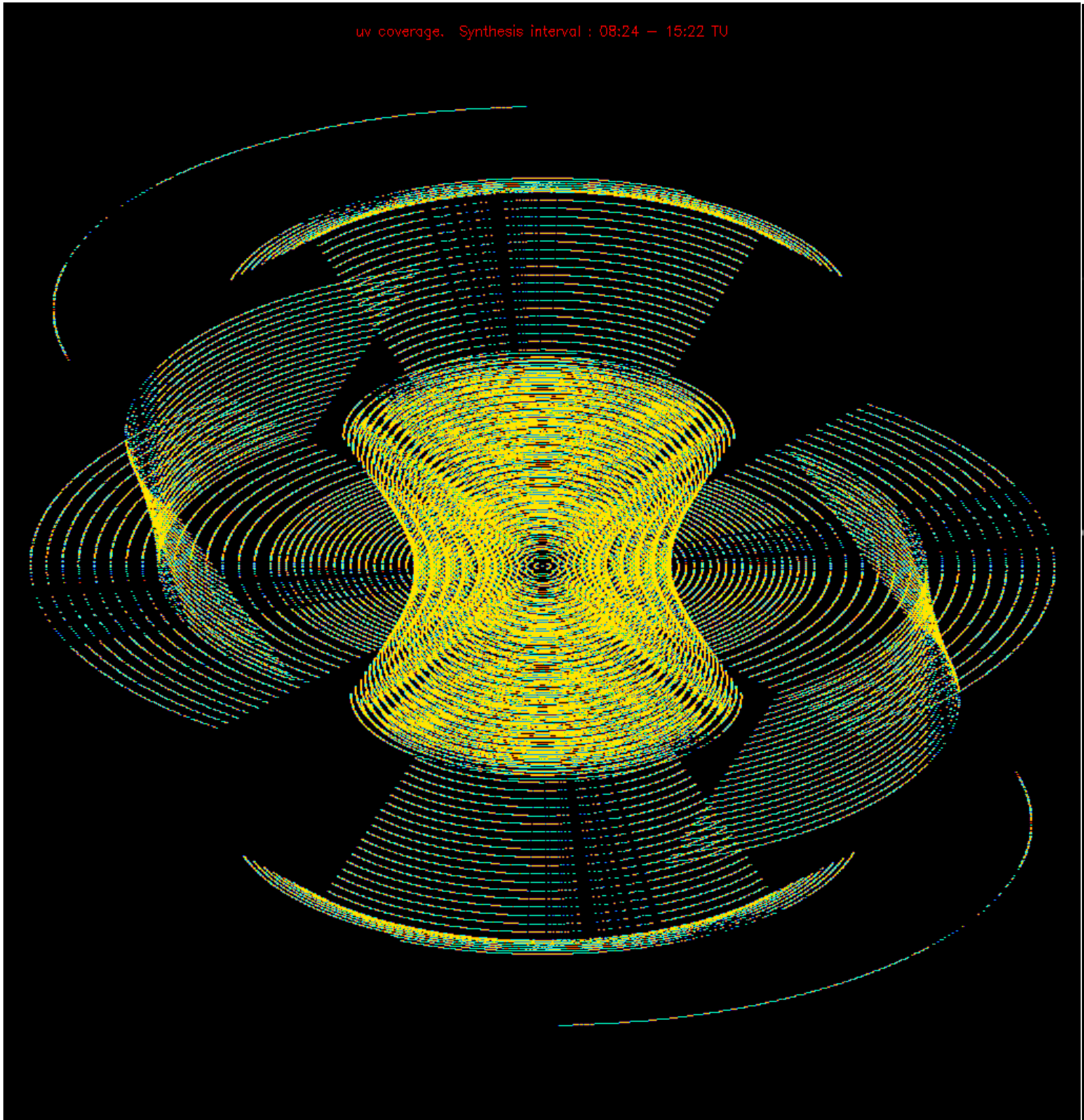

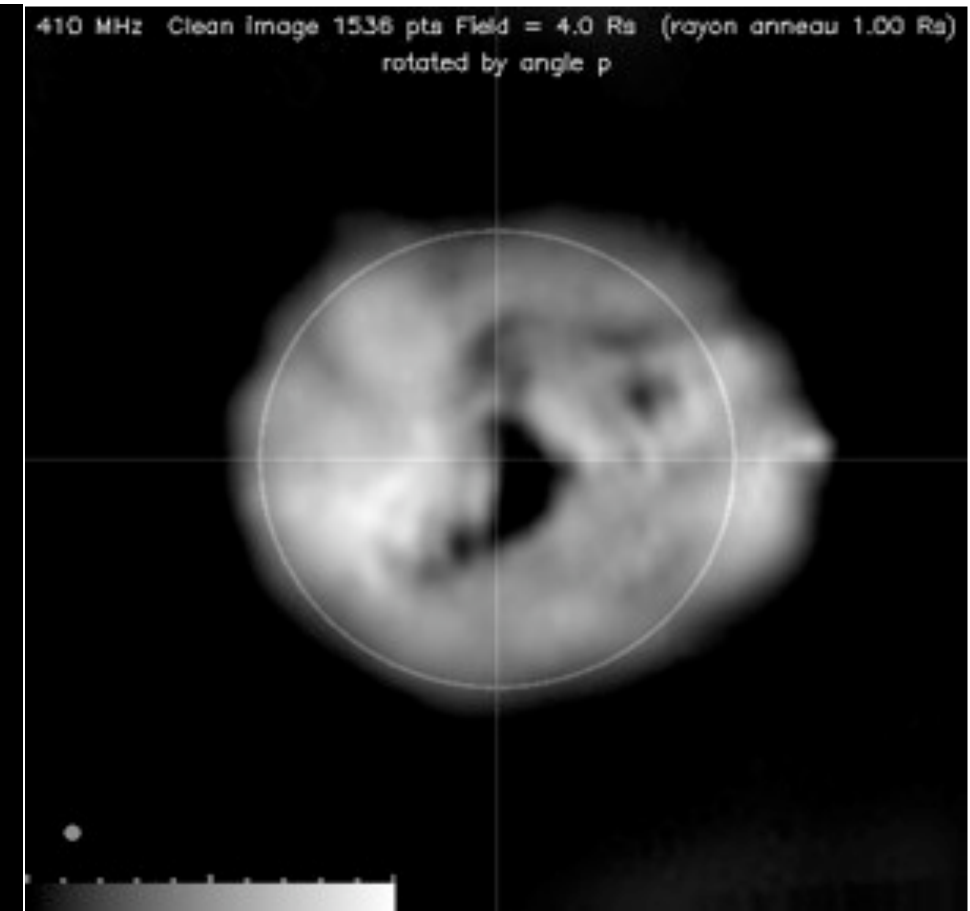

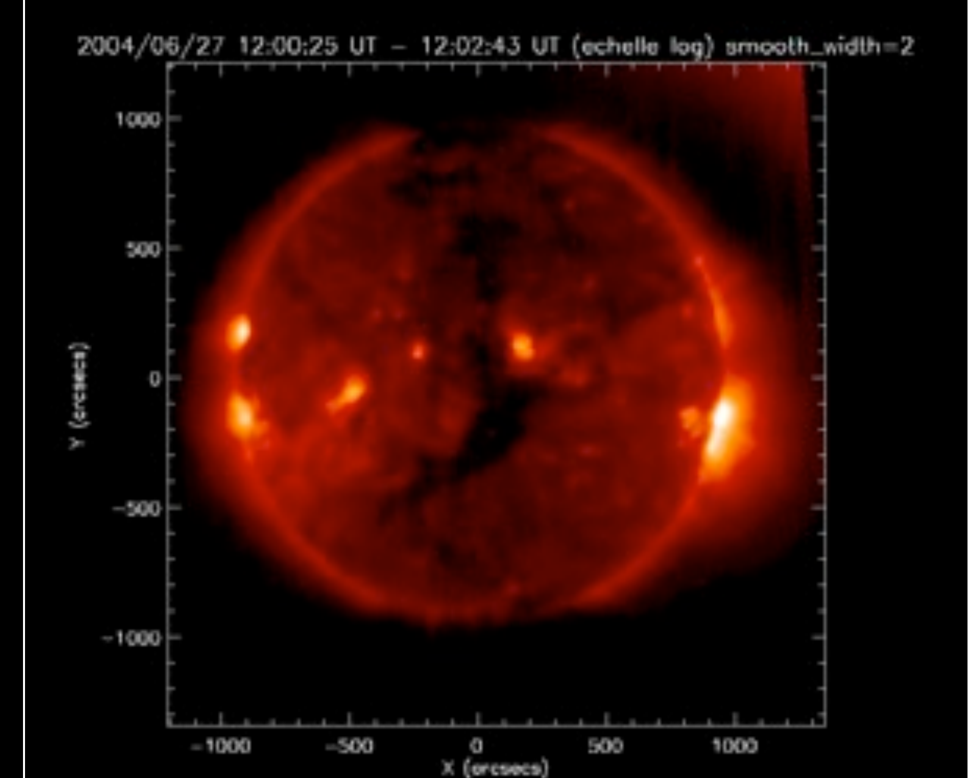

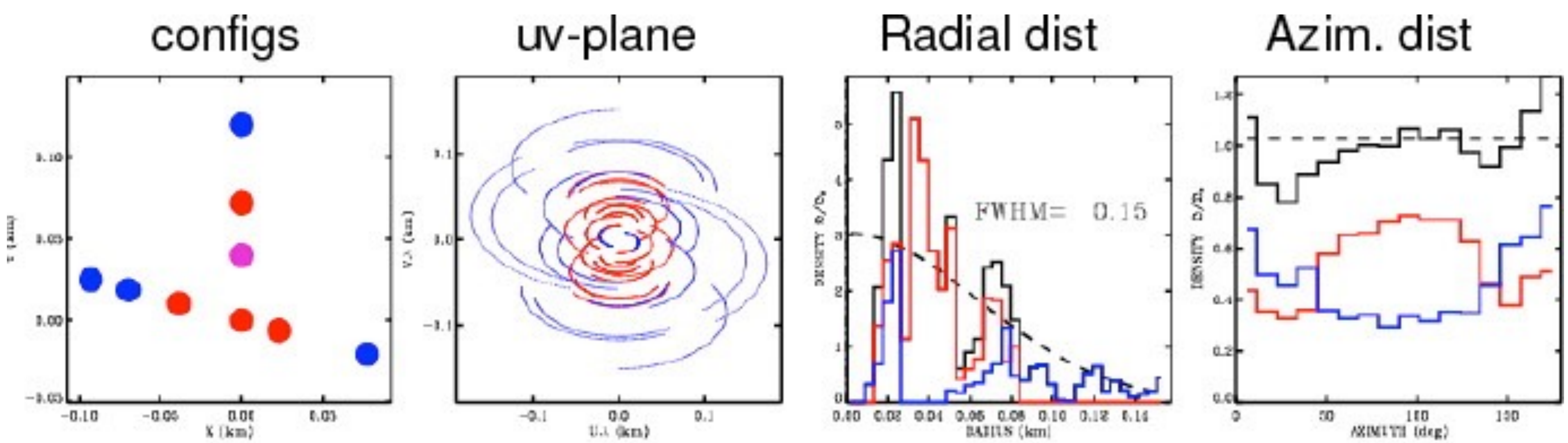

Plateau de Bure observations, supersynthesis + multiconfiguration

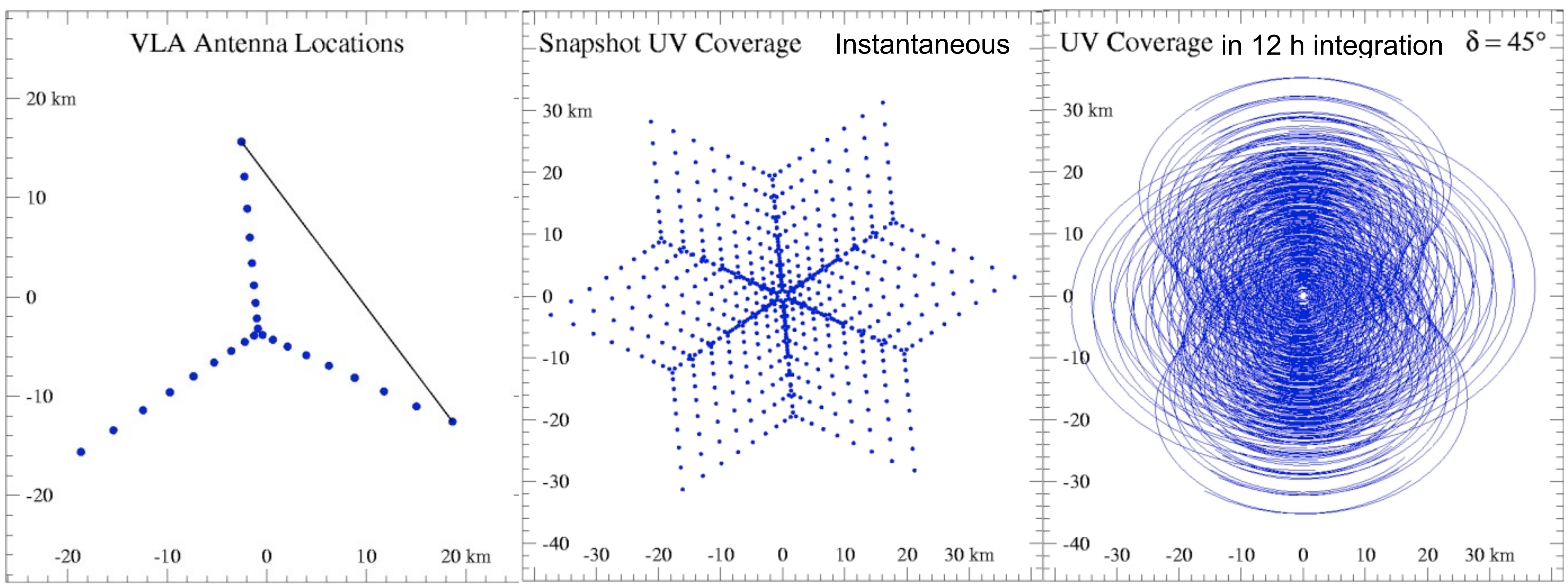

- **Aperture Synthesis Simulator :** https://launchpad.net/apsynsim

• Sensitivity of an interferometer :

Elementary antenna : a_{eff} , $(S/B)_1$

Pair of elementary antennas → 1 interferometric baseline : $2 \times a_{eff}$, $(S/B)_2 = (S/B)_1 \times \sqrt{2}$

N elementary antennas → N(N-1)/2 interferometric baseline s : $N \times a_{eff}$,

$$(S/B)_N = [N(N-1)/2]^{1/2} \times (S/B)_2 = [N(N-1)/2]^{1/2} \times (S/B)_1 \times \sqrt{2}$$

$$\sim (S/B)_1 \times N \qquad \text{for large } N$$

→ similar to a single antenna of effective area : $A_{eff} = N \times a_{eff}$

- <u>V.L.B.I. = Very Long Baseline Interferometry</u>

Problem: increase d to increase maximum resolution (~λ/d)
Real-time correlation ⇒ antennas connected via :
- HF cables → ≤ a few km (losses)
- optical fibres → ≤ a few 10-100 km
- HF radio link → ≤ a few 100 km (propagation effects)

Beyond that, problems of propagation and phase preservation

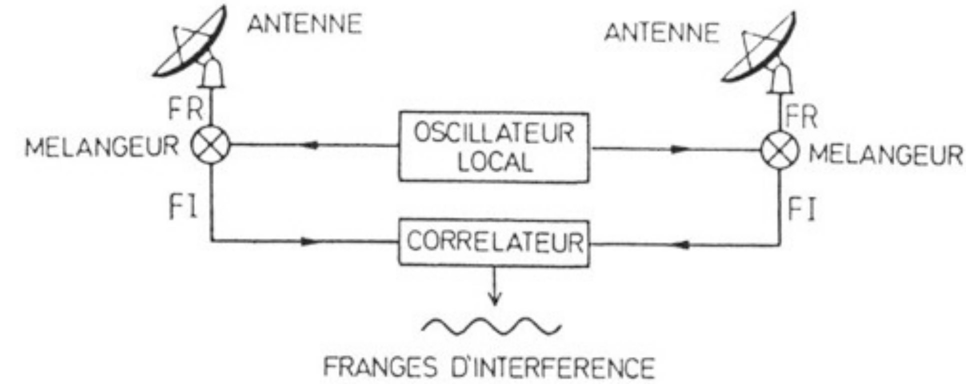

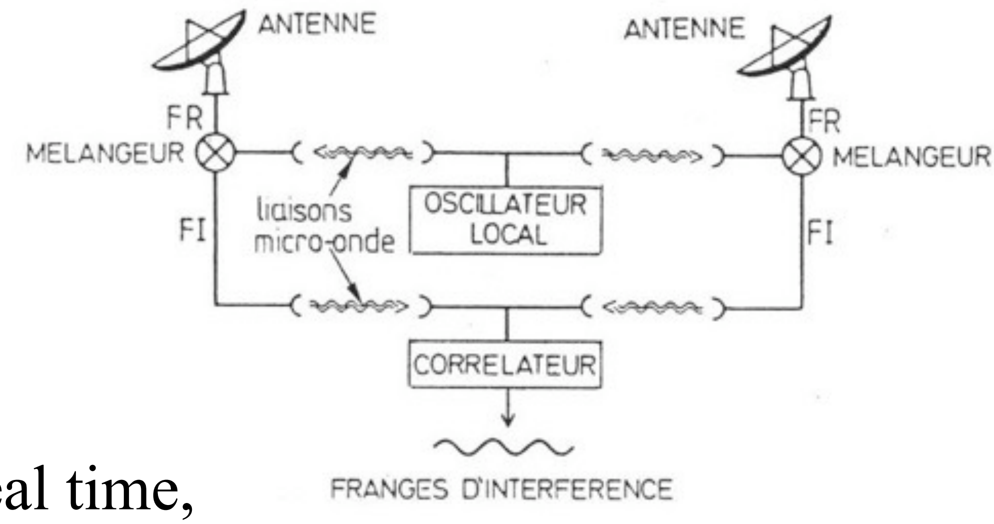

⇒ VLBI technique : instead of correlating (⊗) the signals in real time,
Offline correlation ⇒ recording of signals, possibly digitised (magnetic tape, hard disk) with an "accurate" time reference, then transfer to central computer for later correlation
⇒ if S/N >1 for a given τ (corresponding to $\psi = 2\pi\, d \sin\theta / \lambda = 2\pi\nu\,\tau$), fringes are observed
⇒ measure of $t_A(u,v)$ for the baseline considered
⇒ Intercontinental interferometry is possible = VLBI
On Earth, $d_{max} \approx 12000$ km ⇒ $\lambda/d_{max} = 2\times10^{-8}$ rad $= 4\times10^{-3}$ " at $\lambda = 21$ cm

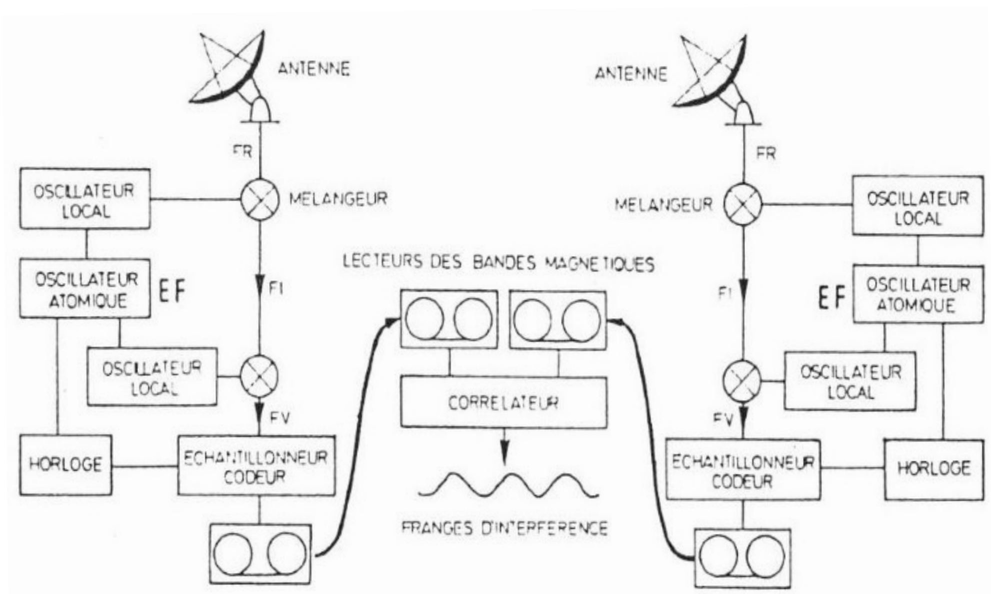

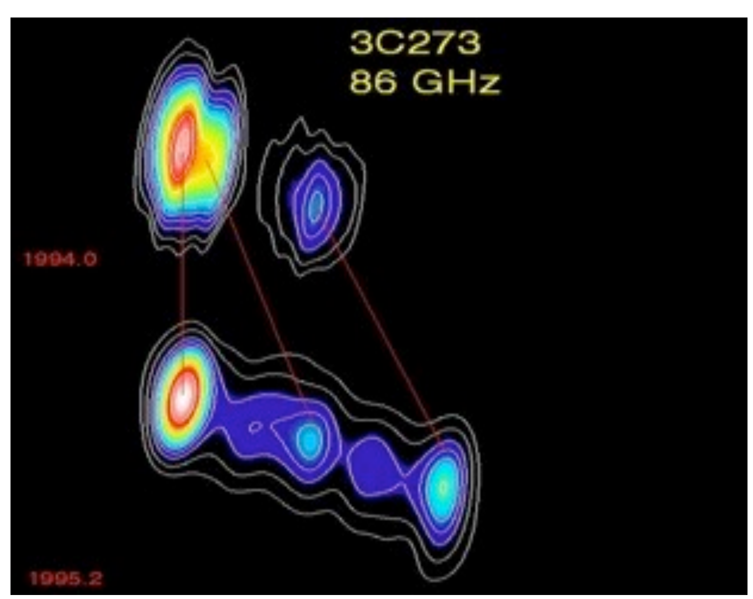

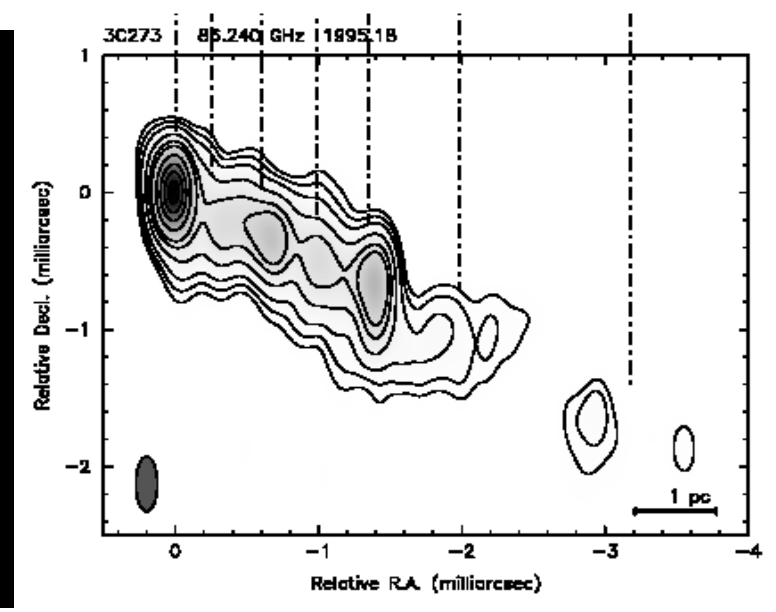

Measurement accuracy: a metrology problem

→ Identical, synchronised VLBI ~ (super-)heterodyne receivers

Precise knowledge of the phase $\psi = 2\pi(\nu-\nu_{LO})t$ of the LF signal of interest (of bandwidth $\Delta\nu \sim \nu-\nu_{LO}$) with $\delta\psi = 2\pi\, \Delta\nu\, \delta t + 2\pi\, \delta\nu_{LO}\, \Delta t$ (Δt = observation duration)

$\delta\psi \ll 1$ requires a clock accuracy $\delta t \ll 1/\Delta\nu$ *(ex: 10^{-6} sec for $\Delta\nu = 1$ MHz)*

The LO of each receiver must have a stability $\delta\nu_{LO} \ll 1/\Delta t$

$$\Rightarrow \underbrace{\delta\nu_{LO}/\nu_{LO}}_{\text{fluctuations of } \nu_{OL}} \ll (\nu_{LO}\times\Delta t)^{-1} \sim (\underbrace{\nu}_{\text{frequency of the radio signal}} \times \underbrace{\Delta t}_{\text{duration of observation}})^{-1}$$

(ex: $\delta\nu_{LO}/\nu_{LO} \ll 10^{-12}$ for 15 minutes of observation at 1 GHz)

LO used :

Rubidium gas lasers : $\delta\nu_{LO}/\nu_{LO} \approx 5\times10^{-12}$ ⇒ 20 sec of coherency at 10 GHz

Cesium lasers : $\delta\nu_{LO}/\nu_{LO} \approx 10^{-12}$

Hydrogen Masers: $\delta\nu_{LO}/\nu_{LO} \approx 10^{-13/-14}$

⇒ precision on knowledge of the baselines : baselines of ~ Earth ∅ must be known at < $\lambda/10$ ~ cm because we need $\delta\psi = 2\pi\, \delta d \sin\theta / \lambda \ll 1 \Rightarrow \delta d \ll \lambda / 2\pi \sin\theta$ to be able to go back to θ (source direction)

→ In the absence of absolute references (t of clocks, φ of LO, or $d_{baseline}$), observation of $|t_A(u,v)|$ during a source transit (fringe visibility for the baseline considered) gives information on the angular dimension of the source.

<u>NB</u>: VLBI very difficult at VLF (decametre range) due to inhomogeneous phase delays $\delta\psi$ introduced by ionospheric crossing $\Rightarrow$ major challenge for LF interferometers (LOFAR, NenuFAR)

<u>VLBI Terminals</u>

History : Mark I, II, III (video, $\Delta\nu$ = 1-56 MHz + digitisation a posteriori); Mark IV (direct digitisation + recording on magnetic tape); Mark V (direct digitisation on hard disk, $\geq$ 100 MHz)

VLBI networks include most of today's large dm-cm radiotelescopes (more difficult on meridian or fixed telescopes):

MERLIN = European network (heterogeneous), VLBA = US network (homogeneous), LOFAR-Eu

VSOP (VLBI Space Obs. Program, Japan): antenna in Earth orbit $\Rightarrow$ d $\approx$ 25000 km

EHT $\Rightarrow$ maximum resolution achieved ~ 10^{-4} " ~ optics

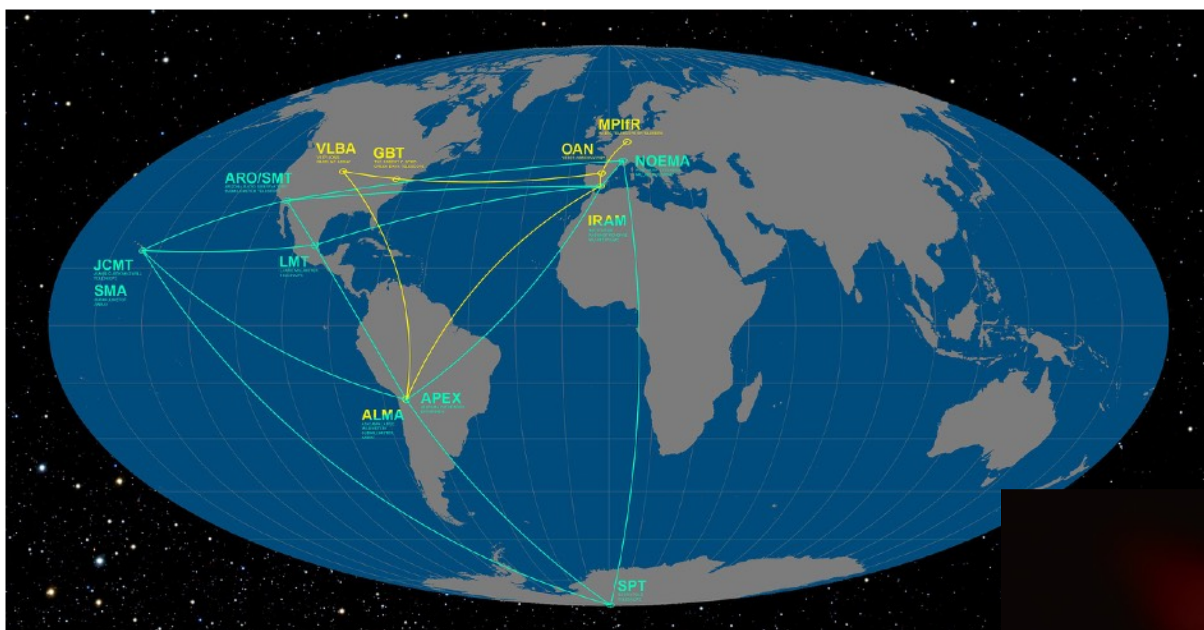

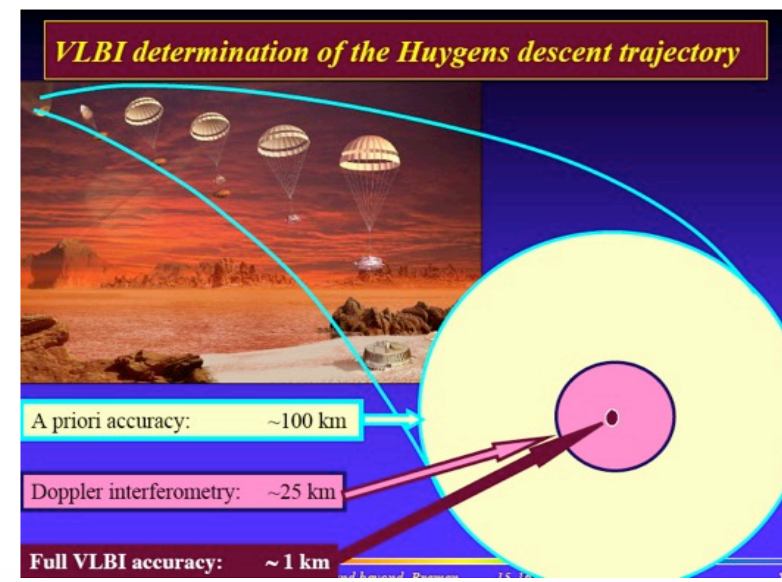

100's microarcsec

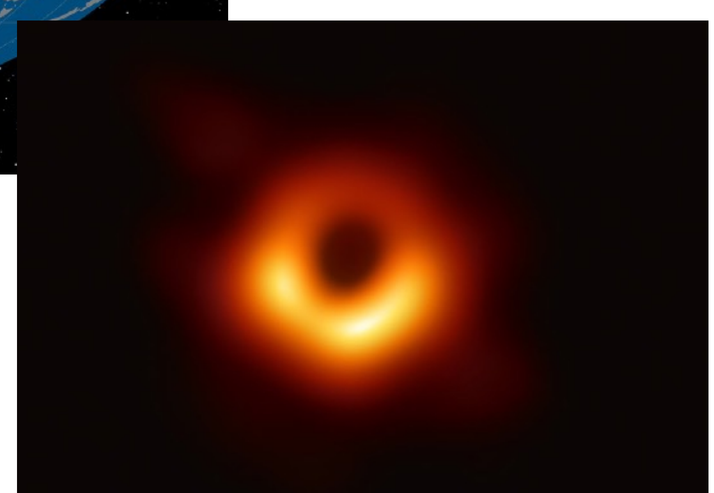

→ M87 in mm VLBI with the
Event Horizon Telescope, 10/4/2019

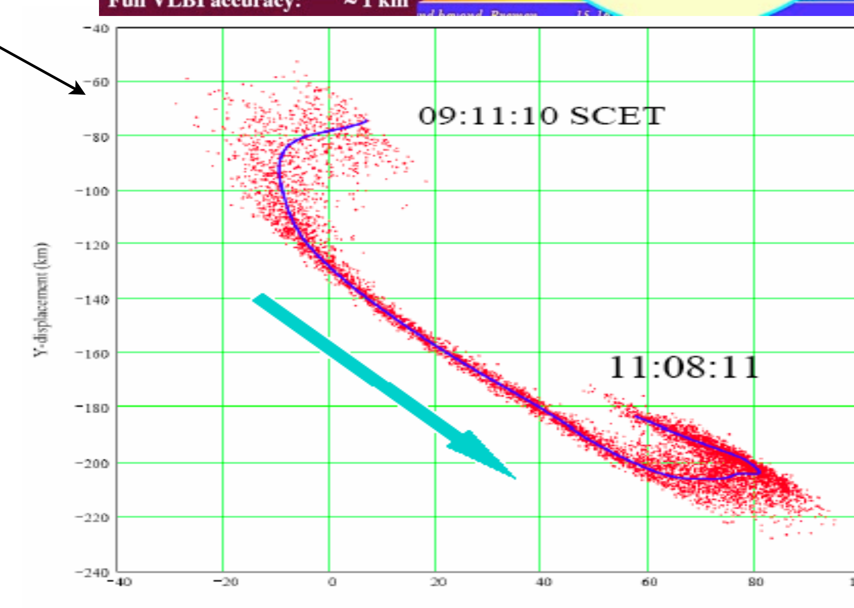

- Introduction (history, interest, specific features)
- Waves & Polarisation
- Plasmas & Propagation (cutoff, dispersion, Faraday effect, scintillations)
- Coherent Signal Detection (measurement theory, antenna temperature, calibration, noise)
- Receivers (heterodyne, system temperature, filtering, gain, RFI mitigation)
- Basics of Radio Astronomy Antennas: Single antennas
- Basics of Interferometry and Aperture Synthesis (phased arrays, electronic pointing, imaging, correlation, coherence, VLBI)
- Observation methods
- Large present & future ground-based radio arrays
- Basics of Space radio astronomy

• **Interferometry & Polarimetry: radio imaging & Stokes parameters** (introduction & remarks)

Relation : measurements ↔ Observables

Explicit equation linking interferometric measurements to S,Q,U,V

derived by (Morris & al. ApJ, 139, p. 551, 1964)

More general mathematical framework proposed by Hamaker et al. *(A&A Supp., 117, 137, 1996)*

→ The « Radio Interferometer Measurement Equation » (RIME)

Basic assumption: linearity of propagation & receiver effects.

$\mathbf{E} = (E_x , E_y) \quad \Rightarrow \quad \mathbf{E' = [J]\, E}$ (propagation)

$\mathbf{V = [J]\, E}$ (reception, with $\mathbf{V} = (V_x , V_y)$)

[J] (ou **J**) is a 2×2 matrix called « Jones matrix »

Single antenna: $\mathbf{V = J\, E} = (V_x , V_y)$ = complex voltages (amplitude & phase) measured by the 2 polarised focal elements (here linearly), from which the "coherence matrix" can be derived :

$$<V\, {}^tV^*>|_{\Delta t >> 1/\nu} = \begin{bmatrix} <V_xV_x^*> & <V_xV_y^*> \\ <V_yV_x^*> & <V_yV_y^*> \end{bmatrix}$$

$$\propto \begin{bmatrix} <E_xE_x^*> & <E_xE_y^*> \\ <E_yE_x^*> & <E_yE_y^*> \end{bmatrix} = \frac{1}{2}\begin{bmatrix} S+Q & U+iV \\ U-iV & S-Q \end{bmatrix} = \mathbf{B}$$

Interferometer : $\mathbf{V_i = J_i E}$ for each element of the interferometer, from which we define the "visibility matrix", which gathers the measurements of a 2-antenna interferometer p,q :

$$<V_p\, {}^tV_q^*>|_{\Delta t >> 1/\nu} = \begin{bmatrix} <V_{px}V_{qx}^*> & <V_{px}V_{qy}^*> \\ <V_{py}V_{qx}^*> & <V_{py}V_{qy}^*> \end{bmatrix} = \mathbf{V_{pq}}$$

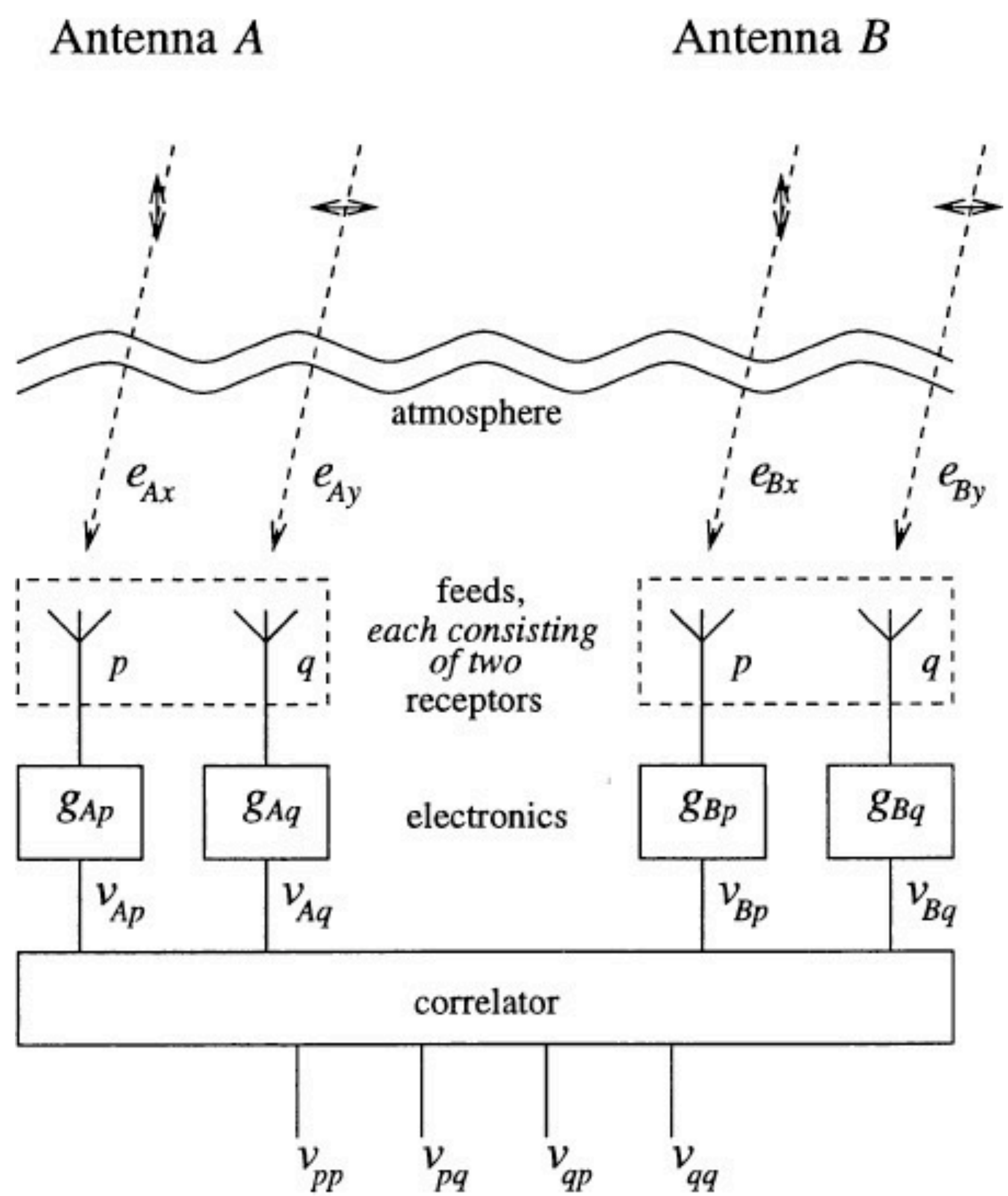

Interferometer block diagram

For an incident electric field $\mathbf{E}$ from a point source, antennas p & q measure :

$$\mathbf{V_p = J_p\, E} \quad \& \quad \mathbf{V_q = J_q\, E}$$

where $\mathbf{J_p}$ and $\mathbf{J_q}$ are the Jones matrices describing the signal transformations between source and receivers.

$\Rightarrow \quad \mathbf{V_{pq}} = \; <V_p\, {}^tV_q{}^*> \; = \; < \mathbf{J_p\, E}\; {}^t(\mathbf{J_q\, E})^*>$

with $\quad {}^t(AB) = {}^tB\; {}^tA$ and assuming that $\mathbf{J_p}$ & $\mathbf{J_q}$ are constante on $< \dots >$

$\Rightarrow \quad \mathbf{V_{pq}} = \; \mathbf{J_p} <E\; {}^tE^*> {}^t\mathbf{J_q}^* = \mathbf{J_p\, B}\; {}^t\mathbf{J_q}^*$

= « Measurement Equation »

(can also be written in circular polarisations)

If we decompose the signal transformations due to propagation and receiver into a product of

(non-commutative) n Jones matrices, e.g. : : $\quad \mathbf{J_p = J_{pn}\, J_{p(n-1)} \dots J_{p1}}$

it comes : $\quad \mathbf{V_{pq}} = \; \mathbf{J_{pn}\, J_{p(n-1)} \dots J_{p1}\, B}\; {}^t\mathbf{J_{q1}}^*\; {}^t\mathbf{J_{q2}}^* \dots {}^t\mathbf{J_{qm}}^*$

The terms $J_{p,q}$ can contain all the transformations undergone by the signal:

- antenna and receiver gain : $\mathbf{G} = \begin{bmatrix} G_x & 0 \\ 0 & G_y \end{bmatrix}$
- phase shifts : $\mathbf{D} = \begin{bmatrix} e^{i\psi} & 0 \\ 0 & e^{i\psi} \end{bmatrix}$
- rotations (of dipoles, Faraday…) : $\mathbf{R} = \begin{bmatrix} \cos\varphi & -\sin\varphi \\ \sin\varphi & \cos\varphi \end{bmatrix}$
- cross-polarisation terms (errors) : $\mathbf{X} = \begin{bmatrix} 1 & \delta_{x\leftarrow y} \\ -\delta_{y\leftarrow x} & 1 \end{bmatrix}$ ...

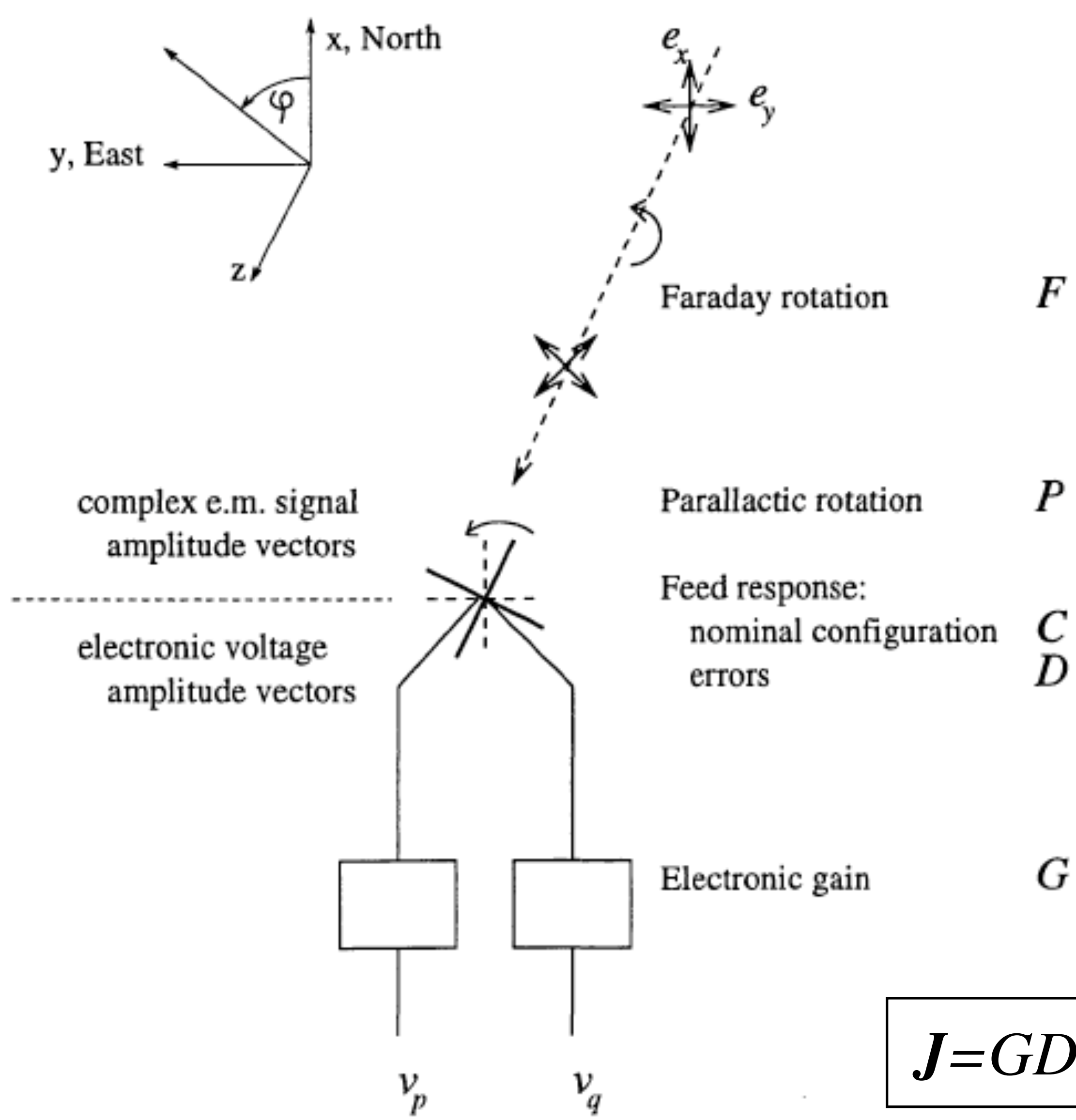

$\boldsymbol{J}$*=GDCPF*

The modelling of a radio interferometer is the determination of the Jones matrices that describe it.

Packages dedicated to a specific type of instrument: AIPS, AIPS++, CASA ...

Examples :

• Observation of a point source with a perfect instrument : :

$\mathbf{V_{pq}} = \mathbf{D_p\, B\, {}^t D_q^*}$

with D the Jones scalar matrix representing the phase shift due to the path difference:

$\psi = 2\pi d \sin\theta / \lambda$

$\Rightarrow \quad \psi_{pq} = 2\pi\, \mathbf{u_{pq}.k} = 2\pi\, (\mathbf{u_q - u_p}).\mathbf{k} = 2\pi\, \mathbf{u_q.k} - 2\pi\, \mathbf{u_p.k} = \psi_q - \psi_p$

Scalar case : $V_{pq} = e^{i\psi_{pq}} \quad \Rightarrow \quad S\, V_{pq} = e^{i\psi_q} S\, e^{-i\psi_p}$

M.E. : $\mathbf{V_{pq}} = \mathbf{D_p\, B\, {}^t D_q^*}$

$<V_{px} V_{qx}^*> = e^{i\psi_q}\, ½\, (S+Q)\, e^{-i\psi_p}$

• For any (extended) source ⇒ decomposition into elementary point sources :

$\mathbf{V_{pq}} = \sum_s (\mathbf{D_p\, B\, {}^t D_q^*})$

⇒ all results obtained for S in imaging from any source apply to the elements of **B**, or equivalently to the Stokes parameters S, Q, U, V

• Variable complex gains (possibly time-dependent) :

$\mathbf{V_{pq}} = \mathbf{G_p}\, \mathbf{D_p}\, \mathbf{B}\, {}^t\mathbf{D_q}^*\, {}^t\mathbf{G_q}^*$ with $\mathbf{G_p} = \begin{bmatrix} G_{px} & 0 \\ 0 & G_{py} \end{bmatrix}$

• calibration of observations = observation of reference sources (known position & size) + interpolation/t $\Rightarrow$ adjustment of antenna gains & phases

Scalar case : $g_p(t)$ & $\phi_p(t)$, with $G_p = g_p(t) \exp[i\, \phi_p(t)]$

M. E. : modeling of $\mathbf{G_p}$ and (iterative) fitting of modeled $\mathbf{V_{pq\text{-}m}}$ to observed $\mathbf{V_{pq\text{-}o}}$:

$\mathbf{D_p}\, \mathbf{B}\, {}^t\mathbf{D_q}^*$ or $\sum_s (\mathbf{D_p}\, \mathbf{B}\, {}^t\mathbf{D_q}^*)$ = « sky model »

$\mathbf{V_{pq\text{-}m}} = \mathbf{G_p}\, \mathbf{D_p}\, \mathbf{B}\, {}^t\mathbf{D_q}^*\, {}^t\mathbf{G_q}^*$ = model including $\mathbf{G_p}$ eand $\mathbf{G_q}$ a given iteration

$\mathbf{V_{pq\text{-}o}} - \mathbf{V_{pq\text{-}m}}$ = residuals

$\mathbf{G_p}^{-1} (\mathbf{V_{pq\text{-}o}} - \mathbf{V_{pq\text{-}m}})\, {}^t\mathbf{G_q}^{-1*}$ = corrected residuals (by minimisation)

$\rightarrow$ improvement of the sky model & iteration.

Simulation of a 10 Jy unpolarised point source (known a-priori = calibrator) observed at the Westerbork Synthesis Radio Telescope @ 1432 MHz with gain errors

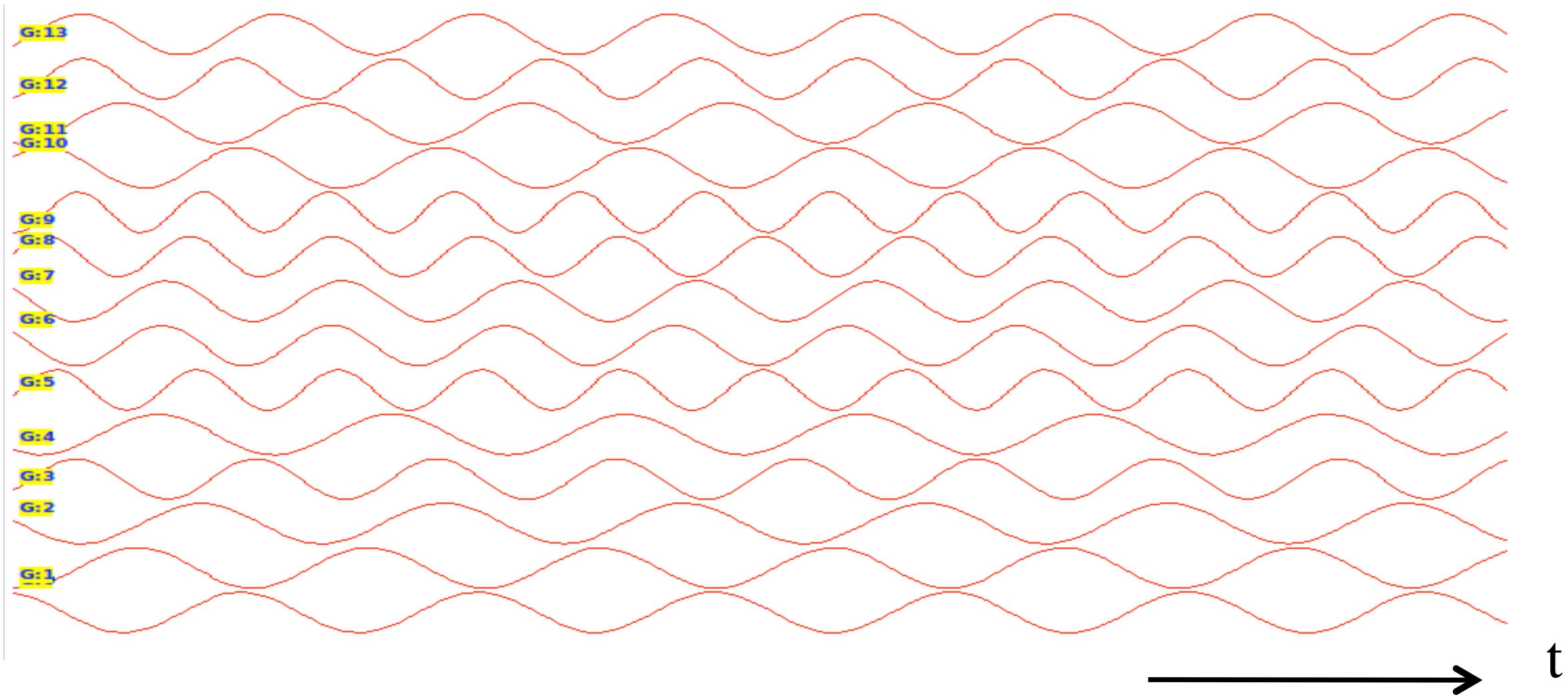

Simulation of a periodic gain error of 20% (0.8-1.2) on each of the 14 WSRT antennas

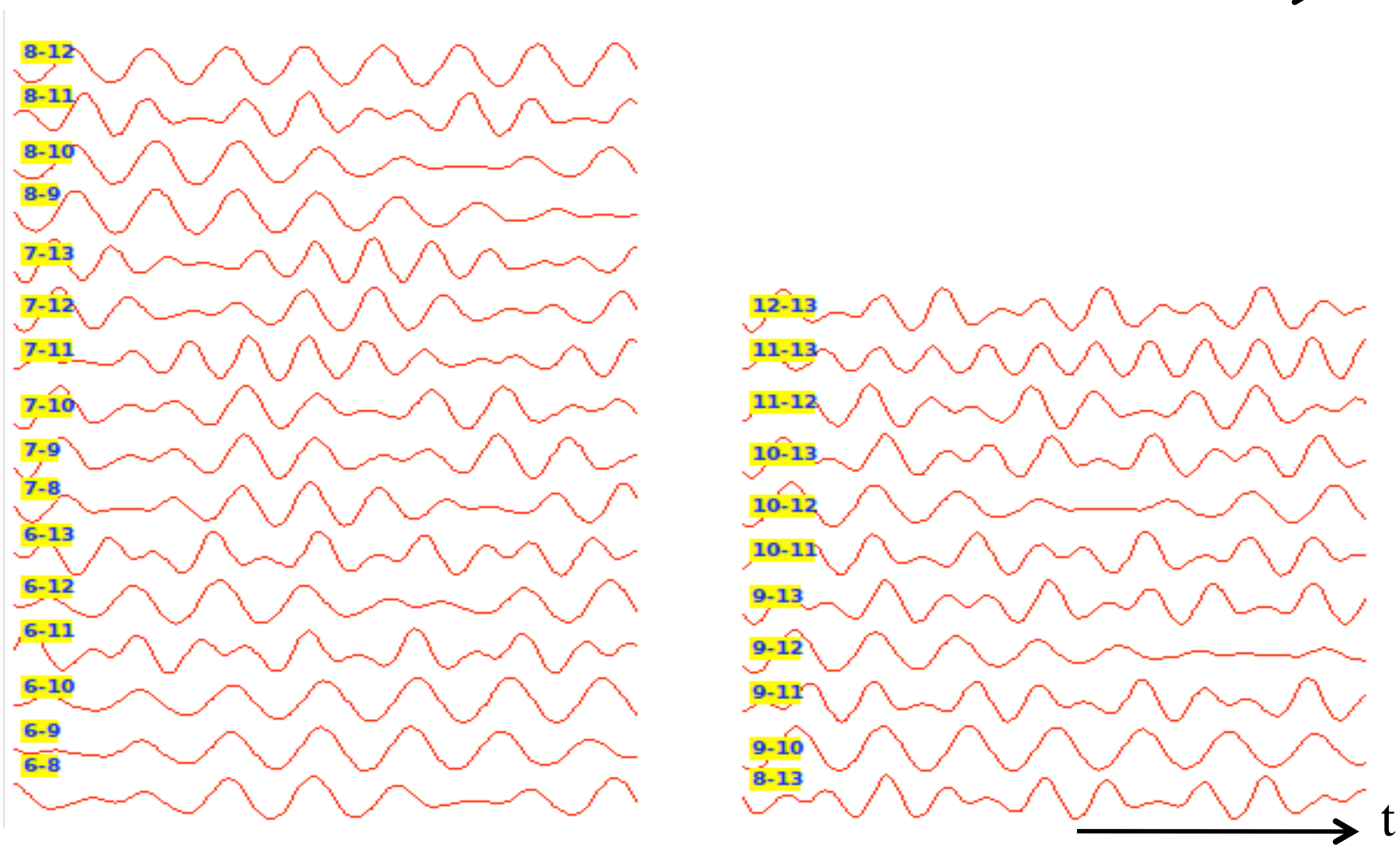

⇒ Visibility amplitude for a few baselines (as a function of t)

Simulation of a 10 Jy unpolarised point source (known a-priori = calibrator) observed at the Westerbork Synthesis Radio Telescope @ 1432 MHz with gain errors

Raw image: $S(\theta,\phi)$, $Q,U,V = 0$ Jy

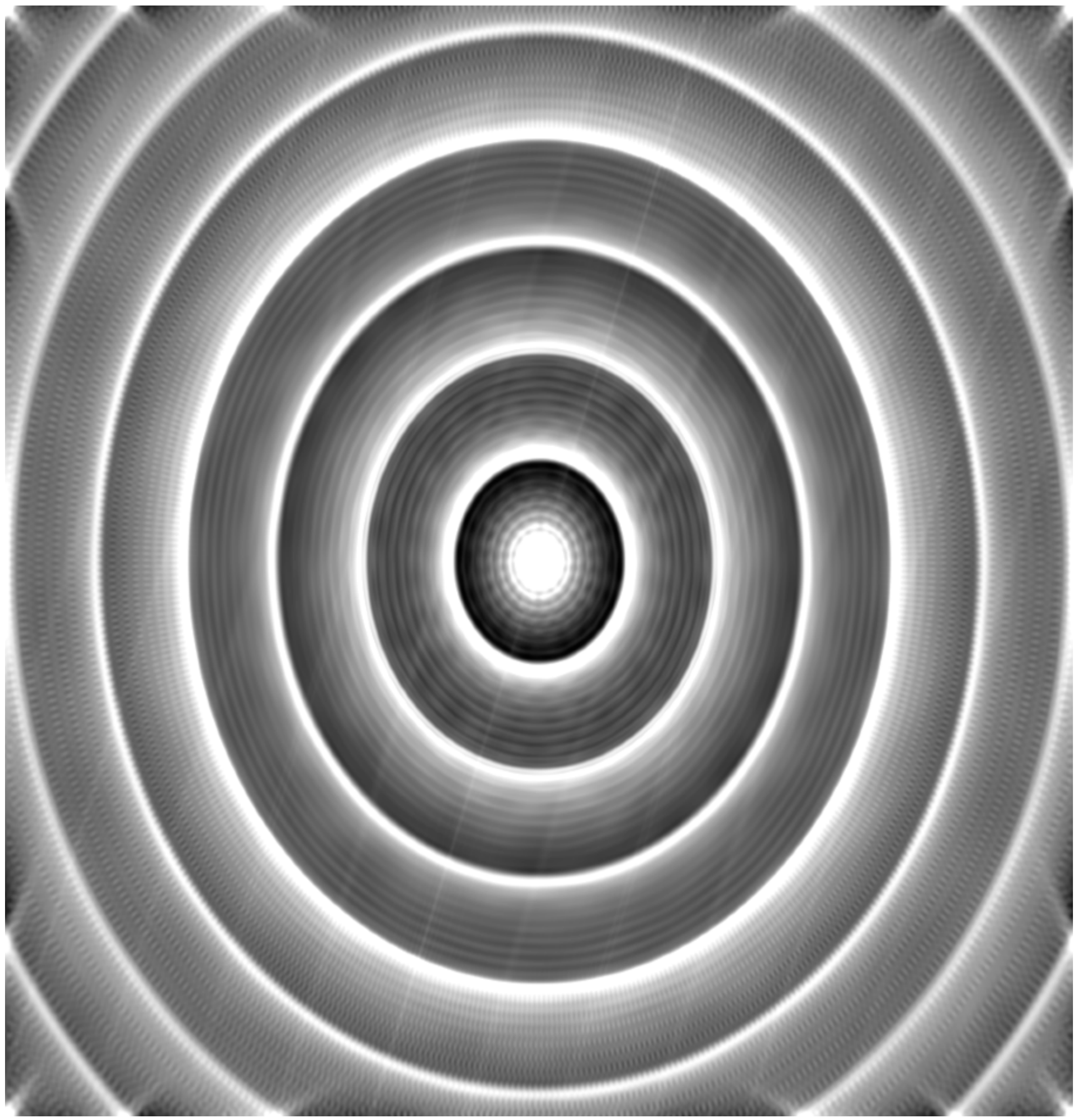

Min=-0.17 Jy Max= 5. Jy

Subtracting a model from the source

Residuals $\delta S(\theta,\phi)$ before Gain calibration

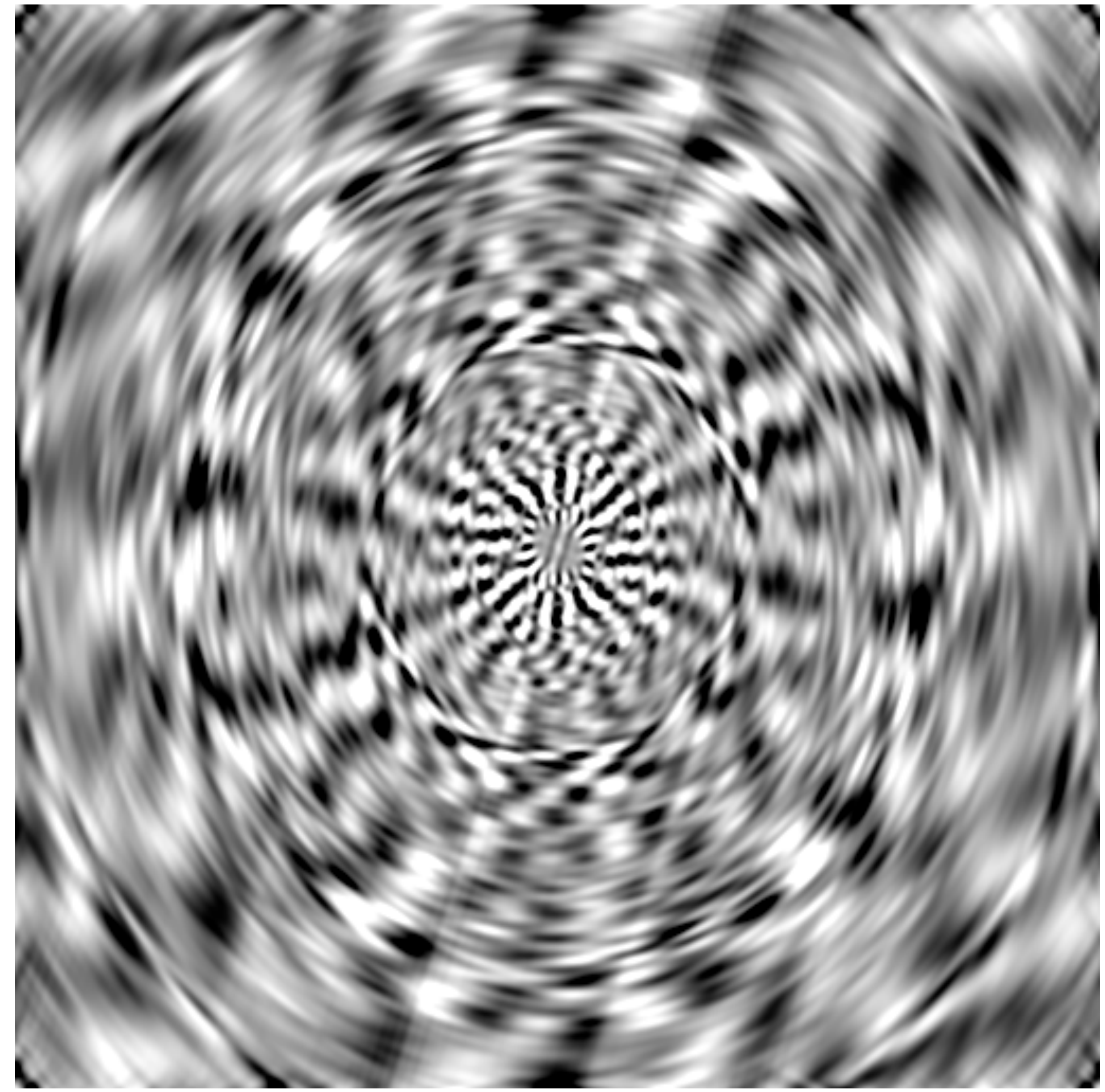

Min = -0.03 Jy Max = 0.03 Jy

⇒ The source has been subtracted, but high residuals (variations in intensity) remain due to artificially introduced and uncorrected gain errors.

Simulation of a 10 Jy unpolarised point source (known a-priori = calibrator) observed at the Westerbork Synthesis Radio Telescope @ 1432 MHz with gain errors

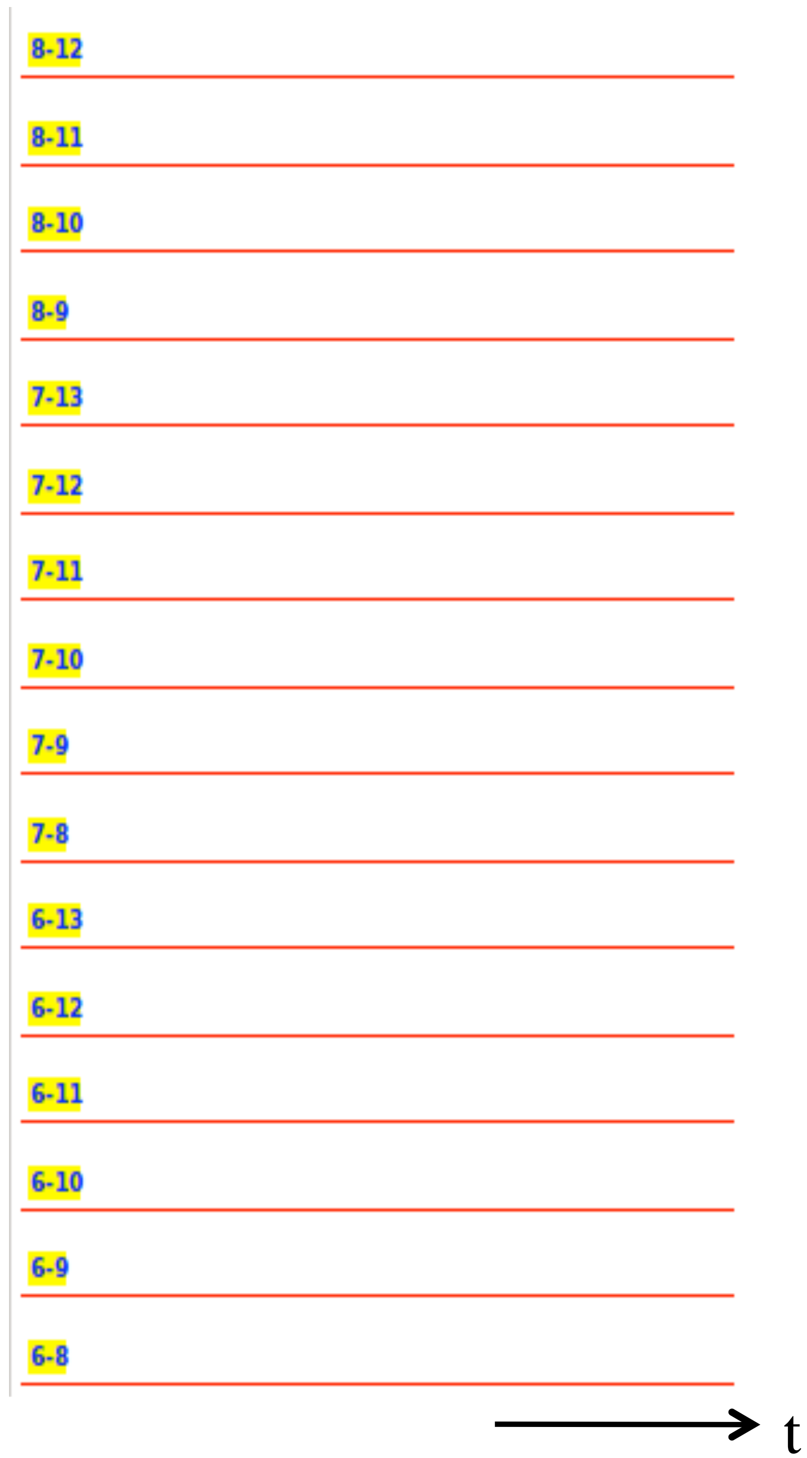

Visibility amplitude for some baselines after source subtraction and gain calibration.

Subtracting a model from the source

Residuals $\delta S(\theta,\phi)$ before Gain calibration (M.E.)

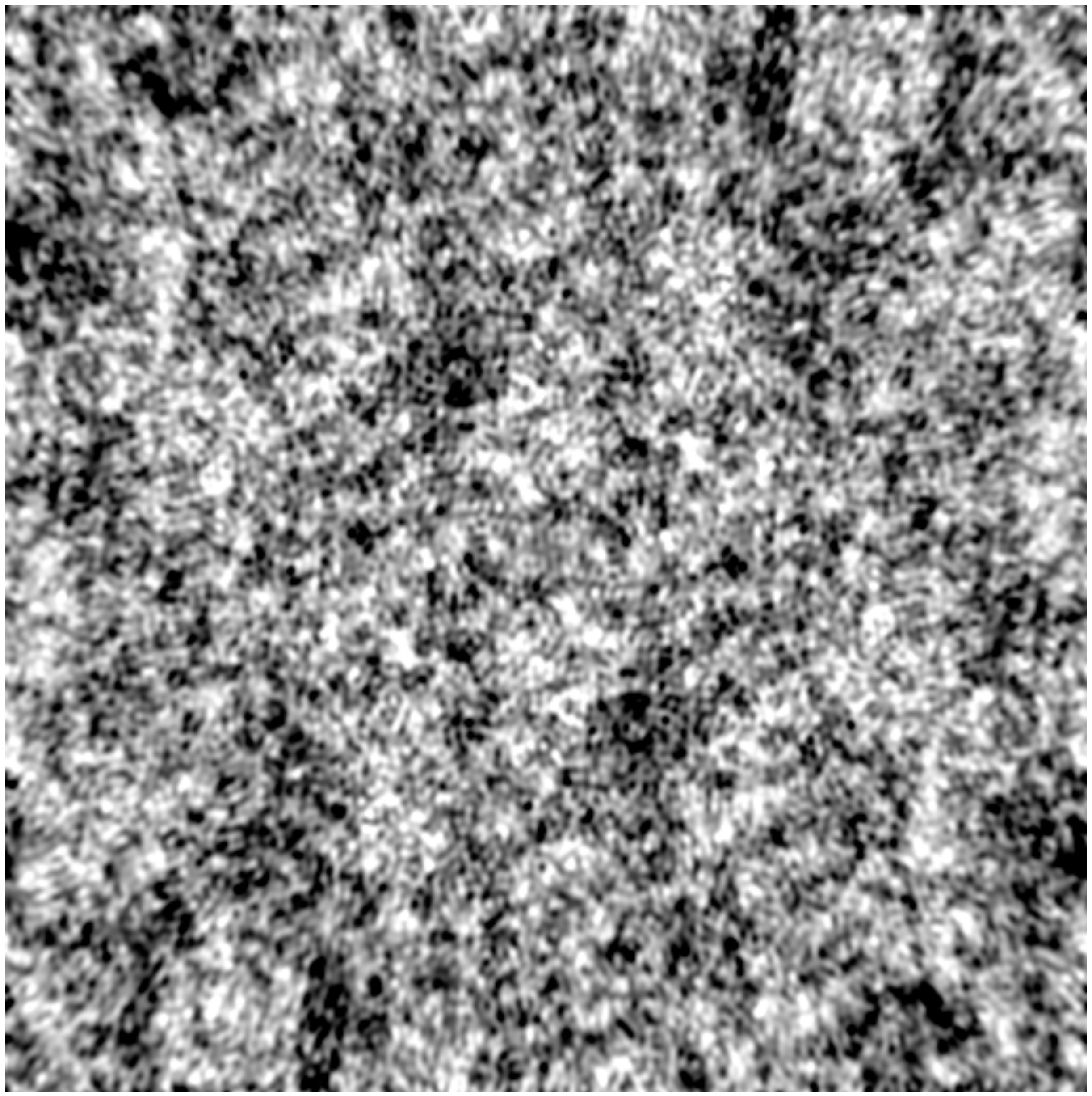

Min = -1.5 10^{-9} Jy Max = 1.5 10^{-9} Jy

$\Rightarrow$ Residuals have Gaussian statistics (numerical error in this case)

Thanks to J. Girard

• Calibration based on observation of the target itself (Self-Cal) ⇒ adjustment of antenna gains (amplitudes and phases) to correct for ionospheric propagation effects

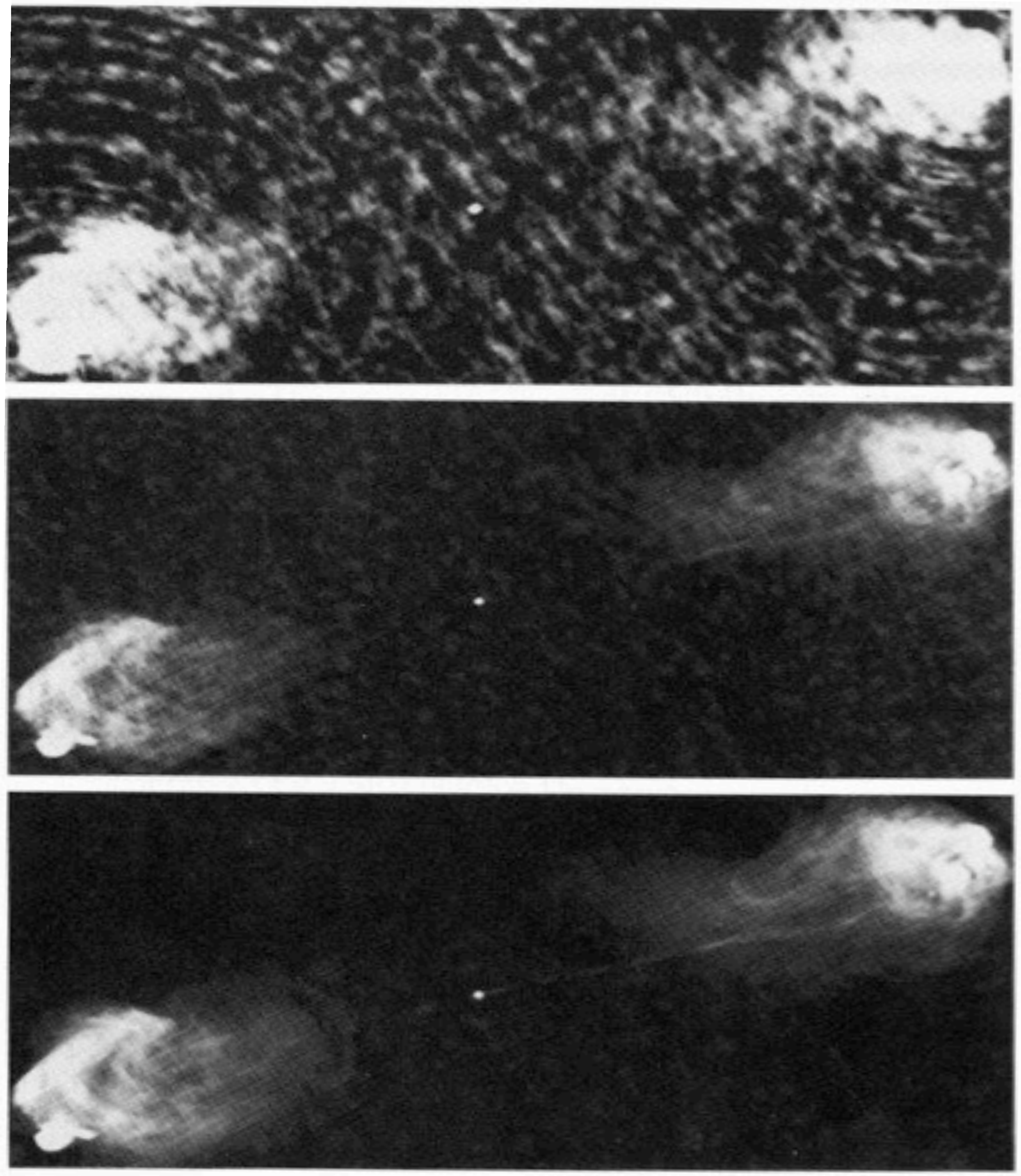

Fig. 8.6. Three images of the radio galaxy Cygnus A, taken with the VLA using all four configurations at 6 cm. In the top panel the interferometer data were calibrated, gridded and Fourier transformed, with no additional processing. Much of the structure is *not* real, but rather due to side lobes of the synthesized beam. In the middle panel, the image was deconvolved using the Maximum Entropy Method (MEM). Note the vast increase in dynamic range. The image in the bottom panel has been self-calibrated. This gives an additional factor of 3 in dynamic range (observed by Perley and Dreher, courtesy of NRAO/AUI)

• Dipole projection effects: described by a Jones matrix

$$\mathbf{L}(\varphi,\lambda) = \begin{bmatrix} \cos\varphi & -\sin\varphi \sin\lambda \\ \sin\varphi & \cos\varphi \sin\lambda \end{bmatrix}$$ with φ = azimuth, λ=elevation

L varies with t, with source position (large field), with antenna position (large array)
+ *antenna radiation pattern, ionosphere, pointing errors*

⇒ requires to solve the Measurement Equation per « facets » (Direction Dependent Effects) as visibility corrections are only valid in one direction…

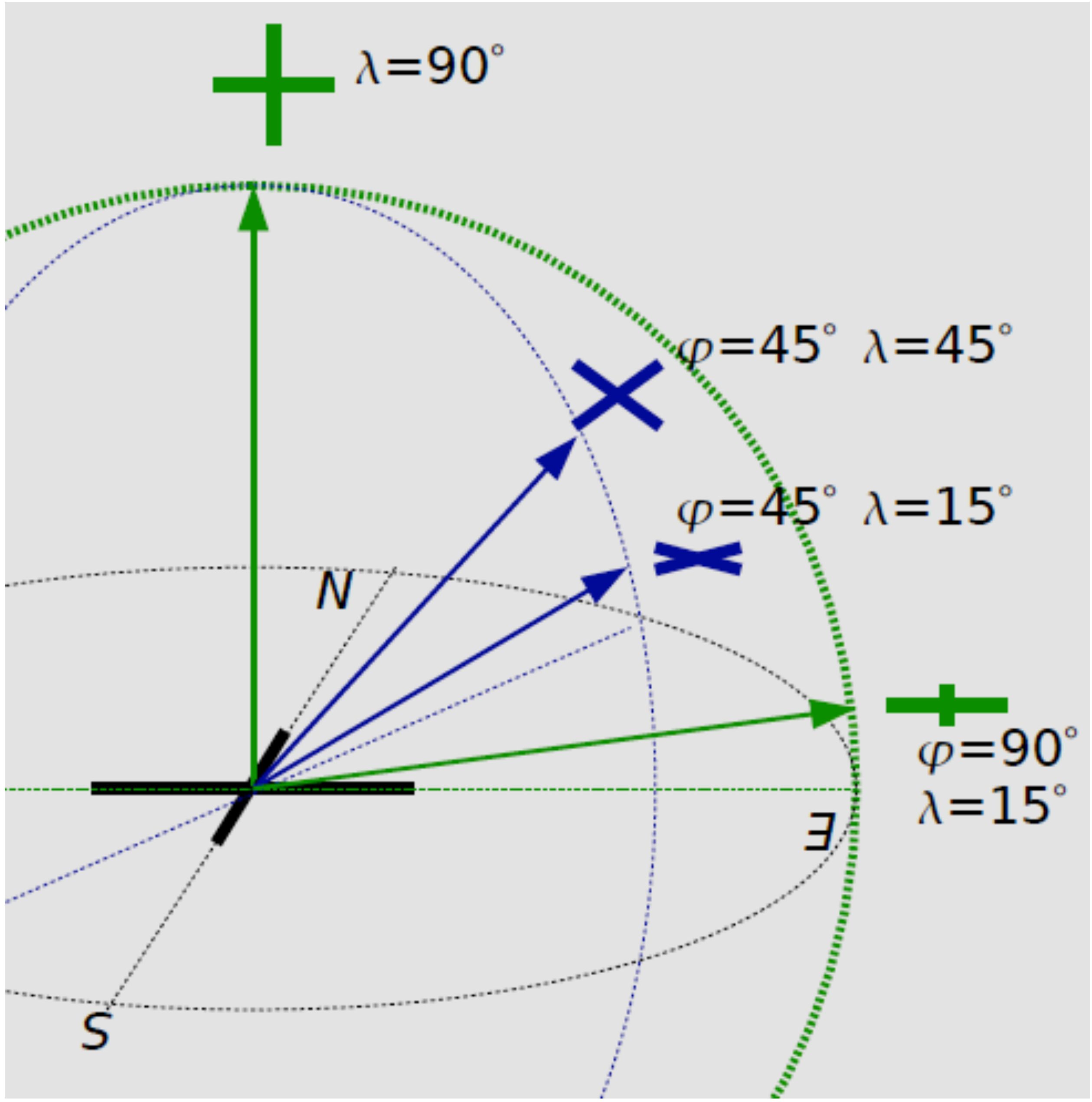

• Imaging techniques

$$\boxed{\begin{array}{c} T_A(\theta,\phi) = 1/4\pi \times [\, g(\theta,\phi) \otimes T(\theta,\phi) \,] \;\Rightarrow\; t_A(u,v) = G(u,v)\,.\,t(u,v) \;\propto V(u,v) \\ \text{with } G(u,v) = 1/4\pi \times TF[g(\theta,\phi)] \;=\; E(u,v) \otimes E^*(u,v) \end{array}}$$

Incomplete (u,v) coverage + noise ⇒ restoration of $T(\theta,\varphi)$ from non unique $t_A(u,v)$

« Main Solution » obtained by setting to 0 unconstrained $t_A(u,v)$ ⇒ $T(\theta,\varphi)_{ms}$

$T(\theta,\varphi)_{real}$ - $T(\theta,\varphi)_{ms}$ = « ghost » or « invisible » solution,

decomposing on portions of the (u,v) plane where $t_A(u,v) = 0$

TF [$t_A(u,v)$ / $G(u,v)$] generally very noisy, as linear deconvolution adds noise due to side lobes of TF [$G(u,v)$] = $g_D(\theta,\phi)$ = « dirty beam » ⇒ high side lobes, linked to the sparse sampling of $G(u,v)$ (dirty beam is dirty !)

⇒ use of non-linear "recipes" to improve restoration

e.g. weighting of $t_A(u_i,v_i)$ by a Gaussian $(u_i^2+v_i^2)^{1/2}$) ⇒ reduction of sidelobes to ~1%

$g_C(\theta,\varphi)$ = « clean beam » = Gaussian approximation of « dirty beam »

Aliasing : FT by FFT $\Rightarrow$ requires interpolation of $t_A(u,v)$ on a regular grid

$t'_A(u,v) = III(u,v).[P(u,v) \otimes t_A(u,v)$ where $t'_A(u,v)$ takes its values on a regular grid $(\Delta u, \Delta v)$

$P(u,v)$ = weighting of $t_A(u,v)$ measurements [e.g. $P(u,v)$ = uniform disk]

$III(u,v) = \Delta u . \Delta v \times \sum_{i,j=-\infty}^{+\infty} \delta(u-i.\Delta u) \times \delta(v-j.\Delta v)$

$\Rightarrow T'(\theta,\varphi) = III(\theta,\varphi) \otimes [\, p(\theta,\varphi) . t_A(\theta,\varphi)\,]$

If $p(\theta,\varphi) \neq 0$ outside the source [e.g. $P(u,v)$ = uniform disk $(u,v) \Rightarrow p(\theta,\varphi) = J1$ (Bessel order 1)]

$\Rightarrow$ artificial signal folding in source image

$\Rightarrow$ ghost images due to « aliasing » (e.g. from unresolved intense point source)

$T'(\theta,\varphi)$ = "dirty map" (generally low dynamics, instability wrt addition of visibility measurements)

• CLEAN : representation of $T'(\theta,\phi)$ by a sum of point sources :

$T'(\theta,\phi) = \Sigma_i A_i\, g_D(\theta-\theta_i,\phi-\phi_i) + t_\varepsilon(\theta,\phi)$ with intensities $A_i > 0$

Iterative decomposition from the most intense peak with a convergence factor γ $(0 < \gamma < 1)$,

converges if $t_\varepsilon \rightarrow$ measurement noise

Clean Image = $(\Sigma_i A_i(\theta_i,\phi_i)) \otimes g_C(\theta,\phi)$ [+ residuals]

NRH @ 327 MHz

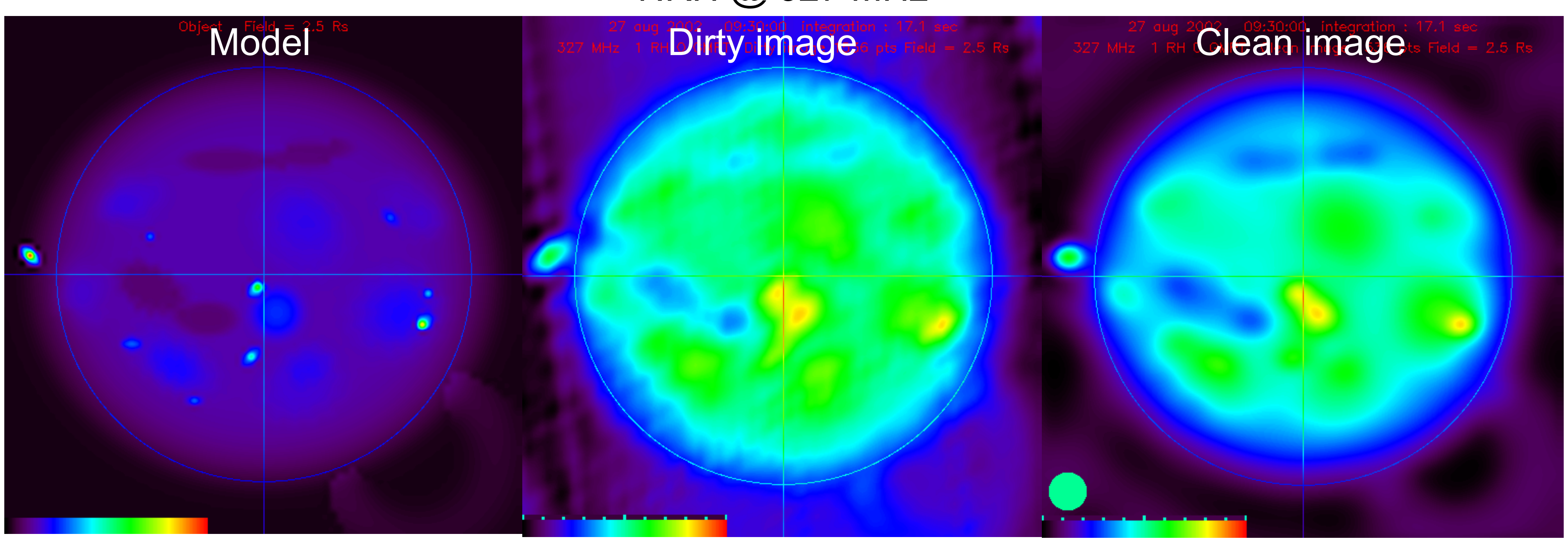

Combination of sets of visibilities from different instruments is possible

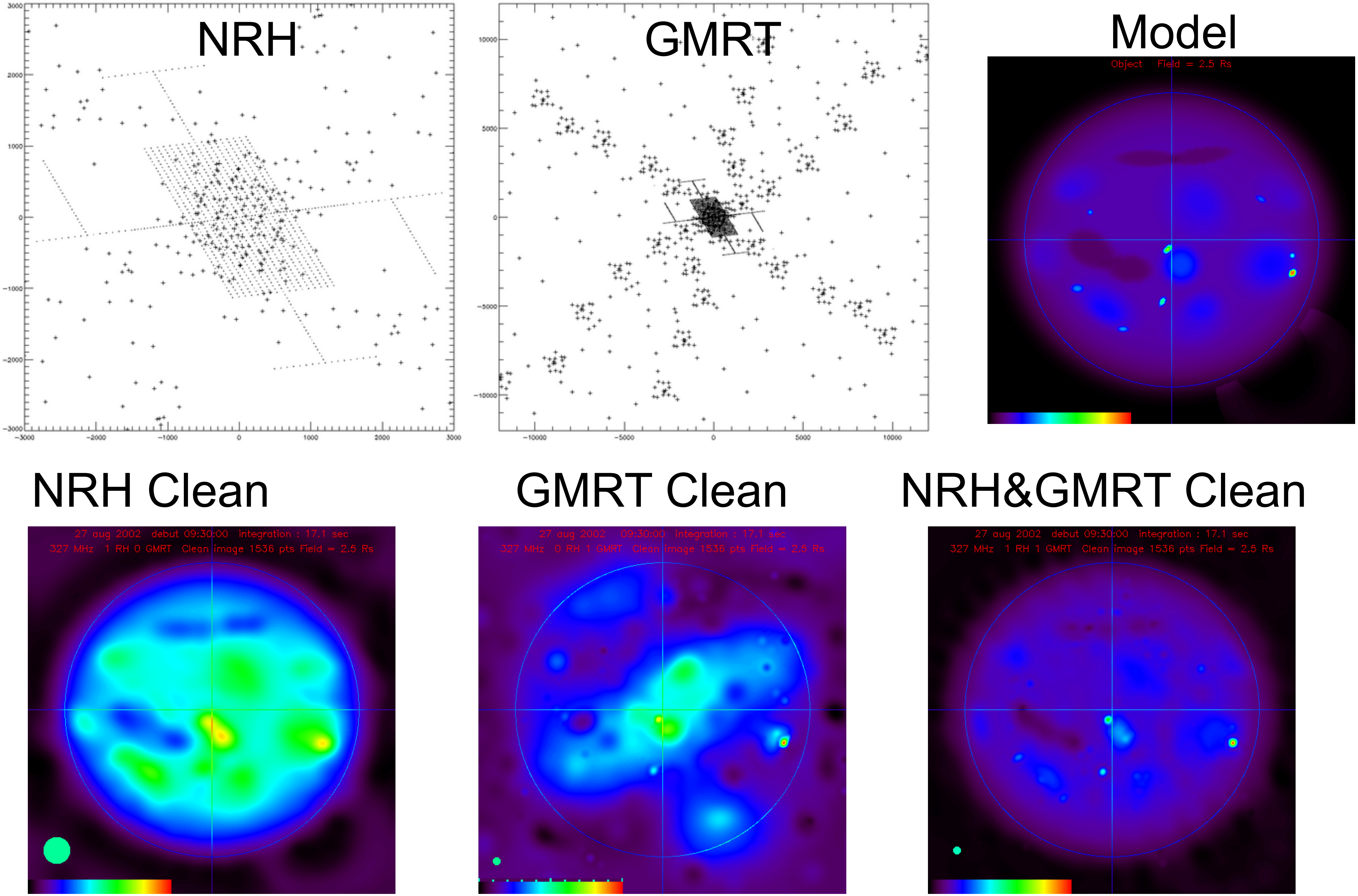

• Other methods: maximum entropy; phase and amplitude closure; compressed sensing ...

• **Spectral measurements** (principle, single dish)

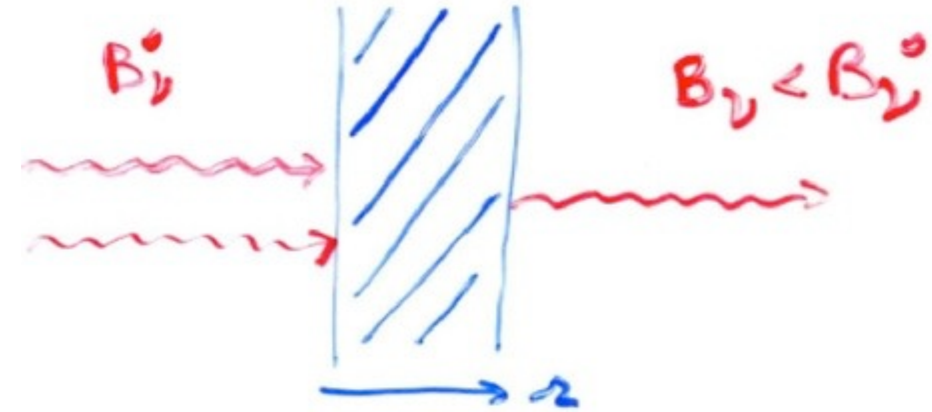

Absorption (photon-matter interaction) :

$dB_\nu = B_\nu - B^o_\nu = - \alpha\, B_\nu\, dr$
$\Rightarrow B_\nu(r) = B^o_\nu\, e^{-\alpha r} = B^o_\nu\, e^{-\tau}$ (τ = optical thickness)

$\rightarrow$ Source of brightness B_S behind an absorbing cloud of optical thickness τ : $B = B_S \times e^{-\tau}$

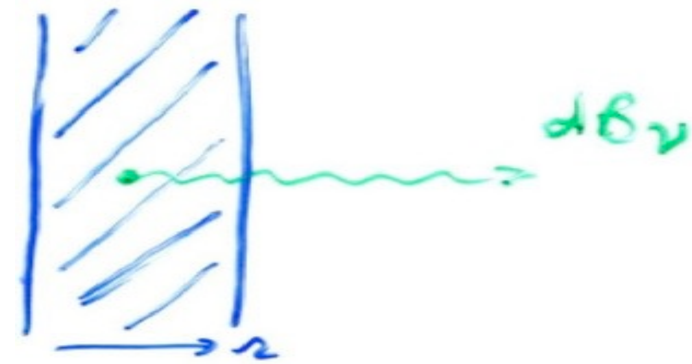

Emission + self-absorption :

$dB_\nu = \beta\, dr\, e^{-\alpha r}$
$\Rightarrow B_\nu = \int_0^r \beta\, e^{-\alpha r}\, dr = \beta/\alpha \times (1 - e^{-\tau})$

$\rightarrow$ Emissive & absorbing cloud with optical thickness τ and temperature T :
$B = 2kT/\lambda^2 \times (1-e^{-\tau}) = B_C \times (1-e^{-\tau}) \rightarrow B_C$ for an opaque medium ($\tau >> 1$)

Real case = combination of the two: $B = B_S \times e^{-\tau} + B_c \times (1 - e^{-\tau})$
In the radio domain (Rayleigh-Jeans) : $T_B = T_S \times e^{-\tau} + T_C \times (1 - e^{-\tau})$

Depending on the cloud's optical thickness : $\tau \approx 0 \Rightarrow T_B = T_S$
$\tau \rightarrow \infty \Rightarrow T_B = T_C \times (1 - e^{-\tau})$
+ intermediate cases

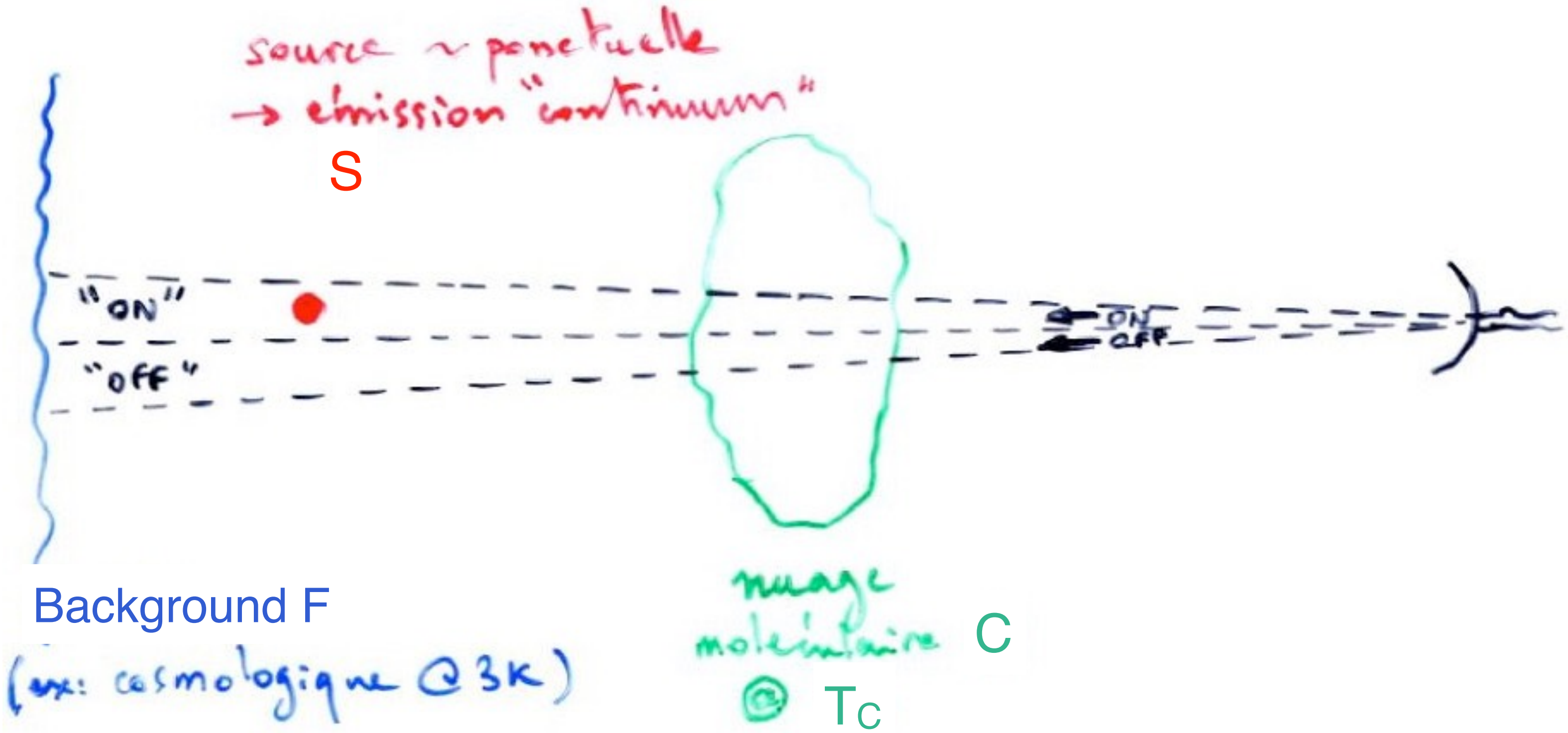

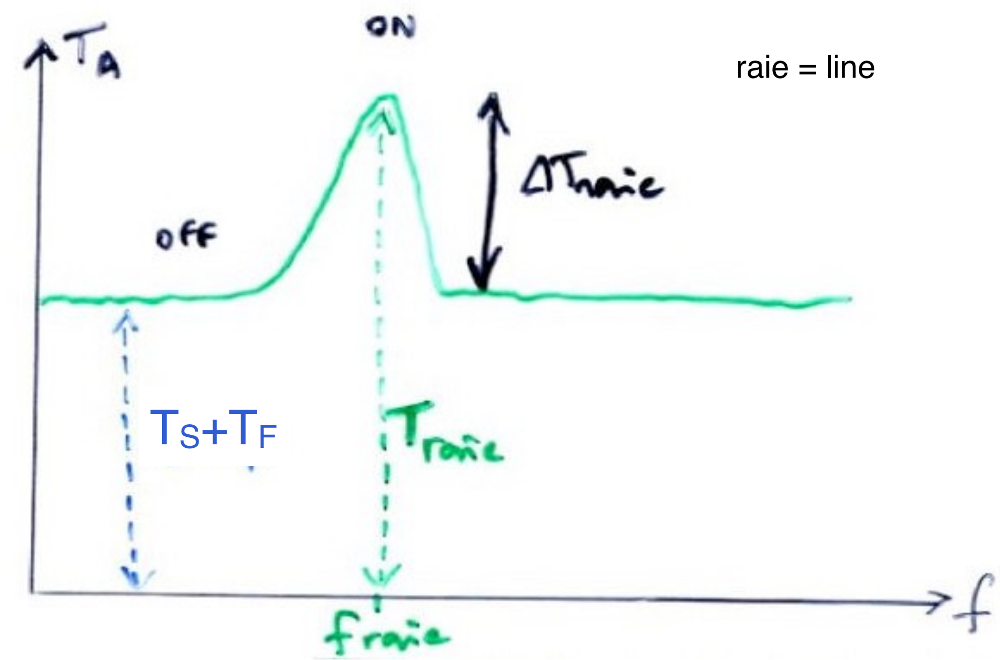

"ON" source : $\Rightarrow$ $T_{line}(f) = (T_S + T_F)\, e^{-\tau} + T_C\,(1 - e^{-\tau})$

"OFF" source (spectrally) : we subtract the background from the adjacent frequencies outside the line $T_{out\text{-}of\text{-}line}(f) = T_S + T_F$

"ON" - "OFF" :

$$\Rightarrow \quad \Delta T_{line}(f) = (T_C - T_S - T_F) \times (1 - e^{-\tau})$$

"OFF" source (spatially) : observation next to the continuum radiosource "S" : $T_S = 0$

similarly we obtain $\Rightarrow \Delta T_{line}(f) = (T_C - T_F) \times (1 - e^{-\tau})$

$\rightarrow$ Combination of "ON" and "OFF" allows us to derive T_C et τ.

NB : the line may appear in emission ($\Delta T_{line}>0$) or in absorption ($\Delta T_{line}<0$) depending on whether T_C is > or < ($T_S + T_F$)

→ From T_C the N_a/N_b ratio of the transition considered is deduced by Boltzmann's Formula :

$N_a/N_b \approx \exp(-\Delta E_{ab}/kT_C)$

with T_C = T excitation of the cloud = T physical if the cloud is at LTE

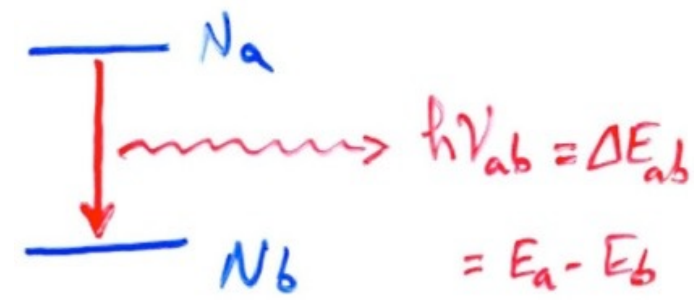

The molecular column density $\int_{\text{line-of-sight}} N.dr$ is deduced from $\int_{\text{profile-of-the-line}} \Delta T_{line}(f).df$

We show that : $N \propto \tau f^2 \Delta f_{line} / [A_{ab} (N_b/(N_a+N_b)) (1-\exp(-h\nu/kT_C))]$

A_{ab} → probability of spontaneous transition a→b

MASER

When a "pump" disturbs ETL and populates high energy levels (collisions / H, IR emission from nearby star or IS dust …)

⇒ $N_a > N_b$ population inversion, then induced de-excitation (cascade)

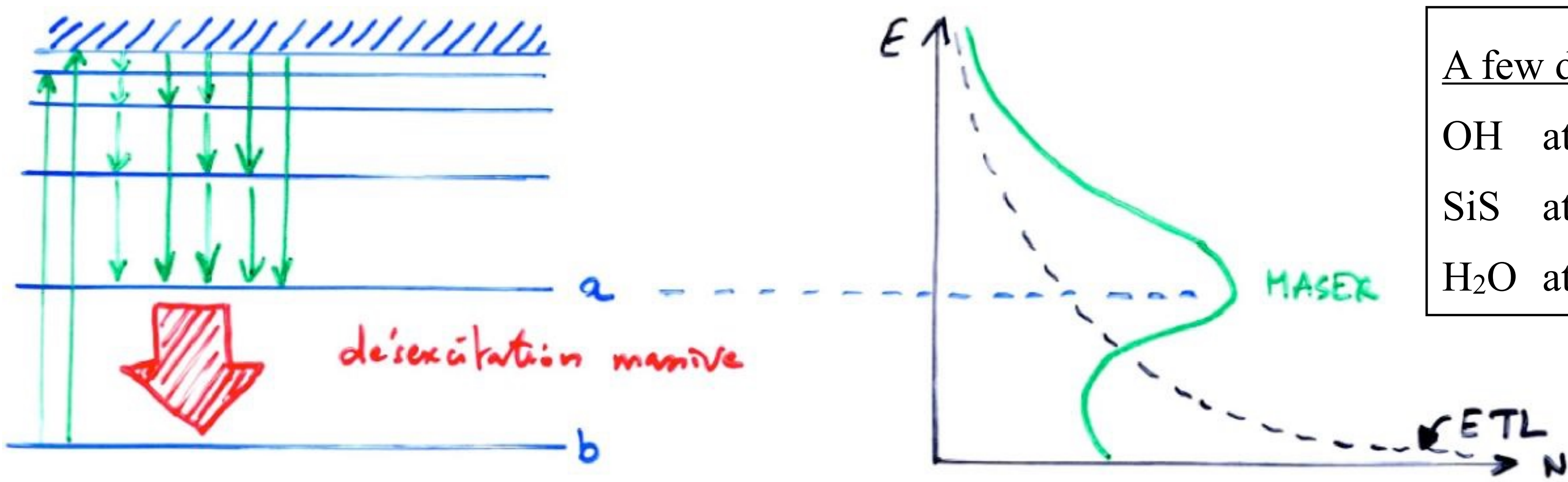

A few detected MASERs:

OH	at	1.665 GHz	CH_3OH	at	25 GHz
SiS	at	18 GHz	SiO	at	43 & 86 GHz
H_2O	at	22 GHz	HCN	at	89 GHz

$N_a/N_b > 1 \Rightarrow T_C < 0$ and $\tau \propto (N_b - N_a) < 0 \Rightarrow \Delta T_{line} > 0 \Rightarrow$ a MASER line is always in emission

Exponential growth ($\propto e^{-\tau}$) of B and T ⇒ T_C can reach $> 10^{15}$ K

Galactic Masers : $L \approx 10^{3-6} L_{Sun}$; Extragalactic Mega-MASERs : $L \sim 10^{6-9} \times$ Galactic ones

→ interacting galaxies? AGN?

- Introduction (history, interest, specific features)
- Waves & Polarisation
- Plasmas & Propagation (cutoff, dispersion, Faraday effect, scintillations)
- Coherent Signal Detection (measurement theory, antenna temperature, calibration, noise)
- Receivers (heterodyne, system temperature, filtering, gain, RFI mitigation)
- Basics of Radio Astronomy Antennas: Single antennas
- Basics of Interferometry and Aperture Synthesis (phased arrays, electronic pointing, imaging, correlation, coherence, VLBI)
- Observation methods
- Large present & future ground-based radio arrays
- Basics of Space radio astronomy

Single dishes and "historical" interferometers

Dénomination et situation	Dimensions	Fréquence de travail maximale	Remarques
I. Antennes uniques			
Amherst (États-Unis)	Diamètre : 14 m	115 GHz	
Arecibo (Porto Rico)	Diamètre : 300 m	5 GHz	Fixe, zénithal
Crawford Hill (États-Unis)	Diamètre : 7 m	115 GHz	
Crimée (Russie)	Diamètre : 22 m	22 GHz	
CSO Hawai (États-Unis)	Diamètre : 10,4 m	690 GHz	
Goldstone (États-Unis) Madrid (Espagne) Tidbinbilla (Australie)	Diamètre : 70 m	9 GHz	*Deep Space Network* de la NASA (poursuite engins spatiaux, mais aussi radioastronomie)
Effelsberg (Allemagne)	Diamètre : 100 m	46 GHz	Plus grande antenne orientable
Green Bank (GBT) (États-Unis)	Diamètre : 100 m	110 GHz	En construction
Green Bank, 140' (États-Unis)	Diamètre : 42 m	22 GHz	
JCMT Hawai (États-Unis)	Diamètre : 15 m	350 GHz	
Jodrell Bank (Royaume-Uni)	Diamètre : 76 m	3 GHz	
Kitt Peak (États-Unis)	Diamètre : 11 m	230 GHz	
Nobeyama (Japon)	Diamètre : 45 m	115 GHz	
Onsala (Suède)	Diamètre : 20 m	115 GHz	
Parkes (Australie)	Diamètre : 64 m	43 GHz	
Pico Veleta (Espagne)	Diamètre : 30 m	350 GHz	
Plateau de Bure (France)	Diamètre : 2,5 m	230 GHz	
Nançay (France)	200 m × 35 m	3,3 GHz	Méridien
SEST (Chili)	Diamètre : 15 m	230 GHz	
Zelenchuk (Russie)	Anneau de 600 m	5 GHz	
II. Interféromètres	(1)		
Australian Telescope (Australie)	6 × 22 m de diamètre	115 GHz	Longueur 6 km
BIMA, Hat Creek (États-Unis)	9 × 6 m de diamètre	230 GHz	Longueur 300 m
Cambridge (Royaume-Uni)	3 × 25 m de diamètre 8 × 14 m de diamètre	1,4 GHz 10 GHz	Longueur 1,6 km Longueur 5 km
Cambridge (Royaume-Uni)	Dipôles sur 40000 m^2	38 MHz	5 km
GMRT, Poona (Inde)	34 × 45 m de diamètre	1,4 GHz	En construction
Lanlherne (Australie)	40000 m^2	3 - 32 MHz	
Merlin (Royaume-Uni)	7 antennes diverses	22 GHz	Sur 240 km
Nançay (France)	43 antennes diverses	450 MHz	En forme de T, solaire
Nançay (France)	144 antennes hélicoïdales, 10000 m^2	110 MHz	
Nobeyama (Japon)	5 × 10 m de diamètre	115 GHz	Longueur 560 m
Ootacamund (Inde)	17000 m^2	300 MHz	Cylindre parabolique
Owens Valley (États-Unis)	6 × 10 m de diamètre	230 GHz	
Plateau de Bure (France)	4 × 15 m de diamètre	230 GHz	Longueur 300 m
Université de Floride (États-Unis)	30000 m^2	26 MHz	
UTR2, Kharkov (Ukraine)	100000 m^2	35 MHz	
VLA, Socorro (États-Unis)	27 × 25 m de diamètre	22 GHz	En forme de Y, branches de 19 km
VLBA (États-Unis)	10 × 25 m de diamètre	22 GHz	Réseau VLBI
Westerbork (Pays-Bas)	14 × 25 m de diamètre	5 GHz	Longueur 3 km

(1) Nombre d'antennes × valeur du diamètre.
BIMA Berkeley Illinois Maryland Array.
CSO Caltech Submillimeter Observatory.
GMRT Giant Meter wave Radio Telescope.
JCMT James Clerk Maxwell Telescope.
UTR2 Ukrainian T-shaped Radiotelescope, Mark 2.
VLA Very Large Array.
VLBA Very Long Baseline Array.

"Historical" low-frequency arrays

Instrument & Localisation	Description	Author & *Year*	Frequency range (MHz)	Effective area (m^2)	Lobe	Polarisation
NDA - Nançay Decameter Array, France	144 antennas log-helicoïdal	Boischot *1977*	10 - 100	~2 × 4000	6° × 10° (tracking)	4 Stokes
UTR-2 array, Kharkov, Ukraine	2040 dipoles in 2 branch (EW & NS)	Braude *1977*	7 - 35	~60000 *(A ~143000)*	30' × 10° (tracking)	1 linear polarisation EW
DKR & BSA Pushchino, Russie	EW cylinder & dipoles	Shitov *1974*	30 - 120 & 109 - 113	~40000 & ~3000	11' × 4.5° & 22' × 48' (16 beams)	1 linear polarisation EW
UFRO Floride	16 log-helicoïdal & 640 dipoles	Carr *1972*	18 - 40 & 26.3 ± 0.2	1200 & 20000	~20° & ~5°	2 circ. polar. & 2 ⊥ lin. polar.
SURA Nizhny Novgorod, Russia	200 MW emitter + receiving dipoles	Tokarev *1980*	4.5 - 9.3	3 × 30000	~10°	?





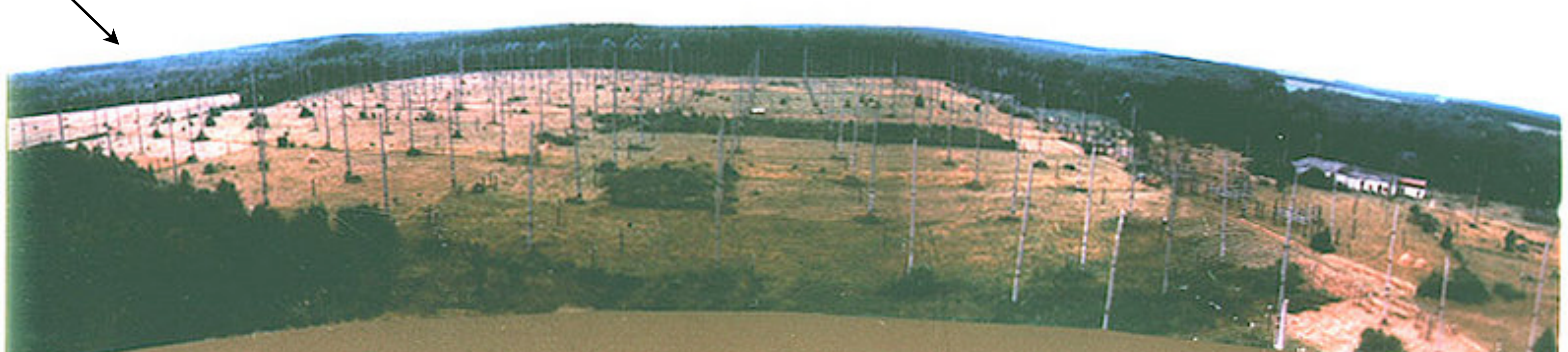


"Classical" moderns interferometers

Westerbork
(ASTRON, The Netherlands)
14 parabolas of 6m
Baseline max: 2.7 km
λ~10cm – 1m
A ~400 m^2

GMRT
(Pune, India)
30 parabolas of 45 m
Baseline max: 25 km
λ~1m, f_{min} = 153 MHz
A ~50000 m^2

VLA
(NRAO, New Mexico)
27 parabolas of 25 m
Baseline max: 36 km
λ~1cm – 1m
f_{min} = 74 MHz
A ~14000 m^2

IRAM
(Pl. Bure, France)
6 parabolas of 15m
Baseline max: ~1 km
λ~1mm
A ~1000 m^2

SMA
(USA – Taïwan)
Hawaïi
8 parabolas of 6 m
Baseline max: 0.5 km
λ~0.5mm
A ~220 m^2

Large instruments in operation / construction / project

- LOFAR, LWA, MWA (≥2010)
- ALMA (≥2013)
- MeerKAT (≥2018)
- SKA (≥2027-8)
- LOFAR-on-the-Moon (?)

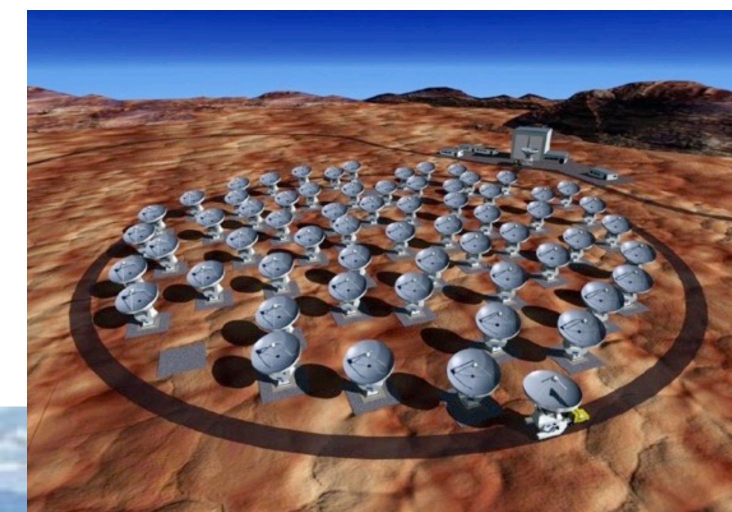

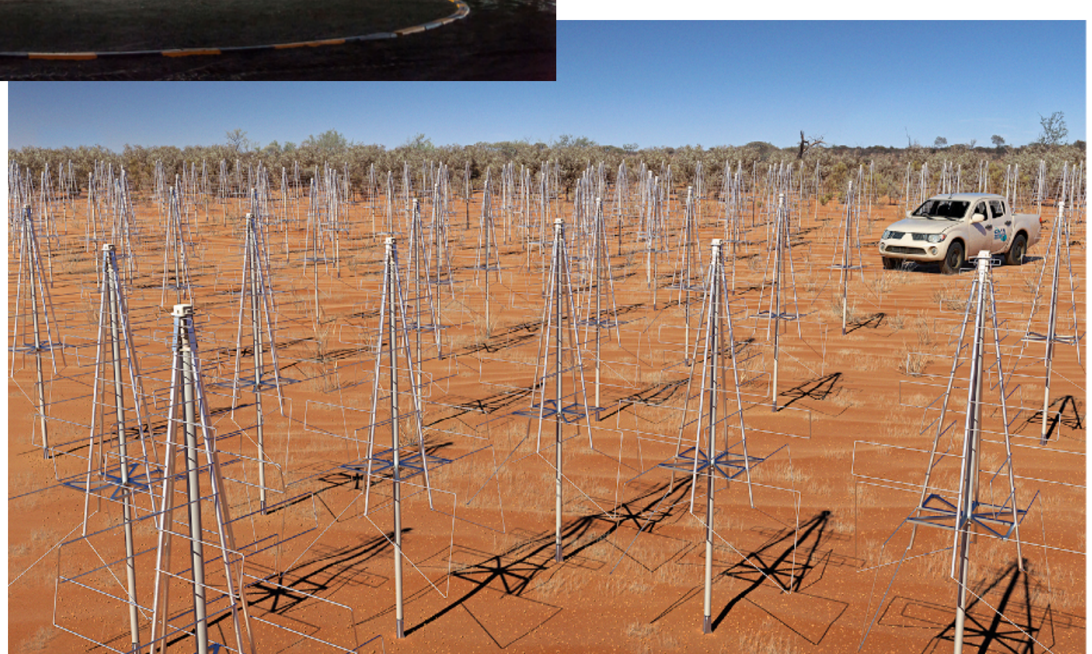

LOFAR (Low Frequency Array)

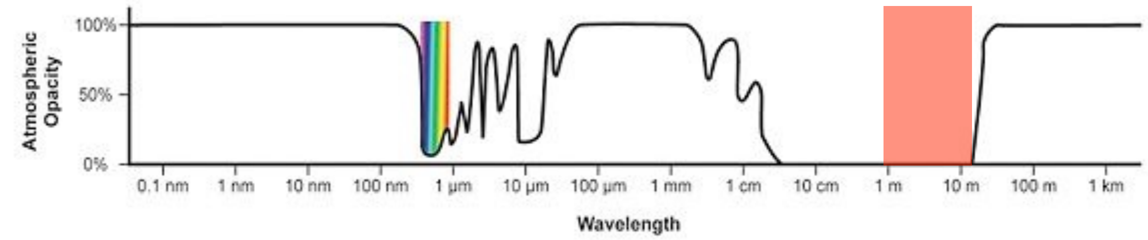

- Phase array interferometer in the Netherlands + Europe
- Diameter ~100 km, European extensions > 2000 km, 24 core stations + 14 remote stations
+ ~15 international stations
- Frequency range = (10)30-80 & 110-250 MHz (λ=1.2-10m)
- A_{eff} ~ 200000 m^2 ($\propto \lambda^2$)
- Resolution ~ 1-10", large fields (sevaral °)
- Imaging mode, Phase array (up to 24 beams in //), Transient Buffer (waveform snapshots)
- Sensitivity < 0.1 mJy, resolutions → 1 msec × 1 kHz
- Full polarization, RFI mitigation
- First "general-purpose" LF imaging spectrometer
- ~ VLBI via Internet in near-real time
- First SKA pathfinder

LOFAR (Low Frequency Array)

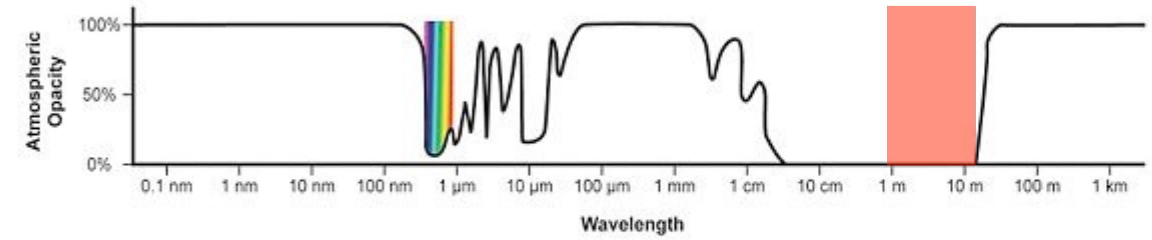

LOFAR station

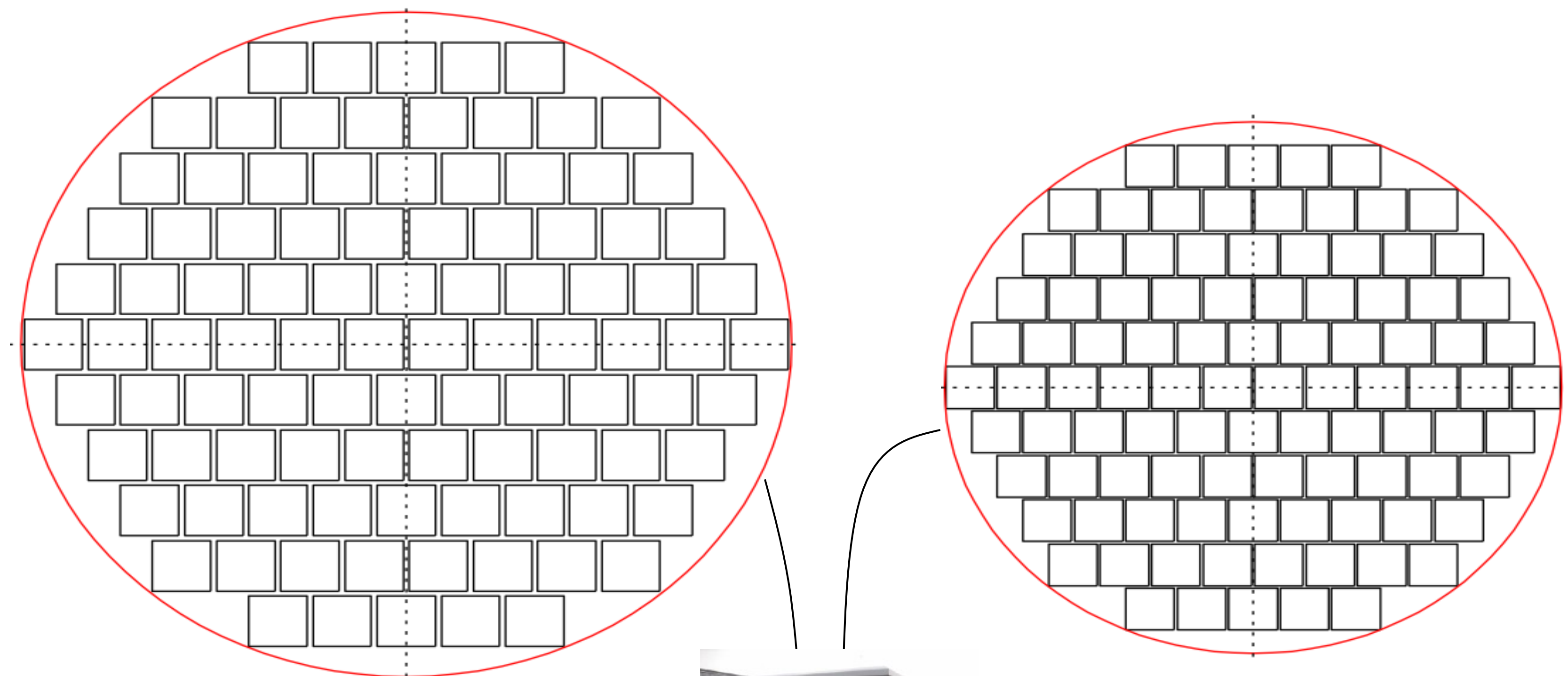

Low-frequency band
(30-80 MHz)

High-frequency band
(110-240 MHz)

60 m

50 m

3 Gbit/sec link

Correlator

Supercomputer B/G ≤2013

CPU/GPU Cluster ≥2014

LOFAR (Low Frequency Array)

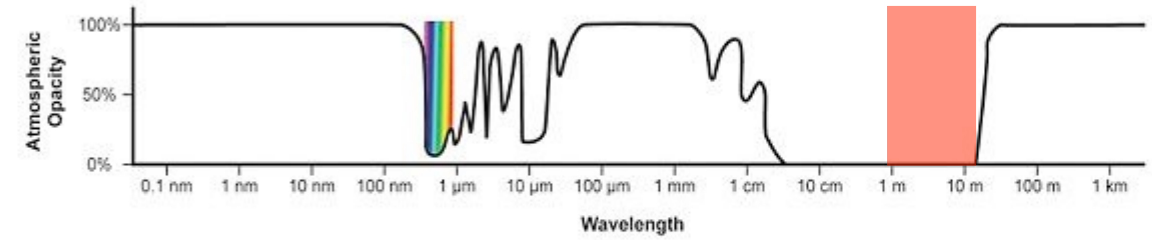

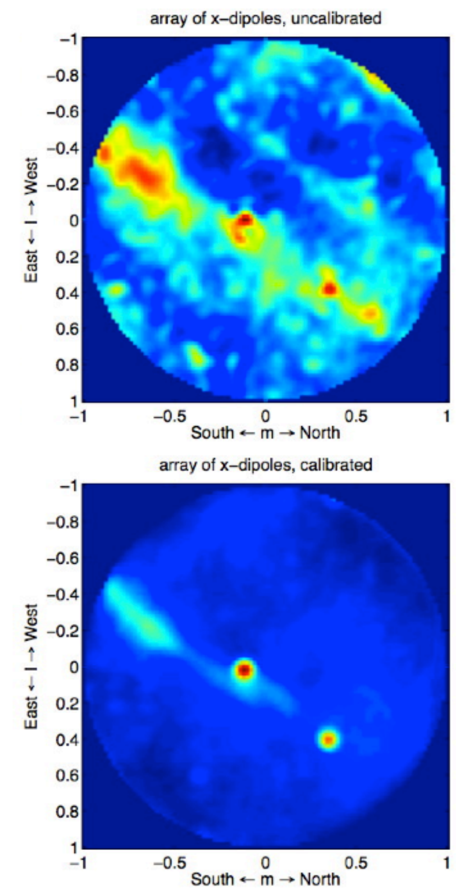

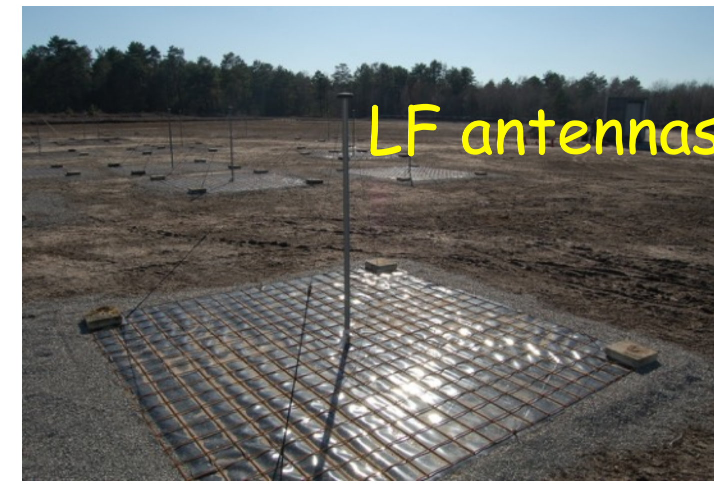

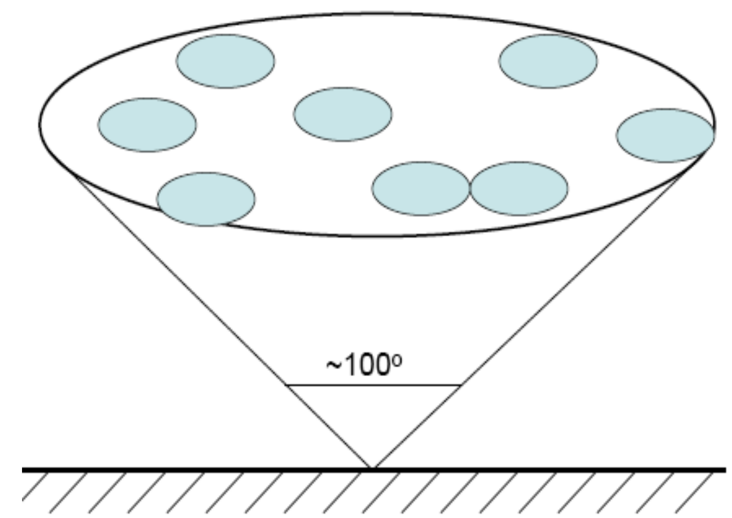

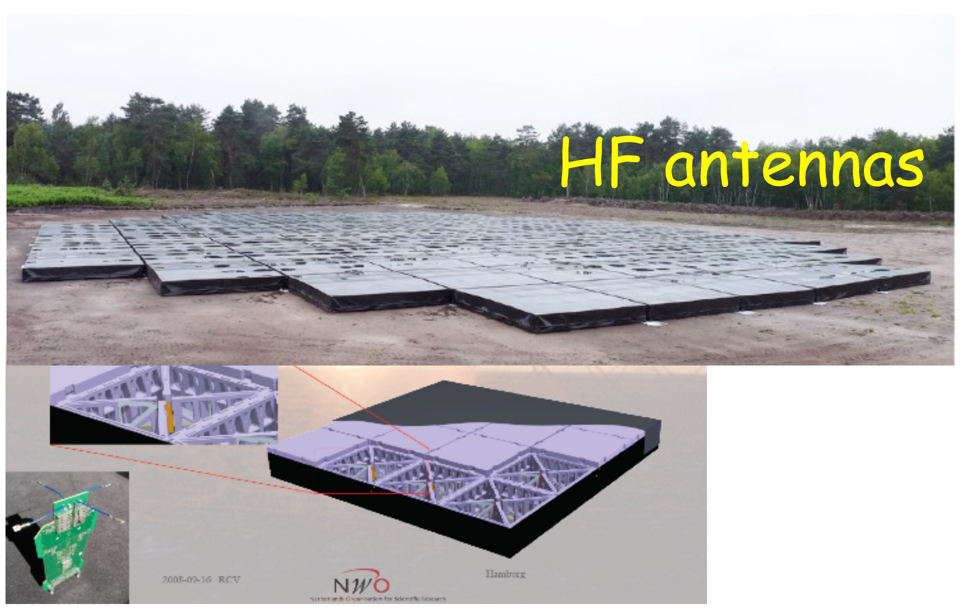

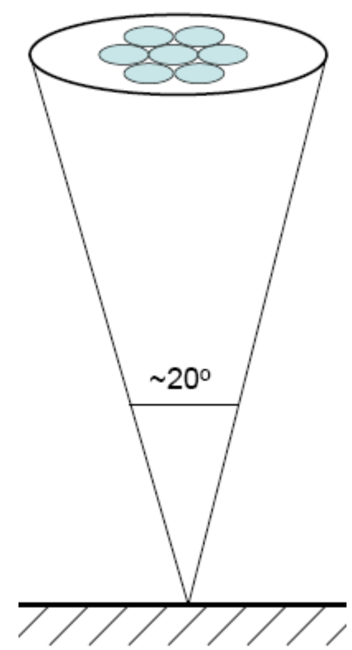

LOFAR (Low Frequency Array)

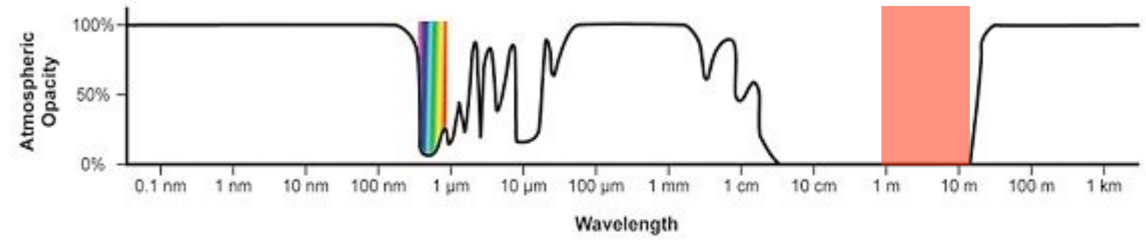

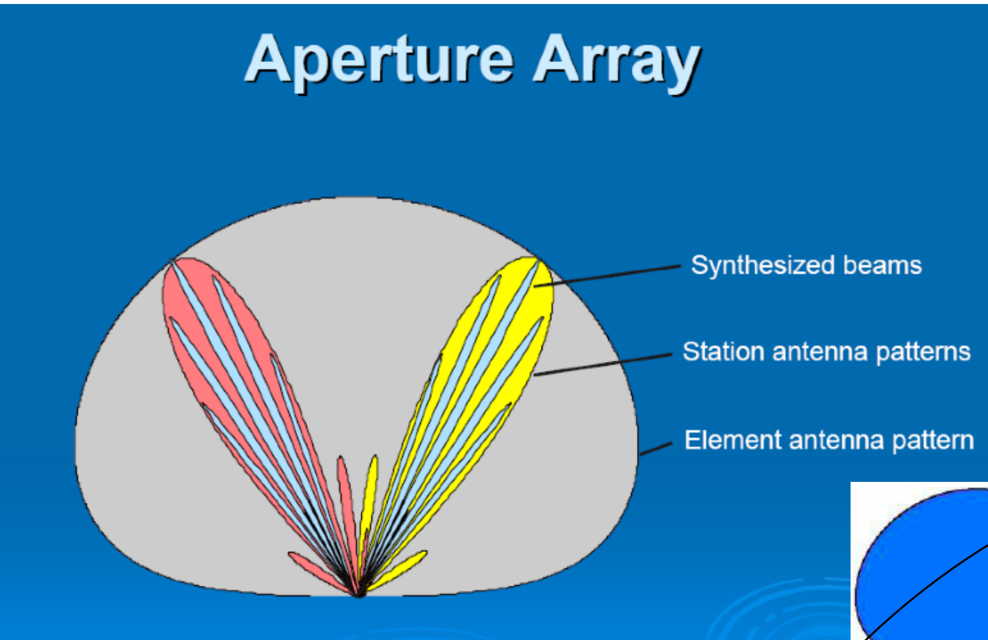

Antenna / station / array lobe

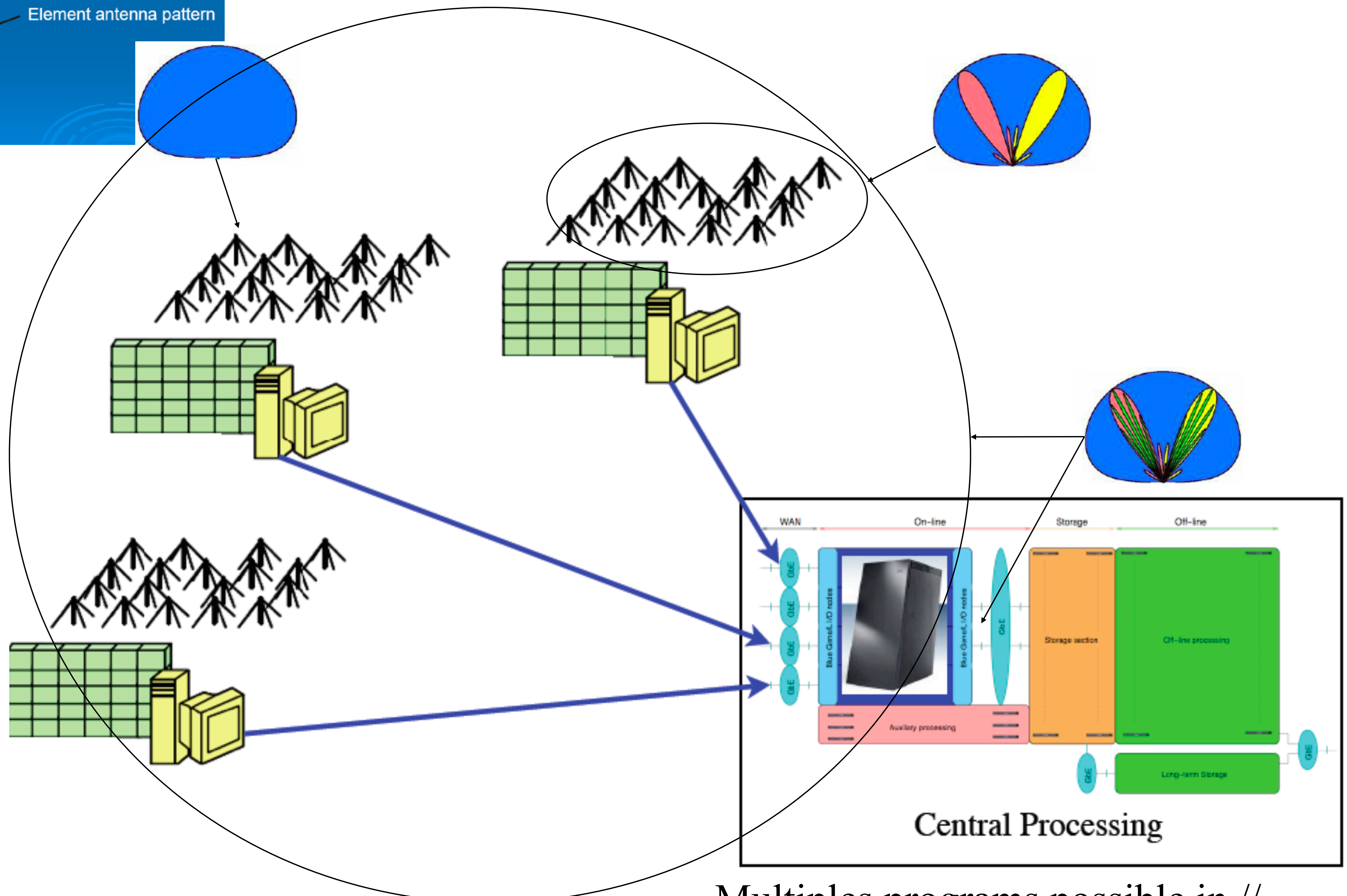

Multiples programs possible in //

LOFAR (Low Frequency Array)

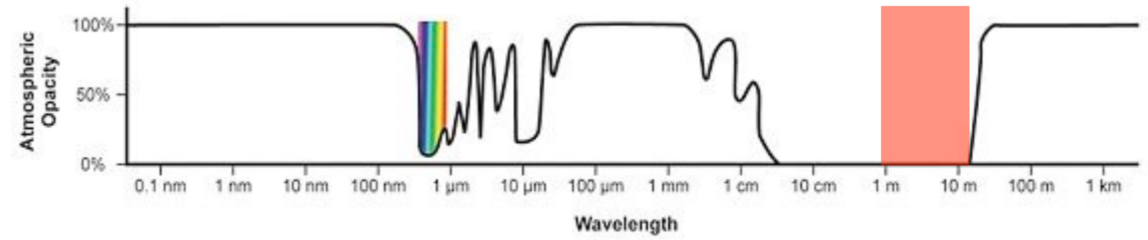

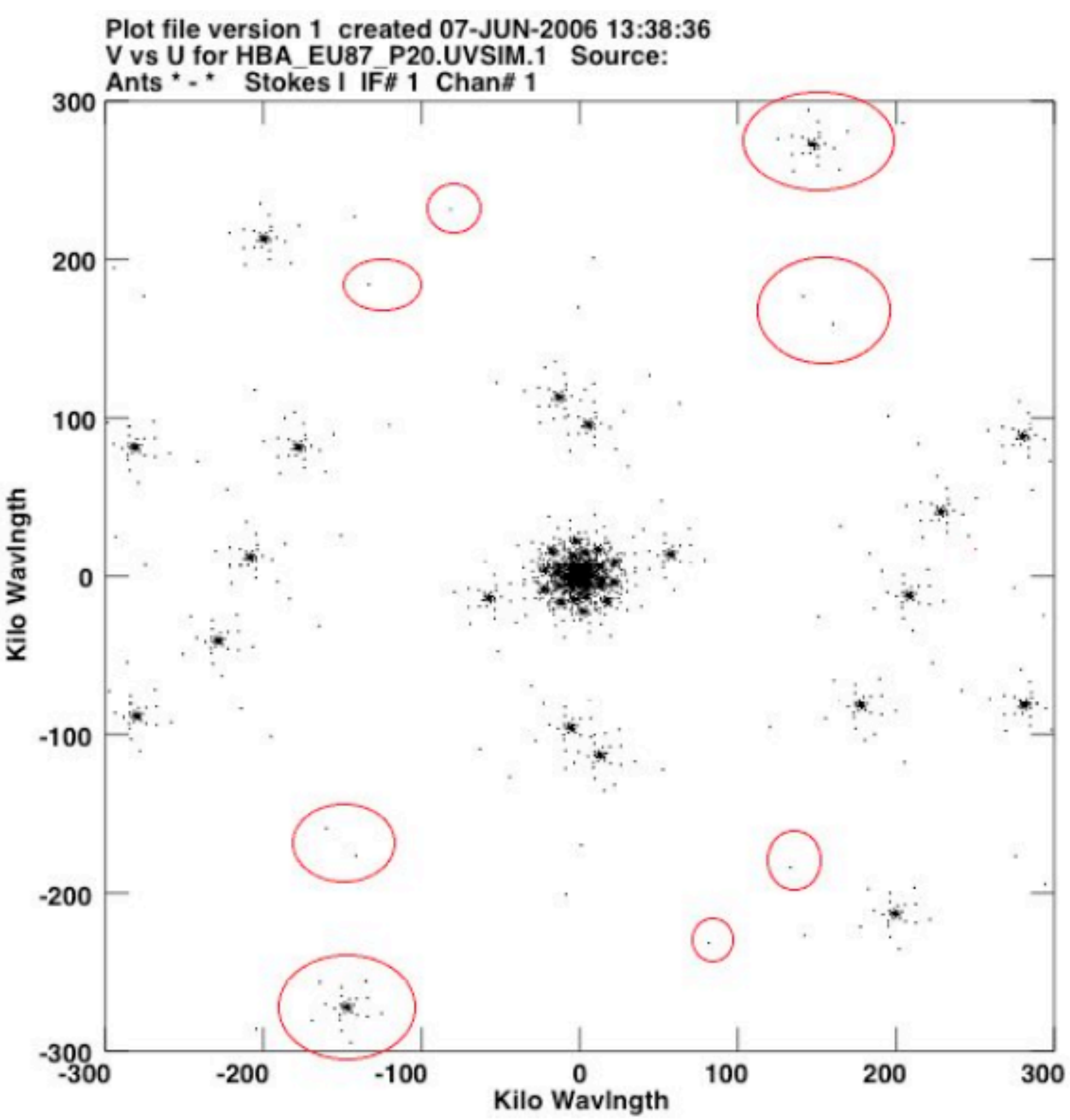

Figure 4 : simulation de couverture du plan u-v de LOFAR incluant les stations prévues en Allemagne et au Royaume-Uni. En rouge l'apport de la station de Nançay. Par intégration sur plusieurs heures, et grâce à la rotation terrestre la synthèse améliore encore la couverture du plan. Couverture instantanée pour H.A.=0 (limitée à une élévation de 45°) pour une déclinaison de 20° à 150 MHz.

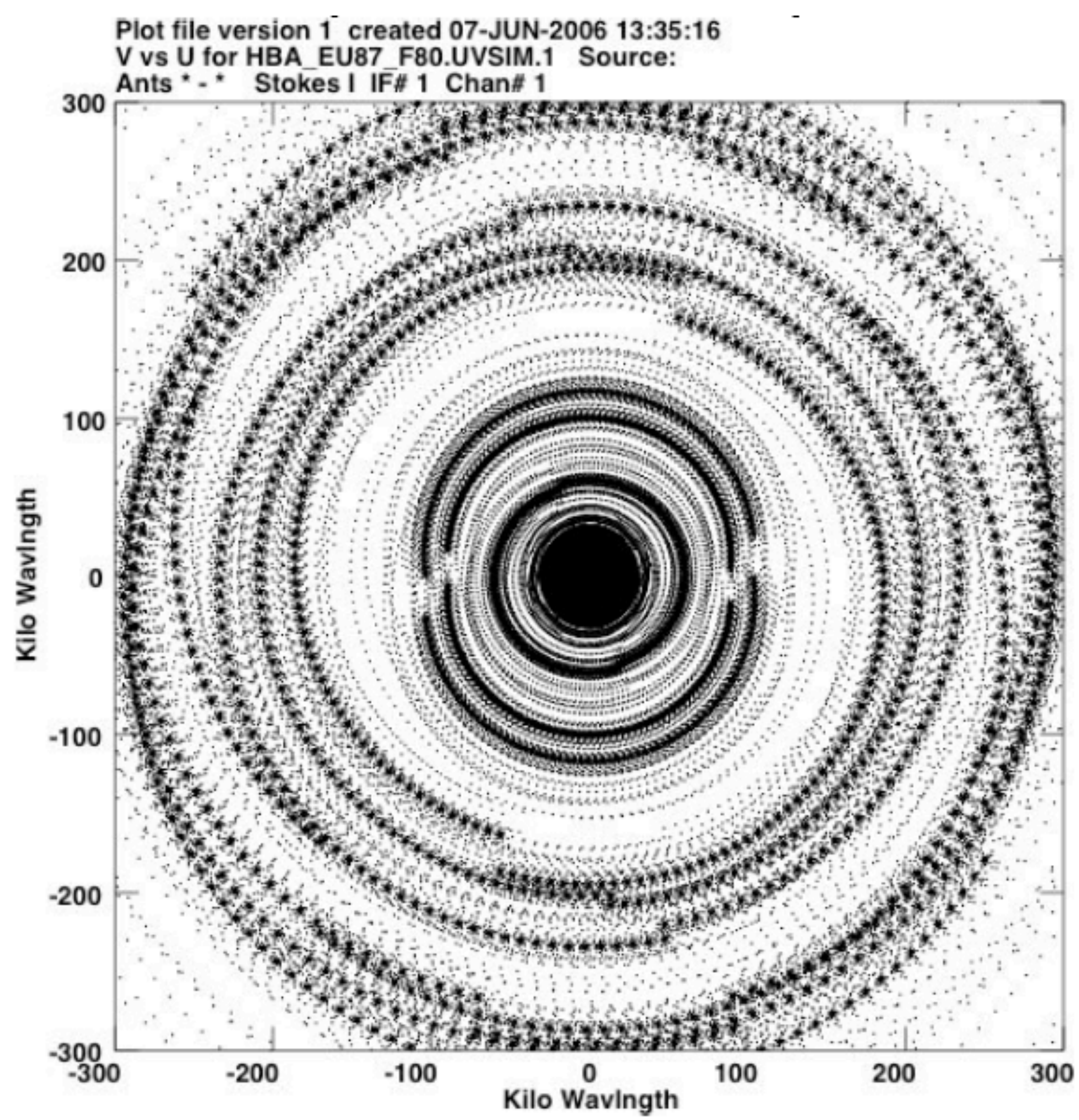

Figure 5 : Couverture du plan u-v pour une déclinaison de 80°, utilisant la rotation de la Terre pour une intégration pendant 8 heures.

(u,v) coverage

LOFAR (Low Frequency Array)

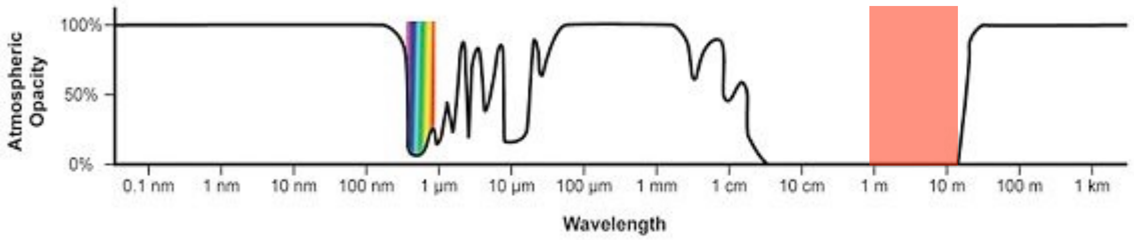

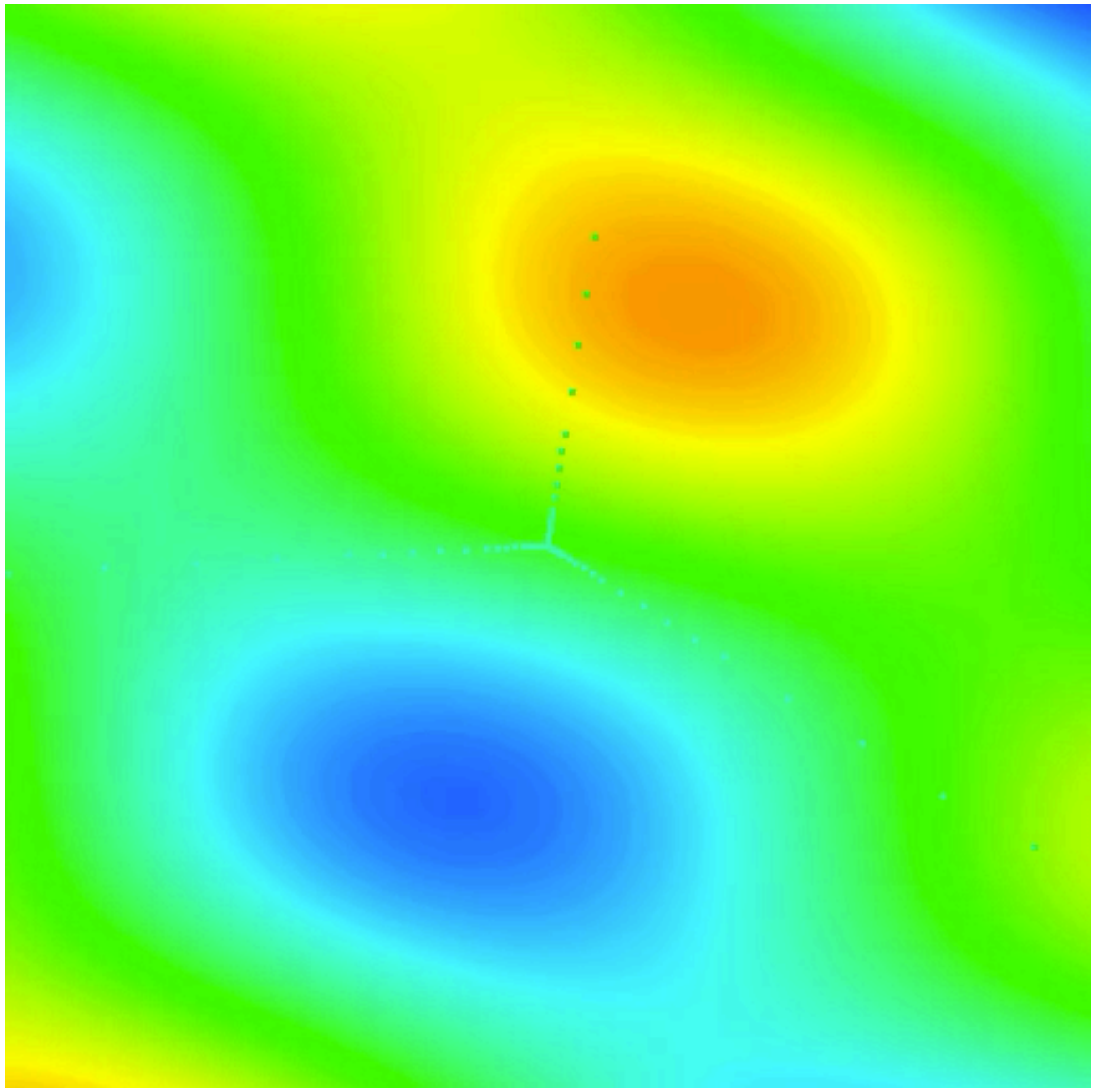

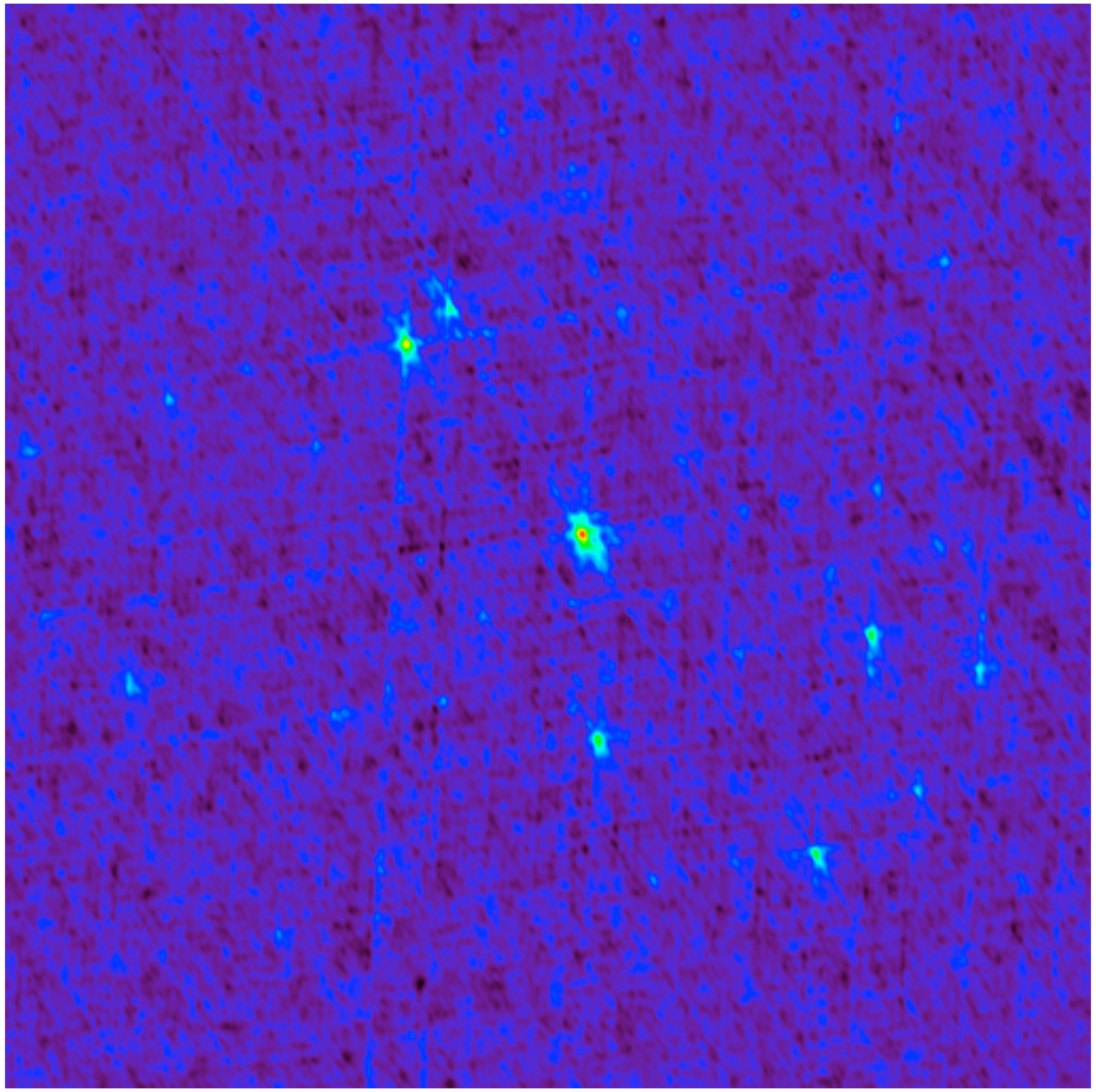

Ionosphere modelling

Calibration problem → solved by using multiple calibrators in each beam

LOFAR (Low Frequency Array)

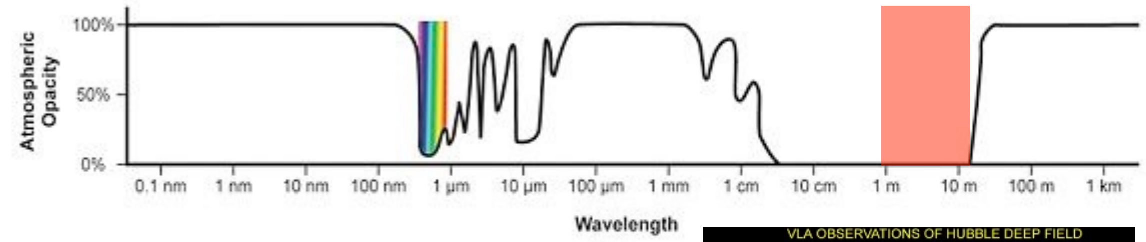

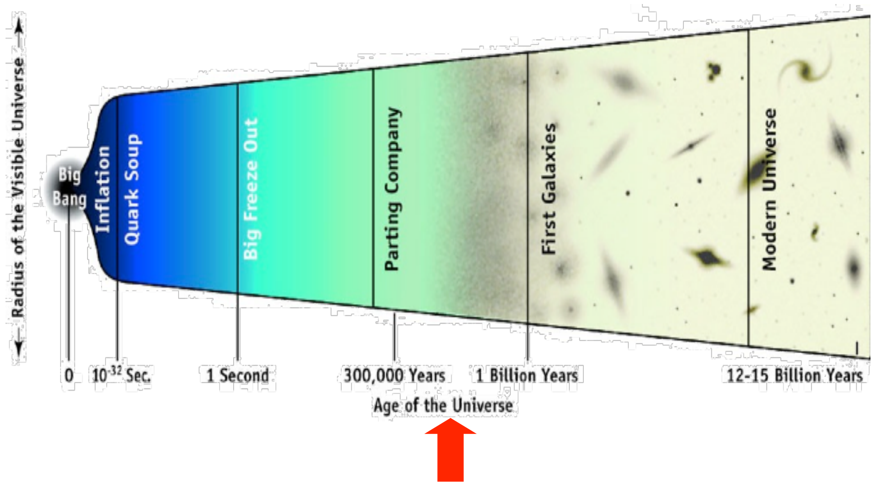

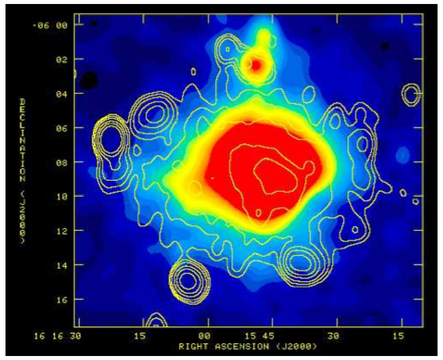

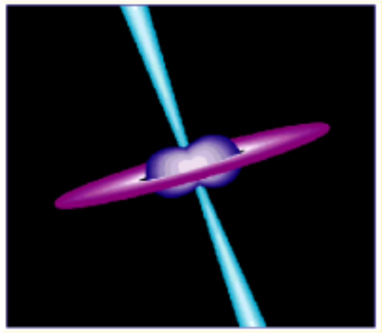

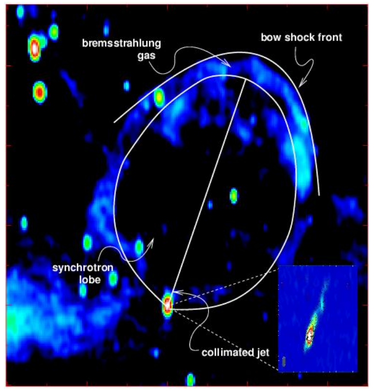

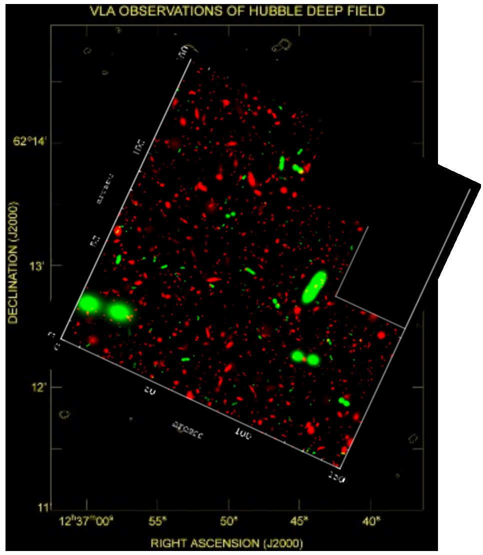

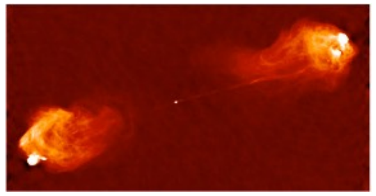

Key Scientific Projects (KSP)

- Cosmology / Reionization, 1st stars (Groningen)
- Deep surveys, stellar formation, AGN, clusters... (Leiden)
- Transients = sporadic sources (Amsterdam...Meudon)
- High-energy particles, cosmic rays, neutrinos impacting the Moon (Nijmegen)
- Galactic magnetism (Bonn)
- Solar & space physics (Potsdam, Ireland)

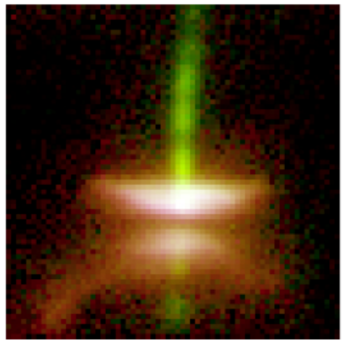

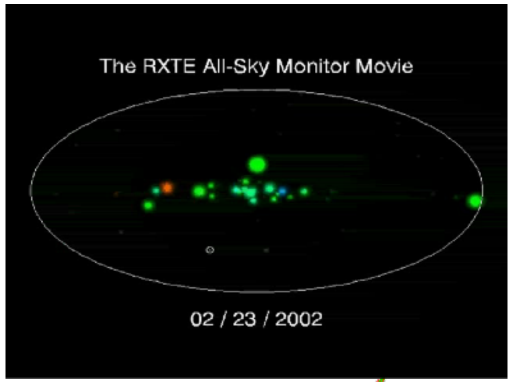

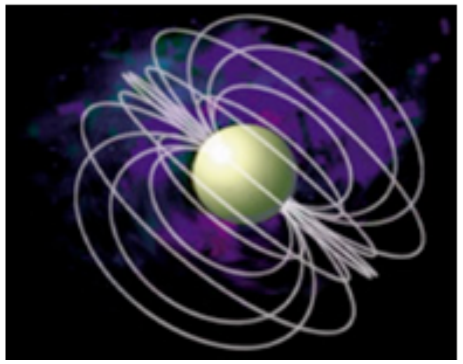

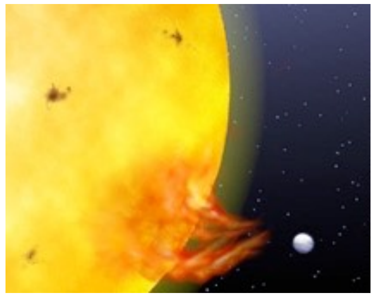

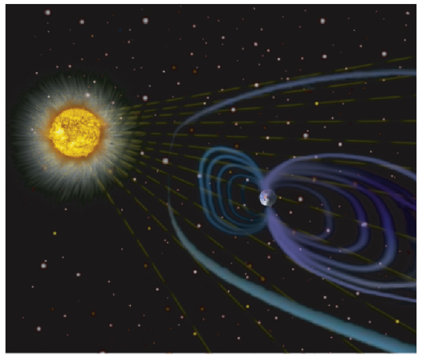

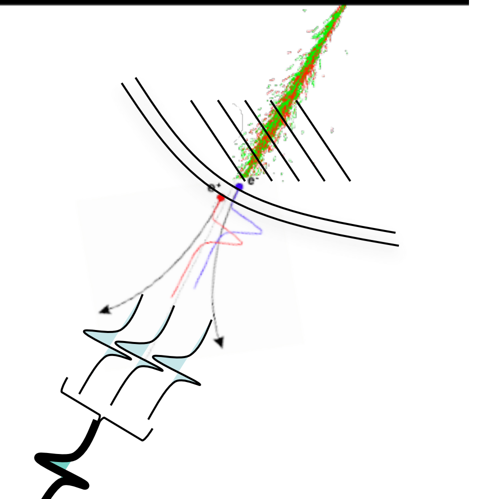

LOFAR (Low Frequency Array)

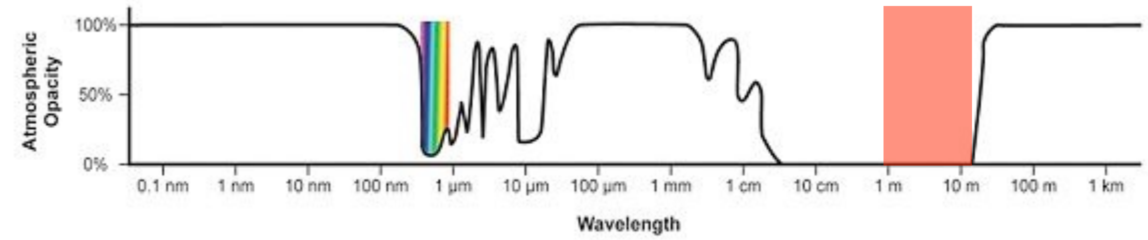

Imaging the Crab nebula (Taurus A)

VLA 5 GHz

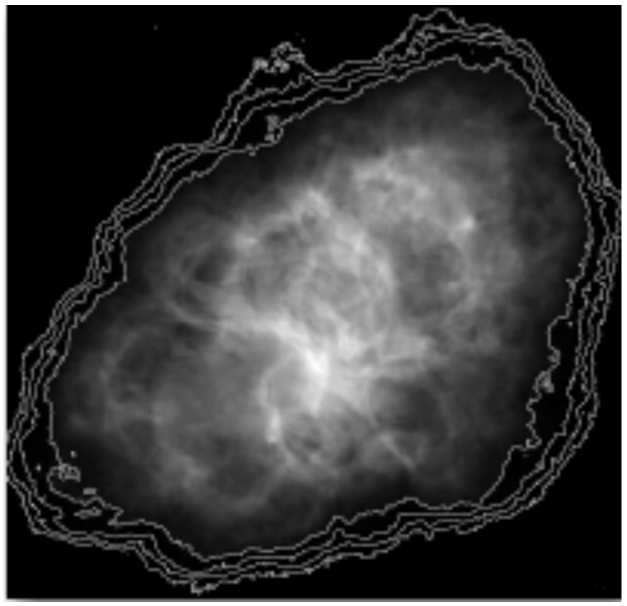

Bietenholz et al., 2004

LOFAR 250 MHz

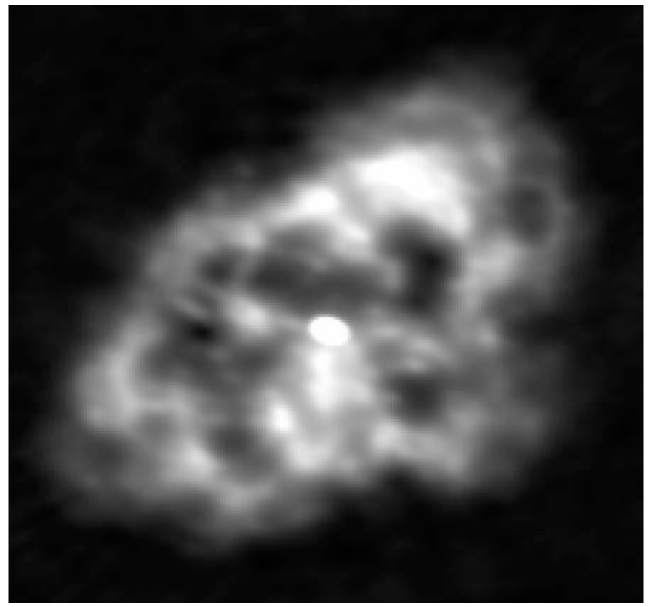

Wucknitz et al., 2011

Discovery of a giant radio galaxy

UGC 09555 triplet

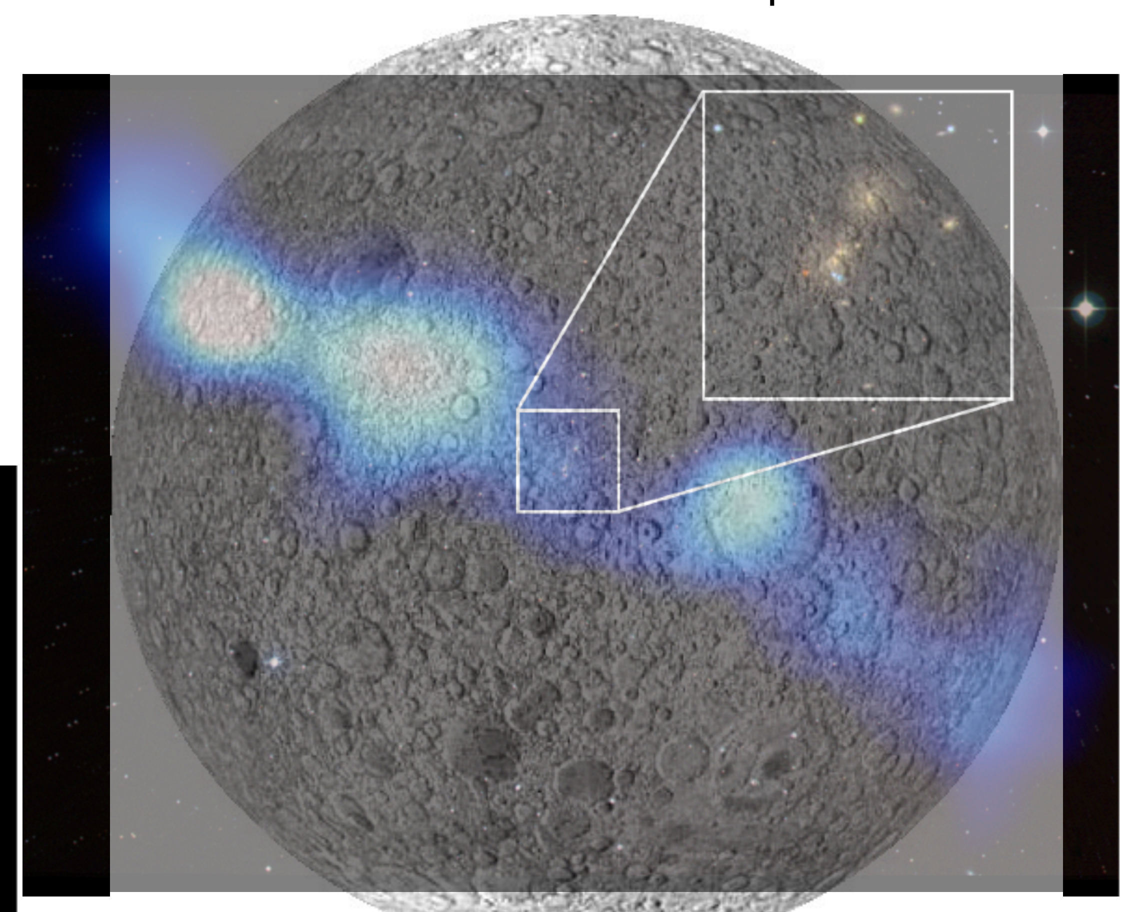

Heald et al., 2013

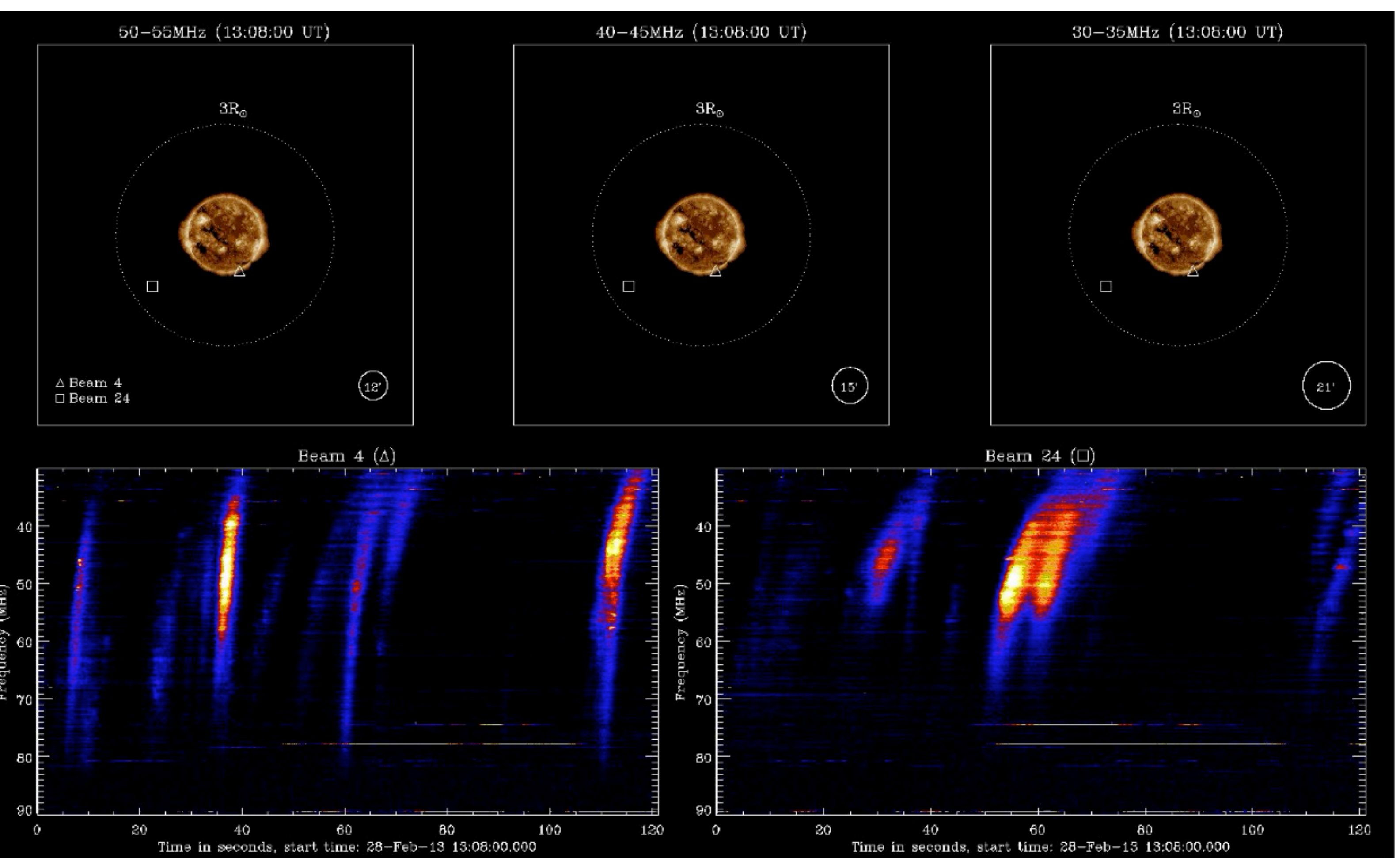

Imaging and simultaneous fast dynamic spectra of the Sun

Morosan et al., 2014

LOFAR (Low Frequency Array)

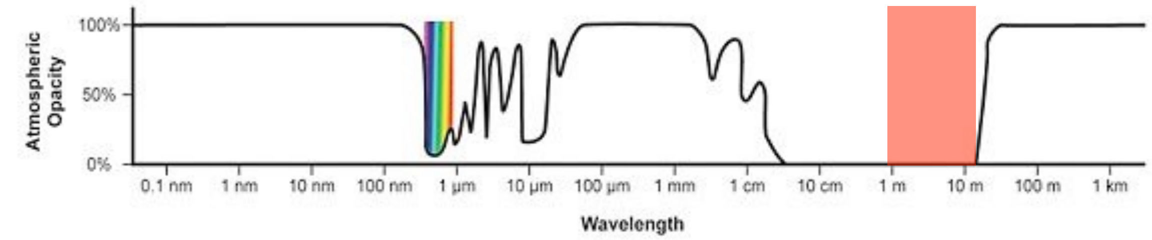

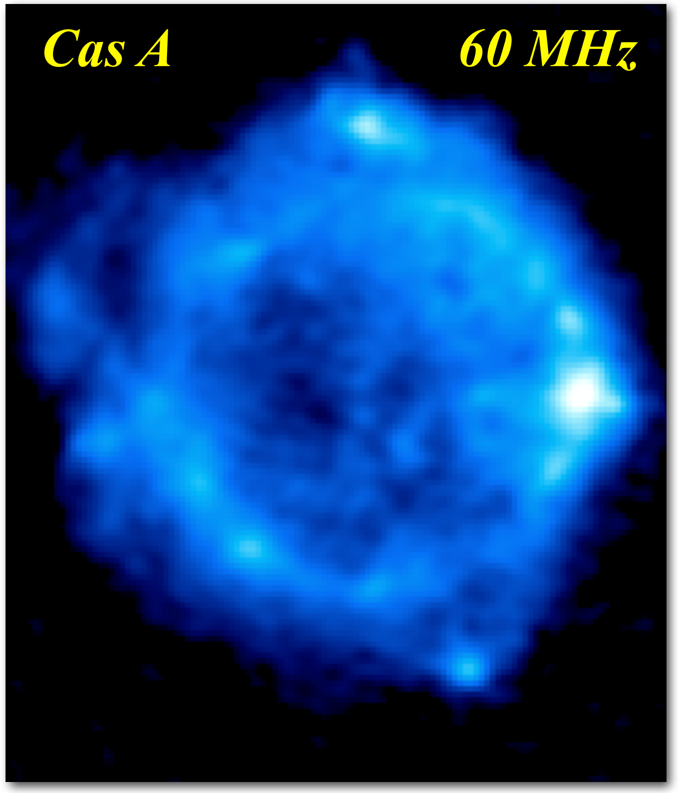

(van Weeren et al. 2014)

RRLs probe the Cold Neutral Medium (CNM)

LOFAR spectrum towards Cas A

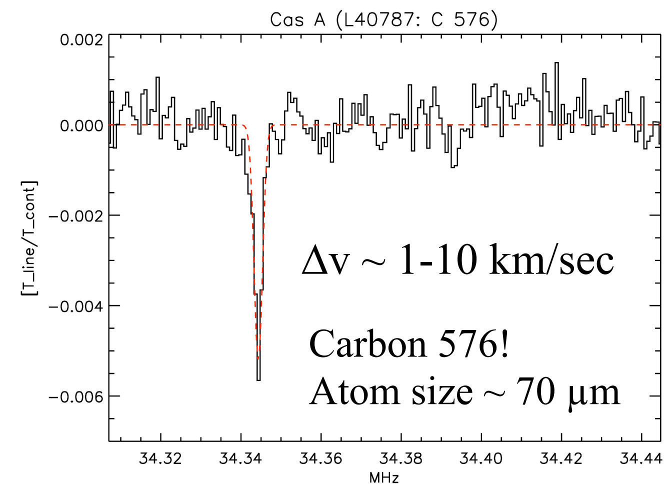

(Asgekar, Oonk, et al. 2013)

C-RRLs actually seen throughout Galaxy!

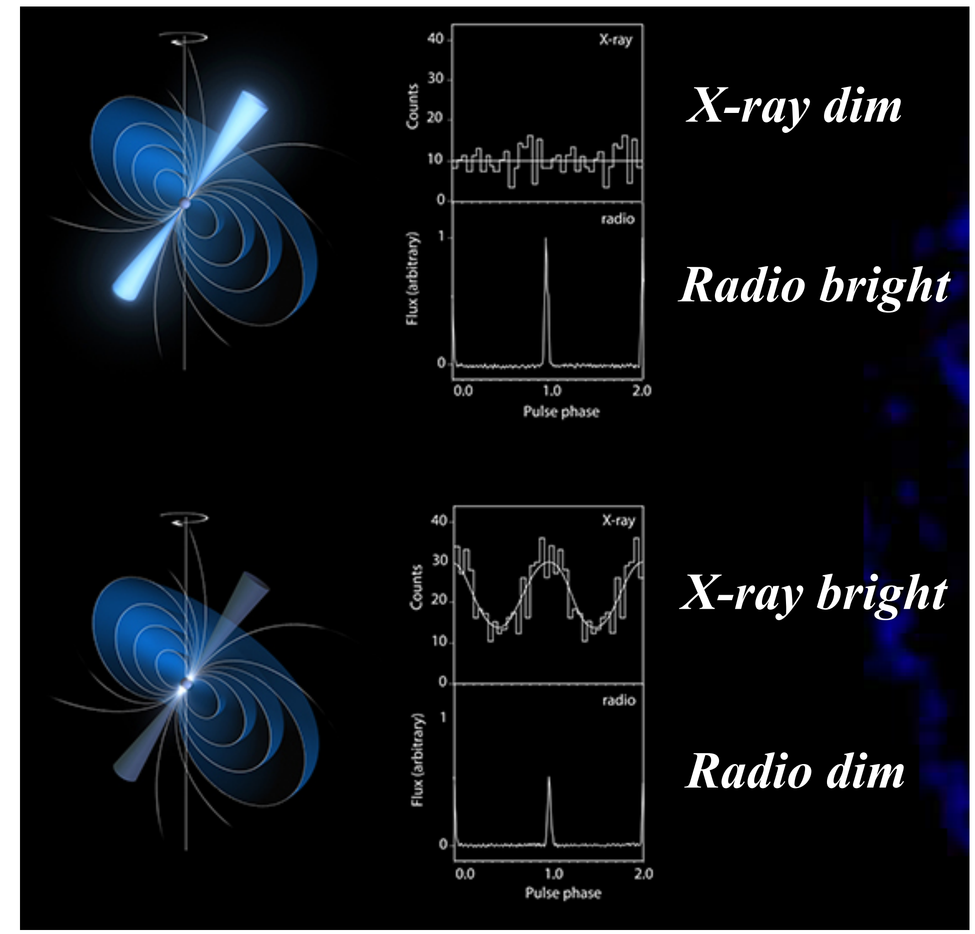

Pulsar

Radio emission from Jovian radiation belts

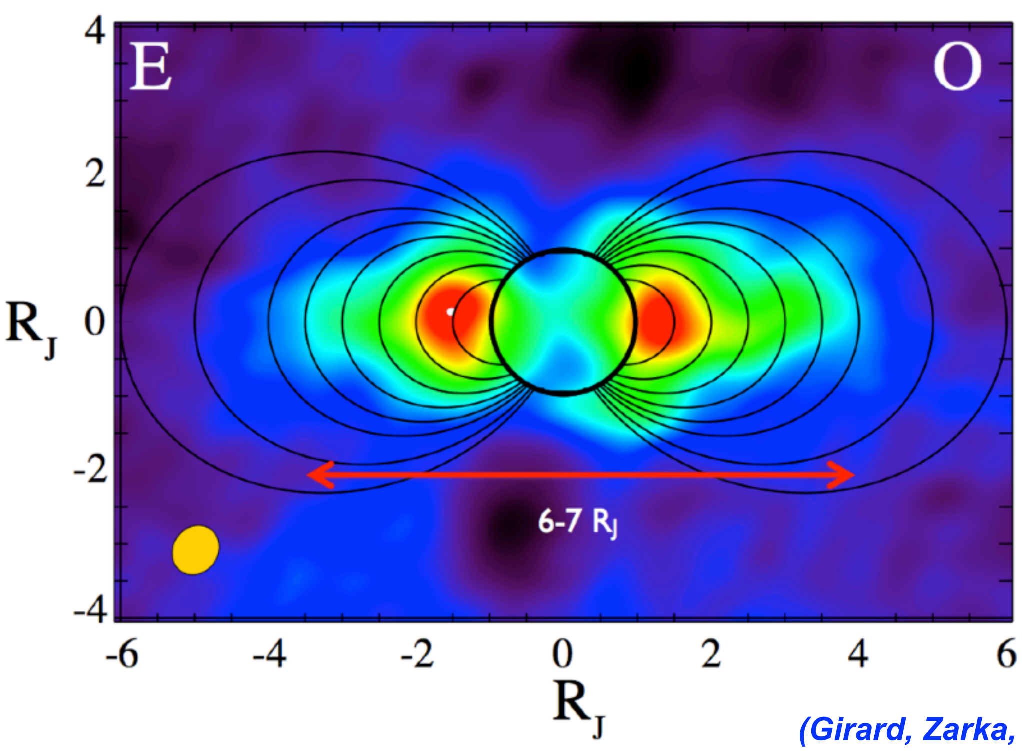

Rotation & frequency averaged image:

Δf = 127-172 MHz,
Δt = 7h
uv= 0-15 kλ
Beam = 17.8”x15.5”
Pixel = 1"
Jupiter disk = 49”

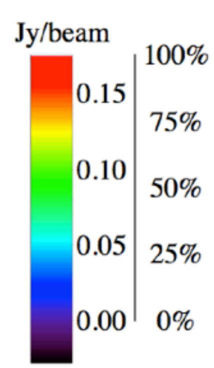

(Girard, Zarka, et al. 2016)

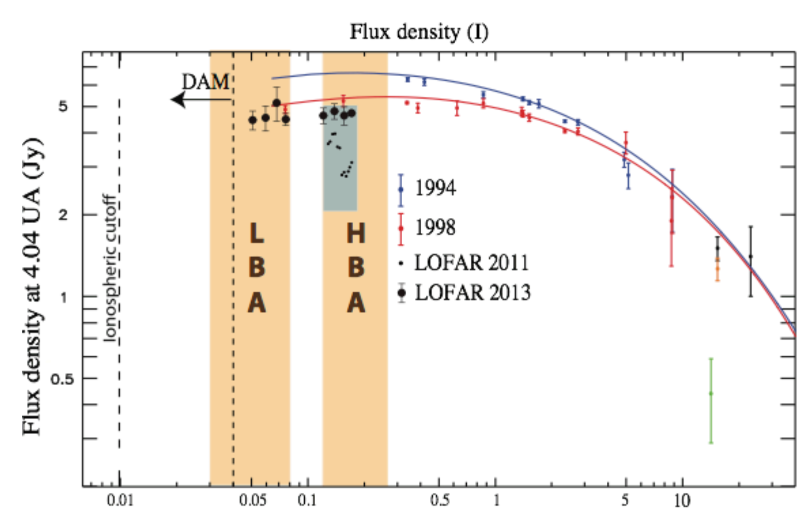

LOFAR (Low Frequency Array)

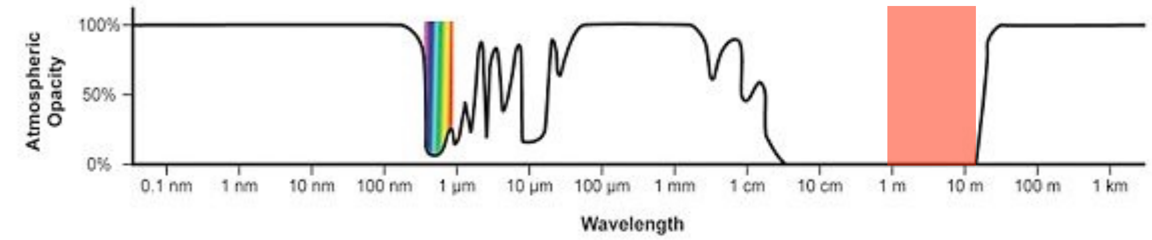

Epoch of reionisation signal ?

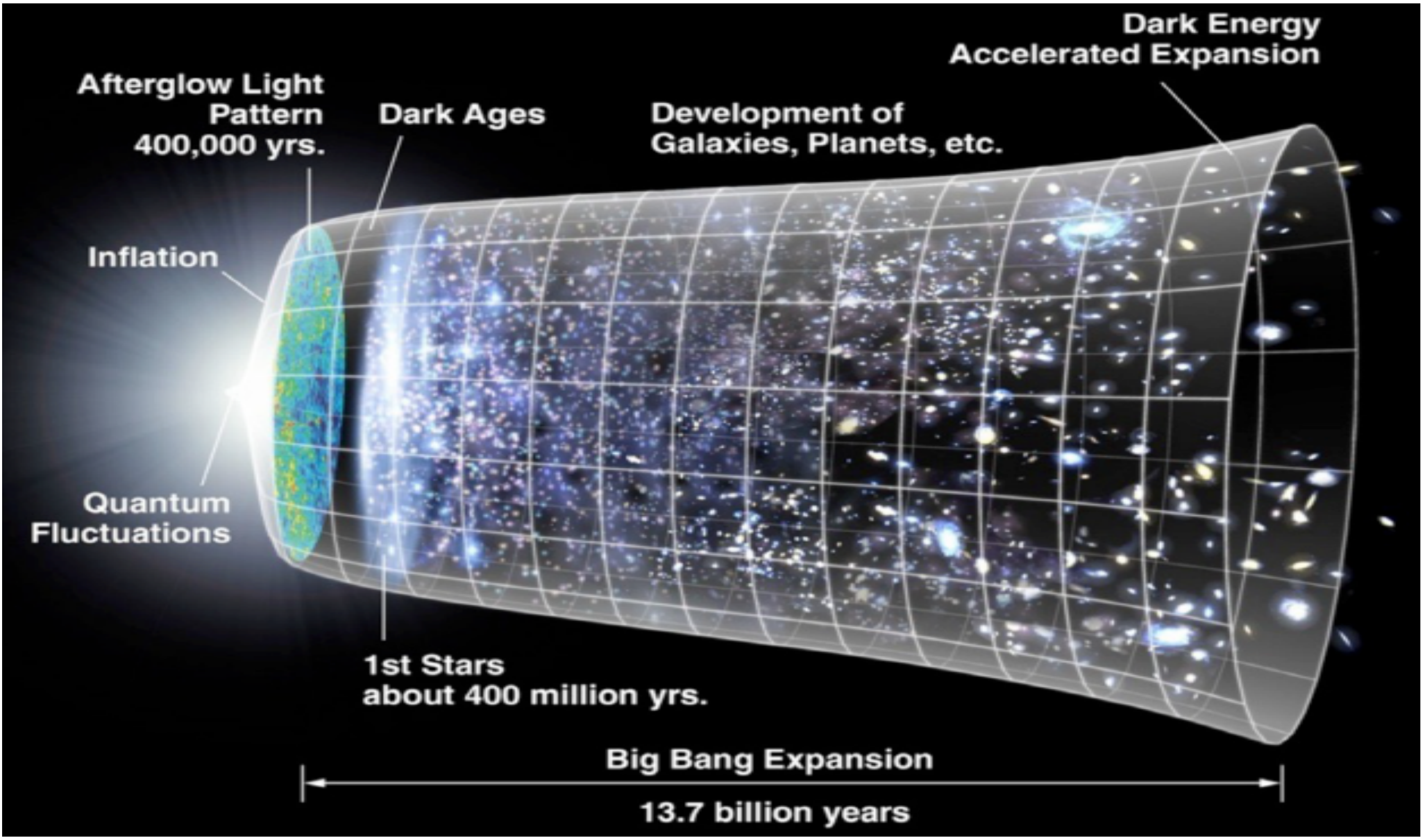

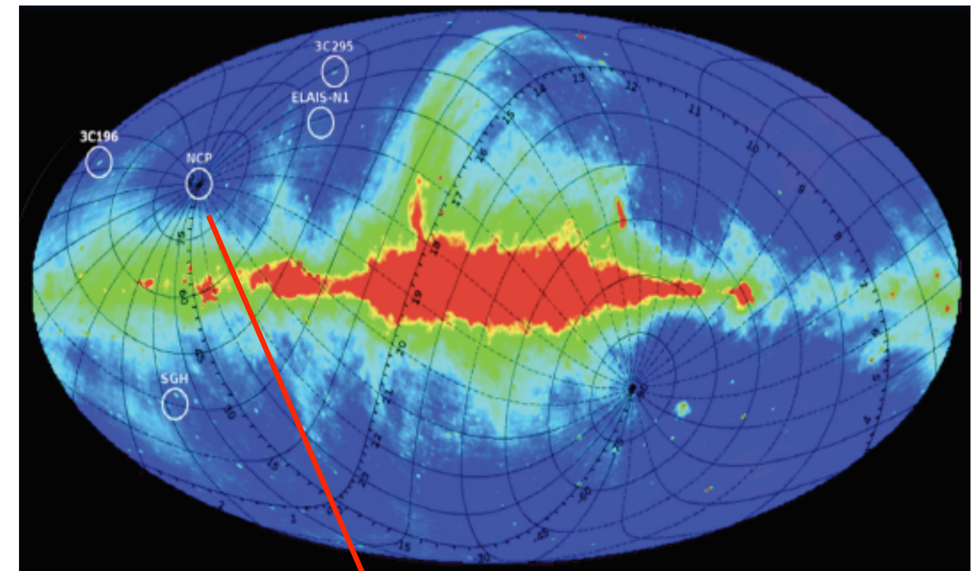

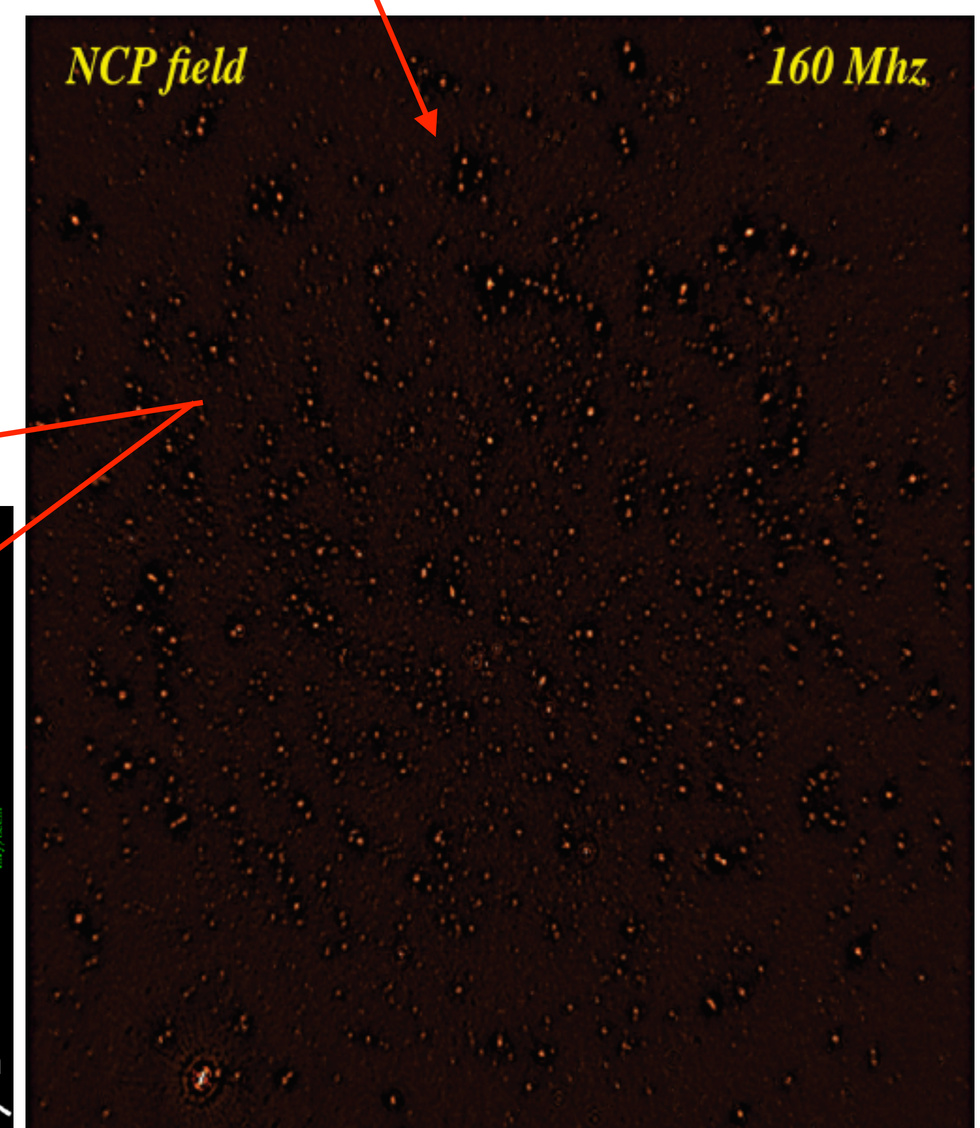

2000 h on 2 FoV → σ = 25 µJy, DR = 10^6 at 30’-60’

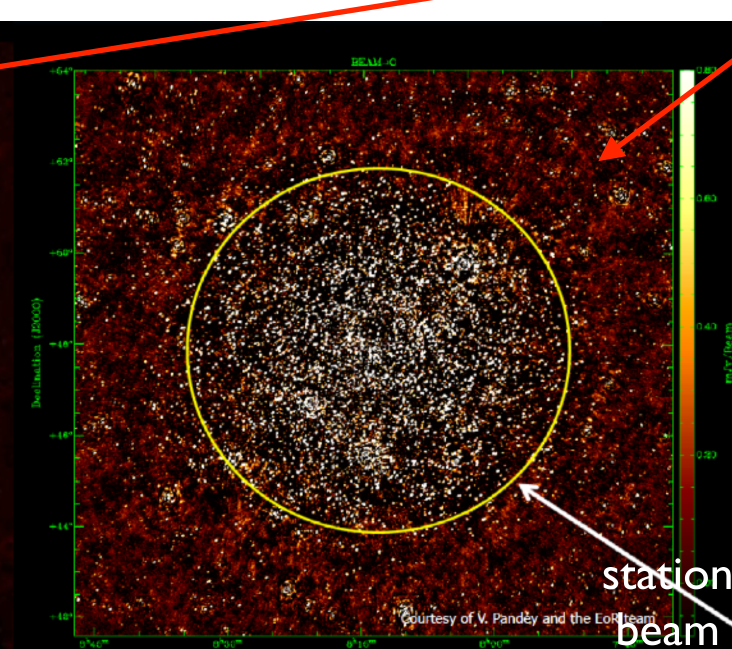

LOFAR (Low Frequency Array)

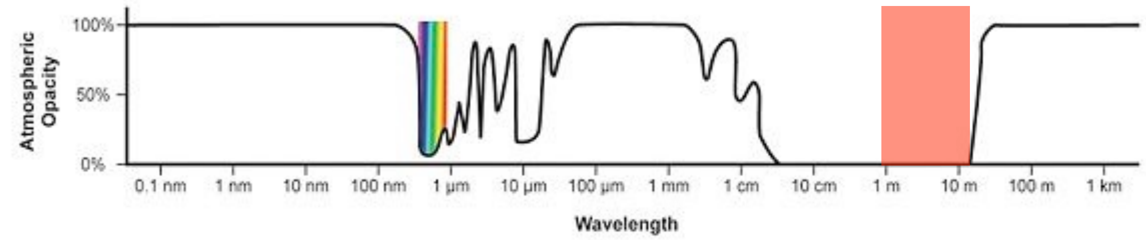

kMS/DDf (2016)

→ instrumental direction-dependent effects
~ digital adaptive optics (with full polarisation)

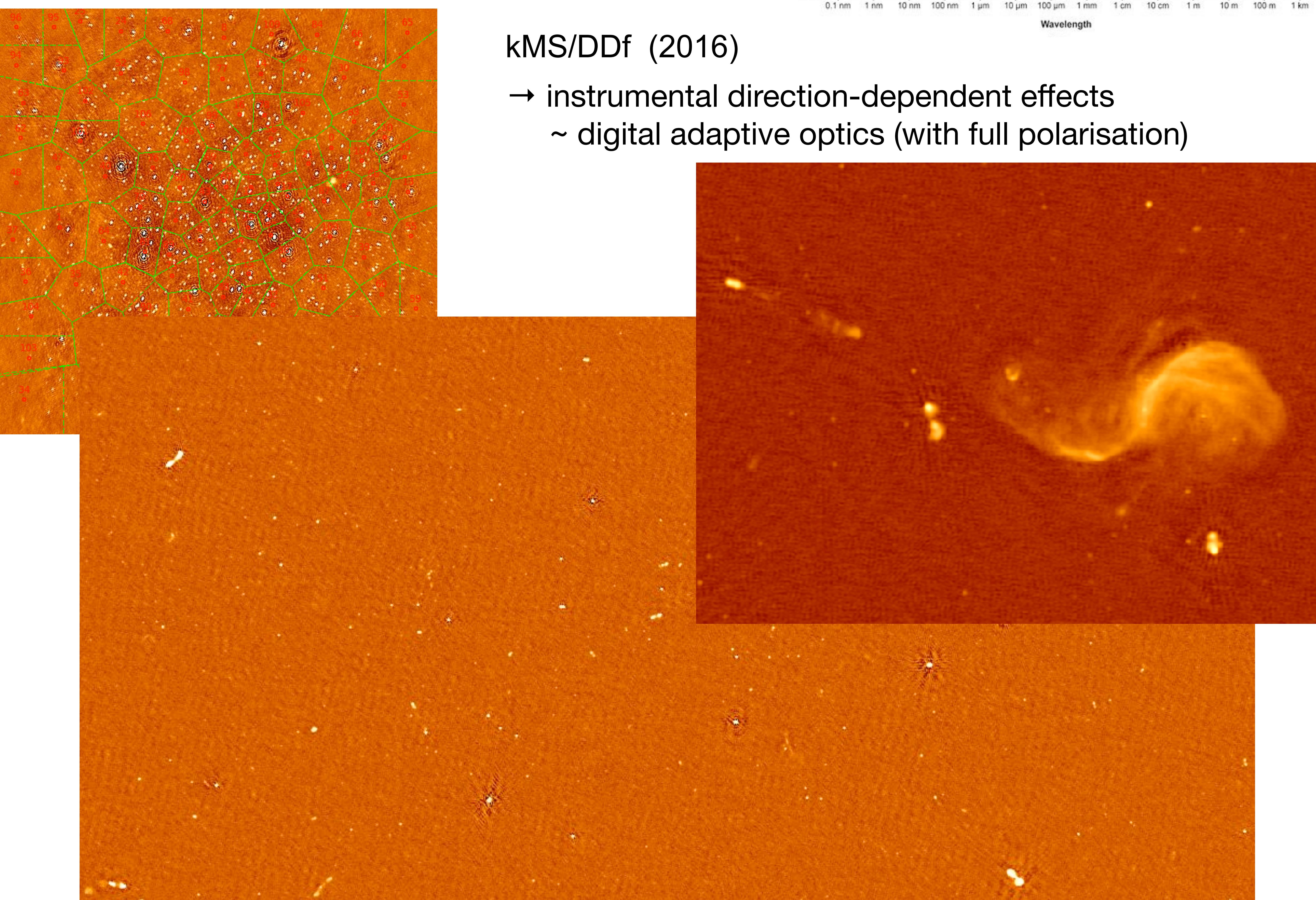

LOFAR Two-meter Sky Survey : LoTSS

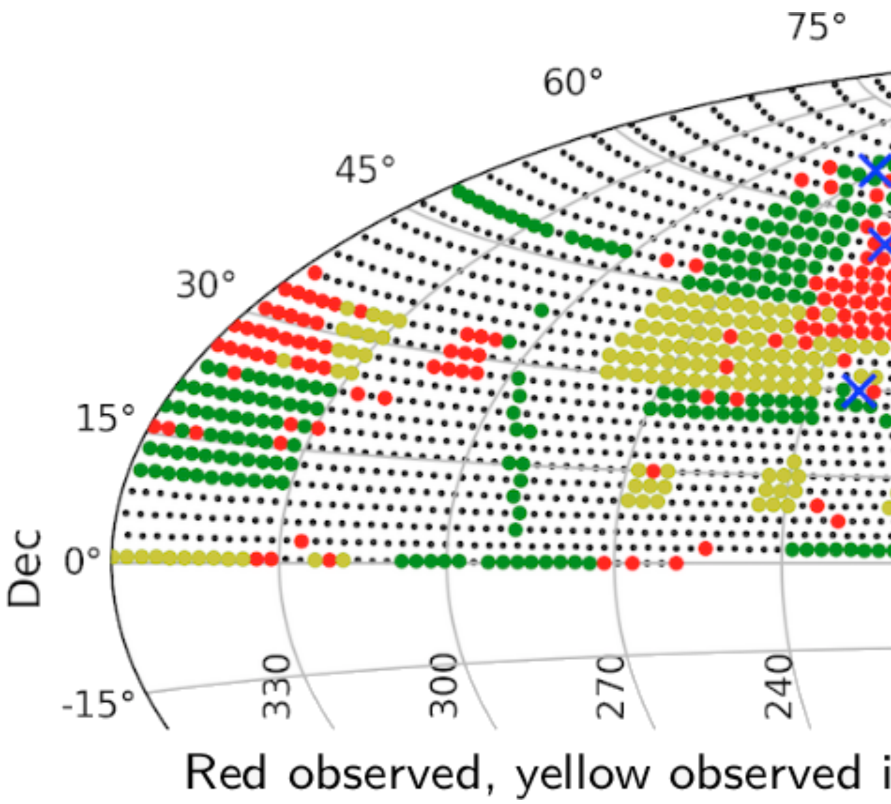

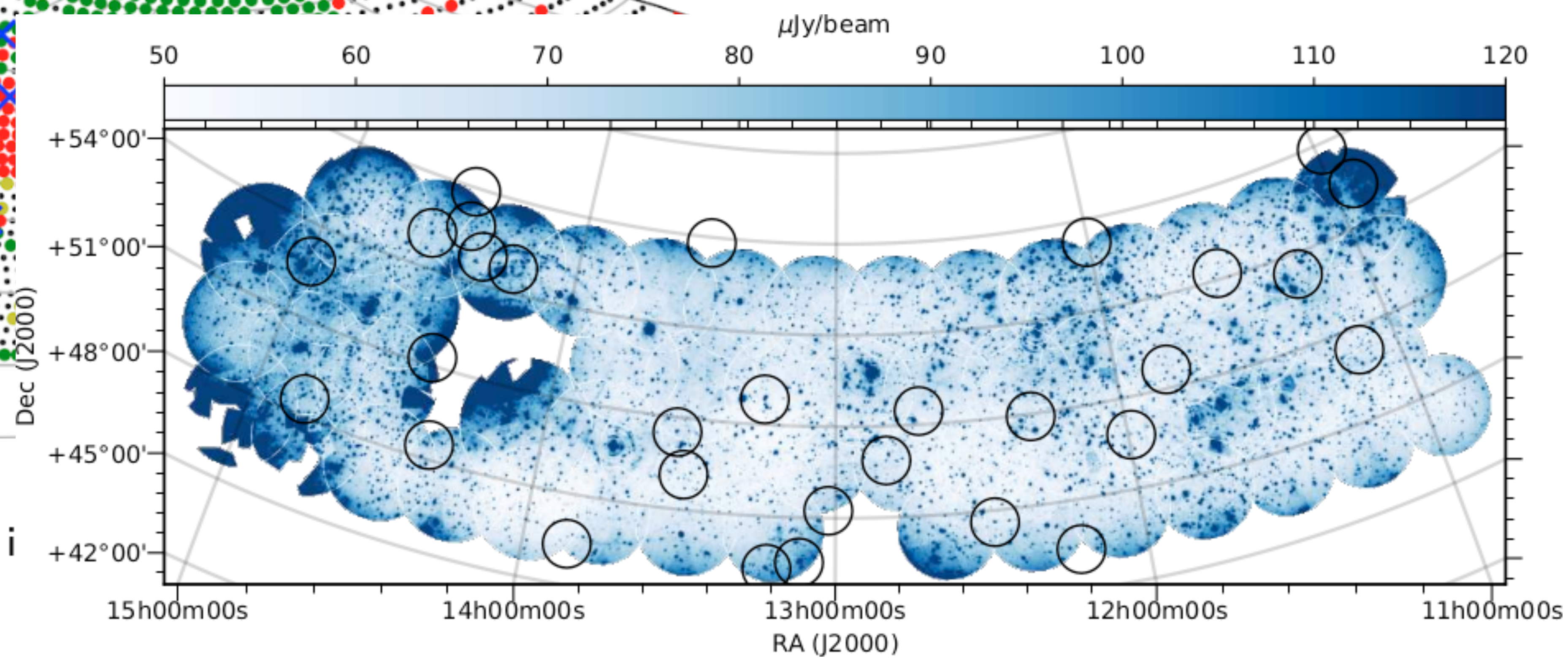

>3000 pointings, Northern hemisphere, Resolution ≈ 5”
Sensitivity ≈100 μJy/beam

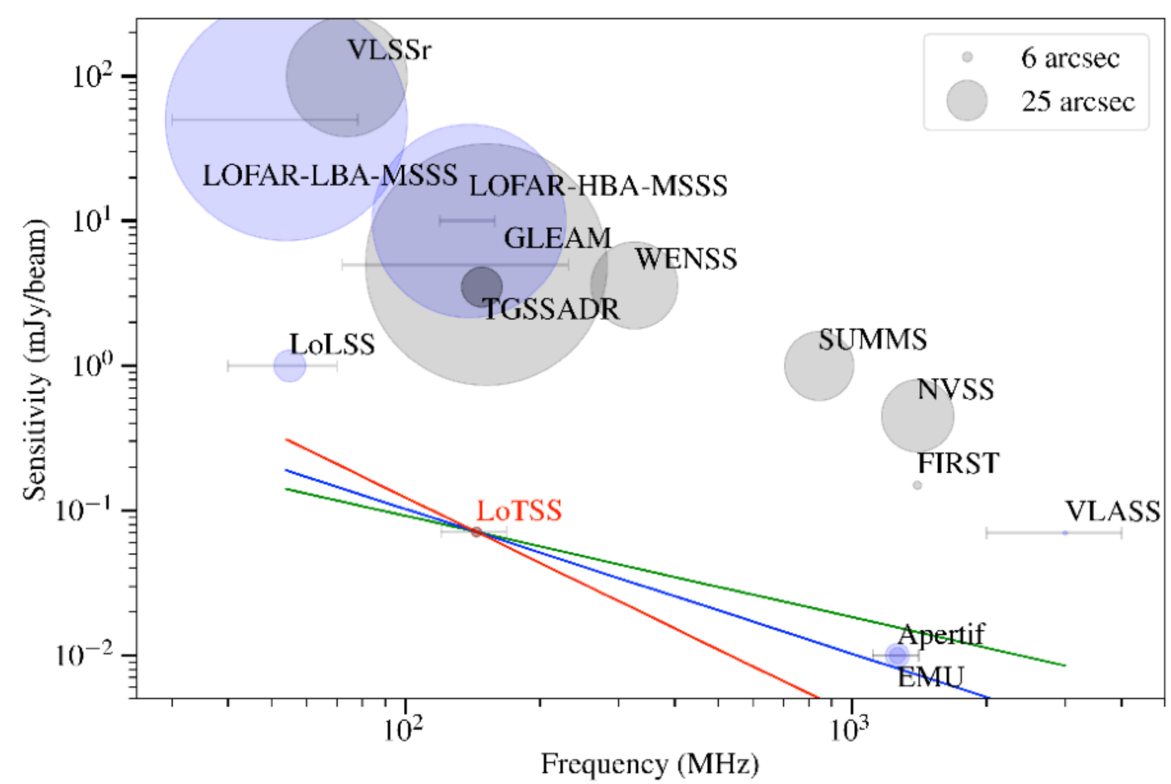

LOFAR Two-meter Sky Survey : LoTSS

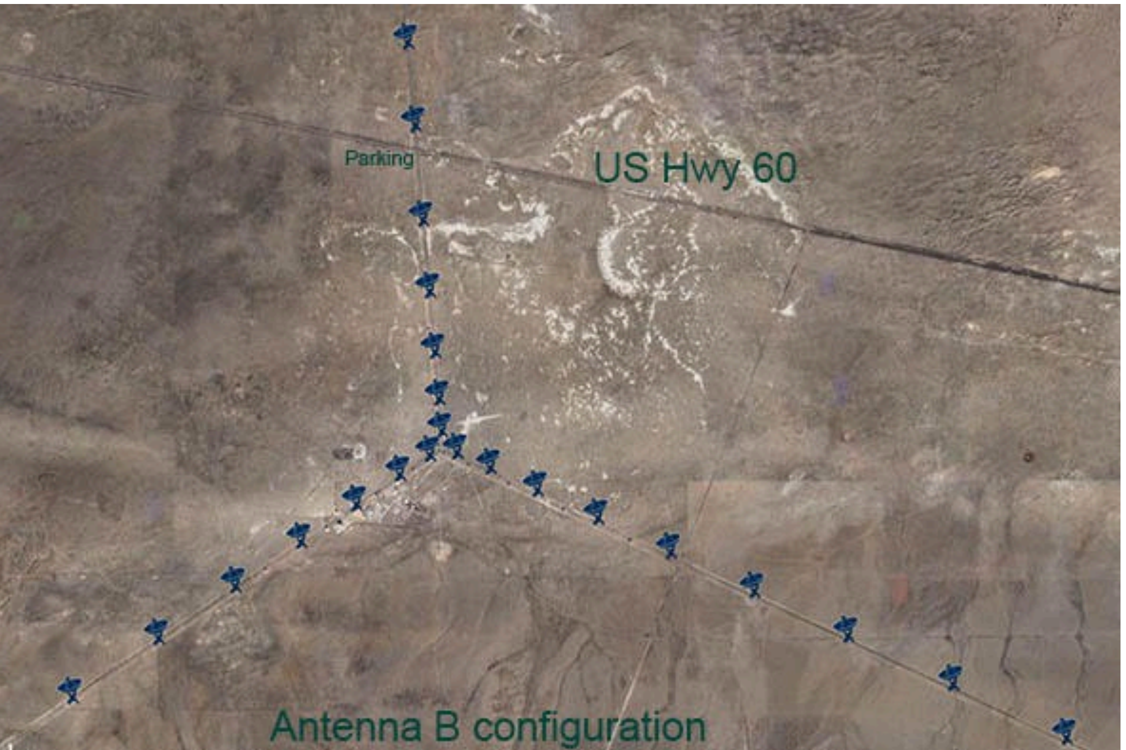

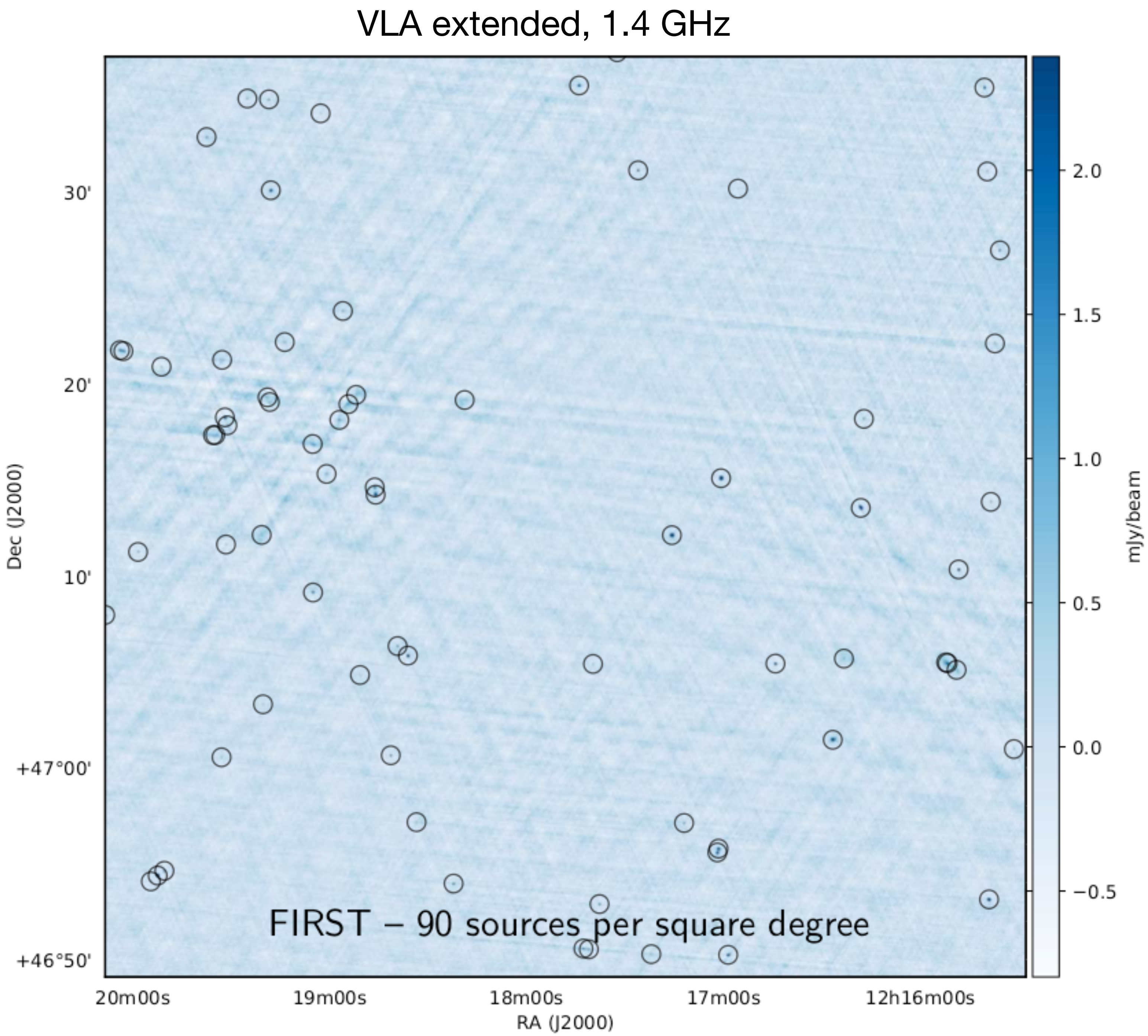

LOFAR Two-meter Sky Survey : LoTSS

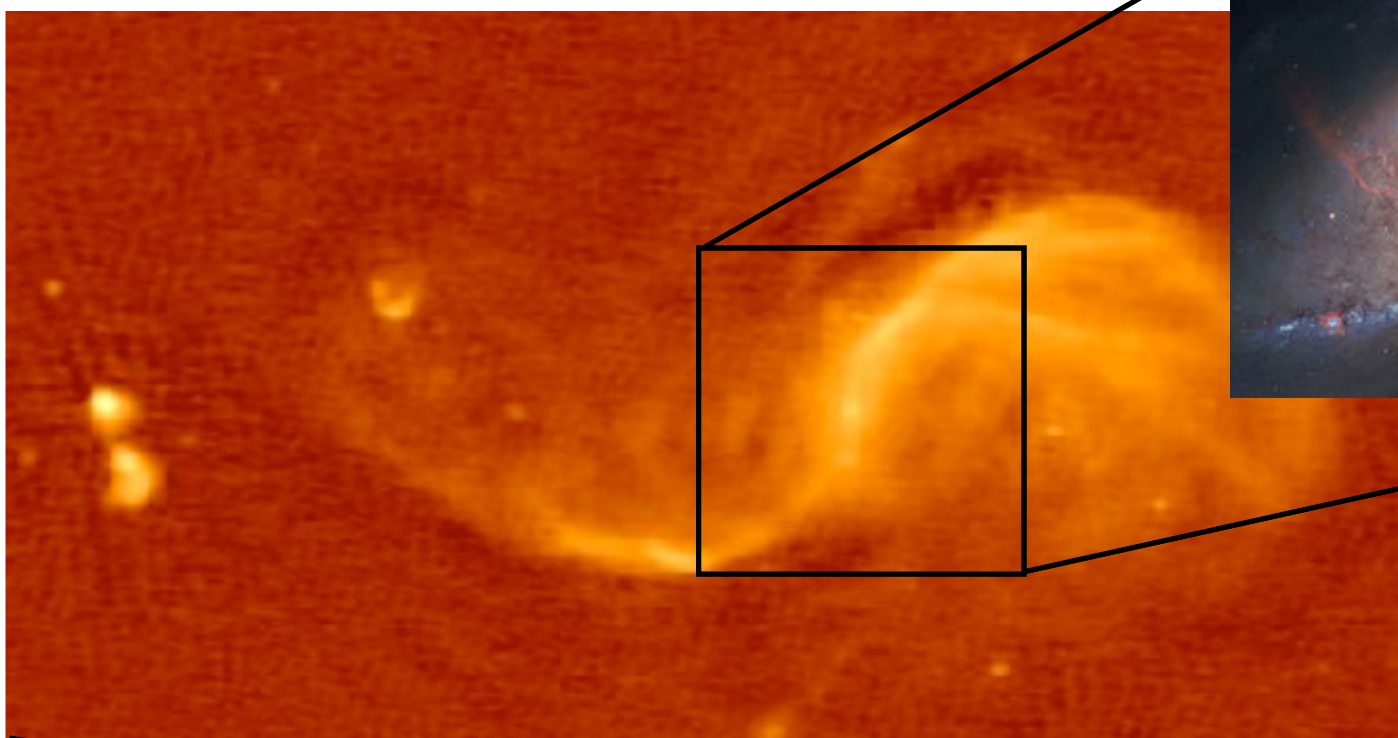

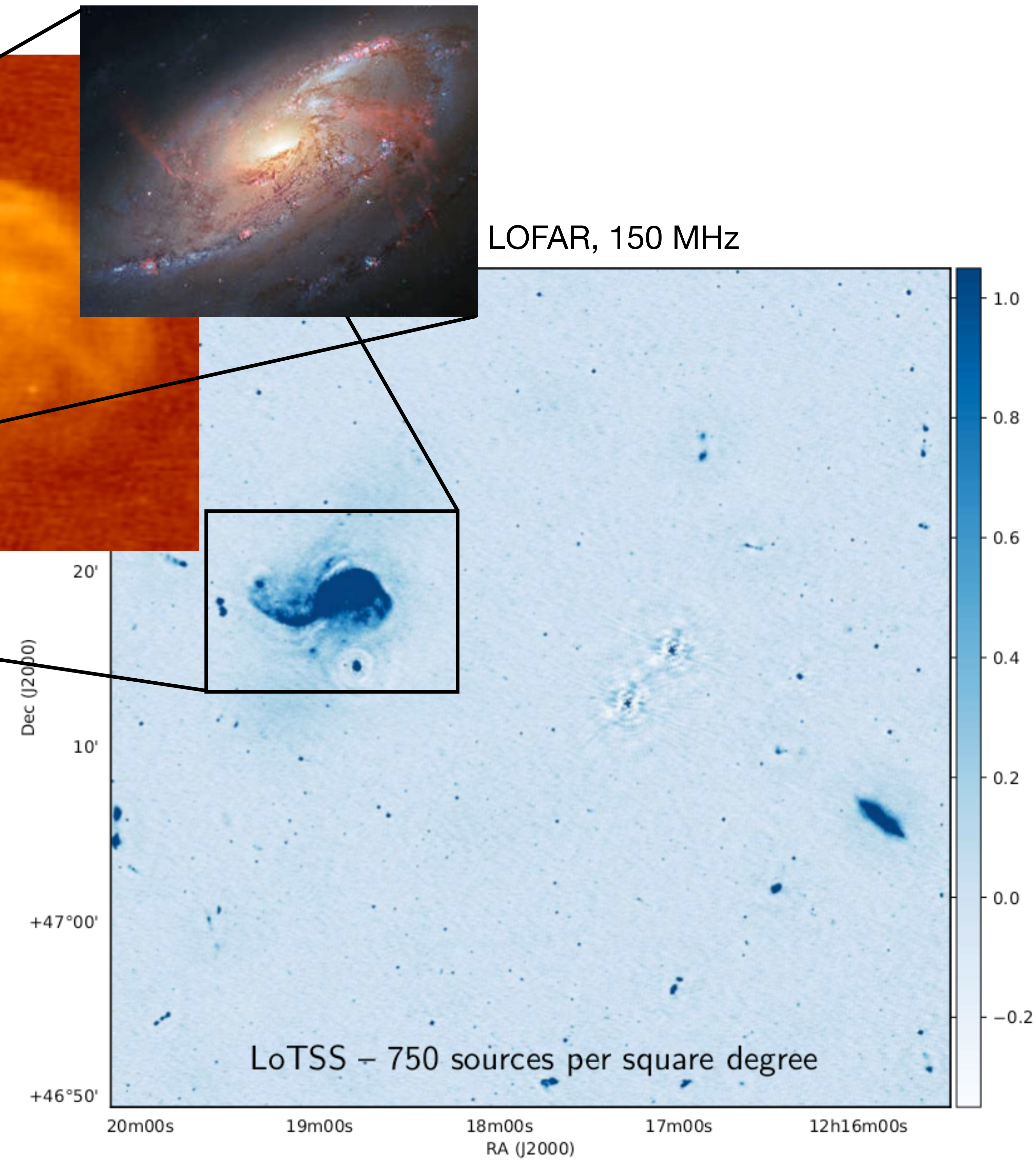

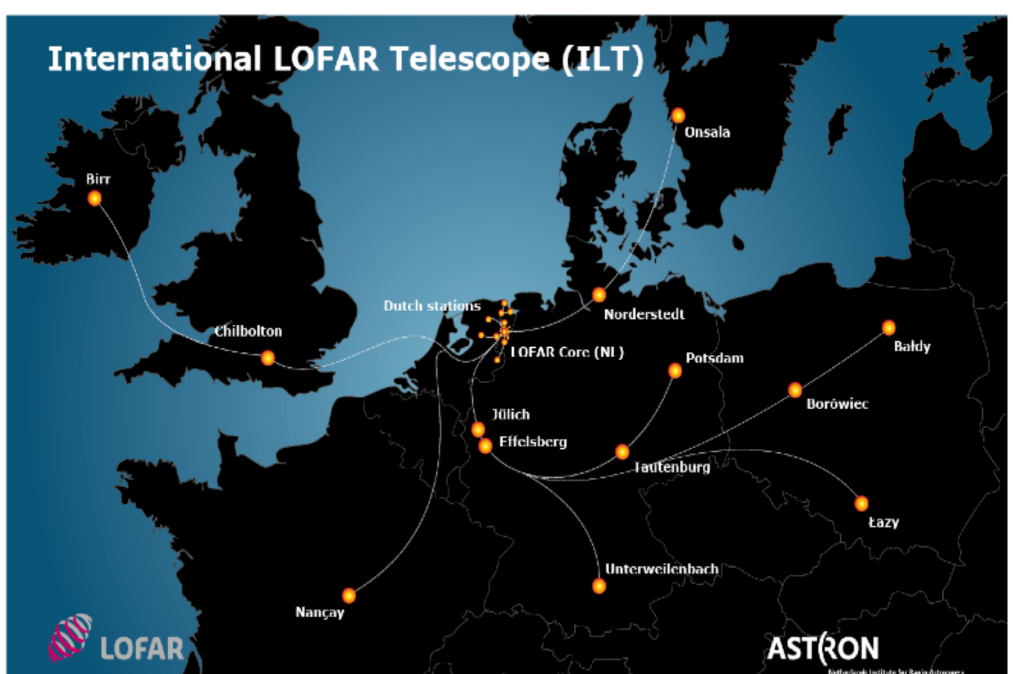

LOFAR Two-meter Sky Survey : Star-Planet interactions & exoplanets in LoTSS

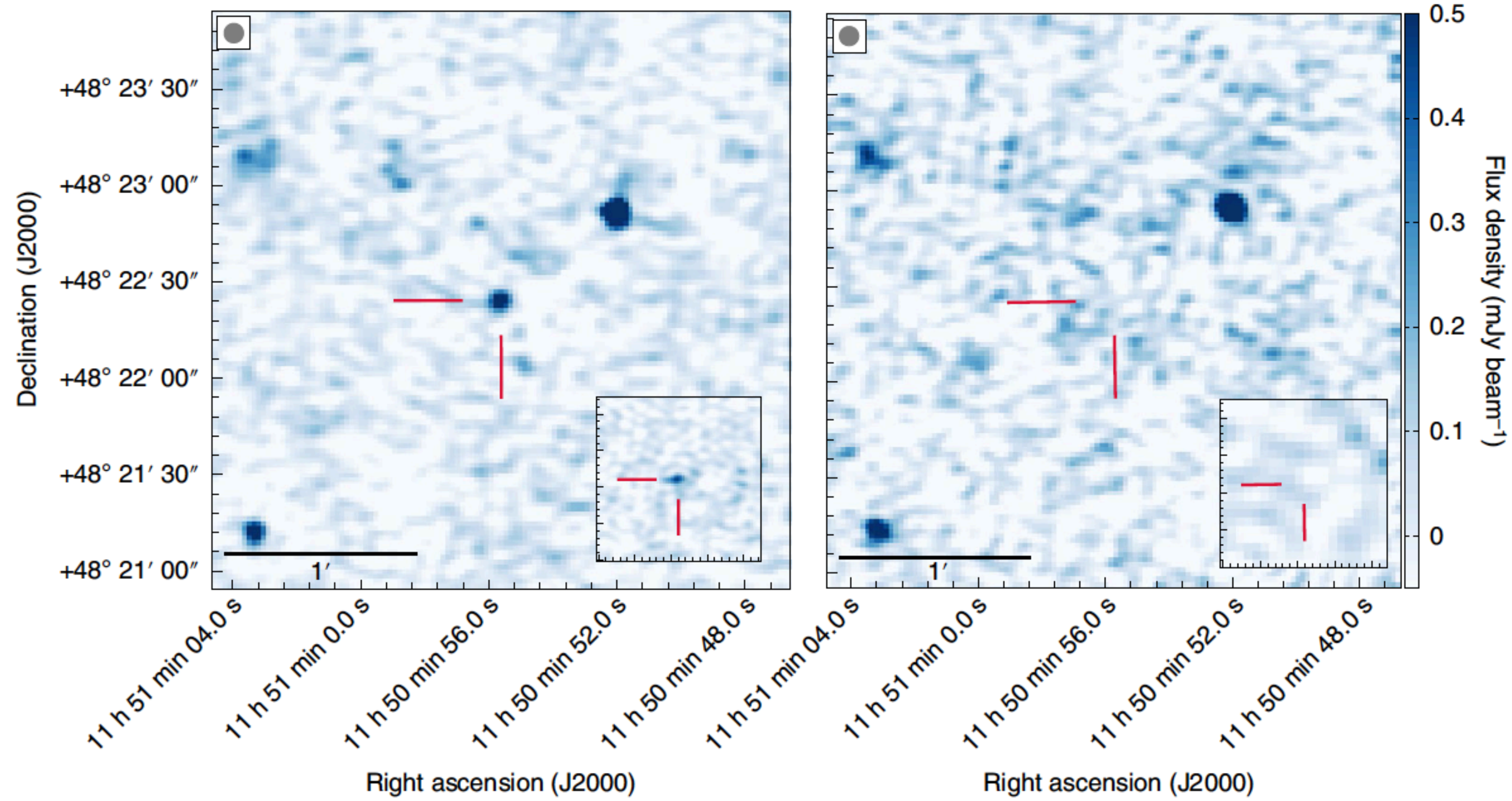

GJ 1151

quiescent red dwarf, P_{rot}~125 d,

variable emission 120-167 MHz,.

circularly polarized

⇒ interaction with a planet of ~2.5 M_E, P ~2 j ?

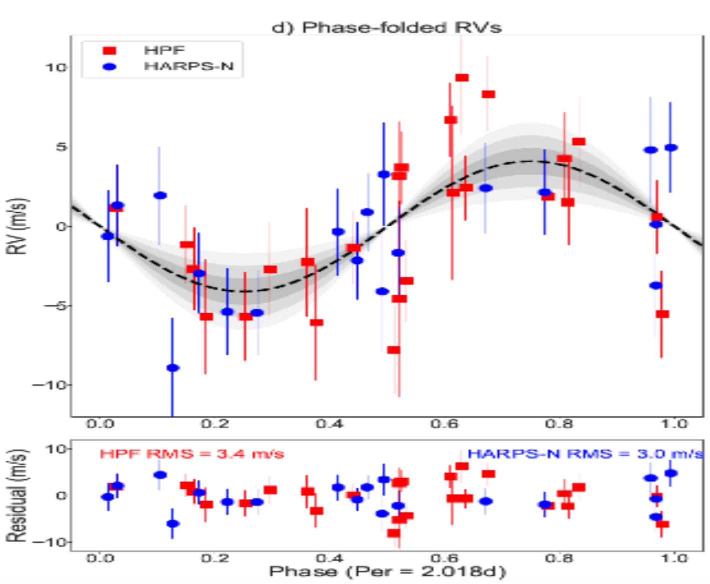

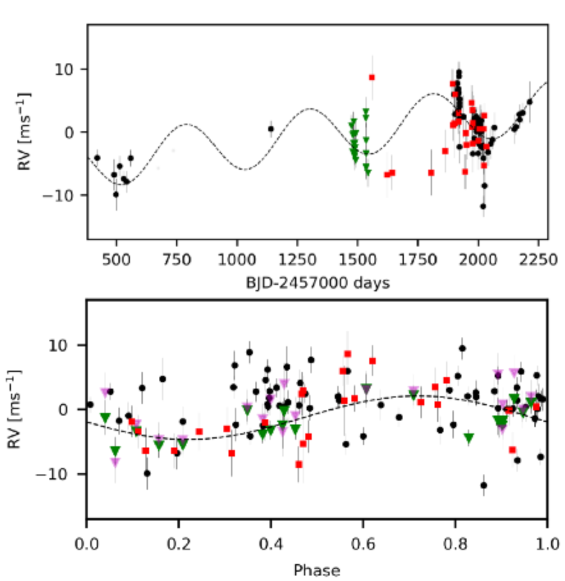

… or maybe not.

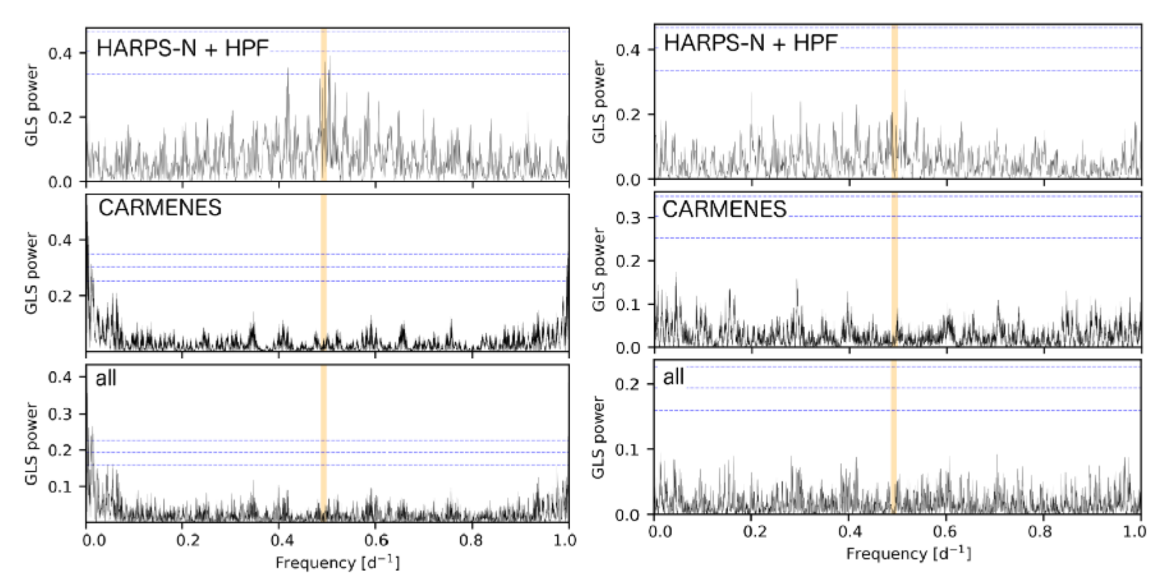

ALMA (Atacama Large Millimeter Array)

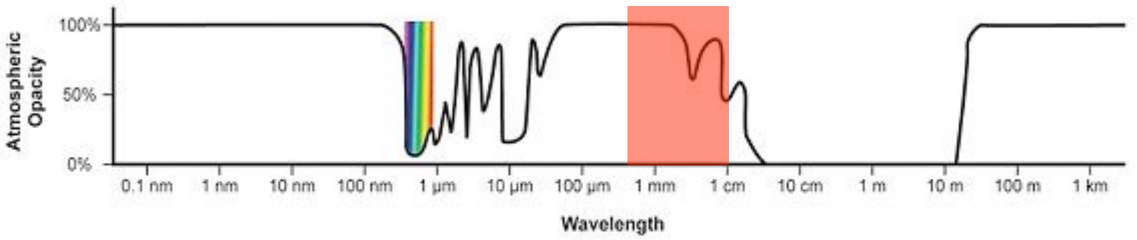

- Chili: 5000m altitude
- 50 parabolas of 12m
- f = [30-900GHz]
- λ= [1 cm-0.3mm]
- S = 5600m²
- baselines ⇒ 14km
- resolution ⇒ 0.007” @ 0.4mm (750 GHz)

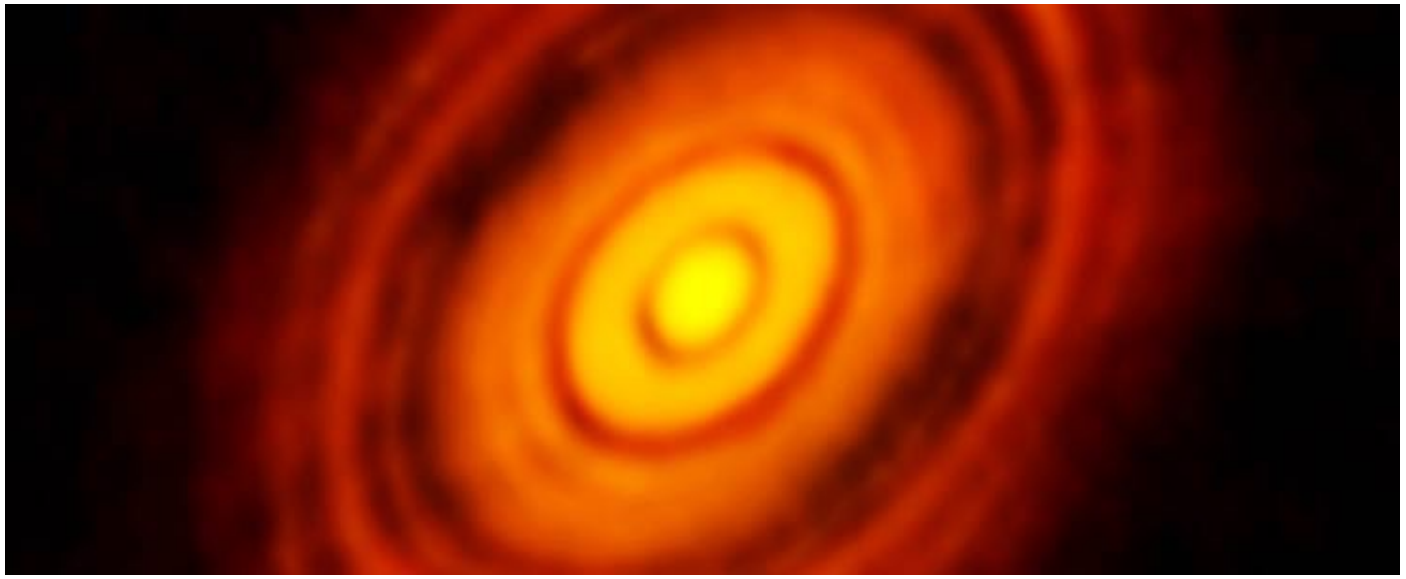

⇒ *Very high-resolution spectro-imaging in the mm/sub-mm range*

LWA

LWA ~ LOFAR LF (USA)

(10-88 MHz)

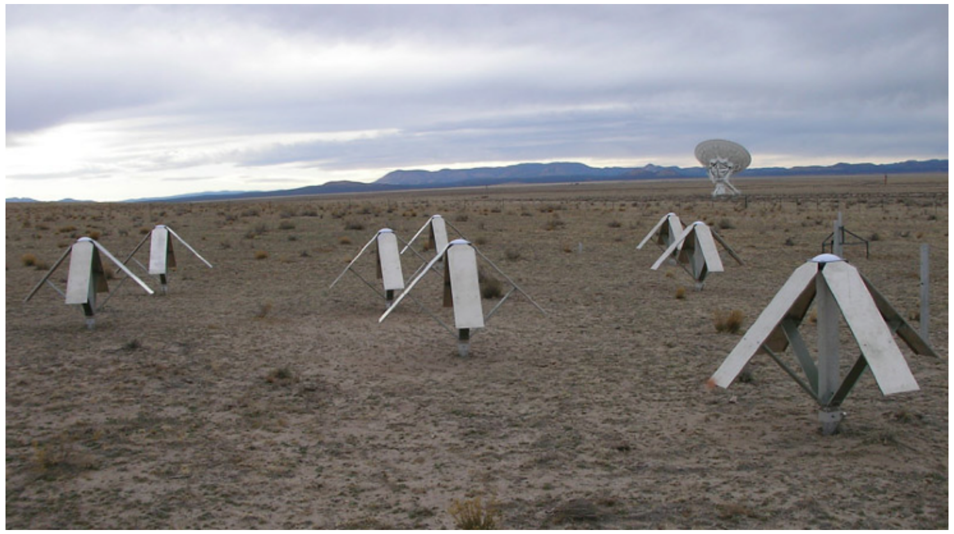

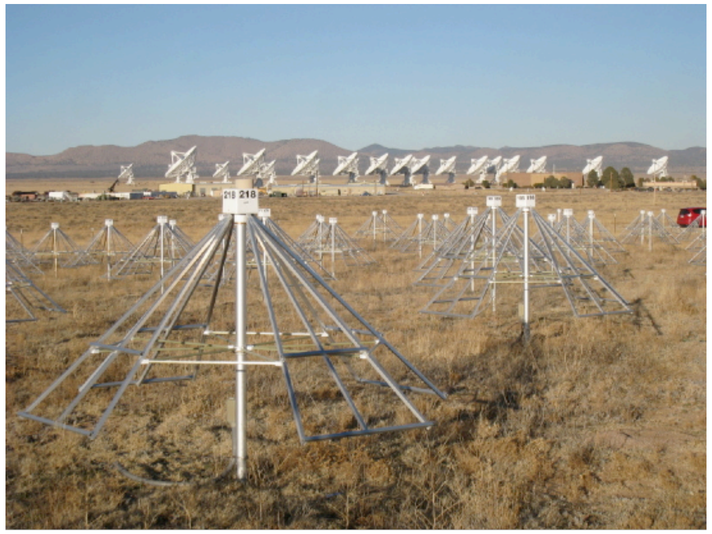

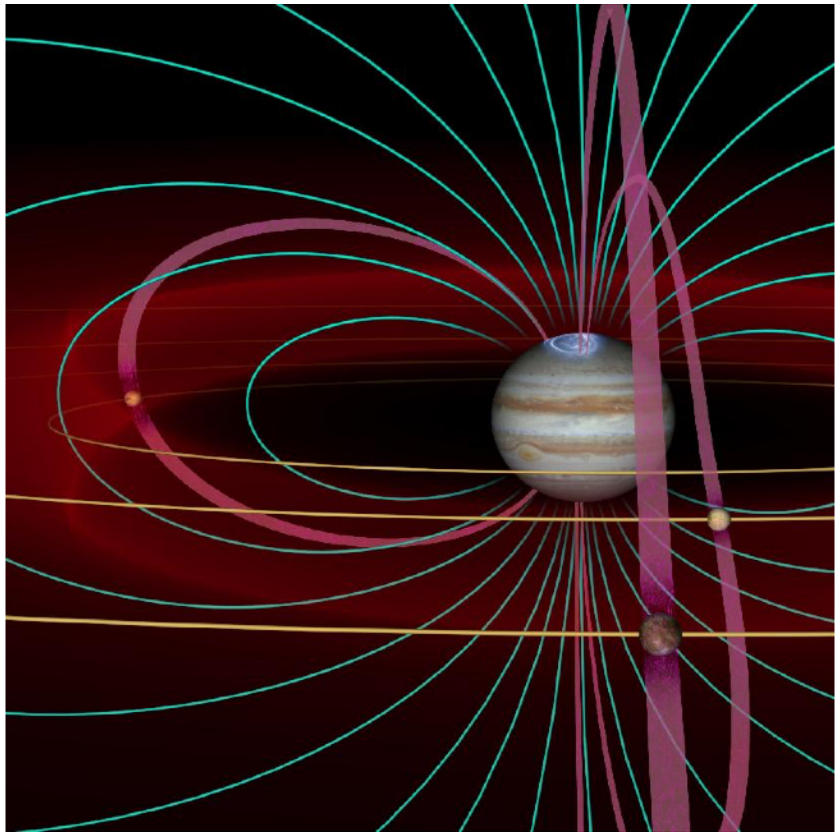

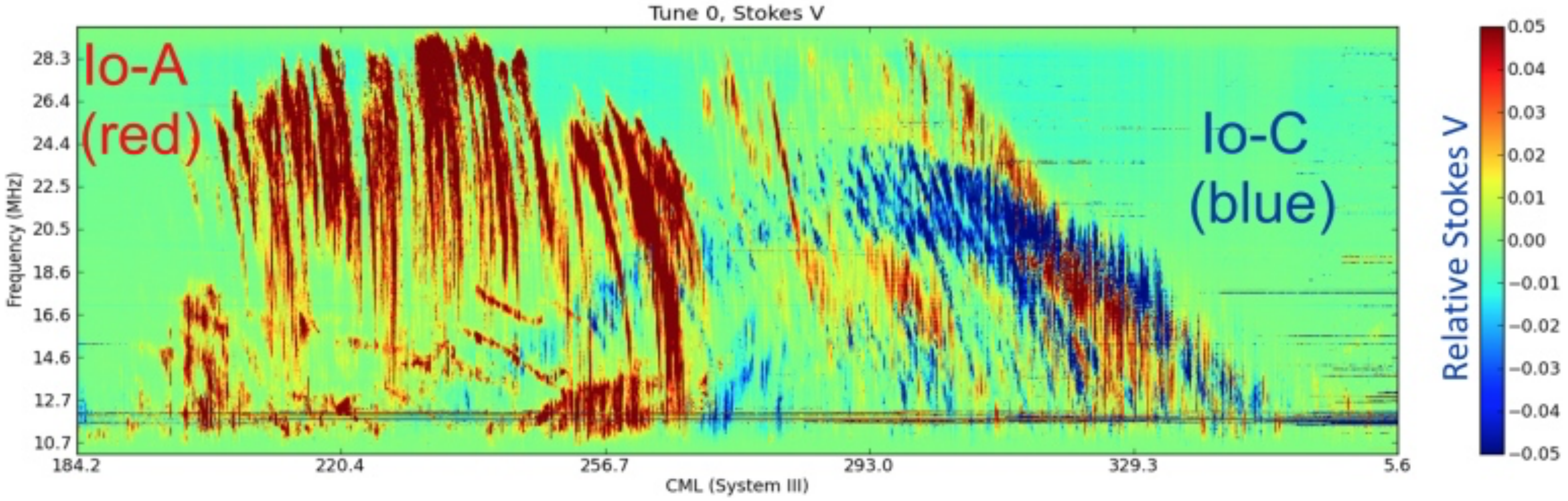

MWA (70-230 MHz, Australia)

GLEAM

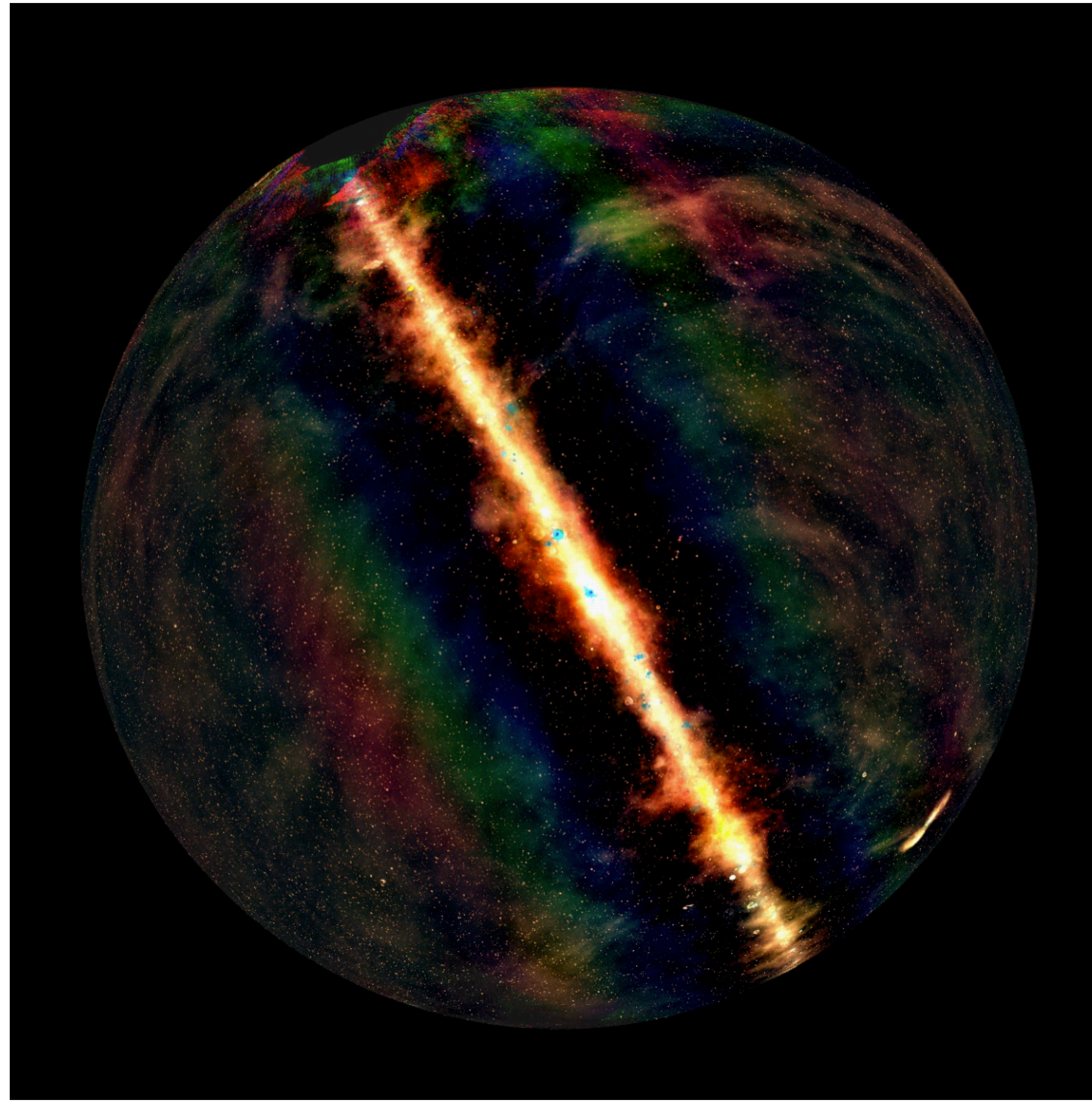

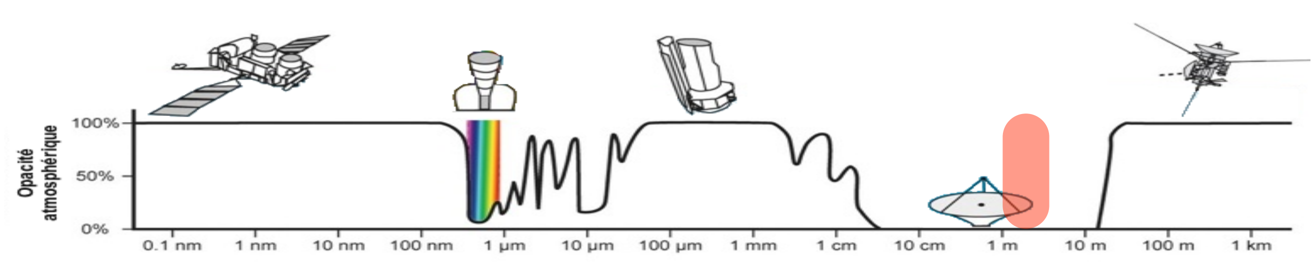

MeerKAT (1-10 GHz, South Africa)

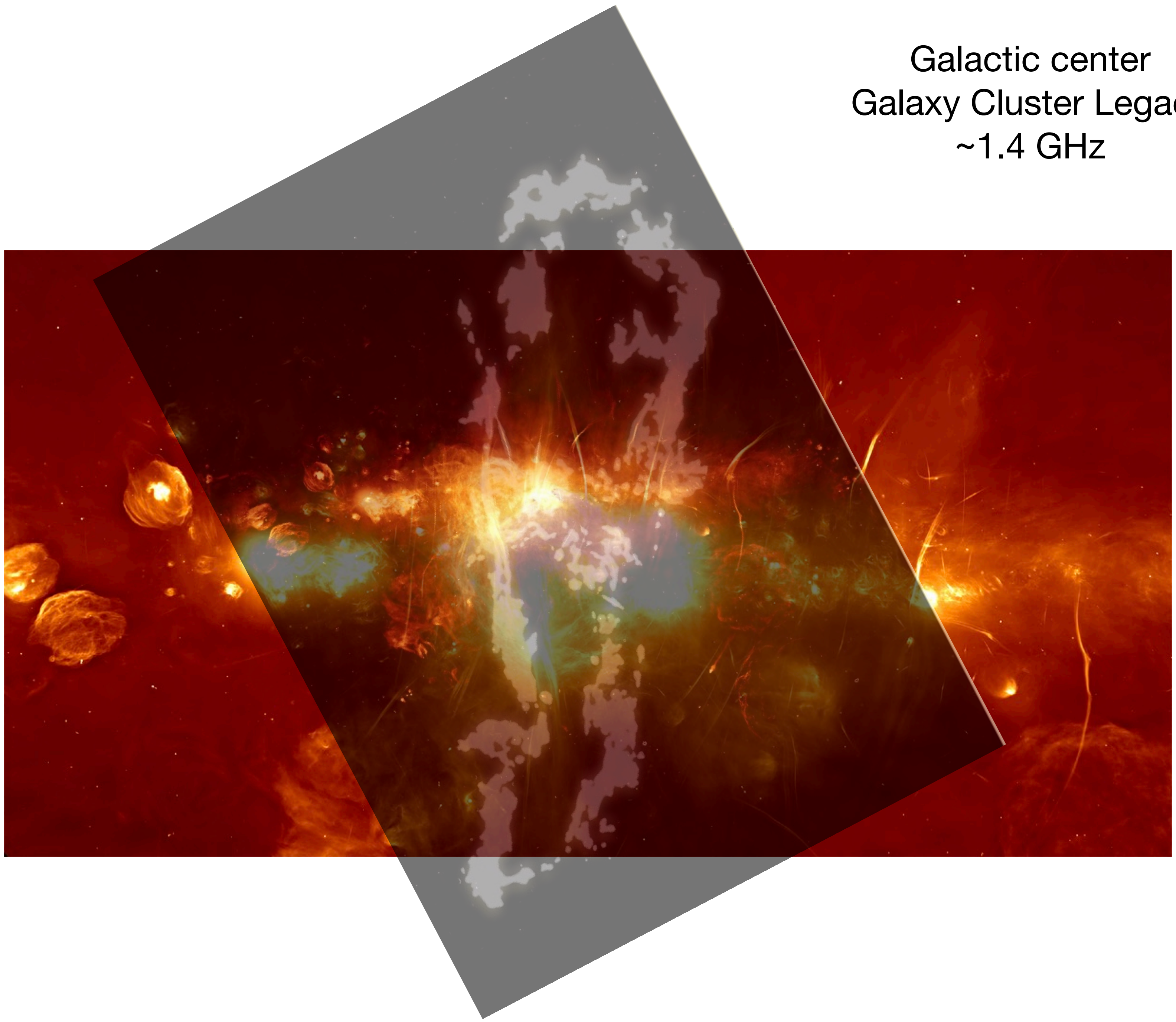

Galactic center
Galaxy Cluster Legacy
~1.4 GHz

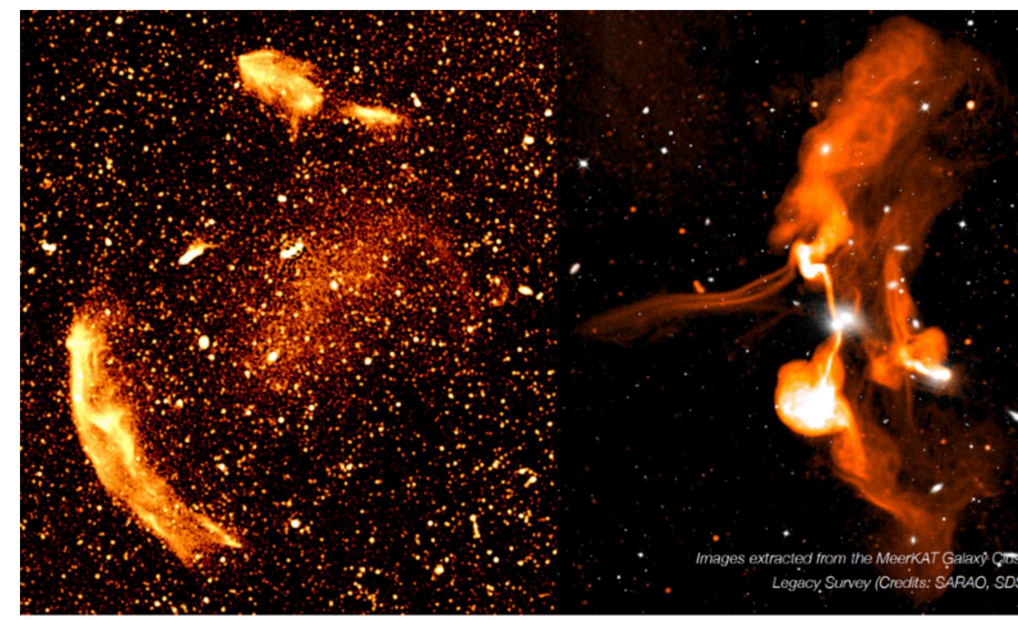

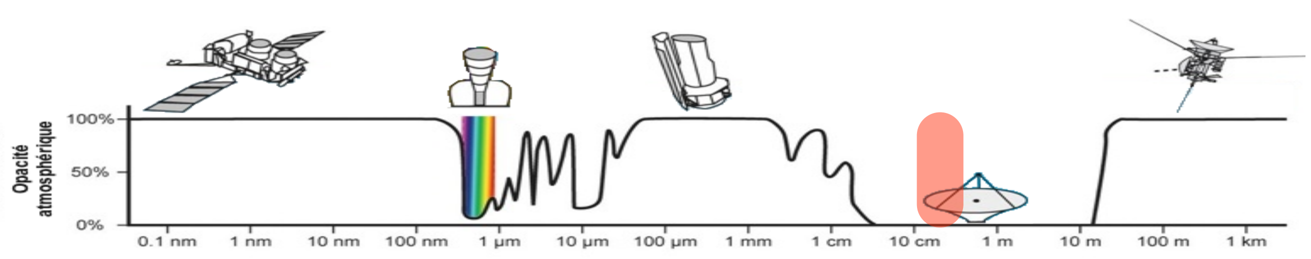

FAST (70 MHz - 3 GHz, China)

500 m diameter, Arecibo-like concept

Radio bursts (AD Leo, FRB…)

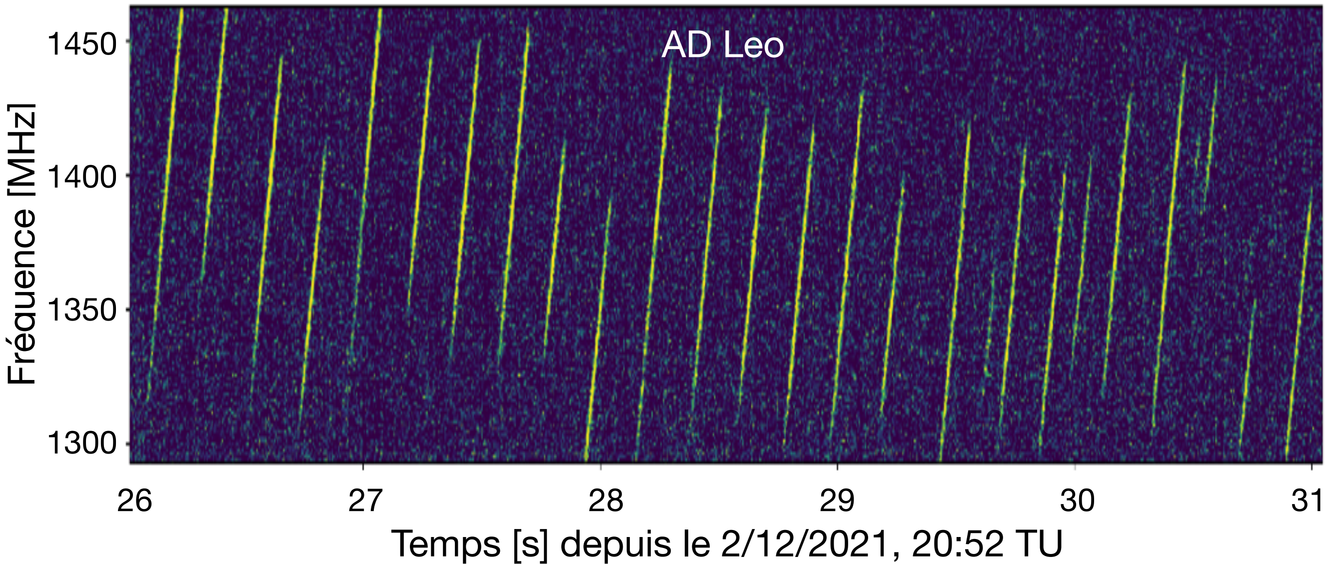

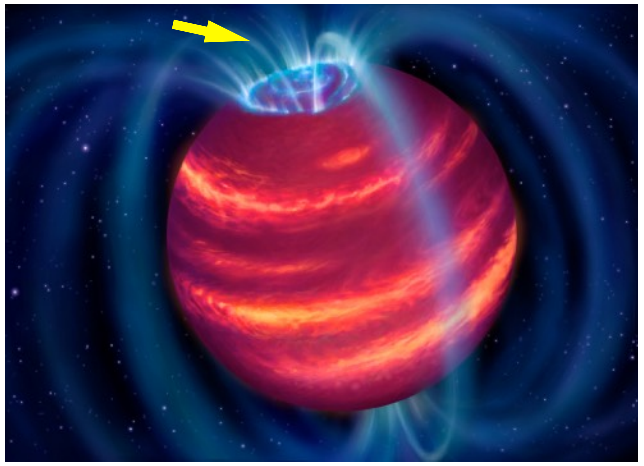

NenuFAR (LOFAR Super Station)

New extension in Nançay upgrading LOFAR

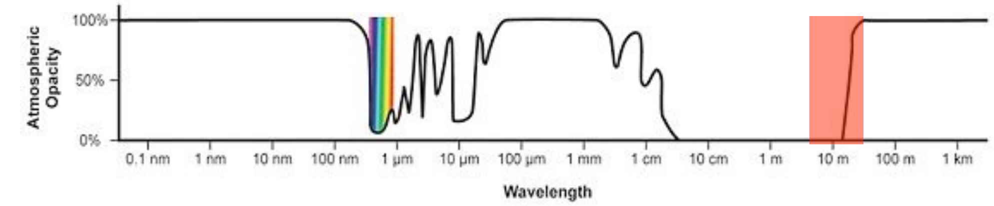

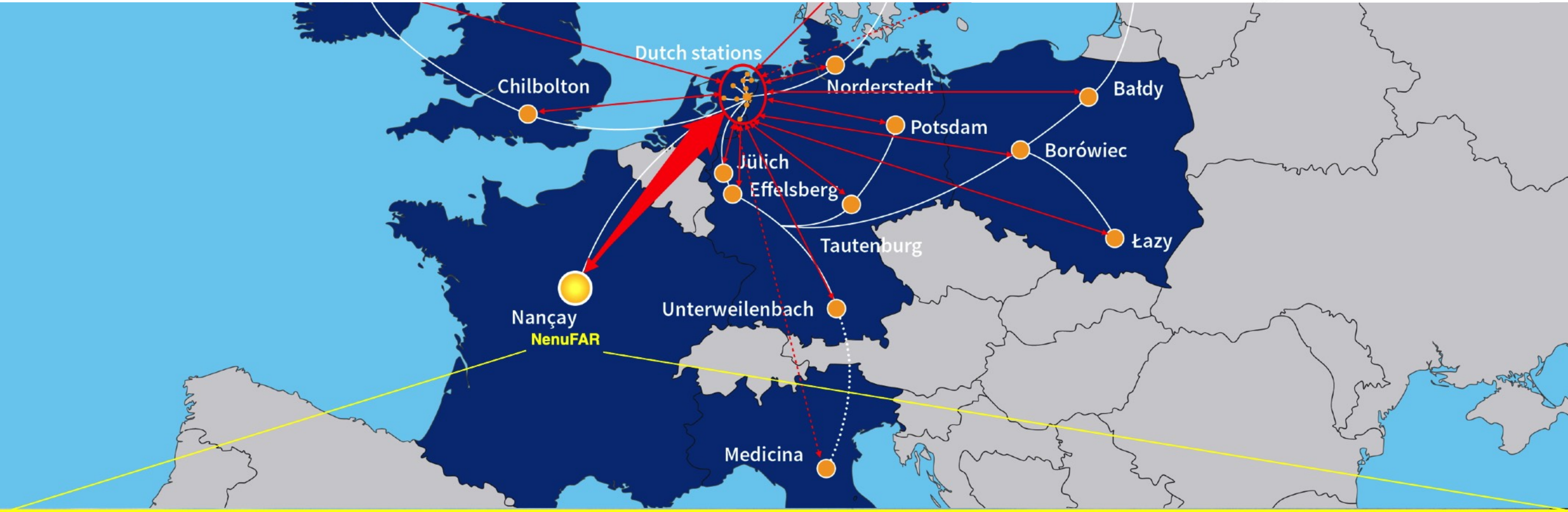

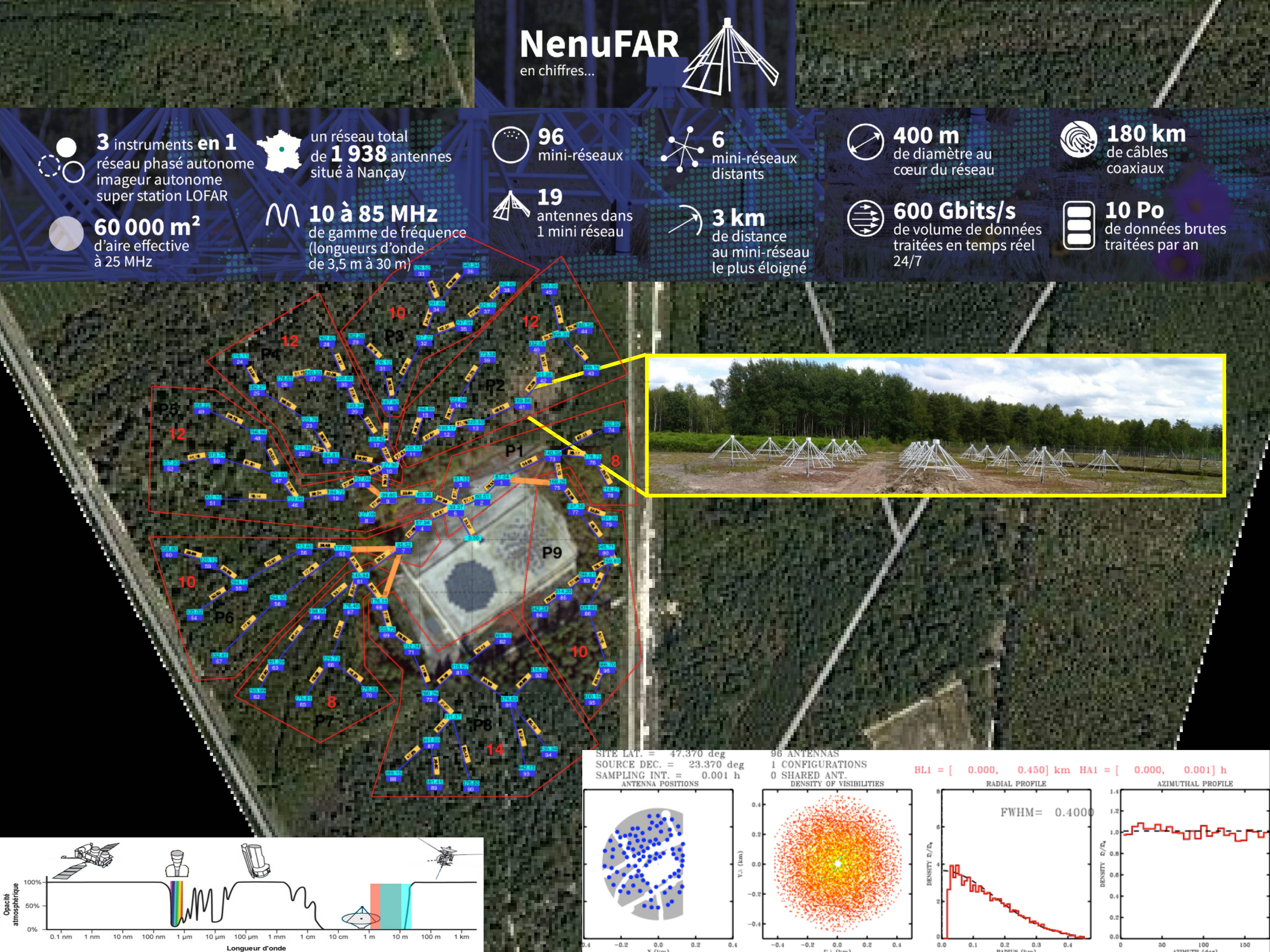
NenuFAR
en chiffres...
3 instruments en 1
réseau phasé autonome
imageur autonome
super station LOFAR
60 000 m²
d'aire effective
à 25 MHz
un réseau total
de 1 938 antennes
situé à Nançay
10 à 85 MHz
de gamme de fréquence
(longueurs d'onde
de 3,5 m à 30 m)
96
mini-réseaux
19
antennes dans
1 mini réseau
6
mini-réseaux
distants
3 km
de distance
au mini-réseau
le plus éloigné
400 m
de diamètre au
cœur du réseau
600 Gbits/s
de volume de données
traitées en temps réel
24/7
180 km
de câbles
coaxiaux
10 Po
de données brutes
traitées par an
P1
P2
P3
P4
P5
P6
P7
P8
P9
SITE LAT. = 47.370 deg
SOURCE DEC. = 23.370 deg
SAMPLING INT. = 0.001 h
96 ANTENNAS
1 CONFIGURATIONS
0 SHARED ANT.
BL1 = [0.000, 0.450] km HA1 = [0.000, 0.001] h
ANTENNA POSITIONS
DENSITY OF VISIBILITIES
RADIAL PROFILE
AZIMUTHAL PROFILE
FWHM= 0.4000
Opacité atmosphérique
100%
50%
0%
0.1 nm
1 nm
10 nm
100 nm
1 µm
10 µm
100 µm
1 mm
1 cm
10 cm
1 m
10 m
100 m
1 km
Longueur d'onde

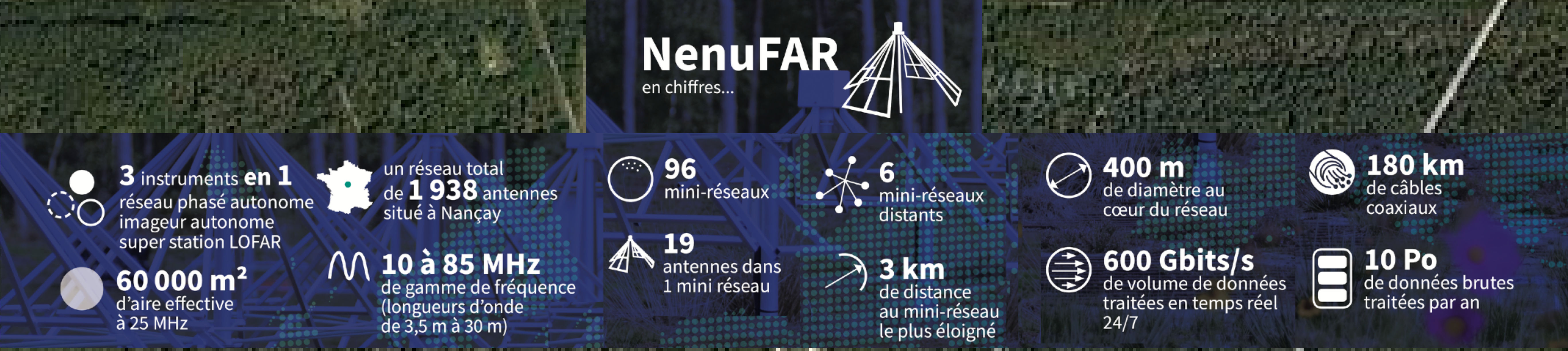
NenuFAR
en chiffres...
3 instruments en 1
réseau phasé autonome
imageur autonome
super station LOFAR
60 000 m²
d'aire effective
à 25 MHz
un réseau total
de 1 938 antennes
situé à Nançay
10 à 85 MHz
de gamme de fréquence
(longueurs d'onde
de 3,5 m à 30 m)
96
mini-réseaux
19
antennes dans
1 mini réseau
6
mini-réseaux
distants
3 km
de distance
au mini-réseau
le plus éloigné
400 m
de diamètre au
cœur du réseau
600 Gbits/s
de volume de données
traitées en temps réel
24/7
180 km
de câbles
coaxiaux
10 Po
de données brutes
traitées par an

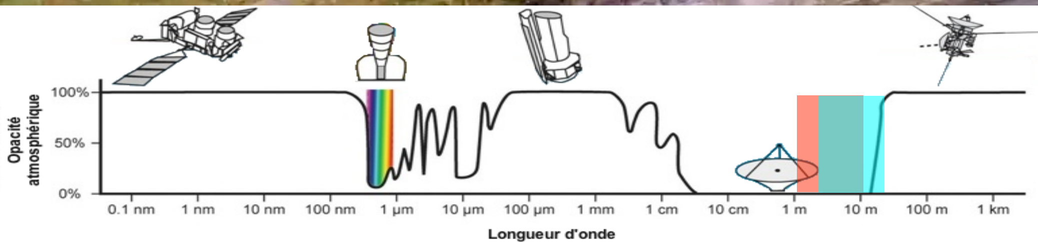
Opacité atmosphérique
100%
50%
0%
0.1 nm
1 nm
10 nm
100 nm
1 µm
10 µm
100 µm
1 mm
1 cm
10 cm
1 m
10 m
100 m
1 km
Longueur d'onde

4 instruments 1n 1: Beamformer / Imager / Waveform / LSS

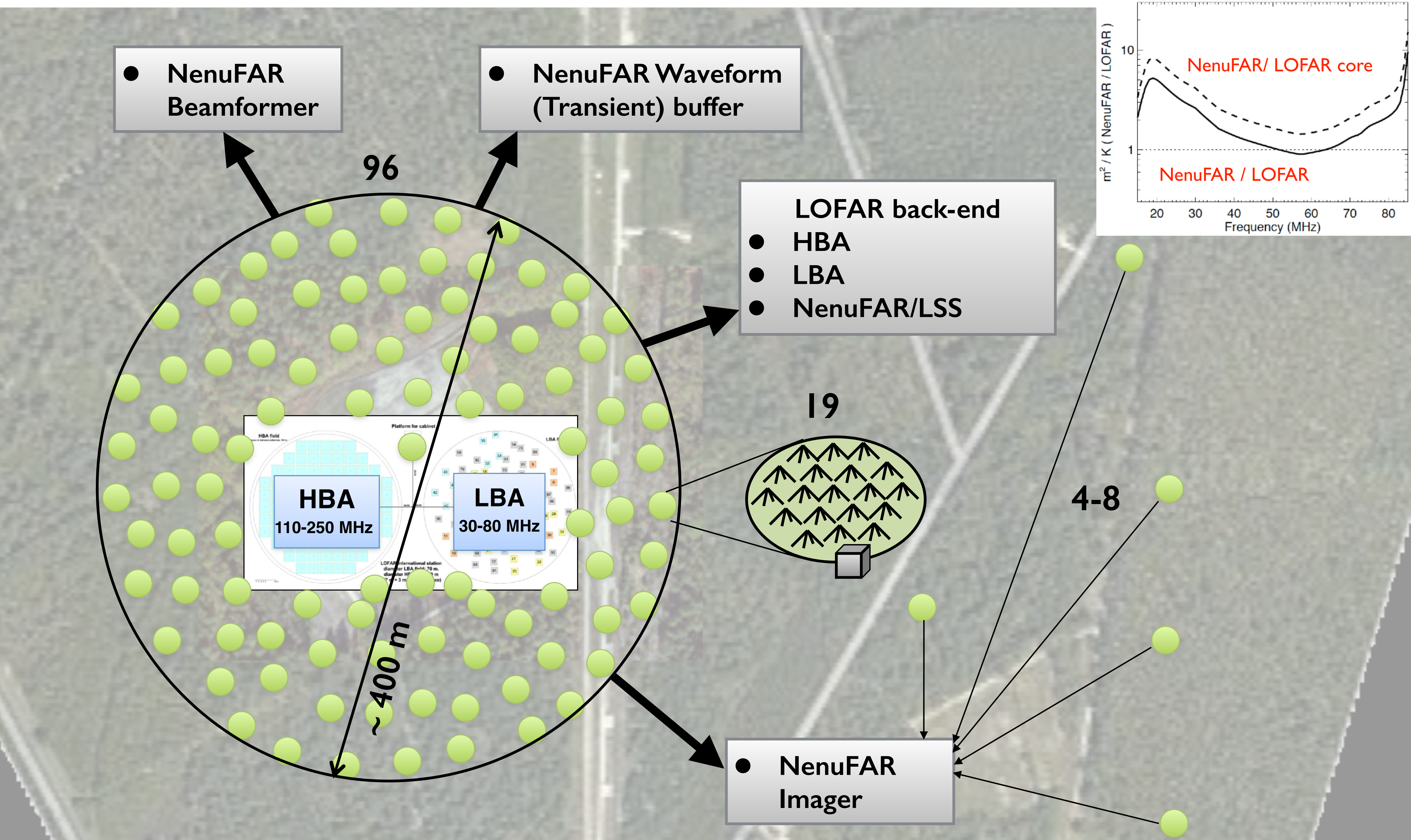

- Large, compact array sensitive to (very) low frequencies
- Large field of view, multi-beam, sensitive to extended structures
- Complementary to LOFAR: high LF resolution with sensitive internatinal baselines

NenuFAR : LOFAR Super Station

Cosmic Dawn with NenuFAR

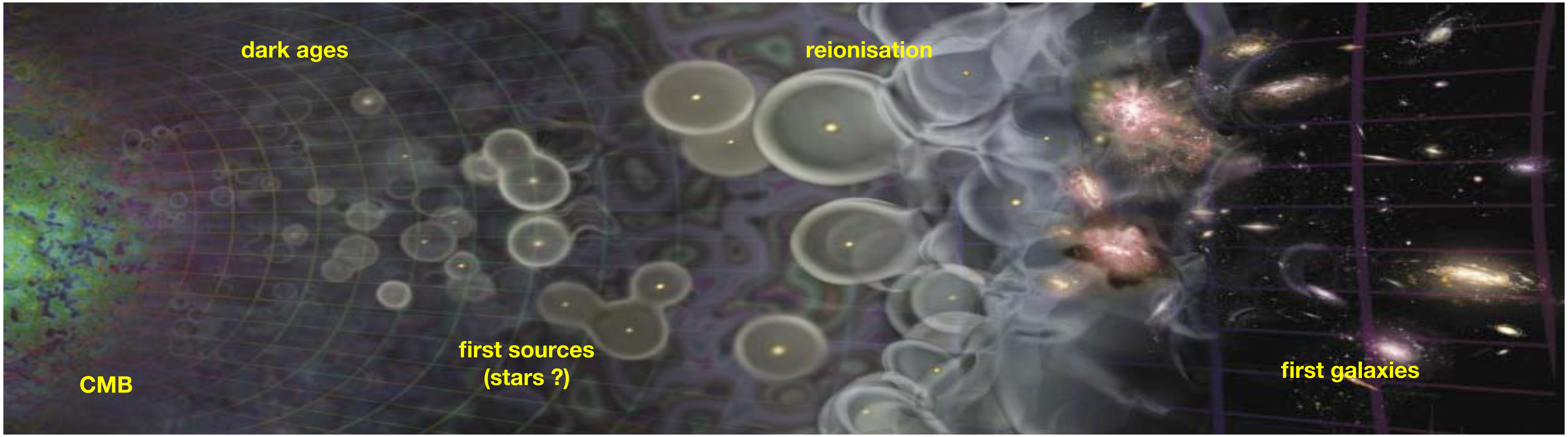

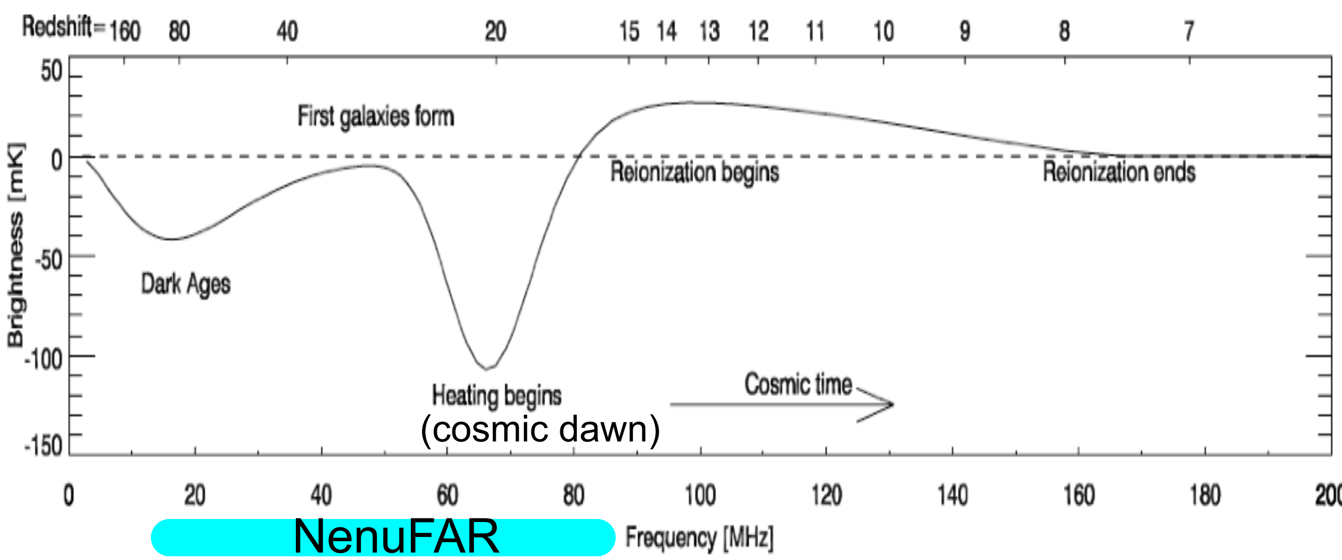

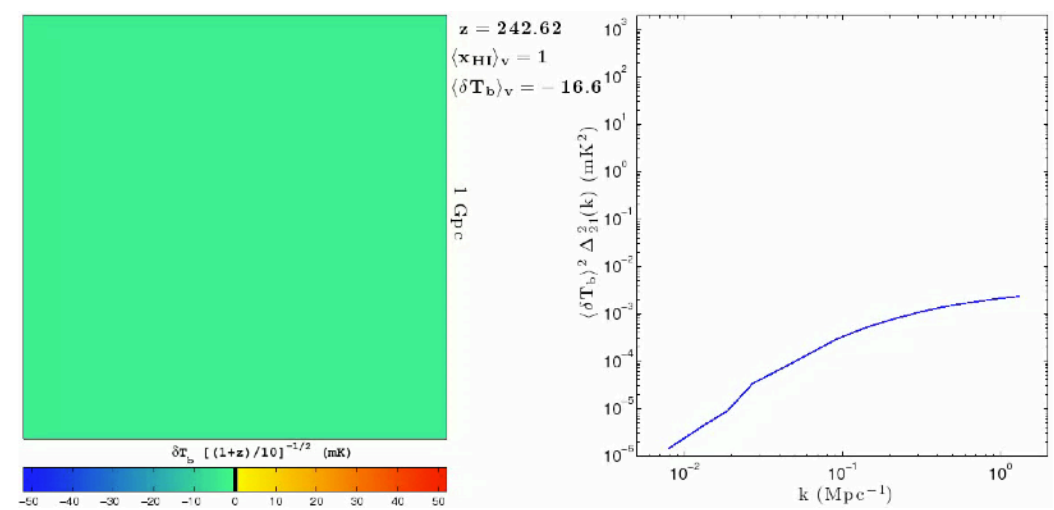

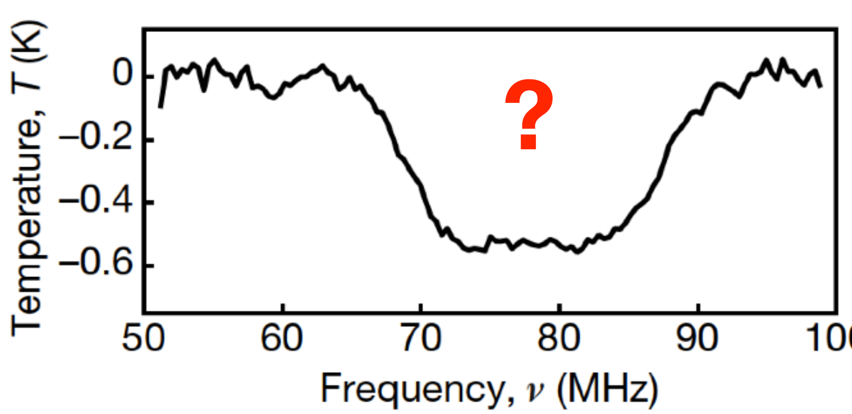

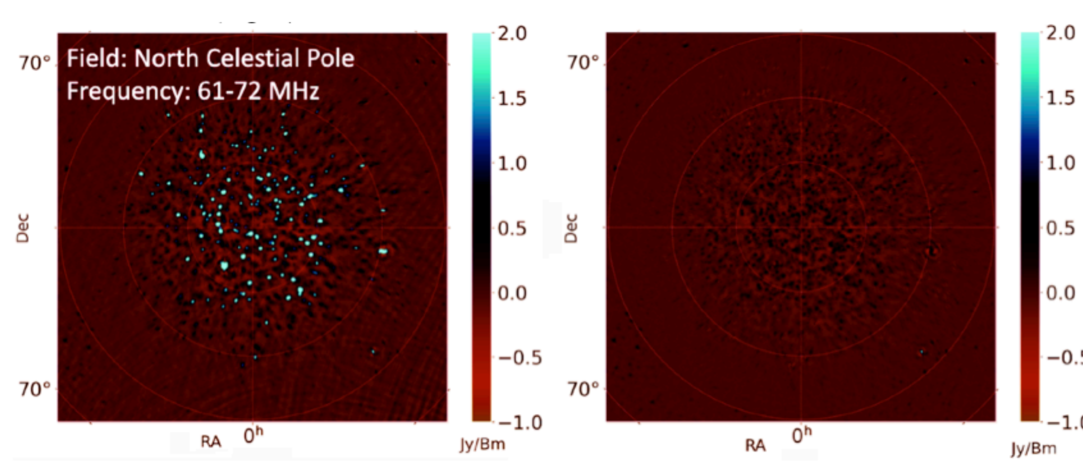

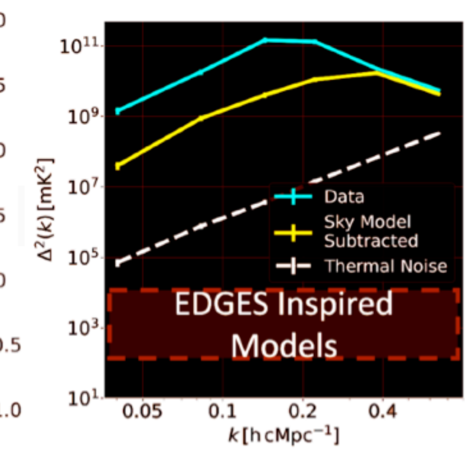

Jupiter observations with NenuFAR

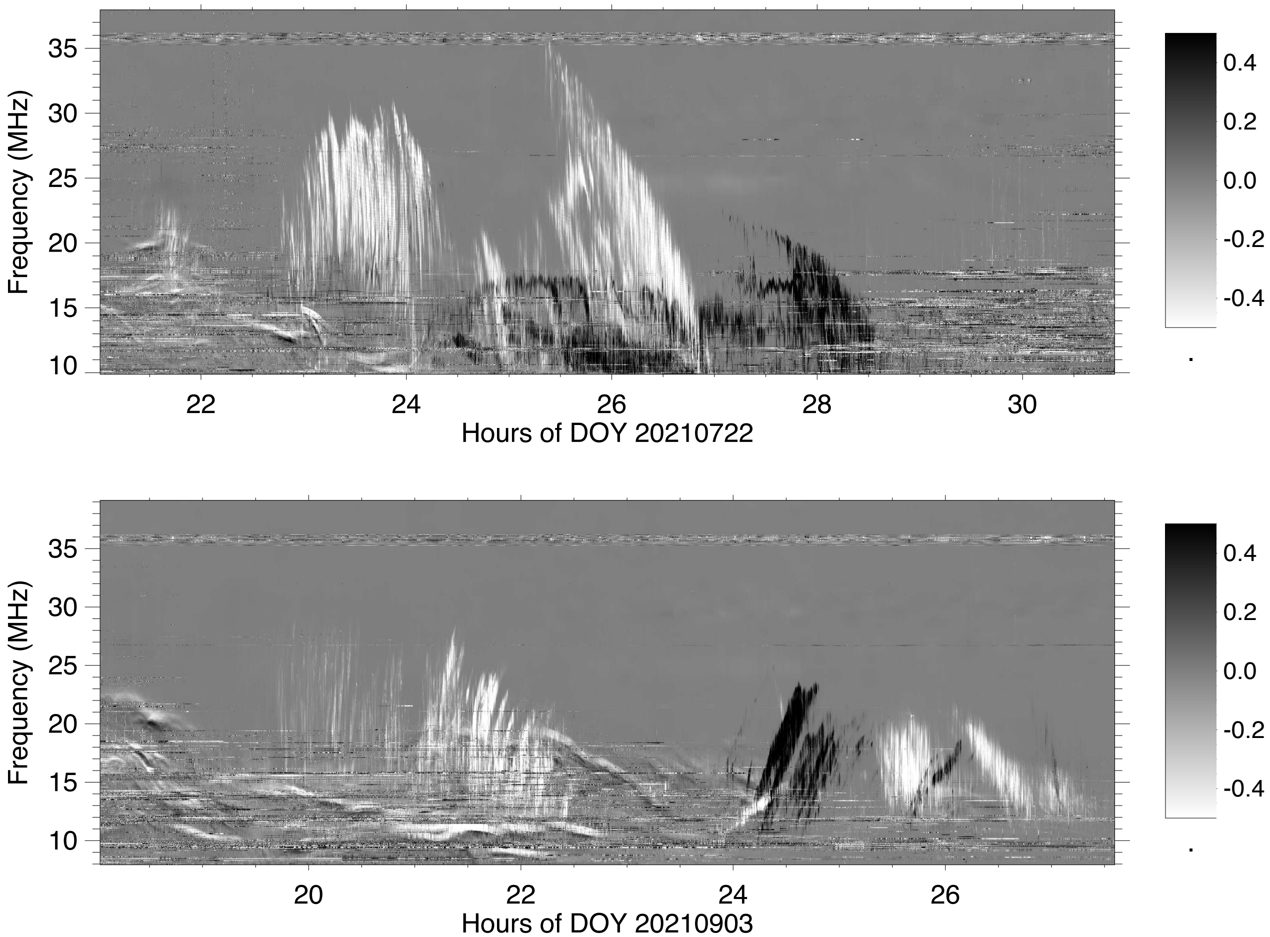

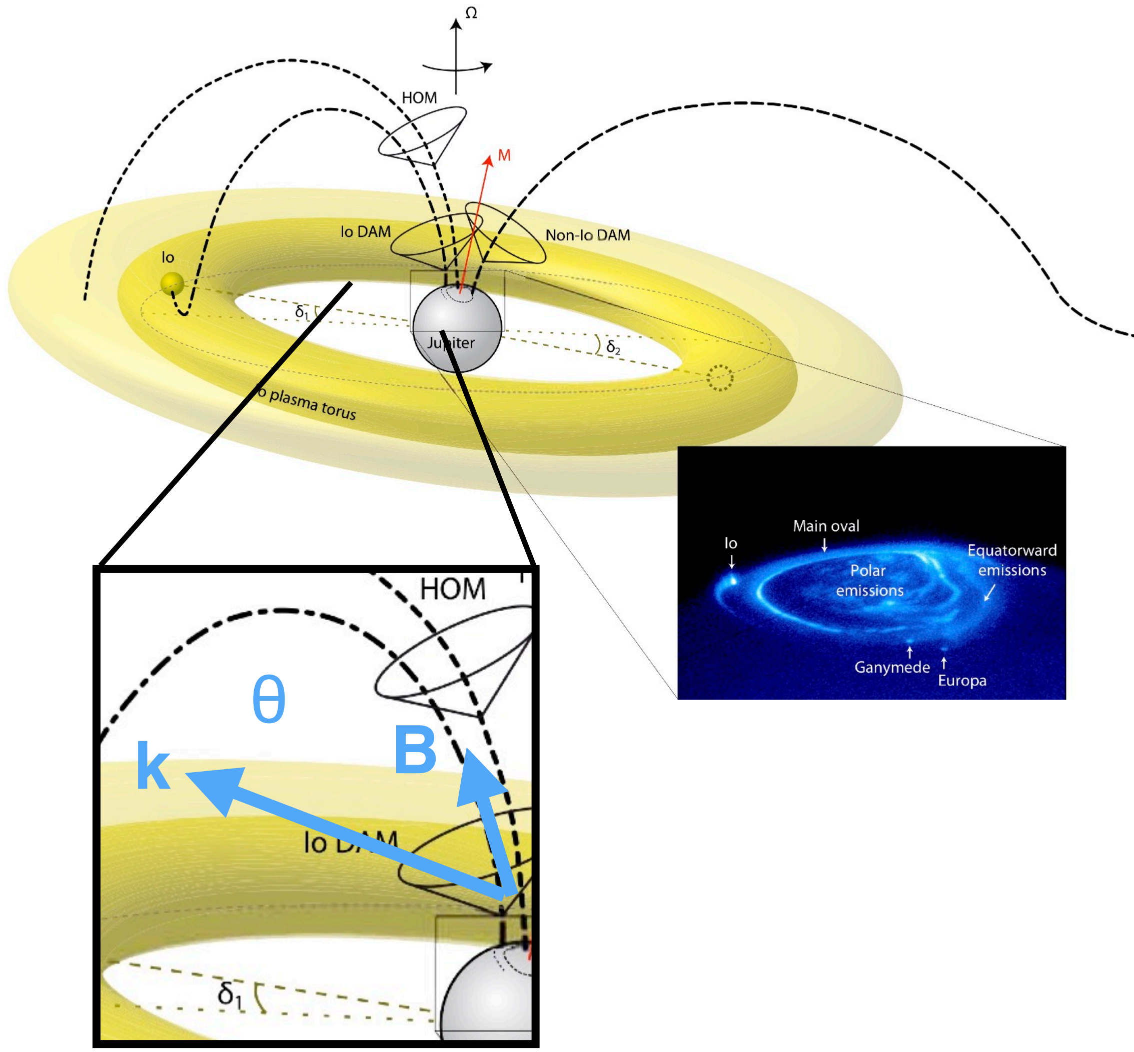

- Radio beaming angle
- Electrons energy
- Ultra-fine structures

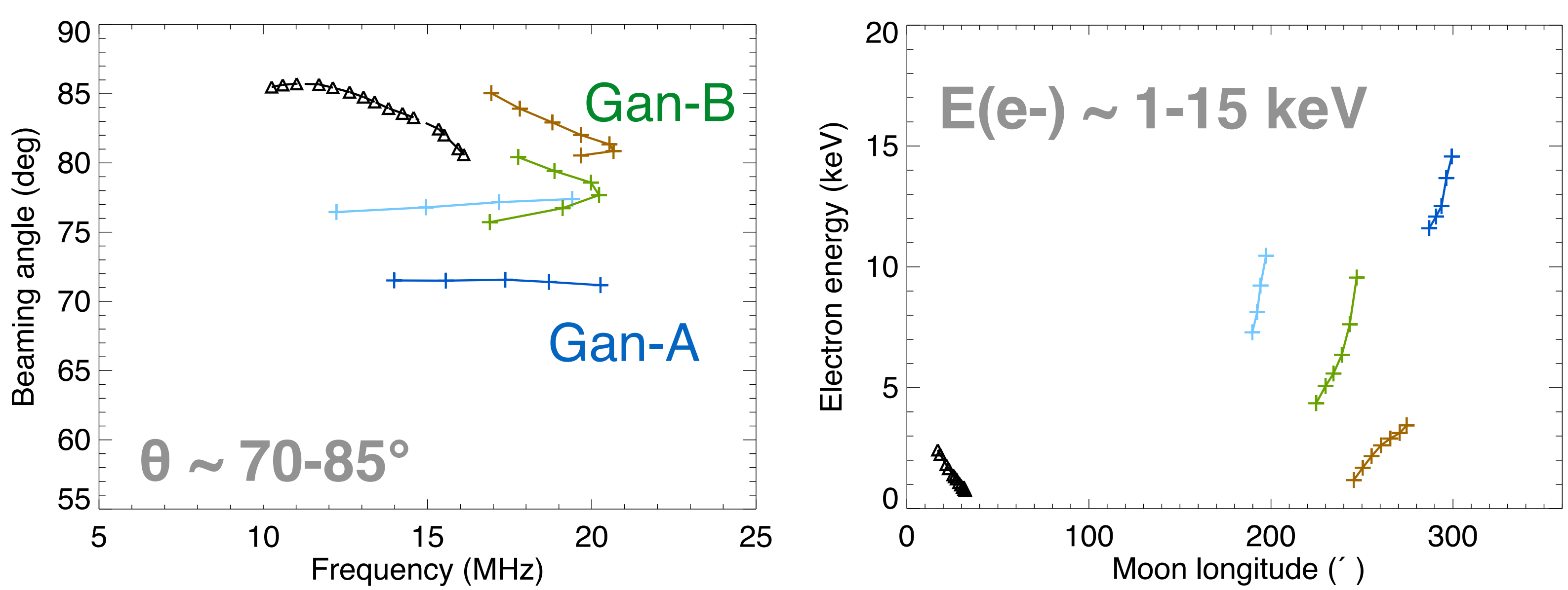

Pulsars with NenuFAR

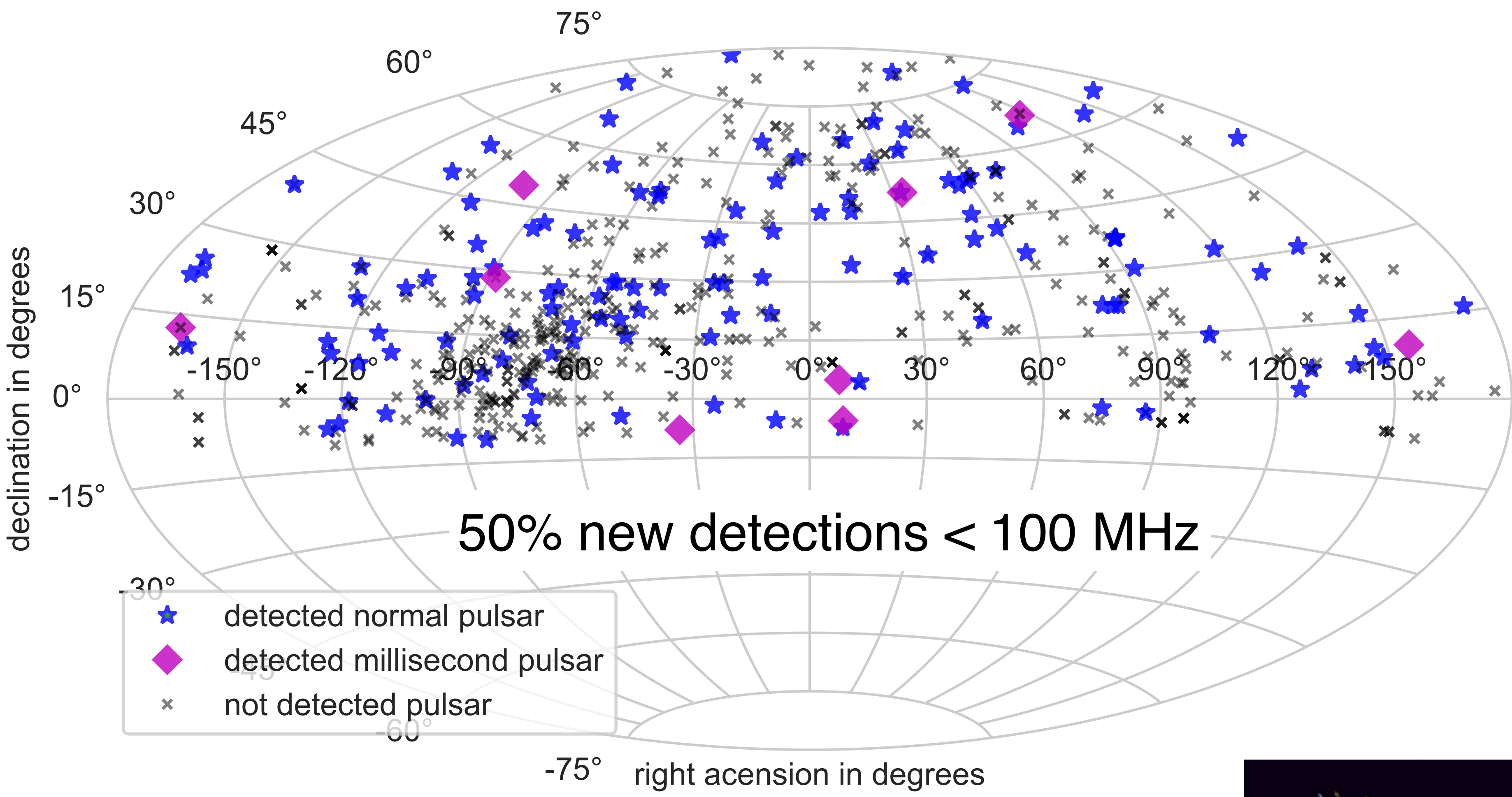

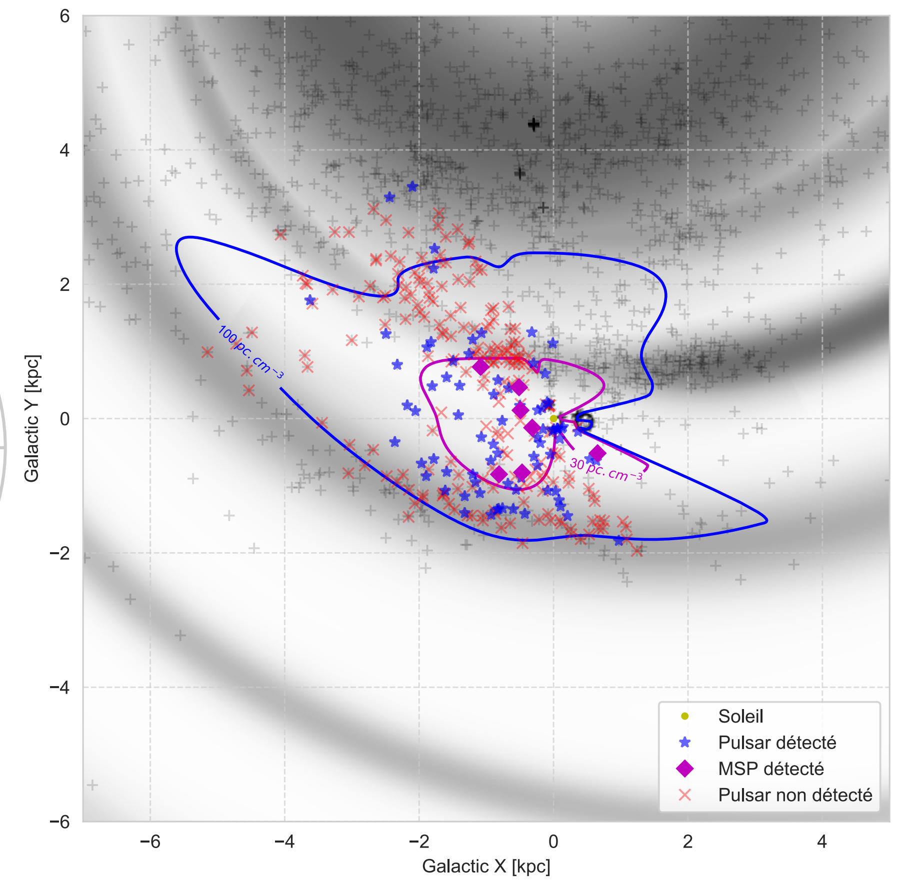

Crab giant pulses

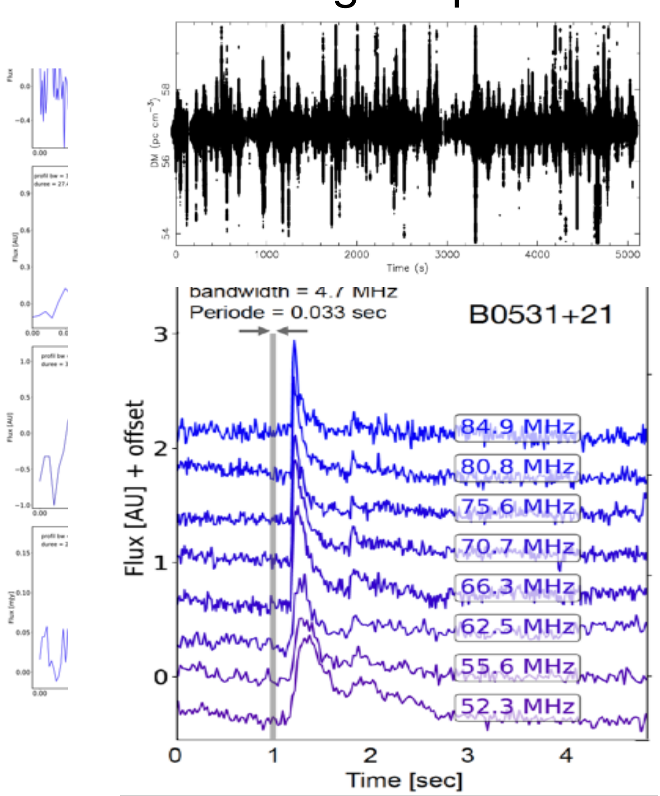

Millisecond pulsars

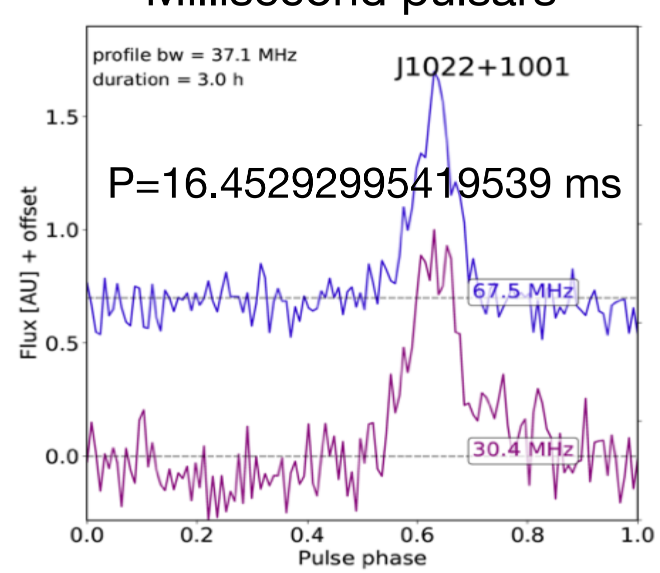

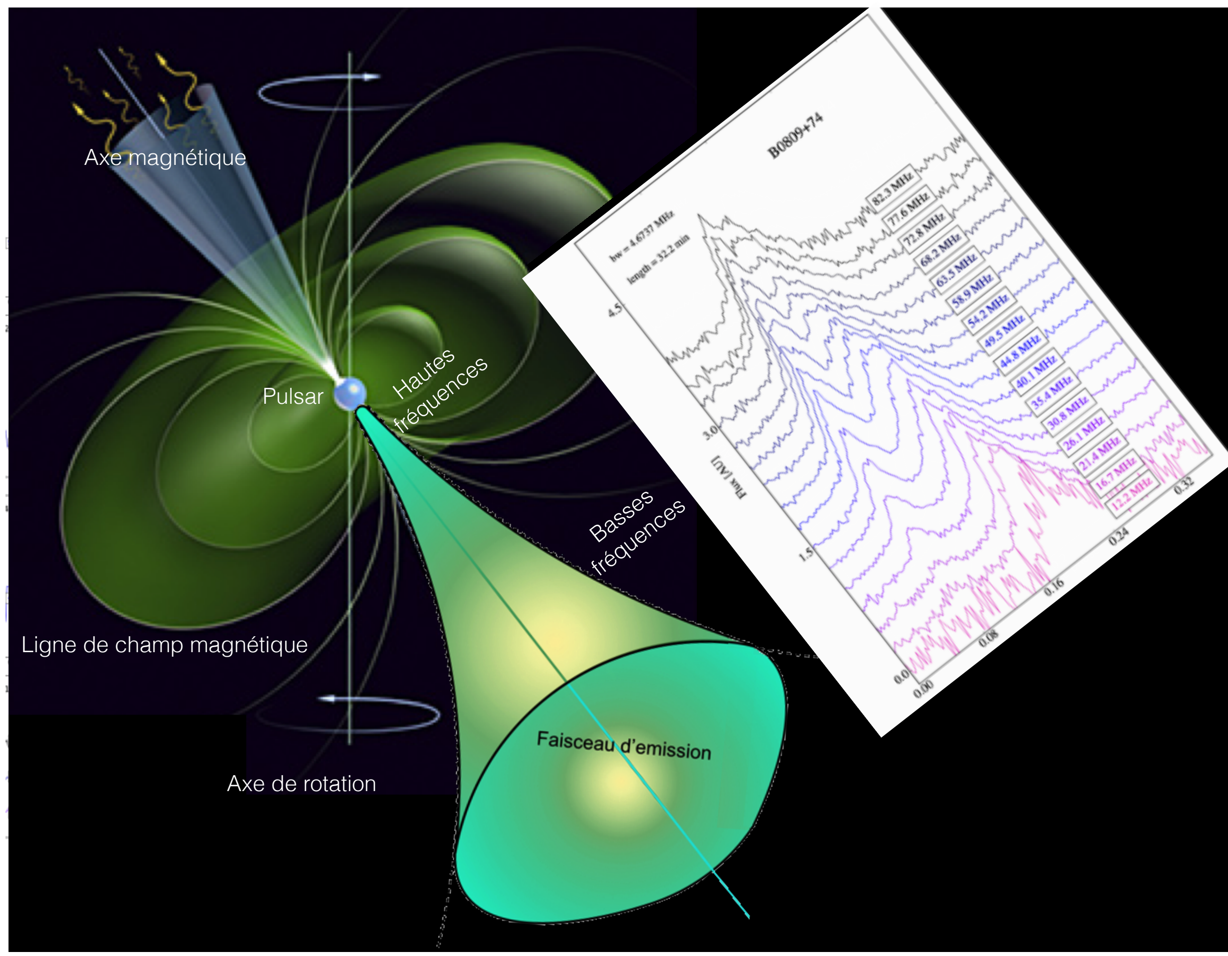

Sun’s observations with NenuFAR

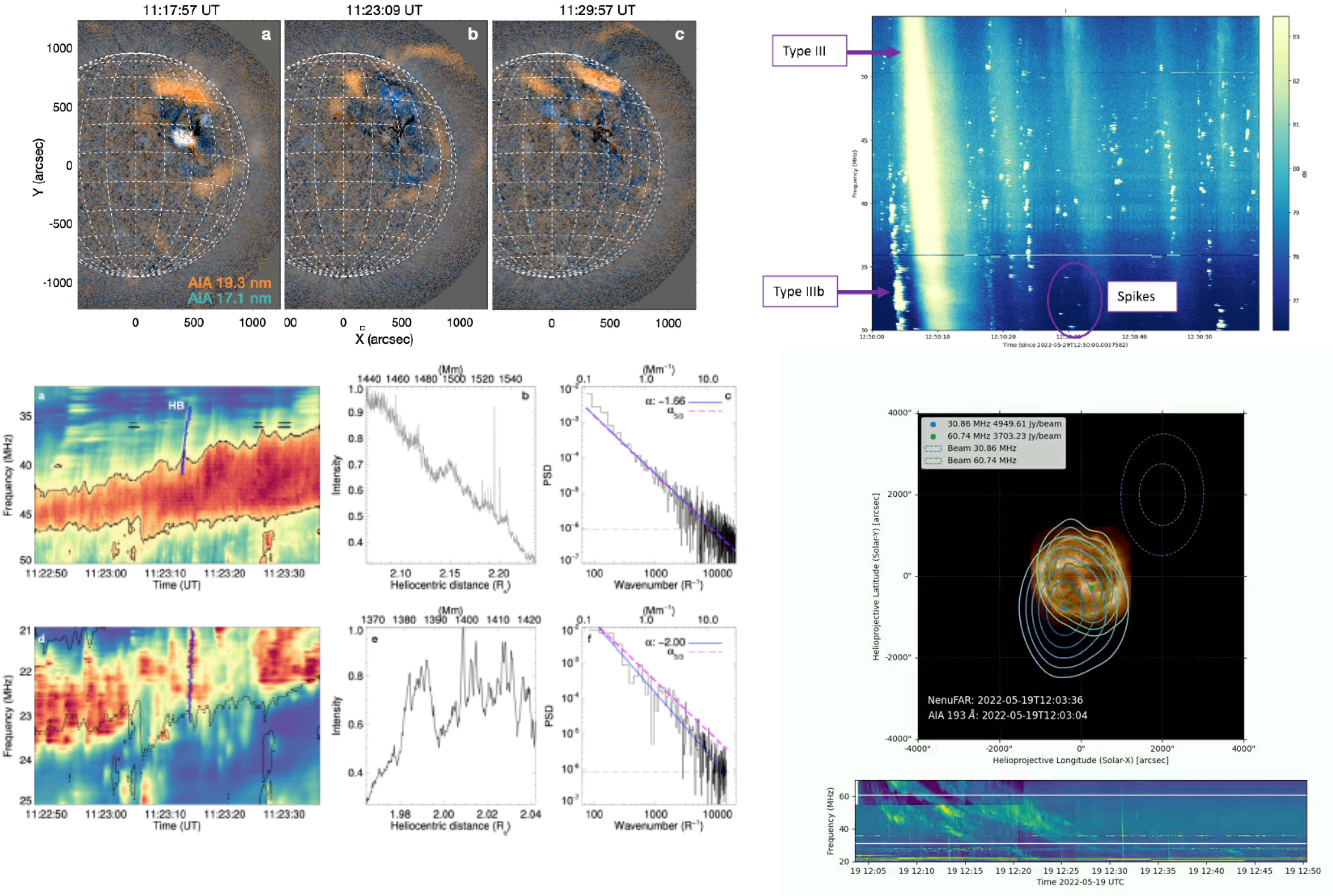

Radio recombination lines in the ISM

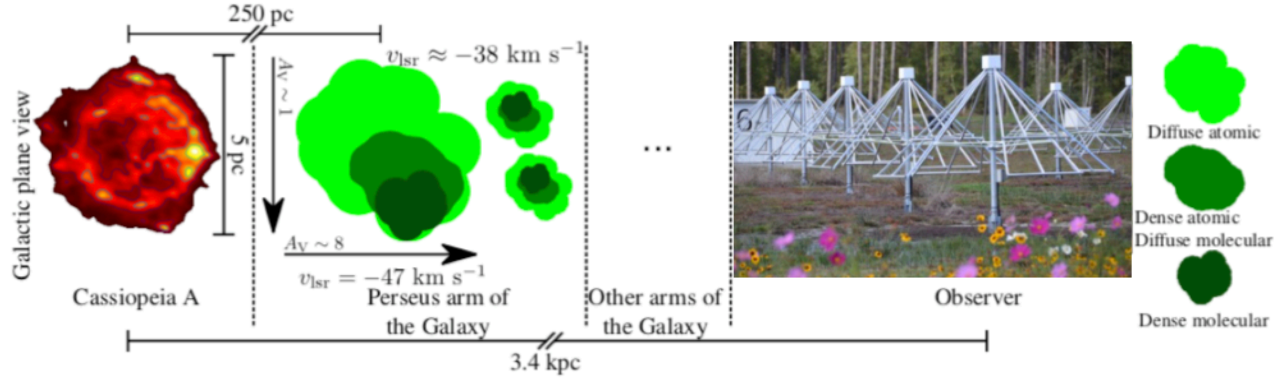

- High SNR detection

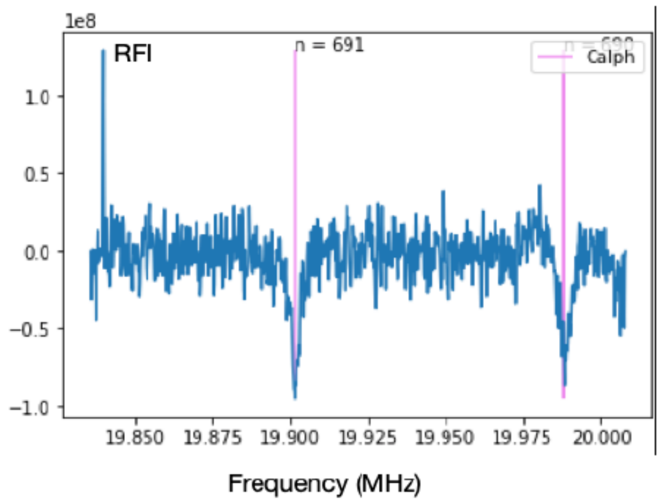

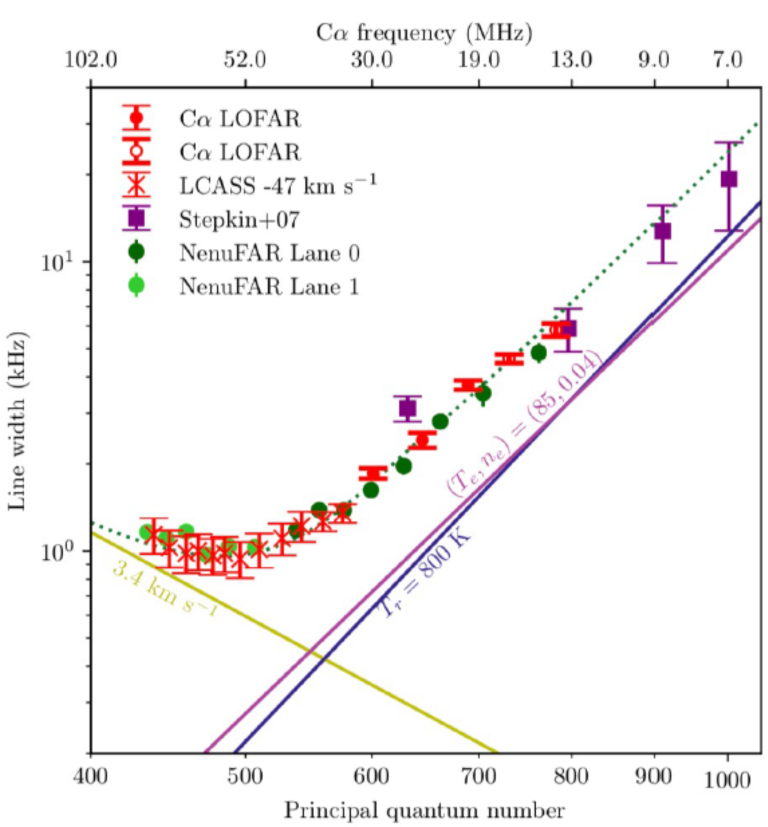

- Tau A : first detection of RRLs

Sensitivity : 8 x 10^{-5}

Line amplitude : 3.3 x 10^{-4} (4σ)

Tau A
December 2021
15 h of observations, equivalent integration 930 h.

C628 alpha -C689 alpha

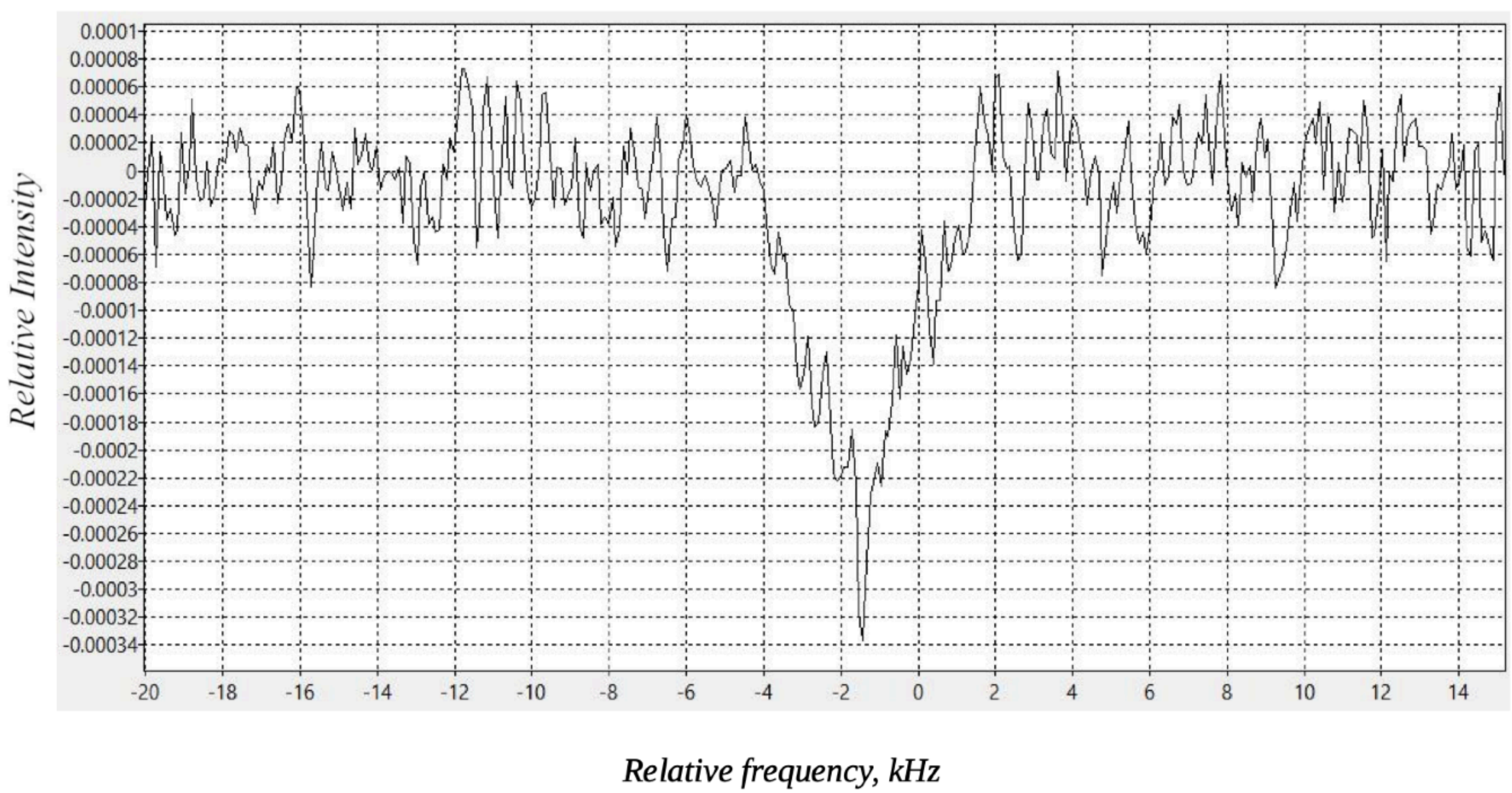

Cosmic Ray showers with NenuFAR

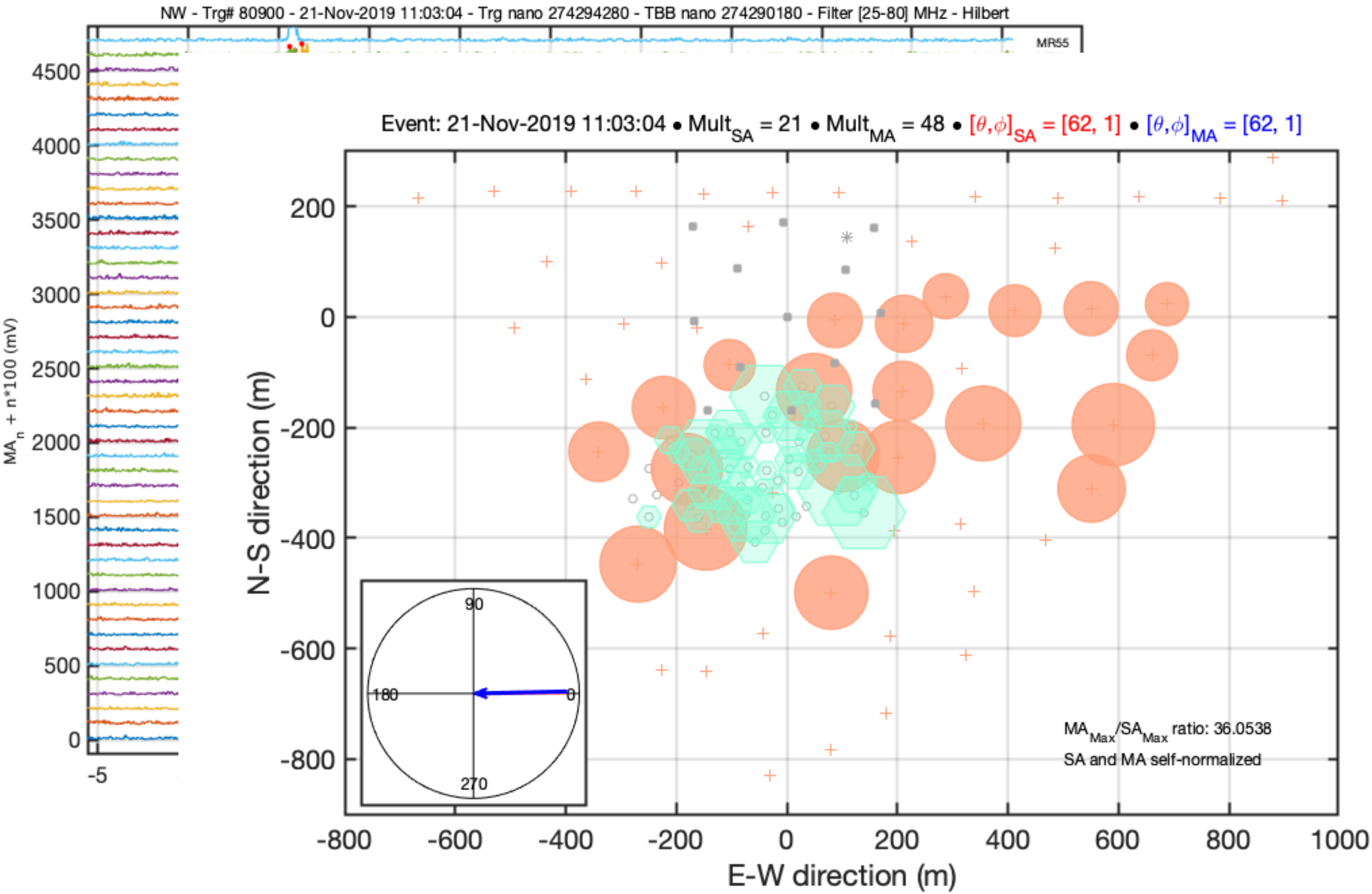

The cost of the digital revolution : data throughput, storage and processing

- Real-time acquisition : From Blue Gene to COBALT (CPU/GPU cluster)

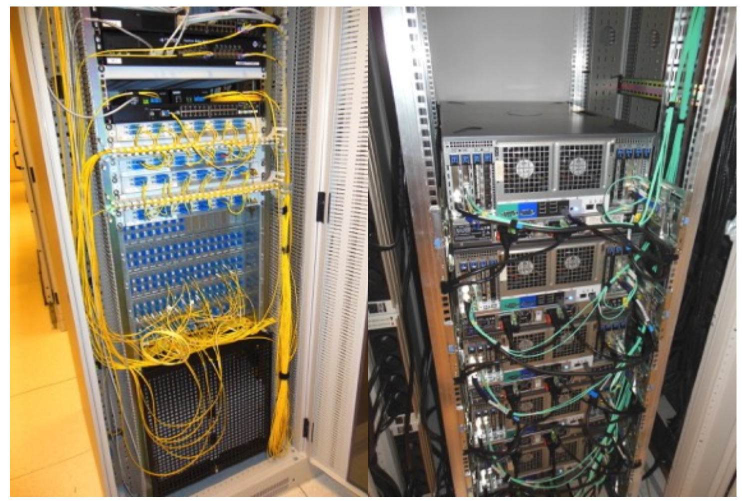

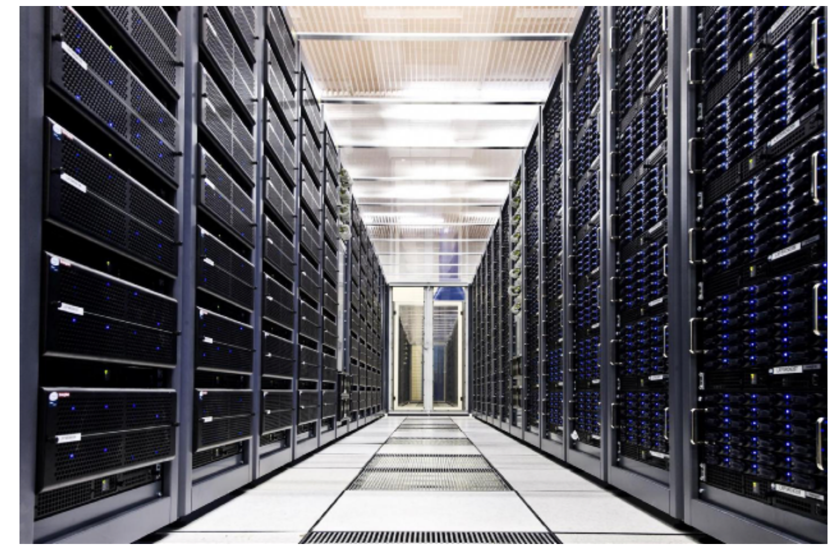

- Post-processing (CPU/GPU cluster)

- Long-term storage (LOFAR) : >30 Po, 3 sites, 10 M data files, > 1 Go/s

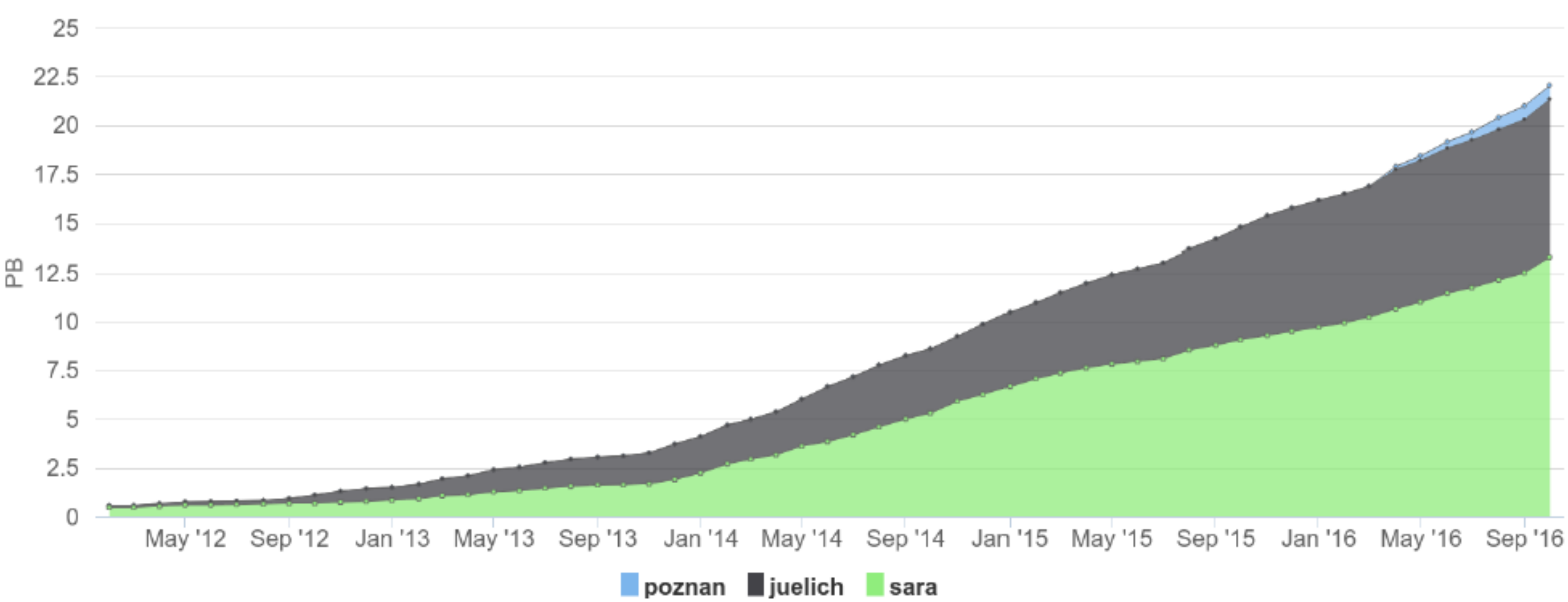

SKA (Square Kilometer Array)

http://www.skatelescope.org/

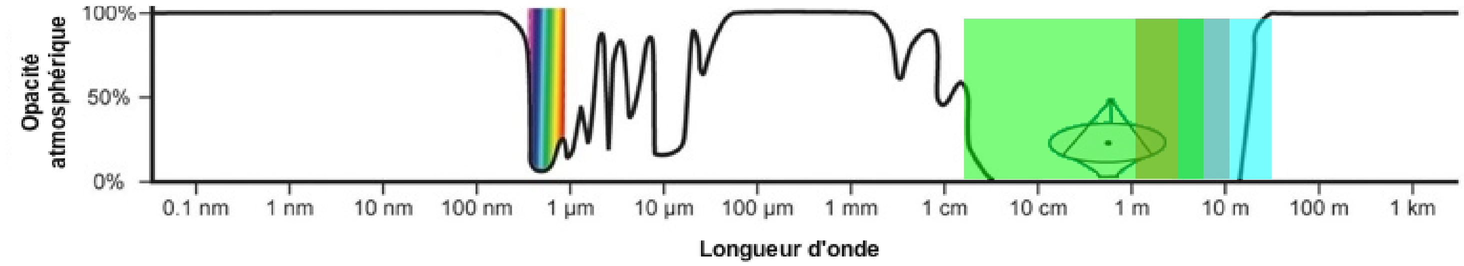

- Australia / South Africa
- Interferometer with many thousand antennas
- f = [50 MHz - 25 GHz]
  λ= [6 m, 1.2 cm]
- A_{eff} = 1 km²
- resolution => 0.001” @ 1.5 cm (20 GHz)
- FoV ~ 1°
- Full polarisation

Colossal data rate :
~500 PB / hour ~ 10000 PB / day
→ raw data storage impossible
→ calibration & real-time imaging = necessary

SKA-Mid : 350 MHz - >20 GHz
200 parabolas, South Africa

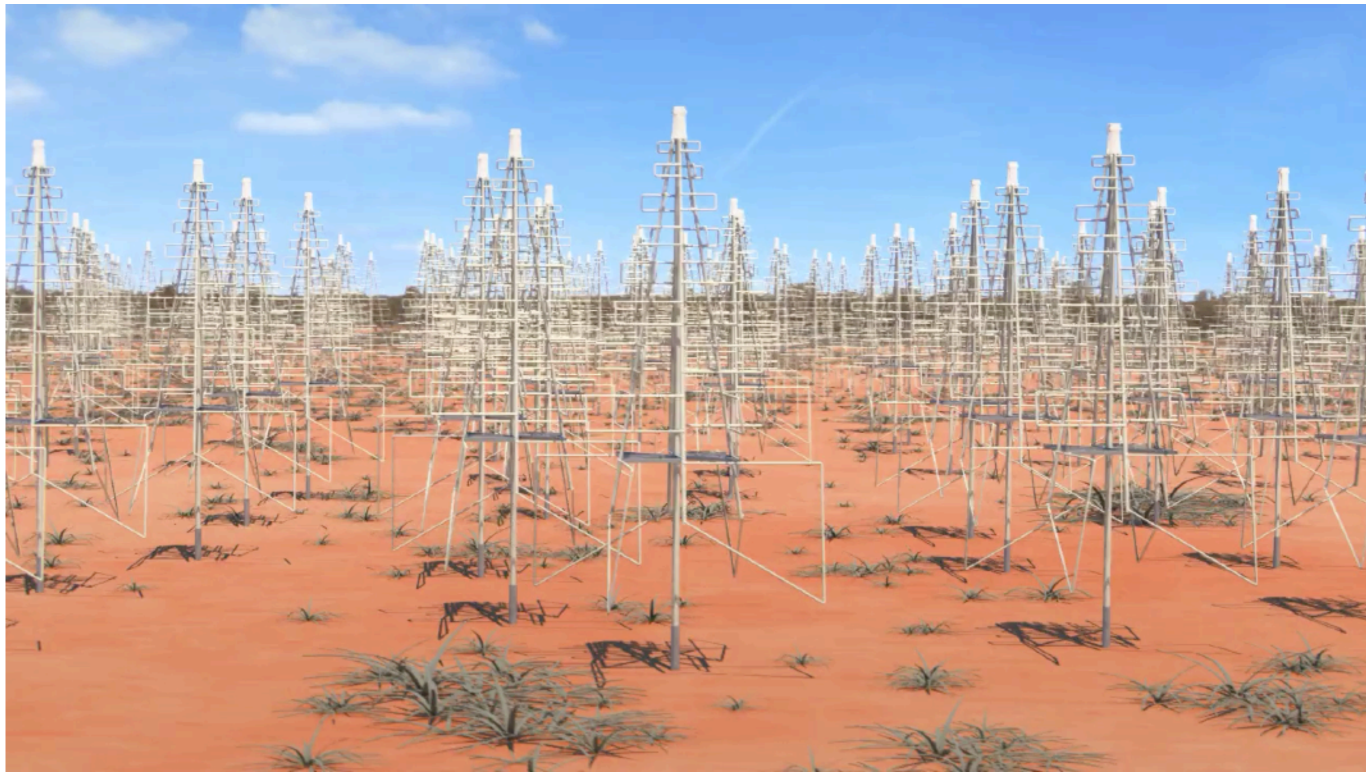

SKA-Low : 50-350 MHz
250000 antennas, Australia

SKA (Square Kilometer Array)

http://www.skatelescope.org/

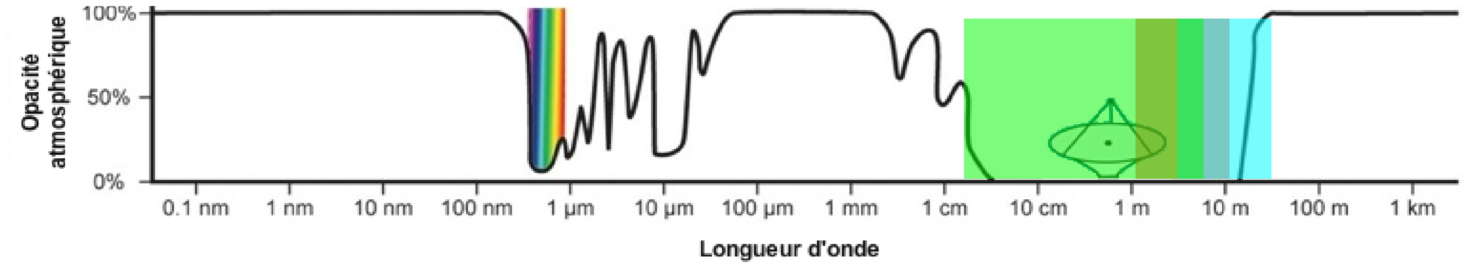

Organisation & Science Working Groups

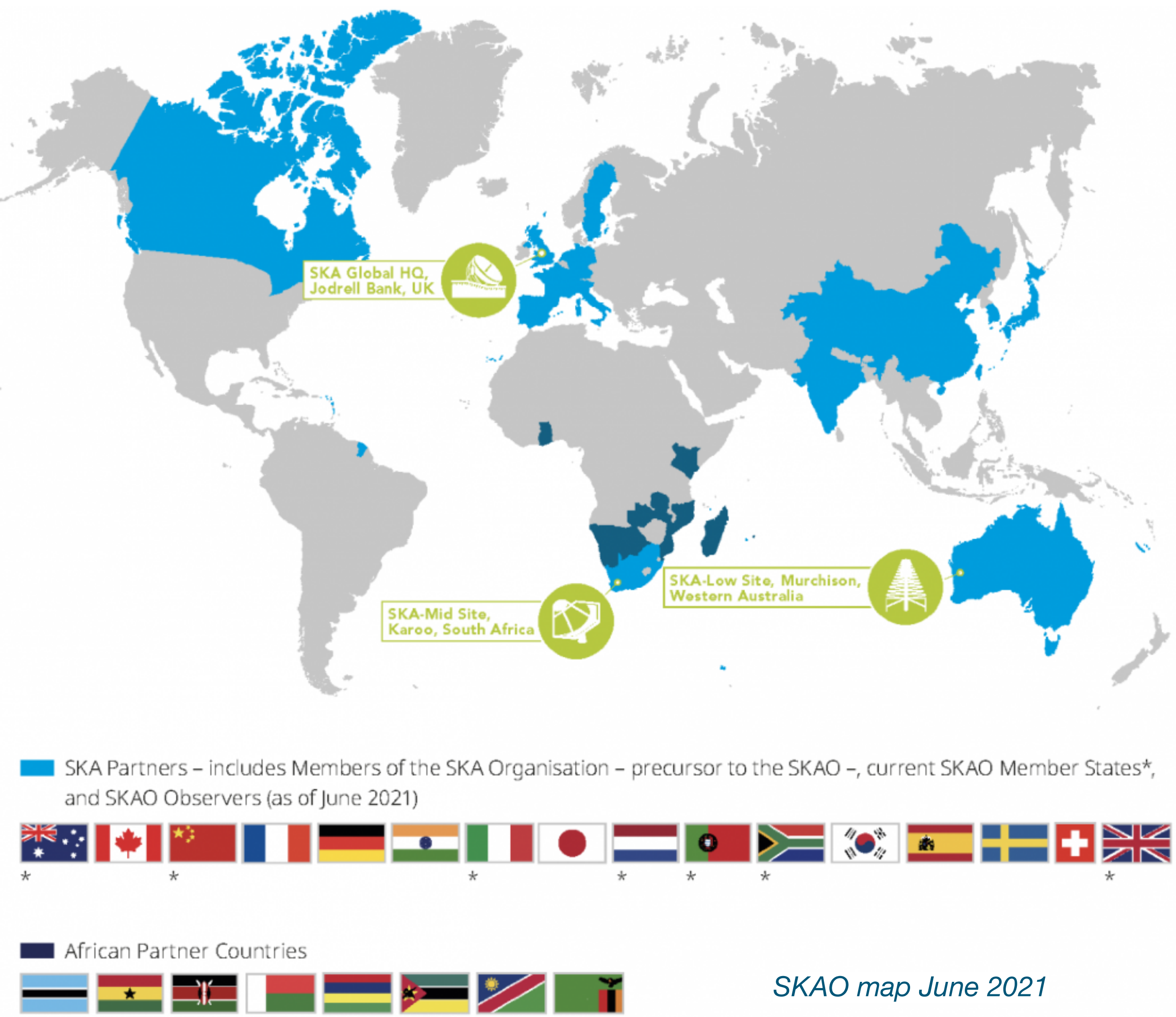

The Science Working Groups

- **Astrobiology ("The Cradle of Life")**
  - *Project Scientist:* Tyler Bourke
  - *Working Group Chair:* Melvin Hoare
- **Galaxy Evolution – Continuum**
  - *Project Scientist:* Jeff Wagg
  - *Working Group Chairs:* Nick Seymour & Isabella Prandoni
- **Cosmic Magnetism**
  - *Project Scientist:* Jimi Green
  - *Working Group Chairs:* Melanie Johnston-Hollitt & Federica Govoni
- **Cosmology**
  - *Project Scientist:* Jeff Wagg
  - *Working Group Chair:* Roy Maartens
- **Epoch of Reionisation & the Cosmic Dawn**
  - *Project Scientist:* Jeff Wagg
  - *Working Group Chair:* Leon Koopmans
- **Galaxy Evolution – HI**
  - *Project Scientist:* Jimi Green
  - *Working Group Chairs:* Lister Staveley-Smith & Tom Osterloo
- **Pulsars ("Strong field tests of gravity")**
  - *Project Scientist:* Jimi Green
  - *Working Group Chairs:* Ben Stappers & Michael Kramer
- **Transients**
  - *Project Scientist:* Tyler Bourke
  - *Working Group Chair:* Rob Fender

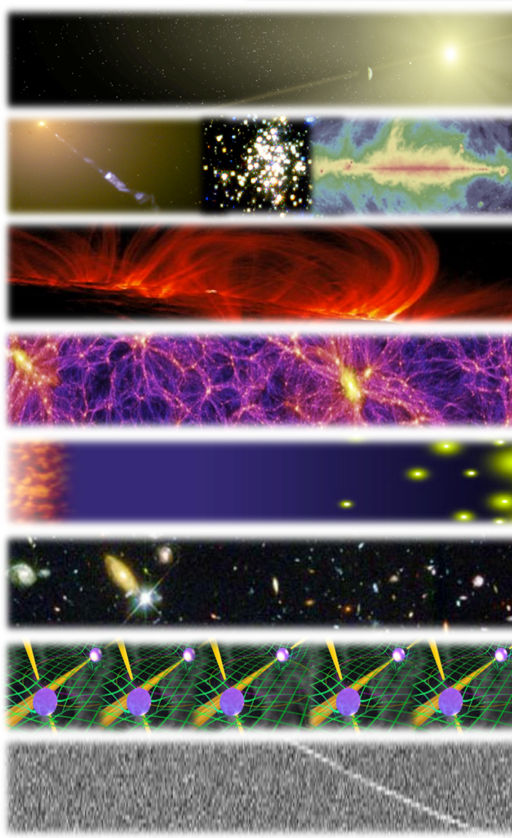

Exploring the Universe with the world's largest radio telescope

Radioastronomy in ~2005

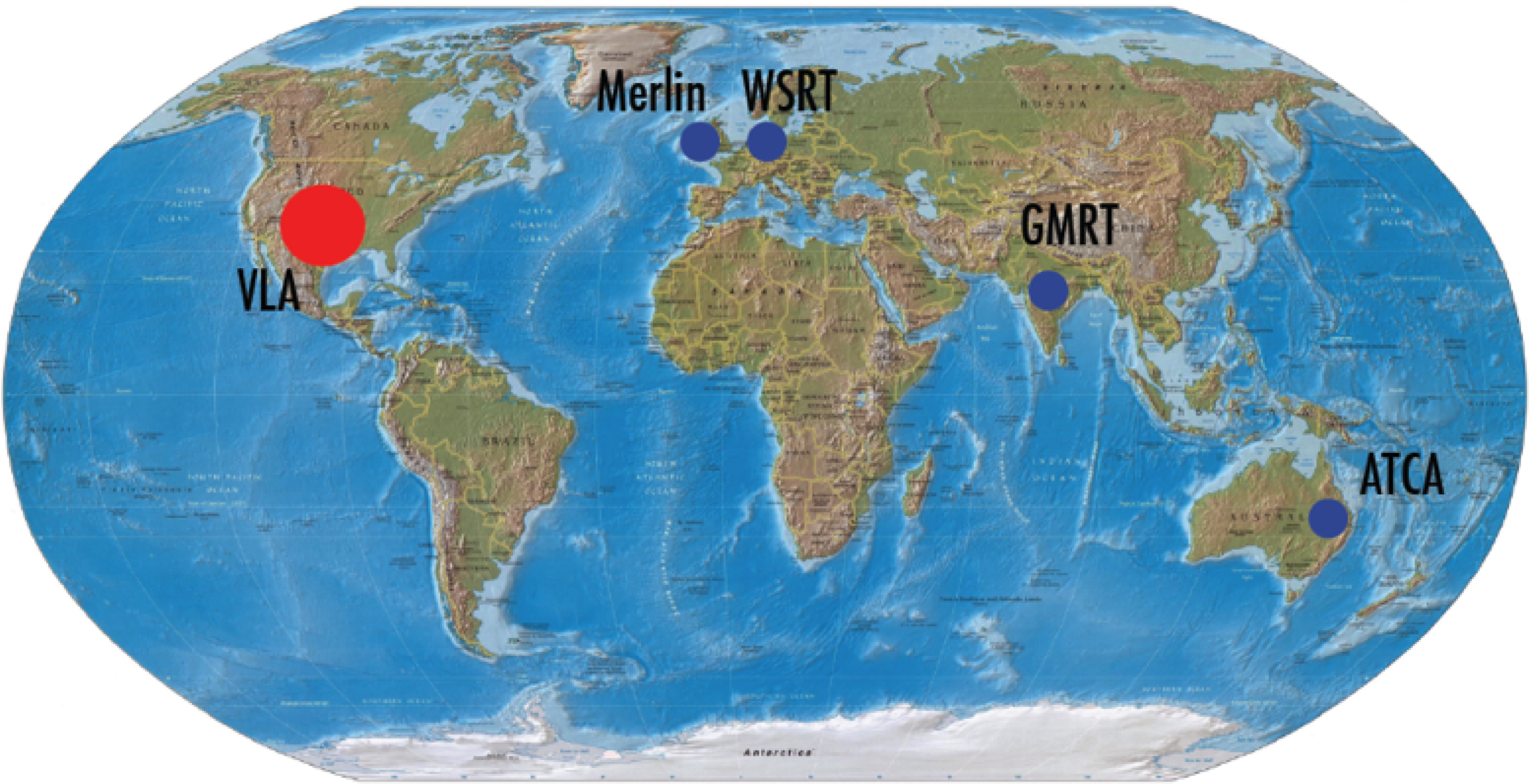

Radioastronomy in ~2010

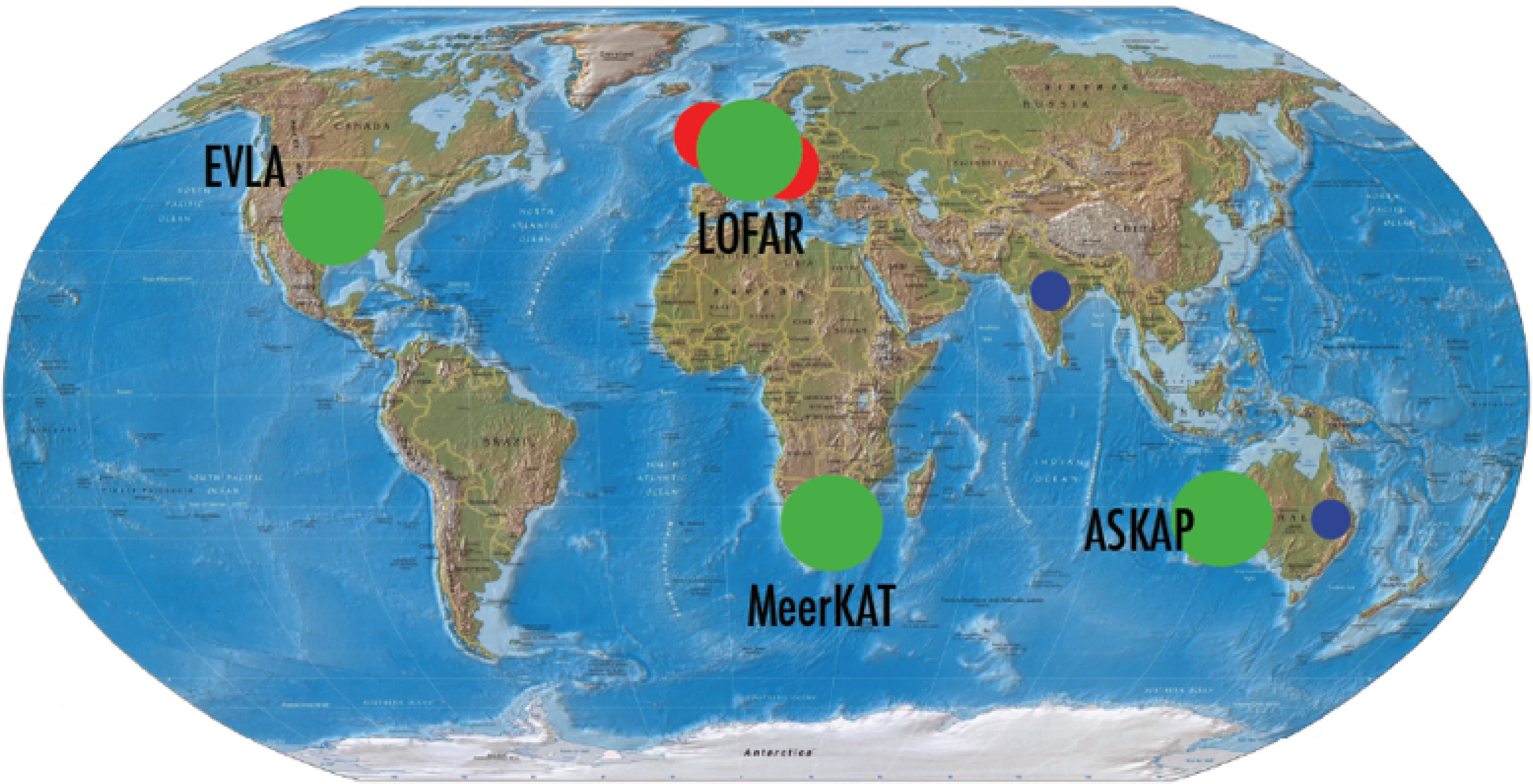

Radioastronomy in ~2015

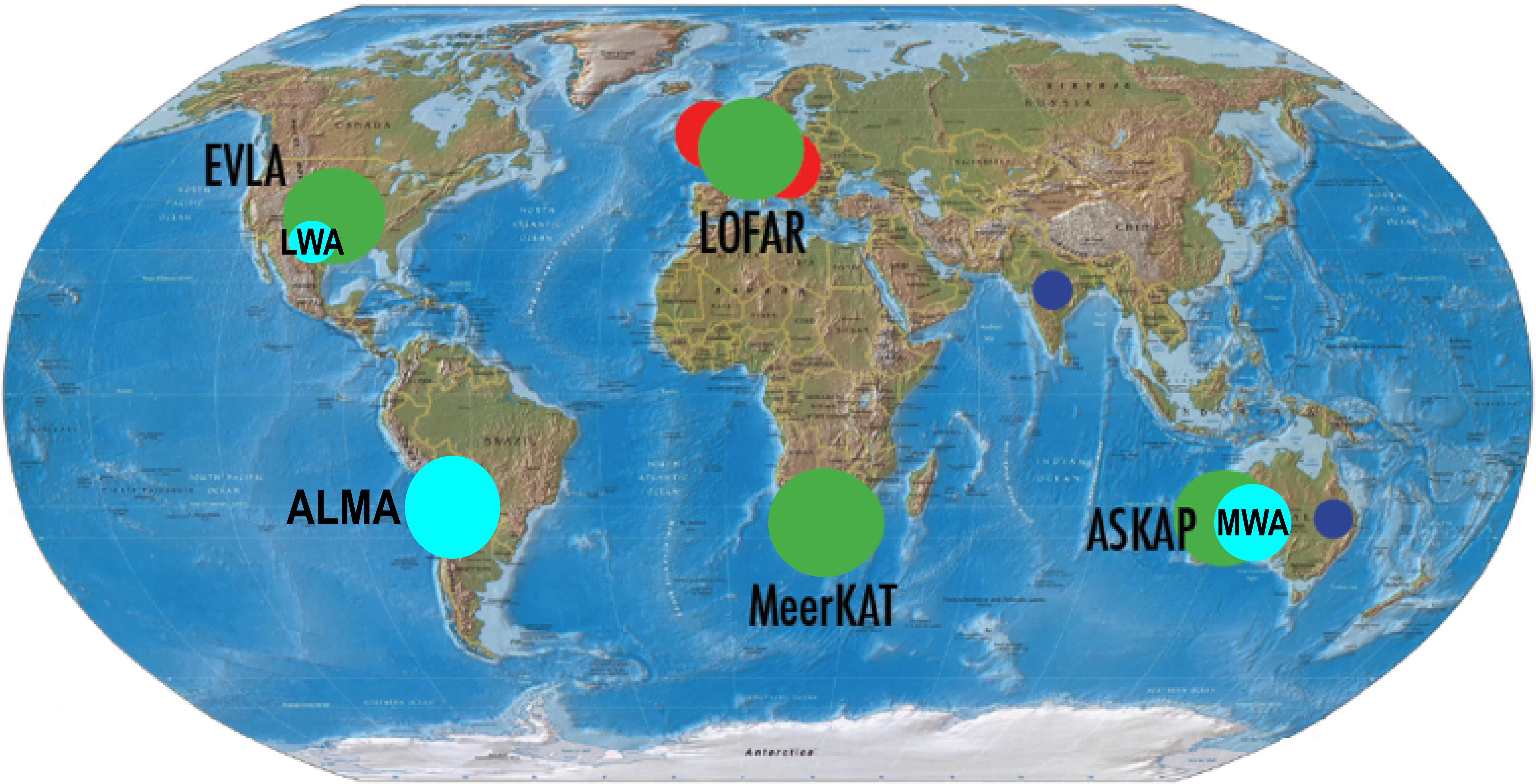

Radioastronomy in 2020+

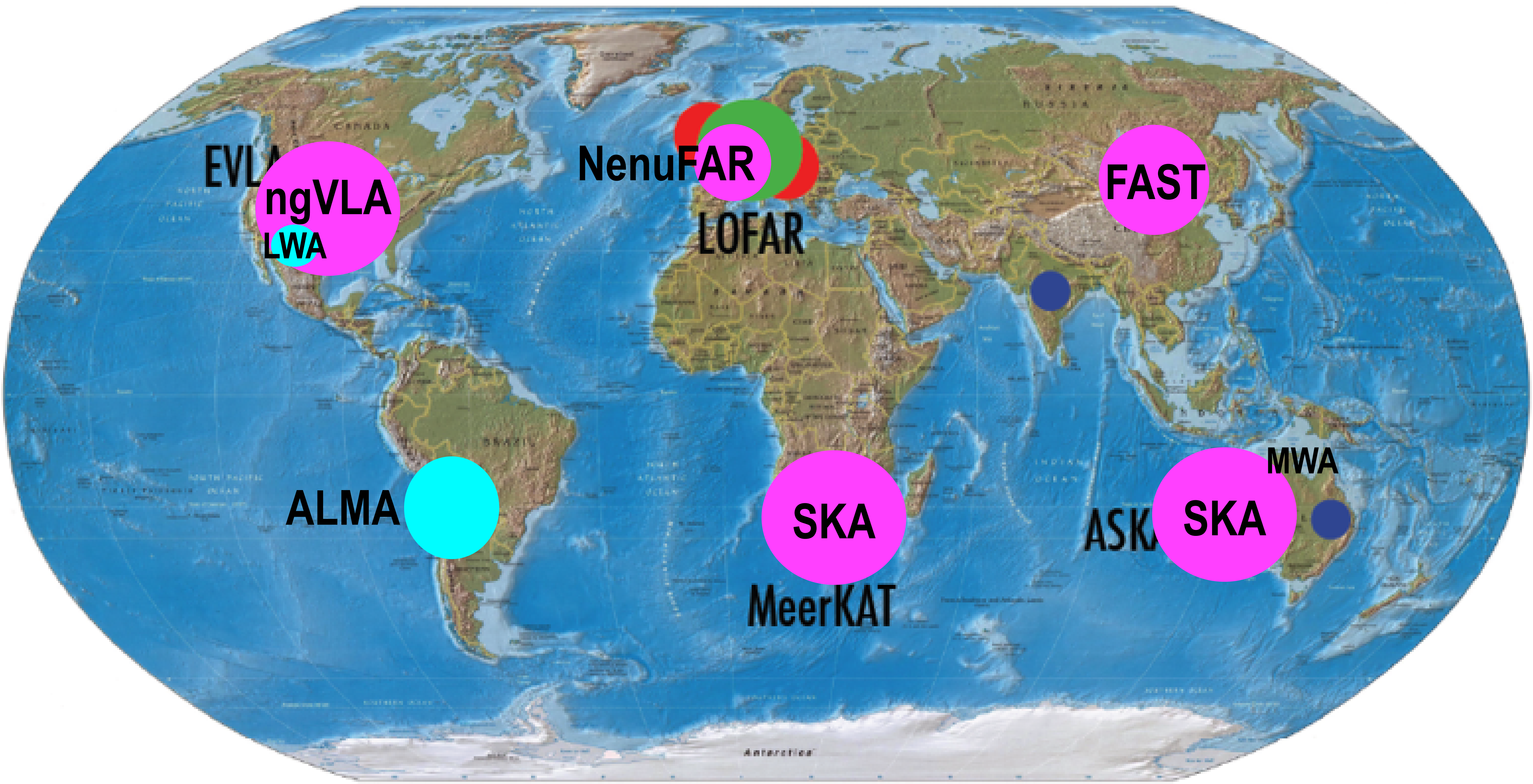

The end of history ?

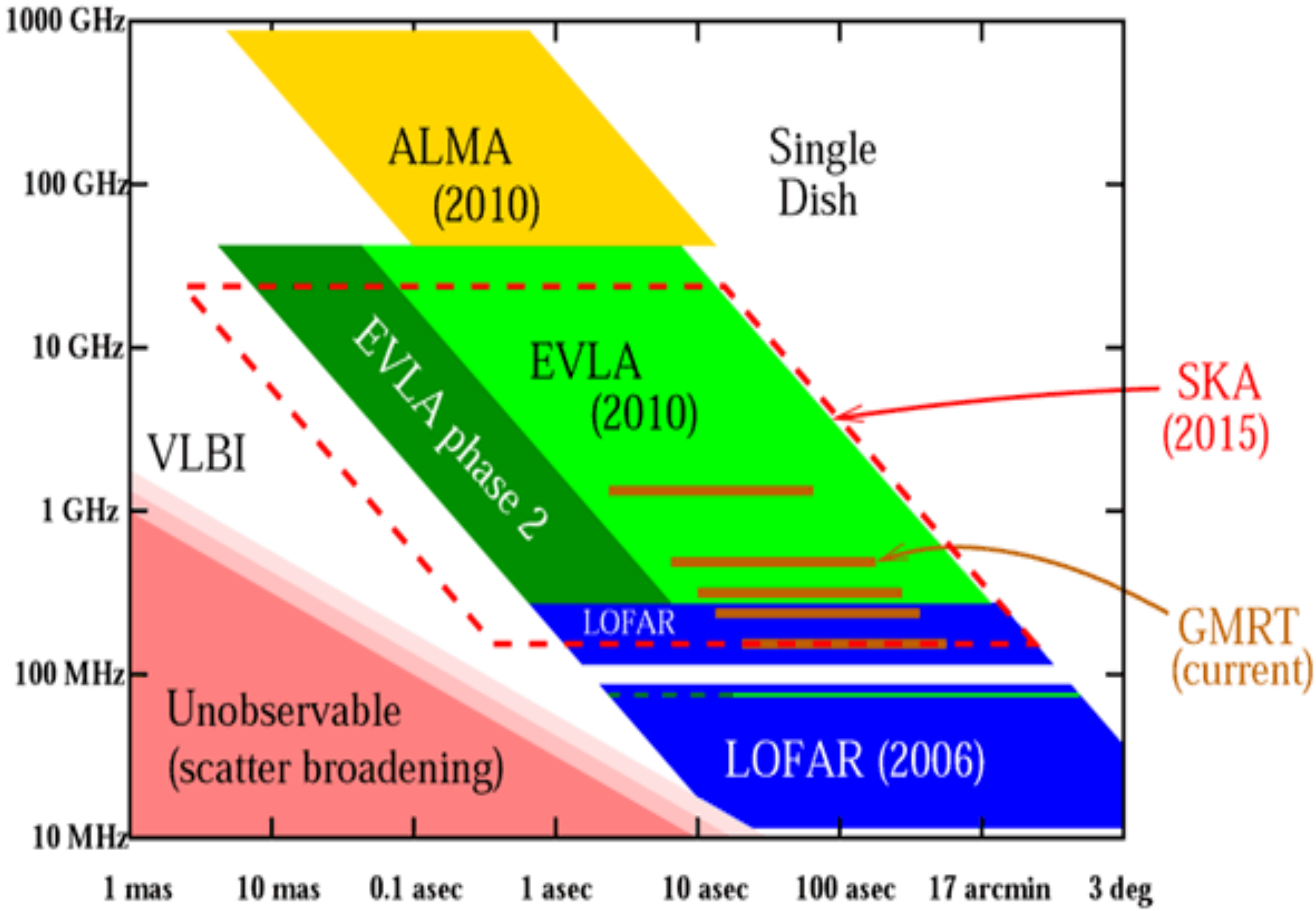

- Introduction (history, interest, specific features)
- Waves & Polarisation
- Plasmas & Propagation (cutoff, dispersion, Faraday effect, scintillations)
- Coherent Signal Detection (measurement theory, antenna temperature, calibration, noise)
- Receivers (heterodyne, system temperature, filtering, gain, RFI mitigation)
- Basics of Radio Astronomy Antennas: Single antennas
- Basics of Interferometry and Aperture Synthesis (phased arrays, electronic pointing, imaging, correlation, coherence, VLBI)
- Observation methods
- Large present & future ground-based radio arrays
- Basics of Space radio astronomy

• Space : access to $\lambda \leq 0.3$ mm & $\lambda \geq 30$ m (up to ~10 km in the Earth's vicinity)

HF - overcoming terrestrial atmospheric absorption

- antennas and receivers ≈ au sol *(e.g. Planck …)*

LF- $\nu \leq 10$ MHz (terrestrial ionospheric cutoff)

- most commonly used antennas: little cumbersome at launch, easy deployment, low mass

⇒ doubles-spheres (DC – ULF) *Cluster, Geotail …*

⇒ booms or wires (LF) *WIND, Ulysses, Cassini, Stereo …*

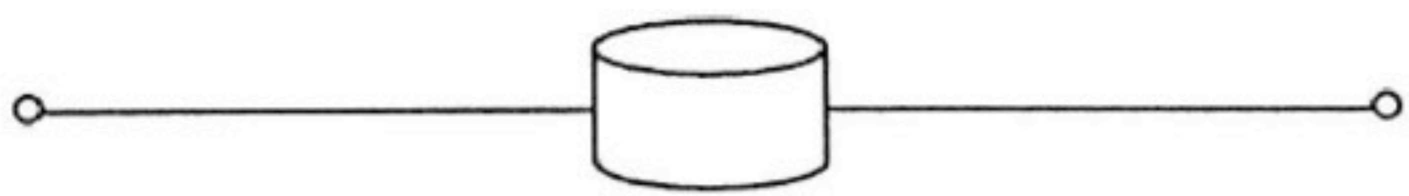

double-sphere probe

Cluster

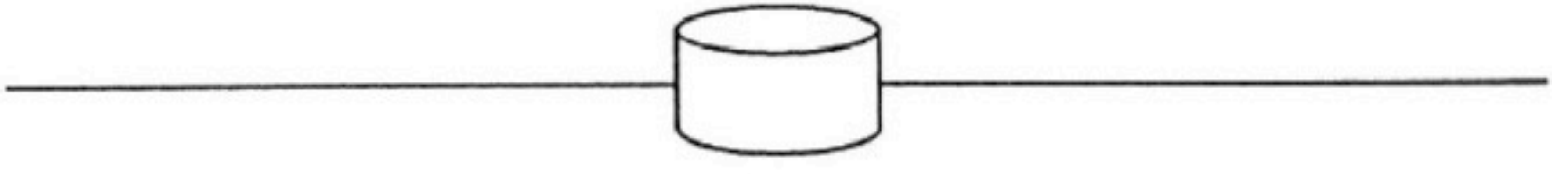

cylindrical antenna

Cassini

- Doubles-spheres antenna

Radiation pattern of 2 spheres in phase ≡ interferometer with 2 antennas :

$P(\theta) \propto \sin^2(\pi\, d \cos\theta / \lambda)$

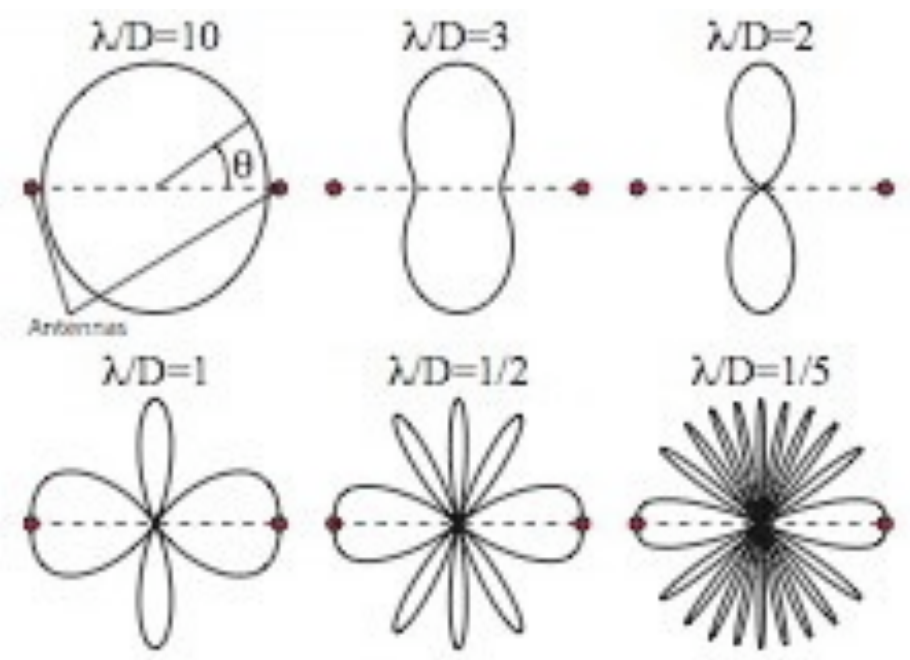

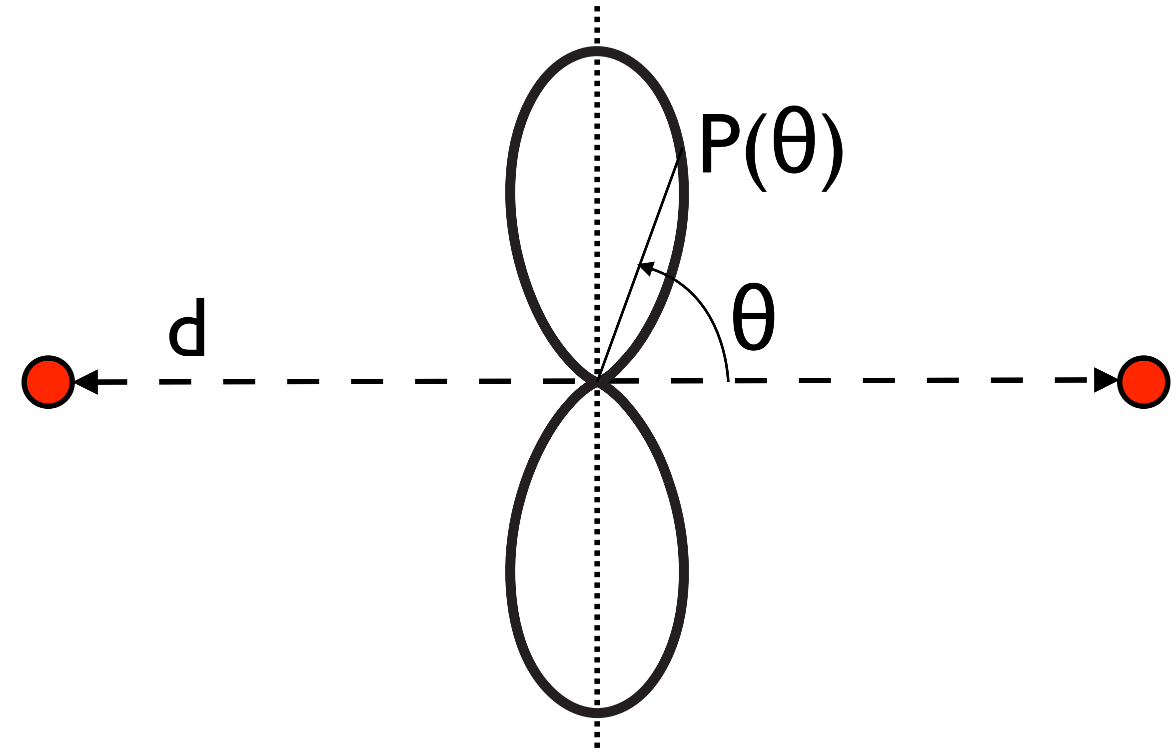

If the spheres are in phase opposition ⇒ diagram rotates by π/2

$P(\theta) \propto \cos^2(\pi\, d \cos\theta / \lambda)$

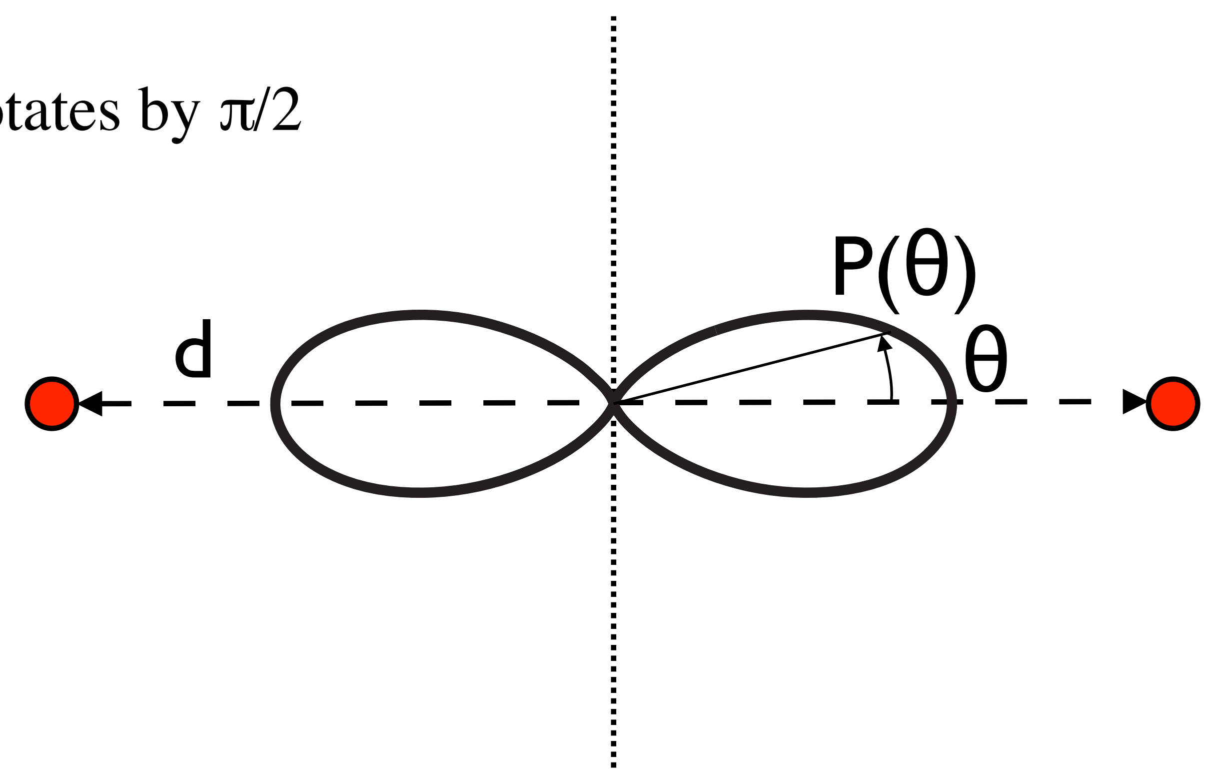

• Short dipole : $h << \lambda$

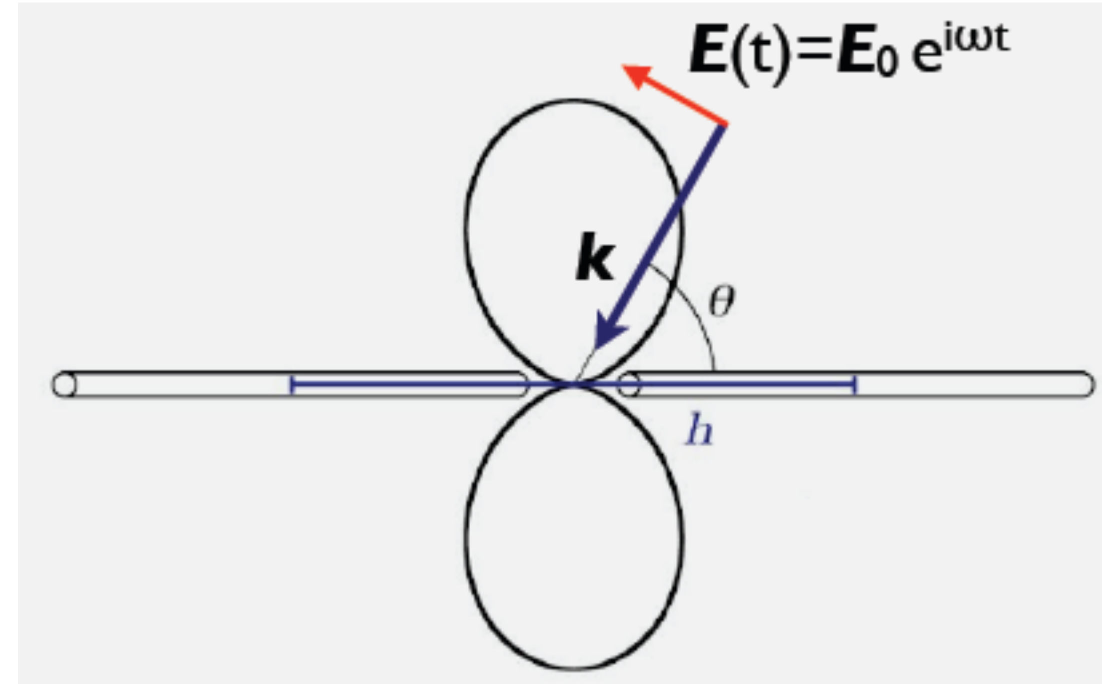

E (transverse) in phase along the antenna

$\Rightarrow$ uniform j along the antenna

We measure the voltage difference between the two wires

$V = \mathbf{h_{eff}.E} = h\ E_o \sin\theta\ e^{i\omega t}$

$\Rightarrow g(\theta) \propto \langle V.V^* \rangle = C \times \sin^2\theta$

3 dB aperture : $g(\theta) = g_{max}/2 \quad \Rightarrow \quad \theta = 45° \ \Rightarrow$ 3 dB aperture = 90°

Directivity : $1/4\pi \times \int_{4\pi} g(\theta)\, d\Omega = 1/4\pi \times \int_{4\pi} C.\sin^2\theta \times 2\pi \sin\theta\, d\theta = 1 \quad \Rightarrow \quad C = 3/2$

Effective area (lossless) : $g_{max} = C = 3/2 = 4\pi/\Omega = 4\pi A_{eff}/\lambda^2$

$\Rightarrow \quad A_{eff} = 3\lambda^2/8\pi$ [m²], unrelated to the geometric surface

Main lobe : $\Omega = 8\pi/3$ [sr]

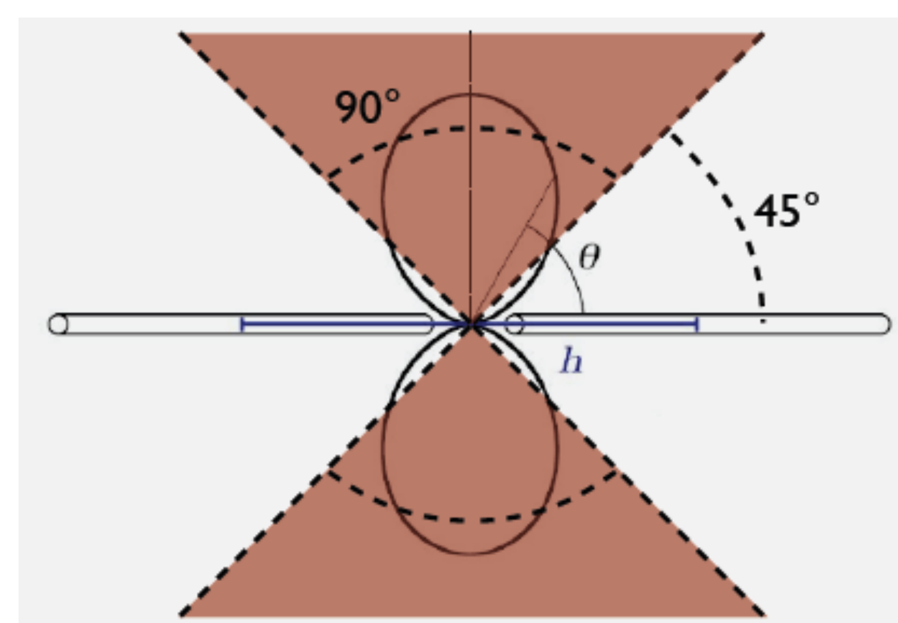

Received flux density : $S = E^2 / Z_o\, b$ [$Wm^{-2}Hz^{-1}$]

$= V^2 / Z_o\, b\, h^2$

with b the reception bandwidth

$= ½\, B\, \Omega = 4\pi/3\, B$

(½ for the polarisation of the antenna)

Sensitivity of the observations :

$(S_{min}\, Z_o\, h^2)^{1/2} = V / b^{1/2}$ [$V.Hz^{-1/2}$] characterises the sensitivity of on-board radio receivers

→ at present ~ 5 – 10 nV/$Hz^{1/2}$ *(LESIA)*

⇒ $S_{min} = 1.5 – 6 \times 10^{-22}\ Wm^{-2}Hz^{-1}$ with antenna length h = 20 m

Sensitivity is limited at high frequencies (≥ 1 MHz) by galactic background noise

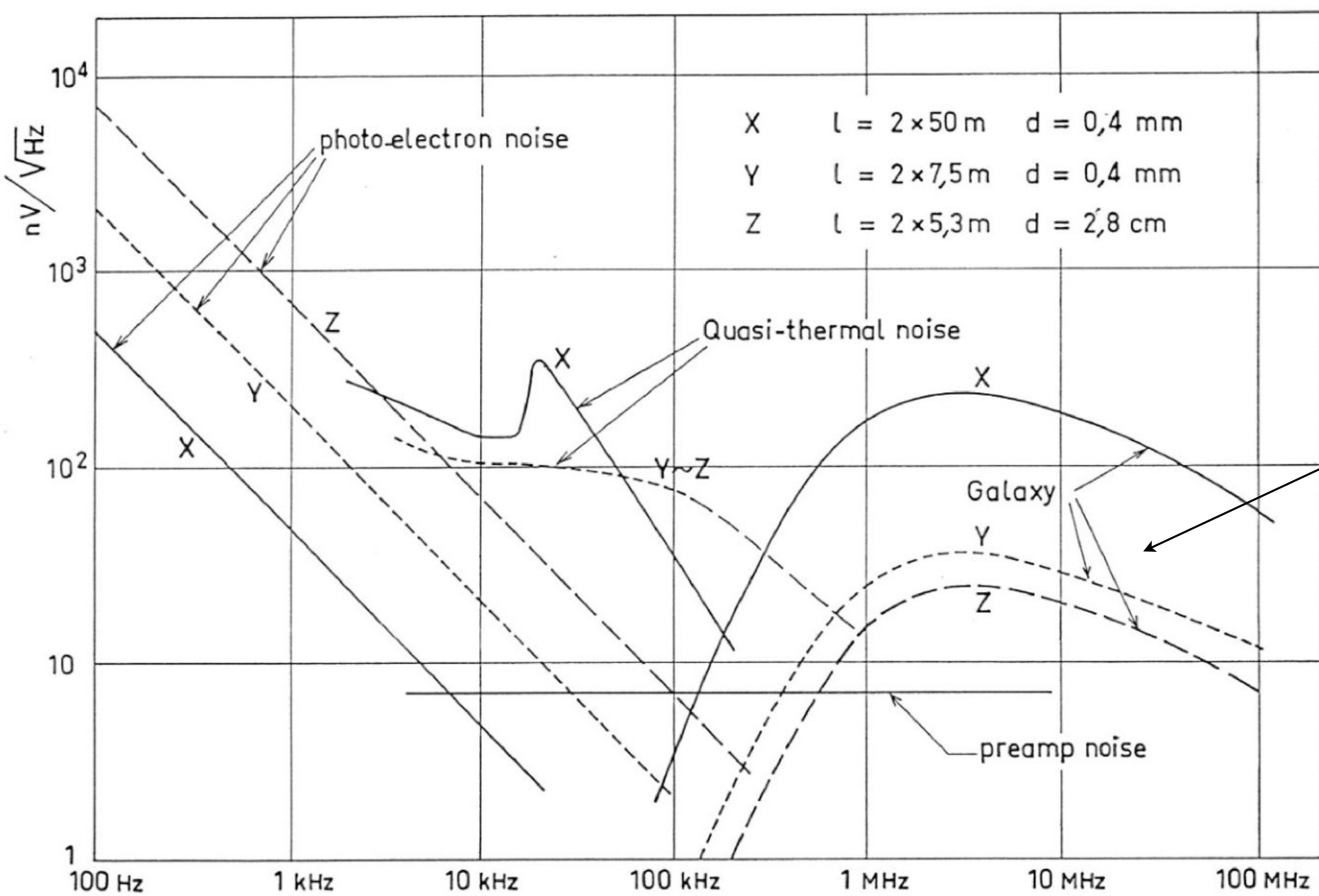

$$S_g = \left[I_g f^{-0.52} \left(\frac{1-e^{-\tau}}{\tau} \right) + I_{eg} f^{-0.8} e^{-\tau} \right] \times \Omega \times \eta$$

0.5 MHz ≤ f ≤ 20 MHz, Ω=8π/3

• Dipole : case $h \geq \lambda$

Non-uniform current distribution on the antenna : $I(z) = I_o \sin [2\pi/\lambda \times (h - |z|)]$

$E(\theta) = \int_{antenne} dE(\theta)$ (contributions of elementary dipoles)

$\Rightarrow$ $g(\theta) \propto [\cos(2\pi L/\lambda \times \cos\theta) - \cos(2\pi L/\lambda)] / \sin\theta$

$\Rightarrow$ apparition of multiple lobes

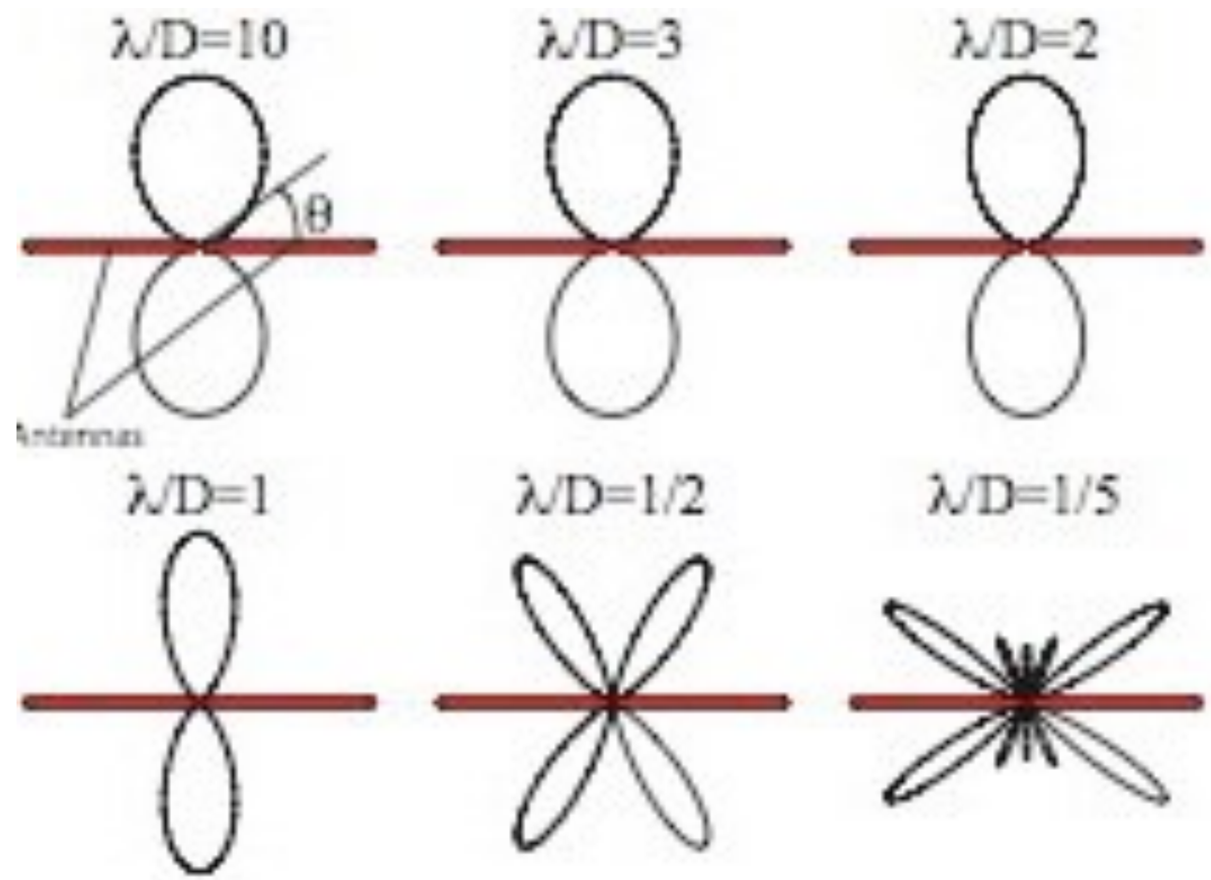

- Antenna configuration / layout

→ 3-axis stabilised spacecraft: *Voyager, Galileo, Cassini, Stereo …*

Tubular antennas (booms) h = 6 – 10 m
Monopoles frequently used (+ spacecraft as a reflecting surface ⇒ response ≈ dipole)
Very poor angular resolution (λ/h >>)
⇒ Development of the « Direction-Finding » technique (Gonio-Polarimetry)
= determination of the **k** vector (+ wave polarisation)
→ restoration of ~1-2° angular resolution (requires precise calibration)

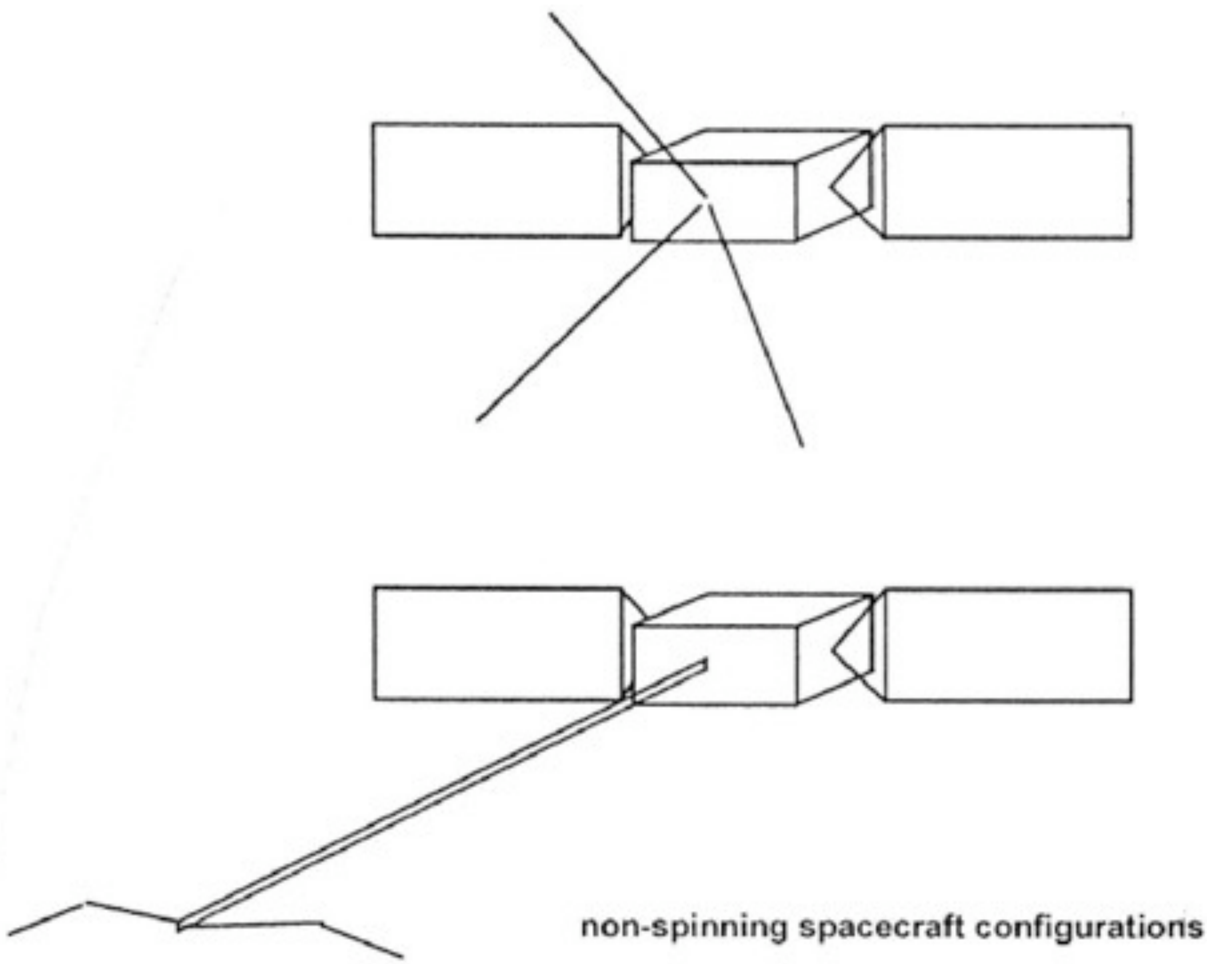

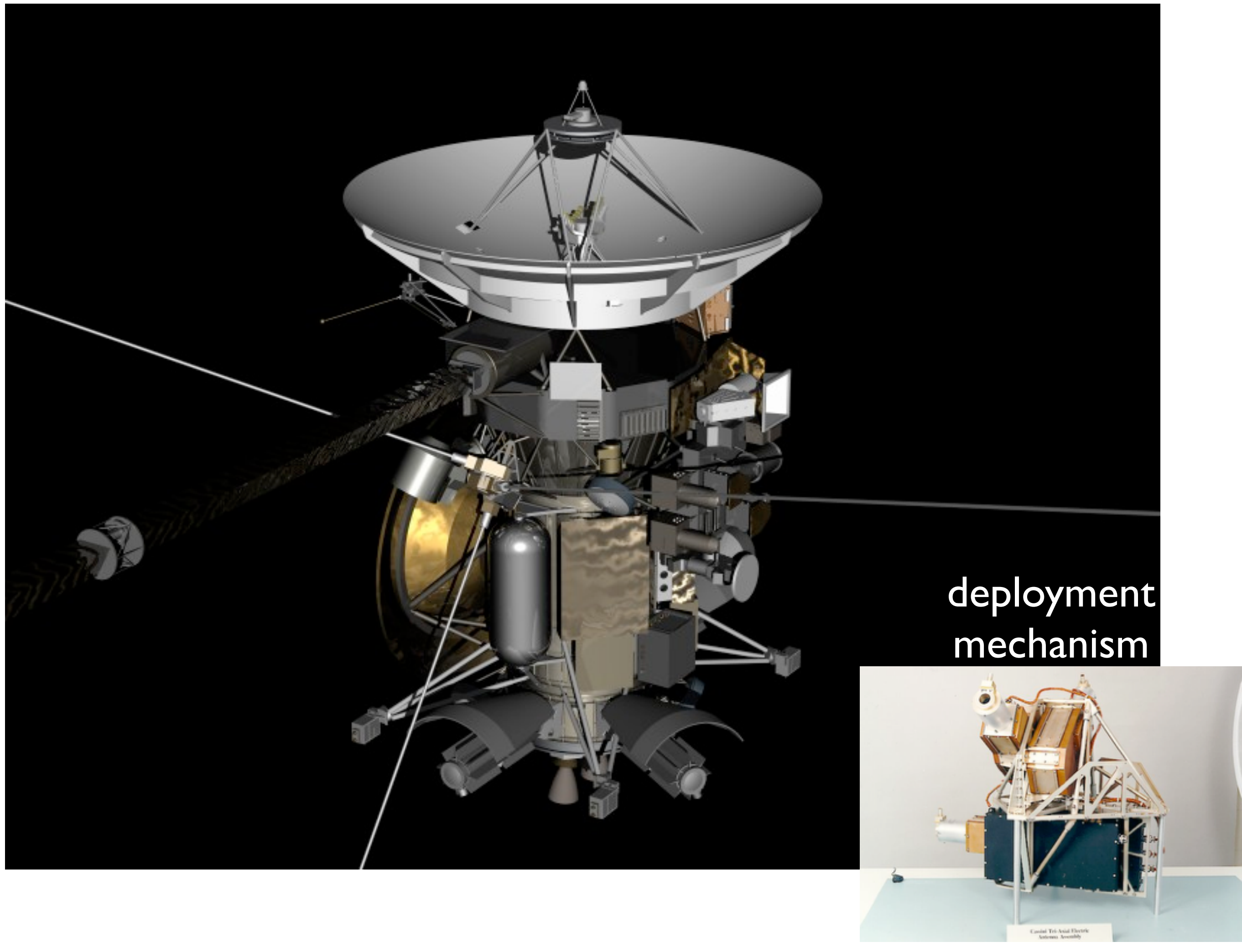

→ Spinning spacecraft: *ISEE, Ulysses, WIND …*

Wire antennas L = 30 – 90 m (centrifugal stabilization)

⇒ possibility of "Direction-Finding" (Gonio-Polarimetry) from variations in amplitude and phase of signal received on rotating antennas
→ restoration of ~1-2° angular resolution (requires precise calibration)

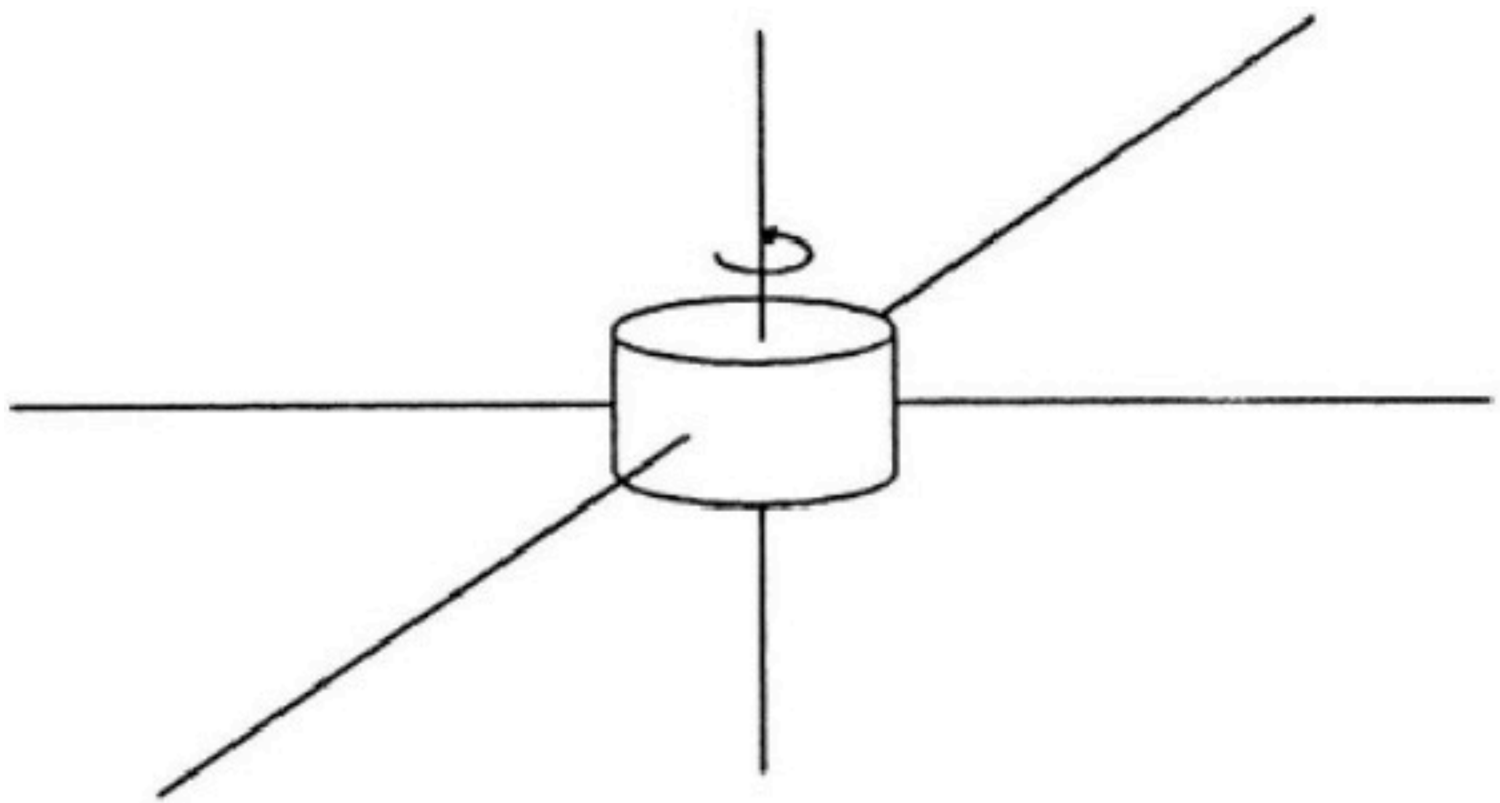

Spinning spacecraft

• Receivers

- in baseband : waveform + FFT or wavelets
- HF : heterodyne
- high dynamic range of LF signals ⇒ use of AGC + digitization with log coding

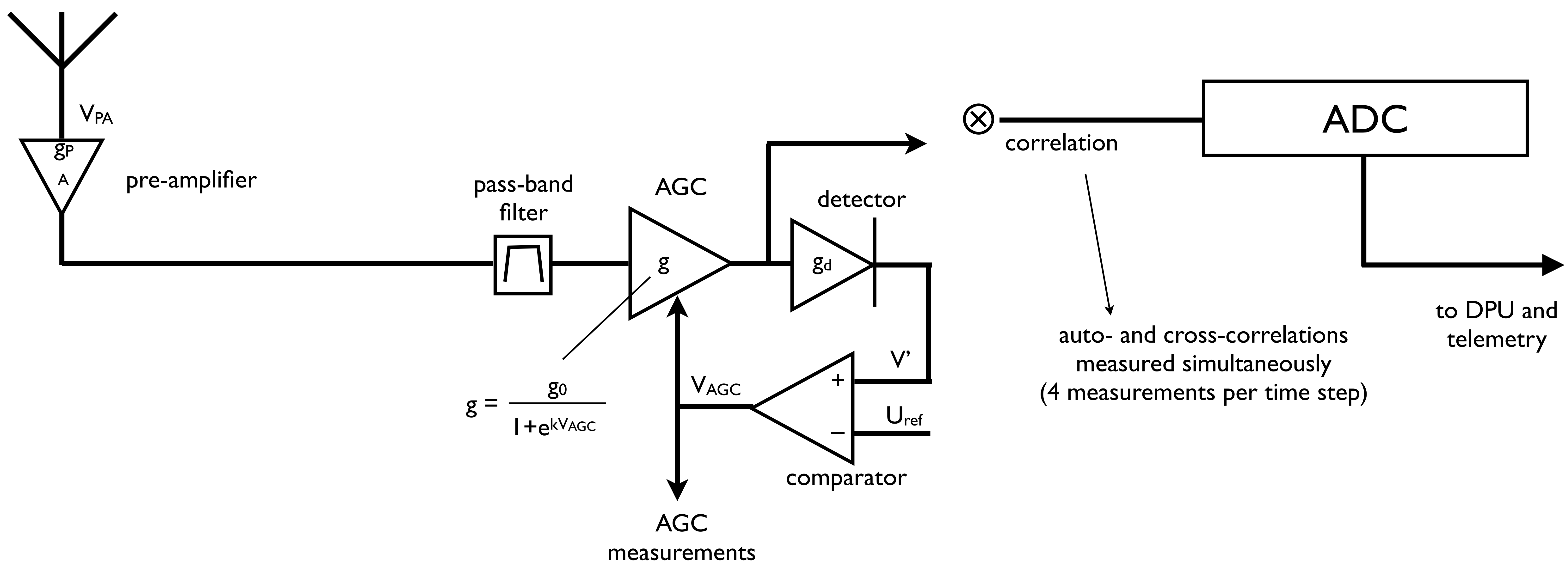

• Goniopolarimetry (or Direction-Finding) :

$\Rightarrow$ Correlation of the signal received from a point source on 2 antennas (dipoles) p,q :

the "coherence matrix" is measured :

$$\langle V_p\,{}^tV_q^*\rangle|_{\Delta t >> 1/\nu} = \begin{bmatrix} \langle V_pV_p^*\rangle & \langle V_qV_p^*\rangle \\ \langle V_pV_q^*\rangle & \langle V_qV_q^*\rangle \end{bmatrix} = \mathbf{V_{pq}} = \mathbf{H_{pq}}\,\mathbf{B}\,{}^t\mathbf{H_{pq}}^*$$

with $\mathbf{B} = \frac{1}{2}\begin{bmatrix} S+Q & U+iV \\ U-iV & S-Q \end{bmatrix}$ & $\mathbf{H_{pq}} = \begin{bmatrix} h_{p\theta} & h_{p\varphi} \\ h_{q\theta} & h_{q\varphi} \end{bmatrix}$

$\mathbf{h_p} = [\, h_{p\theta}\ ,\ h_{p\varphi}\,]$ describes the antenna p
in the reference frame of the incident wave (θ,φ),
z_W axis // wave vector $\mathbf{k}$

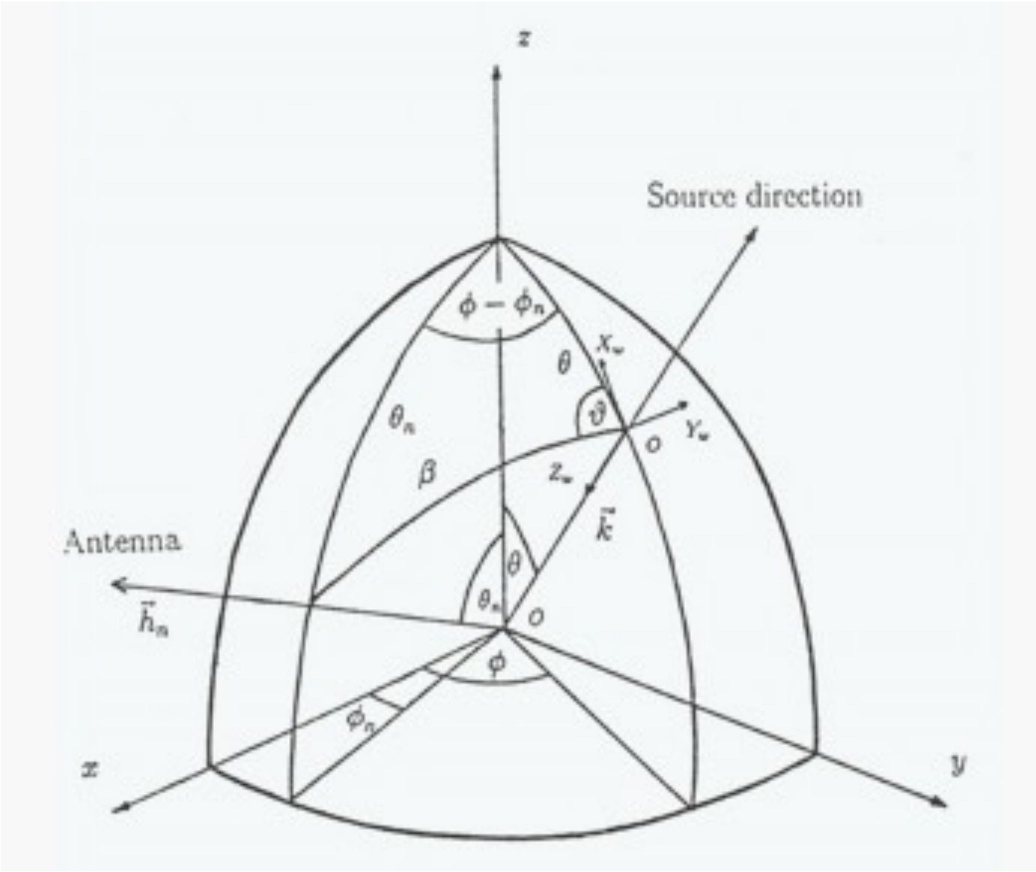

The resolution of this M.E. aims to determine
k & the polarization of the incident wave : S, Q, U, V, θ, φ

NB:

- Polarisation and direction of arrival are inseparable
  $\Rightarrow$ 1°-2° precision achieved on **k**
- **k** is determined for the dominant bright spot of each (t,f) measurement
- Possibility of including a 7th unknown = source size σ (extended, *Ex: uniform or Gaussian disk*)

3-axis stabilised spacecraft : each pair of antennas provides 4 independent measurements :

$<V_pV_p^*>$, $<V_qV_q^*>$, $\mathrm{Re}(<V_pV_q^*>)$, $\mathrm{Im}(<V_pV_q^*>)$

⇒ need 3 antennas (2 pairs) to obtain > 6 independent measurements (e.g. 7 with 2 pairs of antennas including 1 common, e.g. Cassini)

⇒ instantaneous Goniopolarimetriy

With 2 antennas : Goniometry (S, V, θ, φ) under an hypothesis on U & Q (generally =0)

or Polarimetry (S, Q, U, V) under an hypothesis on θ & φ

Spinning spacecraft (at ω) : $h_{p\theta}$, $h_{p\varphi}$, $h_{q\theta}$, $h_{q\varphi} = f(\omega, 2\omega)$

⇒ series of measurements $<V_pV_q^*>$ modulated at ω and 2ω ⇒ determination of S, Q, U, V, θ, φ from Fourier components of $<V_pV_q^*>$ at ω and 2ω (minimum = 2 antennas required)

Antenna calibration

Parameters
- orientation in space
- effective length

Methods
- *Electromagnetic simulations.*
- *Rheometry.*
- *In-flight measurements (on a known point source).*

you need ~1° accuracy on antenna directions to get 1° accuracy for goniopolarimetry.

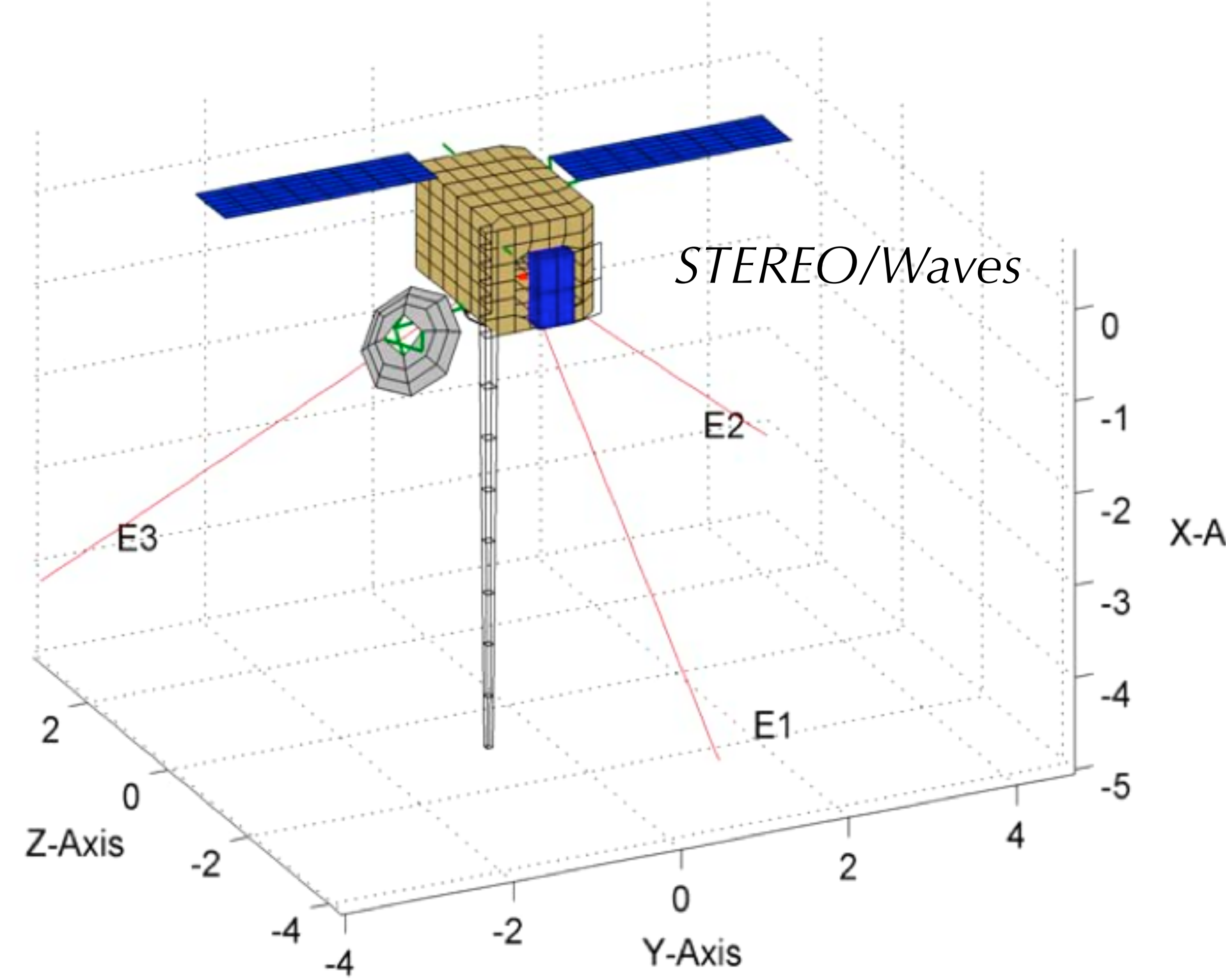

Rheometry

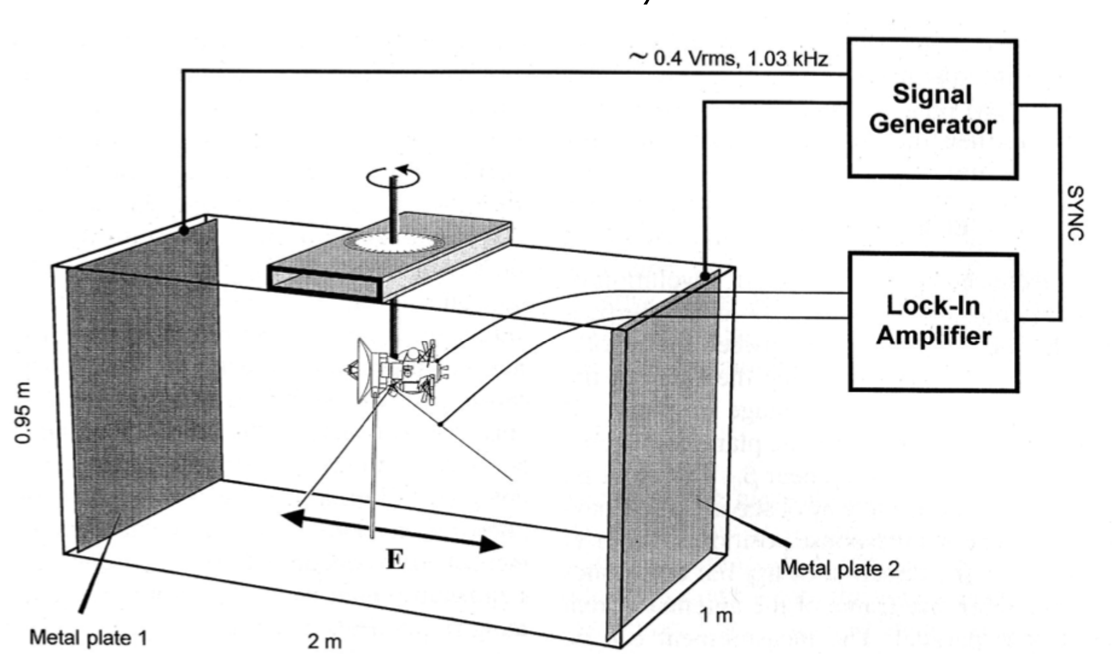

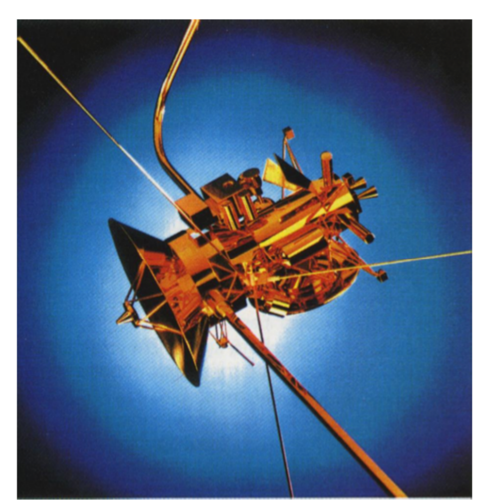

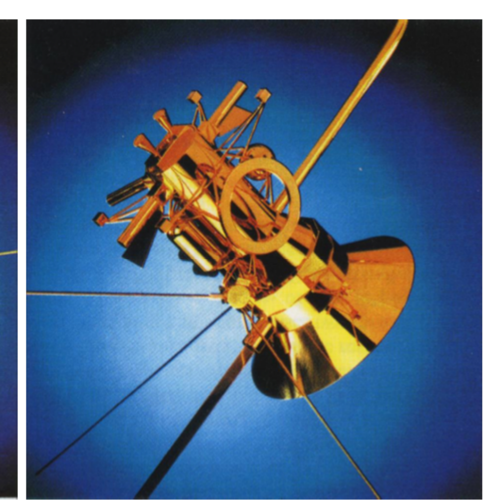

A few results

Earth's auroral radio emissions (1988)

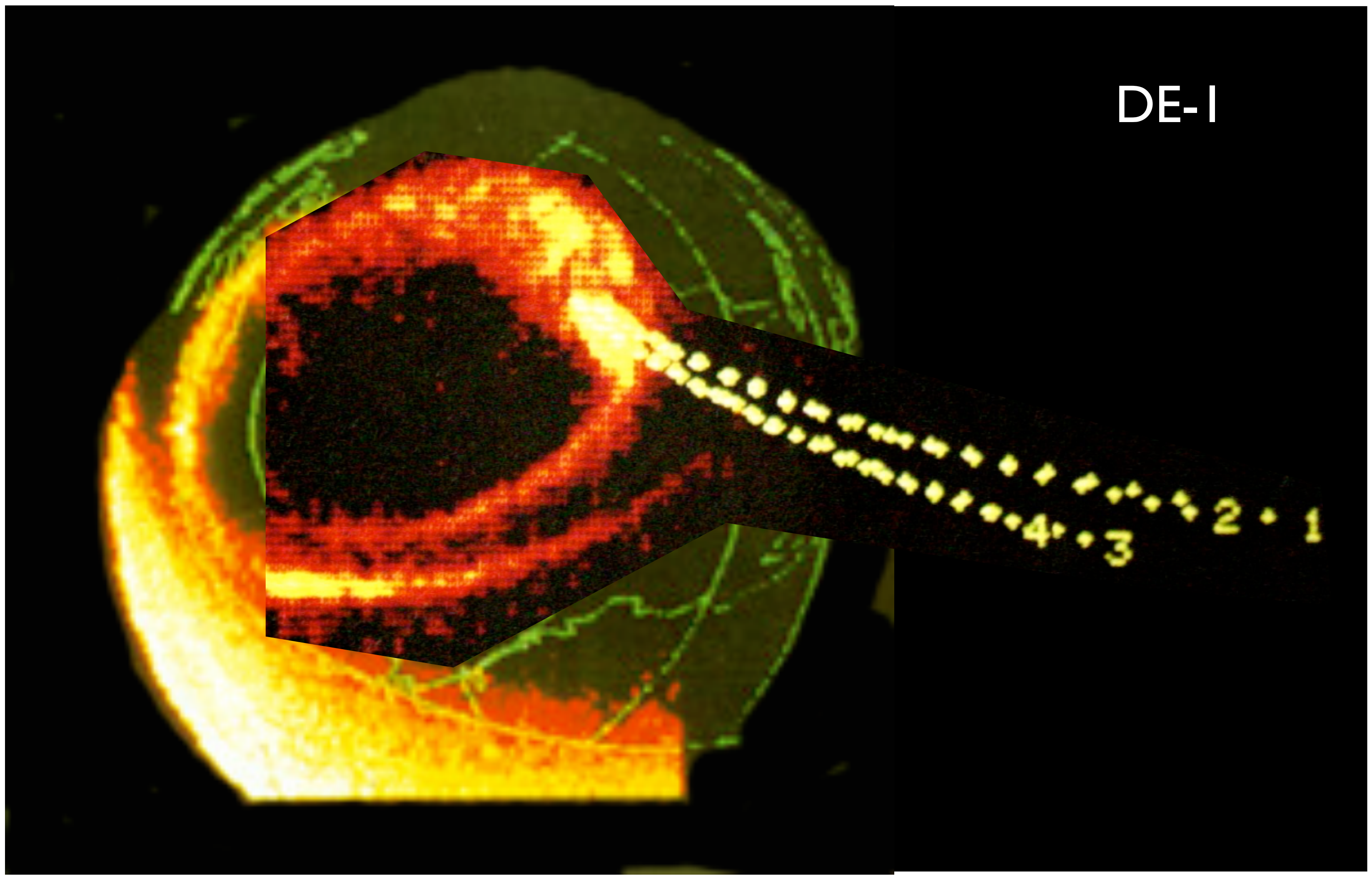

DE-1 (localisation)

Goniopolarimetry via
demodulation
of the spacecraft rotation

A few results

Jupiter: hectometric emission (1994)

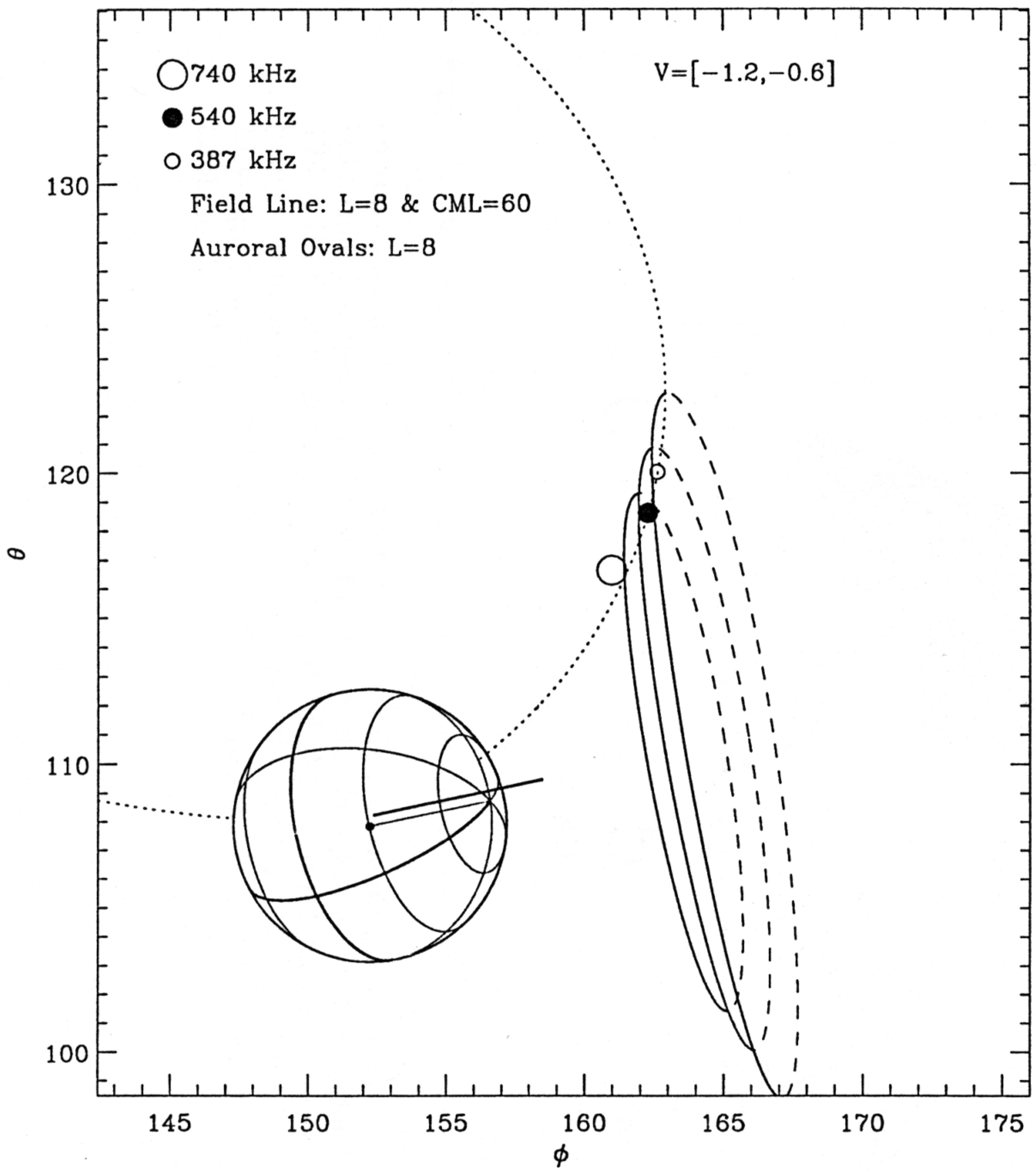

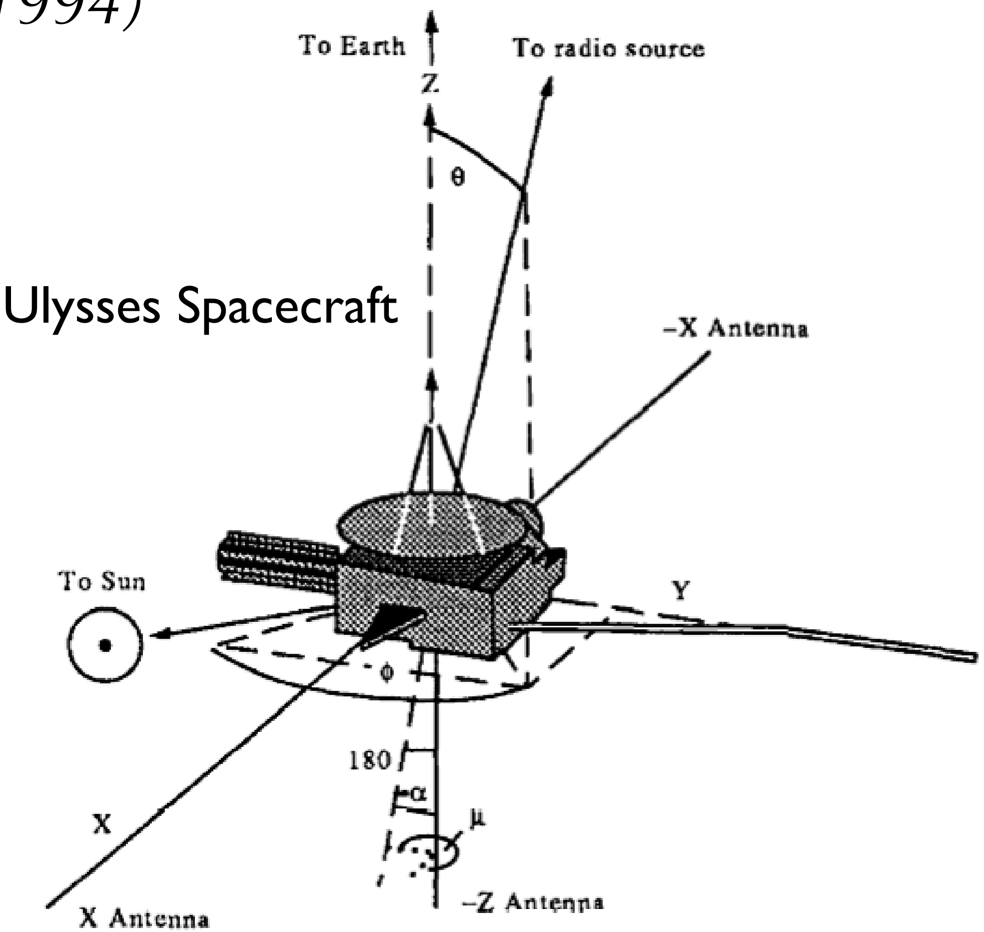

Jupiter flyby by Ulysses

Goniopolarimetry via demodulation of the satellite's rotation

Result: emission at local cyclotron frequency

A few results

Saturn: 3D localisation of auroral radio sources (2009)

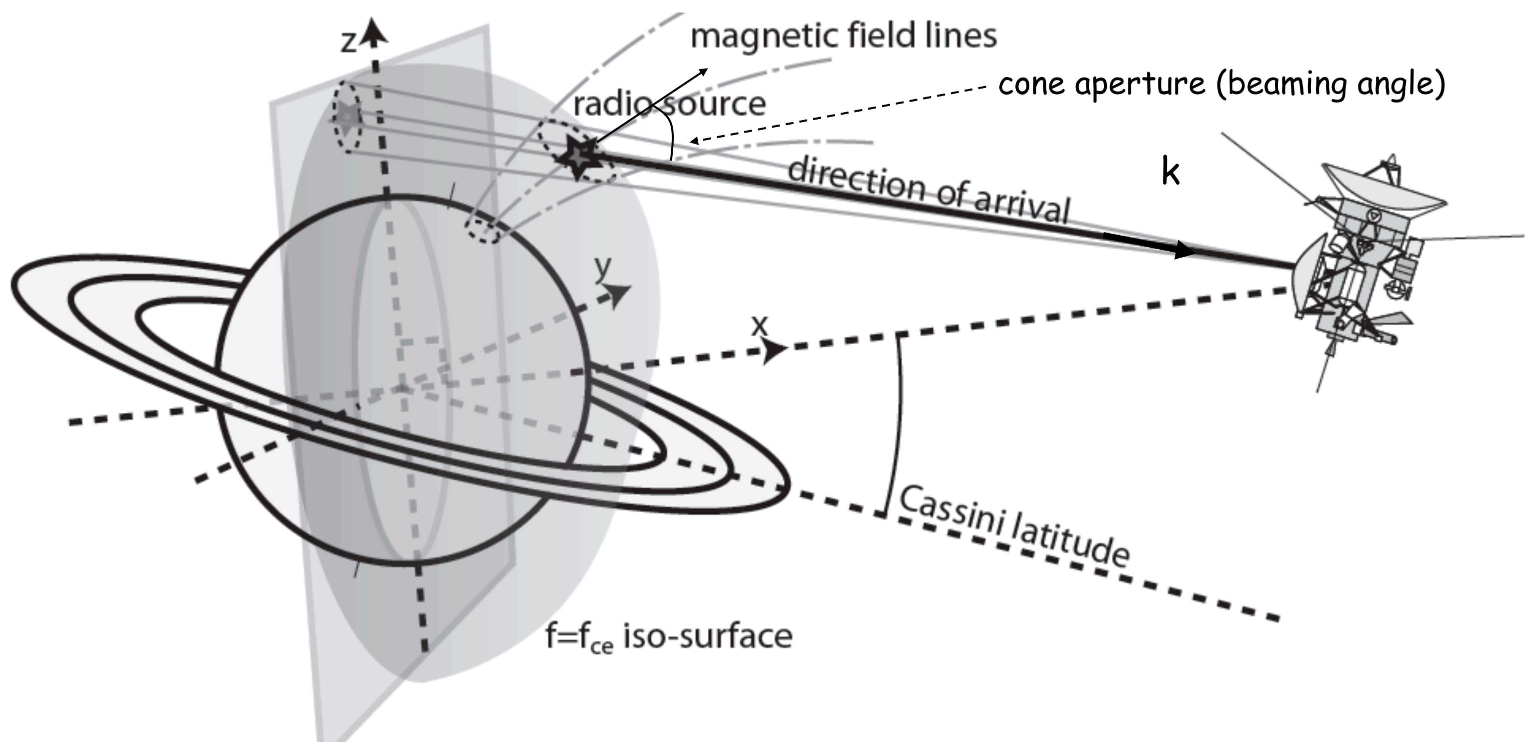

Cassini/RPWS
instantaneous Goniopolarimetry

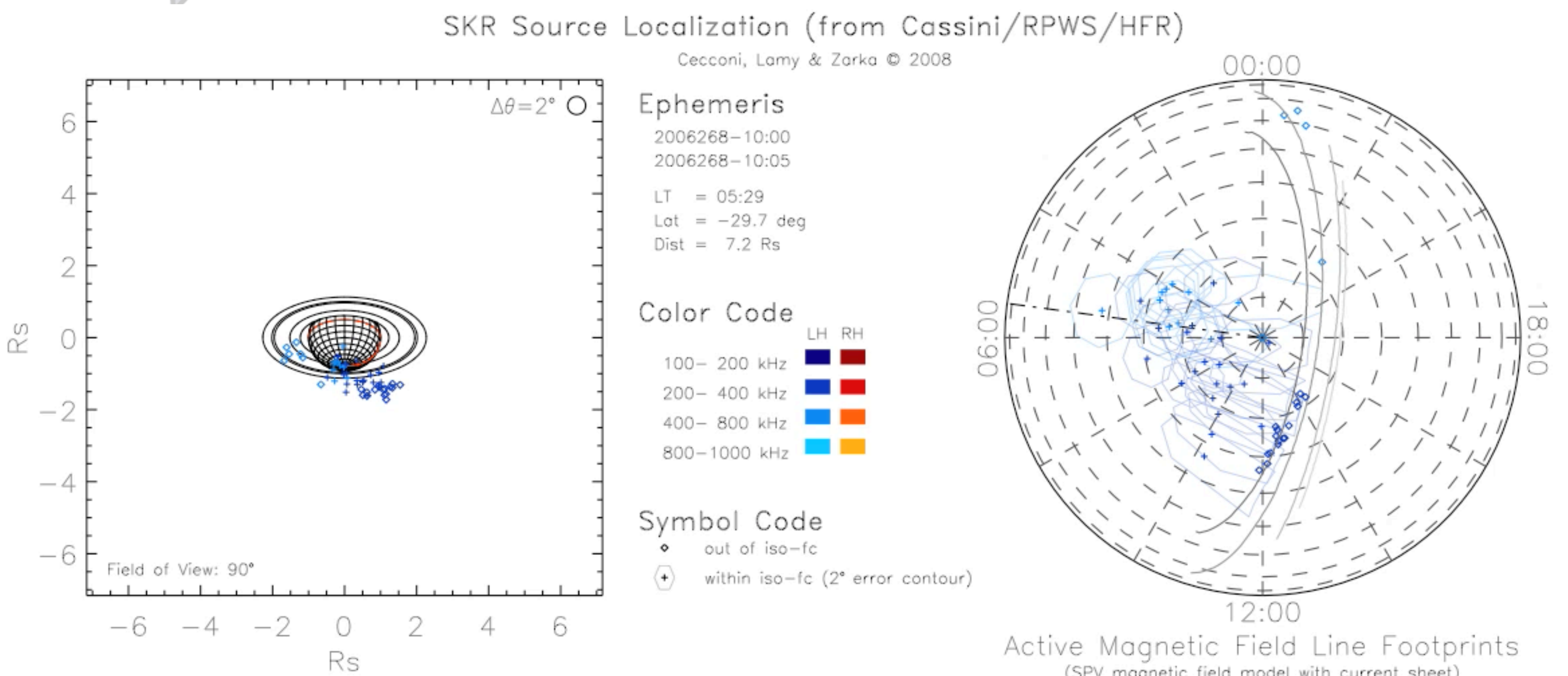

• Specific constraints on space observations

→ L_{max} ⇒ *inertia, deployment, optical shadowing*
→ Mass ⇒ *≤ a few kg*
→ Power consumption ⇒ *≤ a few*
→ Size ⇒ *miniaturisation, ASIC …*
→ Dynamic range ⇒ *2 stages : AGC + numerical analysis*

⇓ ⇓

= gain control loop FFT or wavelets

• Measurements

→ Auto- and cross-correlations of voltages measured at antenna terminals : $\langle V_i V_j^* \rangle$

• Noise sources

→ Quasi-Thermal ⇒ *agitation of free e^- libres in the vicinity of the antenna*
→ e.s. noise with a peak at f_{pe}
→ Photoelectron ⇒ *electrons ejected from antenna or spacecraft by impact of ions or dust grains* (performances of dipoles > spheres)
→ Galactic background ⇒ *dominates ≥ 1 MHz*
→ RFI (onboard) ⇒ *synchronised power converters,*
preamplifiers as close as possible to antennas
(at the foot of the dipoles or in the spheres)

2020+ : LOFAR-on-the-(far side of the)-Moon ?

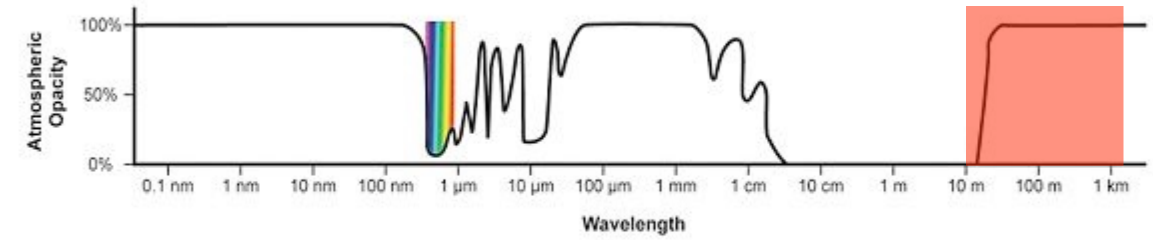

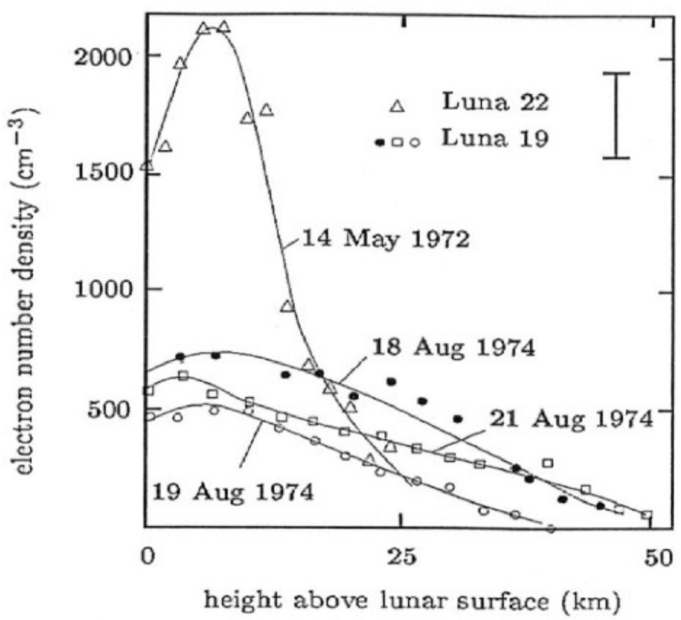

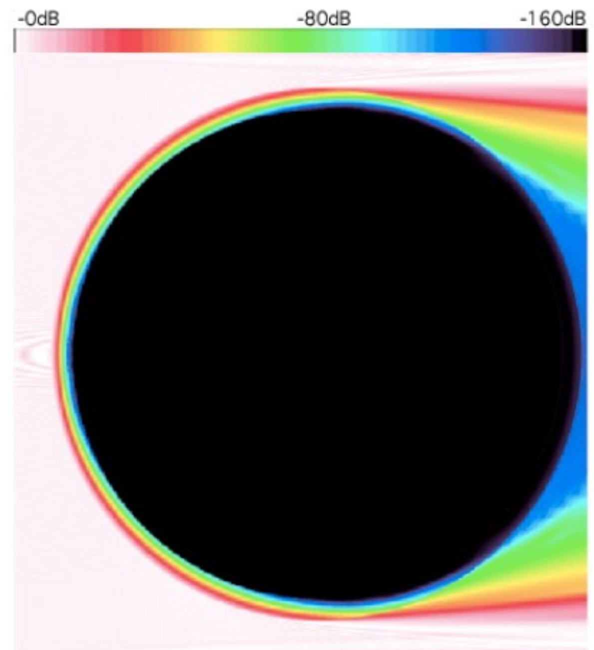

Attenuation of a onde radio wave at 60 kHz

- VLF Astrophysics TBF
- Sky mapping by space interferometry: swarms of small VLF satellites (≥8-16)
  → difficulties = omnidirectional elemental antenna, knowledge/control of baselines
- Lunar VLF interferometer: thin ionosphere, low level of RFI
  → dipoles phasing a posteriori?

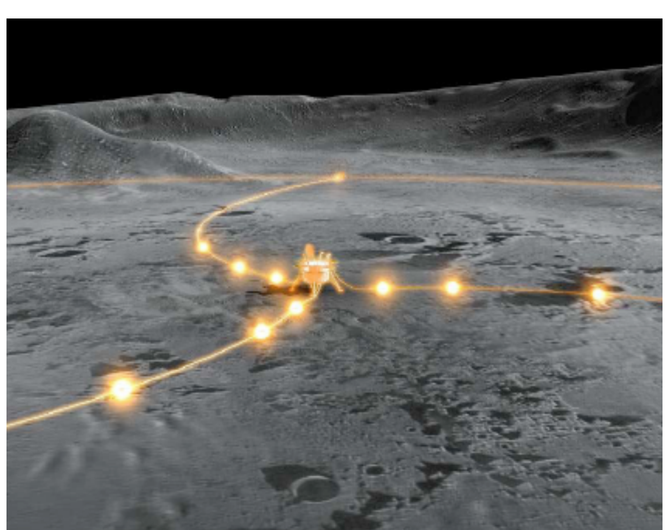

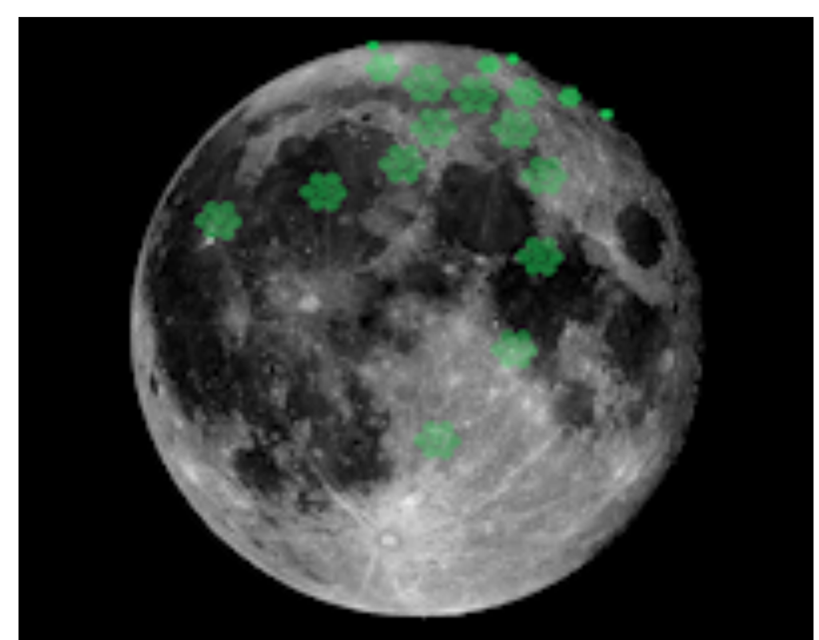

VLF radio interferometry in space

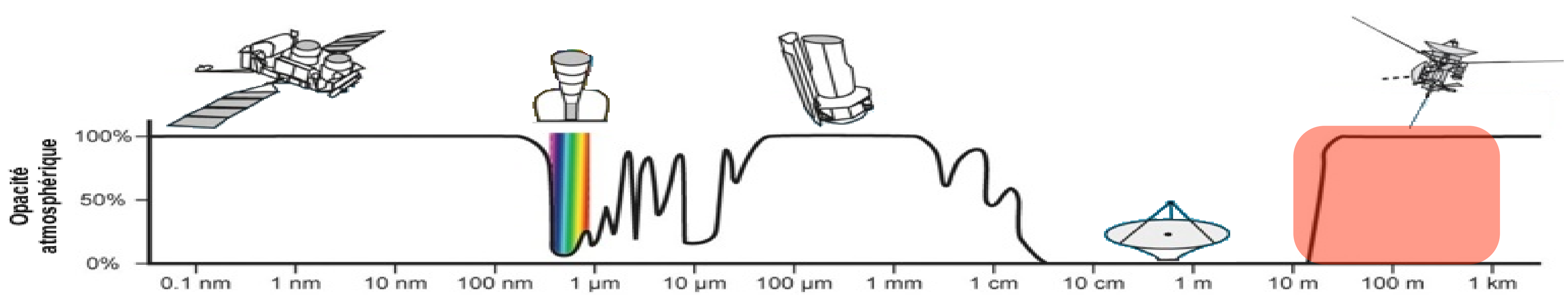

To be continued ...